林業叢刊第203號

2009 海峽兩岸林產科技研討會論文集

Cross Strait Forest Products Technology Symposium Proceedings of the 2009

地點：台北市三元街67號林業試驗所保育大樓

時間：98年10月26日－27日

行政院農委會林業試驗所　中華製漿造紙技術協會　中華林產事業協會

2009 Cross Strait Forest Products Technology Symposium
【Pulp and Paper】
Table of Contents

Section 1: Cellulose Technology

Section 2: Fiber Treatment and Properties

Section 3: Paper Coating

Section 4: Paper Additives

Section 5: Energy and Wastewater

Section 6: Wood Chemistry

Using Ultrasonic to Prepare Cellulose Nanofibers of TEMPO-Mediated Oxidation Directly

Zhongyan Qin, Guolin Tong
Jiangsu Provincial Key Lab of Pulp and Paper Science and Technology,
Nanjing Forestry University, Nanjing 210037, China

Abstract: Cotton linter was used as a native cellulose fibers to be oxidized by the TEMPO-NaBr-NaClO system and 40kHz for 13.5 hours, and individualized cellulose was obtained in the milky white solution directly without post-treatment. The C6 primary hydroxyl group of cellulose fibers was converted to the carboxylate group, whose amount is 1.66 mmol/g. In oxidized processing, the crystallinity of cellulose fibers gradually decreased with the reacted time .Transmission electron microscopic observation shown that individualized cellulose nanofibers 5-10 nm in width and 200-400 in length .individualized cellulose fibers can stabilized dispersed in aqueous solution.

1. Introduction

Cellulose is an important raw material for the synthesis of new carbohydrate with environmentally friendly and biocompatible property, and nowadays the modified cellulose is widely used in various fields. Cellulose nanofibers is a kind of the modified cellulose that has attracted great attention because of it's novel properties in optics, mechanics, surface and thermodynamics. Isogai et al reported that the native cellulose was oxidized to prepare the cellulose nanofibers by TEMPO-NaBr-NaClO system. Based on the present reports, the linter cellulose was processed under ultrasonic in the TEMPO-NaBr-NaClO system were investigated.

2. Material and Methods

The linter pulp was used as native cellulose fibers (Anhui Xuelong, China). TEMPO (Changzhou JiaNa Chemical Co.Ltd, China), sodium bromide(Sinopharm Chemical Regent Co.Ltd ,China), a 5.8-10% sodium hypochlorite solution(Shanghai Jiuyi Chemical Co.Ltd, China), an ultrasonic cleaner was used as ultrasonic generator with working frequency of 40kHz and effect ultrasonic power of 300W (KQ-300DE, Kunshan Ultrasound instrument Co. Ltd, China), and other chemicals were supplied by the laboratory. All chemicals were used without further purification.

The cotton linter pulp(3 g) was dispersed in water (500 ml) with TEMPO (0.048 g, 0.3 mmol) and sodium bromide (0.48 g, 4.8 mmol). The 8.6% sodium hypochlorite solution (30 ml) was added into the mixture and pH was adjust to 10 by adding 0.5 M hydrochloric acid. After pouring the mixtures into a four-neck flask, it was dipped into the trough of the ultrasonic cleaner. The reaction was initiated by setting the power of the ultrasonic cleaner at 100%, the circulating cooling water was used to maintain the reaction at the room temperature and slow stirring is also exploited. The pH was maintained at 10 by adding 0.5 M sodium hydroxide solution. After reaction, the solution was acidified by adding 0.5 M hydrochloric acid and separated by centrifugation at 8000 rpm. The residue was centrifugated in water for three times, and then freezed to stored .

The carboxylate contents of cellulose nanofibers was determined by the electric conductivity titration method.

3. Results and discussion

(1) Preparation of Cellulose Nanofibers with TEMPO Mediated oxidation

The linter pulp was oxidized TEMPO mediated oxidation. The results were shown in Figure 1. Figure 1 shows the relationships between the product of carboxylate and the consumption of sodium hypochlorite with extending reaction. After 2h reaction, the carboxylate content increased from 0mmol/g to 1.1mmol/g, and every 1g cellulose consumed 7 mmol NaClO. Then the carboxylate content further increased up to 1.66 mmol/g after 12 hours and every 1g cellulose consumed only 4.6 mmol NaClO. Finally, no NaClO in the solution was left and

1 mol carboxylate group is corresponding to nearly 7 mol NaClO.

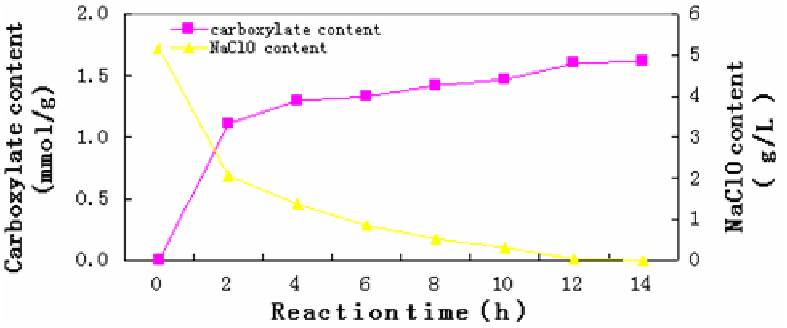

Fig. 1 Association between the reaction time with the contents of carboxylate and the count of sodium hypochlorite in the mixtures when the reaction was carried out by TEMPO-NaBr-NaClO system under the condition of the power 100% of the ultrasonic cleaner, working frequency 40 kHz

Because ultrasonic can destroy the crystal region to increase the accessibility of the reagents, the C6 primary hydroxyl groups of cellulose surface was easily oxidized by the TEMPO, and then the long cellulose fibers were slightly oxidized and rapidly broken down into the small particles duet to the effect of dispersing, mechanical kinetics and fragmentation. Consequently, specific surface area of the particles was larger than that of before, which raise the probability of the C6 primary hydroxyl groups reacted with the TEMPO. As a result, the effects accelerated the oxidation of cellulose. The decrease of the reaction rate can be attributed to the concentration of NaClO, which has been lowered in the solution at last 12 hours.

As shown in Figure 2 & Table 1, the temperature has a profound effect on the preparation of the TEMPO-mediated oxidized cellulose under ultrasonic. If the decomposation was processed at 30-35℃, a mass of NaClO was consumed and the C6 primary hydroxyl group was not sufficiently oxidized leading to the decrease of carboxyl content. When the decomposation was proceeded at 40℃, the C6 primary hydroxyl group of cellulose fibers was oxidized into carboxylic acid and strong decomposation of cellulose is aslo proceeded. However, due to the short reaction time, the carboxylic acid group was retained to some extent. Hence, the content of carboxylic acid group is even higher than that prepared at 30-35℃.

Table 1 Cellulose fibers was oxidized under different conditions

Cellulose(g)	TEMPO(g)	NaClO(mmol)	NaBr(g)	Temperature(℃)	Residues(g)	Time(h)	pH
3.0060	0.0488	35	0.4815	25	2.2506	13.5	10
3.0070	0.0494	35	0.4853	30	2.0320	13.5	10
3.0225	0.0485	35	0.4857	35	1.9562	10	10
3.0544	0.0489	35	0.4820	40	1.9467	6	10
3.0929	0.0490	36	0.4856	25	2.4201	10	9
3.0084	0.0482	35	0.4909	25	2.1035	18	11
3.0694*	—	36	0.4959	25	2.3226	—	10

As shown in Figure 3 & Table1, the pH also affected the content of carboxylic acid group and quality of product. Moreover, it is the higher pH, the longer reaction time will be. When pH was lower than 9, NaClO is relatively easy to be hydrolyzed into HClO and the hydroxyl group tended to be oxidized into carboxylic group. When pH was changed to 11, NaClO completely formed ClO^-, which could select to oxidize C6 hydroxyl group to carboxyl group.

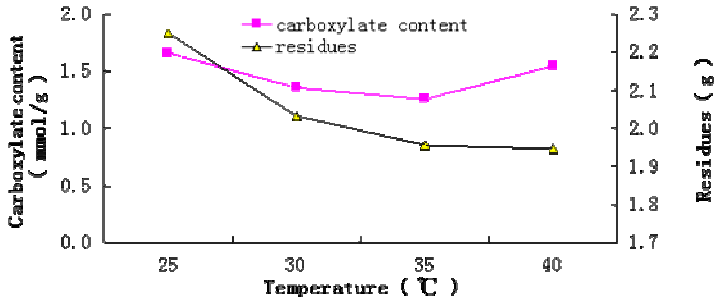

Fig. 2 Association between the reacted temperature with the carboxylate content and the residues

(2) Changing the Crystallinity of Cellulose during the Reaction.

Figure 4 shows the change of crystallinity of cotton fibers before and after reacted in the TEMPO-NaBr-NaClO system under supersonic. Al was the cotton fibers and its carboxylic content was 0 mmol/g, but the crystallinity is the best. In the presence of ultrasonic, the crystallinity of oxidized cellulose correspondingly reduced. The microjet generated by ultrasonic cavitation damaged the surface of cellulose and the fibrillation was generated, hence the surface area was increased and crystallinity was decreased, besides the accessibility of the reagents to cellulose was enhanced. Consequently,it is concluded that the crystallinity of the cellulose is reduced with the reaction time increasing.

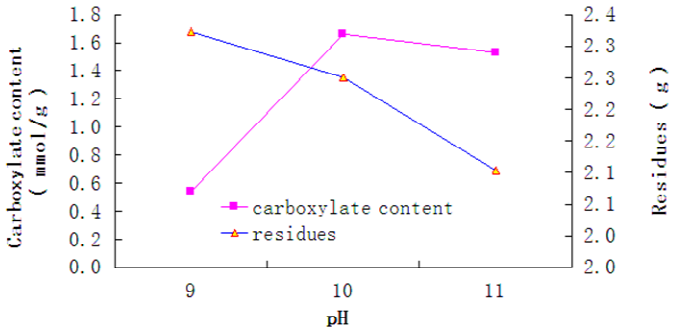

Fig. 3 Relationships between the pH, the carboxylate content and the count of the residues 8h (A3), 13.5h (A4) by the TEMPO-NaBr-NaClO system under the ultrasonic .

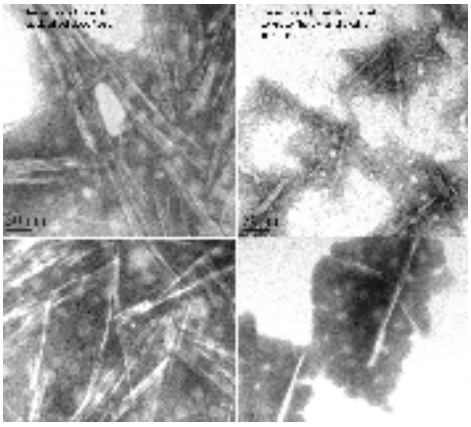

Fig. 4 TEM image of the cellulose nano fibers

Fig. 5 The state of oxidized solution of cellulose fibers

(3) Transmission Electron Microscope Observed Cellulose Nanofibers.

In Figure 4, the appearance of the cellulose nanofibers sample and its dilute sample (diluted to 0.1%) prepared after 13.5h reaction under ultrasonic in the TEMPO-NaBr-NaClO system. In Figure 5, the left bottle

contained the solution obtained directly after reaction, but it all congregated due to the high concentration; the right is the solution which was diluted to 0.1% from the original one and the carboxylic content is 1.66mmol/g. The width of linter is ca. 5-7nm and the density of the primary hydroxyl groups of anhydroglucose units facing the outer side on each cellulose fibril is 3.4 groups/nm^2. From Figure 4, the individualied cellulose nanofibers appeared with the width 5-10nm and length 200-400nm, but not the length only several micron. Under the ultrasonic, the oxidized individualied cellulose fibers have plenty of hydrophilic carboxylic group and its content is about 1.66 mmol/g. It is reported that every chain of cellulose has more than 3000 carboxylic groups of the anhydroglucose units，and the H-bond will be formed between the carboxylic group and H_2O, which will stabilize the individualied cellulose fibers dispersing in the aquaous solution. Meanwhile, strong reation will induce different decomposation degree of cellulose fibers, therefore it prepared the short cellulose nanofibers, but not the long ones.

4. Conclusion

The ultrasonic effect for the oxidation of native cellulose fibers in the TEMPO-NaBr-NaClO system and directly obtain the individualized cellulose nanofibers.

The content of carboxylic groups on cellulose nanofibers could be 1.66mmol/g, and the nanofibers were of width 5-10nm and length 200-400nm.

Vitally, these cellulose nanofibers can stabilize in the solution. The native cellulose was oxidized by the TEMPO-NaBr-NaClO system with the ultrasonic power of 40kHz and pH 10 for 13.5 hours.

Acknowledgement

The financial support from National National Science Foundation of China (30671653) is greatly appreciated.

References

1. Jaehwan Kim, Sungryul Yun. Discovery of Cellulose as a Smart Material.Macromolecules, 2006, 39, 4202-4206
2. Dieter Klemm, Brigitte Heublein, et al .Cellulose: Fascinating Biopolymer and Sustainable Raw Material. Angew. Chem.. 2005, 44, 3358 – 3393
3. Shinsuke Ifuku, Masaya Nogi, et al .Surface Modification of Bacterial Cellulose Nanofibers for Property Enhancement of Optically Transparent Composites: Dependence on Acetyl-Group DS. Biomacromolecules, 2007, 8 (6), 1973-1978
4. Hayaka Fukuzumi, Tsuguyuki Saito, et al. Transparent and High Gas Barrier Films of Cellulose Nanofibers Prepared by TEMPO-Mediated Oxidation. Biomacromolecules, 2009, 10 (1), 162-165
5. Masaya Nogi, Keishin Handa, et al. Optically transparent bionanofiber composites with low sensitivity to refractive index of the polymer matrix. Appl. Phys. Lett. 2005,87, 243110
6. Hiroyuki Yano, Junji Sugiyama et al. Optically Transparent Composites Reinforced with Networks of Bacterial Naofibers. Adv Mater. 2005, 17(2), 153-155
7. Masaya Nogi, Shinsuke Ifuku, et al. Fiber-content dependency of the optical transparency and thermalexpansion of bacterial nanofiber reinforced composites. APPLIED PHYSICS LETTERS, 2006, 88, 133
8. Akira Isogai, Tsuguyuki Saito, et al. Cellulose Single Nanofibers prepared by TEMPO-Mediated Oxidation of Native Cellulose: Fundamentals and Application. Proceeding of International Conference of Pulping, Papermaking and Biotechnology 2008,Nanjing , China's Scientific Culture Press, 124
9. Tsuguyuki Saito, Akira Isogai. TEMPO-Mediated Oxidation of Native Cellulose. The Effect of Oxidation Conditions on Chemical and Crystal Structures of the Water-Insoluble Fractions. Biomacromolecules, 2004, 5 (5), 1983-1989
10. Tsuguyuki Saito, Satoshi Kimura, Yoshiharu Nishiyama, et al. Cellulose Nanofibers Prepared by TEMPO-Mediated Oxidation of Native Cellulose. Biomacromolecules, 2007, 8 (8), 2485-2491

11. Hayaka Fukuzumi, Tsuguyuki Saito,et al .Transparent and High Gas Barrier Films of Cellulose Nanofibers Prepared by TEMPO-Mediated Oxidation.Biomacromolecules, 2009, 10 (1), 162-165
12. Tsuguyuki Saito, Akira Isogai.TEMPO-Mediated Oxidation of Native Cellulose. TheEffect of Oxidation Conditions on Chemical andCrystal Structures of the Water-Insoluble Fractions.Biomacromolecules, 2004, 5 (5), 1983-1989
13. Ma Pibo, Chen Sheng can, et al. Application of ultrasonic wave in sizing of oxidized starch. Progress in Textile Science & Technology, 2008,4,26-28
14. Wang Lan, Jiang Zhixin,Yan Jun. Effect of ultrasonic treatment on the structure and properties of cotton fibers. Journal of Textile Research,2006,27(10),77-79
15. Zhou Gang, Huang Guanbao, Wang Shaopeng. Changes of structure and its dissolution in phosphoric acid of cellulose after pretreated with ultrasonic. Applied Chemical Industry ,2008,37(6),677-679

Homogeneous modification of cellulose in an ionic liquid (BMIMCl)

Huai-Yu Zhan, Chun-Xiang Lin, Ming-Hua Liu and Shi-Yu Fu

State Key Laboratory of Pulp & Paper Engineering, South China University of Technology, Guangzhou 510640, China

The homogeneous modification of cellulose in an ionic liquid, 1-butyl-3-methylinidazolium chloride (BMIMCl), was investigated. Firstly, cellulose chloroacetate (Cell-ClAc), as a macroinitiator, was synthesized by direct acylation of cellulose with chloroacetyl chloride without any catalysts under mild conditions in BMIMCl. Samples were analyzed by NMR and FT-IR. Then, the cellulose-based macroinitiator was used for the ATRP of MMA mediated by the CuBr and 2,2'-bipyridine (bpy) catalysis system. The copolymerization was carried out in BMIMCl without homopolymer by-product. The polymers were easily separated from the catalyst when the ionic liquid was used as reaction medium. The grafting copolymers were characterized by means of ^{1}H NMR and AFM. The grafted PMMA chains obtained by the hydrolysis of the cellulose backbone were analyzed by GPC. The results showed that the obtained copolymers had grafted polymer chains with well-controlled molecular weight and polydispersity, and the polymerization was a "living/controlled" system. Further, through AFM observation, it was found that the cellulose graft copolymer in solution could aggregate and self-assembly into sphere-like polymeric structure.

The macroinitiator Cell-ClAc was synthesized by homogeneous acylation of cellulose with chloroacetyl chloride in BMIMCl as shown in Scheme 1. The homogeneous chloroacylation of cellulose with chloroacetyl chloride can be readily carried out in ionic liquid BMIMCl even at room temperature. To obtain a reasonable reaction speed, a relatively high temperature was adopted.

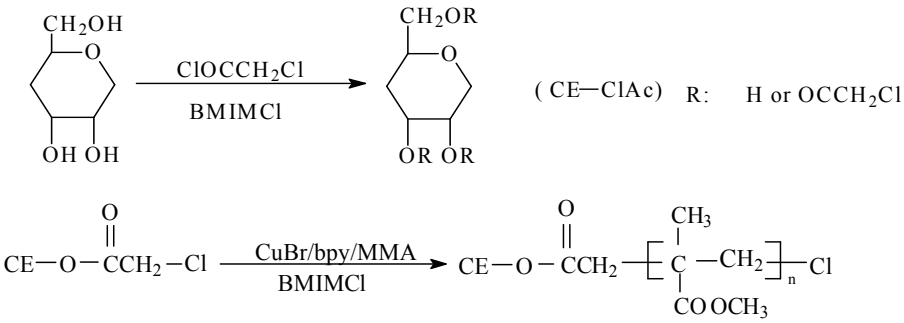

Scheme 1 Synthesis procedure of macro-initiator Cell-ClAc and cellulose graft copolymers

Figure 1 displays the FT-IR spectra for the native cellulose (a) and Cell-ClAc (b). The presence of two new bands at 1750cm^{-1} (–C=O stretching) and at 790cm^{-1} (C–Cl stretching) in the spectrum of Cell-ClAc, in which there is no band for Cell-OH, indicates that the chloroacetyl group has been attached to cellulose.

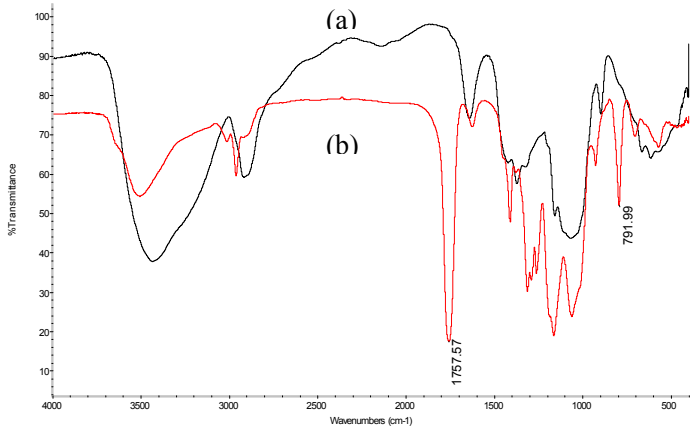

Figure 1 FTIR spectra of underivatized cellulose and macro-initiator Cell-AcCl (DS= 1.87).

The introduction of the chloroacetyl groups on cellulose chains was further confirmed by NMR measurement (Figure 2). The chemical shift at δ = 4.237 ppm in ^{1}H NMR (Figure 2(a)) could be attributed to the ethyl protons of chloroacetyl group. In the ^{13}C NMR spectrum (Figure 2(b)), the chemical shift of carbonyl carbon appeared in the range of 165-171 ppm.

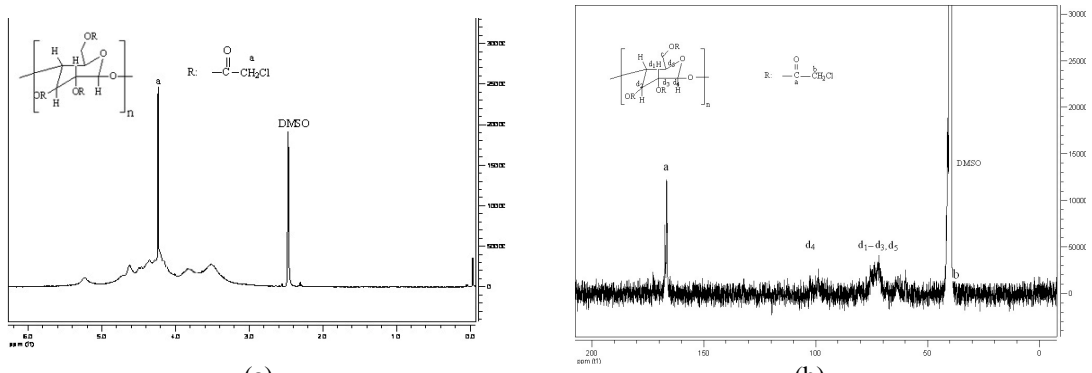

(a) (b)

Figure 2 ^{1}H NMR (a) and ^{13}C NMR (b) spectra of Cell-AcCl (DS =1.87) in DMSO-d_6.

The chloroacetate groups formed from the reaction of the hydroxyl groups on the cellulose backbone with chloroacetyl chloride were known to be an efficient initiator of ATRP (Kamigaito et al, 2001.). A series of polymerizations were conducted using CuBr/bpy as the catalyst system and Cell-AcCl as the macroinitiator, ionic liquid BmimCl as reaction medium. The reaction of grafting on cellulose is indicated in Scheme 1. Chloroacetate groups here act as initiator sites.

The graft copolymers Cell-PMMA was characterized by ^{1}H NMR analysis (Fig. 3). The chemical shift of proton at 3.677 ppm can be observed, which is attributed to protons of -OCH_3 in PMMA.

The ‘‘livingness’’ of atom transfer radical polymerization process can be ascertained from a semilogarithmic plot with the linear first-order kinetics, which reflects the constant concentration of propagating radicals. Semilogarithmic plots of the monomer conversion versus the reaction time for MMA copolymerization with Cell-ClAc macro-initiator is shown in Fig. 4. The variation of $\ln([M]_0/[M]_t)$ is linear with time in the period of 25 to 180 min, where $[M]_0$ is the initial monomer concentration and $[M]_t$ is the monomer concentration at time t, which indicates that within this period the polymerization is of first-order with respect to the monomer. That is, the concentration of the growing radical species in the system is constant during the polymerization. After 180 min, a slight curving occurred. The possible reason might be the polar solvent BMIMCl used and the decrease of radical concentration, which is due to partial termination of living free radicals.

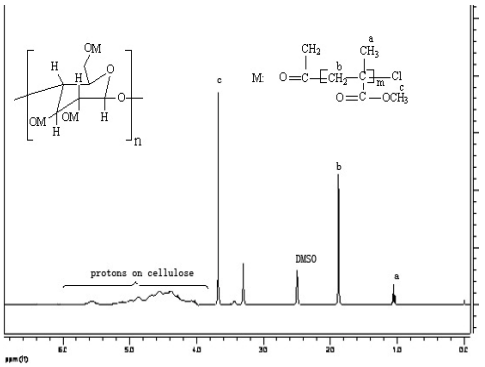

Figure 3 ^{1}H NMR of Cell-PMMA in DMSO-d_6

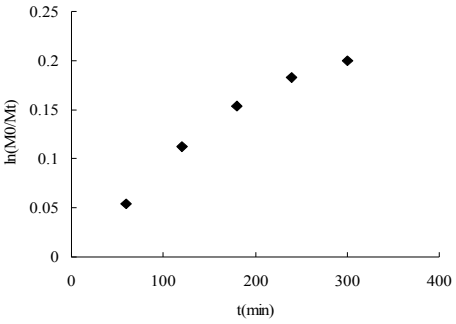

Figure 4 Semilogarithmic plot of monomer consumption versus time for MMA polymerizing in BMIMCl initiated by Cell-ClAc. ([Cell-ClAc]/[CuBr]/[Bpy]/[MMA] =1:1:1:100, temperature 60℃).

Fig. 5 shows the variation of the molecular weight and its distribution of the side chain PMMA obtained by selectively hydrolysis of cellulose in Cell-PMMA copolymers. The molecular weight of the graft copolymer is increased with the monomer conversion, and the M_w/M_n is about 1.6, which is decreased after the grafting polymerization. These results confirm again that the graft copolymerization is living and controlled.

Above discussion indicates that the graft copolymerization of MMA onto the cellulose backbone by ATRP was accomplished successfully in the ionic liquid BMIMCl. At the end of graft copolymerization in this way, homopolymer was not observed in the medium. Consequently, there was no problem over separating the graft copolymer from the homopolymer. This is an important advantage over conventional radical polymerization where homopolymerization and graft copolymerization occur simultaneously. Further, ionic liquids allow a simple process for separation of the metal complex from the polymer mixture at the end of the polymerization, and the ability to recover and reuse the catalyst dissolved in the ionic liquids for subsequent polymerizations was also reported by Traian Sarbu.(Sarbu& Matyjaszewski, 2001.).

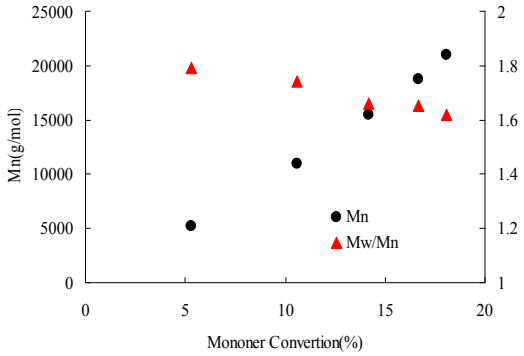

Fig.5 The variation of the M_n and M_w/M_n of side acetone, after chain PMMA with the monomer conversion.

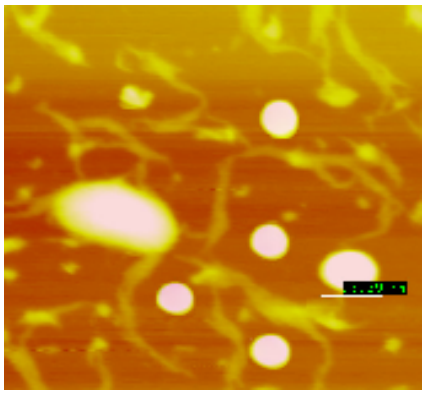

Fig.6 AFM images for Cell-PMMA in solvent solvent evaporation.

The morphology of Cell-PMMA graft copolymer was studied by tapping mode AFM. AFM images in Fig.6 shows the spherical morphology of the aggregates of cellulose-g-PMAA copolymers after the solvent is evaporated at the room temperature. The copolymer in acetone formed discrete, spherical particles and the average diameters of sphere-like particulates derived from the selective solvent acetone is roughly 50-100 nm. It indicates the tendency of aggregation of Cell-PMMA copolymers in solution.

References

1. Barsbay, Murat, Gueven, Olgun, Stenzel, Martina H., Davis, Thomas P., Barner-Kowollik, Christopher&Barner, Leonie.(2007). Verification of controlled grafting of styrene from cellulose via radiation-induced raft polymerization. *Macromolecules*, 40(20), 7140-7147.
2. Kamigaito M, Ando T & Sawamoto M. (2001). Metal-catalyzed living radical polymerization. *Chem Rev,* 101, 3689.
3. Mehmet Coskun&Mehmet Murs¸ itTemuz.(2005). Grafting studies onto cellulose by atom-transfer radical polymerization. *Polym Int,* 54,342–347.
4. Meng T., Gao X.& Zhang J.(2009). Graft copolymers prepared by atom transfer radical polymerization (ATRP) from cellulose. *Polymer*, 50(2), 447-454.
5. Nishio, Yoshiyuki.(2006). Material functionalization of cellulose and related polysaccharides via diverse microcompositions. *Advances in Polymer Science,* 205, 97-151.
6. Sarbu T.& Matyjaszewski K.(2001).ATRP of Methyl Methacrylate in the Presence of Ionic Liquids with Ferrous and Cuprous Anions. *Macromol. Chem. Phys.*, 202, 3379-3391.

Effect of Cellulase-assisted Refining on Properties of Fast-growing Poplar APMP

Gui-Hua Yang [1,2], Jia-Chuan Chen[1] and Feng-Shan Zhang [3]

[1] Key Laboratory of Paper Science and Technology of Ministry of Education of China, Shandong Institute of Light Industry, Jinan, China 250353;

[2] State Key Laboratory of Pulp and Paper Engineering, South China University of Technology, Guangzhou, China 510640;

[3] Huatai Group Co.Ltd, Guangrao, 257335, China

Abstract: The effect of cellulase treatment on properties of fast-growing poplar APMP pulp was studied. The results showed that, compared with the untreated pulp, the beatability of the treated pulp was improved, such as an increase of 1°SR~6.0°SR in beating degree and a decrease of 12.5%~22% in beating energy consumption. Brightness, breaking length, tearing index, bursting index and folding number of the pulp treated were respectively improved by 1.1% ISO, 23.5%, 12.2%, 15% and 67%. Treated by cellulase, fiber length increased partly, fiber width and fines content decresed, fibers torsion increased, and fiber bonding got stronger.

1. Introduction

Compared with other hardwood species, fast-growing poplars have many advantages, such as fsat-growing, better adaptability, easily breeding, and broad application[1]. As important material for pulping, fast-growing poplar species were widely planted and used in China. Saving and reducing of energy consumption is playing an important role in pulp and papermaking industry, and is also one of efficient methods of decreasing productive cost and improving marketable competition. Utilization of biotechnology in pulp and papermaking industry has grown rapidly since the mid-1980s. The utilization of enzyme for drainage enhancement, deinking of secondary fibers, and modification of fibers characteristics are intensively pursued[2-3]. Enzyme treatment can enhance swelling and absorption capbility of fibers, improve refining properties of pulp, and reduce refining energy[4-5]. The effect of cellulase-assisted refining on properties of fast-growing poplar APMP pulp were studied in this paper.

2. Material and Methods

(1) Material

Fast-growing poplar wood chips (length 15-25 mm, thickness 3-5 mm, width 10-20 mm) are from Shandong province, and commercial cellulase was from SUKEHAN company. The chemical components of fast-growing poplar and the properties of cellulase are shown in Table 1 and Table 2 respectively.

Table 1 Chemical components of fast-growing poplar

Cold water extractives /%	Hot water extractives /%	1%NaOH extractives /%	Benzene-ethanol extractives /%	Holocellulose /%	Klason lignin /%	Acid dissolved lignin /%	Pentosan /%
2.31	0.78	17.72	3.69	80.41	17.57	1.89	24.95

Table 2 Cellulase properties and its applicable conditions

Enzyme	Activity	Optimal pH	Optimal temperature
Cellulase	14400IU/g	5～6	50~55℃

(2) Methods

The flow chart of APMP production and cellulase treatment process is shown as follow.

Chemical impregnation → The first stage refining with refiner → High consistency settle → The second stage refining with refiner → Cellulase treatment → Refining with PFI mill → Sheet forming → paper properties measurement

Fig. 1 The flowchart of the production APMP and enzyme treatment with cellulase

Table 3 shows the optimal chemi- pretreatment conditions on wood chips. Cellulase treatmental conditions are showed in Table 4. All dosage of chemicals and cellulose are based on the oven-dry pulp.

Table 3 Chemi- pretreatment conditions

	NaOH /%	H_2O_2 /%	Na_2SiO_3 /%	$MgSO_4$ /%	EDTA /%	Temperature /℃	Time /min	liquor-to-wood ratio
First chemi-pretreament stage	3.3	3.0	1.0	0.2	0.2	75	50	1:4
Second chemi-pretreatment stage	3.0	3.0	2.0	0.3	0.3	70	60	1:4

Table 4 Cellulase treatment conditions

Factors	cellulase dosage /IU·g^{-1}	pH	Temperature /℃	Time /min	Pulp consistency /%
Conditions	20 25 30	6.0	55	90	10

(3) Standard methods

Pulp and paper properties were measured according to the following standard methods. Pulp was refined according to ISO5264-2. Handsheets were made according to ISO5269-2.Beating degree, Schopper-Riegler ISO5267-1; brightness, ISO2470; opacity, ISO2471; breaking length, ISO1924-1; tearing index, ISO1974; bursting index , ISO2578; folding number, ISO5626.

3. Results and discussion

The effects of cellulase treatment on beatability, refining energy, physical strength and optical properties of APMP pulp were mainly studied.

(1) Effect of cellulase treatment refining on beating degree and beating energy of fast-growing poplar APMP pulp

Refining energy, based on PFI revolutions, is related with beating degree. So the change of beating degree and PFI refining revolutions can indirectly express the consumption of refining energy.

Fig.2 and Fig.3 show the effects of cellulase treatment on beating degree and energy consumption.

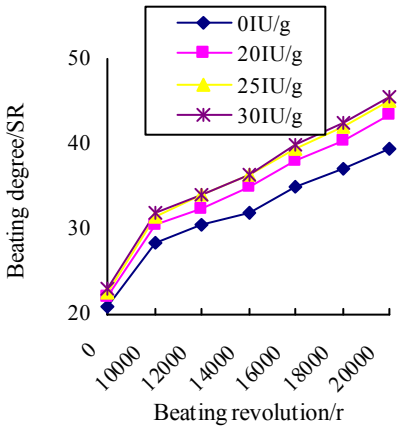

Fig.2 Effects of cellulase treatment on beating degree

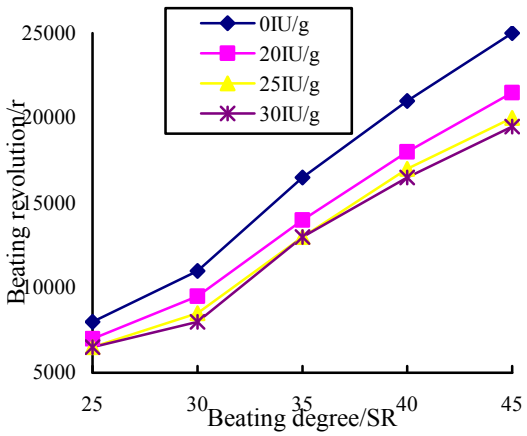

Fig.3 Effects of cellulase treatment on beating revolution

Fig.2 and Fig.3 indicated that, as comparison of properties of the untreated pulp for the same PFI revolutions and beating degree, the treated pulp showed an increase of beating degree in range of 1.0°SR to 6.0°SR, and a decrease of refining energy comsuption from 12.5% to 22%. Cellulase treatment can make fiber softer and more incompact, easier to refine, and reduce refining energy. The effect of cellulase-assisted refining were different in the cellulase dosage of 20IU·g^{-1}, 25IU·g^{-1} and 30IU·g^{-1}.The optimal dosage of cellulase was 25IU/g, in which the effect of cellulase-assisted refining was best.

(2) Effects of cellulase treatment on properties of fast-growing poplar APMP pulp

The differences of properties between the untreated and treated pulp of fast-growing poplar APMP pulp were shown in Table 5.

As can be seen from Table 5, compared with the untreated pulp for the same beating degree as that of treated pulp, the brightness, breaking length, tearing index, bursting index and folding number of the treated pulp were respectively improved by 1.1%ISO, 23.5%,12.2%,15% and 67%.Cellulase treatment led to a slight increase of optical properties, and significant increase of physical strength properties of APMP pulp. The results indicated that cellulase was very good in improving of physical strength properties of fast-growing poplar APMP pulp.

Table 5 Effects of cellulase treatment on properties of fast-growing poplar APMP pulp

Pulp properties	Untreated pulp	Treated pulp
Brightness /%ISO	75.8	76.9
Opacity /%	81.9	82.2
Breaking length /km	2.23	2.76
Tearing index /mN·m^2·g^{-1}	3.59	4.03
Bursting index/KPa·m^2·g^{-1}	1.26	1.45
Folding number/time	3	5

Notes:beating degree, 45°SR. Cellulase dosage, 25 IU·g^{-1}.

Table 6 Analysis of fibers properties of fast-growing poplar APMP pulp beated by cellulase-assisting

Fiber properties	Untreated pulp	Treated pulp
Ln /mm	0.517	0.569
Lw /mm	0.613	0.643
Lww /mm)	0.706	0.771
Fiber width /μm	20.9	20.1
Fibers torsion /mm	0.51	0.59
Fines /%	38.11	33.36

(3) Analysis of fiber properties

Table 6 shows the FQA analysis results of the untreated and treated pulp fibers. The results indicated that, compared with the pulp untreated by cellulase, fiber length (Ln,Lw and Lww)of the treated pulp increased slightly, fiber width and fines decresed, fiber torsion increased, and fiber bonding got stronger. Specific surface area of fines are relatively larger, cellulase can easily touch and degradate these fines, and fiber length of the treated pulp were longer than that of the untreated pulp .Cellulase treatment can make fiber be easily splited and torsioned, avoid cutting during refining and beating process, and improve strength properties of pulp.

4. Conclusion

The optimal conditions of cellulase treatments were pH 6, 55℃, 90min, 25IU/g xyellulase, and 10% pulp consistency.

Compared with the untreated pulp , the beating degree of the treated pulp was increased in range of 1°SR to 6.0°SR, and refining energy consumption decreased by 12.5% to 22%. The beatability of the treated pulp was improved.

Cellulase treatment can obviously improve the physical strength properties ,especially in breaking length and folding number, and increase the brightness by 1.1%ISO. But the opacity of the treated pulp was slightly decreased.

Fiber length of the cellulose-treated pulp increased slightly. Fiber width and fines content decresed. Fiber torsion increased, and fiber bonding got stronger.

Acknowledgement

This work was supported by the National Natural Science Foundation (Grant No.30671648), and the Natural Science Foundation of Shandong Province (Grant No. Z2006B08, Y2007D41) and the Science and Technology Development Program of Shandong Province (Grant No. 2008GG2TC01011-4).

References

1. Zhiqiang Pang; Jiachuan Chen; Guihua Yang. Investigation on fiber morphology and pulp properties of different poplar species with different ages. Thesis for master degree of Shandong Institute of Light Industry. 2004, 6: 66~67.
2. Ying Wang, Yulin Zhao and Yulin Deng.Effect of enzymatic treatment on cotton fiber dissolution in NaOH/urea solution at cold temperature [J]. Carbohydrate Polymers.2008,72:178-184
3. Rafael Vicuñaa, Fabiola Escobarb, Miguel Ossesb and Arnoldo Jarab Bleaching of eucalyptus Kraft pulp with commercial xylanases. Biotechnology Letters, 1997, 19(6): 575–578
4. O. Darcfa,A.L.Torres,J.F. Colom, et al.Effect of cellulase-assisted refining on the properties of dried and never-dried eucalyptus pulp [J].Cellulase,2002,9:115-125
5. Pommier J.C., Goma G., Fuentes J.L., et al. Using enzymes to improve the process and the product quality in the recycled paper industry. Part 2: Industrial applications [J]. Tappi J., 1990, 73 (2): 197

Design of Experiments Application in Fiber Loading

Jiawei Yuan [1] and Yi Jing [1]
Jiangsu Province Key Lab of Pulp and Paper Science and Technology,
Nanjing Forestry University, Nanjing, Jiangsu Province,210037

Abstract: Paper strength reduces with ash increasing. Fiber loading technology is adding $Ca(OH)_2$ into fiber suspension, then adding CO_2 gas into the slurry, and PCC is precipitated into the inner of fiber, which is good for fiber bond and decreases the loss of paper strengths. Design of Experiments (DOE), which can screen out the most important factor in experiments, is used in the study. Four-factors-two-levels experiments, with different pulp concentrations, rotate speed, pressure of CO_2 gas and reacting time, are designed. Results show that rotate speed is the key factor on the ash of paper. Rotate speed and pulp concentration and their interaction are the key factors affecting on Z-bond of paper. Fiber loading method can improve the addition amount of fillers for mechanical pulp, without sacrificing the Z-bond of paper. Compared with the directly adding fillers in mechanical pulp, it can improve both paper strength and ash content.

1. Introduction

Fillers can not only improve the optical property and printability of paper but also reduce the cost of production. The problem of energy shortage is the pressing problem in paper manufacturing industries. Increasing filler and ash content in paper have gradually become the trend of development. However, fillers will weaken the hydrogen bonds among fibers and reduce the paper strength. Researchers adopt fiber loading technology[1-6] to increase paper ash content: one method is that makes the single filler particle directly enter into fiber interior at the high rotating speed. The other method is a chemical reaction by means of $Ca(OH)_2$ reacting with CO_2 in the pulp slurry with high pressure and rotate speed. Calcium carbonate can precipitate in the fiber interior and surface.

The fiber morphology of the mechanical pulp is different from LBKP and NBKP. The mechanical pulp has the following characteristics:

1. the bulk and stiffness of paper
2. the high opacity of paper
3. low cost
4. hollow lumen(be shown as in Fig.1)

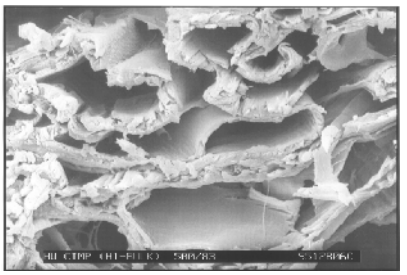

Fig.1 The fiber morphology of the mechanical pulp

Fig.1 shows that the hollow fiber lumen of mechanical pulp can fit the fiber loading technology because of its special lumen structure. If CO_2 can react with $Ca(OH)_2$ in fiber lumen, precipitated calcium carbonate particles can form in the fiber interior. The ash content of paper can increase and the paper strength can not decrease. The application of fiber loading technology in mechanical pulp is not reported so far.

2. Material and Methods

(1) Material

Bleached Chemi-Thermal-Mechanical Pulp (BCTMP)，freeness:250ml.

Alkaline Peroxide Mechanical Pulp (APMP)，freeness: 250-300ml.

(2) Equipment

GSH-2 high pressure reaction kettle, CO_2 gas cylinder, ZQS2-23L Valley beater, JA-1203 electronic balance,etc.

(3) Chemical

$Ca(OH)_2$, NaOH, PCC, CO_2.

(4) Methods

a. Fiber composition

Choose two kinds of mechanical pulp to compare the results of fiber loading with each other. One kind of mechanical pulp is 50% BCTMP(hardwood) and 50% BCTMP(softwood);the other is 100% APMP(hardwood).

b. handsheet formation

(a) fiber loading

Deflake and concentrate the fiber suspension, then pour it into reaction kettle, fiber swelled with NaOH for about 30 min. Add $Ca(OH)_2$ into the fiber suspension(the $Ca(OH)_2$ is totally turned into PCC, the weight of PCC is 20% of dry fiber). Stiring the suspension adequately to make sure that the fiber and $Ca(OH)_2$ is mixed fully. CO_2 is infused into the mixture from the bottom of the reaction kettle.PCC is precipitated at normal atmospheric temperature, under certain rotating speed and CO_2 pressure. The loaded fiber suspension is used to make handsheet without adding any additives. The base weight of handsheet is 60g/m^2.

(b)direct loading

Deflake and add PCC(20% of oven weight of fiber)into fiber suspension, add no additives ,then make and sheet. The baseweight of paper is 60g/m^2.

c. handsheet testing

Thickness(GB451-79),whiteness and opacity(GB/T1543-1988),tensile(GB453-89),Scott, brusting strength (GB/T454-1989) and ash(GB/T463-1989).

(5) Design of experiment

In fiber loading process, there are many factors affecting PCC formation. How to screen out the key factor from numerous factors is very important. It not only saves the cost of experiments, but also shorten time of experiments and improve efficiency of research. These factors include: temperature, the concentration of calcium hydroxide slurry, CO_2 gas pressure, rotating speed, additive, etc. Design of experiment is shown as Table 1 by Minitab software. The aim of DOE is that key factors can be screen out from four factors and analyze interaction between different key factors.

Table 1The design of experiment

Run Order	pulp concentration（%）	rpm	pressure （MPa）	time （min）
1	1.5	400	0.2	8
2	2.5	400	0.2	15
3	1.5	800	0.2	15
4	2.5	800	0.2	8
5	1.5	400	0.3	15
6	2.5	400	0.3	8
7	1.5	800	0.3	8
8	2.5	800	0.3	15

(Normal temperature; NaOH consumption: 0.1%, swelling time:30min;filling content:20%;fiber suspension mixed with calcium hydroxide powder:30min under 400rpm)

3. Results and discussion

(1) Results and analysis of MINITAB software

The fiber composition is 50% BCTMP(hardwood) and 50% BCTMP(softwood).Results of fiber loading are shown as Table 2. shows the results by directly adding solid PCC particles.

a. The key factor affecting the ash content of paper

Fig.2 shows which a factor is the most important one affecting ash of paper among pulp concentration, rpm pressure and time. Minitab can analyze the key factor. The factor appearing on the right side of vertical line is the key factor. Rotate speed is on the right of the vertical line, so it is the factor affecting on the ash of paper.

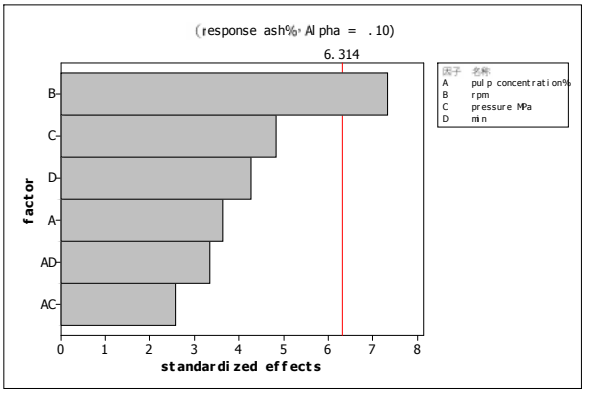

Fig.2 Pareto chart of the standardized effects on ash of paper

The more rotate is, the more strength shear force is. When the shear force changes, the combination between filler and fibers changes. If the rotating speed is too high, the PCC particles adsorbing to the surface of the fiber will drop off. Moreover, CO_2 can not enter into the lumen to react with Ca(OH). But low rotate speed is good for the PCC particles formation. So rotate speed is the key factor .

b. The key factor affecting the Z-bond of paper

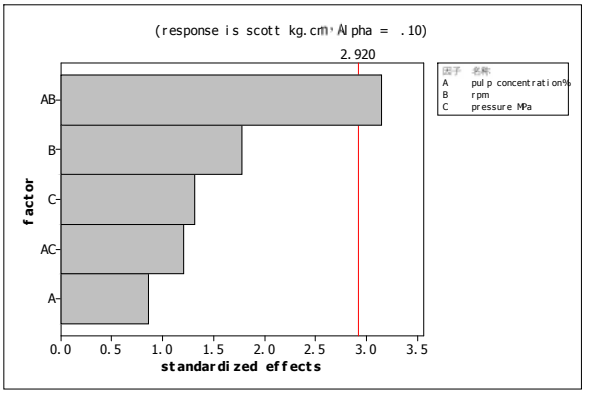

Fig.3 Pareto chart of the standardized effects on Z-bond of paper

Z-bond of paper indicates the bond of fiber layers in the Thickness direction of paper. Fig.3 shows that the key factor affecting on the Z-bond of paper is pulp concentration and rotate speed. Pulp concentration and rotate speed has interaction each other, it can be found that there is a point of intersection between two lines cross from Fig.4.Interaction illustrates that pulp concentration and rotate jointly influence the Z-bond of paper. Two factors have a optimal combination.If there is not interaction between pulp concentration and rotate speed, two lines must be parallel.

Fig.5 is contor plot of Z-bond VS rotate speed & pulp concentration. It shows different combination of rotate speed and pulp concentration with different Z-bond objectives. For example, if Z-bond of paper reachs above

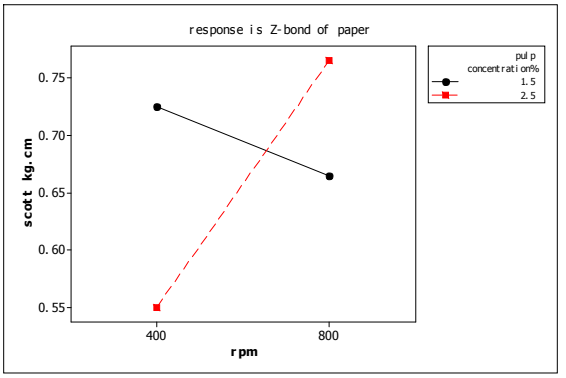

Fig.4 interaction plot for Z-bond of paper

0.75 kg.cm, pulp concentration should be 2.5%,at the same time, rotate speed should be above 200 rpm. The more pulp concentration is, the more fibers touch PCC particles forming by chemical reaction.

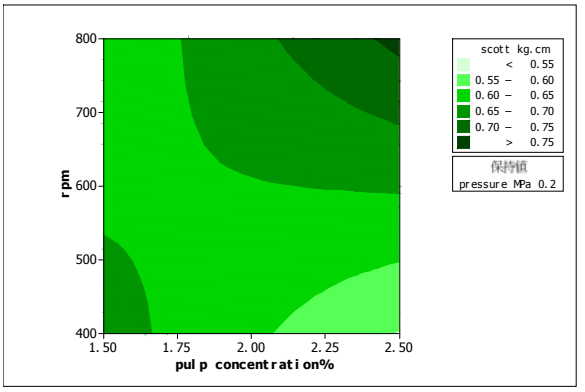

Fig.5contor plot of Z-bond vs rotate speed & pulp concentration

c. Comparison between fiber loading and direct add fillers

Analyzing the comparison of the data between the Table 2, it can find that the ash content of handsheet made from fiber loaded BCTMP is only half increased when compared to the handsheet made from direct loaded BCTMP at same filling content (20%).Because 50% BCTMP made from softwood is used in this experiment, and mechanical pulp made from hardwood is easier for fiber loading[8].The bursting strength are nearly all improved, and Scott is mostly increased. Strength property is improved when ash content is also increased in three groups of order 2,order 4 and order 6.The opacity are nearly all improved, but the whiteness are all reduced. The thickness are partly increased.It is advantageous to improve paper stiffness.

Table 2 The results of fiber loaded handsheets(BCTMP)

RunOrder	thickness(mm)	Whiteness%	opacity（%）	brusting strength（Kpa）	ash（%）	Scott (kg.cm)
1	0.147	78.54	94.68	53	13.87	0.43
2	0.152	77.34	93.26	60	11.79	0.53
3	0.155	72.68	91.69	87	5.99	0.65
4	0.162	75.58	91.12	75	9.12	0.78
5	0.147	74.65	90.89	79	6.44	0.82
6	0.148	76.82	91.72	62	11.13	0.57
7	0.159	74.35	89.97	88	6.08	0.68
8	0.152	75.58	89.76	76	7.54	0.64
Directly add fillers	0.155	79.66	89.91	48	7.94	0.64

4. Conclusion

(1) DOE method was chosen to use in this study. It can screen out the key factor which affects the experiment and interaction between different factors.

(2) Pulp concentration, rotating speed, pressure of CO_2 gas and reacting time were studied and the experiment of four-factors-two-levels was designed. The results show that rotating speed is the key factor on the ash of paper.

(3) Pulp concentration and rotate speed their interaction are the key factors on the Z-bond of paper.

(4) Compared to direct add fillers, fiber loading can improve the paper strength (including Z-bond) and ash content.

References

[1] Klungness,et al.U.S. Pat, 5, 223, 090 (1993)

[2] John H. Klungness et al.In: Proceedings of the 2001 international mechanical pulping conference:04-08(2001)

[3] Silenius, P.Helsinki University of Technology, Espoo, Finland, Report Series A14(2002).

[4] Middleton S.R. et al.Journal of pulp and paper science, 29(7):241-246(2003)

[5] John H. Klungness et al.4th International refining conference,Palazzodella Fonte,Fiuggi,Italy:18-20(1997)

[6] Klaus doelle,Kisslegg(DE),US 0051480 AL(2007)

[7] Zhang Shicheng,etc,Journal of Northeastern University, 21(2):169-172(2000)

[8] Liu Wenxia,Journal of Shandong Light Industry Institute, 8(2):42-46(1994)

Preparation and Characterization of Nanocrystalline Cellulose

Chih-Ping Chang[1], Yuan-Shing Perng[2], I-Chen Wang[3], Chung-Yao Weng[2] and Kuo-Jung Hung[1]

[1] Professor and Graduate student, Department of Forestry, National Chung-Hsing University

[2] Professor and graduate student, Department of Environment Engineering, Dayeh University

[3] Division Head, Division of Wood Cellulose, Taiwan Forestry Research Institute

1. Introduction

Nanotechnology represents a major opportunity to generate new products of forest industries in the coming decades. It transform the forest products industry in virtually all aspects—ranging from production of raw materials, to new applications for composite and paper products, to new generations of functional nanoscale lignocellulosics. By way of nanotechnology, the original material properties will be highly improved and even induced brand-new characteristics. The U.S. National Science Foundation (NSF) predicts at 2004, that within a decade nanotechnology will provide a $1 trillion market, and provide two million new jobs. And Canada had already patronized 64 billion dollars last ten years to endeavor the combination and cooperation of nanotechnology and forest industry.

Cellulose is one of the major components construct the plant cell wall. The cellulose annual yield is about 1×10^{11} tons. Beside the high quantity yield, cellulose provide its particular characters of renewable, biodegradable, environment friendly and great mechanical property which increasing highly interesting in today's world. The cellulose structure consists of long chains of α-d-glucose units joined by β-1,4-glycosidic links consist of crystalline regions linked by amorphous regions. It commonly used as reinforcement in polymer substrates in order to improve mechanical property of composites. Degrade cellulose into nanocrystalline cellulose (NCC) helps the combination between NCC and polymer. By manipulate NCC additives precisely, makes composites with transparency, strength, surface properties and biodegrade possibility.

In this study, cotton pulp was hydrolyzed by sulfuric acid based on 2^4 factorial design. The NCC yields were used as database of ANOVA test and the influence of different factors: acid consistency, solid/liquid ratio, reaction temperature and reaction time were discussed. The NCC produced in this study then examined by DLS, TEM, FTIR and SAXRD, so the NCC size distribution, morphology, functional groups change, cellulose crystalline type and crystallinity were all evaluated.

2. Material and Methods

In this study, high level of acid consistency (A) was settled at 60 %, and low level was 50 %; high level of solid/liquid ratio (B) was 1:20 and low level was 1:20; reaction temperature (C) with high level 55℃ and low level 45℃; reaction time with high level 15 min and low level 5 min. All the experiments were sampling every 5 min, in order to check the tendency of NCC yield.

10 g of cotton pulp was first decomposition by disintegrator and then acid hydrolysis under different condition with 400 rpm continuous stirring. Reactions were terminated by adding DI water and cooling system down to 10℃. All the liquid phase were then centrifugation for 10 min under 10000 rpm. Upper phase then dialysis for 72 hr and adjusted to *p*H 7 by 1% NaOH. All the liquid then frozen dried and calculate the yield and processed ANOVA test.

Under different acid consistency, the products of highest yield condition were selected to equipment analysis. DLS samples were adjusted with DI water into 10% concentration then analyzed directly with DLS Nano S90, Malvern, Britain. TEM sample were adjusted into 5% concentration with 70% ethanol then negative stain by uranyl zinc acetate and then coated on TEM cooper grid and followed by TEM observation with JEM-1400, JEOL, Japan. FTIR examine based on diffuse reflectance principle. The frozen dried sample were well mixed with KBr and then analyzed by Spectrum 100, Perkin Elmer, U.S. The crystal type and crystallinity

of frozen dried NCC were analyzed by XRD-6100, Shimadzu, Japan.

3. Results and discussion

Research results shows that acid consistency, solid/liquid ratio, reaction temperature and reaction time all have significantly affection of NCC yield under significance level α=0.05. When change acid consistency and solid/liquid ratio into high level, or change reaction temperature and reaction time into low level, the influence of NCC yield presented significantly. The main effect (F) of each factor according to priority is: acid consistency＞reaction temperature＞reaction time＞solid/liquid ratio. The NCC yield in initial stage of 55% or 60% sulfuric acid hydrolysis presents rapid decrease and remind stable after 20 min. Furthermore, the yield of 50% sulfuric acid hydrolysis reminds lower and stable level. Depend on DLS and TEM results, the size of NCC is between 50~450 nm, and the aspect ratio from 1:1~1:30 respectively. FTIR spectrum indicated, compare to cotton fiber, absorption intensity at 621 cm^{-1} increased, which means the SO_4^{2-} still slightly remain in NCC and the absorption at 1147 cm^{-1} shows the sulfonic esters loaded on NCC. On the other hand, the intensity of absorption at 2700~3000 cm^{-1} and 1427 cm^{-1} points that CH_2 groups and CH group decreased respectively. The FTIR spectrum of NCC hydrolyzed by 50% sulfuric acid presents no considerable quantities of functional groups changed except the decrease of fiber-OH on 1640 cm^{-1} and the increase of –OH around 3300 cm^{-1}. XRD determined that NCC produced in this study shows cellulose type II and the crystallinity, compare to cotton fiber, raised from 81.8641％ to 85.4969％. The best yield of NCC is 54.42% under acid consistency 60%, solid/liquid ratio 1:20, reaction temp 45℃ and hydrolysis for 5 min.

4. Conclusions

In this study we find out that solid/liquid ratio is lass important then other factors. Consider about the prime cost, further research may choice lower solid/liquid ratio and still obtain similar NCC yield. Varied NCC produced by mean of different acid hydrolysis conditions. According to the NCC morphology, NCC yielded by 55% sulfuric acid hydrolysis has suitable aspect ratio and may able to be used as reinforcement in polymer composites. On the other hand, those NCCs with lower aspect ratio may have the abilities to improve the surface properties of polymer composites. After sulfuric acid hydrolysis, the quantity of hydroxy group and sulfonic esters group were highly increased. For future study, those active functional groups may further modified for different purposes, in order to explore the utilities of NCC.

Table 1 NCC yield based on 2^4 factorial design.

sample	Acid concentration (%)	Solid/liquid ratio	Reaction temp (℃)	Reaction time (min)	Yield (%)
1	50	10	45	5	1.64
2	60	10	45	5	33.23
3	50	20	45	5	1.77
4	60	20	45	5	54.54
5	50	10	55	5	2.00
6	60	10	55	5	7.29
7	50	20	55	5	1.88
8	60	20	55	5	11.60
9	50	10	45	15	2.18
10	60	10	45	15	13.51
11	50	20	45	15	3.51
12	60	20	45	15	18.15
13	50	10	55	15	0.59
14	60	10	55	15	2.20
15	50	20	55	15	1.04
16	60	20	55	15	6.72
17	55	15	50	10	19.47
18	55	15	50	10	19.14
19	55	15	50	10	17.49

Table 2 Results of ANOVA analysis based on 2^4 factorial design.

Source	df	Mean Square	F	Sig.
Corrected Model	15	640.397	661.280	.000
Intercept	1	5002.083	5165.196	.000
A	1	3372.112	3482.073	.000
B	1	231.090	238.625	.000
C	1	1647.129	1700.840	.000
D	1	782.145	807.649	.000
A*B *C *D	1	48.280	49.855	.000

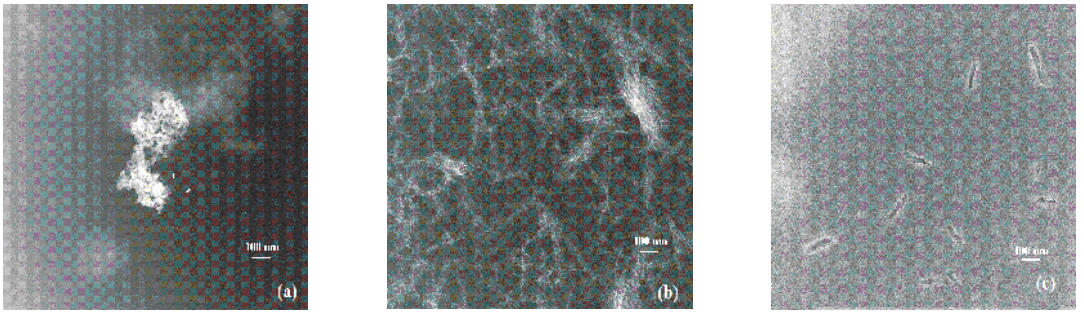

Fig. 1 TEM morphology of NCC produced under different hydrolysis conditions.
(a) Acid concentration 50%, solid/ liquid radio 1:20, 55℃, hydrolysis 5 min.
(b) Acid concentration 55%, solid/ liquid radio 1:15, 50℃, hydrolysis 5 min.
(c) Acid concentration 60%, solid/ liquid radio 1:10, 45℃, hydrolysis 5 min.

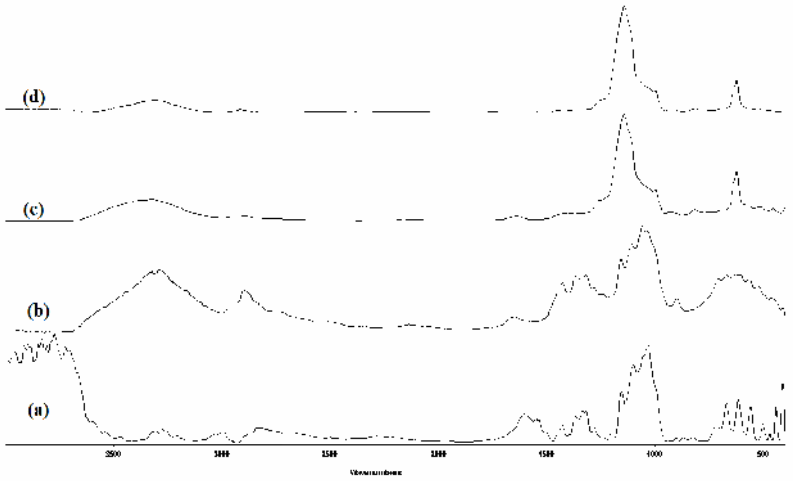

Fig. 2 FTIR spectrum of cotton fiber and NCC
(a) Cotton fiber
(b) NCC hydrolyzed by 50% sulfuric acid
(c) NCC hydrolyzed by 55% sulfuric acid
(d) NCC hydrolyzed by 60% sulfuric acid.

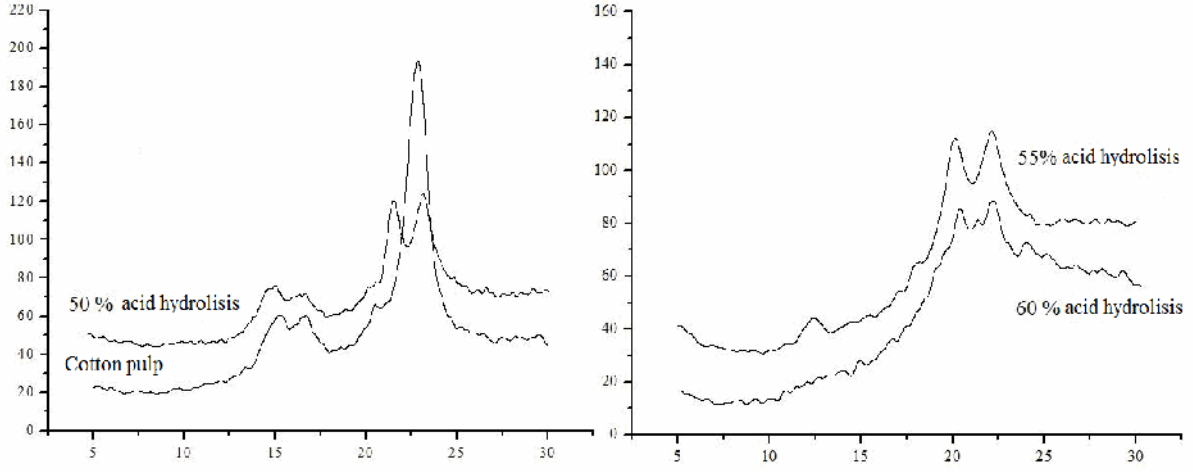

Fig. 3 NCC crystalline type analyzed by x-ray diffusion spectrum.

Fiber Surface Characteristics of Eucalyptus Pulp and Its Effects on Strength Properties

Beihai He, Xiangping Wang, Shangjun Ding,Guanglei Zhao, Junrong Li, Liying Qian and Lihong Zhao

State Key Laboratory of Pulp & Paper Engineering,
National Engineering Research Centre of Papermaking and Pollution Control,
South China University of Technology, Guangzhou 510640, P.R. China

Abstract: Eucalyptus grows fast and behaves well in pulping and papermaking, and the fiber surface analysis of fast-growing eucalyptus is important for the fundamental base of the surface chemistry of wood fiber. Researches were mainly focused on the fiber surface properties of eucalyptus pulp and some modern surface analysis techniques, such as SEM, XPS, and CLSM, were employed in this work, and the relationship between the fiber surface chemistry and the sheet strength properties were also investigated.

1. Fiber Surface Characteristics of Eucalyptus Pulp

Results showed that when the dosage levels of alkaline sodium sulfite were increased to the eucalyptus pulp, the surface chemistry of eucalyptus CTMP pulp was changed (Table 1). Based on the data from XPS, the O/C ratio of the fiber surface was increased and the peak area of C1were decreased respectively, and the strength of paper sheet was improved with the increasing of NaOH charge. This indicated that there were less lignin and extractives, and more carbohydrate on the fiber surface as the alkali dosage were increased (Table 2). Meanwhile, the physics strength of paper sheet were also increased (Table 3).

Table 1 The lignin content and total ion content under different chemical treatment

Na_2SO_3 dosage/%	NaOH dosage/%	Treatment time /h	sulfo group content /%	carboxyl group /%	Fiber surface lignin content /%
15	0	2	85.17	61.51	36.51
15	5	2	93.43	78.52	33.49
15	10	2	99.46	86.25	33.00
15	20	2	103.72	81.08	31.65
15	5	4	113.56	89.31	32.32

Table 2 The O/C ratios and C_{1S} peak areas of CTMP fibers with different chemical dosage

Sample	Na_2SO_3 dosage/%	NaOH dosage/%	Treatment time /h	O/C ratio /%	C_{1S} /%	C1 /%	C2 /%	C3 /%	Surface content	Lignin /%
a	15	0	2	65.0	60.59	14.69	39.63	6.27	36.51	
b	15	5	2	66.6	60.04	13.89	40.99	5.16	33.49	
c	15	10	2	66.9	59.85	13.36	40.23	5.83	33.00	

Table 3 The physical properties of eucalyptus CTMP after treatment

Sample	Beating degree/°SR	Brightness /%	opacity /%	Tensile index/N·m·g^{-1}	Zero span index/N·m·g^{-1}	Tear index /mN·m^2·g^{-1}	Burst indx /KPa·m^2·g^{-1}
a	45.5	49.29	96.35	11.90	70.49	0.92	1.31
b	47	36. 51	96.69	39.75	97.91	2.51	1.94
c	48	35. 27	97.27	41.64	100.13	3.11	2.05

2.1 Effect of Beating Degree on the fiber surface properties measured by XPS

In this work, the effects of PFI beating on the fiber morphology, chemical properties of fiber surface were also analyzed by XPS(X-ray Photoelectron Spectroscopy). Results showed the fiber surface chemistry of eucalyptus pulp were changed with the increasing of PFI mill revolution (Table 4), and the O/C ratio of the fiber surface also increased. when PFI mill revolutions increased from 0 to 14000, The O/C ratio increased from 60.6% to 69.8%, meanwhile the lignin concentration on the fiber surface decreased from 45.47% to 26.98%. It means with the increasing of PFI mill beating degree the surface hydrophilicity of the eucalyptus fiber was also increased, and it had a positive influence on fiber bonding and sheet strength (Table 5).

Table 4 The lignin content and carboxyl groups content with different PFI mill revolutions

PFI Revolution	Beating degree（°SR）	Total lignin content (%)	Surface lignin content (%)	carboxyl group (mmol/Kg pulp)
0	10.5	28.40	45.47	—
2000	12.0	24.00	42.96	—
4000	16.5	22.50	40.55	—
6000	23.0	20.19	36.89	51.03
8000	33.0	18.07	35.20	62.47
10000	45.0	15.67	33.49	78.52
12000	56.5	12.78	32.43	89.68
14000	66.5	8.90	26.98	97.94

Table 5 The O/C ratios and C_{1S} peak areas of CTMP fibers

PFI mill revolutions	O/C ratio (%)	C_{1s}(%)	C1(%)	C2(%)	C3 (%)
0	60.6	62.28	17.86	40.36	4.06
6000	64.9	60.66	14.30	40.83	5.53
8000	65.7	60.35	13.83	41.53	4.99
10000	66.6	60.04	13.36	41.52	5.16
12000	67.1	59.85	13.12	41.30	5.42
14000	69.8	58.89	11.56	41.15	6.18

2.2 Effect of Beating Degree on the fiber surface properties measured by CLSM

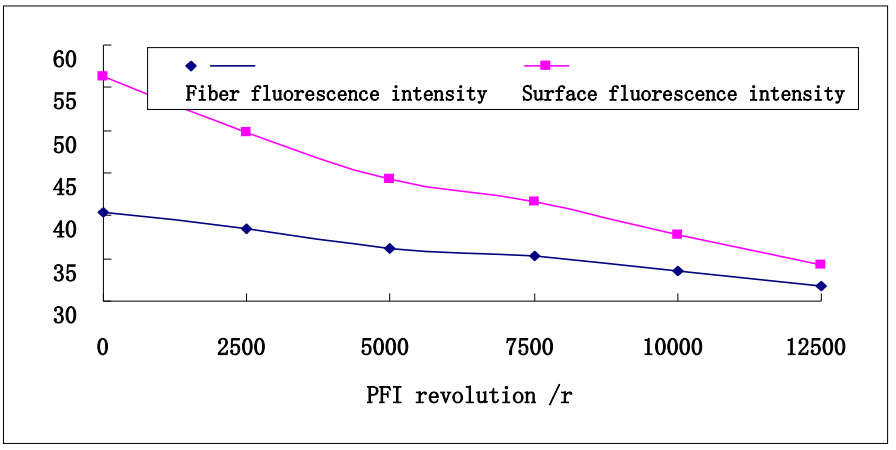

Fig.1 Fiber fluorescence intensity vs different PFI revolutions

Results also showed CLSM is useful fiber analysis technique in this work, with a unique optical slice function, CLSM could give 2D and 3D pictures of wood fiber. In this paper, safranin O was used to dye lignin on the fiber surfaces, and the lignin content on eucalyptus wood fiber were clearly observed from CLSM. And through the establishment of corresponding working curve, the lignin concentration of fiber surface could be easily obtained by CLSM analysis. With the increasing of PFI revolutions, both the fiber fluorescence intensity and surface fluorescence of pulp fiber were decreased, it means that the total lignin content and surface lignin content of were decreased during the pulp beating process (fig. 1). Meanwhile the fiber wall thickness of pulp fiber was also deceased (Table 6).

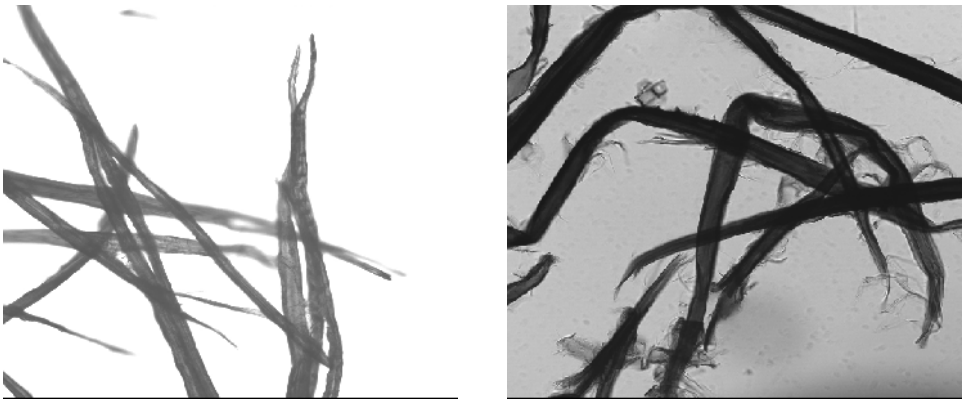

a. before pulp beating b. after pulp beating (14000 revolutions)

Fig.2 Eucalyptus fiber morphology before and after PFI beating process

Table 6 Effects of beating degree on eucalyptus pulp fiber surface chemistry

PFI Mill revolutions	0	2500	5000	7500	10000	12500
Fiber wall thickness /μm	6	5	4	3	2.5	2
Total lignin content /%	28.12	27.67	27.03	26.62	26.15	25.89
Surface lignin content /%	39.09	35.69	32.98	31.41	30.33	29.51

3. Effects of Fiber Relative Bonding Area (RAB) on Paper sheet strength

The paper strength mechanism is one of the interesting topics in paper science research. In this work, an initial research was performed on this area. Based on the famous Page's theory on paper sheet strength, there is a equation as follows:

$$\frac{1}{T} = \frac{9}{8Z} + \frac{12c}{PLb(RBA)} \qquad (1)$$

Where T is paper tensile index, Z a paper tensile index of zero span, C a fiber coaseness, P a fiber perimeter, L a fiber length, b a specific fiber shear strength, and RBA the relative bonding area.

In 1996, Gordon put forward a changed form based on Page's equotion[1],

$$\left[\frac{1}{T} - \frac{9}{8Z}\right]^{-1} = PBSI \qquad (2)$$

In which, PBSI means Page Bonding Strength Index ($N \cdot m \cdot g^{-1}$)

$$PBSI = \frac{PLb(RBA)}{12c} \qquad (3)$$

Based on the equation (2) and (3), it is known that the Relative Bonding Area (RBA) has an affinity relationship with Page Bonding Strength Index (PBSI), so the key work is how to measure the RBA.

One of the methods for detect RBA is Scattering Coefficient Measuring[2]:

$$RBA = \frac{S_0 - S}{S_0} \qquad (4)$$

Where S_0 is the light scattering coefficient before fiber bonding, and S is the light scattering coefficient of paper sheet. In fact, it is difficult to measure S_0 directly, so that an indirect method put forward by Ingman was employed in this work[2]. Based on a series of tests and data fitting, we get S_0=43.32 $m^2 \cdot Kg^{-1}$ (Fig. 3) for eucalyptus pulp fiber.

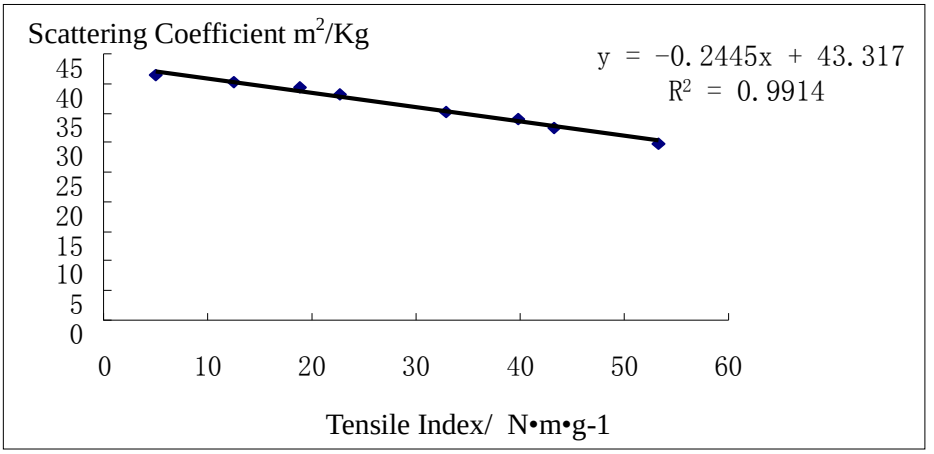

Fig.3 The relationship between tensile index and light scattering coefficient

Table 7 The RBA of the sheet with different PFI mill revolitions

PFI revolution	6000	8000	10000	12000	14000
RBA /%	12.2	18.5	22.7	24.7	30.1
RBA increasing /%	0	51.7	77.4	101.7	153.4
Tensile index / $N \cdot m \cdot g^1$	22.62	32.83	39.75	43.36	53.29
Tensile index increasing /%	0	45.1	75.73	91.68	135.5

Results also showed (Table 7) that with the increasing of PFI revolution, the RBA of paper sheet were also increased, and the amplitude could reached 153% in 14000 revolution of PFI mill. And meanwhile the tensile index and its amplitude was increased to 53 and 135% respectively. It was further proved that RBA is an important factor both in fiber bonding and paper sheet strength.

References

[1] Gordon B..Lingking the fiber characterisitic and handsheet properties of a high-yield pulp[J].Tappi journal,1996,79(1):161-169

[2] Ingman, W.L., and Thode, E.F., Factors contributing to the strength of a sheet of paper[J]. Tappi,1959, 42(1):83-96

The experimental pretreatment of Effluent from BCTMP of Polar with micro-electrolysis method

Xuejing Qu[1], Yunfeng Cao [1], Huifang Xie[1] and Fengshan Zhang[2]

[1] Jiangsu Provincial Key Lab of pulp and paper science and technology, Nanjing Jiangsu Province,210037

[2] Huatai Group in Shandong Province, Shandong Guangrao,257335

Abstract: The experimental pretreatment of effluent from BCTMP of polar with micro-electrolysis method was studied in this paper, and the factors affected on the treatment were discussed. As we can see from the conclusion, pH value was the most important factor to influence the reaction of micro-electrolysis, and other factors, such as Fe/C proportion, reaction time and the ratio of Fe/wastewater had also some effect on treatment efficiency. Under the optimum condition of 3～4 pH value, 0.5:1Fe/C weight proportion,15min reaction time and 0.1～0.125 ratio of amount of Fe/wastewater, the decolorizing rate was 93%, and the COD_{cr} removal rate was about 71%. What's more, BOD_5/COD of wastewater increased from 0.3 to 0.35, which indicated that the biodegradability of wastewater is somewhat improved. The experiments showed that micro-electrolysis method can be used to effectively not only eliminate the color of the wastewater and reduce the COD_{Cr} but also improve the result of the biochemical treatment of the wastewater.

1. Introduction

Bleached chemi-thermal-mechanical pulp (BCTMP) which is low in investment cost and high in yield rate can be used to produce all kinds of papers. This papermaking technology has a great application potentiality because of holding both advantages of chemical pulp and high-yield pulp. However, there are many problems with the treatment of BCTMP effluent. First of all, BCTMP wastewater is not suitable for alkali recovery because of low residual alkali content and high cost for recovering alkali. What's more, some chemicals were added in the process of pulping and bleaching, which made the pollution load of BCTMP wastewater so high that the general biological treatment can not satisfied for the current standard of wastewater discharge. Therefore, it is necessary to develop a suitable treatment of the wastewater.

The micro-electrolysis of iron-carbon method is known as the process of iron scraps and internal electrolysis and iron-carbon reduction technology. It is a kind of electrochemical treatment technology for industrial wastewater, based on the principle of metal corrosion, which is make use of many iron-carbon micro cells created by the crystal structure of iron filings in the electrolyte solution[1]. There are several advantages about using this method treating the effluent. Firstly, it has a wide range of application and costs low and it's easy to maintenance and operation. Secondly, the experimental materials are scrap iron, which in accordance with the policy of using waste to treat waste. Thirdly, not much power resources were consumed during the reaction. The ferric-carbon micro-electrolysis technology was applied more in the treatment of dye wastewater [2-4], however, its application in the pulp and papermaking industrial wastewater has not been reported. This paper studied the treatment effect of decoloration, reducing turbidity, degradation of organic pollutants about effluent from BCTMP of polar with micro-electrolysis method, and several factors affected on the treatment were discussed.

2. Material and Methods

Wastewater for experiment was from the final drainage outlet of the BCTMP plant in a paper mill in Shandong province. The wastewater samples were characterized for the BOD, COD, pH value, suspended solids (SS), color and electrical conductivity as per standard methods of analysis. The measurable results are given in Table 1.

Table 1 The characterizes of the wastewater samples

BOD_5 (mg/L)）	COD_{cr} (mg/L)	pH value	Color (C.U.)	SS (mg/L)	electrical conductivity (μs/cm)
7850	26000	7.8	4500	1950	3800

An pHs-3c precision pH-meter, an 722 grating spectrophotometer, an HANGPING FA1604 analytical balance, an JHR-12 COD thermostatic heater, an 85-2 magnetic stirrer with constant temperature, an Hach2100p turbid meter

a. The determination of wastewater colority: platinum-cobalt standard method.

b. The COD determination: potassium dichromate method

c. The turbidity determination

The mechanism of the micro-electrolysis method

The basic principle of the micro-electrolysis of iron-carbon method is galvanic interaction. Fe-C serves as positive and negative electrodes. Anode in the reaction is performance for losing electrons and would be oxidized, while the cathode would be reduced and get the electrons [5].The electrode reaction formula is:

positive electrode: $Fe+2e \rightarrow Fe^{2+}$ $E^0Fe^{2+}/Fe=-0.44V$

negative electrode: $2H^++2e \rightarrow 2[H] \rightarrow H_2$ $E^0H^+/H_2=0.00V$

The reaction can be displayed in an acidic condition as well as the dissolved oxygen exists:

$$O_2+4H^++4e \rightarrow 2H_2O \qquad E^0O_2=1.23V$$

The products of the electrode reaction have a high chemical activity, the new formed $[H]^+$and Fe^{2+} can occur oxidation reduction reactions with a number of components in waste water, whose products destroyed chromophoric or auxochromic groups of the wastewater; what's more, they broke down macro-molecular material into small molecules and biodegraded the material to be easily biodegradable material, which improve the biodegradability of the wastewater. On the cathode, the organic matter would be reduced when the depolariser existed in the electrolyte solution (waste water). For those organic matter which prone to be oxidized, such as alcohols, aldehydes and phenols. Oxidation reaction occurred at the anode was caused by similar strong oxidants.

3. Results and discussion

(1) The Influence of pH value

By the mechanism of micro-electrolysis, we can see that the $[H]^+$ in the electrolyte solution are response for maintaining the original battery reaction and moving the electrode reaction balance rightward. That's why pH value is a key factor. A comparative test has been done between different pH values under the acidic conditions of the micro-electrolysis experiment, and the treatment effect was shown in Fig. 1.

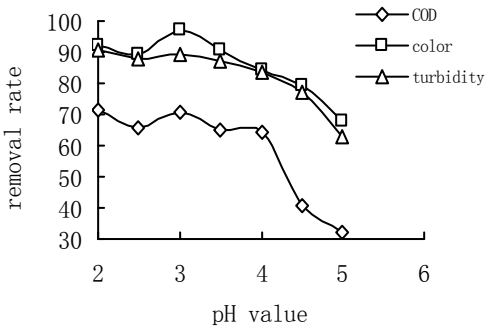

Fig. 1 Influences of pH value (pH 1)

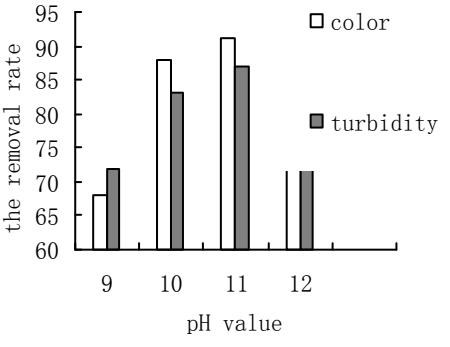

Fig. 2 Influences of pH value (pH 2)

As we can clearly see from the Fig. 1, the effect of the treatment has a significant change with the pH value changes, the removal rate of COD was 71% when the pH value was 3, as well as the removal rate of the color and the turbidity were respectively 97% and 89%; however, when the pH rose to 4, there are almost no changes in the removal rate of the color and the turbidity, and the removal rate of COD dropped to 65%. It is proved in the literature that, generally, in the condition of low pH value, the reaction can be carried out quickly due to a large number of $[H]^+$. But sometimes, it's not true, because the existent form of the product may change by the decrease of pH, which leads to an excessive amount of Fe^{2+} and bad efforts of the treatment. Meanwhile, the lower pH means needing more acid, increasing operating costs and accelerating corrosion of storage tanks and

pipelines. As a result, the optimum pH values is between 3 ~ 4.

After micro-electrolysis reaction, the wastewater was neutralized by the lime, and the products Fe $(OH)_2$ and $Fe(OH)_3$ not only got further precipitation and trapped the pollutants so that the dispersed small organic particles can be settled down by flocculation, but also increased the rate of the removal of the COD_{Cr} and eliminated residual ion particles, such as Fe^{2+}, Fe^{3+}, $SO_4^{2-}$and CO_3^{2-}. The results showed that (Fig. 2): the removal rate of the color and turbidity became higher with the increase of the pH adjustment. When the pH value was more than 10, the removal rate of the color and turbidity was no longer increased with adding the alkali. At this time, it is no effort to improve the result, but only increase costs. Therefore, the pH value of flocculation can be adjusted to 10.

(2) The effects of reaction time

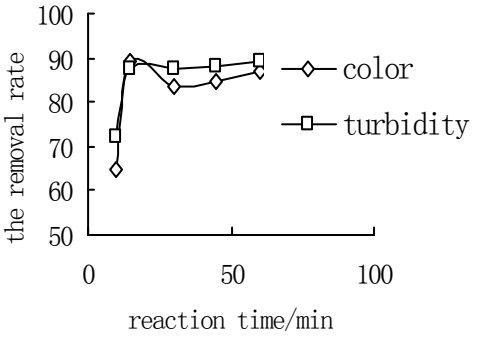

Fig. 3 Effects of reaction time

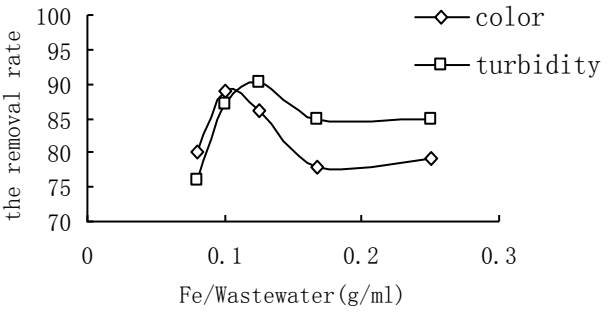

Fig. 4 The effect of the ratio of Fe/wastewater

Micro-electrolysis method is based on iron-carbon primary battery reaction, the longer the reaction time was, the stronger the oxidation-reduction effects would be. However, dissolved iron would increase a lot as the extension of the reaction time, which will increase the dosage of lime and raise the processing costs. It is also said that the remaining Fe^{2+} in solution will be oxidized to be Fe^{3+}in the air O_2, which lead to the forming of the yellow floc Fe $(OH)_3$ by the hydrolysis of Fe^{3+}, and affected the color of the treated wastewater. The results showed that a more suitable reaction time is 15min (showed in Fig. 3).

(3) The effect of the ratio of Fe/wastewater

The dosage of iron also has an impact to the treatment. Theoretically, the treatment effect should be better with the dosage became larger, because the higher the concentration of electrolyte solution was, the faster and the more complete the oxidation-reduction reaction would be. However, it is showed in Fig. 4 by the test data that when the ratio of the iron dosage (g) and wastewater treatment capacity (ml) (the ratio of Fe/wastewater) reached 0.1 or above, the treatment effect deteriorates inversely. This may be because the Fe^{2+} coming out from the anode reaction normally exist by ionized state in neutral and acidic conditions. As the central ion, The Fe^{2+} may occur strong complexation with some chromophore groups of the wastewater rapidly, which can adsorb the metal ions hydrolysed and form larger complex molecules which called alum floc. Therefore, the excess iron added to form the center of the ions may cause the ion spacing so dense that they are not prone to complex and form large flocs. And the effect will be decreased, so it is prefer to control the ratio of Fe/wastewater from 0.1 to 0.125.

(4) The effects of the Fe/C proportion

In the micro-electrolysis reaction, alone with the iron fillings also has bleaching effect, but not as good as the mixture of iron and carbon chips. On the one hand, adding carbon in wastewater treatment could prevent iron fouling phenomenon occurring during the reaction, on the other hand, the original cells is formed by iron plates and activated carbon. What's more, the loss of iron and carbon had to be considered. The test results showed the following reaction conditions: pH value was first adjusted to three, and then transferred to 10; then the processing time would last 15 min; and the ratio of Fe/wastewater was 0.1, the loss of iron was only 5 to 8% of the original quality, however, carbon is almost no loss, inversely, the quality of the carbon particles in theory should increase after drying because the carbon can adsorb tiny particles. The data displayed in Fig. 5 showed

that the optimum iron-carbon mass ratio is around 0.5.

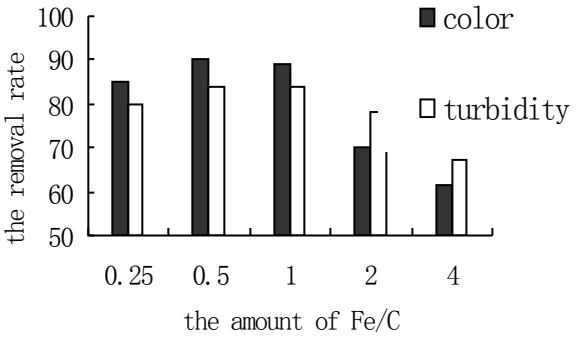

Fig. 5 The effects of the Fe/C proportion

(4) The design of the orthogonal experiment

In order to search for the most important factor among the various process parameters in the micro-electrolysis treatment of poplar BCTMP wastewater, four factors were selected to do orthogonal experiment, which are pH value, Fe / C mass ratio, reaction time, the ratio of Fe/wastewater. Each factor would be inspecting for three levels.

Table 2 Factors and levels of the orthogonal experiments

Level	Factors			
	pH value	Amount of Fe/C	Reaction time /min	Fe/wastewater
1	3	0.25	15	0.1
2	4	0.5	30	0.125
3	5	1	45	0.25

Table 3 Proposals and results of the orthogonal experiments

Number	pH value	Amount of Fe/C	Reaction time /min	Fe/wastewater/ g/ml	the rate of color removal /%
1	3	0.25	15	0.1	90
2	3	0.5	30	0.125	91
3	3	1	45	0.25	93
4	4	0.25	30	0.25	87
5	4	0.5	45	0.1	91
6	4	1	15	0.125	84
7	5	0.25	45	0.125	65
8	5	0.5	15	0.25	63
9	5	1	30	0.1	55
k_1	274	242	237	236	K=719
k_2	262	245	233	240	
k_3	183	232	249	243	
Q	59070	57471	57486	57448	P=57440
S	1630	31	46	8	

By means of an orthogonal test of four factors and three levels which factors are the pH value, Fe/C mass ratio, the ratio of Fe/wastewater and reaction time (showed in Table 2 and Table 3), we concluded that the rate of color removal in the micro-electrolysis treatment was ranged from 55% -90 %, and the most significant factor impacting the treatment effect was the pH value. When the pH value was 3 ~ 4, the color removal rate was about 90%, but when it increased to 5, the color removal rate reduced to below the 60% significantly. The effects of

another three factors which are Fe/C mass ratio, the ratio of Fe/wastewater and reaction time in the treatment on the decolorization are relatively smaller. From these we can see that, during the process of micro-electrolysis experiments, the most critical factor to enhance the treatment efficiency is the adjustment of the pH value of the wastewater.

4. Conclusion

(1) The pretreatment of effluent from BCTMP of polar with micro-electrolysis method was studied, and the optimum process parameters of the experiments were obtained, which were showed as follow: the pH value was about 3 ~ 4, Fe / C mass ratio was 0.5, the ratio of Fe/wastewater was 0.1 ~0.125 and the reaction time was 15min. among these factors, the most critical factor is the adjustment of the pH value of the wastewater

(2) Under the optimum condition of 3～4pH value,0.5:1Fe/C weight proportion,15min reaction time and 0.1～0.125 ratio of Fe/wastewater, the decolorizing rate was 93%, and the CODcr removal rate was about 71%. What's more, BOD_5/COD of wastewater increased from 0.3 to 0.35, which indicated that the biodegradability of wastewater is somewhat improved.

(3) This experiment indicates the possibility of pretreatment of effluent from BCTMP of polar by iron sheets and carbon particles. The iron sheets were from industrial wastes and calcium carbonate power was from alkali recovery plant. It is easy to get the carbon particles because it is no need to grind them which would save grinding and cutting time; furthermore, iron filings is inclined to scale in traditional iron-carbon electrode reaction. As we can see from the UV spectrogram, the conjugated double bonds and the benzene ring appear absorption peaks were found in the formed calcium carbonate and calcium sulfate precipitation, which means the precipitation caused the loss of a part of lignin; After calculating the residue, a small amount of carbon were found to be lost, but the consumption of iron chips is not so much. The reaction can be carried out smoothly as long as the regular complement of quantitative iron and carbon.

(4) The problem existed in the experiment was that, although iron tablets can be used repeatedly, they were easy to rust, especially exposed in the air after the reaction and had to add more acid to remove rust and activate. If it is possibility to do continuous operation, the removal of the rust can be saved, as well as the time and cost. What's more, pay attention to the anticorrosion measures of the equipments and pipelines.

References

1. TANG Xinhu, GAN Fuxing, QIAO Shuyu. The application of iron chips corrosive cell to the treatment of industrial wastewater. [J].Industrial Water Treatment 1998, 18(6) : 4-6.
2. XUE Feng, HU Yanling, LIU Jianhua.Dye sewage treatment based on circular micro-electrolysis technology.[J].Journal of Safety and Environment, 2005,5(5): 117-119.
3. ZHU Hongtao, ZHANG Zhensheng, XU Peiya. Treatment of dyeing and finishing wastewater by ash and iron filings[J].Environmental Science and Technology, 2002, 25(4): 8-9.
4. HAO Ruixia, CHENG Shuiyuan. Study on pretreatment process of dyewastewater using iron fillings filtration and H_2O_2.[J].Techniques and Equipment for Environmental Pollution Control, 2003, 4(4): 15-17, 49
5. HUANG Wu，HU Zhijun. Study on the Decolorizing Technology of Papermaking Wastewater by the Micro-electrolysis Method.[J].South West Pulp and Paper， 2005.Vol.34，No.5
6. HE Song ， LIU Shuaixia ， WANG Jinqi. A Test on the Treatment of Dye Waste by Coagulation-Micro-electrolysis-Biochemical Method [J]Journal of Henan Textile College，2005.Vol.17，No.l
7. QIAO Ruiping，SUN Chenglin etc. Pulp and Paper Effluent Tertiary Treatment by Micro-electrolysis Technology [J] Journal of Safety and Environment, 2007.2, Vol.7, No.1

Effect of mechanochemistry on delignification with Laccase/ Xylanase System

Ji-Xue You, Hai-Lan Lian, Yan-Na Huang and Zhong-Zheng Li

Jiangsu Province Key Lab of Pulp and Paper Science and Technology,
Nanjing Forestry University, Nanjing, Jiangsu Province, 210037

Abstract: The previous research have already proved that Laccase/xylanase system (LXS) from white-rot fungus (Lentinus lepidueus) has the same ability to delignify as Laccase/mediator system (LMS). Mechanochemistry is that the phenomena of the chemical change or physical change was take place in the material by mechanical function. Mason pine (*Pinus massoniana*) pulp was refined in PFI mill, in order to enhanced delignification ability of LXS. The effect of beating on delignification with LXS treatment was investigated，the delignification ability of LXS was compared between before and after beating in this paper. The results indicated that 15 min beating time was optimal time for LXS treatment by comparison of delignification ability before and after beating with LXS treatment. When the enzyme dosage was fixed at 5IU/g and optimal beating time15min , the kappa number of LXS treated pulp after beating decreased by 3 unit and 6.4 unit, the viscosity increased by 8.01% and 6.22% ,the yield decreased by 1.6% and 3.2% respectively compared with LXS treated pulp before beating and original pulp. The SEM images and cellulose crystallinity determination of pulp further illustrated that the mechanochemical effect of delignification was produced with LXS treatment after beating.

1. Introduction

Masson pine is a main papermaking material in South of china. Because its fiber is long and thin, soft, high strengths of pulp, so it is the high-quality papermaking raw material [1-2]. At present the chemical pulp remains a main kind of pulps at home and abroad. The essence of chemical pulping and beaching is delignification in fiber raw materials. But the content of the lignin is relatively high in the chemical composition of masson pine and the cell wall of fiber is thick, so the chemical medicines is difficult to permeate while cooking and beaching, it is more difficult to take off lignin. Thus a large number of chemical medicines were consumed which certainly will cause seriously polluting to the environment. The biotechnology is friendly to environment that for pulping and bleaching field has a importance significance[3-4].

Mechanochemistry is a new developing brim science. Mechanochemistry is that the phenomena of the chemical change or physical change were take place in the material by mechanical function[5-7]. The previous research has already proved that Laccase/xylanase system (LXS) from white-rot fungus (*Lentinus lepidueus*) has the same ability to delignify as Laccase/mediator system (LMS)[8]. Mason pine (*Pinus massoniana*) pulp was refined in PFI mill in this paper, in order to enhanced delignification ability of LXS .The beating played the Mechanochemistry effect here. Thus fiber surface structure, surface nature and surface composition are changed by beating. This should be highly beneficial to enhancement of delignification ability with LXS treatment.

2. Material and Methods

(1) Material

a. Unbleached mason pine (*Pinus massoniana*) pulp

Pulp as dried pulp sheet was obtained from Qingshan Papermaking Mill in Fujian Province.

b. Laccase/Xylanase system (LXS)

Laccase/xylanase system was directly produced by controlling the culture conditions of white-rot fungus. The enzyme activities of laccase, xylanase and cellulase were 156IU/ml, 4.28IU/ml and 0.152IU/ml respectively，the activity of lignin peroxidases or Mn- peroxidases was not found. The LXS was donated by Nanjing Forestry University.

(2) Methods

a. Enzyme treatment

The pulp was treated with LXS in plastic bags. The treatments were carried out at different pH, temperature, pulp consistency, time and enzyme dosage. The control pulp was treated under the same conditions as those of the enzyme treated pulp but without adding any enzyme to it.

b. Alkali extraction of pulp

The enzyme treated pulp was treated with alkali in plastic bags. The alkali extraction was carried out under the following conditions: pulp consistency10%，alkali dosage 1%，temperature 70℃，time 90min。

c. Reducing sugar assay

Reducing sugars in the filtrate were determined by DNS Method [9].

d. Determination of UV Absorbance

The absorbance value was measured at 280nm with UV-751 spectrometer. The absorbance value reflects the relative amount of lignin dissolved in the filtrate.

e. Determination of pulp properties

The yield, brightness and kappa number of pulp were determined according to Chinese National Standards Test Method.

f. Determination of crystallinity

A small amount of control and enzyme treated pulps were made into tablet and then crystallinity was determined with model DMAX-3B X-ray diffractometer.

g. Determination of SEM

The SEM images of both control and enzyme treated pulps were taken with model SEM-505 electron microscope.

3. Results and discussion

(1) Effect of different beating degree on delignification ability with LXS treatment

The previous research have already proved that Laccase/xylanase system (LXS) from white-rot fungus (*Lentinus lepidueus*) has the same ability to delignify as Laccase/mediator system (LMS) [8]. In order to improve delignification ability, the pulps were beating in PFI mill in this paper. The optimum treatment conditions of mason pine pulp with LXS were pH 4.2, temperature 45^{O}C, pulp consistency 3%, time 3h, enzyme dosage10 IU/g (based on laccase). The results can be seen in Table 1.

As can be seen in Table 1, the Kappa number and yield of enzyme treated pulp gradually decreased with increasing of beating degree. The cell wall of fiber produces displacement and out of shape in the course of beating, then P layer and S_1 layer were explode and the fiber was cut off. Because P and S_1 layer contain more lignin in layer, so the lignin was exposed outside after beating that helps to reaction of enzyme and lignin. In addition the longer the beating time, the larger is the surface area of pulp, the effective area of contact of the enzyme and pulp was increased, the reaction of delignification with LXS was promoted, thus the more lignin was take off. The dissolving out of lignin can cause the decline of pulp yield. The kappa number of pulp after alkaline extraction was reduced to 21.8 at beating degree17.5^{o}SR,compared with original pulp and pulp before beating, the kappa number of pulp was decreased 7.1and 2.6 unit respectively. Even by increasing beating time, there was no improvement in lignin removal.

The viscosity of pulp increased with the increasing of beating degree, then it was slightly dropped. When beating degree was set at 21.1 ^{o}SR, the viscosity of pulp was the highest of all. It was explained that the lignin and fiber fines were more dissolved when the pulp was treated with enzyme with the increasing of beating degree, so the viscosity of pulp was increased. If continue beating, then the cutting off of the fiber increases too, so viscosity of pulp was dropped.

The brightness difference of pulp after beating with enzyme treatment can be hardly found, but compared with original pulp , the brightness of that was high slightly.

Table 1 Effect of different beating degree on delignification ability with LXS treatment

Beating time /min	Beating degree /°SR	Kappa number	Brightness /ISO%	Viscosity /mL·g-1	Yield /%
Original pulp	13.0	28.9	25.8	1025.3	100
0	12.5	24.4	26.9	998.3	97.7
10	15.7	23.0	26.6	1021.5	96.8
15	17.5	21.8	26.5	1042.7	96.2
25	21.1	21.5	26.5	1051.0	95.6
30	25.5	21.2	26.5	1018.2	92.3
40	36.5	20.0	26.4	1018.3	90.4

The beating will increase the energy consumption, while beating time was too long. The enzyme treatment result was better with beating time extension, but increasing the beating time will lead to high energy consumption, at the same time the yield of pulp obviously drops.

In summary, it was concluded that 15min beating time was optimal time for LXS treatment。

(2) Comparison of delignification ability before and after beating With LXS treatment

The delignification ability of LXS was compared before and after beating under the optimal treatment conditions for LXS treatment. The delignification ability before and after beating with LXS treatment was compared by detecting the kappa number, viscosity , brightness , yield of pulp and the absorbance value of dissolved lignin ,reducing sugar content in the filtrate. The results can be seen in figures 1, 2, 3, 4 ,5, 6.

Fig.1,2 show the effect of different enzyme dosage treatment on kappa number and yield of pulp before and after beating .The kappa number was determined after alkaline extraction. The results from Fig.1, 2 indicated that the kappa number and yield of both pulp before and after beating were reduced progressively with increasing of enzyme dosage. At LXS dosage 5 IU/g, the delignification reaction already reached higher value. By increasing the amount of enzyme to15IU/g, there was no improvement in lignin removal. The LXS treatment after beating are much more effective in degrading lignin than LXS treatment before beating. When the enzyme dosage was fixed at 5IU/g, the kappa number and yield of LXS treated pulp after beating decreased by 3 unit and 1.6% respectively comparing with before beating and by 6.4 unit and 3.2 % respectively comparing with that of original pulp.

Results in Fig. 3 indicated that the viscosity of LXS treated pulp before beating was the inverse ratio with enzyme dosage. However, the viscosity of LXS treated pulp after beating increased as the enzyme dosage increased. When the enzyme dosage was set at 5IU/g, the viscosity reached maximum and then decreased beyond 5IU/g. It maybe explained that while the pulp was treated by LXS, a few lignin and xylan were dissolved，then some tiny fibers are also dissolved out .So average lengths of fiber were increased by enzyme treatment that caused viscosity to rise. The viscosity of LXS treated pulp after beating increased by 8.01% and 6.22% respectively compared with LXS treated pulp before beating and original pulp. It could be proved that LXS treatment will not cause the negative effect on strength of pulp.

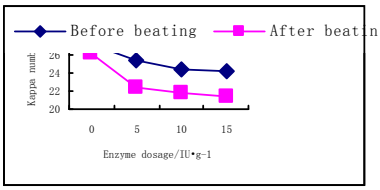

Fig. 1 Effect of before and after beating on kappa number

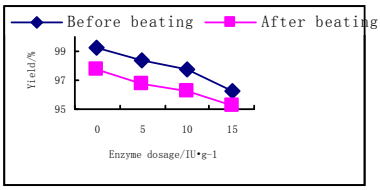

Fig. 2 Effect of before and after beating on yield

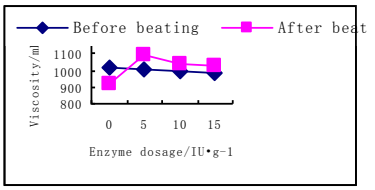

Fig. 3 Effect of before and after beating on viscidity

As shown in Fig. 4, the brightness of LXS treated pulp was not distinctly changed before beating or after beating. Fig. 5 and 6 showed the effect of enzyme treatment before and after beating on absorbance value and

reducing sugar content in the filtrate .The absorbance value of the filtrate can indirectly reflect the amount of the dissolving lignin after enzyme treatment. The detecting of reducing sugar content in the filtrate after LXS treatment can show degradation degree of hemicellulose. As shown in Fig. 5 and 6, the both absorbance value and reducing sugar content in the filtrate increased with the increasing of enzyme dosage. However, the enzyme treatment after beating is much more effective in degrading lignin than before beating under the same enzyme dosage. The absorbance value and the reducing sugar content of LXS treated filtrate after beating were always larger than that of LXS treated filtrate before beating. For example, when enzyme dosage was set at 5 IU/g, the absorbance value and the reducing sugar content of the LXS treated filtrate after beating increased by 76.52% and 103.70% respectively , compared with those of the LXS treated filtrate before beating. Obviously the results showed in Fig. 5 are consistent with result of Fig. 1.

The beating can promote plenty reaction ability of enzyme and pulp, because the surface area was increased by beating. So the delignification ability was obviously strengthened with enzyme treatment after beating. However an improvement in the extent of delignification was obtained by the enzyme treatment after beating , this was quite beneficial to the following bleaching process.

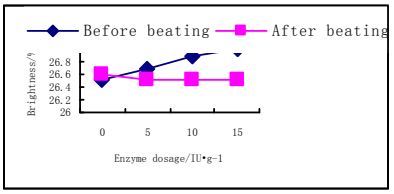

Fig. 4 Effect of before and after beating on Brightness

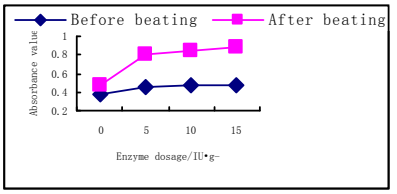

Fig. 5 Effect of before and after beating on absorbance value

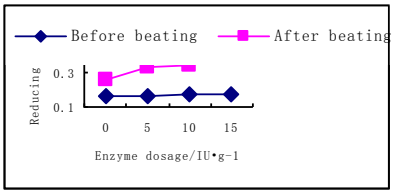

Fig. 6 Effect of before and after beating on reducing sugar

(3) Comparison of crystallinity before and after beating with LXS treatment

Crystallinity of cellulose is the percentage of crystallization region in cellulose structure. As long as the crystallinity increases, the tensile strength, elastic modulus, hardness, density and dimensional stability of fiber will also increase. In this research, crystallinity was determined by X-ray diffraction method. Table2 and Fig.7 showed the change of crystallinity of cellulose before and after beating under the optimal treatment conditions for LXS.

Table 2 change of crystallinity of cellulose before and after beating with LXS treatment

Pulp	Original	LXS treatment before beating	Original after beating	LXS treatment after beating
Crystallinity %	67	68	63	69

*The beating degree of pulp after beating was 17.5 °SR

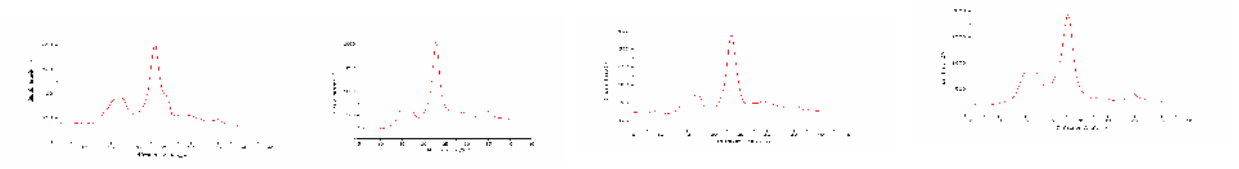

Origina Original after beatting LXS treatment before beatting LXS treatment after beatting

Fig.7 X-ray diffraction patterns of pulps before and after beating With LXS treatment

As shown in Fig. 7, the crystal structure did not change before and after beating with LXS treatment . These results indicated that the small cellulase activity found in LXS had little effect on cellulose. Therefore, the pulp could maintain their crystallinity before beating with LXS treatment and it also explained why the pulp strength did not reduce after enzyme treatment. The crystallinity of cellulose in masson pine pulp slightly drops after beating, but the crystallinity of cellulose after LXS treatment rises to crystallinity of original pulp again. This should owe the credit to the function of mechanochemical effect. It was explained that the contact area of the enzyme and pulp increased, more lignin and xylan were removed that help to arrange closer between the

cellulose that causes the crystallinity of cellulose to rise. It is interest to note that the changes of cellulose crystallinity before and after beating with LXS treatment in Table 2 are consistent with those in Fig.3. At the same time, the mechanochemical effect further illustrated that delignification ability after beating with LXS treatment can was improved.

(4) SEM observation

SEM is a kind of very important surface analyses technologies. The SEM photo can help to observe the change of the micro structure of masson pine pulp before and after beating with enzyme treatment. Fig.8 is the SEM images of surface and cross-section of the pulp treated with LXS before and after beating under optimal conditions. As can be clearly seen from Fig. 8, the surface and cross-section of original pulp were smooth and undamaged, while the enzyme treated pulps had rough surface of fiber, many tiny holes and cracks in the cross section of cell wall, presumably resulted from dissolution of lignin and xylan. Compared the images of the enzyme treated pulps before and after beating , more holes and cracks were found in LXS treated pulp after beating. Especially note worthy is that the delamination of cell wall in enzyme treated pulp after beating has been happened. This is due to the fact that the fibrillation of fiber has produced after beating. The changes of fiber structure lead to the fact that more lignin and xylan are dissolved out. So the enzyme treatment after beating could enhance permeability of bleaching chemicals and dissolved more lignin in subsequent bleaching operation, resulting in reduced chemical dosage and effluent pollution load. In addition compared result of SEM images of enzyme treatment pulp before and after beating was totally unanimous to study result in 2.2 . Also the function of mechanochemical effect has been proved theoretically.

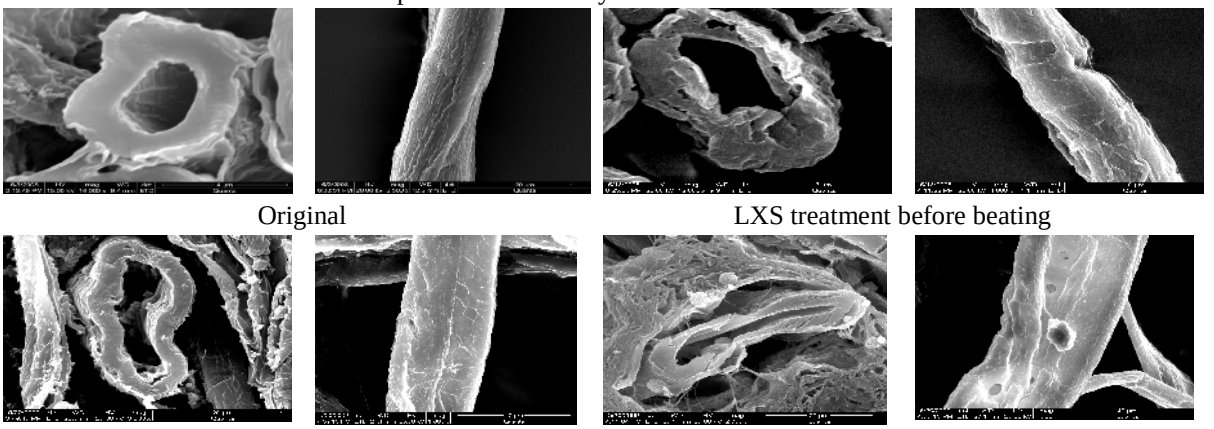

Original LXS treatment before beating

Original after beatting LXS treatment after beatting

Fig.8 SEM images of surface and cross-section of the pulp treated with LXS before and after beating

4. Conclusion

(1) It was concluded that 15min beating time was optimal time for LXS treatment by comparison of delignification ability before and after beating With LXS treatment.

(2) When the enzyme dosage was fixed at 5IU/g and optimal beating time15 min, the kappa number of LXS treated pulp after beating decreased by 3 unit and 6.4 unit, the viscosity increased by 8.01% and 6.22% ,the yield decreased by 1.6% and 3.2% respectively compared with LXS treated pulp before beating and original pulp.

(3) The SEM images and cellulose crystallinity determination of pulp further illustrated that mechanochemical effect of delignification was produced with LXS treatment after beating.

Acknowledgement

This work is supported by National Natural Science Foundation of China (30671654).

References

[1] Wang Zhangrong. Directional select Cultivation of Masson pine papermaking wood [J].China Forestry

Science and Technology，1998,（2）：6~8
[2] You Jixue, Shen Wenying, Ji Wenlan. Evaluation of pulping properties of Masson pine at different ages from Fujian [J]. Chemistry and Industry of Forest Products，1996，16（4）:29~35
[3] Bourbonnais R, Paice M G. Enzymatic delignification of kraft pulp using laccase and a mediator [J].Tappi J, 1996,79(6):199~204
[4] Pratima Bajpai, Pramod K. Bajpai. Application of xylanases in Prebleaching of bamboo kraft pulp[J].Tappi J, 1996,79(4):225~230
[5] Charles R. Hickenboth, Jeffrey S.Moore. Biasing reaction pathways with mechanical force[J].Nature. 2007, 446: 423
[6] A.P.Wiita, R.Perez-Jimenez, J.M.Fernandez . Probing the chemistry of thioredoxin catalysis with force[J]. Nature, 2007,450: 124.
[7] M. K. Beyer ,H. Clausen-Schaumann .Mechanochemistry: The Mechanical Activation of Covalent Bonds . Chemical Review, 2005,105(8): 2921
[8] Jixue You, Jiajia Meng,Xingxing Chen,et al. Study on Direct Delignification with Laccase/ Xylanase System [J]. Journal of Wood Chemistry and Technology,2008,28(3):227~239
[9] Chen, Y., et al., Experimental Method and Technology of Biochemical, Beijing: Science press, 2002, p. 97

Effects of Laccase/Xylanase System and Xylanase Treatments on Oxygen Delignification of Acacia kraft pulp

Yuxiu Wang, Guolin Tong, Hanling Ye and Jixue You
Jiangsu Provincial Key Lab of Pulp and Paper Science and Technology,
Nanjing Forestry University, Nanjing 210037, China

Abstract: The influences of Laccase/Xylanase System (LXS) and Xylanase (X) treatments on oxygen delignification of Acacia kraft pulp were investigated. The comparisons between pre-oxygen delignification and post-oxygen delignification of the two enzymes (systems) were researched respectively. For both of the two enzymes (systems), it clearly showed that the effect of post-oxygen delignification was better than pre-oxygen delignification. Comparing the two enzymes (systems), the effect of X post-oxygen delignification was better than LXS. Both of LXS and xylanase pre-treatment had great effects on the delignification during oxygen delignification. Xylanase was more effective than LXS in the subsequent treatment of oxygen delignification of Acacia kraft pulp.

1. Introduction

Oxygen has been used as an effective delignification and bleaching agent because of its environmental friendly characters. However, as a result of its poor selectivity and ability of lignin degradation, the delignification degree during the reaction is limited. Thus combination of biological technology and oxygen delignification is significant to improve the delignification action and maintain the pulp strength. It has been studied that the laccase/xylanase system produced by controlling culture conditions of the white-rot fungus was effective in degrading of lignin, and xylanase has been used for pulp bleaching.

2. Material and Methods

The unbleached EMCC Acacia kraft pulp, which was produced by Shandong April Ssymb Pulp and Paper Co., kappa number was 11, viscosity was 870 $mL \cdot g^{-1}$, and brightness was 40.76%ISO respectively.

Laccase/Xylanase System provided by the Microbiology Lab was directly produced by the white-rot fungus on the controlled conditions. The purified xylanase was provided by Novozyme Bio-technology Company.

Oxygen delignification was done as the following conditions: oven-dried of the pulp 20g, pulp consistency 10%, $MgSO_4$ charge 0.3% on pulp. The alkali charge, temperature and the reaction time were changed. The pulp was put to oxygen bomb under 0.7MPa of oxygen pressure, and heated to the temperature and kept at this temperature by water bath. At a pre-set time of oxygen reaction bomb was cooled, and the pulp was washed completely, the kappa number, viscosity, and brightness were determined as Tappi methods.

The enzyme pretreatment was done in plastic bag in water bath. The treated pulp was washed with tap water, and the kappa number, viscosity, and brightness were determined as Tappi methods. No mediator was added when LXS was used.

Laccase activity was determined by the method described by Bourbonnais and Paice using ABTS.

Xylanase was assayed according to the method of Bailey *et al*.

3. Results and discussion

(1) Effect of oxygen delignification with LXS pre-treatment

The Laccase/Xylanase System (LXS) was used to pre-treatment for un-bleached EMCC Acacia kraft pulp. After pre-treatment, oxygen delignification was done. The alkali charge, temperature and reaction time during oxygen-alkali delignification with LXS pretreatment were investigated. The results were shown in Table 1, 2 and 3.

Table 1 Effect of LXS pretreatment on alkali charge during oxygen delignification

Alkali charge/%	Kappa Number	Viscosity /mL·g^{-1}	Brightness /%ISO
1.5	8	828.5	49.13
2	7.6	824.9	50.41
2.5	6.8	789.1	54.23
3	7.3	769.4	54.55
3.5	6.7	755.5	54.76
4	6.3	749.3	55.81

Oxygen delignification conditions: pulp consistency 10%, $MgSO_4$ charge 0.05%, oxygen pressure 0.7 MPa, temperature 100 ℃ and treated for 60min.

Table 2 Effect of LXS pretreatment on reaction temperature during oxygen delignification

Tempera-ture/℃	Kappa Number	Viscosity /mL·g^{-1}	Brightness /%ISO
80	8.2	826.3	46.75
90	7.6	805.8	51.08
100	6.8	789.1	54.23
110	6.1	765.3	56.62
120	5.7	720	59.66

Oxygen delignification conditions: pulp consistency 10%, $MgSO_4$ charge 0.05%, oxygen pressure 0.7 MPa, alkali charge 2.5% and treated for 60min.

Table 3 Effect of LXS pretreatment on reaction time during oxygen delignification

Reaction time/min	Kappa Number	Viscosity/mL·g^{-1}	Brightness /%ISO
40	6.9	816.2	53.44
60	6.8	789.1	54.23
80	6.4	760.4	55.75
100	5.9	745.2	58.34

Oxygen delignification conditions: alkali charge 2.5%, pulp consistency 10%, $MgSO_4$ charge 0.05%, oxygen pressure 0.7 MPa, and temperature 100 ℃.

Table 4 Effect of X pretreatment on alkali charge during oxygen delignification

Alkali charge/%	Kappa Number	Viscosity /mL·g^{-1}	Brightness /%ISO
1.5	6.5	748.8	55.81
2	6.3	735.2	55.82
2.5	6.2	732.2	57.27
3	6	726.5	58.47
3.5	5.8	706.6	59.07
4	5.8	697.8	59.28

As shown in table 1, it was clearly shown that when the alkali charge was increased, the kappa number went down and the viscosity was worse. When the alkali charge was set at 2.5%, the delignification was comparably higher and the viscosity was acceptable to keep the pulp a necessary strength. Further more, the brightness of the pulp had an obvious increase at this point. According to Kappa number, viscosity and the brightness of the pulp as well as their trends in Table 2 and Table 3, the optimum temperature and reaction time during the oxygen delignification process were 100℃ and 60 min. It was interesting to find that the optimum temperature and delignification time seemed unaffected by the LXS pretreatment, while the optimal alkali dosage slightly changed.

(2) Comparison of oxygen delignification with LXS pre-treatment and LXS post-treatment

The Acacia EMMC kraft pulp oxygen delignification with LXS pre-treatment, which labeled as LXS+O, and oxygen delignification with LXS post-treatment, which labeled as O+LXS, were done under their optimal treatment conditions respectively. The results were shown in Fig. 1.

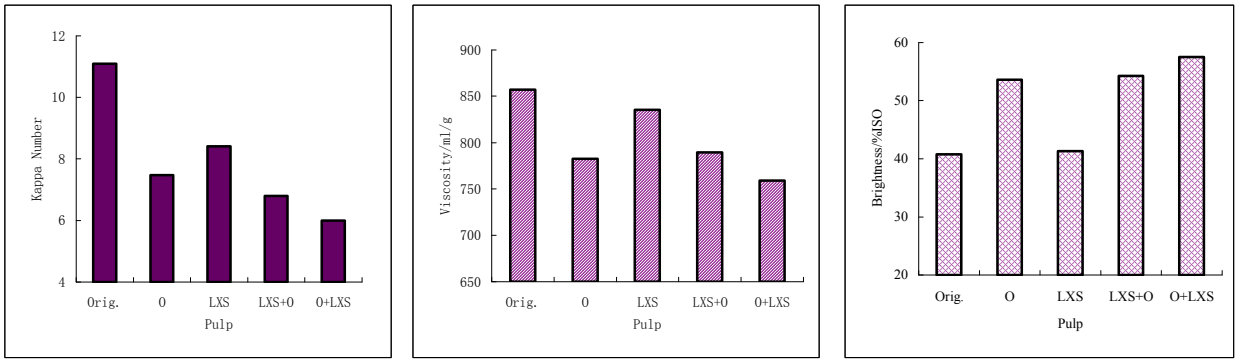

Fig. 1 Comparison of oxygen delignification with LXS pre-treatment and LXS post-treatment

As shown in Fig. 1, LXS treatment had a great effect on the oxygen delignification results whether it is done before or after that. In both of the processes, the kappa numbers of the pulps were much lower and pulp's brightness were higher, comparing with that of the pulp which only through one-staged oxygen-alkali bleaching. As expected, delignification of oxygen was much stronger that that of the enzyme treatment.

Comparing with LXS+O and O+LXS, the O+LXS process was better for a higher delignification degree. The kappa number of the pulp after O+LXS was lower than that after LXS+O, and the brightness was a little higher. Though the viscosity was a little bit lower, in the aspects of maintaining the pulp strength, there was no difference.

(3) Effect of oxygen delignification with Xylanase pre-treatment

As had researched, enzyme pretreatment affected little to the optimum temperature and reaction time in the oxygen delignification process. Thus the optimal alkali charge was only investigated. The results were listed in Table 4.

As shown in table 4, with the increasing dosage of alkali, the kappa number and the viscosity of the pulp gradually decreased and when it was fixed at 2.5%, the brightness leaped to 57.27, which was a considerable increase compared with that 55.82 at 2%. Though a higher alkali dosage was better for the delignification reaction, the lose of the pulp strength can not be balanced in such a mean. So the alkali dosage of 2.5% was just to obtain a relatively ideal pulp property.

(4) Effect of oxygen delignification with Xylanase post-treatment

As was mentioned above, the optimum enzyme dosage and the treatment time may be influenced by the oxygen delignification reaction in the xylanase subsequent treatment process. It was therefore investigated those two conditions for the pulp after oxygen delignification, the results can be seen in Fig. 2 and 3.

5% and X dosage 4 IU·g^{-1}.

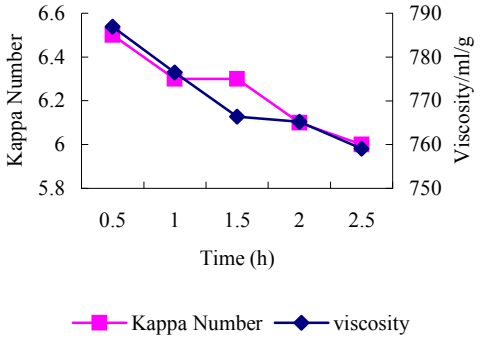

Fig. 2 Effect of oxygen delignification with xylanase post-treatment
conditions: pH 6.0, temperature 50℃, pulp consistency

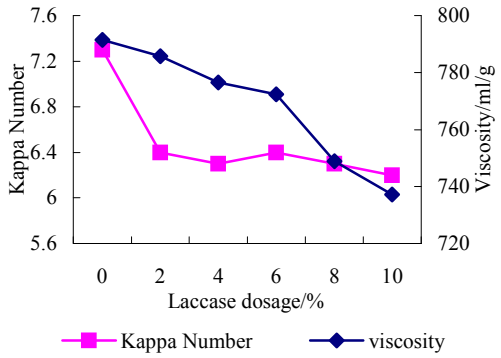

Fig. 3 Effect of X dosage during post-treatment
treatment conditions: pH 6.0, temperature 50℃, pulp consistency 5% and treated for 1 hour.

Fig. 2 showed the influence of treatment time on the pulp properties when it was treated by xylanase after oxygen delignification, Fig. 3 gave these information of the enzyme dosage influence. As shown in Fig. 2, when the reaction time was set between 1 hour and 1.5 hours, the kappa number of the pulp almost had no change, while the viscosity sharply decreased. In Fig. 3, it can be clearly seen that the enzyme applied had a great effect on the properties of the pulp compared with those of the control. When it was set at 4 IU·g^{-1}, the kappa number and viscosity of the pulp decreased by 13.7 %and 1.9% respectively, while the brightness increased about 3% ISO units. So the optimum enzyme dosage and the treatment time for the pulp after oxygen delignification were 4 IU·g^{-1} and 1 hour.

(5) Comparison of oxygen delignification with X pre-treatment and X post-treatment

For both of the pretreatment and the subsequent treatment of xylanase, the comparison of these two processes was done under the optimum conditions respectively. The results can be seen in Fig. 4. (pretreatment

and subsequent treatment of xylanase were labeled as X+O and O+X respectively.)

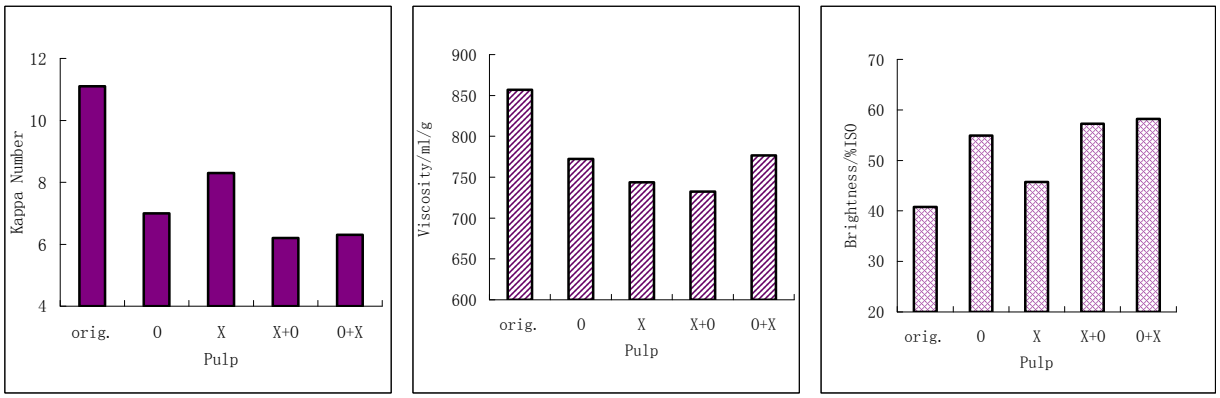

Fig. 4 Comparison of oxygen delignification with X pre-treatment and X post-treatment

As shown in Fig. 4, xylanase treatment had a significant effect on the delignification degree comparing with the single oxygen delignification process, whether it is done before or after that. For these two process, the kappa number of the pulp in X+O seems no difference to that of the pulp in O+X process, while in X+O the viscosity of the pulp was much lower than that in O+X and the brghtness seems a little bit lower. So the X treatment after oxygen dilignification may be more ideal to achieve a relatively higher delignification degree and maintain the pulp strength. Comparing with the original pulp, the kappa number and the viscosity of the pulp decreased by 43.2% and 9.4%, while the brightness incressed around 17%ISO, which is considerable. As is expected, delignification of oxygen was much stronger that that of the enzyme treatment.

4. Conclusion

1. The Laccase xylanase system and xylanase pre-treatment had effects on the delignification during oxygen delignification.
2. The effects of Laccase xylanase system and xylanase subsequent treatments were better than pre-treatment in enhancing the oxygen delignification process.
3. Xylanase was more effective than Laccase xylanase system in the subsequent treatment of oxygen delignification of the Acacia EMCC kraft pulp.

Acknowledgement

The financial support from National National Science Foundation of China (30671653) is greatly appreciated.

References

1. E. W. Bretthauer, H. W. Kraus and A. Domenico. Dioxin perspectives. Plenum Press, New York and London, 1991.
2. EPA's dioxin reassessment. Environ.Sci.Technol.1995, 29:26A.
3. Jixue, You, Jiajia, Meng, Xingxing, Chen, Hanlin Ye. Study on direct delignification with laccase/Xylanase system[J]. Journal of Wood Chemistry and Technology. 2008,28(3):227-239
4. Robert Bourbonnais, Michael G. Paice. Demethylation and delignification of kraft pulp by Trametes versicolor laccase in the presence of 2,2'-azinobis-(3-ethylbenzthiazoline-6-sulphonate)[J]. Appl Microbiol Biotechno. 1992, 36:823-827
5. Bailey, M. J., Biely, P., Poutanen, K. Inter-laboratory testing of methods for assay of xylanase activity[J]. Journal of Biotechnology. 1992, 23:257~270.

Study on Manufacturing of Biodegradable Polylactide from THFA pulp

Chen-Lung Ho[1,2], Tzu-Chao Chien[1], Kuang-Ping Hsu[1], Eugene I-Chen Wang[1] and Yu-Chang Su[2]

[1] Division of Wood Cellulose, Taiwan Forestry Research Institute, 53, Nanhai Rd., Taipei, Taiwan 100

[2] Department of Forestry, National Chung Hsing University, 250 Kuo Kuang Rd., Taichung, Taiwan 402

Abstract: In this study, the tetrahydroxyfurfuryl alcohol (THFA) pulped agricultural and forest wastes, such as rice straw pulp, were saccharified, and then fermented using microorganism to produce lactic acid, and evaluation of the fermentation conditions and lactic acid production rates also conducted. The lactic acid thus produced was condensed to produce polylactide with the optimal conditions evaluated carefully. The results indicated that the optimal conditions of fermenting hydrosate of THA pulp to lactic acid entailed a hydrolyzed sugar concentration of 60 g/L, and by using *Lactobacillus paracasei* subsp. *paracasei* for 72 h to provide the maximum conversion of hydrolyzed sugars，lactic acid production efficiency, and produced lactic acid concentrations were 85.9%, 0.69 g/h, and 49.57 g/L, respectively. Thence, the microorganism strain had high lactic acid production suggesting that the cost of purifying lactic acid produced from the fermentation system might be lowered substantially. As for the polymeric condensation of lactic acid to polylactide, at the synthesize temperature of 140℃, catalyst ($SnOct_2$) concentration of 0.3 wt% yielded the best results to 80%. The average molecular weight of the polylactide could be raised from 18600 to 50300 daltons.

1. Introduction

Among the organosolv processes, the tetrahydrofurfuryl alcohol (THFA) system can be carried out under atmospheric condition, allowing energy saving and low capital cost requirement. THFA boils at 176℃, has low volatility, low toxicity; is biodegradable and water miscible. After pulping, THFA can be recovered from waste liquor. The water layer were treated with acid to separate lignin and carbonhydrate, then pentose and hexose were divided, THFA in water layer were then recovered by other solvent, the consumed THFA can be replenished by converting the dissolved pentosan in the liquor to furfural and then hydrogenated to generate THFA.

This digestion method will not generate combustible organic solvents like methanol and ethanol, and will not generate malodorous gas or liquids [33]. This technology, however, has not yet seen industrial applications. Bogomolove et al.;[34-36] Johansson et al.;[33] and Aaltonen et al.[37] had reported using THFA solutions to delignify birch and pine, and to pulp birch, spruce and eucalyptus. These were pulping of softwoods and hardwoods, whereas, there appears to have no report of applying the method to agroforestry waste like rice straw. In this study, we carried out pulping of rice straw using the THFA method and examined its pulping characteristics and the chemical and physical properties of the pulp in order to establish the feasibility of THFA pulping of rice straw. In this study, rice straw was pulped with the THFA method to examine their pulping characteristics and the chemical properties of the resulting pulp. Upon hydrolysis and saccharification of the pulp, the hydrolyzate was fermented with microbes to produce lactic acid. The fermentation conditions and lactic acid yield, as well as the optimal conditions for polylactic acid formation were evaluated to understand the THFA pulping of rice straw and formation of polylactic acid.

2. Material and Methods

(1) Material

Rice (Oryza sativa) straw, obtained from commercial rice straw ropes of Taiwan which were dissected into segments of ca. 3 cm. The material was air dried before use. The chemical compositions of the rice straw are Holocellulose 68.2% (α -cellulose 50.2%, β +γ-cellulose 18.0%), Lignin 20.1%, Ash 12.6%, Extractive 2.6%

(2) Microbes

Lactobacteria strains studied include *Lactobacillus paracasei* subsp. *Paracasei, L. rhamnosus. L. delbrueckii*, and *L. vaccinosteraus.* The cultural medium used was MRS medium.

(3) Methods

One hundred g (oven-dry mass) of the 3 cm rice straw segments were place in a round-bottom flask and added with 80~95% THFA in water solution having differing amounts of catalyst (HCl, 0.1~0.5%). Adjusting the liquor to material ratio to 10 and 12 (kg L-1), and carrying out digestion at 120℃ for 4 h respectively. After cooking, the pulp was washed thoroughly with water and a 2% solution of NaOH at 70℃ to obtian the pulp. Yields were then determined. In order to compare the delignification rates and yields, digestions at 130 and 150 ℃were also carried out. All test data shown are the average of triplicate analyses.

(4) Evaluation of pulp properties

After pulping, the washed pulp were subjected to chemical analyses, including the kappa number (TAPPI T236 om-85), ash (TAPPI T211 om-93), alcohol-benzene extractives (TAPPI T204 os-76), holocellulose (the Wise method, as stipulated by the Japan Wood Association, 1985), cellulose and hemicellulose content (JIS P9001), and lignin (TAPPI T222 om-88). All test data shown are the average of triplicate analyses.

(5) Carbohydrate analysis of the pulps

Based on the method of Borchardt and Piper[38] and using inositol as an internal standard and prepared acetyl derivatives of the sugars in order to carry out gas chromatographic analysis.

Fermentation

All lactobacteria strains were first activated to serve as inoculums. Sterilized MRS medium (including substrate of 20, 60 and 100 g/l glucose was inoculated with the bacterium and incubated at a 37℃ shaking table at 250 rpm. Every 8 h, a portion of the substrate was withdrew and centrifuged at 5000 rmp for 10 min. The supernatant was isolated for testing the changes in concentrations of lactic acid and glucose.

(6) Composition analysis

a. Total sugar and lactic acid: The centrifuged supernatants were separately derivatized with TMS and methylation to analyse the total sugar and lactic acid. Composition analysis was based on GC, and GC-MS analysis.
b. Optical isomers of lactic acid: Methylated supernatant was analyzed for optical isomers using GC and GC-MS.

Synthesis of polylactic acid: According to the method of Moon et al. (2000).

Determination of PLA molecular weight: Using GPC to fractionate PLC into different average molecular weight fractions.

3. Results and discussion

In this study, we conducted THFA organosolv pulping of rice straw at THFA-water concentrations of 80%~95%, and catalyst (HCl) dosages of 0.15%~0.5%, digestions were carried out at 120℃ for 4 h. At pulp kappa number around 20, pulp yields of 60% or more was obtained, more than 20% higher than those provided by kraft pulping; and the process had excellent pulp ability. In the chemical compositions of the resulting pulps, the higher the THFA concentration, the lower the lignin content tended to become. The higher the catalyst dosage, the greater the degree of delignification was as well. Optimally, 95% THFA with 0.5% HCl at120℃ 4 h cooking of reic straw produced maximum delignification rate of 92% (kappa no. 17.3). When digestion was extended to 300 min, the lignin content change indicated that at the initial stage of the pulping, rapid delignification occurred which differed from typical kraft pulping of wood chips. If 95% THFA and catalyst dosage of 0.5% were employed at 130 or 150℃ cooking, the delignification rate was even faster, however, the pulp yield loss and holocellulose dissolution rate were drastically increased as well. As a consequence, we deemed the conditions with 95% THFA, HCl of 0.5%, temperature of 120℃ and cooking time of 240 min as the optimal. However, if energy and operational efficiency is a factor, then a programmed heating scheme such as using 95% THFA, HCl of 0.5%, temperature of 130℃ and cooking time of 90 min can produce a very good results as well. Additionally, the analysis of sugars in the pulps indicated that in THFA pulping, hemicelluloses were more liable to dissolve

than cellulose, and xylose constituted the main sugar in the dissolved hemicelluloses, which along with increases in the THFA concentration and catalyst dosage, reached as high as 78%. The main constituent of cellulose, glucose, on the other hand, had a dissolution rate of only 11.8% maximum. Finally, on the physical properties of handsheets, the THFA pulp was about 20~30% poorer in strength than the corresponding kraft pulp. This was caused by weaker single fiber strength, but shall not pose any problem in practical application of the pulp.

Subsequently, the organosolv THFA pulped material was sacchrified and fermented with microbes to produce lactic acid, and to evaluate the suitable microbial fermentation conditions and lactic acid formation. The results indicated that one of the 4 strains reached maximum lactic acid production at 72 h, and the other ones between 80 and 96 h. From the transformation rates of THFA pulp upon saccharification, the *L. paracasei subsp. paracasei* had the best performance reaching 85.9%. The maximum lactic acid concentration was also reached by the same strain at a sugar concentration of 60 g/l and a maximum yield of 49.6 g/l. As for hourly lactic acid production rate, the same strain also excelled. At a hydrolyzate concentration of 60 g/l, it reached 0.59 g/l-h. Hence under the optimal rice straw pulp transformation into lactic acid condition, hydrolyzate concentration of 60 g/l inoculated with *L. paracasei subsp. paracasei* fermented for 72 h could reach the maximum lactic acid yield. The high lactic acid yield by the strain means purification cost of the fermentation system is decreased. The lactic acid was subsequently synthesized at a reaction temperature of 140℃ and SnO_{ct2} catalyst at 0.3 wt%, the molecular weight could rise from 18,600 to 50,300.

Optimization of Conditions of Acid-Catalytic Ethanol Pulping of Wheat Straw Using Response Surface Methodology

Zhong Liu and Yanhua Lu
Tianjin Key Laboratory of Pulp & Paper,
Tianjin University of Science & Technology, Tianjin 300457

Abstract: The results of factorial experiment showed that the significant external factors affecting acid-catalytic ethanol pulping of wheat straw were ethanol consistency, pulping temperature, acid dosage and temperature holding time. Based on the results, response surface methodology (RSM) was employed and a second order quadratic equation for pulp yield was built in the present work. The applicability of the model equation for predicting the optimum response values was verified effectively by the validation data. By analyzing the response surface plots and their corresponding contour plots as well as solving the quadratic equation, the optimum process parameters for pulping were obtained as: ethanol consistency 65%, pulping temperature 190 ℃, acid dosage 0.8% and temperature holding time 52.5min.

1. Introduction

Response Surface Methodology (RSM) [i-4] was proposed by Box in the 1950s, which takes regression equation as tools for functional computing. In multi-factors experiments, the interrelation among factors and the results (response value) was expressed by fitting multinomial. So we can analyze the surface of function and explorer the interrelation among factors and results and then optimize them. It is effective method for optimizing reaction conditions and technology parameters and is applied extensively in chemistry, chemical engineering, biological engineering and food engineering. In this paper, we took advantage of RSM method to analyze the factors affecting straw ethanol pulping with acid catalyzing and obtain the optimum conditions.

Organic solvent pulping is an appropriate method for wheat straw pulping with low environmental pollution. There are many solvents for organic solvent pulping. Ethanol is the one among them and ethanol pulping can recover some kinds of value-added byproducts and bring remarkable social and environmental benefit [6] so in this project we optimized conditions of acid-catalytic ethanol pulping of wheat straw using response surface methodology.

2. Material and Methods

(1) Material

The wheat straw used in the project was obtained from Wuji, Hebei province and stored for three months. Stock preparation employed laboratory cutter to cut the wheat straw for about 30mm slice and screened them by 14-mesh screen.

(2) Methods

Ethanol pulping was carried out using batch 4L laboratory digester which can endure maximum pressure 4MPa equipped 300℃ thermometer.

(3) Pulp washing

Washing liquid was prepared according to liquid-to-ethanol 1:8 and the concentration was 65%. Washing was carried out in room temperature and pressure, ethanol solution was used firstly and then fresh water until clean pulp.

(4) Experiment design

Results of earlier experiments showed ethanol concentration, cooking temperature, catalyst dosage, cooking time and ratio of liquid to wood are key parameters to affect yield of screened pulp, so in this project we employed Box-Behnken module[7-10] in response surface methodology. According to the results of mono-factor experiments, we determined the optimum ratio of liquid to wood 1:6 and chose other 4 external factors as independent variable, which were denoted by X_1、X_2、X_3、X_4 respectively. +1、0、-1 were expressed as high,

medium and low level, and according to the function $x_i=(X_i-X_0)/\triangle X$, we coded these independent variables. Among them, x_i was code value of independent variable, X_i was real value of independent variable, X_0 was real value of midpoint of independent variable, $\triangle X$ was changeable step length of independent variable. Factors code and levels were showed in Table 1.

Table 1 Factors, levels and coding

Factors	coding		level		
	code	real value	-1	0	1
Ethanol（%）	x_1	X_1	45	55	65
Cooking temperature（℃）	x_2	X_2	75	85	95
Catalyst dosage（%）	x_3	X_3	0.8	1.0	1.2
Cooking time（min）	X_4	X_4	45	60	75

$$Y = B_0 + \sum_{i=1}^{n} B_i X_i + \sum_{i=j=1}^{n} B_{ij} X_i X_j \qquad (1)$$

If n=4, the above formula can be transformed as $Y=B_0+B_1x_1+B_2x_2+B_3x_3+ B_4x_4+B_{12}x_1x_2+B_{13}x_1x_3+ B_{14}x_1x_4+B_{23}x_2x_3+ B_{24}x_2x_4+ B_{34}x_3x_4+B_{11}x_1^2+B_{22}x_2^2+ B_{33}x_3^2+B_{44}x_4^2$（2）

Therein Y was response value, B_0 was constant, B_1, B_2, B_3, B_4 were linear coefficient respectively, B_{12}, B_{13},B_{14}, B_{23},B_{24},B_{34} were regression coefficient, B_{11}, B_{22}, B_{33},B_{44} were second-order coefficient. This experiment design and data processing were finished by statistics software SAS.

3. Results and discussion

(1) Module establishment and significance test

According to multiple regressions fitting by SAS, we got the quadratic polynomial regression module formula in relation to those four independent invariables. Thereinto Y means yield of screened pulp.

$Y_1 = 48.60667 + 3.2625*x_1 - 1.728333*x_2 - 0.489167*x_3 - 0.903333*x_4$
$- 0.2825*x_1*x_1 - 0.3575*x_1*x_2 - 0.52*x_1*x_3 + 0.135*x_1*x_4 - 1.06125*x_2*x_2$
$- 0.32*x_2*x_3 - 0.4075*x_2*x_4 + 0.7725*x_3*x_3 - 1.0125*x_3*x_4 - 0.77625*x_4*x_4$

According to ANOVA we can see that $F_{regression}=6.31>F_{0.01}(14,10)=4.56$, $p=0.001$. It showed that module had high significance, so the module fitted very well and could be used to analyze and foresee the yield of screened pulp.

(2) Response surface analysis and optimization of screened pulp

The effects of X_1、X_2、X_3、X_4 and their interrelation on the yield of screened pulp were showed in Figure 1 to 3.

In Figure 1 we can see that, when catalyst dosage 1.0%, cooking time 60min, the yield of screened pulp increased with the ethanol concentration going up. When cooking temperature is 177.1℃ and ethanol concentration increased from 45.86% to 64.03%, the yield of screened pulp increased by 6.4% from 45.81% to 52.21%. When cooking temperature is 192.3℃ and ethanol concentration increased by the same level, the yield of screened pulp increased by 5.42% from 43.83% to 49.25. When catalyst dosage 1.0%, cooking time 60min, the yield of screened pulp went down with the cooking temperature went up. When ethanol concentration 45.86%, cooking temperature rose from 177.1℃ to192.3℃, the yield of screened pulp decreased by 1.98% from 45.81% to 43.83%. When ethanol concentration 64.03%, cooking temperature changed same level, the yield of screened pulp decreased by 2.96% from 52.21% to 49.25%, demonstrating that the three factors of ethanol concentration, cooking temperature and their interrelation have great effect on the yield of screened pulp.

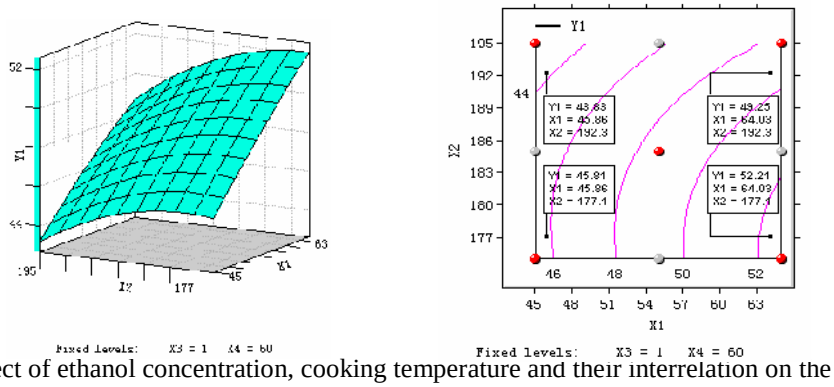

Figure 1 The effect of ethanol concentration, cooking temperature and their interrelation on the yield of screened pulp

In Figure 2, we can see that when ethanol concentration 55%, cooking time 60min，the yield of the yield of screened pulp went down with the cooking temperature going up. When catalyst dosage 0.828%, cooking temperature increased from 176.1℃ to 194.1℃, the yield of screened pulp decreased by 2.53% from 50.07% to 47.54%. When catalyst dosage 1.165%, ethanol concentration increased by the same level, the yield of screened pulp decreased by 3.84% from 49.63% to 46.15%. When catalyst dosage 1.0%, cooking time 60min, the yield of screened pulp went down with the cooking temperature went up. When ethanol concentration 45.86%, cooking temperature rose from 177.1℃ to192.3℃, the yield of screened pulp decreased by 1.98% from 45.81% to 43.83%. When ethanol concentration 55%, cooking time 60min, cooking temperature changed same level, the yield of screened pulp decreased with the catalyst dosage increased. When cooking temperature 176.1℃ and catalyst dosage increased from 0.828% to 1.165%, the yield of screen pulp decreased by 0.44% from 50.07% to 49.63%, demonstrating that the more catalyst dosage is, the less the yield of screen pulp is. And the high cooking temperature can boost this effect.

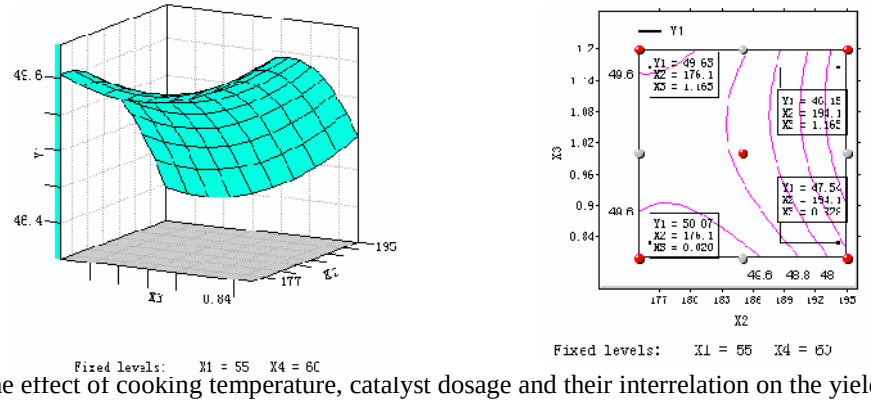

Figure 2 The effect of cooking temperature, catalyst dosage and their interrelation on the yield of screened pulp

In Figure 3 we can see that, when ethanol concentration 55%, catalyst dosage 1.0%, the yield of screened pulp decreased with cooking temperature going up. When cooking time is 46 min and cooking temperature went up from 175.9℃ to 194.2℃, the yield of screened pulp decreased by 3.83% from 48.24% to 44.41%. When ethanol concentration 55%, catalyst dosage 1.0%, the yield of screened pulp decreased with the cooking time increased. When ethanol concentration 55%, cooking temperature 175.9℃, the cooking time changed from 46 min to 73 min, the yield of screened pulp decreased by 0.89% from 49.13% to 44.41%. When cooking temperature 194.2℃, the yield of screened pulp decreased by 2.23% from 46.64% to 44.41%, demonstrating that high cooking temperature can shorten cooking time.

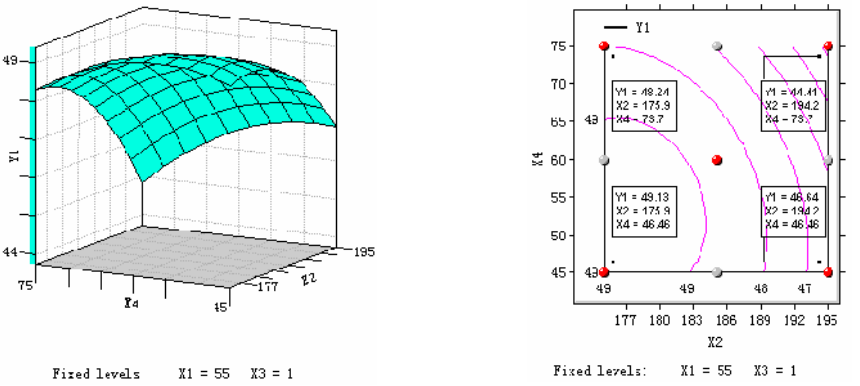

Figure 3 The effect of cooking temperature, cooking time and their interrelation on the yield of screened pulp

(3) Module test experiment

For confirming the effectiveness of module function for evaluating the yield of screened pulp, we took response value 48.61 for optimization and carried out 6 groups experiments for test and the results were listed in Table 2.

From the Table 2, the results from the 6 groups pulping experiments for test are fairly close to the forecast value, approving the response surface methodology was employed to optimize the conditions of acid-catalytic ethanol pulping of wheat straw is practicable.

Table 2 The results from the 6 groups pulping experiments for test

No.	Independent variables				Y		Relative error（%）
	X_1（%）	X_2（℃）	X_3（%）	X_4（min）	Forecast value	Real value	
1	55	185	1.1	60	48.56	47.84	1.48
2	55	185	0.9	45	48.67	46.79	3.86
3	55	185	1.0	45	48.73	48.06	1.37
4	55	175	0.9	45	48.76	47.64	2.30
5	65	195	1.0	60	48.44	46.29	4.44
6	55	185	1.0	60	48.61	48.48	0.27

4. Conclusion

The SAS software was employed to establish the forecast module to optimize conditions of acid-catalytic ethanol pulping of wheat straw using response surface methodology. Through experiments, the module was considered practicable, and using the module response surface the effects of key factors and their interrelation on the yield of screened pulp were discussed. Finally we obtained the external factors affecting the yield of screened pulp are ethanol concentration 65%, cooking temperature 190℃, catalyst dosage 0.8%, cooking time 52.5min。

References

[1]. He zhen, Qi ershi, et al. Improving the products/progress quality combining RSM method [J]. Administration Engineering Transaction, 2001, 15(1):22-25.

[2]. Gao yulong, Wu ning, Jiang hanhu. RSM optimizing food conditions [J]. Food Science, 2004, 25(3): 101-106.

[3]. Li Zongjun, Jiang hanhu. The effects of environmental factors on fermentation [J]. Food Science, 2004, 25(1): 40-46.

[4]. Wang yongfei, Wang chengguo. The application and theory of RSM [J]. Qinghua Transaction, 2005, 14(3): 236-240

[5]. Han qing. Organic solvent pulping of Non-wood materials [J]. International papermaking, 2004, 19(6):7-9

[6]. Myers R H. Response surface methodology [M]. Ann Arbor EdwardsBrothers, 1976.

[7]. Montgomery D C.Design and analysis of experiments. 2nded. [M]. New york, John Wiley, 1991.

[8]. Annadurai G.Raju V.Use of Box-Behken design experiments in the determination of adsorption equilibrium: reactive dye on chitin. In proceeding of the Advances in Chemical Engineering, 8-20. Bhabha Atomic ResearchCenter, Mumbia, India, 1997.

[9]. Annadurai G,Shee ja R Y.Use of Box-Behken design of experiments for the adsorption of vero fix-redusing Biopolymer.BioprocessEng, 1998, 18: 463-466.

Study of Refining Properties of Poplar APMP

Hai-Yong Gong, Xin-Xing Xia and Ying Lin
Shaanxi University of Science & Technology, Xi-an, Shaanxi Province 710021
Shaanxi province key laboratory of papermaking technology & specialty paper

Abstract: The refining properties of poplar APMP were investigated. The result showed that fibers were mainly defibered from lamella during APMP pulping process, and the fibers were stiff. During the refining process, the APMP fibers did little swell and split, however, the fibers were easily broken and formed fine pieces. The paper's tensile index increased as the beating degree rose, which was mainly due to a lot of hydrogen bonds formed between fibers and fine pieces. The tear index also increased as the beating degree rose, and it reached maximum when the beating degree was about 61°SR, then it began to decrease. It showed that the bond among the fibers and fine pieces was the main factor to affect the tensile index and the tear index, then the fibers' length. The density increased and the opacity decreased a little as the beating degree rose.

1. Introduction

APMP pulping method has the advantages of high yields, high utilization of resources and low costs for operation. Therefore, it has been rapidly developing.

Now, softwood has been substituted by hardwood in its dominate of high-yield pulp resources. Production practice and scientific research shows that timbers at the density of about 0.3 ~ 0.5g/cm^3 are suitable for the production of high-yield pulp. In North America, especially in Canada, Poplar, Maple have become the main raw material for production of high-yield pulp [1, 2], as well as Brazil and Australia with eucalyptus [2, 3].

High yield pulps made from hardwood has become a very important paper-making resource. However, so far, it has yet not been deeply studied. This paper mainly studied the refining performance of poplar APMP.

2. Material and Methods

(1) Material

APMP of poplar (17^0SR) was received from Long Feng Paper Co., Ltd. in the city of PuYang in HeNan province.

(2) Methods

a. Apparatus

PFI refiner: DCS-041PT, made in Japan

Multimedia Optical Microscope: Motic-DMB$_5$, produced by MOTIC company in Austrian

Scanning Electron Microscope (SEM): SEMS-570, produced by the company of Hitachi in Japan

b. Beating Process

Poplar-APMP was refined in PFI refiner to reach different beating degree with the concentration of 10%.

3. Results and discussion

(1) Impact of Beating on Fibre Morphology

Fig.1 was multimedia optical microscope photograph of Poplar-APMP with beating degree of 17^0SR, and Fig.7 was SEM photograph of Poplar-APMP with beating degree of 39^0SR. Both pictures showed that the fiber cells were intact, which illustrated that fibre cells were mainly separated from lamella during APMP pulping process.

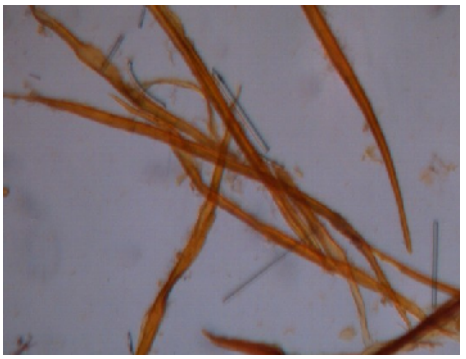

Fig.1 Poplar-APMP(170SR)

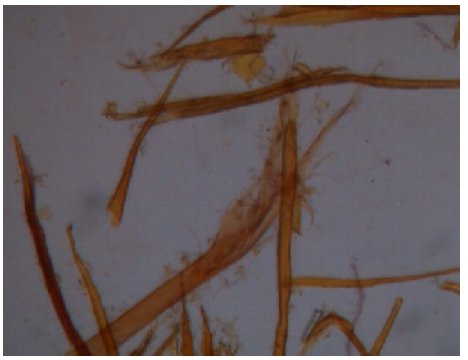

Fig.2 Poplar-APMP(250SR)

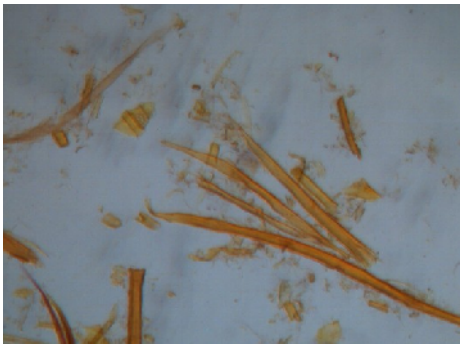

Fig.3 Poplar-APMP(39^0SR)

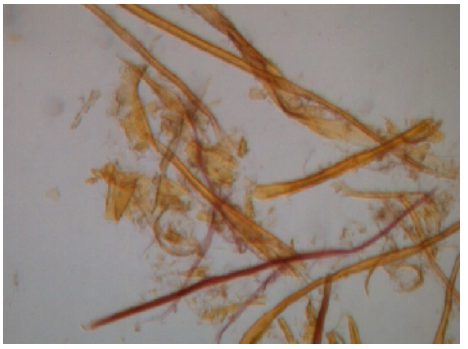

Fig.4 Poplar-APMP(53^0SR)

Fig.5 Poplar-APMP(61^0SR)

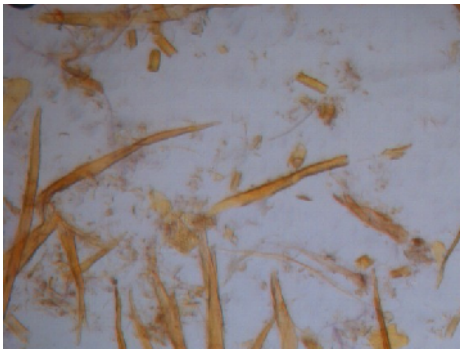

Fig.6 Poplar-APMP(70^0SR)

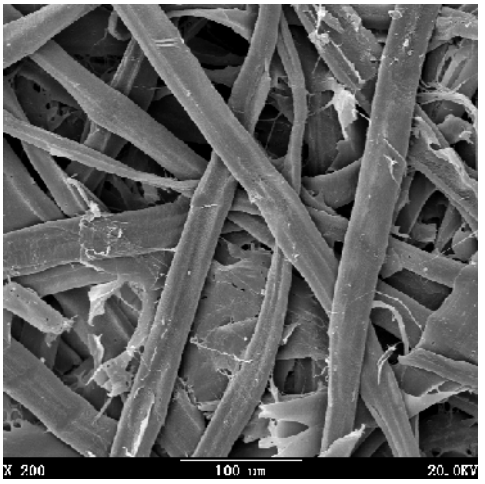

Fig.7 Poplar-APMPSEM photograph(39^0SR)

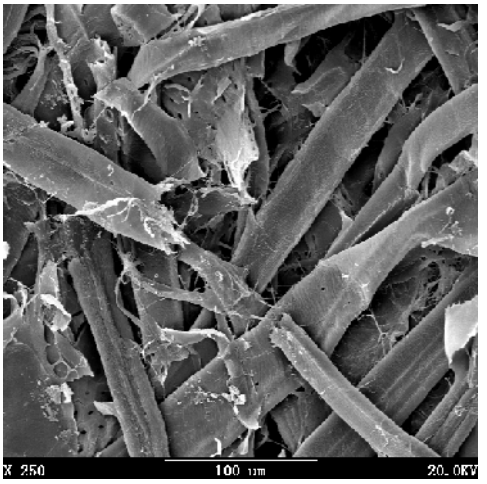

Fig.8 Poplar-APMP SEM photograph(61^0SR)

Fig.2 to Fig.5 optical microscope photographs showed the change of fiber morphology during the process of beating. It was showed that the fiber cells were intact when the beating degree was 17 ^{0}SR. As beating, fibers were gradually broken and appeared more and more fine pieces with the increasing of beating degree. And it was also showed that broken almost totally occurred at the fibers' tips. Therefore, it was proved that fibers were mainly cutted off and appeared lots of fragments during beating of Poplar APMP, and fibers were basically no swell and fibrillation. Even at the beating degree of 61^{0}SR and 70^{0}SR, although lots of fine pieces formed, fibers were yet little swelled and fibrilled. Fig. 7 and Fig. 8 SEM photographs showed that fibers' surface was intact, and no obvious swell and fibrillation at the beating degree of 39^{0}SR and 61^{0}SR. It is because that the yield of poplar APMP pulping is about 85% ~ 90%, so this pulping method keeps most of the lignin, and keeps primary wall and secondary wall-outer layer, and prevented fibers swelled. Therefore, fibers of Poplar APMP are stiff and hard, and are prone to debris at the beating process.

Therefore, during the beating process of poplar-APMP, the fibers were easily broken and formed fine pieces, and little swelled and fibrilled.

(2) Impact of Beating on paper characteristics

Tab.1 paper characteristics made from Poplar APMP with different beating degrees

Beating degree /°SR	Basis weight /g/m^2	Density /g/cm^3	Breaking length /km	Tearing strength /mN.m^2/g	Opacity /%
17	61.3	0.358	1.962	3.26	90.5
25	61.4	0.372	2.113	3.31	90.0
39	61.2	0.384	2.358	3.49	89.2
53	60.9	0.388	2.735	3.62	88.4
61	62.0	0.410	3.041	3.76	87.6
70	61.8	0.412	3.197	3.68	7.1

Tab.1 and Fig.9 showed the physical characteristics of hand-sheets made from Poplar APMP with different beating degrees. It was showed from Figure 8 that the breaking length increased as the beating degree rose, and even at the beating degree 70^{0}SR, the breaking length still showed a tendency to increase, which was because that there appeared lots of fine pieces during refining, and lots of hydrogen bonds were formed among fibers and fine pieces. Therefore, the breaking length was increased as the beating degree rose, though the fibers little swelled and fibrilled at the beating process.

The tearing strength of paper made from Poplar-APMP increased with the increasing of beating degree, and it began to peak off after the maximum. It was seen on Fig.9 and Fig.10 that the tearing strength of the paper made from chemical wood-pulp reached maximum at the beating degree 25^{0}SR, while the tearing strength made from Poplar APMP reached maximum at the beating degree around 61^{0}SR[4], both had a clear difference. Since tearing strength is mainly affected by fibers' bond and the average fiber length, for chemical wood-pulp, fibers are flexible and easy to be swelled and fibrilled at the beating process, so fibers are easy to interweave. Therefore, for chemical pulp, the fibers' length was the main factor to affect the tearing strength, then the fibers' bond. On the contrary, for high yield pulp, fibers are stiff, and hard to interweave. Therefore, for high yield pulp, the fibers' bond was the main factor to affect the tearing strength, then the fibers' length. So the tearing strength increased as the beating degree rose for Poplar-APMP pulp, since the fibers' bond was the major factor to affect the tearing strength. When the beating degree was 61^{0}SR, the tearing strength reached maximum, then it began to peak off, since the average length of fiber had become the major affecting factor.

Paper density increased as the beating degree increased. Since fines increased with the rising of beating degree, which filled among the long fibers, and the density was increased.

Opacity gradually decreased as the beating degree increased. This is because the main factor that affects the opacity is the fibers' bind. However, opacity only reduced about 4% when the beating degree increased from 17^{0}SR to 70^{0}SR, which was due to high stiffness of APMP fibers and lots of spacing among the fibers.

4. Conclusion

During the APMP pulping process, fibers were mainly defibered from lamella, keeping unbroken primary wall and secondary wall-outer layer, and fibers were stiff.

During the refining process, fibers were little swell and fibrillation, but easily broken to fragments.

Breaking length increased when beating degree increased, which was mainly due to lots of fragments appeared in the process of beating.

Tearing strength increased with the increasing of beating degree, it reached maximum when the beating degree was about 61^0SR, then began to decline. The fibers' bond was the main factor to affect the tearing strength, then the fibers' length.

Density increased with the increase of beating degree; opacity declined a little as the beating degree rose.

References

[1] Zhou Yajun. Maple high-yield CMP produce superior grade coated cardboard. China Papermaking, 2003,22 (7): 11

[2] Zhou Y. Overview of HYP in paper and board. Paptac 90th annual meeting. Montreal (Canada), 2004: 143~149.

[3] Hu K, et al. Substitution of HW kraft with aspen HYP in LWC wood-free papers. Paptac 90th annual meeting. Montreal (Canada), 2004: 95~100.

[4] Lu Qianhe. Papermaking Principle and Engineering (2nd edition).Beijing. China Light Industry Press, 2004.

Surface Energy of Aramid Fiber/Pulp and Their Sheets Properties

Fang He, Meiyun Zhang and Sufeng Zhang

Key Laboratory of Papermaking Technology Specialty Paper Development of Shanxi Province, College of Pulp and Papermaking Engineering , Shanxi University of Science & Technology, Xi'an 710021, China

Abstract: The surface contact angle of several meta-aramid fibers and meta-pulps as well as their sheets were measured, and the surface energy of aramid fiber, aramid pulp and sheet was determined according to the harmonic mean –based Wu equation. The relationship between the surface energy and sheet properties in sheet processing was discussed according to the surface energy as well as the interfacial tension and work of adhesion of aramid fibers and pulps. The results show that the surface energy of aramid fibers and pulps is in the range of 35~45mJ·m^{-2}, the surface energy of fibers is slightly higher than that of pulps, the polar component of surface energy is larger than the dispersion one, and the wettability and work of adhesion are enhanced with increase of the surface energy of aramid fibers and pulps, when water and glycol are employed as the testing liquids. The surface energy of aramid sheet decreases during hot pressing process.The better the matching of polar component with dispersion component, the smaller the difference of surface energy and the smaller the interfacial tension, the stronger the adhesion between fibers and pulp with the improved strength of aramid sheet.

1. Introduction

Aramid composite sheet is made by wet forming and hot pressing from aramid fiber and aramid pulp, it is a composite material with good strength, heat resistance and insulation resistance. Studies show that hot pressing soften the surface of part of the aramid fibers and aramid pulps and melt the aramid pulps to bond the aramid fibers together[1-2]. In order to explain the surface and interfacial phenomenon, surface energy is used to represent surface wettability, interfacial bonding and absorption. The larger the fiber surface energy and the closer the surface energy of two phases, the larger polar component and the stronger the wettability, the better to enhance interfacial bonding [3-4]. Many studies show that the properties of composite materials can be enhanced by adding surface active groups and fiber physical chemistry modification [5-6]. Other studies show that carbon fiber surface energy and its polar component is relative to the mechanics properties of its composite materials [7]. However, studies concerning surface energy and hot pressing mechanism of aramid fibers and aramid pulps used in producing composite sheet are very insufficient. In this paper, the relationship between the surface energy of aramid fiber, aramid pulp, its bonding and composite sheet properties is discussed according to the surface energy of aramid fiber which was indirectly indicated by the surface energy of aramid fiber film, combined with interfacial tension, work of adhesion and the influence of hot pressing on surface energy of the composite sheet.

2. Material and Methods

(1) Material

Domestic PMID aramid fibers and aramid pulps are provided by two main manufacturers. They are called as F1 fiber and F1 pulp, F2 fiber and F2 pulp, foreign Nomex paper is provided by Du Pond and called F3 sheet and its aramid fiber and aramid pulp are called as F3 fiber and F3 pulp; the average length of all the aramid fibers is 5~6mm, its diameter is about 12μm, the average length of the aramid pulps is 2~4mm.

(2) Methods

a. Contact angle measurements on aramid fibers

DAT1100 dynamic contact angle tester made in FIBRO Company in Sweden is applied to measure contact angle according to the shape of liquor droplets on the surface of test sample. In the experiment process, aramid fibers are made into film on the Polyethylene plastic plate, then the film is cut into desired dimension and is stuck to the surface of special feeder and sent to the tester.

During the measurement, system will record the dynamic contact angle value and relevant dimension

automatically each 0.02s. Test condition are: test duration, 0.2min; test liquor droplets volume, 4ml; ten different measuring points on each test sample, and arithmetic mean value will be adopted.

b. Surface energy calculation of aramid fibers

According to the harmonic mean presented by S. Wu based on the development of classic geometric mean equation, the surface energy of aramid fibers is calculated using measured contact angles. The theoretical equation is [8]:

$$(b_i + c_i - a_i)\gamma_s^d\gamma_s^p + c_i(b_i - a_i)\gamma_s^d + b_i(c_i - a_i)\gamma_s^p - a_i b_i c_i = 0 \qquad (1)$$

In which, $a_i = \gamma_i(1+\cos\theta)/4$, $b_i = \gamma_i^d$, $c_i = \gamma_i^p$, $\gamma_s = \gamma_s^d + \gamma_s^p$

where a_i, b_i, c_i are testing liquids constant, $_i$ is the testing liquids chosen, and in this study, testing liquids are water and glycol; γ_s^d and γ_s^p is dispersion component and polar component of the sample surface energy, respectively. For the calculation of the surface energy, dispersion component and polar component of the sample, the surface energy, dispersion component and polar component of water and glycol (Table 1) and the surface contact angle of aramid fibers are introduced into equation (1) to obtain simultaneous equations.

Table 1 Surface energy of the testing liquids (20°C)

No.	Surface energy $r_{i/(mJ\cdot m^{-2})}$	Dispersion component $r_i^d{}_{/(mJ\cdot m^{-2})}$	Polar component $r_i^p{}_{/(mJ\cdot m^{-2})}$
water	72.8	21.8	51.0
glycol	48.3	29.3	19.0

c. Forming and molding of aramid sheet

BBC-3 paper former made in German Ernsthaage company is adopted to produce aramid sheet. F1 fiber and F1 pulp, F2 fiber and F2 pulp, F1 fiber and F2 pulp, F2 fiber and F1 pulp are mixed in certain proportion and then are disintegrated, drained and dried to form aramid sheets. The formed aramid sheets are further pressed on the Dp2002 high temperature three- roll soft calender made in Finland DT-Science company. The former two aramid sheets are named F1 sheet and F2 sheet, respectively. Basis Weight of the aramid sheets is about 116 $g_{\cdot m^{-2}}$, the techniques of hot pressing are: pressure, 9~16MPa; temperature, 250°C.

3. Results and discussion

(1) Determination of the surface contact angle of aramid fiber

In the experiment, aramid fiber is made into film on the PE at first, then measure the surface energy of the film to show the surface properties of the aramid fibers indirectly. During the measurement of contact angles, initial contact angle value (0.02s) should be ignored because the shape of liquor droplets on the surface of sample is irregular. Liquor droplets on the surface of sample will be absorbed slowly and disappeared with time. Therefore, the surface contact angles are accepted when the liquor droplets on the sample surface begin to drop steadily. And different testing liquids has different surface energy, the measured contact angles and the changes of surface contact angles are different. The contact angles of water on PE and six aramid fibers decrease rapidly before 0.06s, and the changes slow down after 0.06s, so the surface contact angles of water on aramid fibers would be accepted when the time is 0.06s. When glycol is applied as the testing liquids, the surface contact angles of glycol on aramid fibers would be accepted when the time is 0.14s. Contact angles of aramid fibers are given in Table 2, surface contact angle of water on aramid fiber ranges from 60° to 70°, and surface contact angle of glycol on aramid fiber ranges from 25°to 45°, so it can be determined that aramid fibers have higher hydrophobic property .

Table 2 Surface energy of the aramid fiber and pulp (20°C)

No.	Contact angle θ / °		Dispersion component γ_s^d / mJ·m^{-2}	Polar component γ_s^p / mJ·m^{-2}	γ_s^p / γ_s^d	Surface energy γ_s / mJ·m^{-2}
	water	Glycol				
PE	79.5	60.5	12.1	18.8	1.6	30.9
F1-fiber	63.0	36.7	17. 6	24.9	1.4	42.5
F1-pulp	65.3	44.0	15.0	25.4	1.7	40.3
F2-fiber	61.9	29.9	20.1	24.0	1.2	44.1
F2-pulp	66.2	39.7	17.6	22.9	1.3	40.5
F3-fiber	67.7	41.3	17.4	22.1	1.3	39.5
F3-pulp	68.5	43.7	16.5	22.3	1.4	38.8

(2) Surface energy analysis of aramid fiber

Surface energy of aramid fibers are calculated by establishing theoretical equations with surface energy of testing liquids and solid sample, dispersion component, polar component and the measured surface contact angles of testing liquids on samples .

Surface energy of aramid fibers which satisfied Eq.(1) are calculated and shown in Table 2. Surface energy of six different aramid fibers are very different, this probably result from the different contributions of atoms on the surface of aramid fibers to its surface energy, because the supermolecular structure of aramid fibers are different with different processing [9-10]. The surface energy of F1 fiber, F2 fiber and F3 fiber are larger than F1 pulp, F2 pulp and F3 pulp, respectively, the surface energy of F1 pulp is near to that of F2 pulp, but the surface energy of F3 pulp is lower. Compared to PE, the average surface energy of aramid fibers are 10 units higher. The results show that the wettability of aramid fibers to the same liquid is higher than that of PE. This is because of the introduction of heteroatoms to macromolecular polymer, the sequence of atoms which enhance the wettability of macromolecular polymer is: F<H<Cl<Br<I<O<N[11]. Compared to carbohydrate, there are N atoms on the molecular chains of aramid fibers, so its surface is apt to be bonded with electrophilic atoms and form intensive hydrogen bond, and this will enhance its surface energy.

Moreover, it shows that aramid fibers are moistened by same liquid more easily than aramid pulps because that the surface energy of aramid fibers is larger than that of aramid pulps. During the hot pressing process , aramid pulp melts earlier than aramid fiber and covers the aramid fiber because the morphology and the structure of aramid pulp is different from that of aramid fiber and its molecular chains move rapidly. Aramid fibers are probably moistened by the melted aramid pulps and form good bonding during the short hot pressing process.

In addition, according to Table 2, for the aramid fibers, the larger the surface energy, the smaller the surface contact angle, the higher the wettability and the absorbing capacity The wettability of F2 is the highest and that of F3 is the lowest , and if aramid fibers are moistened by aramid pulps more easily, the work of adhesive of aramid fibers and aramid pulps are higher [3].

(3) Analysis of interfacial tension and work of adhesion of aramid fibers

Chen[3] et al. thought that the larger the surface energy, the stronger the adhesion between aramid fibers and pulps, but the increase of surface energy was not the necessary condition to its surface being moistened. The main factors which determine its surface wettability were interfacial tension and the matching of polar component with dispersion component [12]. In this paper harmonic mean equation is obtained according to the polar component theory of interfacial tension

$$\gamma_{12} = \gamma_1 + \gamma_2 - \frac{4\gamma_1^d \gamma_2^d}{\gamma_1^d + \gamma_2^d} - \frac{4\gamma_1^p \gamma_2^p}{\gamma_1^p + \gamma_2^p} \quad (2)$$

Interfacial tension between aramid fibers and pulps can be calculated by bringing the surface energy, dispersion component and polar component parameters into eq.(2). The lower the interfacial tension, the easier the adhesion between aramid fibers and aramid pulps and the easier one phase is moistened by another one. Then ,work of adhesion (W_a) can be calculated according to the surface energy γ_1、γ_2 and interfacial tension[10]:

$$W_a = \gamma_1 + \gamma_2 - \gamma_{12} \quad (3)$$

W_a is the energy desired to separate the interface of aramid fibers and pulps reversibly, the results are shown in Table 3.

As shown in Table 3, six aramid sheets are made from aramid fibers and aramid pulps with same proportion, and the smaller the difference of surface energy ,the smaller the interfacial tension , the higher the tensile index of aramid sheet. Furthermore, as shown in Table 2 and Table 3, γ_s^p/γ_s^d of F3 fiber and F3 pulp is the minimum, while that of F2 fiber and F1 pulp is the maximum and interfacial tensions of them are the minimum and the maximum, respectively, but tensile index of the sheets are the maximum and the minimum , respectively. It shows that the matching of polar component with dispersion component of aramid fiber and pulp as well as their interfacial tension are relative to their sheet properties closely.

Table 3 The interfacial tension and work of adhesion of aramid and its sheet property

No.	Surface energy difference $\Delta\gamma_s$ / mJ·m^{-2}	Interfacial tension γ_{12} / mN·m^{-1}	Work of adhesion W_a / mJ·m^{-2}	Tensile index / N·m·g^{-1}
F1-fiber/F1-pulp	2.2	0. 20	82.6	51.6
F2-fiber/F2-pulp	3.6	0. 21	84.4	49.4
F1-fiber/F2-pulp	2.0	0.08	82.9	53.0
F2-fiber/F1-pulp	3.8	0. 80	83.7	46.7
F3-fiber/F3-pulp	0.7	0.02	78.3	59.9

Table 4 Surface energy of aramid sheets before and after hot-press process

No.	Surface contact angle θ /°				Surface energy γ_s/ /mJ·m^{-2}		
	Before hot-press		After hot-press		Before hot-press	After hot-press	Drop scope/%
	Water	Glycol	Water	Glycol			
F1-sheet	66.9	29.7	80.1	65.7	42.7	30.2	29.3
F2-sheet	84.0	46.4	87.9	68.1	36.5	26.2	28.4
F3-sheet	76.6	52.9	79.1	72.7	33.5	31.5	5.9

Surface energy of aramid sheet before and after hot pressing process (16MPa) is shown in Table 4. Surface energy of three aramid sheets before and after hot pressing process vary visibly and surface energy of aramid sheets after hot pressing process decreases sharply. The decrease of surface energy mean that the surface structure of aramid sheet is denser and is not easy to be penetrated by liquids. And this decreases the destruction of the surface of aramid sheet by water and other polar molecules and improves the bonding force of molecules, so the mechanics properties and wetting resistance of aramid sheet after hot pressing process is better than that of aramid sheet before hot pressing process. Furthermore, the decrease of surface energy will lead to the decrease of wettability of aramid fibers and the decrease of adhesive force between fibers and pulps during hot pressing process and bring a negative influence on work of adhesion.

4. Conclusion

(1) The surface energy of aramid fibers is slightly higher than that of pulps, the polar component of surface energy is larger than the dispersion component, and the better the matching of polar component with dispersion component, the smaller the difference of surface energy and the smaller the interfacial tension, the larger the tensile index of aramid sheet.

(2) The larger the surface energy of aramid fiber, the better the wettability, the work of adhesion and the adhesive strength.

(3) After hot pressing process, the decrease of surface energy lead to a good wetting resistance of aramid sheet, but it is negative to adhesion process and sheet properties.

References

[1] Heng Peizhi, Tao Shiyi, Wang Liping. The development of polyaramide fiber paper [J]. Paper and Papermaking, 2004, 23(6): 69-73.

[2] Hu Jian, Huang Yilei, Zheng Chisong, et al. Review of Nomex paper cxomposite [J]. Paper Science & Technology, 2003, 22(4): 29-31.

[3] Chen Ping, Lu Chun, Yu Qi. Influenced of fiber wettability on the interfacial adhesion of continuous fiber-reinforced PPESK composite [J]. Journal of Applied Polymer Science, 2006,102(3): 2544-2551.

[4] Liu Yaopeng. Analysis and discussion on optimum condition for bonding [J]. Adhesion in China, 2007, 28(2): 29-30.

[5] Liu Li, Zhang Xiang, Huang Yudong, et al. Effect of ultrasonic treatment on surface characteristics of aramid [J]. Acta Materiae Compositae Sinica, 2003, 20(2): 35-40.

[6] Wang Yang, Li Peng, Yu Yunhua, et al. Interfacial properties of phosphorous acid modified Kevlar fiber reinforced epoxy resin composites[J]. Acta Materiae Compositae Sinica, 2007, 24(3): 7-12.

[7] Hoecker F, Karger-Kocsis J. Surface energetic of carbon fibers and its effects on the mechanical performance of CF/EP composites[J]. Journal of Applied Polymer Science, 1996, 59(1): 139-153.

[8] Wu Renjie. The surface and interface of polymer[M]. Beijing: Science Press, 1998: 1-63.

[9] Zheng Zhiqing, Qian Xianhuo, Wu Xiaohong, et al. The structure and properties of poly-*m*-phenyleneisophthalamide(PMIA) fiber[J]. Synthetic Fiber Industry, 1993, 16(6): 18-21.

[10] Gao Ming, Sunn Fengzhong, Wang Nini, et al. Theoretical analysis on the effect of surface energy upon heat exchanger performance[J]. Energy Engineering, 2006, 27(2):12-14.

[11] Zhao Guoxi. Superficial active substance physical chemistry[M]. Beijing: Peking University Press, 1984: 340-380.

[12] Wu Souheng. Surface and interfacial tensions of polymer melts II: Poly(methyl-methacrylate), poly(n-butymethacrylate) and polystyrene [J]. The Journal of Physical Chemistry, 1970, 74(3): 632-638.

The Effects of the Hollow Plastic Pigment on the Properties of Glossy Ink Jet Paper

Chuan-Shan Zhao, Jian-Tong Cui, Jing-Jing Wang and Quan-Peng Li
Key Lab of Paper Science and Technology of Ministry of Education, Shandong
Institute of Light Industry, Jinan 250353, China
Email:ppzcs78@163.com

Abstract: Traditional cast coated glossy photo paper production process due to its characteristics that the water evaporates from non-coated cast side, so the coating speed is slow, ground paper is non-waterproof paper, therefore the paper products are easy to transmutative, as the cast shows that the formation of dense coatings membrane, the lower ink absorption. To solve such the problems, a novel porous ink receiving layer constituted by a litter amount of a hydrophilic binder(PVA) and a cross-linking agent, a large amount of inorganic pigment(SiO_2) and a hollow structural plastic pigment. In this paper, the effects of the hollow structural plastic pigment rheological properties of the color and the printing and preservation properties of ink jet paper were investigated. Because of the thermoplasticity of the plastic pigment the calendering and dry technology were also studied. From the viewpoint of water-fastness and preventing the penetration of binder, the resin coated paper(being so-called RC paper) is selected as the substrate.

1. Introduction

Hollow plastic pigment is a modified cavity paint，as the air-filled cavity of particles, it's proportion is lighter than the high degree of transparency solid particles[1]. The particles of hollow plastic pigment are well-distributed,the hollow plastic pigment has a lot of strong points that other organic pigment didn't have: high opacity , good stability, good gloss, it can give a good smoothness to paper pages and make the paper have a good printing performance[2]. Coated paper coatings used HP, have a good absorption of printing ink, the glossiness of printing and ink is good. However, the price of HP dope is high, also, it has weaker absorption capacity of pigment ink than the average dopes[3]. This paper use hollow plastic pigment mixed with nano-silica, through changing the using condition to research the effects of the hollow plastic pigment on the properties of glossy ink jet paper.

2. Material and Methods

(1) Material

a. RC-base paper: the norm of base paper is showed in table 1.

Table1 Performance Indicators of Coating Base Paper

fixed amount （g/m^2）	60°glossiness (%)	opacity (%)	whiteness (%)	K&N (%)	Cobb value （g/m^3）
220	49	94.8	93.6	5.29	3.6

b. Pigment :

nano-silica :the performance of nano-silica is showed in table 2:

Table 2 The characteristics of nano-silica which exclusive used in glossy photo paper

performance	norm
BET /m^2/g	200
mean grain size /nm	100
compaction density /g/l	50
volume concentration /g/l	30
pH	3.7-4.7

Plastic pigment HP1055：hollow sphere, ROHM HAAS HP 1055, solid content is 26%, wet density is 1.08 g / mL, dry density is 0.486g / mL, pH value of 8 ~ 9, viscidity is 50～700mPa·s，particle diameter is 1.0 μm (ID 0.82μm), shell thickness is 0.091μm，volume porosity is 55％。

c. Dispersant: Cationic Dispersant A1040：light yellow liquid, solid content is 40%，viscidity is 100mPa·s 。

d. Adhesive: Polyvinylalcohol (degree of polymerization 1700, alcoholysis degree 99％); carboxyl SBR(solid content 49％，PH value 8.3)

e. Trace additive: Cationic fixing agent.

(2) Apparatus

Small coating machine, 3 Roll-ray machine, NDJ-85 digital display discometer, vancometer, spectrodensitometer, whiteness instrument（L&W ELREPHO）.

(3) Methods

a.The Order of Added Paint

In order to prevent each component of the coating flocculating or thickening, the order is :

(a) PVA solution mixed with latex, then add the organic pigments HP1055.

(b) Add the silica dispersion.

(c) Add a fixing agent that other trace additives.

b. Hollow plastic pigment for paints and paper properties

Fixed amount of pigment nano-silica 100 copies, PVA for 30 copies, carboxylated SBR latex for 10 copies, cationic dye-fixing agent of the total coating amount of 2%, prepared in accordance with paint in order to change the amount of hollow plastic pigment, first used high-shear viscometer (NDJ-85 Digital Display Viscometer) measurements coating rheology, and then use small-scale coating machine for coating of the coated base paper ,then use calendering to calendar the paper, after the paper coating, use gloss meter, Elysee optical density meter, whiteness instrument (L & W ELREPHO) to explore the hollow plastic pigment on paper performance.

3. Results and discussion

(1) The effect of hollow plastic pigment on coating rheology

Different contents of hollow plastic pigments effect on the rheology of dope ,the result is showed in fig.1.

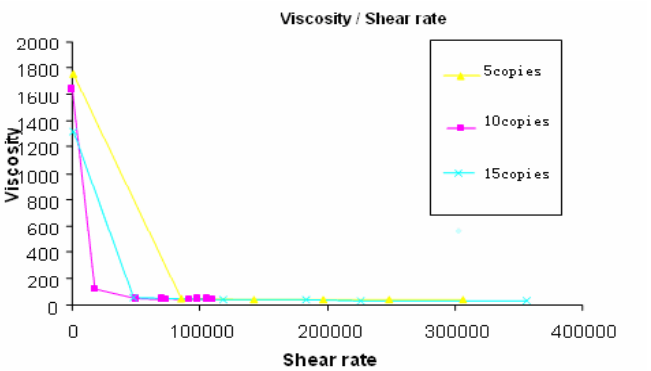

Fig.1 The effect of plastic pigment on the rheology of dope

From the fig.1 we can see that add the plastic pigment, reduces the coating's low shear viscosity, and high-shear leveling, improving coatings pseudoplastic. HP1055 particles hollow core, the moisture sealed in the ball body, though never dry solid content of 26%, but when the coating amount is calculated HP1055, sealed in a sphere of water must be taken into account, the effective solid content so that it is about 56.5 %, so the hollow spherical plastic pigment coating to improve the rheological properties and also can improves the coating solids.

(2) The effect of Plastic pigment on paper properties and print properties

The result are showed in fig.2-fig.5

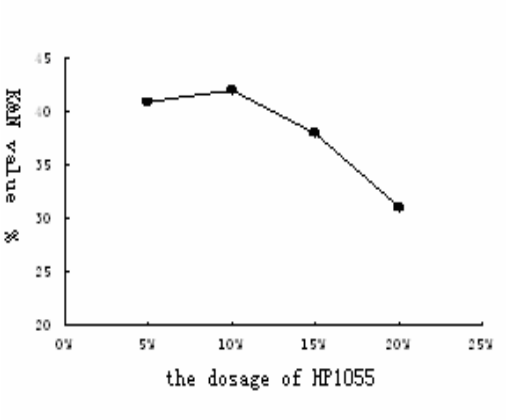

Fig.2 The effect of different HP1055 dosage on K&N value

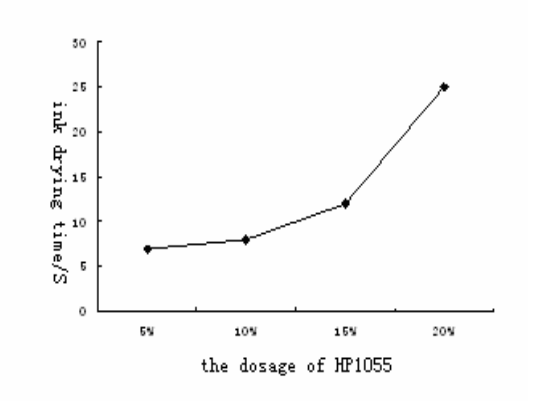

Fig.3 The effect of different HP1055 dosage on ink drying time

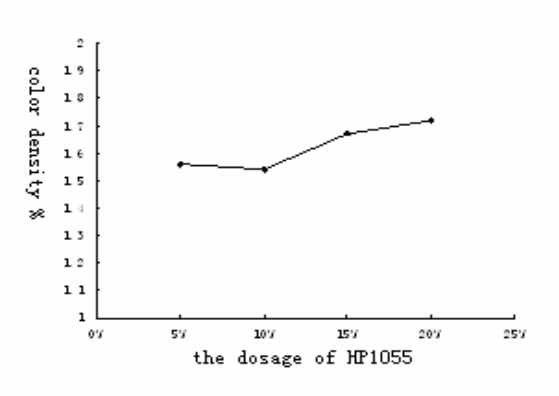

Fig.4 The effect of different HP1055 dosage on color density

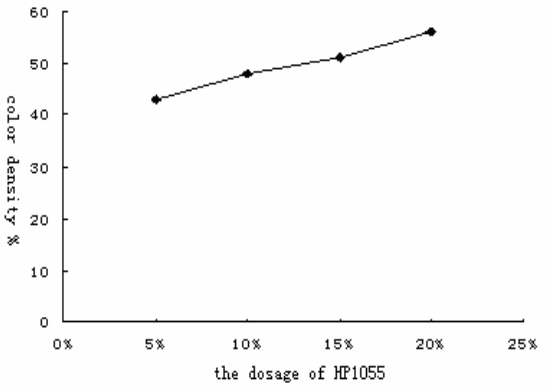

Fig.5 The effect of different HP1055 dosage on gloss

As can be seen from Figure 1.2-1.5, with the HP1055 increased dosage, K & N values and a downward trend in color trends, color density and drying time on the rise because of plastic pigments are styrene and styrene and acrylic acid copolymer, with a certain degree of water resistance, and therefore a lower water-based ink absorption, ink drying time is relatively long. Integrated consider selecting 10% of the amount of the best conditions. Under these conditions, K & N value of the paper, ink drying time, paper, color density and gloss to achieve the best results.

(3) Characteristics of hollow plastic pigment

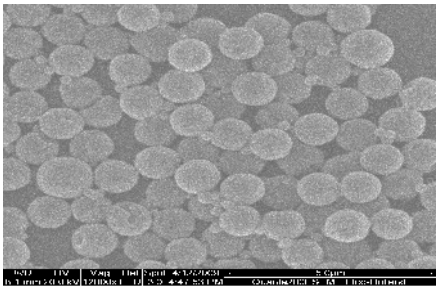

Fig.6 SEM of HP1055

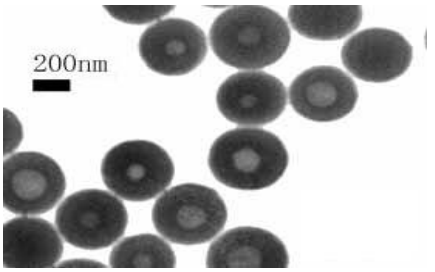

Fig.7 TEM of HP1055

Fig. 6 SEM scanning electron microscope and Fig.7 TEM scanning electron microscopy can be found pigment particles are spherical bodies, and is hollow, the moisture sealed in the ball body, only in dry rooms, at a

certain temperature and pressure, leaving the hollow sphere, so it has less density, greater thickness and plasticity of pine can greatly improve their performance and covered with gloss. Hiding strong, white high, and can give a high gloss paper and printing gloss; coating loose thick, flexible, able to provide excellent print fidelity; to improve the operating conditions, lower pressure and temperature pressure-ray machine ; in the lower coating weight of the coating under the conditions to achieve higher coating results.

4. Conclusion

Hollow plastic pigment due to its own advantage made a large number of applications in the ink-jet printing paper, plastic paint plastic paint usage at 10%, it can improve the performance of coated paper to change the coating surface smoothness and gloss, but the main effect is special effects in the finishing course. Plastic paint itself has a special thermoplastic, so that when in the calendar, the mineral pigments are prone to deformation, so that coating's surface is smooth, porous, high gloss; plastic pigments also can improve the print gloss.

Literature Reference

[1] Sweet R G.. High frequency recording with electrostatically deflected ink-jets [P]. US: 3596275, 1971.

[2] Hyun-kook Lee，Margaret K. Joyce，Paul D. Influence of silica particle size and packing volume on printability of glossy inkjet paper coating. Proceedings of the IS&T NIP19:International conference on digital printing technologies , New Orleans,2003:613-618.

[3] Katri Vikman. Studies on fastness properties of ink jet print on coated papers. Helsinki University of Technology, Laboratory of Forest Products Chemistry. 2004:20-22.

Blends of SA and SB Latexes on the Performance Characteristics of LWC Papers

Sheau-Horng Lin[1]

[1]Department of Wood Science and Design, Pingtung University of Science and Technology, Taiwan

Abstract：The objectives of this study was to investigate the properties of the colors made from mixed latexes at various ratios and to explore the optimum combination ratio of SA and SB that would give suitable printability in light weight coated paper (LWC). The higher the Tg of SA, the better the smoothness and gloss, while dry pick decreased. Higher smoothness and gloss were obtained with the use of SA compared to SB latexes, and the latter gave superior dry pick.Water retention of the coating colors prepared from mixed SA/SB binders was lower than that of the pure components. LWC papers prepared from colors using SA_{250}/SB_{100} (SA of Ps 250 nm mixed with SB of 100 nm Ps) as the binder gave excellent smoothness and gloss before and after printing. Its dry-pick is, however, slightly inferior to that of SA_{100}/SB_{100}. SA/SB at a ratio of 20/80 provided the highest dry-pick, especially when Tg of SA and SB were –9 ^{0}C and 0 ^{0}C respectively. SA at 0 ^{0}C Tg though demonstrated second to the best dry-pick for LWC papers, their printed gloss was excellent while other properties were close to the optimum level. SA_{250} at Tg 0 ^{0}C is recommended to mix with SB to pursue the best printability and lowest cost for LWC paper production.

1. Introduction

With lower basis weight and thus less production cost than regular art paper,light weight coated paper is reported increasingly demanded, especially when the price of pulp is soaring (Fu Bu, 2002). SA is the most popular kind among all latexes from acrylic acid group (Hayes, 1998). SA and SB have never been used jointly as a mixed binder in coating colors preparation to strive for the best properties an LWC could ever expect. The objectives are to investigate the compatibility of the two latexes and seek the optimum combinations for designated paper properties.

2. Materials and Methods

(1) Materials

Styrene, 2-ethylhexyl acrylate (2-EHA) monomers, potassium per-sulfate, anionic surfactant, and SB latex.

(2) Methods

The following four items are the main methods for this study. Preparation of SA latex, measurement of latex properties, mixtures of SA and SB latexes, coating colors preparation and examination of LWC's properties.

3. Results and Discussion

(1) Effects of polymerization conditions on SA's characteristics

The particle size distribution of SA varied with different polymerization processes. The continuous operation showed the narrowest distribution, while shot-growth process the widest (Fig. 1)

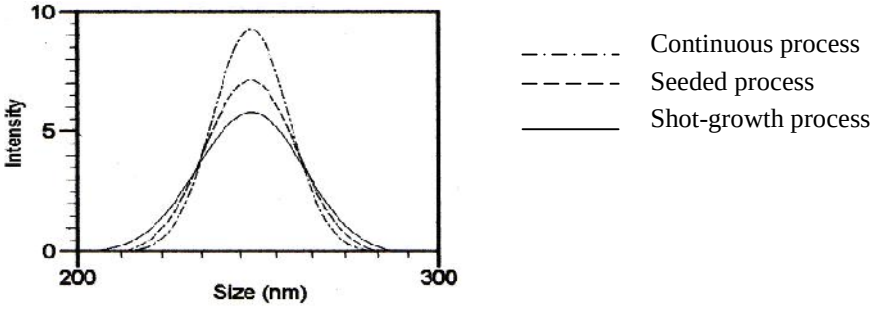

Fig. 1 Effect of polymerization processes on particle sizes distribution of latexes

(2) Effects of SA/SB's characteristics on coating colors' properties

The water retention of the mixed latex is lower than the original ones due to the smaller interspaces between molecules resulted from latexes' entanglement (Fig. 2).

Water retention of SA_{200}/SB_{200} decreased more than that of SA_{100}/SB_{100} because the diminishing of molecular interspaces is more obvious in latex of larger Ps than those of smaller Ps, especially at Tg 0 and –9 ^{0}C (Fig. 3)

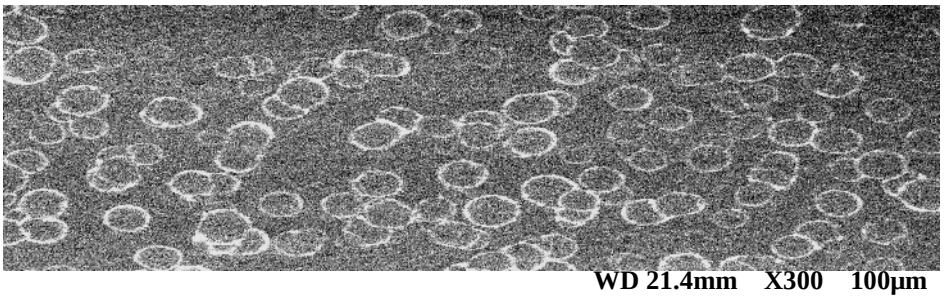

Fig. 2 An SEM image of molecules entangled SA/AB latex

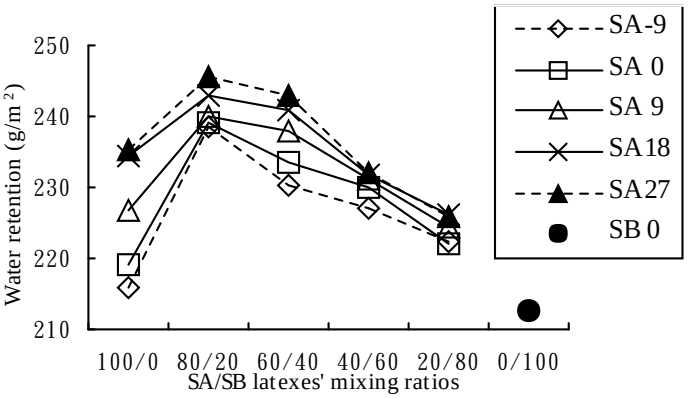

Fig. 3 Tg and mixing ratio of SA_{100}/SB_{100} on the water retention of coating colors.

Sheet gloss indicated same traits as smoothness when SA_{250}/SB_{100} and SA_{100}/SB_{200} were applied in the colors（Fig. 4）. The former combination gave LWC the best gloss, SA_{200} / SB_{200} the worst at 0.05 significant level. Though a ratio of 20/80 would give the highest value, the difference from other combinations is insignificant. Higher SA Tg , e.g. 27 ^{0}C could provide even better sheet gloss.

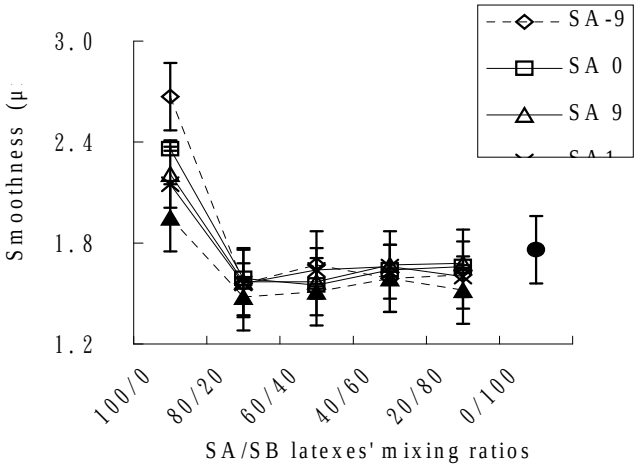

Fig. 4 Effects of SA_{250}'s Tg and its ratio with SB_{100} on the smoothness of LWC

Sheet gloss indicated same traits as smoothness when SA_{250}/SB_{100} and SA_{100}/SB_{200} were applied in the colors. The former combination gave LWC the best gloss, SA_{200}/SB_{200} the worst at 0.05 significant level. Though a ratio of 20/80 would give the highest value, the difference from other combinations is insignificant. Higher SA Tg , e.g. 27 ^{0}C could provide even better sheet gloss. Printed gloss of LWC showed similar trend as of sheet gloss when mixed latexes were used（Fig.5）. The best printed gloss occurred with SA_{250}/SB_{100} after calendaring at 80 ^{0}C.

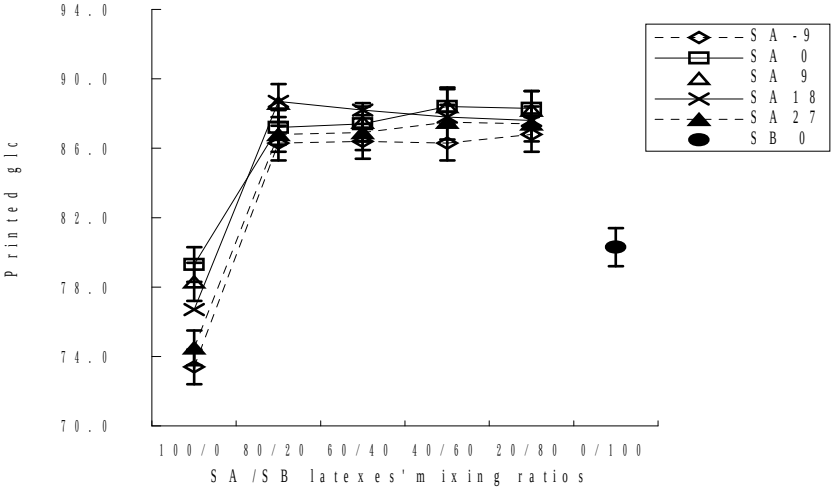

Fig. 5 Effects of SA_{250} 's Tg and ratio with SB_{100} on the printed gloss of LWC.

The integration of SA_{100} with SB_{200}demonstrated lower dry pick than that from sole SA or SB because SA_{100} at Tg –9 and 0 ^{0}C provided higher dry pick than SB. In short, SA/SB gave the highest dry pick, SA_{250}/SB_{100} the second, followed by SA_{100}/SB_{200} and SA_{200}/SB_{200} at a significant level of 0.05 by Duncan's new multiple range analysis. Simultaneously considering coating process and production cost, SA_{250}/SB_{100} at a ratio of 20/80 is the best choice for the manufacturing of SA_{250} is much easier than other particle sizes. LWC using SA/SB mixed latex for the colors undoubtedly showed inferior dry pick strength to sole SA.（Fig.6）

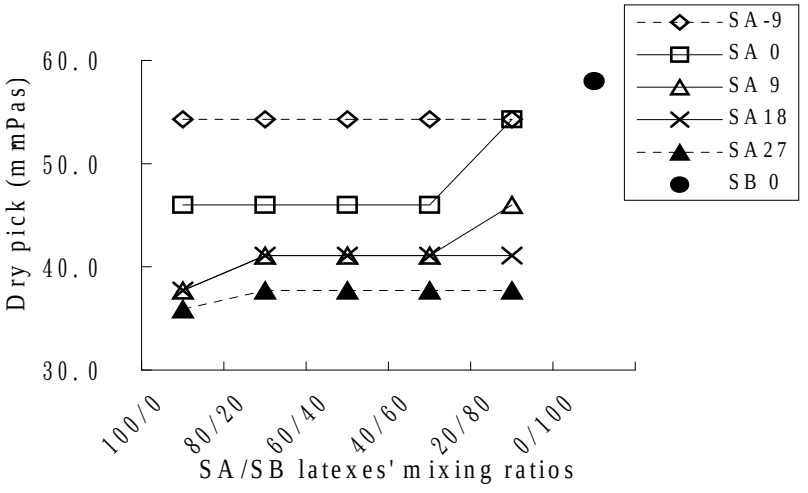

Fig. 6 Effects of SA's Tg and its ration with SB on LWC's dry pick.

References

[1]Fu Bu, *Jappi* 7:35-43 (2002).

[2]Hayes, P.C. *Tappi Course Notes:* 329 (1998).

Effects of Nano-sericite Modified SBR on the Coating Color and Coated Paper Properties

Yuan-Shing Perng[1], Eugene I-Chen Wang[2], Min-Jei Liu[1] and Tser-Ying Teng[1]

[1] Professor and Graduate Student, Department of Environmental Engineering, Dayeh University.

[2] Division Head, Division of Wood Cellulose, Taiwan Forestry Research Institute.

1. Introduction

Sericite is a native mica mineral mined in eastern Taiwan. It is a lustrous layered powder composed mainly of silicon dioxide and aluminum oxide, with the empirical formula of KAl2(Si3Al)O10(OH)2. Upon treatment to become nanoparticles, sericite swells and exfoliates to have very high specific surface area. The purpose of the study was to investigate applying the nanosericite to SBR binder, and examine the effect of modification on SBR. The modified SBR was further used in a LWC coating formulation in a bid to understand the potential functions of such mineral in coating application. The solids content, low- and high-shear viscosities, water retention value (WRV) and pH of the color, and the brightness, opacity, L*a*b* values, gloss and smoothness of the coated paper were examined.

2. Material and Methods

(1) Design

Seven different proportions of nanosericite (0, 0.1, 0.2, 0.3, 0.4, 0.7, and 1.0%) and 3 SBR average particles sizes (120, 130, 185 nm) were combined for a modification experiment. The modified SBRs were measured for their pH, particle size, solids content, and low-shear viscosity. Individual modified SBRs were then added at 11.2 parts to clay/calcium carbonate at 40/60 mix to prepare color. The modified colors were examined for their solids contents, low- and high-shear viscosities, water retention value, and pH. The colors were then used to coat base paper, and the brightness, opacity, L*a*b* values, glass and smoothness of the resulting paper were measured.

(2) Method

The SBR modification entailed putting different proportions of nanosericite to SBR of different average particle sizes. In order not to destroy the structure change of the SBR, the mixing speed of modification was controlled at 1000 to 2000 rpm.

The process of coating color preparation was in the order of pigments (Clay + GCC) + distilled water (high-speed mixing) → dispersant (high-speed mixing) → defoamer (high- and low-speed mixing) → modified SBR (low speed mixing) → hardener/melamine resin (low-speed mixing) → NaOH (low-speed mixing) → distilled water (low-speed mixing). The binder level (latex + starch) was 11.2 parts pigments.

The coating color thus prepared was applied to 21.0 x 29.7-cm base sheets using an automatic bar coater (KRK-motor type). The base sheet was preconditioned for 24 h at 20 °C and 65% RH. The coating amount was adjusted by using bars of different numbers. The coated sheets were immediately placed in an oven maintained at 120 °C for 30 s to dry. Coated paper was supercalendered in one pass with a KRK 30FC-200E single-nip supercalender having a linear nip pressure of 9.807 x 103 kPa and a temperature of 55 °C.

3. Results and discussion

(1) The SBR properties modified by nanosercite

The results of SBR modification experiment indicated that since 3.7% solids suspension of nanosercite at pH 9.0 was used, along with increasing proportions of nanosercite, pH of the SBR also increased, while solids content and low-shear viscosity decreased linearly with the increasing sericite addition.

(2) Properties of coating color

Upon color preparation, the parameters mentioned above were measured. The results indicated that the proportion of nanosericite addition and the intrinsic SBR size had effects on color pH as shown in Fig. 1. The pH was between 8 and 8.5. NaOH was added to bring the pH to 9.0. Their effects on the WRV are shown in Fig. 2.

Along with increasing sericite addition, WRV also increased, suggesting a reduction of water holding capacity. The 130 nm SBR group had WRV increases greater than those of the 185 and 120 nm groups. The effects on the low-shear viscosity are shown in Fig. 3. The low-shear viscosity increased with increasing nanosericite addition, and the effect was more pronounced in the 185 and 130 nm groups than it did on the 120 nm group. The effects on the high-shear viscosity are shown in Fig. 4. The parameter also increased with nanosercite dosage, but the effect on the 120 nm group was more pronounced than the other groups.

The results of optical properties of the coated papers using nanosercite modified SBR are shown in Fig. 5 to 7. Brightness of the paper increased linearly with increasing sericite proportion. The gain, however, was only 1.2% GE. The coarser the SBR particle was, the greater the brightness gain became. Fig. 6 shows the effect of nanosercite modification on the paper opacity. The trend was similar to the brightness and showed linear gains at 1.5% maximum. The same SBR particle size effect also exisited. Fig. 7 shows the gloss effect. The higher the nanosericite proportion, the less the gloss linearly became. The decrease was ca. 1.2%. The larger the SBR particle was, the higher the resulting gloss became

Figure 8 shows the effect of nanosercite proportion and SBR particle size on the coated paper smoothness. The smoothness linearly decreased with increasing sericite substitution; whereas the coarser the SBR particle was, the lower the paper smoothness became.

4. Conclusion

Applying nanosericite to modify SBR can modify the WRV, low- and high-shear viscosities of the color. Hence it may be considered as a rheological modifier for color preparation. Addition the mineral increased paper brightness and opacity, but caused lowering of gloss and smoothness.

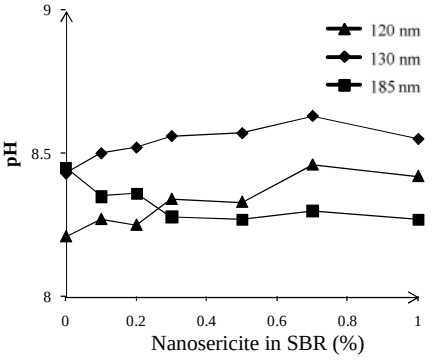

Fig. 1. Effects of nanosericite proportion and SBR particle size on the pH of SBR.

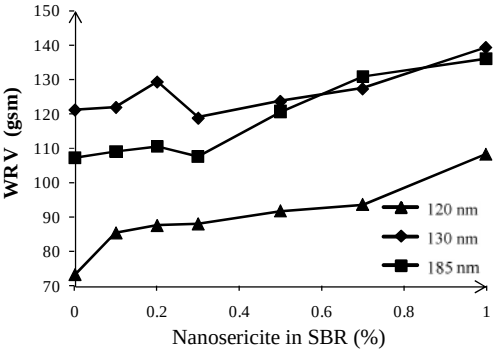

Fig. 2. Effects of nanosericite proportion and SBR particle size on the water retention value.

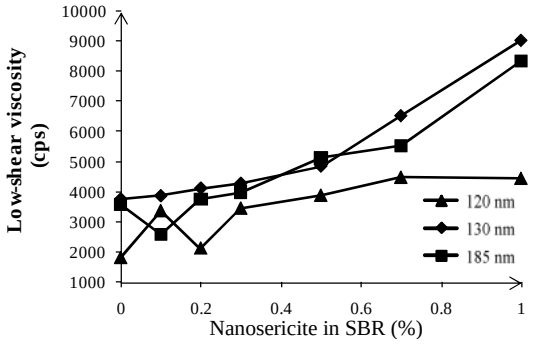

Fig. 3. Effects of nanosericite proportion and SBR particle the low-shear viscosity of SBR.

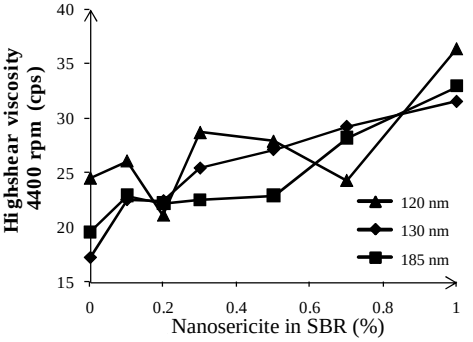

Fig. 4 Effects of nanosericite proportion and SBR particle size on the high-shear viscosity.

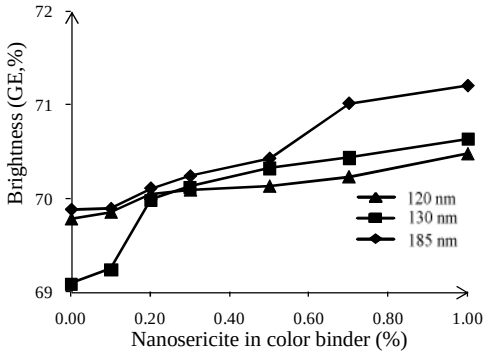

Fig. 5. Effects of nanosericite and SBR particlesize on the coated paper Brightness.

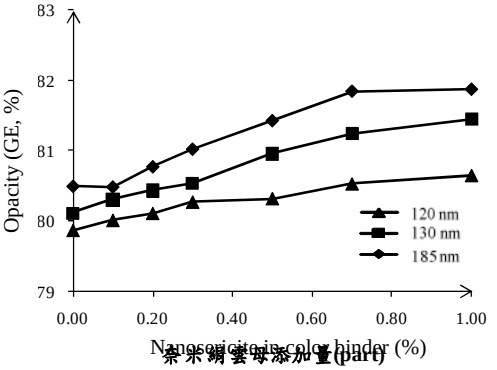

Fig. 6. Effects of nanosericite and SBR particlesize on the coated paper Opacity.

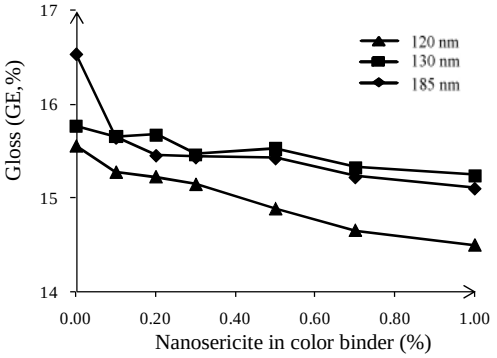

Fig. 7. Effects of nanosericite and SBR particlesize on the coated paper Gloss.

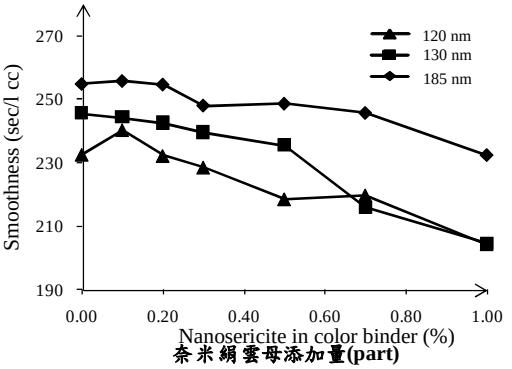

Fig. 8. Effects of nanosericite and SBR particlesize on the coated paper Smoothness.

Improvement on the Softness of Toilet Paper by Starch Gelatinization Treatment

Jinxia Ma, Xiaofan Zhou and Zhongzheng Li

Jiangsu Provincial Key Lab of Pulp and Paper Science and Technology, Nanjing Forestry University, Nanjing , Jiangsu Province, 210037

Abstract: This paper investigates a novel method of enhancing the softness properties of toilet paper by taking the advantage of starch stickiness and its characteristics of sol-gel. In the research, a compound which consists of non-ionic raw starch (the major constituent) and other ancillary reagents were used. Together with the synergistic effect of mechanical force, the starch gel materials can firmly resides on the surface of fiber, which improves the softness properties of paper greatly but only with a minor negative effect on the paper strength properties. According to the shown results, while the usage of maize starch and borax were 3% and 0.5% with a total pulp concentration of 20%, the softness of paper derived from the bleached wheat straw pulp would be improved by 100% and 50% respectively, if compared with the ones of paper derived from the starch gelatinization treated pulp and soft agent treated pulp. Even though those starch gelatinization treated paper have undergone a separate 33.7% and 28.6% decrease in water absorption and paper tensile strength properties, the two deteriorated characters were still superior to those of soft agent treated pulp. Thus this research puts forward an entirely new idea and avenue for the purpose of increasing the paper softness.

1. Introduction

From environmental and supply perspectives, there is increasing interest in using non-woody material sources, such as wheat straw, for pulp and paper. Wheat straw chemical pulp can be used for the production of specialty papers and also for substitution of wood pulp in various applications [1]. In China, wheat straw is the most available raw material for pulp and paper industry and wide used for toilet paper.

The toilet paper belongs to the scope of the widely processed household paper with a plenty of varieties. Besides its high quality requirements of tensile strength and absorption properties, increasingly importance has been attached to the softness property and its tactile quality as well. According to some relevant documents introduced, the softness of toilet paper firstly depends on the characteristic of raw materials. Derived from which the softness of the toilet paper can be sorted in the orders as follows: cotton pulp> wood pulp> rag pulp> waste paper stock> wheat straw pulp[2-5]. And those bleached wheat straw pulp will even worsen the softness of the toilet paper, which is up to the fiber structure of wheat straw pulp. In the raw materials of wheat straw, the high content of nonfibrous cells(close to 40%) and hemicellulose result in the high brittleness, transparency and poor paper softness. Therefore, in order to improve its flexibility of paper, paper industries joint efforts currently underway between chemical suppliers and fabric makers to address these tradeoffs with solutions geared specifically toward increasing softness without sacrificing other sheet properties like wet strength or absorbency—still important to consumers[2-6]. Nowadays soft agent, which is able to boost foaming during toilet paper production and improve the paper's softness is added. However, those agents would take a hit in tensile strength [6]. Thus this paper investigates a novel method of enhancing the softness properties of toilet paper by taking the advantage of starch stickiness and its characteristics of sol-gel. In this research, a compound consisted of non-ionic raw starch (the major constituent) and other ancillary reagents were used [7-14]. Together with the synergistic effect of mechanical force, the starch gel materials can firmly resides on the surface of fiber, which improves the softness properties of paper greatly but only with a minor negative effect on the paper strength properties.

2. Material and Methods

(1) Material

Soft agent was supported by Ciba Chemical company. Bleached wheat straw pulp with beating degree

39^0SR was supported by Shangdong Tralin Paper Co., Ltd. Tapioca starch and maize starch were supported by National Starch company. Borax is analytical reagent.

(2) Pulp treatment process

Bleached wheat straw pulp was disintergrated and adjusted to the certain consistence, mixed with starch and ancillary reagent by dispersing mixer, then heated and cooked in 90℃ for 20 minutes in double roller mixer. Finally treated pulp was scattered with high frequency dispersion. This process was called starch-gelatinization treatment. Soft agent-treatment process was that bleached wheat straw pulp was disintergrated to 1% consistence and added with 0.5% soft agent.

(3) Handsheets

Handsheets with a basis weight 30g/m^2 were prepared from bleached wheat straw pulp treated by starch-gelatinization, the webs were wet-pressed and dried at 105℃ for several minutes. Reference handsheets were prepared from untreated bleached wheat straw pulp and soft agent-treated pulp. Handsheets were thus conditioned at 23℃ and 50% relative humidity for more than one day, then measured paper properties.

Determination of paper properties

Tensile strength, absorbent value and softness were tested according t the TAPPI standard.

3. Results and discussion

As for the unmodified native starch, its dextrin of starch with a high consistency level will get a better viscosity and gelatinization but worst fluidity. Nevertheless, pseidoplasticity can still be demonstrated. In the practical manufacturing process, the external pressure would arise the occurrence of the deformation of starch gel, in other words, the penetration of the colloidal sols may occur on porous substrate or any irregularities so that the starch could penetrate into the three dimensional fiber network and achieve the final redistribution in certain areas. Thus enhance the colloidal sols' dispersibility and its close contact with materials. In addition, such a characteristic has promoted a tightly integration between starch and fiber adherend. At the meanwhile, starch is generally prone to gel with the help of electrolyte [8-15]. Thereby with an aim of improving fiber softness, this paper makes full use of the gel reactions between the higher concentration starch and borax to form starch gels, which were simultaneously accumulated on the surface of the bleached wheat straw pulp uniformly by using the mechanical force from double roller mixer.

(1) Effect of borax amount on paper properties

Borax usage, pulp consistence, and the amount of starch as well as its varieties all have an influence on the treatment effects. And the impact of the borax usage was firstly investigated in this paragraph (seen in Figure 1). During this experiment, Tapioca starch was used with a taken amount of 3% (oven dry stock), but the final concentration of the dextrin of starch and stock was 20%.

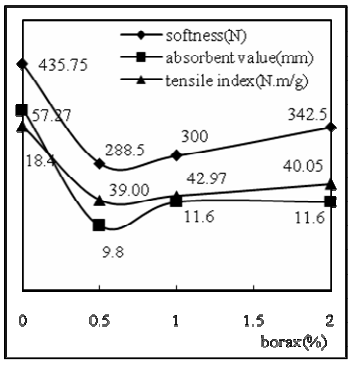

Fig. 1 effect of borax amount on paper properties

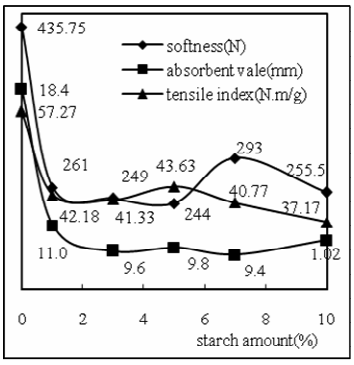

Fig. 2 effect of starch amount on paper properties

According to the information shown in Figure 1, paper softness was dramatically improved whereas negative effects on the tensile strength and absorption ability were drawn when the usage of borage reached 0.5% or below (oven dry stock). Nevertheless, if the amount of usage was over 0.5%, the results of the changing

trends in terms of paper softness, tensile strength and absorption ability were wholly inversive. Theoretically speaking, it is the starch gel, the products of the gel reactions between the higher concentration starch and borax (below 0.5%) that locked the hydroxyl groups on the surface of fiber and deteriorated the inter fiber bonds by accumulating on the surface of the bleached wheat straw pulp uniformly with the help of the mechanical force from double roller mixer. Thus this kind of starch gel accumulation finally arose a drop in the paper tensile strength, however, it also simultaneously contributed to an great improvement on the density and softness of paper, which is mainly due to the starch, the substitute of partial fibers. Moreover, the increased density of paper indicated a deep shrink to the number and size of pores in paper besides the locked hydroxyl groups, resulting in a decrease in the inter fibrous capillary effect followed by a declined absorption ability of paper. On the contrary, as mentioned above, there was a increase in paper tensile strength and absorption ability but a decrease in softness when the amount of borax usage were over 0.5%, and the reason for this may be considered as the increased borax usage leaded to a further decrease in the starch gelatinization level, that is to say, still many ungelled starch, whose surface contained free hydroxyl groups, resided on the surface of fiber so that the inter fiber strength and paper tensile strength were both strengthened. However, the starch gelling strength were rose up, which made a increase in the stiffness of the treated fibers as well as the inter fibrous capillary effect, thus resulted in softness descended but absorption ability improved.

(2) Effect of starch amount on paper properties

When study the effects of starch amount on paper properties, maize starch was used in the experiment with the borax usage 0.5% (dry stock), and the final concentration of the dextrin of starch and stock was 20%.

It can be seen from the Figure 2 that paper softness was dramatically improved while great negative effects on the tensile strength and absorption ability were drawn when the usage of starch reached 3% or below (oven dry stock). Nevertheless, if its amount of usage was over 3%, the results of the changing trends in terms of paper softness, tensile strength and absorption ability nearly leveled out. This indicated that maize starch could have a complete gelatinization, and accumulated uniformly on the fiber surface where the residual starch was not able to be absorbed.

(3) Effect of starch type on paper properties

The comparisons between the results of maize starch and tapioca starch gelatinization treatment were presented in Figure 3, Figure 4 and Figure 5. In the experiment, the amount of the starch usage was 0.5% (oven dry stock), and the final concentration of the dextrin of starch and stock was 20%. Additionally, 0.5% is the optimum borax usage for getting the most preferable paper softness properties with an increasing rate of 100%, but it also brought a huge loss of tensile strength and absorption ability of paper. Compared with the softness of paper derived from maize and tapioca starch gelatinization treated pulp, maize starch gelatinization treatment manifested approximately 18% better value than its tapioca counterparts. It had a close relevant to their polymerization degree of amylose and amylopectin, and in particular with the amylose, the first cause of starch gelatinization. Depending on the dominant amount of amylose, maize starch had better gelatinization ability and better reactions with borax than tapioca starch. Furthermore, the properties of the paper derived from the maize starch treated pulp were all prior to the ones of the paper derived from the tapioca starch treated pulp, in other words, compared with amylopectin gelatinization treatment on the surface of pulp, three crucial properties of toilet paper in terms of softness, absorption and tensile strength are all better if the pulp were treated by amylose gelatinization treatment. While the usage of maize starch and borax were 3%, 0.5% respectively, with the total pulp concentration of 20%, the sharp contrasts between the bleached wheat straw pulp with starch gelatinization treatment and without were not just the improved softness properties of paper derived from those starch gelatinization treated pulp by 100%, but also the decreased tensile strength and absorption ability by 28.6% and 33.7% separately.

(4) Effect of pulp concentration on paper properties

When investigating the effects of pulp concentration on paper properties, maize starch and borax were used in the experiment with a taken amount of 3% and 0.5% respectively. And the final concentration of the dextrin of starch and stock was 20%. As the information shown in the Figure 6, the higher concentration the pulp had, the

better the reactions between the starch and borax would be enhance, which resulted in more hydroxyl groups that were locked. Thus the fiber stiffness was gradually increased. Additionally, the harder the starch gels they were, the stiffer the pulp was, surely the absorption abilities would benefit from the fluffy inter fiber bonds and the enforced inter fibrous capillary effect, but the increased stiffness of fiber was apt to decline the softness greatly. Therefore, according to the figure 6, the optimum pulp concentration was 20%.

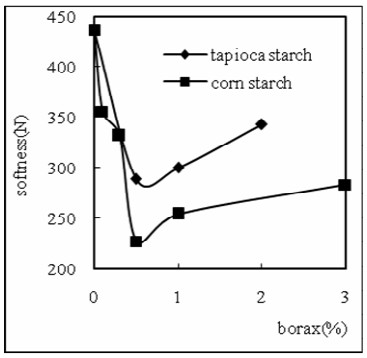

Fig. 3 effect of starch type on paper softness

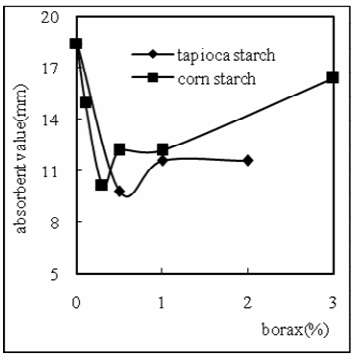

Fig. 4 effect of starch type on absorbent value

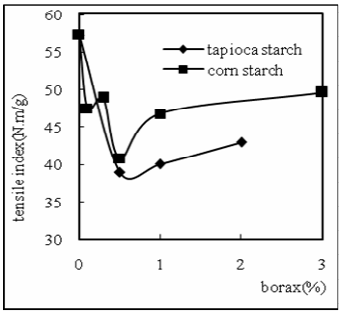

Fig. 5 effect of starch type on tensile strength

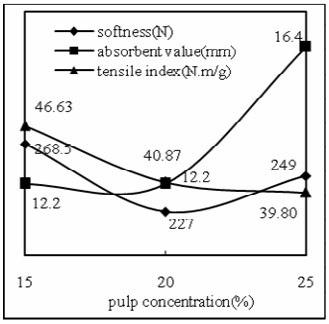

Fig. 6 effect of pulp concentration on paper properties

(5) Comparision of soft agent and starch gelatinization treatment on paper properties

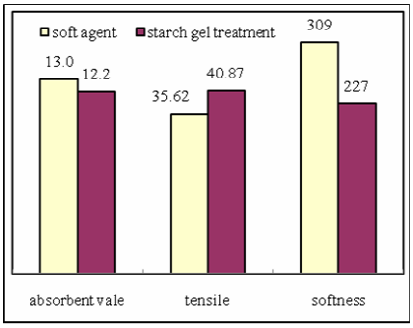

Fig. 7 effect of treatment process on paper properties

When discovering the effects of soft agent on the paper properties, it was found that the paper would get optimum properties if the amount of soft agent usage reached 0.5%. Thereby 0.5%, 3% and 0.5% were taken as the usage amount for soft agent, maize starch and borax respectively, with a final pulp concentration of 20%. According to the Figure 7, paper derived from the pulp with starch gelatinization treatment would get a better softness and tensile strength than that derived from the pulp treated with soft agent. That is because the soft agent had an great impact on the paper strength during the processing of rising up foam formation and improving paper softness. On the contrary, besides the starch gelatinization treatment could make a great improvement of paper softness, it only drove the starch gel accumulating tightly on the surface of the fiber, so as to reduce the free hydroxyl groups, but it did not decrease the paper stiffness, hence the paper strength had only a slight drop.

This investigation demonstrated that fiber treatment with starch gelatinization could improve the softness with only little changes of the paper strength, but also put forward an entirely new idea and avenue for the purpose of increasing the paper softness.

4. Conclusion

1. Borax usage, pulp consistence, and the amount of starch as well as its varieties all had an influence on the gelatinization treatment effects. But maize starch gelatinization treatment had better results than tapioca starch.
2. Pulp concentration of dextrin of starch and starch gels also affected the paper properties, and the optimum pulp concentration was 20%.
3. While the usage of maize starch and borax were 3%, 0.5% respectively, with the total pulp concentration of 20%, the sharp contrasts between the bleached wheat straw pulp with starch gelatinization treatment and without were not just the improved softness properties of paper derived from those starch gelatinization treated pulp by 100%, but also the decreased tensile strength and absorption ability by 28.6% and 33.7% separately.
4. Fiber treatment with starch gelatinization put forward an entirely new idea and avenue for the purpose of increasing the paper softness.

References

1. Vichnevsky, S., Chute, W.. Wheat Straw Pulp Fractions and Their Impact for the Properties of Mechanical Pulp [C]. Proceedings of the 2001 TAPPI Pulping Conference, Seattle, Washington (2001):123-135.
2. Bottiglieri, J. Tissue: Is Softness the Central Concern? [J]. Solutions!, 2002, 85(6):66-68.
3. Lan-sheng Kuo and Yin-lie Cheng. Effects of Creping Conditions on Surface Softness of Tissue Paper - Application of Sled Method [J]. TAPPI Journal, 2000, 83(12):1-12.
4. Cai Hongmin. Productive Practice of Soft Toilet Paper with Wheat Straw Pulp [J].Hunan Papermaking. 2007(1):14-15.
5. Liu Shiliang. Medium Consistency Refining of Wheat Straw Pulp for Paper Towel Production [J]. China Pulp & Paper, 2006(5): 31-33.
6. You Haoliang and Huang Yuying. Research on Application of Chemicals in Household Paper [J]. Hunan Papermaking, 2005(1):20-23.
7. Ge Hanke, Tao Jingsong, Liu Huanbing, Yan Dongbo. Research Progress in Measurement Method of Pulp Fiber Flexibility [J]. Transactions of China Pulp and Paper, 2006, (4):102-106.
8. Lin Haiyan, Luo Xuegang. Research Progresses in Rheelogical Properties and Application of Starch [J]. Science and Technology of Food Industry, 2005, 26(3):182-184.
9. Chen Zhongxiang, Hu Zhengping, Jiang Weifeng. Pastification of Starch and Influence of additives on the Pastification Temperature [J]. Chemistry and Adhesion, 2003(2):91～93.
10. Zhen Guifu, Xu Zhenxiang, Zhou Bing, Qing Zhichun and Chen Xiwu. Study of Physico-chemical Characteristics of Potato Gelatin Starch [J]. Food Science, 2002 (8):77~80.
11. Huan Yanjun. Variations of Starch in Extrusion Cooking [J].Journal of Food Science and Biotechnology, 1997, (4):45-47.
12. Du Xianfeng,Xu Shiying,Wang Zhang. Study on the Mechanical Properties of Starch Gels [J]. Transactions of the Chinese Society of Agricultural Engineering, 2001, (2):16-19.
13. Wang Huizhong. Effects of borax on adhesion property of starch [J]. Jinan Man-made Fibre Technology，1992(1):54-58.
14. Wu Zonghua and Chen Huan. Effects of Inorganic Electrolytes on Adsorption of Starches to Pulps [J]. Journal of Fujian Teachers University (Natural Science), 2001, (4):66-69.
15. A.Z.A., Yusu, Z., Qi, D.. Borax Enhanced Starch Improves Paper Properties [C]. Proceedings of the 2000 TAPPI Papermakers Conference, Atlanta, Georgia, USA (2000):649-653.

The Application of Chitosan on Fungal-resistance of Paper-based Cultural Relics

Tsang-Chyi Shiah[1]

[1] Department of Forest Products Science, National Chiayi University, 300 Syuefu Rd., Chiayi City 60004, Taiwan.

[1] Corresponding author, e-mail：tcshiah@mail.ncyu.edu.tw

Abstract： Paper-based artworks and documents often suffered damage from the growth of fungi. Biological damage is mainly brought about by unsuitable environmental conditions and often results in discoloration, structural damage to the basic component of materials, damage to the essential additive components.

The molded cultural properties on papers belong to one kind of bio-deteriorations; the molded stains on paper not only apparently decrease the life of rare books, paintings and art crafts, but also affect the preservation of cultural relics.

Chitin, next to cellulose, is the second most abundant material in natural. Chitosan is a substance obtained by de-acetylation of chitin, the principal component of many living things, including crustaceans, insects and fungi. Because of the superior properties and abundance, chitosn and chitin are commercial utilization and environmental application on world widely.

Due to the chitosan is a cationic polymer and a cationic polyelectrolyte, it shows superior of antimicrobial properties. The purpose of this study is to investigating the feasibility of chitosan as a possible in the fungal-resistance of paper-based cultural relics. The experimental results are as follows, filter paper treated by 95% de-acetylation of chitosan with 1.5% of concentration shows the best fungal-resistance effect, the lower concentration of chitosan, the less of fungal-resistance effect will obtained. At the same concentration, the higher of de-acetylation of chitosan, the better of fungal-resistance effect will be. The application of chitosan on fungal-resistance of paper-based cultural relics can be a viable alternative conservation medium for paper-based of artifacts and archives.

1. Introduction

Chitin, next to cellulose, is the second most abundant material in natural. Chitosan is a substance obtained by de-acetylation of chitin, the principal component of many living things, including crustaceans, insects and fungi. Because of the superior properties and abundance, chitosn and chitin are commercial utilization and environmental application on world widely.

Paper-based archives and artistic articles comprise the major collections in Taiwanese museums. However, there seems to be a lack of research on the preservation of paper relics with chitosan in Taiwan. Due to the chitosan is a cationic polymer and a cationic polyelectrolyte, it shows superior of anti-microbial properties. The purpose of this study is to investigating the feasibility of chitosan as a possible method in the fungal-resistance of paper-based cultural relics.

2. Material and Methods

(1) Materials

1. Raw materials included handmade Kozo paper (37.82 g/m^2), Newsprint paper (47.87 g/m^2), and Filter paper (92.89 g/m^2, Advantec brand No.1).
2. Chitosan powder: The degree of de-acetylation divided into 80, 85, 90, 95% were supplied by C & B company, Taiwan.

(2) Methods

1. To prepare 0.1, 0.75, 1.5% of chitosan solution in 0.5% acetic solution respectively for paper soaking treatments. specimens (5 × 5 cm) were soaked with different concentration of chitosan solution for 5 min, then put into 50℃ oven to dry.

2. Spores of molds usually found on paper including *Aspergillus niger, Aspergillus flavus, Penicillium* sp., *Trichoderma viride* and *Mucor* sp. were suspended in 200 mL of a water solution and inoculated on chitosan treated and untreated paper specimens placed in petri dishes containing potato-dextrose agar (PDA), then put into a 25℃ dark incubator for 2 weeks of mold-resistance test (TAPPI 1993).
3. Analysis of chitosan soaked paper properties:
   (1) The brightness, CIE L*a*b*, and ΔE* 【(color difference) = $[(L^*-L^{*\prime})^2+(a^*-a^{*\prime})^2+(b^*-b^{*\prime})^2]^{1/2}$】of each paper specimen were measured before and after chitosan treatments.(L*,a*, b*: before treatment, L*',a*', b*': after treatment)
   (2) We also measured color changes (expressed as ΔE*), physical properties, and chemical properties of the various paper specimens before and after 72hrs accelerated aging tests under 85℃ / 85％RH, 105℃ /0％ RH and 313nm UV light respectively.
   (3) The microstructure of each paper specimen was observed with a scanning electron microscope (SEM ; Hitachi S-2400, Japan).
   (4) The variations of chemical functional group of chitosan soaked paper specimens before and after heat aging treatments were analyzed by using Fourier Transform Infrared Spectroscope (FTIR, Bio-Rad, FTS-40) at a resolution of 4cm^{-1}. The infrared transmittance spectra were measured with the range of 800-3000 cm^{-1}.
   (5) The folding endurance and tensile strength of each specimen were measured according to the respective CNS 10378 and CNS 12607 standards.

3. Results and discussion

(1) Fungal resistance of chitosan-treated paper

We inoculated the papers with 5 species of molds: *Aspergillus niger, Aspergillus flavus, Penicillium* sp., *Trichoderma viride* and *Mucor* sp. Paper specimens were placed on a 5 × 5cm round inoculation dish with agar to check the anti-microbial properties of the papers. It was found that paper specimen treated by 95% de-acetylation of chitosan with 1.5% of concentration owns the best fungal-resistance effect, the lower concentration of chitosan, the less of fungal-resistance effect will obtained. At the same concentration, the higher of de-acetylation of chitosan, has the better fungal-resistance effect (see **Table 1**). Experimental results as showed in **Fig.1**, the fungal-resistance effect are in the order of : *Trichoderma viride, Penicillium* sp., *Mucor* sp., *Aspergillus niger* and *Aspergillus flavus.*

(2) Effects of the chitosan soaking on paper color changes

Paper specimen after soaked with different de-acetylation and concentration of chitosan solution were shown just slight reductions in the brightness and slight color changes. The trends of color change increased of filter paper after aging treatments are in the order as follow: 85℃ / 85％RH＞105℃ /0％RH ＞313nm UV light aging. Experimental results are shown as **Fig.2**.

Chitosan solution soaked newsprint paper showed greater color differences after the UV aging treatment than that of Kozo paper and Filter paper (**Fig. 3**).

(3) Effect of the chitosan soaking on the fold and tensile strength of paper specimens

The folding endurance and tensile strength of paper specimen were apparently increased than did untreated papers after soaking of chitosan solution. (**Table 2**).

Table 2 shows that after 105℃ /0％RH and 85℃ / 85％RH of heating for 72 hr respectively, it was evident that chitosan can improve the heat resistance of paper to some extent. In other words, under both of aging tests for 72 hr papers soaked with chitosan had superior aging resistance; still maintain strength on good levels.

(4) Micro-structure observation

From the SEM observation, we found that chitosan soaked paper specimens did not show significant variation on the fiber structure after 72 hr of aging treatments (see **Fig.4** for SEM observations).

(5) FTIR analysis

Experimental results revealed that, the Filter paper specimen of IR absorbance spectra representing amino acid (N-H) and carbonyl group (C=O) at 1542 cm^{-1} and 1650 cm^{-1} respectively, were shown after chitosan

treatment. The carbonyl group were apparently increased after 72 hr of 85℃ / 85％RH, 105℃ /0％RH and 313nm UV light aging respectively (see **Fig.5**).

Table 1 The fungal-resistance effect of chitosan soaked filter paper.

DAc %	Conc %	Fungi inoculated on fillterpaper				
		Penicillium sp.	*Trichoderma viride*	*A. flavus*	*A. niger*	*Mucor* sp.
Blank		3+	5+	5+	5+	5+
80	0.1	2+	4+	5+	5+	5+
	0.75	1+	—	5+	4+	3+
	1.5	—	—	4+	3+	1+
95	0.1	2+	4+	5+	5+	4+
	0.75	1+	—	4+	3+	2+
	1.5	—	—	4+	1+	1+

**Tests were carried out on potato-dextrose agar medium at 25 ℃. * Fungi cultivated for 14 days.

***Penicillium* sp.** (DAC80%)	***Penicillium* sp.** (DAC95%)
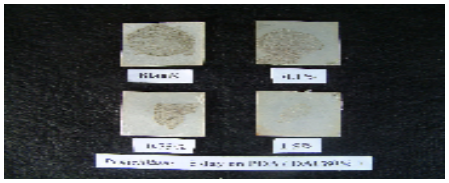	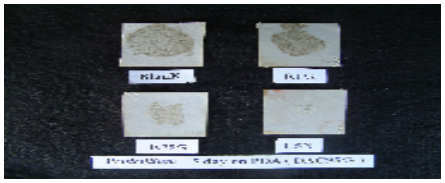
***Trichoderma* viride** (DAC80%)	***Trichoderma* viride** (DAC95%)
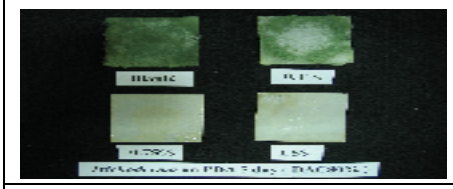	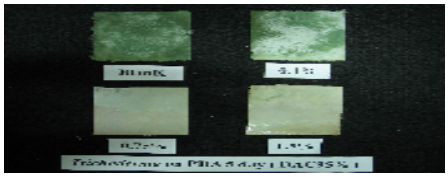
Aspergillus niger (DAC80%)	***Aspergillus niger*** (DAC95%)
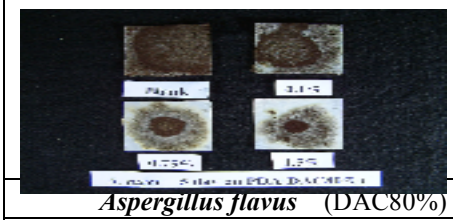	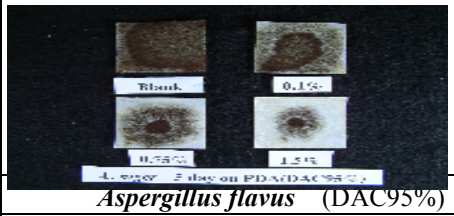
Aspergillus flavus (DAC80%)	***Aspergillus flavus*** (DAC95%)
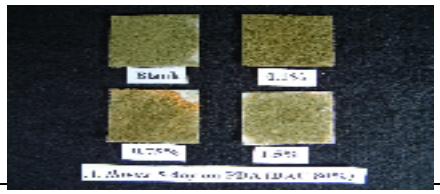	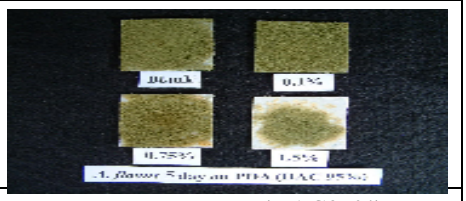
***Mucor* sp.** (DAC80%)	***Mucor* sp.** (DAC95%)
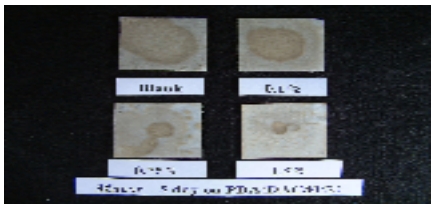	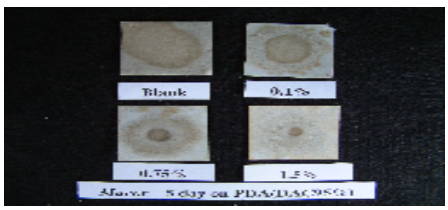

Fig.1 The fungal resistance test of chitosan soaked filter paper on on PDA for 5 days

Effects of Adding Co-ground Talc and Calcium Carbonate on the Retention and Paper Properties

Yuan-Shing Perng[1], Eugene I-Chen Wang[2], Yi-Ting Yang[1] and Yi-Wei Lee[1]

[1] Professor and Graduate Student, Department of Environmental Engineering, Dayeh University.

[2] Division Head, Division of Wood Cellulose, Taiwan Forestry Research Institute.

1. Introduction

There are few reports dealing with the applications of talc powder in papermaking wet end as a filler. Lasmarias and Sharma (2004) investigated using talc to replace a portion of precipitated calcium carbonate (PCC) and clay in the base stocks of a supercalender and coating base sheet, and examined its effect on retention, drainage and paper properties. Their laboratory handsheet study indicated that not only retention increased and drainage became faster, the tensile strength and rotogravure printability were improved as well. As for industrial application cases, the proprietary nature prevent their disclosure. However, it is expected that performance shall be similar to the lab results.

In recent years, a domestic paper filler supplier has developed wet co-grinding of calcium carbonate and talc ore mixture and successfully promoted its application in several domestic paper mills. The wet-ground calcium carbonate/talc was reputed to give higher retention, sizing degree and opacity in the mill trial. Yet, again due to the confidential clause between the supplier and mill, there was no further report.

Thus the main purpose of this study was to examine the effects of replacing 10% of calcium carbonate with talc on the fiber retention, ash retention, sizing degree, paper physical properties, surface properties, and optical properties of handsheets. The filler preparations were either wet co-ground of talc and calcium carbonate or wet-ground calcium carbonate mixed with dry-ground talc. The 100% wet-ground calcium carbonate and 100% dry-ground talc served as the blank groups.

2. Material and Methods

(1) Experimental design

Two methods of preparation were employed to produce the talc/calcium carbonate mixture. They were either proportionally mixed and then wet co-ground together, or they were formed by mixing wet-ground calcium carbonate and dry-ground talc to proportion. The effects of adding calcium carbonate with partial talc replacement to a fine paper stock on the ensuing first pass retention, ash content, sizing degree, bulk, tensile index, smoothness, roughness, brightness and opacity of the resulting handsheets were examined. The 100% wet-ground calcium carbonate and 100% dry-ground talc were used as the blank groups. Filler (GCC + talc) dosages of 10, 20 and 30% were used, and the level of talc replacement was pegged at 10% in accordance with the commercial specification. There were 13 sets of experiments, each set was replicated 10 times for a total of 130 set. The pooled standard deviations of the experiments were: FPR, 1.2%; ash retention, 1.3%; sizing degree, 2.24 s; bulk, 0.03 cm3 g-1; tensile index, 1.37 N m g-1; smoothness, 0.32 s; roughness, 0.10 μm; brightness, 0.25% ISO; and opacity, 0.25%.

(2) Methods

Suitable amounts of filler suspensions were oven-dried at 105℃ for 1 h, a small amount of the dried filler cake was placed on the specimen stage of the SEM, and the specimen operated with 15 kV accelerating voltage for observing the filler shapes.

To a 0.3% consistency pulp stock, 4 filler groups comprised of wet-ground calcium carbonate alone; dry-ground talc alone; wet co-ground calcium carbonate/talc; and wet-ground calcium carbonate plus dry-ground talc, each at 0, 10, 20 and 30% dosages to dry pulp were added separately. Upon thorough mixing, 0.5% AKD sizing agent and 300 mg L-1 of a cationic retention aid were added sequentially. Then handsheets of 60 g m-2 were formed and the first pass retentions measured.

The resultant handsheets were conditioned overnight under a standard atmosphere of 23℃ and 50% relative

humidity (RH) in a constant temperature and humidity chamber. Then the paper grammage, caliper, bulk, ash content, sizing degree, tensile strength, smoothness, roughness, brightness, opacity etc. were determined.

3. Results and discussion

(1) Wet co-ground effects

The SEM micrographs of the 4 experimental filler groups delineated above are shown in Fig.1. From the micrograph and the properties of average particle diameters, brightness, and specific surface areas, wet co-ground calcium carbonate-talc appeared to have talc particles with more evenly distributed size and smaller average particle diameter of ca. 6.32 μm than the dry-ground talc. In addition, the plates of talc had generally smoother, less jagged edges. Average particle diameter of the wet co-ground calcium carbonate-talc also was finer, ca. 1.34 μm, than the wet-ground calcium carbonate alone. Among the groups, the ranking for particle size distribution, brightness and specific surface area were in the order wet-ground calcium carbonate; wet co-ground calcium carbonate-talc; wet-ground calcium carbonate and dry-ground talc; and dry-ground talc.

(2) First pass and filler retentions

Effects of different filler groups and different filler dosages on the first pass retention of the handsheets are shown in Fig. 2. Adding fillers apparently decreased FPR and ash retention of the system. Among the 4 filler groups, wet-ground calcium carbonate had the poorest FPR and ash retention, while the dry-ground talc had the best performance. The wet co-ground mixed filler had the second best FPR and ash retention, ahead of the middling post-mixed GCC and dry ground talc. The probable reason for the good performance of co-ground GCC-talc was the more uniform and diminutive size distribution which appeared to be particularly helpful with the retention of fillers. Our experimental results are in agreement with those of Lasmarias and Sharma (2004) noting added talc to calcium carbonate filler enhanced retention rates.

(3) Paper bulk

Among the 4 groups, the bulk of handsheets containing only GCC had the least bulk; while the dry-ground talc only group had the highest bulk. There was no significant difference between the wet co-ground filler group and the post-mixed GCC and talc on their contributions to paper bulk.

(4) Sizing degree

The results indicated that talc enhanced sizing degree. However, along with increased ash content, sizing degree decreased. Among the 4 groups, GCC had the least size, and dry-ground talc the highest. The post-mixed calcium carbonate and talc had the middling performance. Wet co-ground GCC and talc, however, produced handsheets with higher sizing degree than the post-mixed group. This phenomenon might be related to the specific surface area of the respective minerals. The larger the specific surface area, the slower the AKD maturation rate became, leading to degradation of the sizing agent. Thus with protracted reaction time, the AKD was less able to react with fiber surface and react in turn with water molecule to become hydrolyzed and consequently resulting in a reduced sizing degree.

(5) Tensile index

Ash/filler content appeared to decrease the tensile index of paper since filler particles generally interfere with fiber-to-fiber bonding. Among the 4 filler groups, the GCC-only group had the least tensile index. The mixed GCC and talc groups had higher tensile index than either pure filler groups. Wet co-ground calcium carbonate and talc appeared to have the best tensile index, slightly better than the post-mixed GCC and talc group. In the middle was the dry-ground talc only group, and the GCC only group performed the poorest in this regard as well. The more uniform and diminutive particle size distribution might be a contributing factor. In addition, the 10% larger-sized talc particle might assist in aligning fibers forming a 3-dimensional bonded structure which increased the tensile index of the paper. The experimental results supported the conclusions of Lasmarias and Sharma (2004) that incorporating co-ground talc improved tensile index of the paper.

(6) Smoothness and roughness

Increased ash content appeared to decrease the smoothness and increase the roughness of the paper. The trends, however, were not consistent. Among the 4 groups, dry-ground talc along caused the lowest smoothness,

whereas the post-mixed GCC and dry talc had the highest smoothness. GCC was the second best in smoothness. With regard to the roughness, at relative low ash content, mixed filler groups had higher roughness values than either fillers alone groups. At high ash content, however, the dry-ground talc alone group had the highest roughness.

(7) Brightness and opacity

The results indicated that increased ash content led to higher brightness and opacity of the handsheets. For paper brightness, the wet co-ground GCC and talc had the highest value; whereas the dry-ground talc along produced paper with the lowest brightness. It appeared that substituting 10% of calcium carbonate with talc increased the brightness of the paper. Based on the additive principle, the brighter filler pigment shall elevate the fiber-filler mixture, in other word, the filled paper. Intrinsic brightness of the pigments thus appeared to dominate the observed effects.

As for the paper opacity, among the 4 filler groups, GCC-only had the highest opacity, and dry-ground talc-only the poorest. The mixed GCC-talc groups had middling opacities. Substituting 10% of GCC with talc decreased the opacity of the paper. The phenomenon might relate to the size distribution of the pigment particles. GCC had the smallest average particle diameter (1.46 μm), which increased the frequency of light passing through air-to-filler interfaces and increased light scattering, hence the increased opacity. Adding 10% of larger particle talc (averaging 8.61 μm) to GCC caused an increase in the average particle size, hence reduced opacity of the paper. There appeared to be comparable effects between the 2 mixed filler groups.

4. Conclusion

The experimental results of replacing 10% of calcium carbonate with talc indicated an increased first pass retention, filler retention, bulk, sizing degree, tensile index, and brightness of the resulting handsheets. However, at the cost of decreased smoothness and opacity of the handsheets. Wet co-ground talc and calcium carbonate produced a more uniform and smaller particle size than the corresponding mixed wet-ground calcium carbonate and dry-ground talc. Furthermore, the outer edges of the filler particles appeared to be smoother in the former group as well. The wet co-ground filler gave paper with better filler retention, sizing degree, tensile index, and brightness than the group with separate filler diminution and then mix treatment.

(A) $CaCO_3$ (GCC) (B) Talc (C) Wet co-ground $CaCO_3$/talc (D) GCC+talc

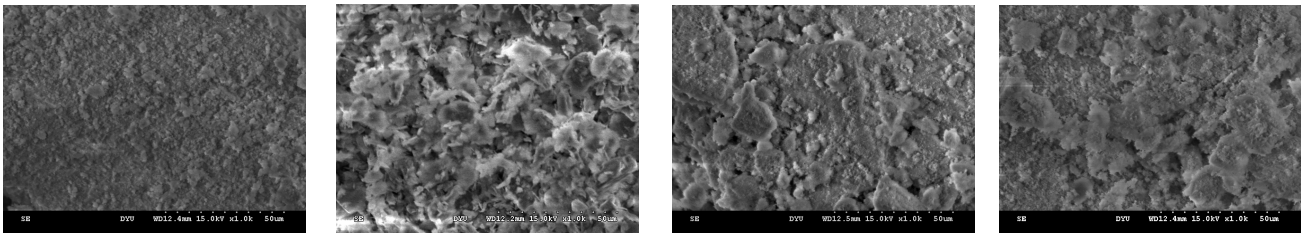

Fig. 1 SEM photomicrographs of the 4 types of filler (x1000).

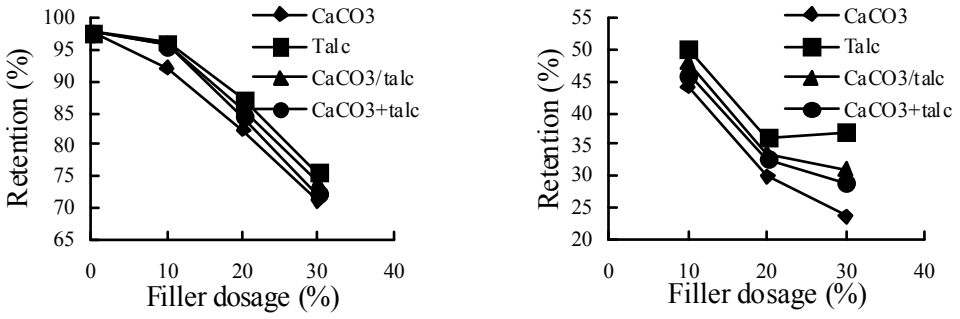

(A) First pass retention (B) Filler retention

Fig. 2 Effects of filler type and dosage on the first pass retention (A) and ash retention (B).

Essential Oil Compositions and Antimicrobial Paper Activities of the Various Parts of *Litsea cubeba* (Lour.) Persoon from Taiwan

Chen-Lung Ho[1,2], Kuang-Ping Hsu[1], Tzu-Chao Chien[1], Eugene I-Chen Wang[1] and Yu-Chang Su[2]

[1] Division of Wood Cellulose, Taiwan Forestry Research Institute, 53, Nanhai Rd., Taipei, Taiwan 100

[2] Department of Forestry, National Chung Hsing University, 250 Kuo Kuang Rd., Taichung, Taiwan 402

Abstract: The leaves, fruit, flowers, stems and twigs of *Litsea cubeba* were extracted either by the hydrodistillation or headspace-GC methods. Compositions and yields of the essential oils were determined and the oils applied to antimicrobial activities and antimicrobial paper capabilities evaluations. A total of 53, 50, 76, 94 and 90 compounds were identified respectively from the leaf, fruit, flower, stem and twig oils of the tree by the hydrodistillation method, and their yields were 13.93 ± 0.09, 3.97 ± 0.03, 10.39 ± 0.05, 0.09 ± 0.01 and 0.36 ± 0.02 ml/100 g of the oven-dried (o.d.) materials, respectively. The headspace-gas chromatography (HS-GC) method, on the other hand, generated 41, 29, 50, 54 and 61 identified compounds respectively from the leaves, fruit, flower, stem and twig of the tree. Yields of essential oil were determined using the multiple headspace extraction (MHE) method and found to be 13.91 ± 0.05, 3.99 ± 0.05, 10.39 ± 0.02, 0.09 ± 0.00 and 0.37 ± 0.01 ml/100 g of o.d. materials for the leaves, fruit, flower, stem and twig, respectively. The main compounds based on the 2 methods were similar and those in the leaves, flowers and twig were 1,8-cineol, in fruit was citral, and in the stem were limonene, citronellal, citronellol etc. When tested for their antibacterial activities using the paper disc diffusion method, oils from all parts showed excellent activities, particularly the fruit oil. When the oils were infused on filter paper and tested for their antimicrobial paper capability according to the JIS L1902 method, the results indicated that fruit oil exhibited excellent antimicrobial paper activities. Citral was deemed the main cause of its antimicrobial activity. In the day and age of multiplicity of contagious diseases and prevalent in-hospital contagions, these essential oils present a potentially good choice as antibacterial agents. We think that essential oils of the species are capable of multipurpose applications.

1. Introduction

Litsea cubeba Pers belongs to the family of Lauraceae, and genus of Litsea. It is a deciduous bush or small tree, mostly distributed in the East Asia region. In Taiwan, it is distributed in the central and eastern mountainous terrains ranging in elevations from 300 to 2,300 m. The whole plant possesses a pungent gingery odor. Leaves of the species oblong lanceolate; fruit globulous drupe turns black when mature, and possess a pungent odor. The Atayal tribe of Taiwan's indigenous people call this plant "Makauy," and wont to eat its leaves, roots and fruit. The roots are reputed to cure headache and the fruit aid digestion as well as substitute for salt. The whole plant parts can be effective spices to cover unpleasant fishy odors. The Saisiyat people, another indigenous tribe, also add the tender leaves of *L. cubeba* to soups, making use of it as a condiment.

L. cubeba oil is a pale yellow, volatile essential oil with an intense lemon-like, refreshing, sweet odor which is insoluble in water. It is used as a fragrance enhancer in foods, cosmetics, and cigarettes and also as a raw material in the manufacture of citral, vitamins A, E, and K, ionone, methyl ionone, perfumes, and other essential oil mixtures. [1] Literature pertaining to various parts of the plants abound. [2~14] However, most reports concentrated on the essential oils from leaves, flowers, and fruit. There are few reports on the stem and twig oils of the species. The essential oils from various plant parts also belong to different chemotypes, such as the cineole, linalool and linalool/citronella types of leaf oils. [2~5, 7~9, 11, 14] Thus, it is apparent that the essential oils of the species possess fair amount of variability.

This species is regarded as a medicinal plants in China. The 1977 compilation of Chinese herbal medicine dictionary talked about the antibacterial and anti-inflammation activities of *L. cubeba*; [15] subsequently, a few reports also noted that *L. cubeba* essential oils had extensive antibacterial and antifungal activities. [16~18]

Yet there are very few literature regarding *L. cubeba* essential oils from Taiwan. Furthermore, the

antibacterial activities of the oils were unreported as well. Thus, we firstly endeavored to examine the extraction of essential oils from 5 parts of leaves, fruit, flowers, stems and twigs of Taiwan grown *L. cubeba* using the hydrodistillation and headspace-GC methods separately, as well as analyze their compositions. In the headspace-GC method, the multiple headspace extraction (MHE) method was used to determine the oil yields and to serve as the basis for chemotyping classification. In the 2nd part, the antimicrobial activities of these 5 parts were assayed and filter papers with the oils added separately were evaluated for their antimicrobial paper capability and feasibility. The information thus obtained may serve as the basis for a multipurpose approach of developing *L. cubeba* parts for practical applications.

2. Material and Methods

(1) Materials

The collection site of all experimental *L. cubeba* parts were obtained from the Lienhuachih Research Center of the Taiwan Forestry Research Institute.

(2) Methods

a. Extraction of essential oils and compositional and yield determinations

(a) Hydrodistillation

1 Kg each of The leaves, fruit, flower, stem and twig was placed in a round-bottom flask and added with 3 L of distilled water. The water was heated to boil and refluxed for 8 h.

(b) GC and GC–MS Analysis

According to Ho et al. [23] (2008).

(c) HS-GC analysis

According to Ho et al. [23] (2008).

(d) Yields of essential oils

According to Kolb[24] (1985) and Ho et al. [23] (2008), the matrix effect can be eliminated by using the MHE method.

b. Antimicrobial activities of the essential oils

(a) Microbial strains

The microbial strains were obtained from the Culture Collection and Research Center of the Food Industry Research and Development Institute, Hsinchung city, Taiwan. The bacterial cultures included 5 types of gram-negative bacteria: *Escherichia coli* (IFO 3301), *Enterobacter aerogenes* (ATCC 13048), *Klebsiella pneumoniae* (ATCC 4352), *Pseudomonas aeruginosa* (IFO 3080), and *Vibrio parahaemolyticus* (TCC 17803); and 3 gram-positive bacterium: *Bacillus cereus* (ATCC 11778), *Staphylococcus aureus* (ATCC6538P), and *S. epidermidis* (ATCC 12228); and 1 yeast: *Candida albicans* (ATCC 10231).

(b) The paper disc diffusion method

This test was carried out in accordance with the method of Cimanga et al. [25] (2002).

Evaluation of the antimicrobial activities of Standard processed textile products using the JIS standard test (JIS L 1902: 2002) [26]

According to JIS standard test (JIS L 1902: 2002).

3. Results and discussion

We extracted essential oils from the leaves, fruit, flowers, stems and twigs of *Litsea cubeba* plant parts using both hydrodistillation and HS-GC methods. Leaf oil provided the highest yield (13.93 ± 0.09 ml/100 g), flower the next (10.39 ± 0.05 ml/100 g), then fruit (3.97 ± 0.03 ml/100 g), twig (0.36 ± 0.02 ml/100 g) and stem (0.09 ± 0.01 ml/100 g) in decreasing order. Compositions of the oils were varied. From the leaf oil, 53 and 41 compounds were respectively identified by the hydrodistillation and HS-GC methods, with 1,8-cineol predominated. From the fruit oil, 50 and 29 compounds were respectively identified by the 2 methods, and citral was the predominant component. The flower oil of the species produced 76 and 50 identified compounds respectively by the 2 methods, and 1,8-cineol was also the main component. From the stem oil, 94 and 54

identified compounds were respectively produced by the 2 methods, and limonene, citronellal and citronellol led the list. Finally, in erstwhile unpublished twig oil, we found 90 and 61 identified compounds respectively by the 2 methods, also with 1,8-cineol predominated. The experimental results confirm the viability of using HS-GC as an effective means of essential oil analysis and phytochemical typing applications.

In the antibacterial assays, we used paper disc diffusion method. The results suggested that the oils from all parts of the *L. cubeba* possessed excellent antibacterial activities, particularly the fruit oil. We have also confirmed the source of the activity derived from citral compound.

Furthermore, we infused the oils of different concentrations from various *L. cubeba* plant parts onto paper squares and tested for antimicrobial paper capacities using the method of JIS L 1902. The results indicated that fruit oil exhibited excellent antimicrobial paper activities. In this day and age of prevalent in-the-hospital contagions, the essential oils might be good choices for containing the problem, leading to multipurpose utilization of the *L. cubeba* plant oils.

Developing Highly Cationic Starches for Controlling Dissolved and Colloidal Substances in Papermaking Systems

Lijun Wang, Lingzhi Luo and Siwei Xing
Tianjin Key Lab of Pulp and Paper, Tianjin University of Science & Technology, Tianjin, 300457
*Corresponding author: wangchem@tust.edu.cn

Modern papermaking mills using higher ratios of recovered fiber and high yield pulps, together with more tightly closed whitewater recirculating system often face serious pitch and stickies deposit problems. Chemical or enzymatic biological methods have been used to prevent their deposition in the system, among them the chemical fixation method is an active player and it has been widely used in paper mills, mainly due to its convenience and effectiveness in using. However, the dissolved and colloidal substances (DCS) always decrease paper strength properties, after being successfully fixed onto paper fibers[1]. Therefore, it is beneficial to find new kinds of fixing agents which not only have better DCS controlling effects but also avoid the decreasing of paper strengths.

On the other hand, cationic starches are well-known dry strength agents for papermaking, but often their charge densities are too low to neutralize or fix dissolved and colloidal substances which are highly anionic. For this purpose, starches must be highly cationized. In our study, highly cationic starches with degree of substitution (DS) as high as 0.60-0.90 were made by etherification of corn starch with 2, 3-Epoxypropyltrimethylammonium chloride. Using a HCS with DS of 0.80 as fixing agent in old newsprint pulp showed that the molecular weight of the HCS was so large that it performed much more like a flocculant[2](See Figure 1). Enlightened by the literature that HCS with lower molecular weight may behave better in fixing DCS[3, 4], and since starch is composed of amylose and amylopectin, it is reasonable to think that HCSs made from starches with different amount of amylose and amylopectin would have different properties. Therefore, general corn starch, amylose and amylopectin were used to prepare highly cationic starches, their molecular weights degraded by acid hydrolysis (See Table 1); and the effects of the resulted HCSs on DCS controlling and paper strengthening were investigated[5]. The result showed that HCSs with lower molecular weight interacted more effectively with pulp fibers with less adsorbing to the fiber (See Figure 2 a-d)), leaving more degraded HCSs to interact with the DCS in the liquid phase, resulting in better controlling performances (See Figure 3a-d). The degraded HCSs made from relatively pure amylase and amylopectin, i.e., the nearly totally linear and totally branched starches, seemed to have unique properties, in that the degraded linear HCS had better performance in controlling DCS, while the degraded branched HCS had better performance in paper strengthening (See Table 2).

Furthermore, the effects of low-molecular-weighted HCS (LHCS) on controlling polysaccharide-based anionic trashes were investigated by treating it with model compounds such as pectin, oxidized starch and degraded hemicellulose and measuring the absorbance, zeta potential and monosaccharide composition of the supernatants of the model compounds[6] (See Figure 4). The results showed that, compared with the traditional anionic trash catcher such as polyamine, the LHCS had much better effects in controlling the polysaccharide-based anionic trashes, owing to its extra hydrogen bonding effect with the polysaccharides.

References

1. Francis, D.W. and Ouchi, M.D. - Effect of dissolved and colloidal solids on newsprint properties, *J. of Pulp and Paper Sci.* **27** (9): 289 (2001)
2. Li-Jun Wang, Fu-Shan Chen, and Lin-Jie Zhou.- Performance of fixing agents in controlling microstickies in newsprint pulp, *Proc. 2006 Pan Pacific Conf.*, June 6-9, Asem Hall, Coex Convention, Seoul, Korea, P111 (2006)
3. Bobacka, V., Kreutzman, N. and Eklund, D. - The use of a fixative in combination with cationic starch in peroxide-bleached TMP, *J. of Pulp and Paper Sci.*, 25 (3): 100 (1999)
4. Vihervaara, T. and Jouko K., - A new generation of starch based cationic polymers for controlling wet end

chemistry, *Proc. Tappi 1994 Papermakers Conf.* Tappi Press, Atlanta: 529 (1994)

5. Lingzhi Luo, Lijun Wang, DCS controlling and paper strengthening effects of highly cationic starches with different branching degrees and molecular weights, *Appita Journal*, In press (2009)
6. Wang, Li-Jun; Luo Ling-zhi, Xiao he, Controlling Polysaccharide-based Anionic Trashes Using Low-molecular-weighted HCS, *China Pulp and Paper*, 25(7): 1 (2006)

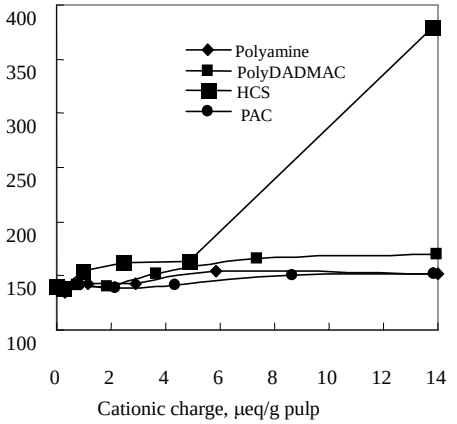

Figure 1 Fixing agents on fiber flocculation (Flocculation was measured indirectly by the formation index with a 2D Lab Formation Sensor, Techpap Co. Ltd., France, on handsheets made from 100% domestic ONP. Higher L.T (look through) means worse formation)

Table 1 Molecular information of the HCSs as characterized indirectly by the flow time of 0.1% HCS solution in the capillary of a Ubbelohde viscometer (GB1632 non-dilution 4-0.57 type)

HCS	Flow time in capillary (sec)
undegraded normal HCS	172.9
degraded normal HCS	123.4
undegraded linear HCS	219.0
degraded linear HCS	122.1
undegraded branched HCS	152.3
degraded branched HCS	118.6

Table 2 Effect of degraded HCSs (0.2% odp) on paper strengths

HCS		Tensile index		Burst index		Folding times		Tearing index	
		Average (N.m/g)	p value	Average ($kPa.m^2/g$)	p value	Average	p value	Average ($mN.m^2/g$)	p value
Control		26.47	1.00	1.66	1.00	12	1.00	9.27	1.00
Degraded HCSs	Normal	27.05	0.75	1.68	0.86	8	0.09	8.45	0.07
	Linear	26.94	0.60	1.76	0.48	7	0.05	7.63	0
	Branched	33.28	0	1.66	0.98	11	0.70	9.08	0.64

Note: p values were obtained from a statistical t-test calculated with Microsoft Excel 2003. $p<0.05$ means the difference is statistically significant between two sets of data.

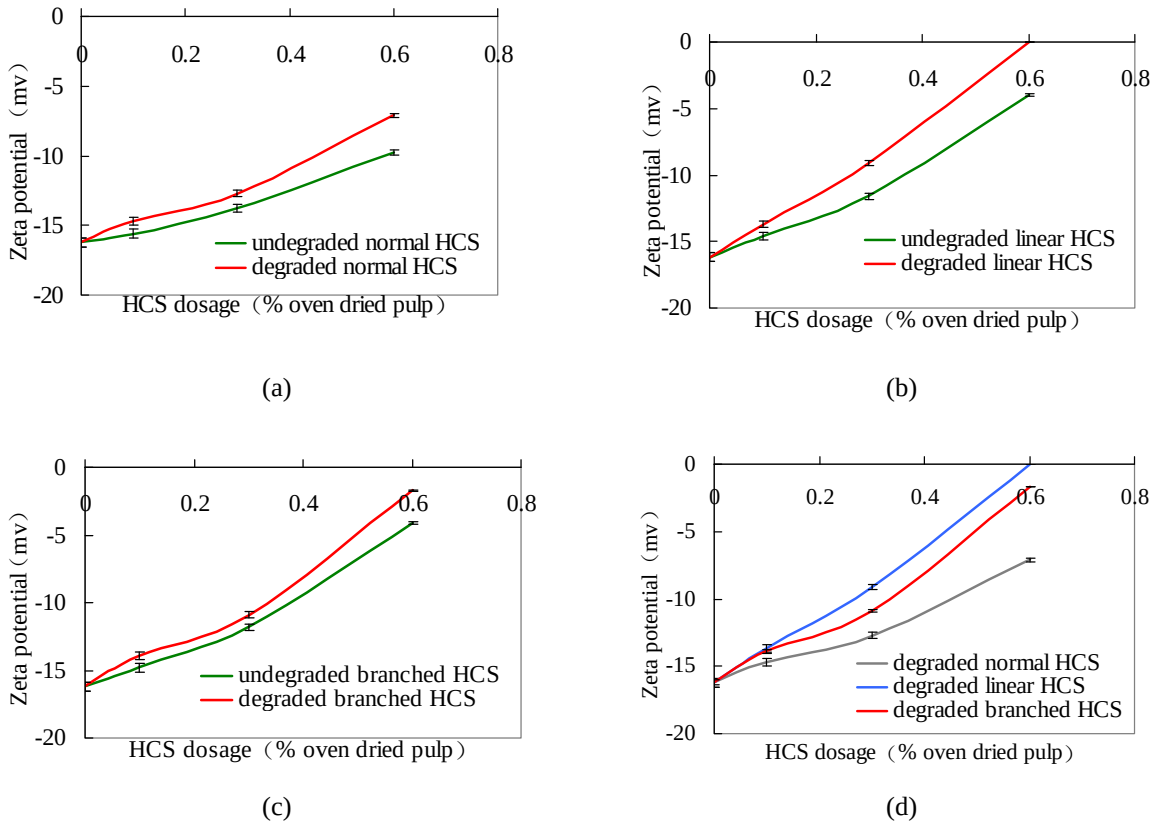

Figure 2 Effects of HCSs with different branching degrees and molecular weights on pulp ζ-potential (ζ-potentials were measured respectively by a Mütek SZP-06 System Zeta Potential Tester. The degraded HCS made the pulp ζ-potential more positive, and the dosage to neutralize the pulp was always lower than for the undegraded HCSs, meaning that if the dosage of the HCSs is at the same level, more degraded HCS will be left in the water phase to react with the DCS, resulting in a better DCS controlling effect)

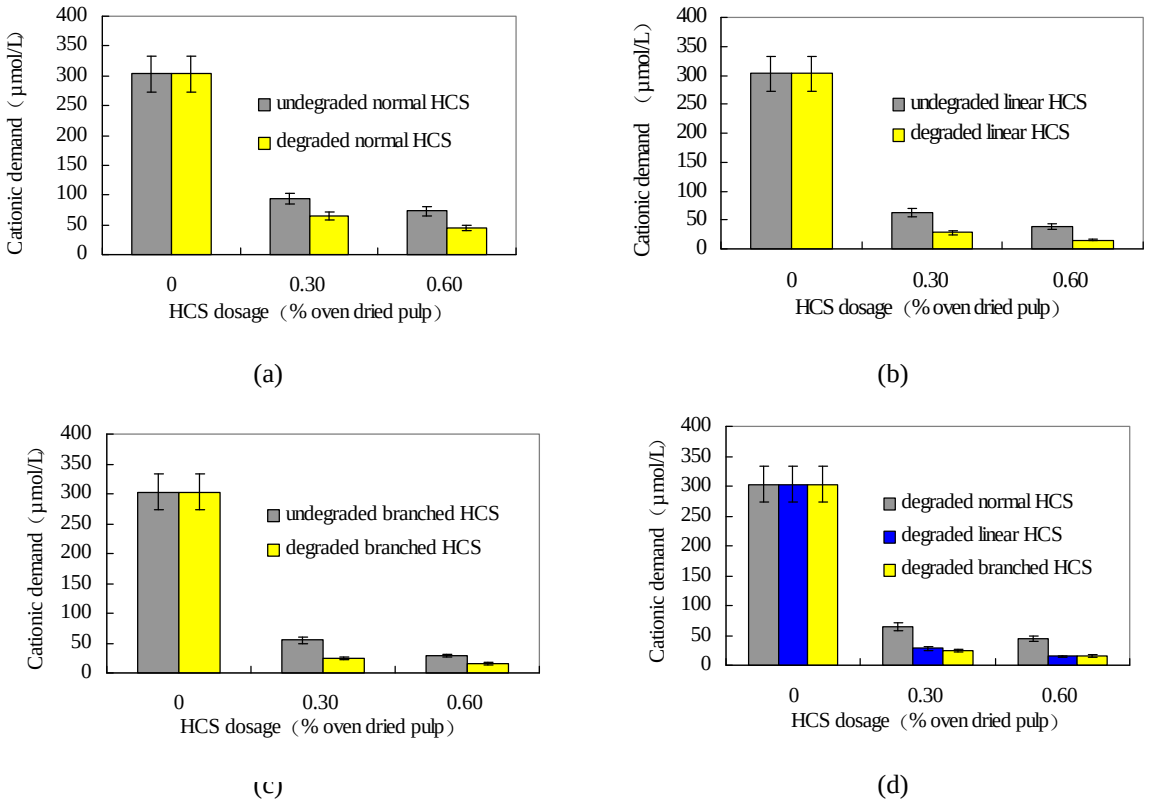

Figure 3 Effects of HCSs with different branching degrees and molecular weights on cationic demand of filtrate (The cationic demands were measured with a Mütek PCD 03 Particle Charge Detector from BTG Group, Sweden. Both the degraded and undegraded HCSs decreased the cationic demands of the deinked pulp, and the degraded HCSs showed better performance than their corresponding undegraded ones)

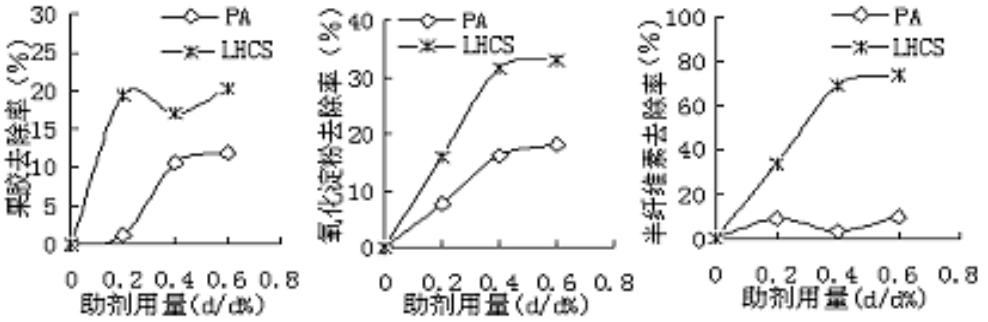

Figure 4 The effect of polyamine (PA) and low-molecular weighted highly cationic starch (LHCS) on removing polysaccharide-based anionic trashes (Clearly LHCS showed better performance in removing such anionic trashes)

A Energy System Integrative Optimization Platform for Energy-saving in Pulp and Paper Industry

Huanbin Liu[1,2] and Jigeng Li[2]

[1] Professor and Former President of South China University of Technology, Foreign Menber of the Russian Academy of Engineering.

[2] South China University of Technology, Guangzhou , China 510640

Pulp and paper production is an energy-intensive activity and energy costs can represent up to 25% of the total manufacturing cost. Paper industry is the six largest consumer of commercial energy in China. There are two key reasons made higher energy consumption in Mainland China's pulp and paper industry in comparison of developed countries: one is lower degree of energy system optimization, another is lower level of integration in process technologies. Advanced process control is one of the options for reducing process variability and specific energy consumption. It was developed that a energy system integrative optimization information platform for energy-saving embedded in MES level of advanced process control system by the South China University of Technology.

1. Energy System Analysis Method

The three-link method was used to analysis pulp and paper process energy flow system. According to the process trait of energy, it is divided three-link: Energy-conversion link, Energy-use link and Energy-recovery link, as Fig. 1 and Table 1.

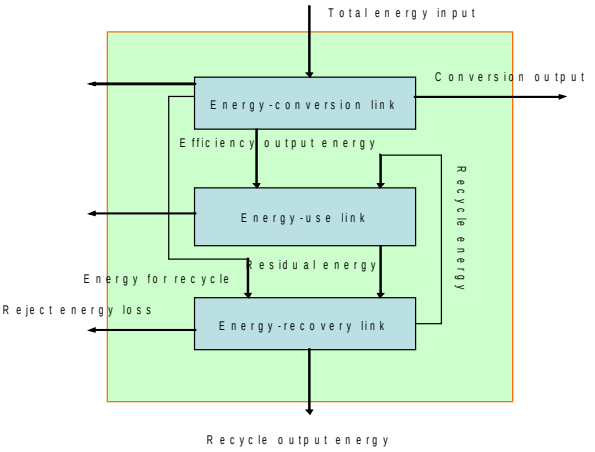

Fig.1 The three-link method

link	Operation Unit
Energy-conversion link	boiler, steam turbine, alkali recovery boiler, etc.
Energy-use link	digester, refiner, bleach, de-inking,beating, paper machine, water treatment, office, etc.
Energy-recovery link	condensed water, cycle heat from dry section, cycle heat from blow tank section

Table 1. The division of three-link

2. Paper Mill Energy Optimization Platform (PMEOP)

(1) MEOP Fuction Module

PMEOP consistend of 10 modules showing as Fig2.

(2) PMEOP Function

The PMEOP have the following function:

- Communication among "information islands"
- Paper mill energy flow transparent
- Compare and analysis historian data and optimize operation set points
- Compare the energy operation figure with benchmarking
- Use "three-link" method to analysis and diagnosis the bottle-neck
- Optimize and match stepped utilization of energy

- Uniform to supervise great energy consumption equipment and process
- Dynamic optimize and distribute the energy flow
- Reduce the schedule and unscheduled downtime for reducing the energy consumption and the fiber material consumption
- Energy consumption predict and Planning (Option).

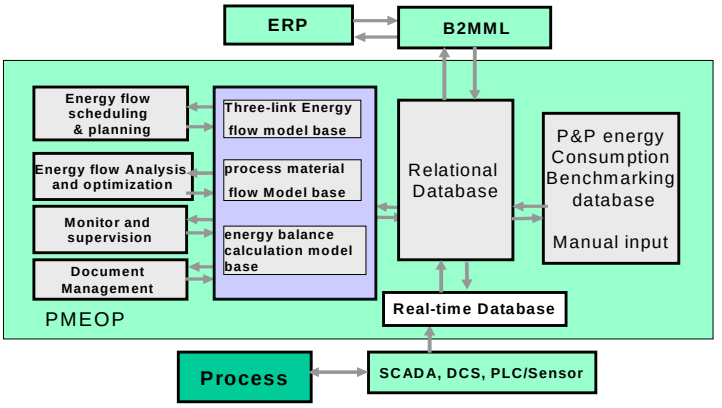

Fig.2 PMEOP Software Struture

(3) PMEOP Hardware Structure

PMEOP Hardware Structure show as Fig.3

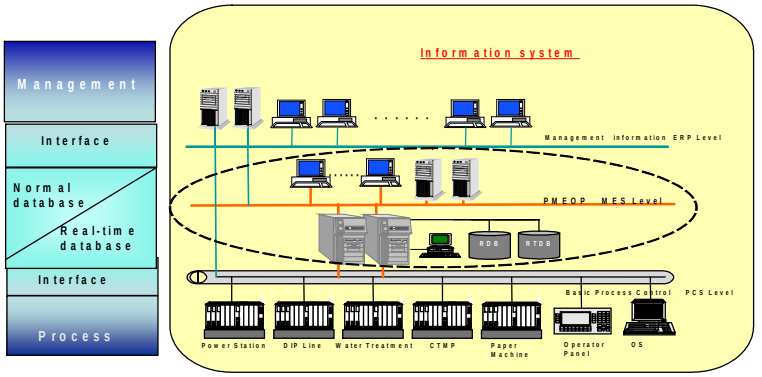

Fig.3 PMEOP Hardware Structure

3. Conclusion

The PMEOP comprises of high-end algorithms, included “three link” energy models, process simulation, process variable estimation (soft-sensors), monitoring, diagnostics and optimization algorithms, to achieves balance between throughput and quality, to reduce process variability and specific of energy consumption.

Polydiallyldimethylammonium Chloride Impact on Dissolved and Colloidal Substances

Lu Dai, Hongqi Dai and Hui Chen

Jiangsu Province Key Lab of Pulp and Paper Science of Nanjing Forestry University, Nanjing, China

Abstract: PDADMAC's impact on DCS is studied under different conditions. It can be concluded that charge density of PDADMAC is constant within wide pH range, and hardly influenced by inorganic salt, and optimum charge exists in order to have preferable drainage ability of pulp. DCS effects flocculation of fines and jeopardizes retention and drainage performance. Meanwhile, high pH value enables the release of anionic particles, hence increases cationic charge demand.

1. Introduction

For the past few years, the degree of closed system of white water in papermaking system is higher and higher, Functional agents' ability, paper quality and production stability are badly effected by fines in white water, anionic disruptors and accumulation of inorganic salt[1]. The research of impact of anionic trash disruptors and controlling technique are the hot topics for paper makers these years. In China, there are few researches concerning PDADMAC used as ATC. And particle surface charge density in wet-end or paper machine system and charge of all kinds of soluble electric substance are key factors of determining accumulation of particles and ability of functional agents. Till now, there are two wildly used ways to measure colloid charge- electrical Methods and potentiometric titration. Research indicates that[2-3] ability of agents can be improved dramatically by adding PDADMAC in pulp with high CD value. Paper machines operate under the best condition when Zeta potential near zero by adding PDADMAC. By testing pulp Zeta potential, CD value and drainage performance, anionic trash catching abilities of cationic starch, PDADMAC, PEI and PAC, and it finds out that PDADMAC has the best performance, and it has less influence on Zeta potential when decreasing CD value, so it has better selectivity. In the research, PDADMAC's impact on DCS is studied under different conditions. Drainage performance, turbidity, CD value and Zeta potential of pulp with anionic trash simulacrum are studied. PDADMAC's catching efficiency and its adaptability are fully considered.

2. Material and Methods

KP bleaching eucalyptus pulp(Goldfish, Brazil) washed and made with deionized water. PDADMAC (Kemira), relative molecular mass 40 thousands, charge density 4.45meq/g. Sodium oxalates (Kelong Chemical reagent plant in Chengdu, anionic charge density is -0.05 meq/g). 1000ml of 0.3% density of pulp(1% DCS to dry pulp) is added into dynamic drainage jar, mixed at the speed of 1500rpm, keep this speed, and adding ATC under different experiment design. Freeness is measured with Canadian standard freeness tester, filtrate is collected, and tested with 2100P Turbidi Meter for turbidity. And the measurement of Zeta potential by Zeta potential meter (Germany mütek Company).

3. Results and discussion

(1) DCS's impact on wet-end characteristics

DCS causes many problems in the operration of wet-end such as minoring or even eliminating abilities of cationic agents. And retention and drainage performance are affected because of its high anionic charge. Each process of papermaking is connected tightly, deteriorism of wet-end operation will influence processes such as pressing, drying and so on, and finally effect paper quality even cause serious problems like dropping of strength index, and affect normal production[4]. In the experiment, DCS's impact on pulp freeness, turbidity, CD value and Zeta potential is discussed, and its results can be seen from Figure 1 to Figure 4.

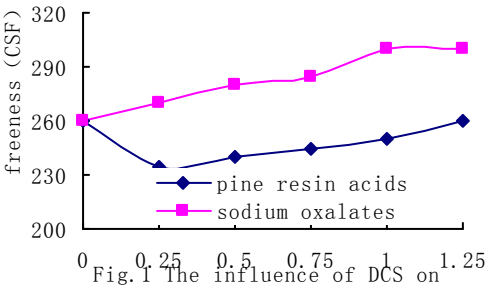

Fig.1 The influence of DCS on pulp freeness

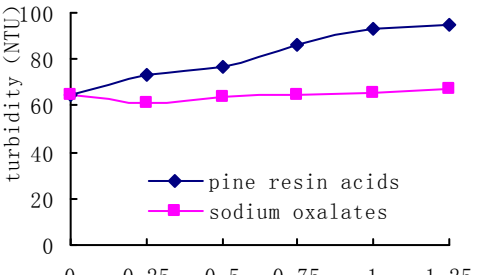

Fig.2 The influence of DCS on filtrate turbidity

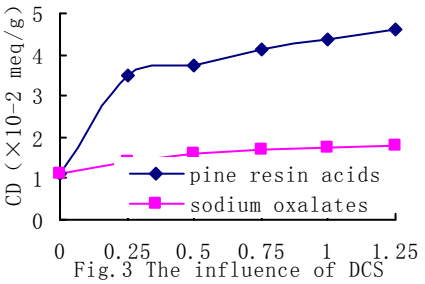

Fig.3 The influence of DCS on pulp CD value

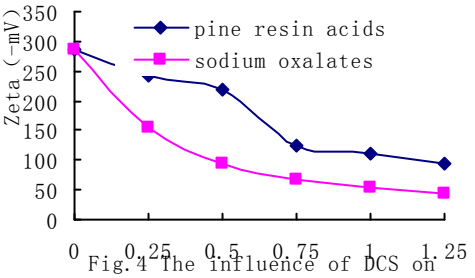

Fig.4 The influence of DCS on pulp Zeta potential

It can be seen from the figures that freeness and turbidity are increasing when the density of DCS is increasing. It shows that accumulation of DCS has bad impact on retention and drainage performance. Because DCS causes high anionic charge in the system in order to affect flocculation of fines in the pulp and jeopardizes retention and drainage performance[5]. From Figure 3, when resin acid density is from 0 to 0.25%, CD value increases dramatically, but over 0.25% slowly. For sodium oxalates, CD value is much smaller than that of resin acids; it is probably because that sodium oxalates have weaker electronegativity and lower ionization extent. Figure 4 shows that Zeta potential reaches zero then the charge of DCS is increasing, maybe flocculation ability in improving and particles transfer towards fiber.

(2) PDADMAC's catching efficiency on DCS

PDADMAC's catching efficiency on DCS can been seen from Figure 5 to Figure 8. PDADMAC is added in pulp with different concentration of DCS, changing trends of pulp freeness appears the same way when charge of PDADMAC is increasing-rise to some value and gradually decline; filtrate turbidity is declining when charge of PDADMAC is increasing, but when charge is over 0.1% to 0.2%, turbidities of resin acids and sodium oxalates are almost stable, it proves that PDADMAC neutralize DCS efficiently.

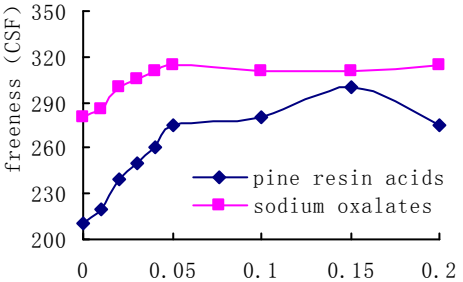

Fig.5 The influence of PDADMAC on pulp freeness

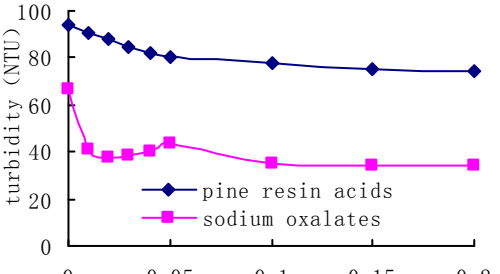

Fig.6 The influence of PDADMAC on filtrate turbidity

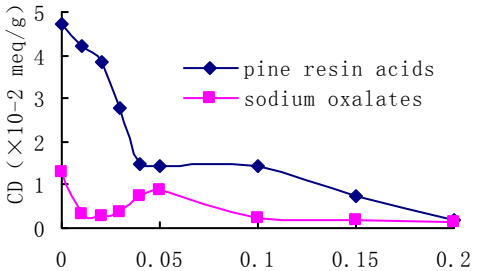

Fig. 7 The influence of PDADMAC on pulp CD value

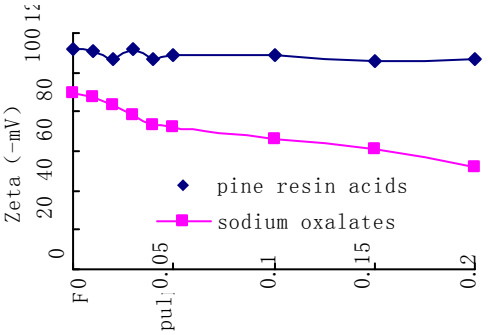

From Figure 7, it can be seen that CD value is slowly declining when the charge of PDADMAC is increasing, but when the charge reached some point, the change of CD value becomes smooth. Before reaching the optimum charge, PDADMAC neutralize DCS qualitatively and selectively. And the compounds will set on fiber and be brought on paper sheets. As a result, the amount of anionic substances decrease, and it causes the declining of CD value. However, when the charge of PDADMAC is over 0.1%, DCS is completely neutralized with PDADMAC, so if adding excessive PDADMAC, it will neutralize with anionic fiber. And it turns out that cationic agents do not have enough adsorption sites to react with fiber, so excessive PDADMAC becomes cationic trash. Zeta potential of resin acids is almost stable, but the increasing trend of sodium oxalate Zeta potential is obvious. On Figure 8, Zeta potential is declining, and it shows that flocculation ability of the system is improving.

(3) pH value's impact on pulp drainage ability and electrical properties

pH value of papermaking system in which aluminum, vanadium and pine resin sizing is applied is about 4.5, and pH value of AKD sizing alkaline papermaking system is from 8 to 9. So the pH range in this research is selected from 4 to 10. The charges of PDADMAC and DCS in resin acids are 0.05% and 1%, and they are relative to dry pulp; the charges of PDADMAC and DCS in sodium oxalates are 0.01% and 1%, and they are relative to dry pulp. NaOH and HCl are used to adjust pH value of pulp, and the result can be seen from Figure 9 to Figure 12.

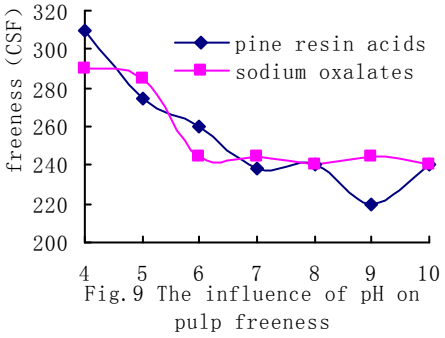

Fig. 9 The influence of pH on pulp freeness

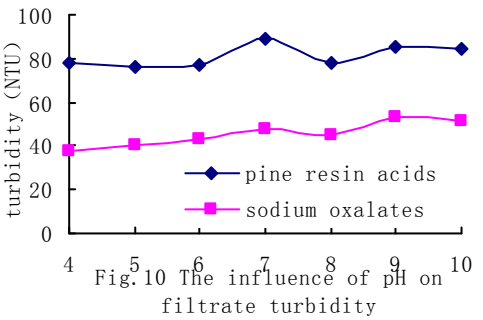

Fig. 10 The influence of pH on filtrate turbidity

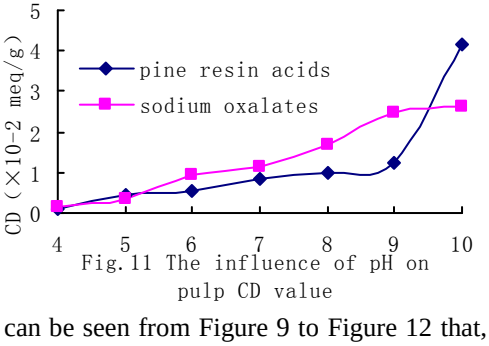

Fig. 11 The influence of pH on pulp CD value

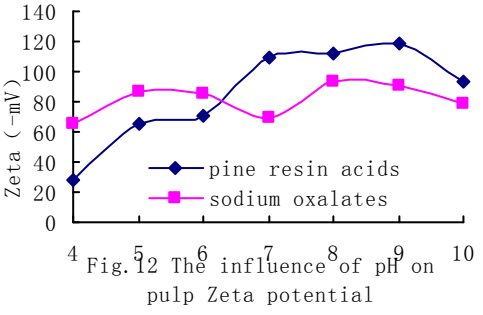

Fig. 12 The influence of pH on pulp Zeta potential

It can be seen from Figure 9 to Figure 12 that, the increasing of pH value causes decline of pulp freeness, meanwhile, turbidity is increasing when pH value is increasing. The amount of anions is increasing when pH

value is increasing, so the CD value is increasing. For resin acids, it can be seen from Figure 11 that when the pH value is between 4 and 9, CD value of the system if increasing stably, but when it is over 10, CD value increases dramatically. It just enough testify the turning point of Zeta potential at the same point. It may be because of the ionization of resin acids, and it increases the CD value of the system.

The change of pH value not only influences electrical properties and structure characteristic of high molecular weight hydrophobically associated cationic, but also influences chemical structure and electric double-layer of colloid surface in the suspension system[6]. So the change of retention and drainage ability in different pH value is the result of the influence from the two aspects. When the pH value is decreasing, modulus of Zeta potential is decreasing, it improves flocculation ability of retention and filter aid. When pH value is about 4, Zeta potential is near zero, electric double-layer is pressed smaller[6,7], suspended colloid particles can collide and congregate easily.(Refer to Figure 12)

4. Conclusion

In the water system with fixed amount of DCS, charge density is increasing proportionally while the charge of PDADMAC is increasing with the same proportion. It shows that there are neutralization reactions between PDADMAC and resin acids. DCS causes high anionic charge in the system in order to affect flocculation of fines in the pulp and jeopardizes retention and drainage performance. Optimum charge exists in order to have preferable drainage ability of pulp. But if adding excessive PDADMAC, it will neutralize with anionic fiber. And it turns out that cationic agents do not have enough adsorption sites to react with fiber, so excessive PDADMAC becomes cationic trash. When the pH value is decreasing, modulus of Zeta potential is decreasing, it improves flocculation ability of retention and filter aid. But more anionic groups are ionized from anionic trash when the pH value is increasing and the CD value is increasing.

Acknowledgement

This research was founded by National Natural Science Foundation of China (contract grant number: 3081995) and Jiangsu Provincial Key Lab. of Pulp and Paper of Science and Technology(200818) are greatly appreciated.

References

[1] LI Hui, LI Youming, WANG Rui, ZHAO Yu. The Non Process Elements in Paper Industry [J]. Paper and Paper Making，2004，1（1）：38

[2] Brouwer P. H.，The relationship between zeta potential and ionic demand and how it affects wed-end retetion [J]．TAPPI，1991（1）：170-179．

[3] Glittenberg D.，Hemmes J. L.，Bergh N. O.．Cationic starches in systems with high levels of anionic trash [J]．Paper Technology，1994，35（7）：18-27．

[4] LIU Zhong. Effect of Anionic Trash on Newsprint Properties and the Measures of Diminishing the Effect [J]. World Pulp and Paper 21(3).

[5] GAI hengjun, HU kaitang. The anionic trash at the wet of papermaking [J]. Shanghai Paper Making, 2002,(03).

[6] MA qingshan, Chemical flocculate and flocculant，Bei Jing: Chinese Environmental Science Press，1988.

[7] ZHANG guanghua．The chymist theory and application at the wet of papermaking [M]．Bei Jing: Chinese Light Industry Press，1998.

Application of a Pilot-Scale Pulsed Elecrocoagulation System to Pulp Mill Beaching OE Stage Effluent

Yuan-Shing Perng[1], Eugene I-Chen Wang[2], Yuan-Chang Hsieh[1] and Meng-Kuan Hsiao[1]

[1] Professor and Graduate Student, Department of Environmental Engineering, Dayeh University.

[2] Division Head, Division of Wood Cellulose, Taiwan Forestry Research Institute.

1. Introduction

Pulp mill is water use intensive, requiring substantial amount of water to produce a ton of product. The hindrances toward fuller reuse of the post-treatment effluents are mostly related to residual ionic species (e.g. chloride, potassium, metals/transition metals and calcium) and coloration from ligneous fragments and dissolved organic solids. This will result in fouling and scaling of the black liquor evaporators, fouling and plugging of the kraft recovery furnace, corrosion and increased use of bleaching chemicals.

The purpose of this study was to assess the possibility of using pulsed electrocoagulation technology to treat the effluent of a bleaching oxygen extraction (OE) stage in the kraft pulp mill for water reuse. For the study, a medium-sized pulp mill was selected which produces 400 t/d of bleaching kraft hardwood and discharges 20,000 m^3/d of wastewater. Experiments were carried out in a pilot-scale pulsed electrochemical reactor followed by an aerator, a flocculation tank, and a sedimentation tank. Effects of the operating parameters, viz. electrode material, current density and hydraulic retention time (HRT) of the system, and water quality indicators (electrical conductivity, suspended solids (SS), chemical oxygen demand (COD), true color and hardness) of the treated wastewater were investigated.

2. Material and Methods

(1) Materials

a. Wastewater

The bleaching sequence of a cooperating pulp mill was: cooking stage→oxygen alkali extraction stage (OE) → chlorine dioxide stage (D1) → chlorine dioxide stage (D2). The wastewater stream test-treated in the experiment was from the OE-stage effluents of the Taiwan Pulp and Paper Inc., Hsinyin, at southern Taiwan. The mill produces mostly bleached hardwood pulps containing often eucalypt and other mixed hardwoods. The OE stage effluent is known for its dark brown coloration and high electrical conductivity. There were substantial variations in effluent qualities measured daily. In order to avoid spurious variations that might affect the treatment results, a combined effluent of 1,000 L was equalized in a homogenization tank before use in each set of experiments.

b. Treatment system

Figure 1 presents the schematic diagram of the treatment system used in the study. The system was composed of a perfectly mixed homogenization tank of 1000 L, a 65 L pilot-scale alternating electrocoagulation reactor; a 78 L aerator; a 100 L flocculation tank, allowing flocs sufficient time to grow; and a 120 L sedimentation unit.

c. Pulsed electrocoagulation reactor

A pulsed electrochemical reactor (Model JC-10) developed by Jye-shi Environmental Technologies & Engineering Inc. of Taiwan was used in the study. The reactor is shown in Figure 2 and is capable of treating 0.1~0.5 m^3/h of wastewater with a HRT between 0.13 and 0.65 h.

There are 16 electrolytic cells inside the reactor, separated by cast iron or aluminum plates as electrodes. Figure 3 shows the setup of the electrodes. The operational current density for the reactor was between 66.7 and 266.7 A/m^2, and the electrical potential was 5-18 V for iron electrode and 18-32 V for aluminum electrode.

d. Operating Conditions

The values of three operating variables studied were listed below:

- Electrode materials: cast iron and aluminum electrode plates;

- Current density (A/m^2): 0, 66.7, 133.3, 200, and 266.7; and
- HRT in the reactor (min): 6.5, 8.13, and 16.25.

3. Results and discussion

(1) Wastewater Characteristics

The combined OE stage effluents properties observed during a period of 2 months. As shown, the variations in electrical conductivity, filtered COD and true color were substantial. The properties of OE stage effluent had very high conductivity, temperature, colored substances and strongly alkaline conditions.

(2) Effects of Operating Variables on the Treatment Performance

a. Electrical conductivity removal

The results indicate that the removal increases with increasing current density and HRT in both electrode materials. At HRTs of 6.50 and 8.13 min, the electrical conductivity removal by the aluminum electrode set was ca. 15% higher than those obtained with cast iron electrode set. At an HRT of 16.25 min, however, the 2 sets of electrodes produced similar electrical conductivity removal rates. With the aluminum electrodes, the highest conductivity removal achieved was 63.2% (from the original 6,390 μs/cm to 2350 μs/cm), which was obtained at a 266.7 A/m2 current density and an HRT of 16.25 min. With the cast iron electrodes the highest conductivity removal achieved was 70.1% (from the original 6,390 μs/cm to 1,910 μs/cm), obtained also at a 266.7 A/m^2 and an HRT of 16.25 min. Electrical conductivity reflects the concentration of ions in a solution. The decrease in conductivity indicates a reduction in the amount of ions. Thus, during treatment in the reactor, the reduction in conductivity of wastewater was due to the charge neutralization of ionic species contained in it. The charge neutralization de-charges ionic species causing them to become insoluble substances, which are removed through induced micro-aggregation and coagulated macro-aggregation (floc formation) .

b. SS removal

The removal increased with increases in current and in HRT. At low current density (< 133.3 A/m^2), both sets of electrodes had SS removal rates of < 80%. The aluminum electrode set outperformed the iron one. At high current densities (> 200 A/m^2), both electrode had SS removal > 80%, however, the iron electrode set tended to do better than the aluminum set. These phenomena might impact on future economic efficiency assessment in application. With the aluminum electrodes, the highest removal achieved was 92.9% (from the original 140 to 10 mg/L), which was obtained at 266.7 A/m2 and an HRT of 16.25 min. With the iron electrodes, the highest removal rate was 96.4% (from the original 140 to 5 mg/L), which was also obtained at 266.7 A/m2 and an HRT of 16.25 min. The post-treatment values < 20 mg/L SS meets most national and regional effluent discharging standards.

c. COD removal

Similar to cases of electrical conductivity and SS removal, COD removal also increased as current density or HRT increased. In the cast iron electrode set, at an HRT of 16.25 min, the COD removal was far greater than those at HRTs of 6.50 and 8.13 min. In the aluminum electrode set, however, both HRTs 8.13 and 16.25 min gave COD removals much greater than that of HRT 6.50 min. With the aluminum electrodes, the highest COD removal rate was 75.7% (from the original 1,150 to 279 mg/L), which was obtained at 266.7 A/m2 and an HRT of 16.25 min. With the iron electrodes, the highest COD removal was 81.1% (from the original 1,041 to 197 mg/L), which was also obtained at 266.7 A/m2 and an HRT of 16.25 min. The removal of COD might have been due to the attachment of dissolved substances to polarized suspended solids and polarized colloidal particles which form flocs with the flocculation action of the $Fe(OH)_3$ in the reactor. This was supported by the observation that at the moment when the Fe and Al electrodes reached limiting ionization capacities, the removal efficiency of COD showed marked increasing trend. The deduction also was congruent with the experimental results and hypothetical reaction mechanisms .

d. True color removal

Similar to the cases of conductivity, SS and COD removals, true color removal also increased as current density or HRT increased. In the iron electrode set, the 16.25 min HRT produced much greater true color

removal than those at the 6.50 and 8.13 min HRTs. Similar to the COD removal situation, in he aluminum electrode set, both HRTs 8.13 and 16.25 min produced true color removal rates much greater than that at 6.50 min HRT. With the aluminum electrodes, the highest true color removal rate was 86.4% (from the original 2,551 to 346 Pt-Co units), which was obtained at a current density of 266.7 A/m2 and an HRT of 16.25 min. With the iron electrodes, the highest true color removal rate was 86.6% (from the original 2,325 to 311 Pt-Co units), which was obtained at a current density of 266.7 A/m2 and an HRT of 16.25 min.

e. Hardness

Certain metal ions interferes with the titration process, causing the end point color to fade, become indistinct, or consume excessive EDTA, the same is true also for certain suspended and colloidal organic substances. As a consequence, our hardness determinations were interfered and the end points largely indistinct. The accuracy of the data was affected.

The results indicated that the removal increased with increasing current density and HRT in both electrode materials. With the aluminum electrodes, the highest hardness removal rate was 89.5% (from the original 135.8 to 14.2 mg/L), which was obtained at a current density of 266.7 A/m2 and an HRT of 16.25 min. With the iron electrodes, the highest hardness removal achieved was 79.6% (from the original 183.9 to 37.6 mg/L), which was obtained at 266.7 A/m2 and an HRT of 16.25 min. Hardness is mainly composed of concentrations of Ca and Mg ions. As both these ions are easily polarized and form flocs to be removed, hence hardness removal was generally higher than the corresponding electrical conductivity.

4. Conclusions

The results obtained during the study were encouraging and showed that electorcoagulation technology can be used to treat effluent of an OE bleaching stage for water reuse. Under the operating conditions studied, the removals of conductivity and COD always increased with an increase either in current density or HRT. The highest removals obtained at 266.7 A/m2 and an HRT of 16.25 min for electrical conductivity, SS, COD, true color and hardness were 63.2%, 92.9%, 75.7%, 86.4% and 89.5% for aluminum electrode and 70.1%, 96.4%, 81.1%, 86.6% and 79.6% for iron electrode, respectively.

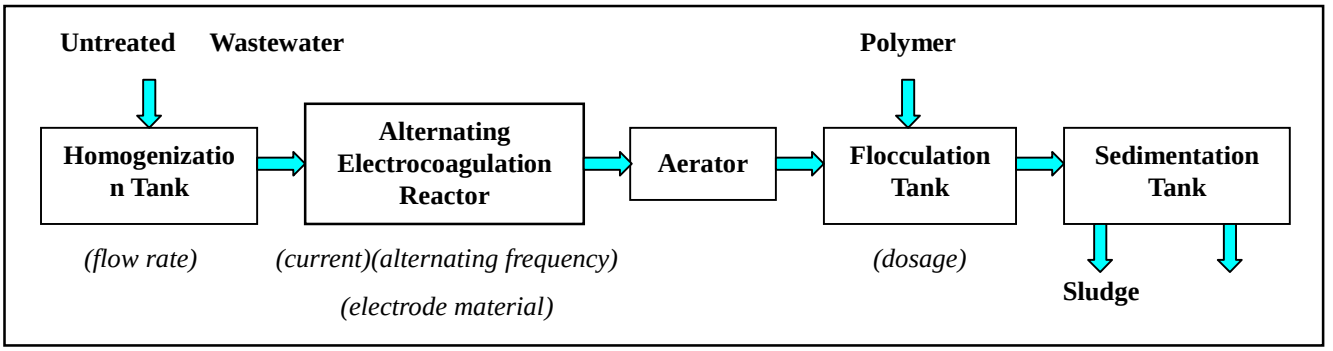

Fig. 1 Schematic diagram of the pulsed electrocoagulation treatment system.

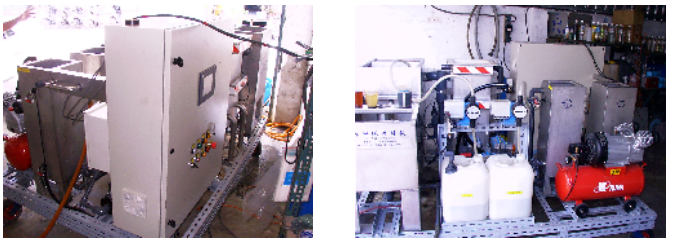

Fig. 2 Photos of the pilot-scale pulsed electrocoagulation treatment system.

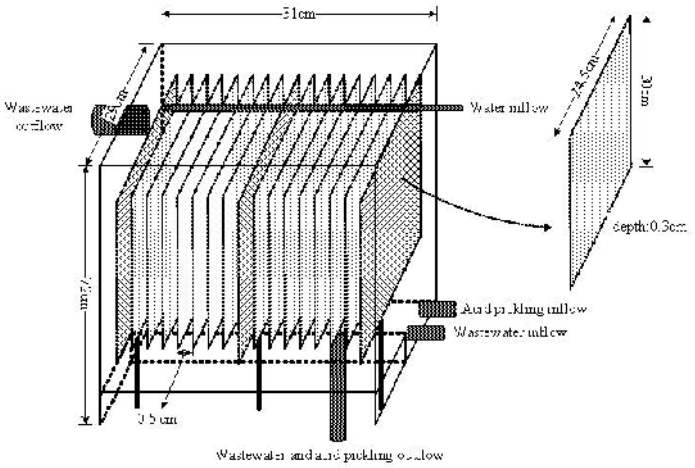

Fig. 3 Diagram showing the electrodes inside the alternating electrocoagulation reactor.

The Analysis on Wet-end Chemical Features of "Zero Discharge" Papermaking Mills

Xiaofan Zhou, Jiesheng Wu and Wei Zhang
College of Paper & Printing Science and Engineering, Nanjing Forestry University, Nanjing, 210037

Abstract: In this research, furnish samples were collected from different parts of two "zero discharge" papermaking mills. Variations in pulp consistency in different parts of paper machine were studied under the condition of zero discharge. The study showed, in this completely closed white water system, furnish consistencies in head box, in white water and in machine chest are 2.80%, 1.95%, and 5.22%, respectively. All of these numbers were higher than those in manufacture processes of papermaking enterprises with incompletely closed circulation. Further study showed the stock in the whole process had high levels of fines, no matter in machine chest or in head box. The fine content of the head box in one paper machine was as high as 83.8%. That is the main reason why the consistencies of both furnish and white water is high in the closed circulation system. It also explain why paper sheet with good formation could be achieved when head box consistency has reached as high as 2.8%. This study also briefly predicted and analyzed the future development trend of wet end chemistry under the condition of zero discharge.

1. Introduction

In the process of making paper, it is the consistent task to researchers to reduce the amount of used water for paper making as well as increase white water circulation. With the enhancing the strength of environmental legal system and public realization of environmental protection, the clean paper making process has to be expedited. Gradually, the degree of water consumption per ton paper and white-water closed is regulated strictly. There has been much related information and research about zero discharge at home and abroad, however, much is about circulation the waste water after purification treatment. A new homeostasis-producing technology with short process and zero discharge has been developed by paper making department in Nanjing Forestry University through 3 years of research, which has been used in more than 30 middle or small paper mills in China. Nevertheless, there are still many issues need to be studied. For example, what is the characteristic of wet-end chemistry in the producing process? What is the difference between this method and non zero discharge production? Also, it is controversial whether this new technology could be used in large modern paper machine. This article is aimed to investigate the character of wet-end chemical, find the inherent mechanism, and afford sufficient theory to justify the utilization of this new technology on large paper machines, through investigating this homeostasis-producing technology with short process and zero discharge.

2. Material and Methods

(1) Material

Instruments used were: DDJ tester; PCD 03, pH particle charge tester (Mütek Company, Germany); 7230G infrared spectrophotometer; WYZ－300 paper tension tester; YQ-Z-23A bursting strength tester; PTI Bauer-McNett fiber classifier.

(2) Methods

Measurement on content of fine component

A dynamic drainage tester (DDJ) is used to determine the content of fine fibers. The pulp consistency is 0.5%, accurate amount of OD pulp was put in the DDJ and dilute to 0.5% consistency, which is stirred at the constant revolutions of 1500 rpm to avoid pulp flocculation. When the drainage starts, water was continuously added to the stirring DDJ until the filtrate turned clear. The filtrate was collected, evaporate to dryness and weigh for the weight of fines. The fine content was calculated:

Content of fine fibers (%) = weight of fine fibers in filtrate/ weight of absolutely dry fibers*100

(The content of fine fibers in waste paper pulp is 25.1% on the average)

3. Results and discussion

In this experiment, pulp and water samples were taken from both Nanjing Luhe Xingguang Paper Mill and Wuxi Paperboard Mill, both producing corrugated paper. The paper machine at both mills is a 3500/110 multi-rotary screen cylinder paper machine with 3 round screens in forming section and pneumatic mortar paper flow box, which could produce corrugated paperboard with a basis weight in the range of 60～150 g/m^2. The press section has 3 bi-rolling presses, resulting in paper web dryness of 45% entering the dryer section. The dry section is composed of 24 dryers of 1500 mm diameter. Besides, there is a surface sizing press in the middle of dry section.

The homeostasis-producing technology collects and reuses all water streams including the water used for cloth cleaning and screen washing to ensure that no waste water is released besides the minor amount from the reject streams of cleaners for light and heavy impurities. This closed-circulation system of wasted water has achieved the goal of zero discharge and economical production as compared with the traditional waste water treatment at the end of the pipe. As a result of the closed water system, pulp consistencies increased due to the acumination of fine fibers as shown in Table 1. As can be seen, the content of fine fibers in the whole process is very high. Taking the data of Luhe paper mill, for example, pulp consistency of the flow to the head box is high at 2.8%, of which the fine fibers account for 1.8%, or 63.83% of the 2.8%. In Wuxi paper mill, fine fibers account for 83.9% of the total fibers to the head box. All white water and washing water streams have very high consistency but consist almost exclusively of fine fibers. Thus, in this production system using homeostasis-producing technology, accumulation of fine fibers results in extremely high consistencies in all paper making streams whereas almost all long fibers leave the system in the first pass.

Table 1 Data comparison of Luhe and Wuxi paper plant

location	pulp concentration		fine fiber concentration		comparatively proportion of fine fiber	
	Luhe	Wuxi	Luhe	Wuxi	Luhe	Wuxi
flow box	2.82%	2.80%	1.80%	2.35%	63.83%	83.93%
white water under screen	1.81%	1.95%	1.79%	1.93%	98.90%	99.49%
Water collection pool	1.46%	1.53%	1.45%	1.53%	99.32%	100%
machine chest	5.12%	5.22%	2.24%	3.52%	43.75%	67.43%
white water used for pulp shredder	2.04%		2.00%		98.04%	
water for washing cloth	1.25%		1.25%		100%	
water taken from cloth	1.24%		1.24%		100%	
Finished paper			29.70%	36.33%		

Compared with the traditional paper mill with incomplete closed water system, this homeostasis-producing technology would cause high pulp concentration in each section of paper making, resulting from the acumination of fine fibers. For instance, the consistency of pulp arriving at the screen is about 1.0% for the former as compared to 2.8% for the latter. If one subtracts fines content (1.8%) from the 2.8%, the consistency of the long fibers to the flowing box is about 1%, which is close to that of the traditional system. Thus, there is no significant difference in long fiber content in the flow box between the two systems. Besides, from the analysis of the evenness of corrugated paper produced has no distinct change after the production system was converted to the zero discharged system.

In this new completely closed process, the waste water in the whole system is recycled and reused with no

waste water being discharged. Assuming the input waste paper and the corrugated paper produced has the same moisture content, the production system has only one inlet of make-up water to compensate for the water evaporated in the dryer section and water associated with cleaner reject of the pulping system. In the beginning of production, the system is not in a balanced situation. The fine content and the pulp consistency at the head box is low. This is also true for the fine content of the corrugated paper produced. As the time goes on, the fine content of pulp at various streams of paper machine increase steadily, causing also an increase in pulp consistency. The system eventually reaches equilibrium when the amount of input pulp reached equilibrium with the amount of finished paper per unit time. The fine contents and the pulp consistencies also reach steady state, which are shown in Table 1. It is noteworthy that the proportion of fine fiber were 63.8% and 83.9% in Luhe and Wuxi mills, respectively.

The closed circulation of white water would be expected to induce a significant increase in negative charge and dissolved organics in the whole production system. Thus, it is necessary to determine the stead state contents of negative charges of the pulp samples and of the COD of the effluents in the production process. The results are shown in Table 2 and 3.

Table 2 content of negative charge in pulp sample of Luhe and Wuxi paper plants

location	**content of negative charge C/L**	
	Luhe	**Wuxi**
flow box	154.4	146.5
machine chest	137.0	150.2
white water under screen	117.2	120.2

Table 3 Comparison of COD in Luhe and Wuxi paper plants

location	**COD content mg/L**	
	Luhe	**Wuxi**
water collecting pool	10000	10210
white water used for pulp shredder	9445	10000

As shown in Table 2, the negative charge content of the pulps is so high that it would have an influence on the efficiency of retention and drainage aid. The COD content of the effluents is extremely high, reaching a level of 10000 mg/L in both mills. Discharging these effluents in to the releasing water would induce environmental pollution unless a costly advanced waste water treatment system is employed. In this respect, the zero-discharge system could solve this problem by making waste water circle without releasing.

Table 4 Pulp beating degree in some section in Luhe plant

location	pulp beating degree (°SR)
machine chest	21.5
flow box	25.5

Because of the acumination of fine fibers in the closed system, the drainage property of pulp deteriorates from machine chest to the flow box as shown in Table 4. This could cause declination of drainage rate of the paper machine due to the increase of fines in flow box. However, in the real production, most fines in the pulp in head box could pass through the forming screen of 200 mesh, inducing little significant influence on the rate of drainage.

Based on the analysis of the results on wet-end chemistry, the authors may make the following predictions:

1. After arriving at the balance, the amounts of added pulp, fillers and chemicals are the same as those in the finished paper, which means all those added could be wholly retained in the finished paper. So, the mill

could produce finished paper according to the prescription.

2. Stability of chemicals in the system will be an important issue. Some retention and drainage aid and sizing chemicals would become ineffective due to decomposition. Thus, the dosage of a given chemical addition should be determined according to its stability in the system.
3. Water in the production serve as the carrier pulp, fillers and chemicals, and exert the effect of dispersing the pulp fibers during forming. In this respect, this zero discharge system could work stably as long as the quality of water in the system remains unchanged.

4. Conclusion

1. Under the conditions of zero discharge, recycled water in the whole system has a huge amount of fine fibers. Due to the acumination of fines, the pulp consistency in every streams increases significantly as compared to the corresponding streams in the traditional system with incomplete closure.
2. Under the condition of zero discharge, the steady state concentration of COD and negative charge are both high in the recycled water. However, this kind of water could be used continuously without releasing to the environment. This not only eliminates the requirement for waste water treatment, but also minimizes the loss of fibers, fillers as well as chemicals, resulting in considerable saving in production cost and decreased water pollution.
3. After the realization of zero discharge, added fibers, fillers and chemicals could be retained completely. In this way, paper mill could produce paper according to the formulation.

Effect of Hot Water Pre-extraction on Eucalyptus Alkaline Pulping and Peroxide Bleaching

Zeng Zhang, Congcong Chi, Weiwei Ge

State Key Laboratory of Pulp & Paper Engineering, South China University of Technology, Guangzhou, 510640

Abstract: The influences of hot water pre-extraction on the followed alkaline pulping and peroxide bleaching were investigated. Eucalyptus chip was adopted as raw materials. The cooking results indicate that with the hot water pre-extraction process, the pulp with obviously lower kappa number can be got under the conditions of lower alkali charge and shorter cooking time. The peroxide bleaching results show that the pre-extraction process before cooking can increase the pulp brightness by 7 ISO% in 2 hours bleaching with 4% H_2O_2 charge. By the (AQ)P bleaching sequence the consumption of H_2O_2 is decreased obviously and the pulp brightness can be over 83%ISO with 4% H_2O_2 charge and 4 hours at 95℃.

1. Introduction

The topic of biorefinery has been paid attention in recent years and the viewpoint of Integrated Forest Biorefinery (IFBR) was presented. One of the ideas in IFBR is to reasonably obtain hemicellulose sugars, including polysaccharides or monosaccharides, simultaneously in the chemical pulping process [1]. In this study eucalyptus chips were adopted as raw materials and the influences of hot water pre-extraction on the followed alkaline pulping and peroxide bleaching were investigated.

2. Material and Methods

Eucalyptus chips (*Eucalyptus ABL 12*) were provided by Leizhou forestry bureau, Guangdong province, China.

Hot water pre-extraction was processed with M/K 609-2-10 digester. The conditions is as follows: maximal temperature:150℃; time to the temperature:55min; time at the temperature:150min; ratio of water to o.d.chip: 5:1. With these extraction conditions the pentose yield is about 28% [2].

Soda-anthoquinone cooking and kraft cooking were carried out with M/K 609-2-10 digester. Plastic bag and water bath were adopted for the experiments of bleaching and (AQ) pretreatment. The bleaching conditions are described in the following results. The (AQ) pretreatment conditions are as follows: A(Acid treatment)：pH≈2; 70℃; 30min; consistency 10%. Q(chelating reagent treatment)：pH≈5.5; 0.2%DTPA; 70℃; 60min; consistency 10%. No washing is processed between A and Q.

The pulp properties and chemical components were determined with Chinese Standard Methods and Tappi methods. The content of hexeneuronic acid group was determined with the method introduced in reference [3].

3. Results and discussion

(1) Effect of hot water pre-extraction on alkaline pulping

Soda-AQ pulping (S) and kraft pulping (K) were processed and parts of the results are shown in Table 1. When cooking with the original chips (OC) , the alkali charge should be over 18% for obtaining the regular pulp without obvious rejects. Pulping with extracted chips (EC) results in obviously lower kappa number and lower pulp yield. The alkali consumption is decreased. The content of hexeneuronic acid (C_{HexA}) is much lower in the pulp sample produced from extracted chips, which can partly explain the decrease in kappa number.

Table 1 Cooking conditions and results

Chip sample	Original chips (OC)		Extracted Chips (EC)	
Pulp sample	OC-S	OC-K	EC-S	EC-K
Alkali charge （Na_2O%）	18	20	16	18
Sulfididy (%)	—	30	—	30
Anthroquinone (%)	0.05	—	0.05	—
TAT (min)*	90	120	90	90
Pulp yield (%)	47.6	48.4	44.2	42.9
Kappa number	20.0	21.0	13.9	15.7
Viscosity (mL /g)	870	950	920	970
Alkali consumption (Na_2O %)	15.4	18.1	14.1	17.0
C_{HexA} (μmol /g o.d.pulp)	54.5	52.8	12.9	11.2

*Other cooking conditions: TTT 90min; T_{max} 165℃; ratio of liquid to wood 4:1.

The pulp strength and the chemical components in pulp and chip were determined. The results of pulp strength determination indicate that some negative effects are induced by hemicellulose loss in water pre-hydrolysis. The phenomena in beating experiment indicate that when the pulp produced from extracted chips is used, the beating time should be double for obtaining the same beating degree as that of the pulp from original chips. The determination of chemical components shows that in the extracted chips the contents of holocellulose, lignin and ash are decreased. But obvious increase in the contents of benzene-ethanol extractives and 1%NaOH extractives are presented.

(2) Effect of hot water pre-extraction on peroxide bleaching

Peroxide bleaching was carried out for investigating the influence of hot water pre-extraction on bleaching results. The contents of transition metal in different pulp and chip samples were determined. Parts of the results are showed in Table 2. The difference of metal content is not obvious between the original chip sample (OC) and the corresponding soda-AQ pulp (OC-S). Distinct content changes of manganese and copper can be found when the original chips and extracted chips are compared. The difference between pulp samples OC-S and the relative pulp sample EC-S is also obvious. The acid-chelating pretreatment (AQ) can eliminate more manganese and copper, but give less effect on iron content.

Part results of bleaching experiments are also shown in Table 2. With the same 4%H_2O_2 charge and 2 hours retention time, the brightness of pulp sample EC-S is 7 units higher than that of pulp sample OC-S. The results also show the benefit from (AQ) pretreatment. When comparing the results of EC-S with that of EC-S-(AQ), the brightness of EC-S-(AQ) is 10%ISO higher and obviously more residual H_2O_2 content can be determined. These may be partly explained by the less content of manganese in EC-S-(AQ).

Table2 Transition metal content and bleaching results

Pulp & chip	Transition metal Content (mg/kg pulp)			Bleaching conditions**		Brightness (%ISO)	Residual H_2O_2 (%)
	Mn	Cu	Fe	NaOH:H_2O_2	Time (h)		
OC-S	6.04	1.25	24.30	0.6	2	61.73	≈0
EC-S	1.16	0.16	19.91	0.6	2	68.76	≈0
				0.75	2	66.31	≈0
EC-S-(AQ)*	0.11	0.17	21.18	0.6	4	83.07	19.8
				0.75	2	76.92	30.7
				0.75	4	83.79	15.4
Original chip (OC)	5.44	1.83	24.07	---	---	---	---
Extracted chip (EC)	2.80	0.34	22.16	---	---	---	---

*EC-S-(AQ) is the EC-S pulp sample pretreated with (AQ) sequence.

**Other bleaching conditions: 4%H_2O_2; 3%Na_2SiO_3（40°Bé）; 0.5%$MgSO_4$; 95℃; consistency 10%

4. Conclusion

When the pre-extracted chips are used for alkaline cooking, the pulp with obviously lower kappa number can be got under the conditions of lower alkali charge and shorter cooking time. The content of hexaneuronic acid in pulp is decreased distinctly. Some negative effects are induced on pulp yield and strength by hot water pre-extraction process. Higher energy consumption is presented in the beating process. More investigation should be made for selecting suitable sugar yield in pre-extraction stage and optimizing the following cooking conditions to find the balance between the pre-extraction and the following pulping.

The peroxide bleaching results show that when chip pre-extraction is processed before pulping, the pulp brightness after bleaching can be increased by 7 ISO% under the same conditions of 4% H_2O_2 charge with 2 hours bleaching time. The consumption of H_2O_2 is decreased obviously which means the H_2O_2 charge can be reduced for certain brightness target. When (AQ)P bleaching sequence is adopted the pulp brightness can be over 83%ISO with the conditions of 4% H_2O_2 charge and 4 hours retention time at 95℃.

Acknowledgement

The authors would like to acknowledge the National Natural Science Foundation of China (No.30671647) for financial support of this research project.

References

[1] Adriaan van Heiningen, Converting a kraft pulp mill into an integrated forest products biorefinery, Pulp & Paper Canada, 2006, 107(6): 38-43

[2] Yu, J.-R., Zhang, Z., Chi, C.-C., An inquiry into a quick determination method for the pentosan in hemicellulose preextraction liquor from eucalyptus Chips, China Pulp and Paper, 2007, 26(11):10-13

[3] Chai X-S, Zhu J-Y and Li J, A Simple and Rapid Method to Determine Hexeneuronic Acid Groups in Chemical Pulps, Journal of Pup and Paper Science, 2001, 27(5): 165-170

Novel Green Liquor Pretreatment of Loblolly Pine Chips to Facilitate Enzymatic Hydrolysis into Fermentable Sugars for Ethanol Production

Shu-Fang Wu[1, 2], Hou-Min Chang[1, 2], Hasan Jameel[1] and Richard Philips[1]

[1]Department of Wood & Paper Science, North Carolina State University

[2]Jiangsu Provincial Key Lab of Pulp and Paper Science and Technology, Nanjing,

Abstract: Generally, softwood species have been found very recalcitrant to enzymatic hydrolysis of the carbohydrate fractions to monomeric sugars. To solve this, loblolly pine chips were pretreated with green liquor at 16% TTA (as Na_2O on wood) at 170℃ for 800 H-factor. The yield of resulting pulp was 77% and the lignin content decreased from 29.2 to 21.6% and the total polysaccharide decreased from 62.6 to 53.8%, all based on the weight of original wood. When the pulp was subject to enzymatic hydrolysis using 40 FPU/g, only 44% of the polysaccharides in wood were converted to monomeric sugars. This conversion figure is much lower than that of mixed southern hardwoods (+75%) treated under similar conditions. If the green liquor treated pulp was further subject to either oxygen delignification or mechanical refining prior to the enzymatic hydrolysis, the conversion rate increased to 52% and 59%, respectively. Furthermore, combination of oxygen delignification and refining further increased the total sugar conversion to 76% of the total sugar in wood, approaching that of the mixed southern hardwoods.

1. Introduction

Lignocellulosic biomass is the most abundant renewable resources on earth. In the past decades, there has been a growing interest in using this biomass as feed stock for the production of bioethanol.[1, 2] Lignocellulosic biomass cannot be converted directly to ethanol, requiring several unit operations. First the polysaccharides (cellulose and hemicelluloses) are hydrolyzed to fermentable sugars, followed by fermentation of the resulting sugars to ethanol and distillation of the dilute ethanol broth to the final Product. Utilization of cellulolytic enzyme system for hydrolysis of the polysaccharides is currently an active research and development topic for bioethanol production technology. However, lignocellulosic biomass, especially softwood, has natural resistance to biological degradation because of its morphological structure and chemical composition. Thus, some kind of pretreatment is required to obtain high conversion of polysaccharides to fermentable sugars.[3, 4] Many pretreatment methods have been researched, including acid hydrolysis[5-6], wet oxidation[5, 7, 8], steam explosion[5, 9], SO_2 pretreatment[10], oxygen delignification[11], peracetic acid pretreatment[12], ammonia explosion[4] and lime pretreatment[4]. These pretreatment methods affect enzymatic hydrolysis of biomass differently, and also introduce different degrees of complexity in process technology and chemical cost / recovery. A novel pretreatment method based on green liquor was developed in our laboratory at North Carolina State University (patent pending). While the green liquor pretreatment alone works well with hardwoods[13], it gave relatively low fermentable sugars under the same conditions for softwood. In this paper, we report a novel combination of the green liquor pretreatment with two additional unit operations, oxygen delignification and refining for softwood chips that gives high conversion rate of fermentable sugars in the subsequent enzymatic hydrolysis, and requires only proven process steps, with chemicals completely compatible with a traditional kraft recovery system..

2. Material and Methods

(1) Material

Loblolly pine from a mill in southeastern United States was used in this study. The chips were screened and the accepts from 3/8” and 5/8” holes were used for pretreatment.

(2) Methods

a. Pretreatment

Pretreatment was carried out in a 7-liter M&K Digester with 700 OD grams of chips. The chips were

cooked with green liquor at three different alkali charges (12, 16 and 20% TTA as Na_2O on wood, 25% sulfidity) and the contents pulped to the target H Factor of 800 at a maximum temperature of 170 ^{o}C with liquor to wood ratio of 4. After pulping the samples were washed overnight. The yield was measured by centrifuging the chip mass and measuring the consistency and total weight. The chips were then disintegrated using a refiner at .005 inch gap and then screened using a .008 inch screen plate. The rejects were refined with a disk gap of .001 inch and then added back to the accepts. The pulp was then centrifuged and fluffed for further processing.

b. Oxygen delignification

Oxygen delignification was carried out in a 2.8 L reactor in an oven heated by blowing hot air. GL pulp (100 g OD) was treated with 5% NaOH on pulp at 10% consistency under100 psig oxygen pressure and at 110 ^{O}C for 60 min. (excluding time to temperature of 45 min). After delignification, the pulp was washed with cold water, centrifuge and fluffed. Pulp yield was measured by the consistency and total weight.

c. Refining

Pulp (30 g OD) was refined in a PFI mill at 10% consistency for 9,000 revolutions. After refining, pulp was collected and hydrolyzed with enzyme without washing.

d. Enzymatic hydrolysis

Enzymes used in this work were kindly provided by Novozymes. An enzyme mixture was prepared by mixing cellulase (NS50013), xylanase (NS50014) and β-glucosidase in the ratio of 1 FPU:1.2 FXU:1 CBU, respectively. This enzyme mixture was used throughout this work. Enzyme dosage is expressed in FPU, but it includes the other two enzymes in the ratio shown above.

Enzymatic hydrolysis was carried out with 2 g of pulp at 5% consistency with 40 FPU at pH 4.8 (acetate buffer) and 50 ^{O}C for 48 hours. After enzymatic hydrolysis, the mixture was centrifuged. The supernatant was collected, boiled for 5 min. and centrifuged again. The aliquot of the supernatant was used for determination of sugar content. The residue from the enzymatic hydrolysis was washed and centrifuged (3 times), freeze-dried in water suspension and weighted for weight loss.

e. Analytical methods

Sugar analysis was carried out with ion chromatography (ICS-3000, Dionex) using CarboPac^{TM}PA1 (2×250mm) as analytical and CarboPac^{TM}PA1 (4×50mm) as guard column. Sodium hydroxide solution (0.1 mole/L) was used as eludant. Aliquots of Klason lignin filtrate and enzyme hydrolysate were used to determine sugar content for GL pulps and enzymatic hydrolysate, respectively.

Lignin content is determined according to the TAPPI Standard Method T222.

3. Results and discussion

One special feature of the present process that differs from other pretreatment methods is the use of green liquor (GL) from a pulp mill as a pretreatment chemical. The inorganic chemical used is recovered and the dissolved organics and residual lignin are burned to produce energy, thereby the operating costs are minimized. The process and the equipment used are all proven technologies used in many pulp mills and thus involve low risk for investment. The second special feature is that, unlike other pretreatment methods, all fermentable sugars are recovered in a single step, the enzymatic hydrolysis stage. This feature avoids the need to collect fermentable sugars from both pretreatment and enzymatic hydrolysis stages, resulting in diluted sugar concentration for fermentation to ethanol. This second feature requires that the pretreatment retains as much polysaccharides as possible in the pulp while at the same time facilitate the subsequent enzymatic hydrolysis for high sugar conversion.

Chemical composition of wood, green liquor pretreated pulps at 3 different temperatures (GL pulps) as well as oxygen delignified GL pulps (GL-O) are given in Table 1. As can be seen, the lignin content decreased from 29.2% to 20.2-22.4%, a decrease of 7-9% based on wood, depending on TTA charged. Approximately about equal amount of carbohydrates was also lost during the pretreatment, mainly mannan as expected due to well known peeling reactions. It is noteworthy that little glucan was lost during the GL pretreatment. Surprisingly, subsequent oxygen delignification only removed an additional 2% lignin (on wood) and is accompanied by 1-4

% lost in polysaccharides.

Table 1 Yield and chemical composition of GL pulps and oxygen delignified GL pulps

	Polysaccharides (% on wood)					Lignin %	Total %	Yield % on wood
	Glucan	Mannan	Other Hexosan	Pentosan	Sum			
Wood	44.3	10.0	1.8	6.5	62.6	29.2	91.8	
GL20	44.0	3.4	1.0	5.4	53.8	20.2	74.0	76.5
GL16	44.4	3.6	1.0	5.5	53.8	21.6	75.4	77.0
GL12	44.0	4.1	1.1	5.8	55.0	22.4	77.4	78.6
GL20-O	41.4	3.3	0.9	5.3	50.4	18.5	68.9	72.3
GL16-O	41.2	3.3	0.9	5.3	50.7	19.5	70.2	73.8
GL12-O	43.4	3.9	1.1	5.5	53.9	20.1	74.0	77.0

The effects of GL pretreatment, oxygen delignification and refining on weight loss of enzymatic hydrolysis and total fermentable sugar yield in the hydrolysate are shown in Table 2. Both weight loss and total sugar yield are indicators of the enzymatic hydrolysis efficiency. As can be seen in Table 2, the numbers are very close in every treatment, indicating that weight loss is as good an indicator of enzymatic hydrolysis as the total sugar yield in hydrolysate. These results also indicate that little lignin becomes soluble during the enzymatic hydrolysis. Green liquor pretreatments resulted in conversion of 45% of the polysaccharides in wood into fermentable sugars. Total alkali charge (TTA) in GL pretreatment appeared to have only minor effect. Both refining (R) and oxygen delignification (O), each carried out alone, significantly improved enzymatic hydrolysis efficiency. In both cases, the effect of TTA in GL pretreatment became significant, higher TTA giving higher sugar conversion. When both refining and oxygen delignification were employed with GL pretreatment, over 75% of the total polysaccharides in wood were converted to fermentable sugars. The synergetic effect of the combined oxygen delignification and refining on total sugar conversion is especially noteworthy.

Table 2 Enzymatic hydrolysis of GL pretreated pulp

	Weight loss (%)		Total sugar yield in hydrolysate (%)		Sugar conversion* (%)
	On pulp	On Wood	On pulp	On wood	
GL20	38.4	29.4	37.7	28.8	46.5
GL16	33.4	25.7	35.6	27.4	44.3
GL12	30.8	24.2	34.0	26.7	43.6
GL20-R	51.0	39.0	51.3	38.9	63.5
GL16-R	47.2	36.3	47.4	37.0	59.0
GL12-R	43.8	34.4	42.6	33.1	51.1
GL20-O	49.3	35.6	47.0	34.0	54.9
GL16-O	44.5	32.8	43.3	32.0	51.7
GL12-O	35.1	27.0	33.2	28.6	41.4
GL20-O-R	65.9	47.7	64.2	46.4	75.3
GL16-O-R	66.4	49.0	63.6	46.9	76.3
GL12-O-R	59.4	45.7	60.0	46.2	74.6

* Sugar conversion=Weight loss (on wood) / Total sugar in wood×100%

4. Conclusion

Enzymatic hydrolysis efficiency of softwood can be greatly improved by green liquor pretreatment followed by oxygen delignification and refining, all being proven technologies. Over 75% of the total polysaccharides in wood can be converted to fermentable sugars.

Acknowledgement

This research is financially supported by a consortium of industrial members (Wood to Ethanol Consortium) through a grant to North Carolina State University. The authors are grateful to the members of the Consortium.

References

[1] Ragauskas AJ, Williams CK, Davison BH, Britovsek G, Cairney J, Eckert CA, Frederick Jr WJ, Hallett JP, Leak DJ, Liotta CL, Mielenz JR, Murphy R, Templer R, Timothy Tschaplinsk. The path forward for biofuels and biomaterials [J]. Science, 2006, 311: 484–489

[2] Faaij A. Modern biomass conversion technologies. Mitigation and Adaptation Strategies for Global Change, 2006 (11): 343-375

[3] Wyman CE, Dale BE, Elander RT, Holtzapple M. Coordinated development of leading biomass pretreatment technologies. Bioresour Technol, 2005, 96: 1959-1966

[4] Mosier N, Wyman C, Dale B, Elander R, Lee YY, Holtzapple M, Ladisch M. Features of promising technologies for pretreatment of lignocellulosic biomass. Bioresour Technol, 2005, 96: 673-686

[5] Thomsen MH, Jørgensen ATH. Preliminary results on optimization of pilot scale pretreatment of wheat straw used in coproduction of bioethanol and electricity. Appl Biochem Biotech, 2006, 130: 448-460

[6] Mielenz JR. Ethanol production from biomass: technology and commercialization status. Curr Opin Microbiol, 2001, 4(3): 324-329

[7] Varga E, Schmidt AS, Réczey K, Thomsen AB. Pre-treatment of corn stover using wet oxidation to enhance enzymatic digestibility. Appl Biochem Biotech, 2003, 104: 37-50

[8] Klinke HB, Ahring BK, Schmidr AS, Thomsen AB. Characterization of degradation products from alkaline wet oxidation of wheat straw. 2002, Bioresour Technol, 82: 15-26

[9] Kurabi, A, Berlin, A, Gilkes, N, Kilburn D, Bura R, Robinson J, Markov A, Skomarovsky A, Gusakov A, Okunev O, Sinitsyn A, Gregg D, Xie D, Saddler J. Enzymatic hydrolysis of steam-exploded and ethanol organosolv-pretreated Douglas-fir by novel and commercial fungal cellulases. Appl Biochem Biotech, 2005, 121-124: 219-230

[10] Sassner P, Galbe M, Zacchi G. Steam pretreatment of Salix with and without SO_2 impregnation for production of bioethanol. Appl Biochem Biotech, 2005, 124: 1101-1117

[11] Draude KM, Kurniawan CB, Duff SJB. Effect of oxygen delignification on the rate and extend of enzymatic hydrolysis of lignocellulosic material. Bioresour Technol, 2001, 79: 113-120

[12] Teixeira LC, Linden JC, Schroeder HA. Alkaline and peracetic acid pretreatments of biomass for ethanol production. Appl Biochem Biotech, 1999, 77-79: 19-34

[13] Jin, Y., Chang, H-m., Jameel, H. and Phillips, R. J., Green Liquor Pretreatment of Mixed Southern Hardwoods to Enhance Enzymatic Hydrolysis for Bioethanol Production, manuscript under preparation.

On the Similarities between Juvenile Wood and Compression Wood in Loblolly Pine (*Pinus taeda* L.)

Ting-Feng Yeh[1,2], Barry Goldfarb[3], Hou-min Chang[2], Ilona Peszlen[2], Jennifer L. Braun[4] and John F. Kadla[4]

[1] Current address: School of Forestry and Resource Conservation, National Taiwan University

[2] Department of Wood and Paper Science, North Carolina State University

[3] Department of Forestry and Environmental Resources, North Carolina State University

[4] Forest Science Center, University of British Columbia

1. Introduction

Due to the environmental concern, the land available for wood production is depleted. In order to meet the wood demand for the future challenges, more wood with target characteristics will be produced from limited forestland by intensively managed fast-growing plantation. Forest product has shifted from old-growth to short-rotation juvenile stock. In softwood, juvenile wood (JW) is always accompanied with compression wood (CW). They both have high lignin content, low cellulose content, and low pulp yield. There is a common belief that JW is the same as CW. In order to resolve whether JW is truly identical to CW, twenty-four rooted cuttings of one loblolly pine clone were planted in Phytotron unit for 9 month under normal, artificial bending, and windy condition. Our analyses showed that JW is very different from CW in morphological structures. The metabolites profiling showed that CW has quite different metabolites level when compared to JW. Further chemical analyses showed that JW and CW are very different in chemical compositions. In addition to discussing the chemical compositions, milled wood lignin (MWL) from each different group of woods is isolated, and the detail chemical structures of lignin are quantified and compared. These results provide new evidences that whether JW is truly the same as CW.

2. Material and Methods

Twenty-four rooted cuttings of one loblolly pine (*Pinus taeda*) clone were grown in Phytotron (North Carolina State University) for 9 months. The chamber photoperiod and temperature were 18 hr at 28°C under incandescent lighting, and 6 hr at 20°C in the dark. The trees were assigned randomly into three environmental conditions, i.e. control, bending, and augmented wind. The control and bending trees (8 trees each) were in the reduced wind chamber. Another 8 trees were in the augmented wind chamber with two oscillating fans. The tree sway frequency was about 5 times/min. The bending trees were rendered at 45° to the perpendicular stems, when the new growth stem reached about 30 cm, another bending was applied. The tress were bent a total of 3 to 4 times during the 9-month period. All wood samples were collected from the same relative height of each of the stems. They were separated into 5 groups, control normal wood (CTNW), bending opposite wood (BOW), bending compression wood (BCW), windy opposite wood (WOW), and windy compression wood (WCW).

Wood blocks from the same relative height of stem were softened in water and sliced (10μm in thickness) along the radial direction using a microtome (Spencer Lens Co., Buffalo, NY). The microtome slices were stained with Safranin O and photographed with a Nikon light microscope (model: Eclipse E200). Fiber length, width, coarseness, kink and curl indexes were recorded by a fiber quality analyzer (FQA, Op Test Equipment, Inc., Hawkesbury, ON). Wood extractives were removed according to TAPPI standard T265 om-88. The total lignin content was determined by the Klason lignin method. Both Klason lignin and acid soluble lignin were combined to give total lignin content. The holocellulose samples for fiber quality analysis (FQA) are prepared according to Yokoyama *et al.* [*1*]. The monomeric sugar analysis was carried out according to the procedures of Coimbra *et al.* [*2*]. Nitrobenzene oxidation was performed according to the method of Chen [*3*]. The stereo structures (*erythro* and *threo* forms) of arylglycerol-β-aryl ether linkages of lignin were determined by ozonation analysis according to the method of Akiyama *et al.* [*4*]. MWLs are prepared according to the method of Björkman [*5*]. The preparation of acetylated MWLs were carried out according to Adler [*6*]. All NMR spectra

were recorded on a Bruker AVANCE 300MHz spectrometer at 300K using DMSO-d_6 as the solvent according to Capanema *et al.* [*7*]. The polar phase metabolite analysis of xylem tissue by GC-MS was carried out by the protocol of Morris *et al.*[*8*].

3. Results and discussion

In order to resolve whether juvenile wood is truly identical to compression wood, loblolly pines were planted in 3 different environments, constrained bending, excess wind and the unaltered control, yielding 5 different wood specimens. Our results show that juvenile wood is different from compression wood in morphology and chemical characteristics, including tracheid shape and length (Table 1), sugar composition, and lignin structure (Table 2). Compared to the compression wood produced by artificial bending, the wood produced in the windy environment can be classified as a mild type compression wood. In fact, metabolic profiling of these two wood samples from the same trees that were analyzed for chemical analyses in developing xylem in this study shows they are similar in metabolic complexities (Figure 1). Our metabolite results support this similarity and extend it to metabolite pools during wood formation.

References

[*1*]Yokoyama, T.; Kadla, J. F.; Chang, H. M. (2002) Microanalytical method for the characterization of fiber components and morphology of woody plants. *J. Agric. Food Chem.* 50:1040-1044.

[*2*]Coimbra, M. A.; Delgadillo, I.; Waldron, K. W.; Selvendran, R., Isolation and analysis od cell wall polymers from olive pulp. In *Modern Methods of Plant Analysis*, Linsken, H. F.; Jackson, J. F., Eds. Springer-Verlag, Berlin, 1996; Vol. 17, pp 33-44.

[*3*]Chen, C. L., Nitrobenzene and cupric oxide oxidation. In *Methods in Lignin Chemistry*, Lin, S. Y.; Dence, C. W., Eds. Springer-Verlag, Berlin, 1992; pp 301-321.

[*4*]Akiyama, T.; Sugimoto, T.; Matsumoto, Y.; Meshitsuka, G. (2002) Erythro/threo ratio of b-O-4 structures as an important structural characteristic of lignin. I: Improvement of ozonation method for the quantitative analysis of lignin side-chain structure. *J. Wood Sci.* 48:210-215.

[*5*]Bjorkman, A. (1956) Studies on finely divided wood. Part I. Extraction of lignin with neutral solvents. *Svensk Papperstidn* 59:477-485.

[*6*]Adler, E.; Brunow, G.; Lundquist, K. (1987) Investigation of the acid-catalyes alkylation of lignins by means of NMR spectroscopic methods. *Holzforschung* 41:199-207.

[*7*]Capanema, E. A.; Balakshin, M. Y.; Kadla, J. F. (2004) A comprehensive approach for quantitative lignin characterization by NMR spectroscopy. *J. Agric. Food Chem.* 52:1850-1860.

[*8*]Morris, C. R.; Scott, J. T.; Chang, H. M.; Sederoff, R. R.; O'Malley, D.; Kadla, J. F. (2004) Metabolic profiling: a new tool in the study of wood formation. *J. Agric. Food Chem.* 52:1427-1434.

[*9*]Balakshin, M. Y.; Capanema, E.; Goldfarb, B.; Frampton, J.; Kadla, J. F. (2005) NMR studies on Fraser fir lignins. *Holzforschung* 59:488-496.

Table 1. Different fiber properties[#]

Group	Length, mm[$]	Width, μm	Coarseness, mg/m	Curl index	Kink index
CTNW	1.221 A*	29.1 A	0.128 A	0.0179 A	0.03 A
WOW	1.317 A	29.8 A	0.142 A	0.0195 B	0.04 A
WCW	1.043 B	24.8 B	0.210 B	0.0283 C	0.28 B
BOW	1.088 B	23.5 B	0.134 A	0.0183 BC	0.03 A
BCW	0.852 C	19.4 C	0.200 B	0.0276 C	0.35 C

[#]: Each property of each group is expressed as the mean value.

[$]: Length weighted length

[*]: The letters (A,B,C) indicate significant differences using Tukey-Kramer HSD test at α=0.05 level.

Table 2. Major differences of functional groups and inter-unit linkages between five MWLs [$].

Structures[#]	CTNW	WNW	WCW	BOW	BCW
Total H units	0.05	0.04	0.11	0.04	0.12
Conjugated	0.01	0.01	0.02	0.01	0.02
Non-conjugated	0.04	0.03	0.09	0.03	0.10
Total OH	1.42	1.43	1.47	1.40	1.48
Phenolic OH	0.28	0.28	0.31	0.28	0.31
Aliphatic OH	1.14	1.15	1.16	1.12	1.17
5-5’ etherifed	0.10	0.12	0.15	0.09	0.14

[#]: The peak assignments and calculations are according to the works of Capanema et al. [7] and Balaksihn et al. [9].

[$]: The numbers are expressed as per aromatic ring.

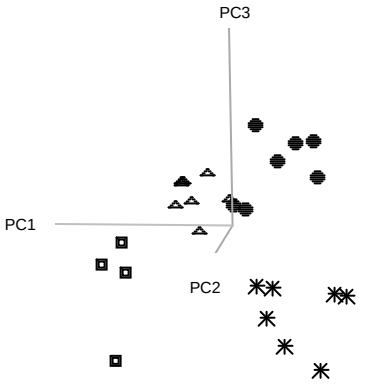

Fig. 1 Metabolic phenotypic clustering results for different xylem tissues: △, control normal wood (CTNW); ✳, bent compression wood (BCW); ●, bent opposite wood (BOW); □, windy wood (WW).

The Preparation and Characterization of New high-temperature fire-resistant insulation board

Chuan-Shan Zhao, Jin-Jiang Pang, Jing-Jing Wang and Zhi-Qiang Li

Key Lab of Paper Science and Technology of Ministry of Education, Shandong Institute of Light Industry, Jinan 250353, China

Email:ppzcs78@163.com

Abstract: This paper through the wet forming Vacuum filter process, uses the aluminosilicate fiber-based materials and high temperature resistant adhesive binder to prepare for aluminosilicate -fiber insulative materials which have high-performance and high-temperature , in the good adhesive and grout concentration conditions, add no glues, added fiber, researches that how the cycle time influences the concentration of glue, cardboard bulk density, the impact of adhesive retention rate, and studies how the thermal conductivity influences the board density. The best experimental conditions for the liquid concentration is 9.41 percent, cycle time is 28h (after the glue to be added), when the bulk density fiberboard for aluminosilicate is 290 ± 5kg/m^3, the insulation board can have a good CD and can be resistant 1200 ℃

Thermal insulation material is usually a light, loose, porous, small thermal conductivity. Because of its unique insulation, thermal insulation, fire safety, this is widely used in steel, furnaces, pipelines and chemical industry. [1].

Aluminosilicate refractory fiber insulation for industrial kilns as the earliest and most widely used application areas,[2]. However, the production of aluminum silicate fiber mostly by hand, this process step was simple, but wasting a lot of manpower, material resources, and a lower yield. For this problem, this paper, the application Zhangqiu Anlert ecological ceramic fibers produced by silicate fiber paper machine, add the laboratory-made high-temperature adhesive conditions, automated production to meet market demand.

1. Experimental materials and apparatus

Aluminum silicate fibers, Fiber Co., Ltd. Shandong Zhangqiu Anlert eco-production, a diameter of 2 ~ 6um, whose main component is Al_2O_3 content of ≥ 46%, Al_2O_3+SiO_2 content of ≥ 99%, the other as ≤ 1%, long-term use temperature of to 1260 ℃.

High-temperature adhesives, made in laboratory, PH=10, can be stored for a long

Anlert ecological Ceramic Fiber Co., Ltd in Zhangqiu. aluminum silicate fiberboard continuous production equipment.

Thermal conductivity detector

(1) Process

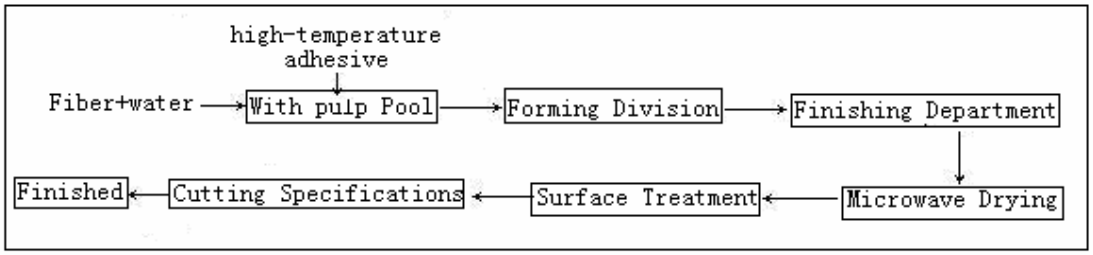

(2) Determination of thermal conductivity

Experimental steady-state thermal conductivity of test plate method, steady-state plate method measuring principle for the Fourier heat conduction law, for a thickness of δ, cross-section area S of the parallel plate, both sides maintain a stable temperature T_1 and T_2 (T_1>T_2), d, within a circular plate specimen to generate a pass along the vertical one-dimensional heat flow q, according to the Fourier heat conduction equation can be obtained with a one-dimensional vertical heat flow circular plate thermal conductivity of the sample λ formula:

$\lambda = (d \times q) \div [\Delta T \times (\pi \times d^2) / 4]$

q—a unit of time flowing through S($S=\pi d^2/4$) area of heat flow, w.

ΔT—a diameter d of the circular plate specimen thickness δ along the direction of the temperature difference (T_1-T_2), K.

2. Results and discussion

(1) High Temperature Characterization of aluminum silicate fiber insulation board

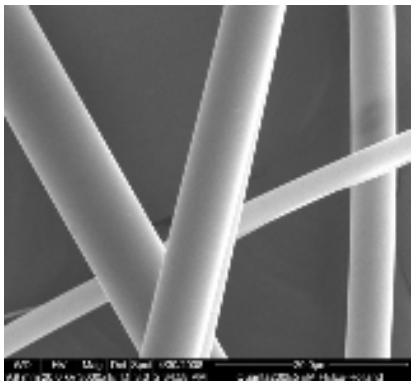

Fig. 2 Microstructure of aluminum silicate fibers SEM diagram (× 3000)

From the figure it can be found in the surface of aluminosilicate refractory fibers in a smooth, showing glassy state, not easy to bond with each other, in the uniform adhesive solution, the fiber surface to be wet and soaking, to increase the cohesive force between the fibers. The system of regulating the viscosity and consistency, it has to form a uniform porous network structure. After drying, due to adhesive bonding and fiber between the intertwined, overlapping role in the formation of a certain skeleton structure of aluminum silicate fiber products.

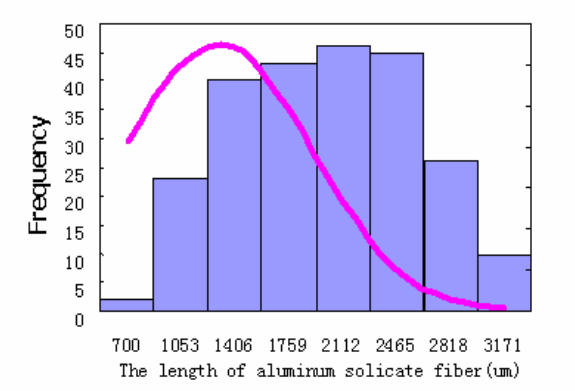

Fig.3 Histogram of silicate fibers

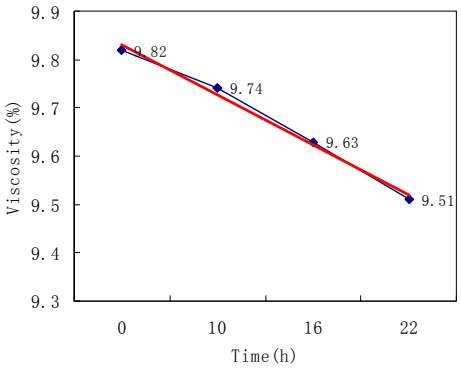

Fig.4 Cycle time of the glue concentration

Take plants out of aluminum silicate fiber injection in conventional microscope, for the length of statistics, and then in the EXCLE function to handle any application of Frequency Figure 3, from the previous figure can be, aluminosilicate fiber length in the range of 1406 ~ 2465μm, the fiber length the frequency of relatively frequent, and coniferous wood fiber length of 2.0 ~ 3.2mm, width of 30 ~ 75μm, broad-leaved wood fibers around 1mm, a width of 60μm below the aluminum silicate fiber length of wood fiber and broad-leaved coniferous wood fiber length of between the width of the microscopic measurement of value is 17μm.

(2) The cycle time of the glue concentration

Slurry from the headbox by forming the Department of suction, the finishing department press processing, plate containing glue accounts for 60% of wet-plate, this part of the glue can not be pumped into the recovery tank, reuse, cardboard The adhesive can only be played with the cardboard into the microwave drying the role of connecting fibers. From Figure 4 shows the growth over time, glue concentration decreased and lower in this part of the glue is the Retention play in cardboard binders role in enhancing the strength and hardness of

cardboard.

(3) The cycle time of the bulk density of adhesive retention rate

Table 1 At different times of the retention rate and bulk density

Time/h	Viscosity of Adhesive C/%	Before drying quality M1/kg	After drying quality M2/kg	The poor quality M1-M2/kg	Volume $V/\times10^{-3}$ m^3	Volume weight kg/m^3	Retention L/%
0	9.82	3.26	0.9	2.35	3.132	287	25.6
10	9.74	3.40	0.8	2.6	3.193	250	31.65
16	9.63	2.25	0.65	1.6	2.801	232	23.7
22	9.51	1.81	0.6	1.2	2.243	268	19.4
28	9.41	1.91	0.72	1.19	4.391	271	15.5

Note: The slurry concentration of 1%

Can be drawn from Table 1, the longer the cycle time, will continue to decrease in the concentration of adhesive, resulting in the adhesive aluminum silicate fiber retention rate decrease, when the cycle of 28 hours after the glue concentration dropped to 9.41%, glue Retention rate of 25.6% fell to 15.5% in the original, this time able to meet the strength requirement aluminosilicate fiber surface, and feel good, plate-like as shown in Figure 6, experiment with the concentration of glue at this time is better, and then copy the process of paper plates Addconstantly adhesive glue to keep the concentration of 9.41% volatility.

Tible 1shows the difference over time, changes in bulk density also will analyze the reasons may be the following situations: First, the concentration of slurry concentration process in the copy made, and there is no consistent plasma concentration fluctuations occur, such as in the boot 16 hours after the board The bulk density of 232kg/m^3, to speculate at this time the lowest possible plasma concentration; second, the speed issue, because the Ministry of molding forming process, the suction power of a larger, making network speed is not synchronized with the fabric, making sheet jointed, after a whole After pressing department decorated, there will be changes in bulk density issues; three are taken from plate-like size, due to plate in the board machine wet-plate sampling, may be operated manually weighing and measurement error. Several factors can cause the above bulk density changes.

Fig.5 Aluminosilicate fibers plate-like Digital photos

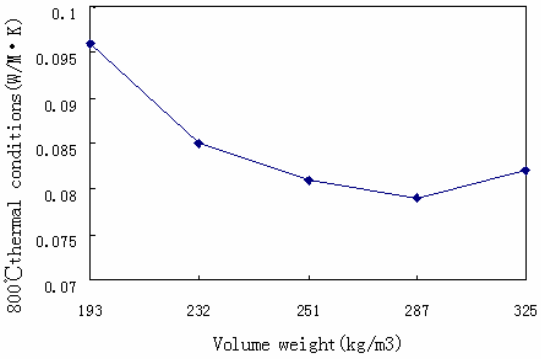

Fig.6 bulk density on thermal conductivity of aluminum silicate fiber

(4) bulk density effects on thermal conductivity

For a certain process conditions for a given insulation material, its composition, structure and fibrous tissue such as have been designated. At this time in a certain atmospheric pressure affect its thermal conductivity is the density and temperature of the main factors [3].

As can be seen from Figure 6, with the bulk density increases, 800 ℃ under the thermal conductivity of

aluminum silicate fiber gradually reduced to the most under the value, there is an upward trend in high-temperature silicate fiber insulation board generally solid phase aluminosilicate fiber and high-temperature adhesives, as well as containing 75% or more of the gas phase of the composition, density of the thermal conductivity of silicate fibers effect, in essence, reflected mainly the porosity, pore size and pore properties of the thermal conductivity rate. See Figure 7 is evident from the high-temperature insulation board, in the 190kg/m^3 ~ 290kg/m^3 bulk density within the aluminum silicate fiber thermal conductivity of the material increases with the bulk density was decreased trend.

3. Conclusion

1. With the cycle time of adhesive growth and reduce the concentration of glue, adhesive silicate fiberboard in a retention rate has also reduced the experiment to determine the optimum cycle time of 28h, the concentration of 9.41% at this time glue, adhesive retention rate for the 15.5%.
2. The thermal conductivity increased with the increase in bulk density after the first, to reduce the rising trend, the best test weight of 290 ± 5kg/m^3, the thermal conductivity of 0.079 W / M • K.
3. The use of laboratory-made high-temperature adhesive aluminum silicate fiber board can be ≤ 1200 ℃ to use, 800 ℃ plate method under steady-state thermal conductivity, bulk density of 285 ~ 290 kg/m^3 paperboard thermal conductivity of 0.079 W / M • K, and the cardboard can be cut with a good nature.

References

[1] Liu Xiaochun. Thermal insulation materials, development and construction applications. Fujian Building Materials, 1997, (4) :18-21

[2] Teneyck, John D.Seamless ceramic fiber composites articles and method and appatatus for their production：US ,4435468 [P].1984-03-06

[3] Seiji Sakurai, Kaoru Umino.Fibrous composite material for fused aluiminum:US，4622070 [P].1986-11-11

Effects of Na_2SO_3-HCHO Pretreatment on the Chemical Composition and Enzymatic Hydrolysis of Rice Straw

Lei Jing[1], Yongcan Jin[1], Hou-min Chang[2] and Zhongzheng Li[1]

[1] Nanjing Forestry University, Nanjing 210037, China

jinyongcan@njfu.edu.cn

[2] North Carolina State University, Raleigh, NC 27695, US

1. Introduction

A great deal of work has gone into the development of biofuels[1, 2]. The extent to which biofuel production competes with food production has been greatly questioned, which has led to great interest in "second generation" biofuels, derived from non-food materials, particularly lignocellulosic biomass [3-6]. Potential sources of such material include agricultural and timber industry waste, waste paper and purpose-grown plant material derived from rapidly growing non-food plants such as scrub willow, switchgrass and Miscanthus, which can be grown on land unsuited to food production[7].

Cell walls of lignocellulosic biomass have natural resistance, often called "recalcitrance", to microbial and enzymatic deconstruction. The recalcitrance of lignocellulose is a major barrier to the economical development of biobased fuels and products[8]. Processes and platforms that can efficiently and economically convert woody biomass to fuel ethanol are still lacking. Existing efforts are focused on alkaline, dilute acid, steam explosion, ammonia, and organosolv pretreatment technologies which have achieved some level of success[9, 10].

Sulfomethylation of lignin occurs while formaldehyde is added in sulfite cooking. Delignification of lignocellulotic fiber material is greatly improved since the reaction takes place on C5 of lignin structure at relatively low cooking temperature[11, 12]. The effect of sodium sulfite/formaldehyde pretreatment on chemical compositions of mixed southern hardwood was investigated, as well as on acceleration of enzymatic saccharification was evaluated in this paper.

2. Material and Methods

(1) Material

Rice straw was generously provided by Jiangsu Shenda Shuangdeng Paper Co., Ltd. Whole rice straw without classification, including stem, knot, leaf and sheath was cut to a length of 3-5 cm for pretreatment and enzymatic hydrolysis.

(2) Sodium sulfite-formaldehyde (SF) pretreatment

A ten-bomb lab-scale pulping system with oil bath was used with batch capacity of oven dry rice straw of 80 g per bomb. Rice straw was directly subjected to pretreatment using sodium sulfite and formaldehyde with molar ratio 1:1 at 150˚C and 160˚C for 1 h with Na_2SO_3 charge from 4% to 16% on the basis of bone-dry straw. Pulps obtained in accordance of above condition are expressed as SF Temp-Na_2SO_3, in which Temp and Na_2SO_3 are pretreatment cooking temperature (150 and 160˚C) and Na_2SO_3 charge (4, 8, 12, 16%), respectively. The ratio of cooking liquor to rice straw was 6 (v/w). The straw was first impregnated with the pretreatment liquor at 60˚C for 30 min. Immediately after impregnation, the temperature was raised to cooking temperature and maintained for 60 min. At the end of the pretreatment, the solid was collected and washed with hot water to remove residual chemicals and dissolved straw compounds. Pretreatment yield was calculated according to the solid loss determined from the measured wet weight and moisture content of the collected solid. The pretreatment spent liquor was collected for pH analysis.

(3) Enzymatic hydrolysis

A laboratory blender was used to defiberize the pretreated rice straw to produce substrates. Enzymatic hydrolyses of the substrates were carried out at substrate consistency of 5% (w/w) in sodium acetate buffer (pH 4.8) at 50˚C using a shaking incubator at 180 rpm. Enzyme cocktail dosage was 5 to 40 FPU/g substrate based on cellulase activity. An enzyme cocktail mixed by cellulase 50013, xylanase 50044 and β-glucosidase 50010 (1

FPU:1.2 FXU:1 CBU) was used for enzymatic hydrolysis. Excessive 50010 was used to prevent cellobiose accumulation[13]. Around 0.3% sodium azide, based on substrate slurry weight, was added into the system as antibiotic. Enzymatic hydrolysis residue and hydrolysate was separated by centrifugation. The residues were washed by deioned water three times to remove the protein and other dissolved substances. Vacuum dried residues were weighed to evaluate enzymatic hydrolysis efficiency. Hydrolysates were sampled for monomeric sugar (glucose, xylose and mannose) analysis. Each data point was the average of duplicate experiments.

(4) Analytical methods

Cellulase activity of celluclase 50013 was determined by the filter paper method[14]. Whatmann No. 1 filter paper was used as a standard substrate. Manufacturer specified activity of Novozymes 50044 and 50010 was directly used to calculate loading. Enzymatic hydrolysate was cooked in boiling water for 5 min. The hydrolysate was diluted 2000 times with the addition of fucose as internal standard. Monosaccharides were determined using an improved high-performance anion exchange chromatography (ICS-3000, Dionex) with pulsed amperometric detection (HPAEC-PAD) method. An 18 mmol/L NaOH solution prepared with degassed super-purified deionized water was used as eluent at a flow rate of 0.25 mL/min. Aliquots (5 μL) were injected after passing through a 0.22 μm nylon syringe filter. The column was reconditioned using 200 mmol/L NaOH after each three analysis. Monosaccharides were quantified with reference to standards using the same analytical procedure. The concentration of monosaccharide was corrected by calibration curve of standard sugars. The average of duplicate runs was used in reporting. Data of glucose, xylose and mannose contents were corrected to glucan, xylan and mannan for sugar yield calculation.

Klason lignin content was determined according to the TAPPI T-222 standard method. The solid materials were milled using a Wiley mill before acid hydrolysis. The hydrolysate from this determination was retained for analysis of sugars and acid-soluble lignin. Sugars were determined as described above. Acid-soluble lignin was determined by absorbance at 205 nm in a 765 UV-VIS spectrometer.

3. Results and discussion

(1) Effect of SF pretreatment on chemical compositions of rice straw

Cooking temperature and chemical charge play an important role on pulping yield. Table 1 shows that SF pulp yield levels down with the increase of sulfite and formaldehyde charge. The yield of pulp pretreated at 150˚C is around 6% to 7% higher than that pretreated at 160˚C. The pH value of spent pretreatment liquor raised with the increase of sulfite charge (Table 1) as a result of the formation of NaOH in sulfite and formaldehyde system[13, 14]. Spent liquor pH of 160˚C pretreatment is lower than that of 150˚C pretreatment, which attribute to more straw components are degraded to acidic substances at a high temperature. The pH value of 150˚C and 160˚C pretreatment spent liquor inclines to the same while Na_2SO_3 charge is over 16%.

Table 1. Effects of temperature and sulfite charge on sugar degradation, %

	SF 150-04	SF 150-08	SF 150-12	SF 150-16	SF 160-04	SF 160-08	SF 160-12	SF 160-16
Yield, %	82.7	76.7	66.8	59.8	80.3	69.1	60.6	55.2
pH	6.8	7.3	7.9	8.6	5.8	6.7	7.4	8.4

Delignification of lignocellulose is beneficial to enzymatic saccharification, but strong pulping condition also causes to serious degradation of polysaccharide. The selectivity of delignification ought to be considered to obtain more monomeric sugar in enzymatic hydrolysate. Figures 1 and 2 illustrate the effects of temperature and sulfite charge on lignin and polysaccharides degradation. With the raise of sulfite charge, the increasing range of delignification drops, while degradation of polysacchrides increases steadily. Though the removal ratio of lignin is much higher than that of sugar, too much carbohydrate loss will lower the final monomeric sugar yield.

Residual lignin in SF pulp pretreated under 160˚C is about 1% higher than that pretreated under 150˚C in pulp yield range of 55% to 85% (Fig.3). Nevertheless, polysaccharides in 160˚C pretreated pulp is lower than that in 150˚C pretreated pulp, especially at a relatively high pulp yield (Fig.4). The result clearly indicates that, the delignification selectivity of SF pretreatment under 150˚C is better than that under 160˚C.

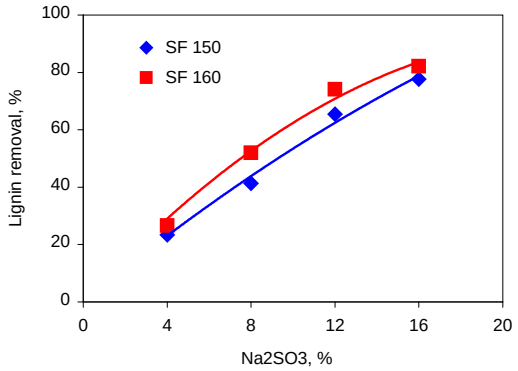

Fig.1 Effect of Na_2SO_3 charge on delignification

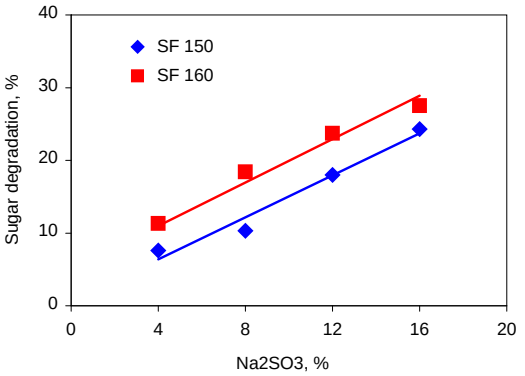

Fig.2 Effect of Na_2SO_3 charge on sugar degradation

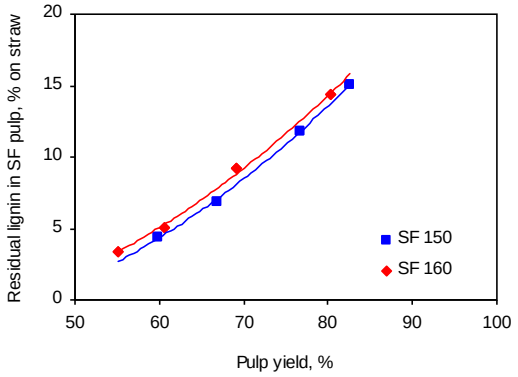

Fig.3 Relationship of yield and residual lignin of SF pretreated pulp

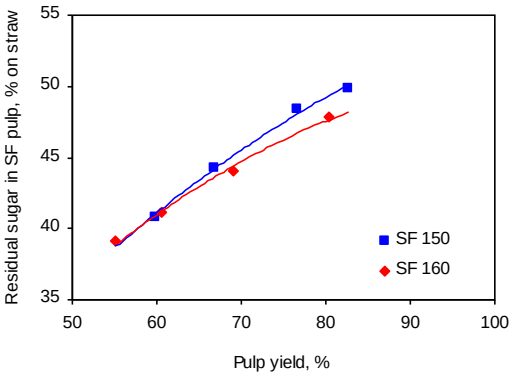

Fig.4 Relationship of yield and residual sugar of SF pretreated pulp

Table 2 Effects of temperature and sulfite charge on sugar degradation, %

Na_2SO_3	Temperature 150˚C					Temperature 160˚C				
%	Arabinan	Galactan	Glucan	Xylan	Total sugar	Arabinan	Galactan	Glucan	Xylan	Total sugar
4	12.2	34.6	7.4	5.3	7.6	28.0	46.0	9.7	9.6	11.3
8	11.0	42.7	9.4	9.7	10.3	31.8	55.7	13.9	22.4	18.4
12	29.4	58.0	13.7	21.9	18.0	40.8	66.6	16.0	32.9	23.7
16	45.1	69.2	17.3	31.6	24.3	47.9	73.0	19.5	36.5	27.5

The stability of different polysaccharides is rather different in SF cooking. The degradation degree of glucan, xylan, arabinan and galactan are listed in Table 2. Galactan and arabinan are easy to be dissolved, it does not significantly affect final enzymatic saccharification for their low content in rice straw. Glucan and xylan are the two main polymeric sugars in lignocellulose. The degradation degree of glucan and xylan is not as high as that of galactan and arabinan, however, it will directly lower the total sugar yield of enzymatic hydrolysis. While rice straw is pretreated by sulfite-formaldehyde under a strong condition, the degradation degree of glucan is over 15%, and that of xylan over 30%. Fig.5 shows the lignin and polymeric sugar content of rice straw and SF pretreated pulp on the basis of original straw.

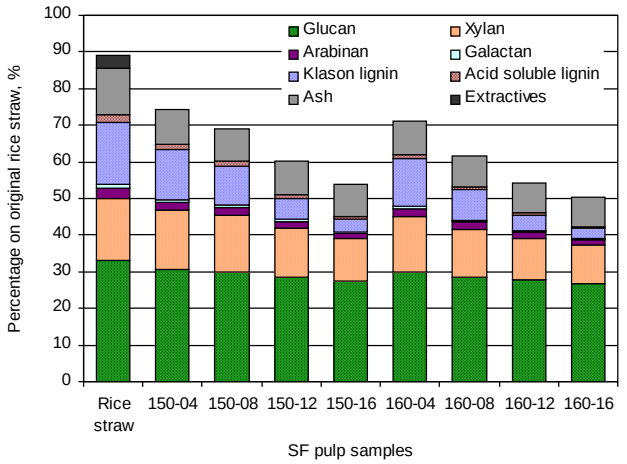

Fig.5 Main chemical compositions of SF pretreated rice straw pulp

(2) Effect of SF pretreatment on enzymatic hydrolysis of rice straw

The enzyme cocktail mixed with cellulase, xylanase and β-glucosidase was applied to investigate the effect of sulfite-formaldehyde pretreatment on improvement of enzymatic saccharification. Only 0.6% to 1.2% arbinose and no galactose were detected in all enzymatic hydrolysate. Glucose and xylose are the two main monomeric sugars in the hydrolysate. Total sugar yield corrected as the sum of glucan, xylan and arabinan based on original rice straw at different enzyme dosage is shown as Fig.6. It is clearly that more total sugar could be obtained in enzymatic hydrolysate with increasing enzyme dosage. At cellulase dosage 40 FPU/g, enzymatic hydrolysis of SF pulps pretreated by 16% Na_2SO_3 under 150˚C, and 12% Na_2SO_3 under 160˚C, reach the highest yield of about 42%. No significant sugar yield could be obtained while enzyme dosage increase from 20 to 40 FPU/g.

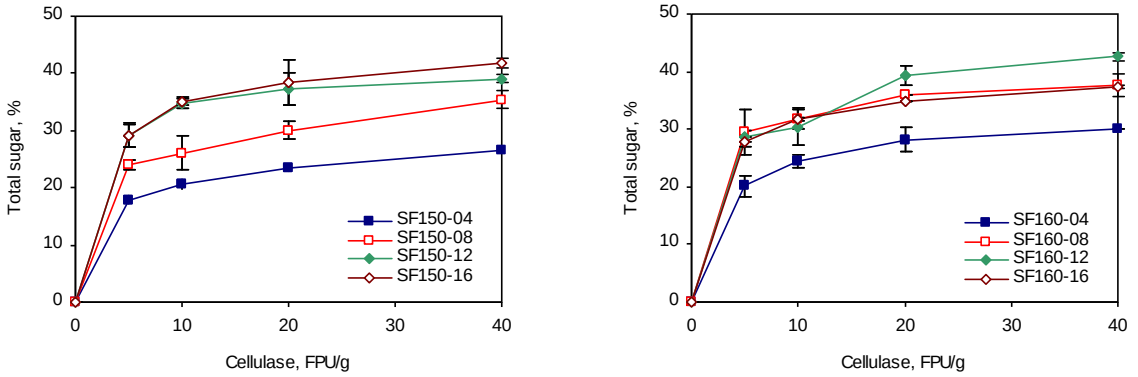

Fig.6 Effect of enzyme dosage on total sugar yield of enzymatic hydrolysis, % on original rice straw

The enzymatic hydrolysis conversion of glucan, xylan and total sugar on the basis of sugars in original rice straw are shown in Tables 3 to 5. Conversion ratio of glucan is higher than xylan due to more xylan is removed in pretreatment. More than 75% of polymeric sugars are converted to monosaccharides under optimized pretreatment and enzymatic hydrolysis conditions. It indicates that sulfite-formaldehyde pretreatment greatly improves the efficiency of enzymatic sacharification.

Table 3 Enzymatic hydrolysis glucan conversion, % on glucan in original rice straw

FPU/g	SF 150-04		SF 150-08		SF 150-12		SF 150-16		SF 160-04		SF 160-08		SF 160-12		SF 160-16	
pulp	avg	stdev	avg	stdev	avg	stdev	avg	stdev	avg	stdev	avg	stdev	avg	stdev	avg	stdev
5	38.3	1.3	49.0	1.8	60.5	3.7	60.2	4.1	41.9	3.9	60.9	7.6	60.3	1.6	58.3	1.4
10	43.2	1.8	53.3	5.5	71.9	1.9	73.4	1.7	50.5	2.5	65.7	3.7	64.2	7.0	67.5	0.5
20	48.6	1.0	61.3	2.4	77.6	5.7	79.8	6.1	58.4	4.4	73.9	0.1	82.2	3.0	73.9	0.4
40	54.4	0.2	71.7	2.8	80.6	0.9	86.5	1.7	61.9	0.0	77.0	3.3	88.8	1.4	78.5	0.5

Table 4 Enzymatic hydrolysis xylan conversion, % on xylan in original rice straw

FPU/g	SF 150-04		SF 150-08		SF 150-12		SF 150-16		SF 160-04		SF 160-08		SF 160-12		SF 160-16	
pulp	avg	stdev	avg	stdev	avg	stdev	avg	stdev	avg	stdev	avg	stdev	avg	stdev	avg	stdev
5	27.6	1.0	41.0	1.3	48.8	4.2	49.3	4.2	34.3	2.8	50.4	7.8	46.9	2.5	46.2	1.4
10	33.2	1.3	44.8	5.4	58.4	1.2	58.4	0.6	41.5	2.0	53.6	2.4	49.3	5.2	51.0	0.3
20	38.8	1.2	51.8	3.4	62.2	4.9	65.5	7.3	48.5	4.2	62.0	0.1	65.5	3.5	56.3	0.3
40	45.0	0.2	62.3	2.6	66.8	2.4	72.1	1.5	52.2	0.2	65.4	5.3	71.7	1.7	61.7	0.2

Table 5 Enzymatic hydrolysis total sugar conversion, % on polymeric sugar in original rice straw

FPU/g	SF 150-04		SF 150-08		SF 150-12		SF 150-16		SF 160-04		SF 160-08		SF 160-12		SF 160-16	
pulp	avg	stdev	avg	stdev	avg	stdev	avg	stdev	avg	stdev	avg	stdev	avg	stdev	avg	stdev
5	33.1	1.2	44.4	1.5	54.1	3.8	54.0	3.9	37.4	3.4	54.8	7.3	53.1	1.9	51.6	1.4
10	38.1	1.6	48.4	5.3	64.4	1.6	65.1	1.3	45.2	2.2	58.8	3.1	56.3	6.0	58.8	0.4
20	43.3	1.0	55.7	2.7	69.1	5.2	71.4	7.4	52.3	4.1	66.7	0.1	72.8	3.0	64.5	0.1
40	49.0	0.2	65.7	2.6	72.5	1.3	77.7	1.6	55.7	0.1	69.7	3.7	79.0	1.4	69.1	0.4

4. Conclusion

1. Lignin in rice straw could be effectively removed in SF pretreatment. Sugar loss reaches 15% to 20% at 50% lignin removal. Delignification selectivity of SF pretreatment under 150˚C is better than that under 160˚C.
2. At cellulase dosage 40 FPU/g, enzymatic hydrolysis of SF pulps pretreated by 16% Na_2SO_3 under 150˚C, and 12% Na_2SO_3 under 160˚C, reach the highest yield of about 42% based on original rice straw.
3. A great improvement of enzymatic sacharification of SF pretreated rice straw is obtained. More than 75% of polymeric sugars are converted to monosaccharides under optimized conditions.

References

[1] Antoni, D, Zverlov, VV, Schwarz, WH. Biofuels from microbes. Appl Microbiol Biotechnol 2007; 77: 23–35.

[2] Dale, B. Biofuels: thinking clearly about the issues. J Agric Food Chem 2008; 56: 3885–3891.

[3] Chang, MCY. Harnessing energy from plant biomass. Curr Opin Chem Biol 2007; 11: 677–684.

[4] Kumar, R, Singh, S, Singh, OV. Bioconversion of lignocellulosic biomass: biochemical and molecular perspectives. J Ind Microbiol Biotechnol 2008; 35: 377–391.

[5] Wackett, LP. Biomass to fuels via microbial transformations. Curr Opin Chem Biol 2008; 12: 187–193.

[6] Yuan, JS, Tiller, KH, Al-Ahmad, et al. Plants to power: bioenergy to fuel the future. Trends Plant Sci 2008; 13: 421–429.

[7] Heaton, EA, Dohleman, FG, Long, SP. Meeting US biofuel goals with less land: the potential of Miscanthus. Global Change Biol 2008; 14: 2000–2014.

[8] Himmel, ME, Ding, SY, Johnson, DK, et al. Biomass recalcitrance: engineering plants and enzymes for biofuels production. Science 2007; 315: 804–807.

[9] Mosier, N, Wyman, C, Dale, B, et al. Features of promising technologies for pretreatment of lignocellulosic biomass. Bioresour Technol 2005; 96: 673–686.

[10] Pan, XJ, Arato, C, Gilkes, N, et al. Biorefining of softwoods using ethanol organosolv pulping: preliminary evaluation of process streams for manufacture of fuel-grade ethanol and co-products. Biotechnol Bioeng 2005; 90: 473–481.

[11] Ohi, H., Nakano, J., Ishizu, A. Sodium sulfite-formaldehyde-quinone cooking. II. Delignification of softwoods and hardwoods. Mokuzai Gakkaishi 1990; 36(2): 112-119.

[12] He, W, Tai, D, Lee Z. Effect of formaldehyde during alkaline sulfite pulping of wheat straw. Trans China Pulp Paper. 1994, 9: 1–7.

[13] Emmel, A, Mathias, AL, Wypych, F, et al. Fractionation of Eucalyptus grandis chips by dilute acid-catalysed steam explosion. Bioresour Technol 2003; 86: 105–115.

[14] Wood, TM, Bhat, M. Methods for measuring cellulase activities. In: Colowick, S.P., Kaplan, N.O. (Eds.), Methods in Enzymology. Biomass (Part a, Cellulose and Hemicellulose), vol. 160. Academic Press, New York, 1988; pp. 87–112.

The current status and tendency of waste paper recycling in China

Q. X. Hou, W. Liu, Y. M. Hong
Tianjin Key Laboratory of Pulp & Paper,Tianjin University of Science ＆ Technology,
Tianjin 300457, China

Abstract: The current status and tendency of waste paper recycling and processing technologies in China's paper industry are analyzed. It is pointed out that China's paper industry has been facing the problem of high dependence on imported waste paper resources. The relative measures that should be taken are proposed in order to improve domestic waste paper recycling.

The recycling of waste paper can bring substantially economic and environmental benefits such as less contamination, lower consumption of virgin fiber and energy and better protection of forest resources. It has become an essential aspect of sustainable development strategy. The waste paper has taken about 40% of the total fiber resources all around the world, and it is predicted that the world's waste paper consumption would be up to 225 million tons till 2010. But the low usage and high reliance on imported waste paper has been a critical problem in China.

The current status of waste paper recycling in China mainland

Table 1 2001-2008 waste paper recycling Stat.

Year	2001	2002	2003	2004	2005	2006	2007	2008
Output of paper &board/ million tons	32.0	37.8	43.0	49.0	56.0	65.0	73.5	79.8
Consumption of paper &board/ million tons	36.83	44.15	48.06	54.39	59.30	66.00	72.90	79.35
Consumption of pulps/ million tons	29.80	34.70	39.10	44.55	52.00	59.92	67.69	73.60
Quantity of recycling/ million tons	10.13	13.38	14.62	16.51	18.09	22.63	27.65	31.28
Rate of recycling/%	27.5	30.3	30.4	30.4	30.5	34.3	37.9	39.4
Usage of recycled pulp/ million tons	13.10	16.20	19.20	23.05	28.10	33.80	40.17	44.36
Proportion of recycled pulp/%	44.0	47.0	49.1	51.7	54.0	56.4	59.3	60.3
Quantity of waste paper imported/ million tons	6.24	6.87	9.38	12.30	17.03	19.62	22.56	24.20

Note：Quantity of recycled pulp=Quantity of waste paper×0.8

It is apparent that the waste paper utilization rate of the mainland is going up with the development of paper making industry in an investigation of China Paper Association. As it is shown in Table 1 that the usage of waste paper rises to 44.390 million tons in 2008 from 13.100 million tons in 2001, and the growth is 239%. The utilization rate of recycled pulp rises by 16.0% from 44.0% in 2001 to 60.3% in 2008. And the proportion of imported waste paper has a significant growth of 288% from 6.240 million tons in 2001 to 242.00 million tons in 2008.

There are three main driving factors for the rapid growth of waste paper usage: the national industrial policy adjustment, the lackage of wood resources and the better quality of imported waste paper than that of domestic.

The most important cause for the rapid growth of waste paper usage is the fast-growing consumption of paper and cardboard. We consumed 79.350 million tons of paper and paperboard in 2008 and 36.830 million tons in 2001, so the growth is 115%. The importation of wood pulp is 9.520 million tons in 2008 (Table 2) and in 2001 it is 4.900 million tons. It accounts for only 13% of the total pulp consumption though it rises by 94.3%. The domestic non-wood pulps maintain at about 13.000 million tons with a declining proportion of the total usage of pulps. So the rapid growth of waste paper consumption and modest increase of domestic wood pulp output is necessary to make up the pulp consumption gap especially against the background that the consumption

structure is continuously optimized and the environmental requirements gets increasingly strict.

Table 2 China's consumption of pulps in 2008

Types of pulps	2007		2008	
	Consumption/million tons	Proportion/%	Consumption/million tons	Proportion /%
Total	67.69	100	73.60	100
Wood pulp	14.50	22	16.24	22
Imported wood pulp	8.45	12	9.52	13
Recycled pulp	40.17	59	44.39	60
Imported recycled pulp	18.05	27	19.36	26
Non-wood pulp	13.02	19	12.97	18

The national industrial policy adjustment is also an important drive. It asks for increasingly recycling of domestic waste paper and larger proportion of wood pulp. The higher content of wood pulps and nearly no non-wood pulps in the imported waste paper leads to the better quality of imported waste paper than that of domestic.

The current status and tendency of waste paper processing technologies in China's paper industry

The waste paper processing technologies in mainland developed relatively slowly, particularly the deinking and thermal dispersion. But we made great progress in the recent 10 years, including increasingly sophisticated technologies and advanced equipment overseas. At the same time, China's scientific research institutes and some machinery plants are working hard to produce the key equipments in the recycling pulp production. At present, the complete sets of equipments for small or medium-scale paper recycling projects and some of the large-scale projects can be produced domestically. Just take the former Huayi Light Industry Machinery Co. Ltd. as an example, it developed a "400 tons / day cardboard box waste treatment system" and a "150 tons / day deinking line".

In the hydraulic pulping process, the main aquapulpers used are the horizontal drum aquapulper and the vertical D-aquapulper. The horizontal drum aquapulper which has a continuous, large handling volume, high yield and good stability characteristics can reach more than 1,000 tons/day of processing capacity. The vertical D-aquapulper is intermittent, and it has a mild chemical treatment and the chemicals can be accurately measured. In the deinking processes, the flotation de-inking method still accounts for most cases because of its easy controlling, good stability and equipment's adaptability. Enzymatic deinking process has certain prospects, but it is not so popular at present because its application is restricted by the types of waste paper and inks. Thermal dispersion equipments can be grouped into two categories, one is the disc mill disperser and the other is the kneading machine. The disc mill disperser, such as the device produced by Andritz, disperses the stickies uniformly into the almost invisible micro-particles. The kneading machine is always placed between deinking and bleaching processes. The main purpose is to remove the thermally dissolved substances and at the same time improve the bleaching efficiency.

The main problems of recycling of waste paper

The papermaking industry has a great dependence on imported waste paper, but from another point it also shows that there is still a great potential of China's waste paper recycling.

The other problem is that the level of industrialization needs to be improved in the following areas: its lack of supportive policy and poor industrial base; the quality and scale of waste paper at present are difficult to meet the industry requirements; the lack of uniform standards for waste paper classification; the lack of industry standards and unified supervision.

Measures to improve China's waste paper recycling

First of all, we should step up the propaganda efforts. The significance of paper recycling should be emphasized, making it equal to the development of circular economy, the protection of forest resources, the

maintenance of ecological homes and the benefit of future generations. Secondly, the key equipments of pulping system should be researched and developed such as large-scale and efficient deinking equipments, high concentration of hydrogen peroxide bleaching system and recycled fiber quality testing and monitoring system. Thirdly, some abundant financial companies can introduce advanced technology and equipments to produce high quality recycled pulp according to their existing equipments, technology and production varieties. But the quality of imported waste paper should be strictly controlled to protect the legitimate interests.

The usage of new papermaking chemicals is also of great importance. More attention should be paid into the research of new deinking agent, strength agent and bleaching agent in order to further enhance the value of waste paper. The application fields of recycled fiber should be expanded. A large number of studies have shown that waste paper has a bright future in the material fields such as packaging materials, composite materials and functional materials.

The prospects of the waste paper recycling

Affected by the global financial crisis, China's paper industry has also suffered an enormous blow in September 2008. In 2009 the government has adopted some measures including the support in the export tax rebate, technological innovation and solving the excess inventory. 2009 is the year full of both opportunities and challenges. China's paper industry will accelerate the technological innovation, the implementation of energy-saving and emission-reduction, the elimination of the backward enterprises to achieve industrial upgrading. China's paper industry will be recovered with the national economy recovery.

References

(1) Guo Y.X.. China's paper industry status and development proposals in the international financial crisis. Paper & Paper Making, 2009, 28(3):1-3

(2) The annual report of China's paper industry in 2008. China Pulp & Paper Industry, 2009, 30(9):6-17

(3) Zhang C.H.，Wang R.H.，Sun K.W.. Development of Utilization of Waste Paper in Material Field. Resources Regeneration, 2009, 3:42-44

(4) Gu M.D.. Light industrial restructuring plan for the revitalization and stable development of paper industry. Paper Information, 2009, 4:18-21

(5) Shen Z.H.，Chen Z.Q，Zhao T.. Improved recycling technology for high quality recycled pulps and new uses. World Pulp and Paper, 2008, 27(2):9-15

(6) Yin Z.H.，Tian M.H.，Song W.M.. Research on Chinese Import of Waste Paper in Large Quantities .Forestry Economics, 2008, 4:46-50

Consumption Analysis of Wood Materials in Taiwan

Yi-Chung Wang[1] and Jiunn-Cheng Lin[2]

[1] Department of Forestry and Nature Conservation, Chinese Culture University. 55 Hwa Kang Rd. Yang Ming Shan, Taipei,11104 Taiwan.

[1] Corresponding author: ycwang@faculty.pccu.edu.tw

[2] Taimali Reserch Center, Taiwan Forestry Research Institute.

Wood materials are important to daily life as well as to the development of the wood-based industry. The demand for wood products increases dramatically due to economic advancement, changes in industrial structure, and higher national income. Wood materials are processed to produce furniture and wood equipment. Due to the emerging ecological awareness in Taiwan, the forest industry has adopted a management policy conforming to ecological protection and national security trends. In the early years, large-scale timber harvesting was encouraged in support of the policy of "improving business and industry through agriculture and forestry" (Lin *et al.* 2005) . In recent years, however, harvesting in natural forests is prohibited, annual quotas are imposed, and land protection is reinforced, leading to the gradual decline in annual wood production. The demand for wood is rising in Taiwan as supply decreases continually (Lin and Lee 2003). Thus, the logical resort was to increase import. However, this leads to a higher reliance on imports. Furthermore, due to decreasing forest resources and better ecological awareness around the world, timber exporting countries are treasuring their forest resources and imposing restrictions on exports, greatly influencing the supply and demand curve (Iskandar *et al.* 2006). In the future, the timber demands of countries can only be satisfied through artificial fast growing forests (Azizi 2008, Azizi *et al.* 2009). Forest products are important carbon pools. Woodbury *et al.* (2007) indicated that wood products comprise only 3% of total stocks but account for 27% of carbon sequestration. The raw materials used for production include timber, fuel wood, wood materials such as lumber, plywood, composite boards (particle boards and fiber boards), pulp, paper, and wood chips. The flow and storage of forest harvests and forest products play a crucial role in the worldwide carbon cycle (Jenkins *et al.* 2003, Hu *et al.* 2008). The flow of carbon dioxide is decided by the speed with which plants and the soil release this substance (Böswald 1998, Burschel *et al.* 1993, McFarlane and Ford-Robertson 2001). Meanwhile, forest harvesting causes a change in the carbon dioxide present in plants, greatly influencing the carbon cycle (Row and Phelps 1991, Winjum *et al.* 1998, Heath and Smith 2000). The carbon found in plants may be released when harvesting timber, creating forest products, or using forest products. Carbon is released back into the atmosphere when burning wood or using forest products even for a short period of time. Similarly, forest products used for an extended period oxidize due to decay. Through forest reproduction after harvest or when the capacity of products used for an extended period increases, carbon dioxide is absorbed back into plants or the products themselves (Burschel *et al.* 1993). Thus, the proper management of forest resources and forest products can influence the carbon dioxide emissions level of forest resources, and even entire nations (Woodbury *et al.* 2007, Obersteiner 1999, Thompson and Matthews 1989). Forest products not only store carbon but also release relatively little amounts of carbon dioxide and consume relatively little energy during the production process (Obersteiner 1999). If wood materials were used to substitute other raw materials, it will lead to lower energy consumption and slow down the release of carbon into the atmosphere. For these reasons, wood can be a suitable substitute for metals, aluminum, cement, and other materials.(Jaakko 1999) When managed properly, wood can postpone the release of carbon into the atmosphere. These materials are often referred to as ecological materials. Due to its environmentally-friendly applications, the use of ecological resources Taiwan has now become the center of focus for many advanced countries.

This study analyzed the consumption rate of wood materials in Taiwan to investigate the consumption trends in the country. Additionally, the results of the study can provide administrators and policy makers with in-depth information regarding wood consumption and its applications and serve as a reference for forestry administration entities when they evaluate the wood material needs of the country. The evaluation of the

consumption rate of wood materials in Taiwan, the analysis of applications of wood materials and forest products, and the observation of domestic wood production levels are conducive to projecting future wood consumption levels and understanding the future role of domestic wood resources.

This paper investigated the consumption rate of wood materials, analyzed the flow of consumption of wood materials and forest products, and studied the statistics of domestic wood production in Taiwan. For the analysis of consumption rate, wood materials were further classified as log, lumber, plywood, composite board, wood chips, and pulp. Results showed a steady decline in annual log imports, a slight fall in lumber imports, a steady demand for plywood over the past decade, a constant demand of composite boards, a steady rise in wood chips demand, and a decline in pulp imports since 1989, especially hardwood pulp. An analysis of consumption of wood materials and forest products showed that in the wood processing industry, log, lumber, and plywood were used primarily for construction and decoration at 68.5%, 44.7%, and 70.7% respectively. Domestic consumption of composite board in the wood furniture industry occupies as much as 76.7%. In the wood processing industry, wood chips are mainly used to produce a variety of forest products, chiefly for the production of incense, perfumes, spices, and barbeque chips. In 2008, the wood processing industry consumed 49,000m^3 of log, 1.725 million m^3 of lumber, 1.962 million m^3 of plywood, 479,000 m^3 of composite board, 142,000 m^3 of wood chips, and 3.995 million m^3 of pulp. Thus, the total consumption rate of wood materials in the wood processing industry is 8,352,000 m^3 as shown in Table1. Timber harvesting in Taiwan peaked at 1.790 million m^3 in 1972 and gradually declined to a mere 70,000 m^3 in 1993.

Table 1. Quantity and percentage of wood materials flow to wood processed manufacturing. (2008)

Item	Log	Lumber	Plywood	Composite board	Chip	Pulp	Total
Quantity (10^4 m^3)	4.9	172.5	196.2	47.9	14.2	399.5	835.2
WF （%）	6.3	12.4	17.3	76.7	0.0	0.0	11.1
WP（%）	3.4	9.4	1.7	1.6	0.0	0.0	2.5
WC（%）	6.6	26.9	9.3	0.1	0.0	0.0	7.8
OWP（%）	15.3	6.6	1.0	15.2	100.0	0.0	4.3
CF（%）	68.5	44.7	70.7	6.4	0.0	0.0	26.6
PP（%）	0.0	0.0	0.0	0.0	0.0	100.0	47.8
Total（%）	100.0	100.0	100.0	100.0	100.0	100.0	100.0

WF: wooden furniture industry, **WP**: wood processing industry, **WC**: wood container manufacturing industry, **CF**: construction and decoration industry, **OWP**: other wood processing related industries, **PP:** paper and paper product industry

Since timber harvesting in Taiwan reached its peak in 1972 at 1.79 million m^3, log production has been on the decrease. The harvest volume has remained constant at 50,000-60,000 m^3 over the past decade. This is due to lower log prices, the harvesting of mixed wood trees, priority over tree trunks, and lower income that could not cover the harvesting costs.

Technology and mechanism of silicon-transition pulping restrained by Oxide Using SEM-EDAX

Yongjian Xu, Xuanjian Li, Gang Pan and Jiao Wang

College of Papermaking Engineering, Shaanxi University of Science and Technology
Shaanxi province key laboratory of papermaking technology and specialty paper
Key Laboratory of Auxiliary Chemistry & technology for Chemical industry, Ministry of Education，
shaanxi, xi'an, China, 710021

Abstract: Soda-AQ pulping with adding aluminum trioxide was studied to reveal mechanism of silicon-transition-restrain using SEM-EDAX. Aluminum trioxide is able to restrain silicon transition to black liquor especially when the amount of aluminum trioxide is more than 3% and the amount of ash and silicon in pulp increase correspondingly. The optical microscope image show silicon cells remain between epidermises, and there are a lot of epidermises as bundles in the pulp, which is the main reason for increasing the pulp ash. SEM-EDAX result reveals in deep that the silicon dioxide is restrained into black liquor and the pulp remains a large amount of ash and silicon content possibly based on the reaction of silicon dioxide and aluminum trioxide, and the reaction product of them precipitates on the silicon cell surface which prohibits the silicon resolved into black liquor, it is the reason for some epidermises as bundles during alkaline cooking.

1. Introduction

With the developing and practice of the straw pulp alkaline recovery system, powerful global papermaking groups pay much attention to non-wood pulp. Therefore, Non-wood pulp production capacity in China does not decrease but increases gradually, and non-wood fiber pulp must play an important role in recent development of papermaking industry, even though the non-wood papermaking and alkaline recovery still face much more difficulties [1, 2]. Silicon content in the black liquor from wood pulping is only 0.22%, and recovery rate is up to 95%~98%，whereas silicon content in non-wood pulp black liquor is very high, which results black liquor in high viscosity, easy scaling, difficult evaporation, burning, and also difficult clarification of white liquor and high residual alkali in white mud. All above are the main reasons for the low extraction of black liquor，low recovery rate and high chemical consumption in non-wood pulping system [3,4,5]. There are three main sources for silicon into black liquor [6, 7]: the first is named combination silicon, 90% of silicon in black liquor comes from the raw material [8]; the second is named non-binding silicon, that is, the sediment in the material; the third is the accumulation of silicon in the black liquor system [9], silicate scale from evaporator cleaning come back to the weak black liquor tank which is the reason for the silicon accumulation in the black liquor system. There is also 10% of the silicon from causticization. The combination silicon from raw materials largely exists in the epidermis of stem, leaf, node, and sheath. The part of raw material with high silicon content is removed in the preparation, but the residual silicon is still enough to deteriorate alkaline recovery system. Epidermis tissues of non-wood materials consist of the epidermis cells with the cork cells and silicon cells between them [10], and epidermis cells were completely separated in the conventional alkaline pulping due to the silicon dissolution. It was found that the silicon dioxide could be effectively remained in Soda-AQ pulping with adding aluminum trioxide, which is characterized by its significantly increase in ash content. The goal of this article is to reveal the mechanism of aluminum trioxide on silicon retention, providing with possible theory and evidence to optimize alkaline pulping technology and reduce the cost on silicon retention.

2. Material and Methods

(1) Material and cooking conditions

Wheat straw was used for the pulping from Shaanxi in China, and prepared into sizes for their mill cooking process.

Cooking condition: cooking temperature 155℃; AQ:0.05%; Liquor ratio：1：5；heating time：60min;cooking

time：30min.

(2) Instruments and equipments

ZQS electrothermal rotating cooking tank （four 1 L stainless steel tank）

Multimedia microscope: Motic model of B5 series

SEM-EDAX: JEOL JSM-6400models Scanning electron microscope and Energy Dispersive Spectrometer

S150 sprayer: spraying time: 120s.

Standard dispersion device: L&W disperser, model 969939.

(3) Chemicals

Aluminum trioxide: analytical reagent

NaOH: analytical reagent

(4) Detection of the chemical composition and fiber morphology

Unscreened yield and kappa number were measured according to GB/T1546-1989, and the measurement of the content of pulp ash and silicon dioxide was according to GB/T742-1989. Fiber morphology was observed according to GB/T10336-1989.

3. Results and discussion

(1) Study on the effect of aluminum trioxide on silicon retention.

Silicon could be remained in the Soda-AQ pulp by adding aluminum trioxide, and the effect of aluminum trioxide on silicon-transition-restrain was evaluated based on the measurement of silicon dioxide and ash content in the brown pulp. In order to eliminate impact of the possibly residual aluminum trioxide on the measurement of the ash and the silicon dioxide content, either the pulp were washed in acidic water or the pulp slurry was decanted to remove the residual aluminum trioxide before the ash and silicon dioxide content in the pulp were measured. The so-called decantation is to fully disperse the pulp in the standard disperser and let the residual aluminum trioxide precipitate on the bottom due to its high gravity, then decant the pulp. Acidic wash is to use acidic water to remove the residual aluminum trioxide in the pulp. Both results were shown in Figure 1 and Figure 2. It can be found from figure 1 and figure 2 that the ash content is almost equal to the silicon dioxide content for Soda-AQ pulp, which was due to the main component of ash in non-wood raw materials is silica dioxide. Compared with the Soda-AQ pulp, the ash content and silicon dioxide increased by adding aluminum trioxide into the cooking system and much more increased with increasing the amount of aluminum trioxide, which indicated the good effect of aluminum trioxide on silicon-transition- restrain, especially the amount of aluminum trioxide is more than 3%.

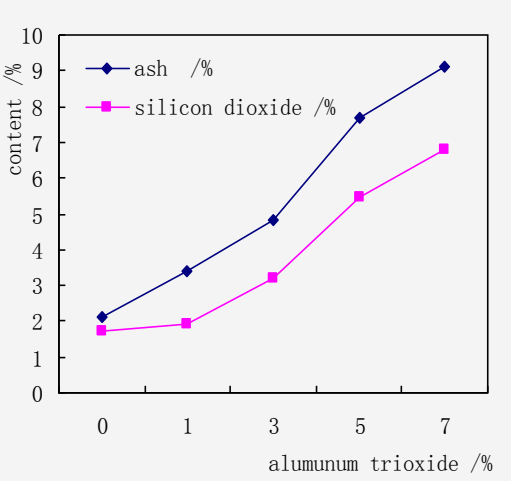

Fig.1 the effect of the amount of aluminum trioxide on the ash and silicon dioxide content in the pulp. （After decantation）

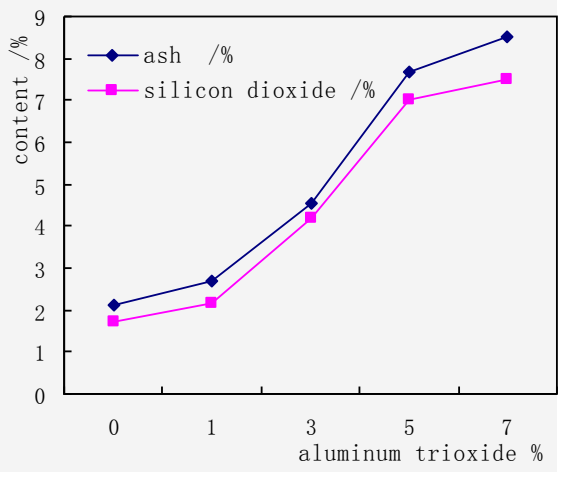

Fig.2 the effect of the amount of aluminum trioxide on the ash and silicon dioxide content in the pulp. （After acidic wash ）

Comparing figure 1 and figure 2, with the amount of aluminum trioxide increasing, the difference between silicon dioxide content and the ash is getting larger and larger; the difference between the ash and silicon dioxide content measurement based on decantation method is much more than that based on acid wash. The ash content obtained from decantation is higher than that from acidic wash at the same amount of aluminum trioxide possibly because calcium oxide and magnesium oxide were also removed from the pulp aside from aluminum trioxide; that the silicon dioxide content from decantation is less than that from acidic wash may be due to the acid hydrolysis of carbohydrates in the pulp.

(2) The mechanism of aluminum trioxide on silicon retention

a. Effect of silicon content and the distribution of mineral element in raw material on silicon transition

The aluminum trioxide could restrain the silicon dioxide into black liquor in alkaline pulping process, and it inferred that a certain compound formed between aluminum trioxide and silicon dioxide under alkaline and cooking temperature condition. If this hypothesis is possible, the effect of aluminum trioxide on silicon-transition-restrain would be affected by chemical composition of wheat straw and the mineral element distribution and content in different botanical parts of wheat straw such as wheat straw stalk, node, leaves, and panicle. The composition of wheat straw and the element distribution in different morphological area is shown in Table 1 and Table 2.

Table 1 The chemical composition of whole wheat straw

Ash /%	Holocellulose /%	Hemicellulose /%	Lignin /%	alcohol-benzene extractive /%
8.78	65.86	22.09	22.11	2.18

Table 2 Element contents of different botanical parts of wheat straw unit :10^{-6}g/g o.d. sample

Position	Si	Mg	Ca	Al	Mn	Cu	Fe	Na	Co	Ni
Stalk	14005	1535	2325	63.3	9.1	5.4	64	122	<0.1	1.78
node	17827	3937	3995	170.9	16	4.27	106	294	<0.1	1.61
Leaves	4032	4376	5061	54.1	40	4.61	329	357	<0.1	2.35
panicle	19422	1421	1421	662.5	30	3.0	279	132	<0.1	1.21

It could be seen from table 1 and table 2 that ash content in wheat straw is much higher than that of wood raw materials, among which 60% to 70% was silicon dioxide. The silicon dioxide distribute in the different morphological parts of wheat straw, and leaves, node, panicle with a high level; calcium and magnesium element were relatively high, and would dissolve into the black liquor during cooking. The distribution of other minor elements were also different in various parts of wheat straw, copper and nickel element content were almost even, manganese, iron and aluminum element content in the stalk were very low, iron and manganese element content in the leaves were the highest, while aluminum element content is lower. Qiu studied the distribution of mineral element in the wheat straw and found that silicon content as high as 56.3% in external surface of internodes stem is significantly higher than that in the inner surface [14-16]. The silicon content in the node and panicle were also high, and the silicon content in fiber cells was the lowest，about 1/30 ~ 1/140 of that in external surface of the wheat straw. Eroglu et al [14 ~ 15,17] found that silicon and other mineral elements in external surface of the wheat straw were readily removed up to 60%~70% even under a relatively modest alkaline pre-treatment condition. Liu et al [12] found silicon content in the middle layer of wheat straw stalk is the highest， which may be due to the high silicon content in the parenchyma. So it inferred that the mechanism and effect of aluminum trioxide on silicon dioxide restrain in different morphological region are different.

b. The mechanism of aluminum trioxide on silicon retention using optical microscopy

Epidermis tissues of non-wood raw materials consist of the epidermis cells with the connection between cork cells and silicon cells [10], and epidermis cells were completely separated in the conventional alkaline pulping due to the silicon dissolution into the black liquor from the epidermis cells. Based on the image of optical microscope，a large number of epidermal cell bundles still linked by silicon cells could be observed in the pulp from Soda-AQ pulping with adding aluminum trioxide as shown in Figure 3. Soda-AQ wheat straw fiber and epidermis cell are shown in Figure 4, not the epidermis bundles but completely individual epidermal cell could be seen. In comparison，it infer that the main reason for silicon retention is epidermis cell bundles linked

by silicon after cooking but not silicon dissolved into the black liquor possibly due to a certain insoluble compound formed between the aluminum trioxide and silicon dioxide. The mechanism of this reaction may be that aluminum trioxide dissolved in alkaline solution, then reacted with silicon cells to form a insoluble substance，and epidermis cells were still connected together. These epidermal cell bundles would not drain in the pulp washing, and still retain in the pulp, which was the reason for increasing pulp ash and silica content.

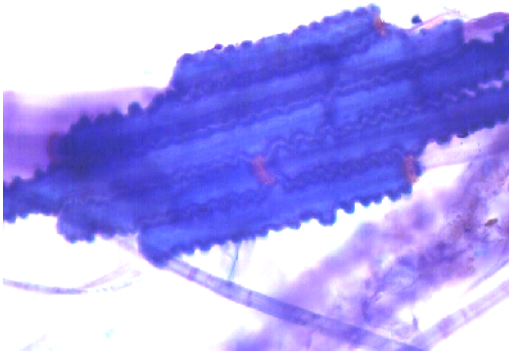

Fig. 3 epidermis bundles from the Soda-AQ pulping with 3% aluminum trioxide addition

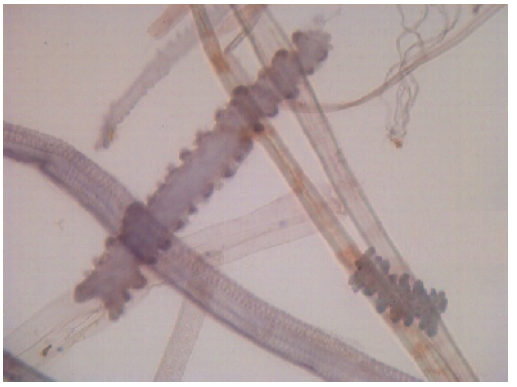

Fig. 4 individual epidermis cell in the Soda-AQ pulp

c. The mechanism of aluminum trioxide on silicon retention using SEM-EDAX.

The results of optical microscope observations can not fully explain the reaction between aluminum trioxide and silicon dioxide during alkaline cooking, but only show the existence of epidermis cells. It was the critical to reveal the mechanism of aluminum trioxide on silicon retention whether the aluminum trioxide-silicon dioxide compound in existence or not between epidermis cells. Therefore, the chemical composition of epidermis cells, especially the silicon compound between epidermis cells in the pulp was analyzed using SEM-EDAX, and the results were shown in figure 5 and figure 6. Figure 6 is the energy photography of region A in figure 5.

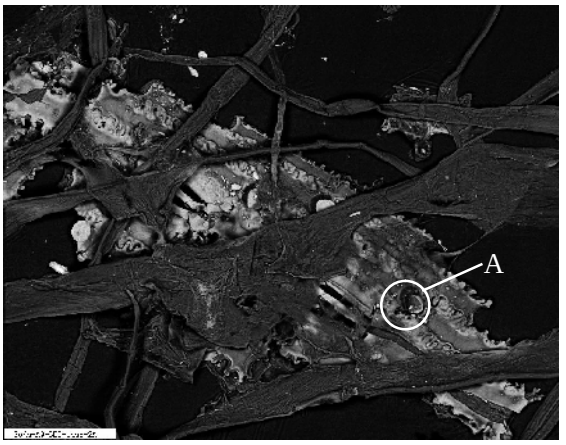

Fig.5 SEM image of epidermis bundles from the Soda-AQ pulping with 3% aluminum trioxide addition

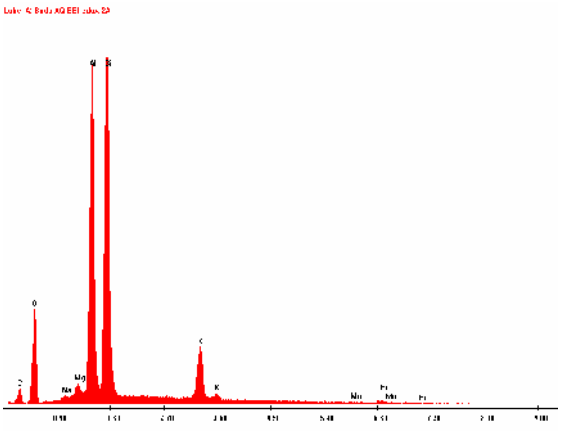

Fig.6 the energy photography of region A in figure 5

It can be seen that the there is a large epidermis cell bundle, and more than one silicon cells existed between epidermises. These silicon cells are still in connection with the epidermis cells the same as that in wheat straw. In Figure 6，the signal peak of aluminum and silicon were stronger than that of other elements, it could be inferred the existence of aluminum in the region A. The aluminum content in wheat straw is very low compared to silicon in Table 2, so the strong signal of Al in the region A only showed it related with the aluminum. Both the elements aluminum and silica are in the region A, it suggested that the reaction may occur between aluminum trioxide and silicon dioxide under alkaline and high temperature conditions. Tutus et al [8] indicated that the aluminum trioxide and silicon dioxide generated similar minerals such as kaoline or talc. The chemical

composition of kaoline is $Al_2O_3 \cdot 2SiO_2 \cdot 2H_2O$, Al_2O_3 and SiO_2 will be combined in various proportions, but always close to 1:2, so Tutus proposed the principle of silicon retention as follows: SiO_2 dissolved in alkaline solution to generate Na_2SiO_3, and then Na_2SiO_3 and Al_2O_3 would form reaction product similar to kaolin minerals under alkaline conditions according to equation (1)

$$2Na_2SiO_3+Al_2O_3+4H_2O \rightarrow Al_2(OH)_4Si_2O_5+4NaOH \quad \text{（equation 1）}$$

Qiu et al [14, 15] found that the silicon in epidermis tissue of wheat straw is dissolved into the black liquor in the early of cooking. Associated with Tutus et al research, silicon dioxide content in pulp increase when adding the aluminum trioxide into cooking system，which means that the reaction between silicon dioxide and aluminum trioxide may occur under the conditions of alkaline and high temperature. The experimental result provided a theoretical evidence for the views of Tutus. Of course, the possibility was not excluded that aluminum trioxide adsorbed onto colloid silicon dioxide. The results showed that the compound covered the surface of silicon cells which hindered further dissolution of silicon dioxide into sodium hydroxide solution either the chemical reacting with or physical adsorbing aluminum trioxide. Taking into account aluminum trioxide as the amphoteric compound, it was expected that a certain insoluble substance would form between aluminum trioxide and silicon dioxide which will not dissolve in alkaline solution under alkaline and high temperature conditions. And the existence of epidermis cell bundles is to support the inference.

Alumina trioxide has the ability to inhibit the silicon dioxide dissolved into cooking liquor, the mechanism of alumina trioxide restraining silicon dioxide transition was initially revealed. The silicon dioxide retention is obvious when the amount of aluminum trioxide is more than 3%, how much is there reaction products of aluminum trioxide and silicon dioxide or the covering layer of aluminum trioxide adsorbing onto colloidal silicon dioxide and how much silicon dioxide has been dissolved into the black liquor before the reaction of the aluminum trioxide and silicon dioxide? All the above need further study.

4. Conclusion

(1) In the alkaline pulping process, the Al_2O_3 can inhibit the transition of silicon. When the amount of Al_2O_3 added to the soda-AQ pulping is up to or more than 3% based on the technology research, it can give significant effects on silicon retention, with a large number of silicon retention in the pulp.

(2) The silicon cells still exist between epidermises in the pulp similar to the status in the wheat straw based on the optical microscope image, and there are a lot of epidermis cell bundles in the pulp from Soda-AQ pulping with adding aluminum trioxide, which is the main reason for a large number of silicon retention in the pulp, and also can explains why ash content increases in the pulp.

(3) The result based on SEM-EDAX image show that on the surface of the silicon that in the junction

The react production or absorption layer between silicon dioxide and aluminum trioxide cover the surface of silicon cells between epidermises among epidermis cell bundles, and the react production or absorption layer further hindered the dissolution of the silicon dioxide into sodium hydroxide, thereby the epidermis cells remains to be linked. The restrain effect of aluminum trioxide on silicon transition is achieved possibly by the reaction with silicon dioxide.

Acknowledgement

The authors would like to acknowledge the financial support to this research from National Natural Science Foundation of China, Shaanxi Natural Science Foundation and Doctoral Fund of Shaanxi University of Science and Technology.

References

1. Zhong,X. Fiber resource restructuring for papermaking in China[C], Proc. Appita Symposium “the fiber trail”, Rotorun, 2002.
2. Li Jinhua Song Hongzhu Xue Yongchang Zhang Qiwen Li Shenggang
Present Situations and Development Strategy on Raw Material of Wood Fiber for Pulp and Paper Industry in

China；World Forestry Research; 2003（16）.6：32-35.
3. Zhang Ke Wang Ping; Some Key Problems Concerning the Increase of the Alkaline Recovery Rate from Wheat Straw Pulp Black Liquor[J]；CHINA PULP & PAPER INDUSTRY; 1999，3：24-26.
4. Li Hui Li Youming Chen Zhonghao Bi Yanjin；Study on Influence of the Enrichment of Non-Process Elements in Clean Bleaching[J]；Guangdong Pulp &Paper; 2003，22（6）：30-34.
5. Zhang Taoyun，Silicon Interference and Technology of Silica Removal from Black Liquor of Straw Pulp[J]，Paper and Paper Making，1999，4：45-46
6. Tandon,R.,Grupta,A. Kulkarni, A.G.,et al. properties of black liquors form pulping of non-woody raw materials[J], Proc. Intl Seminar and workshop on desilication,1989,23-35
7. LIN Xian-cun; LIU Shu-chai；The accumulation of inert deposit in alkali recovery and its influence on the production[J]；China Pulp & Paper Industry; 26(9):62-64(2005).
8. Tutus A. and Eroglu H. A practical solution to the silica problem in straw pulping [J], Appita，2003，56(2)：111—115 .
9. Jia Yuanyuan Gao Zhennan Li Xiulun；Ingredients and Forming Mechanism of the Scale in the Evaporator for Wheat Straw Black Liquor Evaporation[J]；Transactions of China Pulp and Paper; 2003，18（1）：56-58
10. Yang Shuhui; Plant Fiber Chemistry[M]; China Light Industry Press; 2001.1
11. XU Yong-jian, ZHANG Mei-yun LIU Zhen-hua；Recent Advance in Non-Wood Fiber Pulping Technology for Controlling Silicon Transfer；China Pulp & Paper; 2007.11，26（11）:40-43
12. XU Yong-jian PU Wen-juan ZHANG Mei-yun LIU Zhen-hua；The Technology and Mechanism of Restrained Silicon-transition Pulping[J]；Transactions of China Pulp and Paper, 2007.12，22(4):36-39
13. XU Yong-jian; PU Wen-juan; ZHANG Mei-yun；Recent Advances in the Technology and Mechanism on Producing High-Silicon Non-Wood Pulp[J]；Paper and Paper Making 2007.3，26（2）：8-10
14. Yun Na Qiu Yugui Chen Fengyuan Dou Zhengyuan Cheng Zhiwei Dong Hui ；Transferring Feature of the Mineral Elements in Wheat Straw Material during Cooking Process[J]；Guangdong Pulp & Paper 2003，22（6）：11-17
15. Qiu Yugui,Yun Na,Lin Lu,Dou Zhengyuan; Study on the Mineral Elements of Wheat Straw by Means of SEM-EDAX; TRANSACTIONS OF CHINA PULP AND PAPER 2003，18（2）：1-5
16. YAO Jie; XU Xin-wu and FENG Yu-ying; FTIR Studies on the Chemical Composition of Wheat Straw in Different Layers; Spectroscopy and Spectral Analysis 2003，23（1）：58-60
17. Eroglu，H. and Deniz, I. Predesilication of wheat straw with NaOH[J], Das Papier, 1993，47(11):645-650.
18. Tutus A. and Eroglu H. An alternative solution to the silica problem in wheat straw pulping [J], Appita，2004，57 (3): 214-217

2009 Cross Strait Forest Products Technology Symposium
【Forest Products】
Table of Contents

Section 1: Wood anatomy, carbon sequestration

Section 2: Wood properties, structure

Section 3: Wood chemistry

Section 4: Wood composites

Section 5: Preservation, wood processing

Section 6: Wood-plastic, charcoal, finishing

Poster

A Kind of NN Modeling Method of Relational Model of Chinese Fir Microstructure and Its Material Characteristics

Yucheng Zhou

Department of Research Institute of Wood Industry, Chinese Academy of Forestry, Beijing

Abstract: This document explains and demonstrates how to prepare your camera-ready manuscript for *Trans Tech Publications* The best is to read these instructions and follow the outline of this text. The text area for your manuscript must be 17 cm wide and 25 cm high (6.7 and 9.8 inches, resp.). Do not place any text outside this area. Use good quality, white paper of approximately 21 x 29 cm or 8 x 11 inches (please do not change the document setting from A4 to letter). Your manuscript will be reduced by approximately 20% by the publisher. Please keep this in mind when designing your figures and tables etc.

1. Introduction

The Relativity of the wood quality and internal structure has become the focus of attention of experts and academicians in the field of wood industry and engineering worldwide [1-5]. As to the absolutely necessary resource of human life and manufacture, it is in great need of educing wood quality from its internal structure, which means to find out its physics, mechanics and dry shrinkage properties [1]. Besides traditional experiments, such relationship could be worked out based on the research of wood property and its forming mechanism, can be determined.

However, it is virtually difficult to keep such a kind of complicated wood systems in hand although so many people have been dedicated to that, and traditional research was confined to several parameters and unable to work out accurate model. Wood model of internal structure and its physics, mechanics, dry shrinkage property, as a kind of complex system [6], its external wood property was closely related with its microstructure [5], which differentiated in different trees. Virtually, as an organism, a variety of uncertain nonlinear relationship could be found in wood [7], which means that each microstructure parameter will influence wood quality more or less, but the relativity degree is hard to trace and forecast [8]. References [3] and [4] presented a pine tree relational model of basic density and growth ring, in which basic density variation was clearly expressed in different wood internal position through the research of growth ring. Thus a certain kind of mapping relation from wood structure to one of wood physics named basic density was actually presented.

In this paper, a certain kind of Neural Network modeling method [9] with high precision and efficiency is introduced into modeling tasks. Based on NN modeling method, a series of relational models of wood structure and wood property are presented, which has broken through the traditional research approach of working on single binary relation. And principal component analysis and stepwise regression analysis are also applied to the relational models, which can help achieve high precision models and practical models. The modeling tasks were divided into the following several steps. Firstly, the relation models are established following the analysis and preprocess of experimental data, and the performance of NN is assessed by linear regression analysis between network output and target output. Secondly, according to sample distributing characteristic, the data are grouped by growth ring. The radial variation is reflected and the desired approximation degree is achieved in the sub-models based on wood age. Further, a certain mathematical method named stepwise regression is applied to analyze leader-follower inputs. In this way a series of reduced models are provided. When the overall model, sub-model based on wood age and key variable group model was accomplished, the inherent relationship between wood internal and external properties was found out roundly and accurately.

2. Problem description

Experimental data of Chinese Fir can be classified into four kinds of microstructure, physics, mechanics and dry shrinkage property, with totally 25 parameters. In the experiment, wood amount is 20, wood age is 30, data gathering spot is 1-10 position, and sample number is 143. Here its microstructure data was taken as input

vectors, and its physics, mechanics and dry shrinkage as output indexes. The desired relational model was supposed to present the mapping from 18 inputs to 7 outputs of Chinese Fir with high precision and efficiency.

A kind of forward-propagation neural network was adopted in this paper, which is Radial Basis Function (RBF) network instead of BP. The radial basis neural network is absolutely superior to BP for its approximation ability, classification ability and learning rate. Generalized Regression Neural Network (GRNN), as a kind of normalized RBF network, is universally applied in function approach, by which high efficiency can be reached [10].

After the statistics and analysis of training data set, it was supposed to work out the Overall model, the Sub-model based on wood age, and the Key variable group model, so as to make clear its internal relationship in depth. Before modeling, there are several steps of data preprocessing, including data normalization, Principal Components Analysis (PCA) and Stepwise Regression Analysis (SRA). Data normalization is a general method in mathematical modeling, which can get training data ready for modeling. PCA is adopted here for sake of efficiency and precision. SRA functioned well in screening key variable group.

3. Modeling and regression analysis

The modeling task in this paper was developed surrounding the supposed three kinds of models, in detail speaking, which represent Chinese Fir overall relational model, sub- model based on growth ring (8 sub-models) and key variable group model (corresponding to 7 output indexes of Chinese Fir, several optimized groups were given respectively) .

(1) Overall model

As to overall model of generalized regression neural network, the normalization of training data set should be followed by principal component transformation. Here the level of significance was set as $\alpha = 0.05$. This model finally achieved the mapping $R^{R'} \to R^{S}$, where $R' < R$, R is input dimension.

It is indispensable to implement the following process of modeling, in consideration of network performance assessment. Such process is realized through the linear regression analysis between network outputs and target outputs, which is shown in Fig.1.

The performance of a trained network can be measured to perform a regression analysis between the network response and the corresponding targets. The routine Post-Training Analysis (postreg) is designed to perform this analysis.

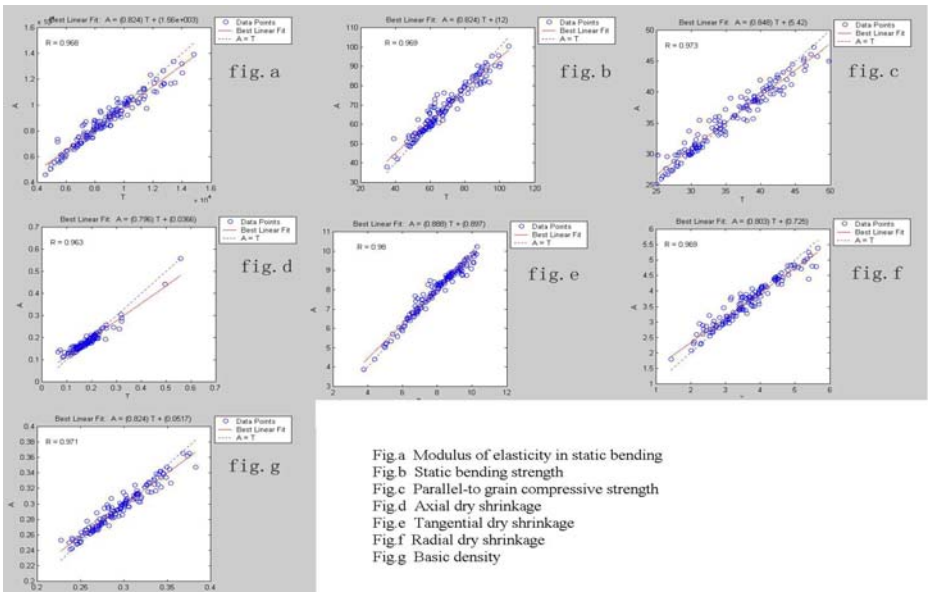

Fig. 1 Regression curve of Chinese Fir Property-Structure model.

Here we pass the network output and the corresponding targets to postreg. It returns three parameters. The first two, m and b, correspond to the slope and the y-intercept of the best linear regression relating targets to network outputs. If we had a perfect fit (outputs exactly equal to targets), the slope would be 1, and the y-intercept would be 0. In this example, we can see that the numbers are very close. The third variable returned by postreg is the correlation coefficient (*R-value*) between the outputs and targets. It is a measure of how well the variation in the output is explained by the targets. If this number is equal to 1, then there is perfect correlation between targets and outputs. In our example, the number is very close to 1, which indicates a good fit. The following figure illustrates the graphical output provided by postreg. The network outputs are plotted versus the targets as open circles. The best linear fit is indicated by a dashed line. The perfect fit (output equal to targets) is indicated by the solid line. In this example, it is difficult to distinguish the best linear fit line from the perfect fit line, because the fit is so good.

In the above expression in Fig. 1, *A* is the $1\times Q$ network output matrix, *T* is the $1\times Q$ target matrix, *M* is the slope of linear regression, *B* is the y-intercept of linear regression, *R* is the regression *R-value*, which expresses the correlation coefficient of network outputs and target outputs. It can be seen from Fig.a to Fig.g that *R-value* is 0.968, 0.969, 0.973, 0.963, 0.98, 0.969, 0.971 respectively.

(2) Sub-model model based on wood age

The distinct radial variation is one of nonnegligible characteristics of wood structure. In order to make clear the considerable difference of wood properties at different wood age, the original experimental data were classified by experimental spot. Therefore, eight sub-models of Chinese Fir based on wood age were achieved, and the regression curve of Chinese Fir property-structure submodel 1 is shown in Fig. 2 for example, in which the desired approximation degree is achieved in the sub-models. From Fig. 2, it can be seen that the network performance of the above sub-models is satisfactory.

(3) Key Variable Group Modeling

The Chinese Fir samples analyzed in this paper include 18 microstructure parameter and 7 indexes of its physics, mechanics. However, as to these 7 outputs of Chinese Fir, each microstructure parameter has influence on those outputs by different levels. In order to find out the relational model proposed in this paper in depth and detail, a series of key variable groups were presented.

It is clear that the performances of those reduced models are not so good as the front two kinds of relational models. However, most of the reduced models are predicatively practical, and the final outputs will also help experts do relevant research work.

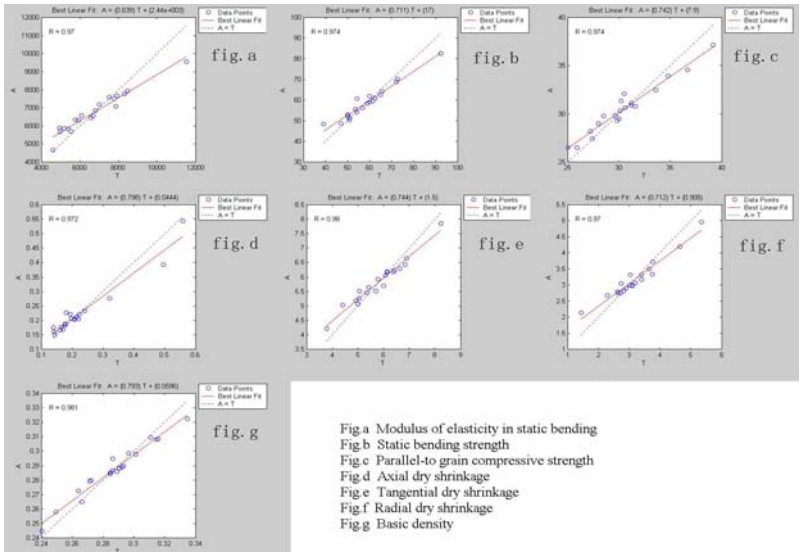

Fig. 2 Regression curve of Chinese Fir Property-Structure submodel 1.

4. Summary

Based on a group of Chinese Fir samples of microstructure, physics, mechanics and dry shrinkage, this paper presented a kind of Neural Network modeling method aided by PCA and SRA. The overall model, sub-model based on wood age and key variable group model worked out here clearly find out the inherent relationship of Chinese Fir internal and external characteristics. Neural Network models established in the research work proved considerably well through regression analysis.

5. References

(1) J. E. Melo, P. J. Pellicane, M. R. Souza, Goodness-of-fit analysis on wood properties data from six Brazilian tropical hardwoods. *Wood Science and Technology*, Vol.34 (2000)

(2) C. Lundgren, Microfibril angle and density pattern of fertilized and irrigated Norway Spruce. *Silva Fennica*, Vol.38(1) (2004)

(3) X. Tian, D. J. Cown, M. J. F. Lausberg, Modeling of Pinus Radiata Wood Properties Part 1: Spiral Grain. *New Zealand Journal of Forestry Science*, Vol.25(2) (1995), p:200-213

(4) X. Tian, D. J. Cown, M. J. F. Lausberg, Modeling of Pinus Radiata Wood Properties Part 2: Basic Density. *New Zealand Journal of Forestry Science*, Vol.25(2) (1995), p:214-230

(5) X. L. Liu, X. M. Wang, X. M. Jiang, Y. F. Yin, Anatomical and physico-mechanical properties of Hippophae rhamnoides L. *Journal of Beijing Forestry University*, Vol.26(2) (2004), p:84-89

(6) Y. C. Zhou, F. Cheng, X. Q. Li, Robust Asym ptotic Tracing of a Nonlinear System. *China Wood Industry*, Vol17(5) (2003), p:11-13

(7) Y. C. Zhou, J. Han, Yin, Robust Control of Nonlinear Uncertain Systems with Constraints. *Control and Design*, Vol.13(2) (1998), p:115-119

(8) Y. C. Zhou, F. Cheng, T. J. Xiao, J. H. Yang, Robust Asymptotic Tracing of a Kond of Nonlinear Systems Containing Uncertain Diathesis. *Scientia Silvae Sinicae*, Vol.39(2) (2003), p:130-136

(9) J. L. Liu, J. Z. Qi, L. P. Zhang, F. L. Zhao, Analysis on the W ood Comparative Anatomic and Properties of Populus davidiana Dode and Populus davidiana var. macrophylla. *Journal of Jilin Forestry University*, Vol.28(4) (1999), p:17-23

(10) H. Zhou, L. G. Zheng, J. R. Fan, K. F. Chen, Application of general regression neural network in prediction of coal ash fusion temperature, *Journal of Zhejing University (Engineering Science)*, Vol.38(11) (2004), p:1479-1482

Microcosmic Structure Analysis of Ash in the Longitudinal Compression Procedure

Kuiyan Song and Jian Li
Northeast Forestry University, Harbin

Abstract: The article is based on the process of Ash longitudinal compression and analyzes the change of compressed wood and uncompressed wood through electron microscope. The result indicates: The elastic character of wood is prominent at the beginning of compressing. This elastic transmutation is caused because of micro-fiber sliding on cellular wall and this sliding will bring tiny transmutation of cell layer. The mutation will increase and crease will appear on the cellular wall with increasing of stress. This mutation is eternal without stress. If continue to apply stress, cellulose molecule will crimp or frame filler of cellulose will break.

1. Introduction

The purpose of wood longitudinal compressing is to get minimal bending radius and many-direction bending. When wood is under the function of longitudinal stress, micro-fiber will slide. Many-direction bending is carried out on the base of cellular wall crease. There is anfractuous relationship between technical conditions and cellularity and cellular wall micro-fiber structure mutation[1,2,3,4].

On the initial stage of wood longitudinal compressing, transmutation has direct ratio increase with stress increasing. The elastic character of wood is remarkable after removing the stress and this elastic transmutation happens instantly[5,6,7]. After the critical point σ_P, mutation will reach elastic-plastic transmutation. The initial period of wood cellular wall crease is very short, namely very tiny curve between stress and transmutation. The maximum mutation is ε_T at the end of this tiny curve. In the procedure of continuative longitudinal compressing relation of stress and transmutation is nearly direct ratio. Maximum transmutation is ε_S when stress will reach the maximum σ_S. Cellular wall crease begins to engender, increase evenly and reach the maximum point. At this moment the main transmutation is elastic-plastic and plastic mutation. With the increasing of stress the sample will be broken [1,2,3,4,5].

2. Materials and Methods

The specimens are taken from logs with an average diameter of 24-26cm in the middle. The logs are ash from northeast Xing'anling, and the specimens choosed are 1.2-1.9 meter high above the ground. The size is 270×16×16 mm.

Universal mechanical testing machine and longitudinal compressing mould are used in the longitudinal compressing test. The compressing speed is 2 mm/min.

We use electron microscopes to observe transmutation of cellular wall before and after longitudinal compressing. One electron microscope is made by SEM from Japan with model JSM-5610LV and another electron microscope is made by FEI from America with the model QUANTA2000. The average moisture of specimens is 8.15%, tested on the middle section.

3. Results and Discussion

Fig. 1 shows the vein holes of non-compressed wood on the drive section. In the process of longitudinal compressing, the vein holes on the catheter wall are compressed, but because of a small distance between each vein hole, a bigger compressing ratio can not receive. As the pressure increased, the cellular wall without vein holes has folded regularly (Fig. 2, Fig. 3). Then, with the increase of stress, the strain becomes bigger (Fig. 4). It is the process of vein holes compressed and cellular wall folded. When the longitudinal compressive pressure goes beyond the allow stress of cellular wall, a glide appears on the surface of specimens, a fold and track appear on the cellular wall of the drive section, and the wood fibers become contorted. Obviously, the wood cells

collapse (Fig. 5, Fig. 6).

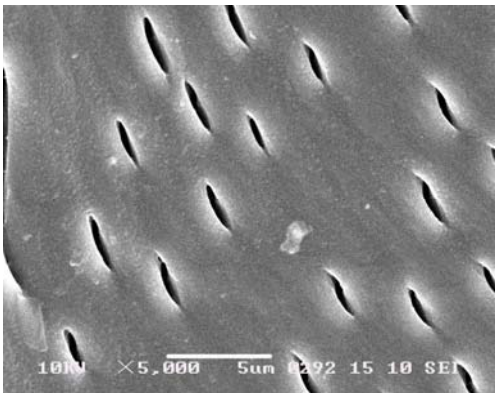

Fig. 1 The cellular wall of non-compressed wood on the drive section.

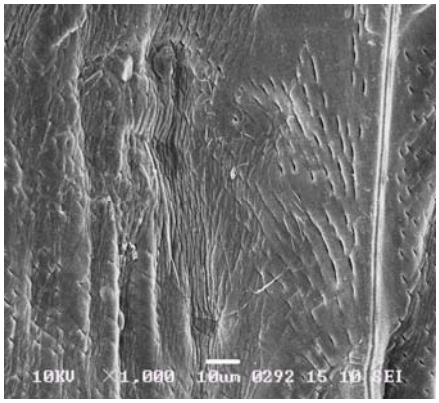

Fig. 2 The cellular wall of compressed wood on the drive section.

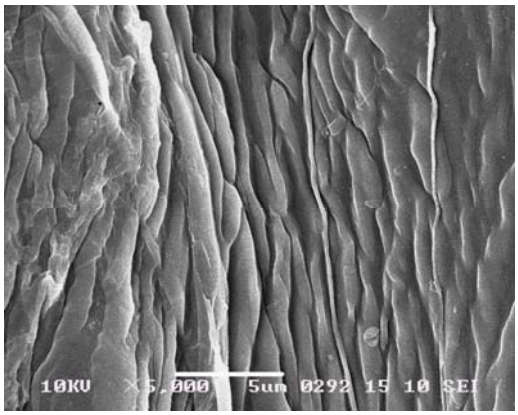

Fig. 3 The cellular wall of compressed wood on the drive section.

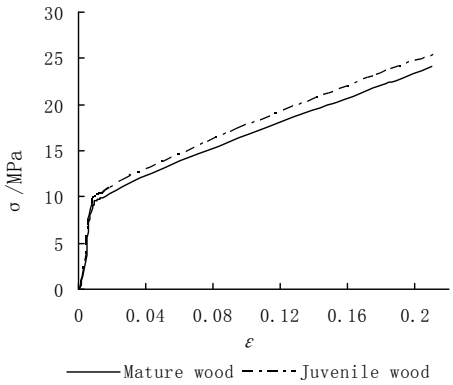

Fig. 4 The relationship between stress and strain of ash longitudinal compression.

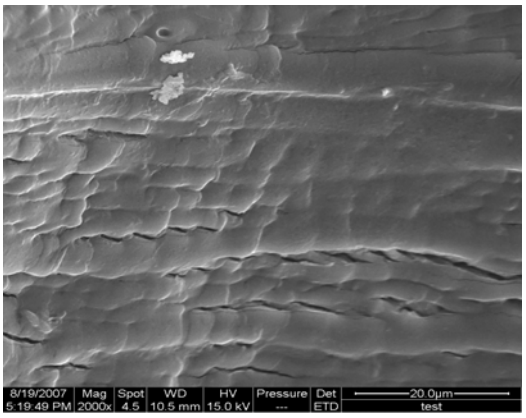

Fig. 5 The cellular wall of compressed wood on the drive section.

Fig. 6 The wood fiber of compressed wood on the drive section.

In the beginning of compressing, elastic character of wood is distinct. Through the relation of stress and strain (Fig. 4), we can find the mutation is elastic mutation. This mutation is caused by sliding of cellular wall's micro-fibers and this sliding will bring tiny mutation of cellular wall. But this mutation is not eternal, or eternal for only a while. After removing of stress, the mutation will disappear. Later the strain will go up highly with stress increasing. Folds appear on the cellular wall and the it can not come back totally. Eternal transmutation happens. With the stress increasing, the fold will go up beyond the limitation. It will bring on huge crimping of

cellulose and avulsion of framework filler of cellulose. The fact is sharp debasement of stress caused by stave of cellular wall and wood fiber.

4. Conclusion

In the wood longitudinal compressing procedure crease will appear on cellular wall on the range of allowable stress. But the cellular wall crease must be controlled to certain extent. This aim can be carried out by measuring stress and other compressing technical conditions.

5. Reference

(1) Li Qing. Development of Compressed Wood from Domastic Elm: China Wood Industry Vol. 14(2000), p. 38-39
(2) Song Kuiyan: *The Technology of Wood Compressing and Multi-Direction Bending* (Northeast Forestry University, Harbin 2003)
(3) Song Yuhong: *Study of F.mandshurica Multi-direction Bending* (Northeast Forestry University, Harbin2003)
(4) Song Kuiyan, Wang Fenghu, Song Yuhong. The Techniques of Elm Longitudinal Compressing and Bending: Scientia Silvae Sinicae Vol. 40(2004), p. 126-130
(5) Tao Junlin, Jiang Ping, Yu Zuosheng. On The Static Constitutive Relation of Wood With Large Deformation: Mechanics and Engineering Vol. 22(2000), p. 25-27
(6) Wang Fenghu: *The Rheological Theory of Wood*. (Northeast Forestry University, Harbin1997)
(7) Liu Yixing, Norimoto Misato, Morooka Toshiro. Quantitative Expression On The Large Transverse Compressive Deformation Relationships Between Stress And Strain of wood: Scientia Silvae Sinicae Vol. 31(1995), p. 436-442

Study on Variations of Tracheid Morphological Characteristics in *Metasequoia glyptostrobides*

Jinqiu Qi, Jianfeng Hao and Haiqing Zhang
Sichuan Agricultural University, Yaan, Sichuan

Abstract: The length, double wall thickness, diameter of tracheid were measured in *Metasequoia glyptostrobides* in Zhong Li of Ya'an city, Sichuan province. The results showed that the fast-growing period of *Metasequoia glyptostrobides* was about 16 years. Its latewood ratio was low, which was 7.3% in average. The mean of tracheid length, tracheid width, tracheid double wall thickness and tracheid diameter was respectively 4.13mm, 4.13 mm, 40.7μm and 32.3 μm, 7.7μm。The mean of tracheid length-width ratio, tracheid double wall thickness–diameter ratio and tracheid diameter-width ratio was 100, 0.48 and 0.75. In addition, the mean of mature age for tracheid length and ring width as assessed indicator was respectively 14.9a and 16.1a, and for tracheid width and tracheid diameter as assessed indicator was respectively 14.9a and 14.4a.

1. Introduction

Metasequoia glyptostrobides belonging to Taxodium family, deciduous trees, was considered as unique and rare relics in China, characterized by fast growing, straight trunk and high yield. It can grows into a mature wood during 10～15 years. At present, research on *Metasequoia glyptostrobide* includes introduction and cultivation, afforesting technology, biomass and so on, but there are few researches on the variation of its tracheid morphology. Tracheid is the main cell of coniferous tree, and accounts for more than 90 percent of timber volume. The paper aims to provide a definitely theoretic support for its oriented cultivation and rational utilization by research on variations and mature age of wood tracheid morphology for *Metasequoia glyptostrobides* and by measurement on tracheid length, tracheid double wall thickness, and tracheid diameter and so on.

2. Materials and methods

(1) Experimental materials

Experimental materials were from zhongli of yaan city, Sichuan province. The planting density of *Metasequoia glyptostrobides* is 3×2.5m. According to the country standard, five typical sample trees were selected, and 10cm-thick discs were cut down from each sample tree at the parts of their DBH (it is 1.3-meter long from the DBH to the apex along the stem) after felled.

(2)Experimental methods

A. Measurement of tracheid length

Small pieces from the parts of earlywood and latewood of each ring were cut down after thin wood pieces through the pith were softened in boiling water, and putted into test tube with mixture of 10% nitric and 10% chromic acid. Tracheid length was measured using micro-projector until the small pieces were separated into individual cells for 10～20 hours at room temperature. 60 measurements of tracheid were recorded for each ring of earlywood and latewood.

B. Measurement of ring width, latewood ratio, Tracheid diameter and tracheid double wall thickness

Some thin softened wood pieces were cut into small pieces with the rings, then made into permanent slices. Photos were taken with the magnification of 100～200 times by OLMPUS Microscope. Ring width, latewood ratio, tracheid diameter and tracheid double wall thickness were measured by wood image analysis program.

C. Definition of mature age

By number of rings as independent variable, and tracheid length, tracheid width, tracheid diameter and rings width as dependent variables respectively, tracheid length(sample A,C), tracheid width, tracheid diameter were fitted function into 4 times from pith to lateral, then rings width, tracheid lendth(sample B,C,D) were fitted

function into 2 times. Finally, extremum of four function and two function was calculated, which is mature age.

3. Results and discussion

(1)Radial variation of ring width and latewood ratio

As shown in Fig. 1. It showed ring width from pith to the10th year increased rapidly, and reached the maximum at the 10th year (8.2mm), then leveled off after 16 years（Fig.1）. In general, average ring width is 4.96mm. The mean of ring width was 5.75mm from pith to the 15th year, 2.42mm from 17th to the 21th year. The Latewood ratio from pith outward of *Metasequoia glyptostrobides* increased slowly with the variation range from3.2% to 14.3%. The maximum of latewood ratio was at the 16th year.

The ring width of *Metasequoia glyptostrobides* relatively leveled off after 16 years, which means the rapid growth period is about 16 years. Mean of latewood ratio of *Metasequoia glyptostrobides* is 7.3％. the wood can't be used as structural material due to its low latewood ratio and soft quality. The latewood ratio could be used as index to measure the intensity of soft wood.

(2) Radial variation of tracheid length

As shown in Fig. 2. Variation curves of tracheid length in earlywood and latewood were similar, and tracheid length of earlywood was less than that of latewood. Tracheid length increased with ring number from pith outward, and leveled off after 16 years, which means that the elongation growth of initial cambium cells levels off. Mean of tracheid length wais 4.13 mm. The trachaid length at the part of latewood of the 19th year is the longest.

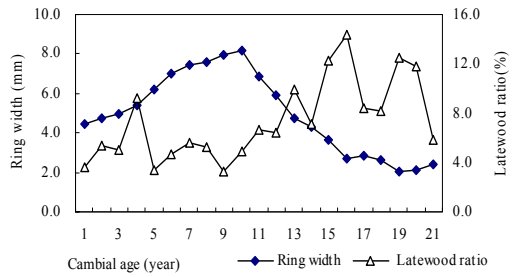

Fig.1 Radial variation of ring width and latewood ratio with cambial age.

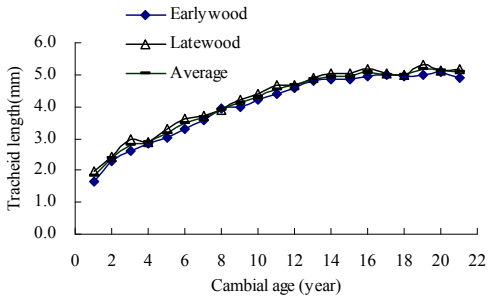

Fig. 2 Radial variation of tracheid length with cambial age.

Sudo[1] divided the variations of tracheid length in mature wood into 3 types: type I, tracheid length of mature wood remained unchanged generally; type II, it increased slowly in straight line; type III, It changed irregularly. Variation of tracheid length of *Metasequoia glyptostrobides* after 16 years was the same to type II. which was similar to variation pattern of tracheid length of *Metasequoia glyptostrobide* of Hubei of Xu Youming[2]. It showed that the radial variational patterns of Tracheid length of *Metasequoia glyptostrobides* in different areas are similar.

(3) Radial variation of tracheid width, tracheid diameter and tracheid double wall thichness

As shown in Fig. 3. Tracheid width of both earlywood and latewood trended to increase from pith outward. Tracheid width increased rapidly for early wood, and slowly for late wood from pith to 10th year, then both leveled off after 10 years. Tracheid width of early wood is bigger than that of latewood. Mean of tacheid width of earlywood was 47.3μm，that of latewood was 18.6μm. Average tracheid width of *Metasequoia glyptostrobide* was 40.7μm.

Tracheid diameter of earlywood trended to increase from pith outward, that increased 22.7～44.5μm from pith to the 10th year, then leveled off from the 11th to 21st year (44.0～49.0μm)(Fig. 3). Variation of tracheid diameter

of latrewood increased slower than that of earlywood, and a slight increasing from pith to the10th year, then declined slowly from 10th year, which ranged from 6.1μm to 10.1μm, and 8.05μm in average. Mean tracheid diameter was 32.3μm。

Tracheid double wall thickness of earlywood increased 5.6～6.9μm from pith to the 3rd ring, then increased slowly (Fig. 3). Tracheid double wall thickcess of latewood increased rapidly with number of rings from pith to the 6th ring (7.1～12.1μm), and leveled off later. Tracheid double wall thickness of latewood was bigger than that of earlywood. Mean of tracheid double wall thickness of earlywood is 6.9μm, that of latewood was 10.6μm. Average tracheid double wall thickness of *Metasequoia glyptostrobide* was 7.7μm.

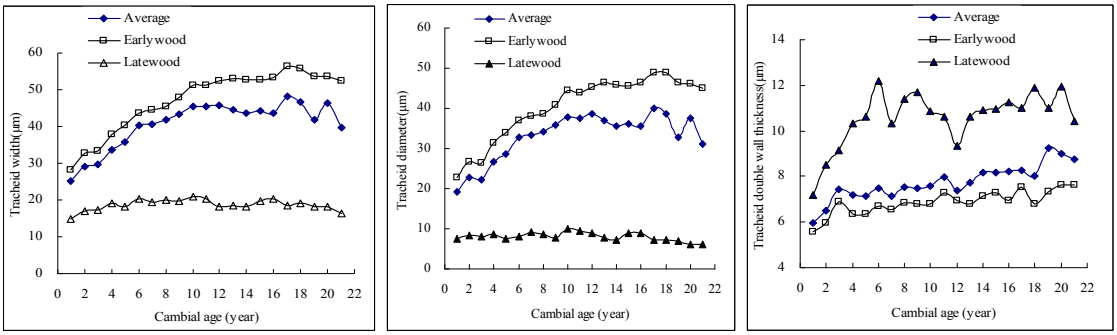

Fig. 3 Radial variation of tracheid width, tracheid diameter and tracheid double wall thichness with cambial age.

(4) Radial variation of tracheid length-width ratio, tracheid double wall thickness–diameter ratio and tracheid diameter-width ratio

As shown in Fig. 4. Tracheid length-width ratio of earlywood increased slowly from pith outward (58～99). Tracheid length-width ratio of latewood increased rapidly from pith outward (134～314)(Fig.4). Mean of tracheid length-width ratio of earlywood was 84, that of latewood was 225. The mean of tracheid length-width ratio was 100. The varition of tracheid double wall thickness-diameter ratio increased very slowly from pith to 13th year (0.35～0.48), and began to increase after 13 years(Fig.4). The mean of tracheid double wall thickness-diameter was 0.48 from pith to the 21st year. The variation of tracheid diameter-width ratio increased very slowly from pith to 13th year, and began to decline after 13 years. The mean of tracheid diameter-width ratio was 0.75 from pith to the 21st year.

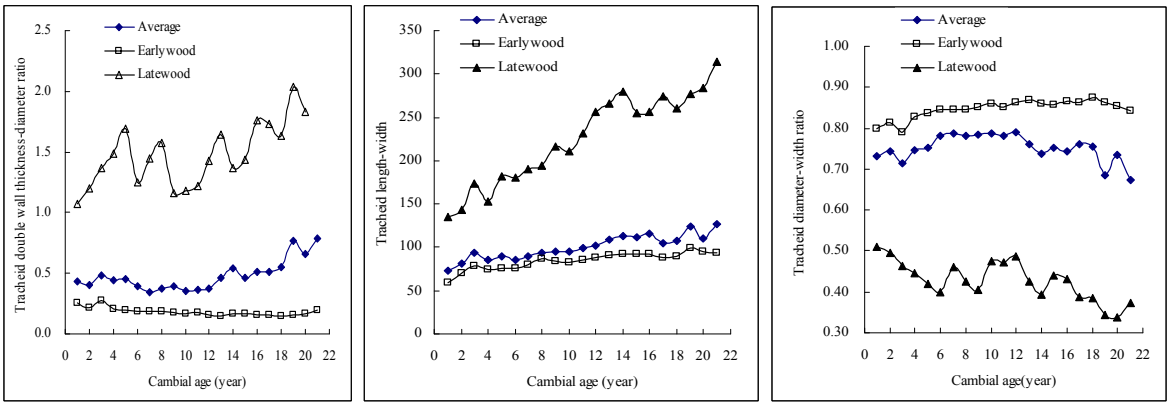

Fig. 4 Radial variation of tracheid length-width ratio, tracheid double wall thickness–diameter ratio and tracheid diameter-width ratio with cambial age.

Tracheid length-width ratio, tracheid double wall thickness–diameter ratio and tracheid diameter-width ratio are considered the standard for paper making fiber material.Many scholars thought that the fibre material with

more than 30～40 length-width ratio, less than 1 tracheid double wall thickness- diameter ratio, more than 0.75 tracheid-diameter ratio fitted for making paper. Length-width ratio of *Metasequoia glyptostrobid* was 100, tracheid double wall thickness-diameter ratio was 0.48, tracheid diameter-width ratio was 0.75, which larger length-width ratio, smaller double wall, thickness-diameter ratio were fitted for paper making. So *Metasequoia glyptostrobid* is a kind of excellent material of making paper.

(5) Definition of mature age

At present, lots of scholars defined mature age underlying with tracheid length, microfibril angle, wood density as main assessing index[3-4]. In this study, assessment index was mainly due to tracheid length, tracheid width, tracheid diameter and ring width. The means of mature age were 16.9a and 16.1a when tracheid length and ring width were used as assessment index. While, the means of mature age were 14.9a and 14.4a when tracheid width and tracheid diameter were used as assessment index. Mature age with index of tracheid width and tracheid diameter was less than that of tracheid length and ring width, which indicates that tracheid length, tracheid width, tracheid diameter and ring width could be used as index for assessing mature age of *Metasequoia glyptostrobid.* For ring width is very easy to be measured, assessment for mature age of *Metasequoia glyptostrobid* can make use of relative stable period of ring width. However, because relative stable period of ring width is more impacted by site condition, the using of this index should be lined with different conditions.

Table 1 Maturation ages of wood tracheid length, tracheid width, tracheid diameter and ring width.

Sample No.	DBH (cm)	No. of rings	Maturation age (year)			
			Tracheid length	Tracheid width	Tracheid diameter	Ring width
A	23	18	15.9	16.7	16.3	16.5
B	22.2	20	16.2	15.4	14.5	17.1
C	21.2	21	19.7	16.4	15.6	18.9
D	26.5	21	16.8	13.9	13.7	14.6
E	22.6	17	16	12.1	11.7	15.4
Mean			16.9	14.9	14.4	16.1

4. Conclusion

(1) Fast-growing period of *Metasequoia glyptostrobid* is about 16 years, and latewood ratio is low , 7.3％ in average.

(2) The means of tracheid length, tracheid width, tracheid double wall thickness and tracheid diameter were 4.13mm, 4.13 mm, 40.7μm, 32.3 μm and 7.7μm. The means of tracheid length-width ratio, tracheid double wall thickness–diameter ratio and tracheid diameter-width ratio were 100, 0.48 and 0.75. *Metasequoia glyptostrobid* can be used as material for making paper.

(3) Relation of wood properties and wood rings was obvious by fitting four function and quadratic function. The means of maturation age were 16.9a and 16.1a with index of tracheid length and ring width, 14.9a and 14.4a with index of tracheid width and tracheid diameter.

5. References

(1) Sudo,S.: Mokuzai Gakkaishi.1970,16(4):162-167

(2) Xu, Y.M.: Journal of Northeast Forestry University. 1996 , 24(6): 50-56

(3) Li Jian,L Ju Yixing.: Journal of Northeast Forestry University. 1999 , 27(4): 24-28

(4) Siokura,T.:Mokuzai Gakkaishi. 1982,28(2):85-90

Conducting Wood Esthetics Study to Propel Wood Anatomy Going Further

Jianju Luo
Forestry College of Guangxi University, Nanning

Abstract: This paper first reviewed the history and evaluated current situation of wood anatomy science in China, then brought forward the concept of "wood aesthetics". For the long-term development, study contents of wood aesthetics at present stage were schemed out and study means of wood macro-aesthetics and wood micro-aesthetics were introduced. The study of wood aesthetics should be carried out in aspects of theory and application. In theory, efforts need to be focused on the elements of wood aesthetics and the basic composition principles of wood aesthetics; in application, firstly, a deep study of the macro- and micro-structure of wood from the aesthetic point of view needs to be carried out, then, innovative design of wood figure patterns and its application in daily life should be conducted extensively. The author pointed out that wood aesthetics would have a broad developing space and an attractive prospect in application. The development of wood esthetics will open a new space for the traditional wood science and bring a strong vitality to wood anatomy science.

1. Introduction

The study of wood science in China initiated from the famous wood scientists Mr.TANG Yao who went to Peiping and worked in Fan Memorial Institute of Biology and was appointed to engage in the research of China wood science in 1931[1,2]. Till now, the development of wood science in China has a history of more than 70 years. Over the past 70 years, a wide range of researches on the wood anatomy of the main natural forest tree species in China were carried out by a large number of wood anatomy experts such as CHENG Junqin[3], LIU Songling[4], XIE Fuhui[5], HE Tianxiang and WANG Binquan[6]. Followed the elder generation, more profound researches on wood anatomy of the main plantation forest tree species in China, including macro, micro and ultramicro-structure, were conducted by a group of wood anatomy experts such as YANY Jiaju, JIANG Xiaomei, FANG Wenbing, LUO Liangcai, XIAO Shaoqiong and XU Yongjie[7,8].

As wood anatomy science developed to the present stage, systematical and profound researches have already been made on almost all the tree species of natural and plantation forest. Under such a situation, how to develop wood anatomy science further is a practical problem faced by wood anatomy teaching and researching members. Drived by such factors and inspired by the experience obtained from the project of wood science course construction, the conception of 'wood aesthetics' gradually came into being.

2. Contents of wood aesthetics study

The study contents of wood aesthetics will continue to develop as study in this field goes on. At current stage, the study should be carried out in aspects of theory and application, and the following contents need to be focused on.

(1) Exploration on aesthetic elements of wood

Inside wood, there are lots of aesthetic elements, including knots, tree forks, tree warts，annual rings, wood rays, the distribution of wood parenchyma, arrangement of pores, and also ultra-microstructural features, such as pits and spiral thickenings on the cell wall, and so on. Such kind of aesthetic elements are very rich inside wood. However, such aesthetic elements need to be discovered, explored and analyzed by our wood scientists actively, and need to be collected and filed systematically.

(2) Research on the basic composition principles of wood aesthetics

Analysis and research on the aesthetic composition principle of various wood patterns should be carried out by applying aesthetic theory. After extensive researches of this kind, the nature of beauty of wood can be recognized and revealed according to esthetic theory, and the theory and knowledge basis for the long-term development of wood aesthetics can be established.

(3) Research on macro and micro-structure of wood from the point of aesthetics

A widely study of the macro and micro-structure of wood had been made by the traditional wood anatomy science, however, it had been studied in terms of wood identification and wood material application. The results will be quite different if studies on macro and micro-structure of wood were made from the point of aesthetics. In the past, in order to identify the wood species, wood was studied in the standard surfaces of cross section, radial section and tangential section. In the study of wood aesthetics, wood slices can be studied in any different direction and angle, and this will result in various kinds of wood patterns. The wood patterns revealed in this way will be not only completely different from but also more plentiful than the traditional ones.

In addiction, the study and utilization of wood aesthetics is focused on non-material property of wood, and so, no large diameter timber is needed. In terms of wood aesthetics, the study of wood structure is not limited in large diameter timber, all kinds of woody plants can be used as study objects, including small arbor, shrub and woody vine. Therefore, wood aesthetics will widely broaden the research field of wood anatomy.

(4) Innovative design of wood aesthetic patterns

A large sum of wood aesthetic elements can be attained from the research analysis of wood structure and wood aesthetic elements. Taking these wood aesthetic elements as the basic unit, plenty of new wood aesthetic patterns with distinctive design thoughts can be acquired if recreations were carried out by applying art design theory and computer graphic technology into the recreation process.

(5) Study on application of wood aesthetic patterns

Long-term development of any academic field needs close combination with practical application and industry development. For the long-term development of wood aesthetics, extensive studies are needed in aspects of wood aesthetic pattern application and its industrialization.

3. Study means of wood aesthetics

Wood aesthetics can be divided into wood macro-aesthetics and wood micro-aesthetics. Wood macro-aesthetics mainly discusses the studies and exploitation utilization of aesthetic value at gross structure level, and wood micro-aesthetics mainly discusses the studies and exploitation utilization of aesthetic value at minute structure level.

(1) Study means of wood macro-aesthetics

The study of wood macro-aesthetics includes the following steps.

A. Material selection: using the theoretical knowledge of wood structure, and selecting the wood with special organization structure as experimental materials.

B. Surface processing: using the theoretical knowledge of wood esthetics constitution, and machining the selected wood to obtain the wood surface which can display ideal texture patterns.

C. Photo shooting: shooting the obtained wood surface by using common photography method or stereomicroscope to gain the digital photographs of texture patterns.

D. Aesthetic analysis on the photos: analyzing the gained digital photographs of texture patterns by using the theoretical knowledge of wood esthetics, and extracting the needed wood aesthetic elements from these photographs.

E. Wood aesthetic pattern recreation: with these wood esthetic elements as basic materials, recreations of wood aesthetic patterns are carried out by using art design theory and computer graphics technology according to designers' own ideas, and ideal wood aesthetic patterns with artistic innovation effect can be finally acquired.

(2) Study means of wood micro-aesthetics

The study of wood micro-aesthetics includes utilization of aesthetic elements of wood micro-structure, so micro-structure pictures of wood is needed. This requires technology of wood microscopic photography to be applied. The specific steps are as follow.

A. Wood sampling: selecting the wood with special organization structure as experimental materials,

sampling wood blocks of 6-15mm in width (tangential), 8-20mm in height (radial) and 10-30mm in length from the experimental materials.

B. Softening treatment: softening (immersion or cooking) the wood blocks to suitable extent with some chemicals (such as the mixture of glycerin and alcohol, etc.) which can soften the wood blocks to facilitate the follow-up wood slicing.

C. Wood slicing: microtoming the softened wood blocks in certain direction and with certain angle to get slices of 10-20μm in thickness.

D. Wood slices processing: Firstly, wood slices are stained in order to obtain the promising color effects by immersing in a staining solution (such as safranin, fast green, etc.). Then, the stained wood slices are dewatered step by step with alcohol solutions of different concentrations to removal the water gradually. Finally, the completely dry wood slices are treated with agents such as clove oil and xylene to improve wood slices' transparency and facilitate the follow-up microscopic photography.

E. Wood slices sealing: the above prepared wood slices are set and glued permanently with neutral resin between the glass slide and glass cover specially manufactured for biological slice. Thus wood glass slides are prepared, which can be used repeatedly and stored permanently.

F. Microscopic photography of wood structure: observing and analyzing the above wood glass slides under a photomicrography system, and taking photomicrographs of wood structure with aesthetic values.

The other aspects of study means of wood micro-aesthetics are similar to those of wood macro-aesthetics, so no need to repeat here.

4. Conclution

Study and utilization of wood aesthetic values will be a revolutionary innovation to traditional wood anatomy. It has a great theoretical significance in keeping the development of wood anatomy science going on, and also has the practical significance in enriching and beautifying people's life and meeting the social needs of people's pursuing in the enjoyment of spiritual culture.

Wood aesthetics is a new field of wood science, and it will develop gradually as people's living standard continuously improving and computer and other modern technology continuously advancing. Wood aesthetics should have a broad developing space and an attractive prospect in application. The development of wood esthetics will open a new space for the traditional wood science and bring a strong vitality to wood anatomy science.

5. References

(1) Juncheng Zhang, Zhiqin Tang, Tang Yao(1905-). Graduates from the Department of Plant in National Southeast University in1927 [J/OL]. 2002-06-02 [2008-4-28]. (http://seuaa.seu.edu.cn/s/14/t/33/a/2317/info.htm.)

(2) Youming Xu, Wood Science [M] .Beijing: China Forestry Press, 2006

(3) Junqin Chen, Nong Li, Chenzhi Sun. etc. The Identification, Properties and Utilization of Chinese Tropical and Sub-tropical Wood [M].Beijing: Science Press, 1980

(4) Songlin Lin, etc. The Wood Structure and Property of Cathay Silver Fir [M]. Changsha: Hunan Science and Technology Press, 1983

(5) Fuhui Xie, Feng Xu. The Wood Structure and Property of Wood Species [M]. Beijing: Academic Books and Periodicals Publishing House

(6) Bingquan Wang. Wood Identification [M].Xi'an: Shanxi Science and Technology Press. 1983

(7) Fuchen Bao, Zehui Jiang, etc. Wood Properties of Main Species from Plantation in China [M]. Beijing: China Forestry Press, 1998

(8) Xiaomei Jiang,etc. Wood Property and Processing of Eucalyptus and Acacia Plantation in China [M]. Beijing: Science and Technology Press.2007

Construction Mechanism of Reticular Structure of Plant Fiber

Yongqun Xie[1], Queju Tong[2] and Yan Chen[1]

[1]College of Material Engineering of Fujian Agriculture and Forestry University, Fuzhou

[2]Forintek Division of FPInnovations, Quebec, Canada

Abstract: This paper investigated and validated the mechanisms and principles for constructing reticular structure of plant fiber through frothing solution approach. After process, plant fibers became low-density reticular-structured block with all properties meeting Chinese standards for cushion packing materials. The bonds between fibers acted as knots in a truss and were strong enough to keep space occupied by bubbles in the frothing solution from shrinking in the subsequent draining process. The formation of the reticular structure depends mainly on the pressure difference between inside and outside bubble, the effect of surface adsorbent force on bubble film, and hydrogen bond among fiber hydroxide.

1. Introduction

White pollution resulting from intensive use of cellular plastics has brought various codes and acts into effect for limiting the use of cellular plastics in many countries. The R&D for substitute material is becoming an important issue. As traditional packing materials, plant fiber-paper products and plant fiber-starch products are not suitable as cushioning material thanks to their various shortcomings such as large specific gravity, great brittleness, low modulus of elasticity, poor resilience and buffer coefficient, pitiable impact strength, sensitive to moisture content, liable to mold and high cost (Wang and Wang 2005; Lawton et al. 1999; Shogren et al. 2002). Plant fiber, such as wood fiber and fiber from agricultural residuals, is renewable and can be obtained easily and cheaply, thus is an ideal raw material to make substitute cushioning material. Several studies (Cao and Wu 2005; Wang 2004; Dai and Dai 2004; Xie et al. 2004) have been conducted using plant fiber (e.g., bamboo fiber, bagasse fiber and wood fiber) as raw materials for making packaging material. The reticular-structured cushion material made from plant fiber discussed in this paper takes advantages of truss-like structure that integrates fibers and reinforces the material. This material is highly satisfied for its environmentally friendly characteristics, adequate physical and mechanical properties and economical viability.

The construction of the reticular structure of plant fiber makes use of the principle of liquid frothing (Leja 1985). When liquid froths, interspaces are created inside the solution with "extruding" effect thanks to air pressure difference between inside and outside bubble; at the same time, fiber gathers around the bubbles and forms "arches" (Wu 1991); by orienting fiber around the bubble, an effective inter-fiber bonding can be realized. This helps form a stable reticular structure with necessary physical and mechanical properties after the liquid is drained.

(1) "Extruding" effect of bubble

Under equilibrium condition, a single bubble in liquid takes the shape with the lowest system free energy, i.e., least gas/liquid interface area (approximately a sphere). The pressure difference between inside and outside bubble can be expressed as follow (Young-Laplace equation):

$$p_1 - p_2 = \gamma_{gas/liquid}\left(\frac{1}{R_1} + \frac{1}{R_2}\right)$$

The bubble diameter is usually very small (0.1~0.5 mm in diameter) and the film is very thin, so the pressure difference should be large enough to push fiber apart and thus to create space between fibers.

(2) Fiber "arches" around bubble

Fiber is adsorbed around the bubble under the adsorption effect of bubble surface (Wu 1991). Bubble adsorption is related to its surface tension, which is formulated below (Gibbs' Equation):

$$\gamma = f^{s} - \sum \Gamma_{i} \mu_{i}^{s}$$

For the nonionic surface-active agent (surfactant), the Gibbs's Equation gives the relationship between surface tension, logarithmic activity of surfactant and its residual:

$$-d\gamma = \sum RT\left(\Gamma_{s} - x_{s}\Gamma_{H_2O}\right)d\ln a_{s}$$

It is the adsorption effect of bubble on fiber that makes fiber gather on the bubble surface and form arches around the bubble.

(3) Orientation and bonding of fiber

"Slow beating" process (Casey 1980) can maintain fiber's original length and make fiber and its two ends adequately broomized, thus enrich hydroxide radicals at fiber ends. The attraction between hydroxide radicals with the effect of water-bridge, plus extremely low surface friction, makes fiber re-oriented. Then the removal of water brings hydroxide radicals closer thus facilitate hydroxide radical bonding and stable reticular structure establishing.

The objective of this paper is to propose the theory and approach for making low density reticular structure material and validate the theory and approach. This will enable effective use of plant fiber and production of low density, high performance, environmentally friendly material, thus allow for reduced use of non-environmentally friendly materials.

2. Materials and methods

Chinese-fir fluff pulp from Jiangle Senrong Fluff Pulp Plant of Fujian, sulphate chemical pulp from Canada and fibre for medium density fiberboard from Furen Wood Ltd. of Fujian were mixed up at the proportion of 6:3:1 in absolute dry weight and refined to beating degree of 40ºSR. Moisture content of the fiber was then adjusted to 8%.

When blending pulp, terpene frothing agent, nonionic alkyl surfactant and FPC compound resin were added into the pulp in order at the amount of 7.2, 11 and 85 mg per litre frothing solution, respectively. After the pulp frothed adequately (approx. 5 minutes), 1100 ml frothed pulp was measured with a quantifying box and then transferred to a forming box. After laid aside for 3 minutes, the formed mat was drained and then dried to below 6% in moisture content. Fig. 1 shows a picture of the final product suggesting fine integration of the mat. The laboratory process for producing reticular structured mat is presented in Fig. 2.

Fig. 1 A picture of sample mat.

Following the national standards for packing materials, sample products for packing ADSL broad-band modems and digital cameras were tested in Fujian Product Quality Test Center.

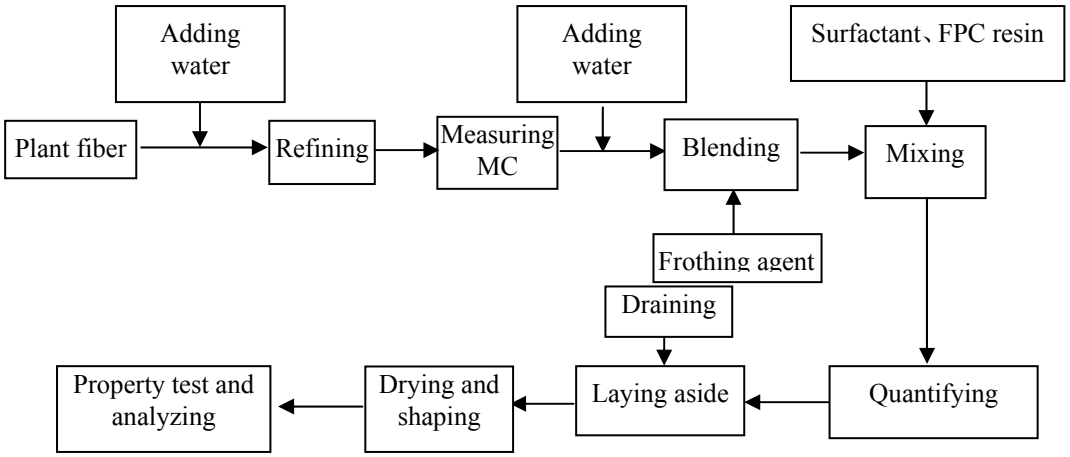

Fig. 2 Laboratory process for producing reticular structured mat.

3. Results and Discussion

Microscopic image showed that the reticular structure of fiber plant had evenly distributed knots (connected fiber) and lumens inside the mat (Fig. 3). A further examination under scanning electron microscope suggested the effectiveness of fiber bonding (Fig. 4). This implied that using solution frothing approach is an effective way to make reticular structured mat from plant fiber.

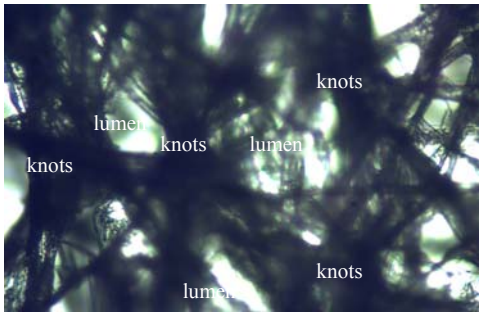

Fig. 3 Microscopic structure of sample mat.

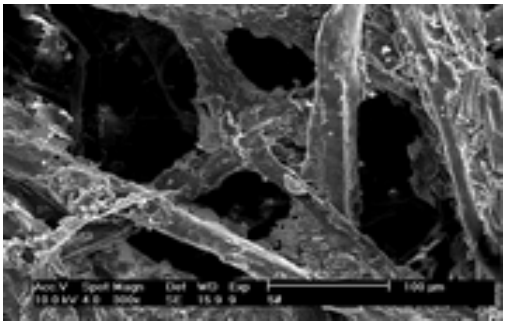

Fig. 4 SEM image of reticular structure.

Test results indicated that all tested properties met the requirements for cushion packing materials (Table 1). The density (0.033 g/cm^3) was much lower than the required (0.2 g/cm^3). The extremely low mat density resulted from the effective bond between fibers and consequent reticular structure. This structure made up with knots and lumens (Fig. 3) which were the oriented fiber around bubbles and spaces occupied by bubbles in frothing solution, respectively. Mat density depends on the size of lumen, which depends on the size of bubble and the effectiveness of fiber bonding. The bond between fibers played a role of knots in a truss, which was strong enough to prevent lumen from shrinking during subsequent draining process. As the size and amount of bubbles are controllable by adjusting production parameters and using different amount of assistant agents, the density of mat can be controlled to range from 0.001 to 0.08 g/cm^3. Materials with such density and structure can be used as a cushion packing material for the excellent properties in shock resistance, vibration absorption and reduction. They can also be used as heat insulation material. The produced mat from this study had a coefficient of heat conductivity between 0.028 and 0.041 W/m·K.

Table 1 Sample mat properties following national standards of China for cushion packing materials.

Test		Requirement	Test result
Sense index		No peculiar smell	No peculiar smell
Density (g/cm^3)		≤0.2	0.033
Free-drop test (from height 800 mm)	ADSL（1kg）	No damage	No damage
	Digital Cameras (220g)		No damage
Stacking test (stacking height: 2.50 m)	ADSL（1kg）	No apparent deformation / damage	No apparent deformation / damage
	Digital Cameras (220g)		No apparent deformation / damage
Vibration at a constant frequency [1)]	ADSL（1kg）	No abnormal damage	No abnormal damage
	Digital Cameras (220g)		No abnormal damage
Vibration at variable frequencies [2)]	ADSL（1kg）	No abnormal damage	No abnormal damage
	Digital Cameras (220g)		No abnormal damage
Compression strength (10% deflection) (kPa)		/	2.5
Moisture absorption (%) (under 50℃, 95%RH for 96 hours)		<28	17
Consistency		No degeneration	No degeneration
Contact corrosion		≤1	0
PH value		5~8	7.6
Ash content (%)		<1	0.35

1) Test frequency: 5 Hz for 1 hour with amplitude of 1 mm)

2) Test was carried out at 5, 10, 20 and 30 Hz for 1 hour each with amplitude of 1 mm)

4. Conclusions

Based on the results following conclusions can be drawn:

(1) A reticular structure of plant fiber can be established with solution frothing approach;

(2) An effective bond between fibers can be realized with the effect of hydroxide radicals;

(3) Material produced had a density between 0.001 to 0.08 g/cm^3 and density is controllable. The produced material had excellent properties that meet the Chinese standards for cushion packing materials.

5. References

(1) Cao, S.W. and Q.Y. Wu. 2005. The buffering packaging material from foaming plant fiber. China Packaging Industry, 99(9): 8-11

(2) Casey, J.P. Ed. 1980-83. Pulp and paper - chemistry and chemical technology. New York: Wiley-Interscience, 3rd Ed..

(3) Dai, H.M. and P.H. Dai. 2004. Study on the key technologies of products from foaming plant fibre. Packaging Engineering (China), (2): 9-11

(4) Lawton, J.W., R.L. Shogren and K.F. Tiefenbacher. 1999. Effect of batter solids and starch type on the structure . Cereal Chem,, 76(5): 682-687

(5) Leja, J. 1985. Surface chemistry of froth flotation. Metallurgical Industry Press, Beijing, China Shogren, R. L., J.W. Lawton and K.F. Tiefenbacher. 2002. Baked starch foams：starch modifications and additives improve process parameters, structure and properties. Industrial Crops Products, 16(1): 69-79

(6) Wang, L.Y. and J.Q. Wang. 2005. Study on properties of starch-fiber biodegradable packaging materials. Packaging Engineering (China), (2): 7-9

(7) Wang, N.Y. 2004. Characteristics of foaming packaging material from plant fiber. China Packaging, 24(1): 103-104
(8) Wu, H.H. 1991. Surface chemistry. Peking University Press, Beijing, China
(9) Xie, Y.Q., Y. Chen and B.G. Zhang. 2004. Study on foaming material from plant fiber. China Wood industry, 18(2): 30-32

Study of Puffing Cell Walls

Jian Qiu[1], Jeanran Gao[1] and Monlin Kuo[2]

[1] College of Wood Science and Technology, Southwest Forestry University, Kunming

[2] Department of Natural Resource Ecology & Management, Iowa State University, USA

Abstract: Since wood is porous it also is a good heat and sound insulating material. Puffing the cell wall may lose certain level of mechanical properties but would increase its insulation properties. In this study, *Trema orientalis* wood was first treated with nitric acid aqueous solution to damage the S_3 layer of cell walls, followed by puffing the cell wall inward with saturated urea and $ZnCl_2$ solutions. Results indicated that treating *Trema orientalis* with 10% nitric acid at 100 ^oC for 20 minute damaged the S_3 layer of cell walls, and the subsequent treatment with urea and $ZnCl_2$ saturated solutions caused the fiber tracheid walls to swell up to 76%. Then, the swollen material was dried with critical CO_2 fluid to obtain puffed wood. SEM examinations of nitric acid-treated samples showed that lignin were removed from the S_3 layer surfaces and S3 mirofibrils were ruptured causing the entire secondary walls to swell inward.

1. Introduction

Microfibrils are the skeletal components in the cell wall that provide strength and other physical properties of wood. Wood is an excellent heat and sound insulation material due to its porosity. These insulation properties would be enhanced if the cell wall can be swollen beyond the normal extent so that additional voids are created in the cell wall. It is the S2 layer of secondary cell walls determines how much the cell wall swells. Due to constraint of the S1 and S3 layers, there is a limit how much the S2 layer is able to swell. Thus, microfibrils in the S1 and S3 layers must be fractured for the S2 layer to swell freely. The S1 layer is inaccessible; thus fracturing the S3 layer may allow the S2 layer to swell toward the lumen. This paper reports results of such an attempt.

2. Materials and methods

(1) Materials

Trema orientalis trees with approximately 20 growth rings at the butt ends were harvested near Pur City, Yunnan Province, China. Boards cut from the sapwood were air-dried before further cutting them into 20 mm x 20 mm x 5 mm (L) samples.

(2) Nitric Acid and Swelling Treatments

Test samples were saturated with 5%, 10% and 15% nitric acid aqueous solution within one hour at room temperature with the aid of intermittent vacuum. Then, the nitric acid-saturated samples were heated in the corresponding nitric acid solution at 40, 70 or 100 ^oC for 20, 40 or 60 minutes. Samples were treated with each of the nitric acid concentration/temperature/duration condition as listed in Table 1. After washing the acid-treated samples completely with distilled water, five samples each were immersed in saturated urea and zinc chloride aqueous solution for 3 weeks, followed by removing urea and zinc chloride with distilled water.

(3) Microscopy

Samples treated with nitric acid and subsequently with saturated solutions of urea and zinc chloride were cut into small specimens [3 mm x 3 mm x 5 mm (L)] and embedded in polyethylene glycol (PEG 1450), and 10 m-thick transverse sections were cut with a sliding microtome. Sections were mounted in 50% aqueous glycerin without staining and studied with a Nikon Eclipse light microscope. Double-cell-wall thickness of fiber tracheids were measured with the aid of Motic Software. The same procedure was done for untreated samples to measure the un-swollen cell wall thickness. One hundred cell wall thickness measurements were made for each

acid/swelling treatment, and percent swelling efficiency of each treatment was calculated based on the untreated cell wall thickness.

Scanning electron microscopy of samples treated with 10% nitric acid at 100 ^{o}C for 20 minutes were done following the method of Kuo et al (1988). Briefly, the samples were embedded in polyethylene glycol (PEG 1450), followed by cutting smooth radial surfaces with razor blade and removing PEG with water.

3. Results and discussion

Many organic liquids and saturated salt solutions are able to swell wood beyond the swelling capacity of water (Stamm 1964). Swelling of the S2 layer, however, is restricted by the presence S1 and S3 layers. In this study, urea and zinc chloride saturated solutions were chosen to swell the cell wall and nitric acid was used to damage the accessible S3 layer to allow the S2 layer to swell into lumen. Results in Table 1 show that condition of the nitric acid treatment is critical in maximizing cell wall swelling. As shown in Table 2, the effects of acid concentration, temperature and duration of heating were all highly significant during the nitric acid treatment. The maximum cell wall swelling with both urea and zinc chloride saturated solutions after the acid treatment achieved was about 75%.

Table 1 Cell wall swelling efficiency of nitric acid treated samples.

Nitric acid treatments			Cell wall swelling efficiency (%)	
Concentration (%)	Temperature (^{o}C)	Duration (minutes)	Urea	$ZnCl_2$
15	100	60	38	24
15	70	40	44	36
15	40	20	44	33
10	100	40	66	56
10	70	20	71	76
10	40	60	45	44
5	100	20	78	72
5	70	60	60	36
5	40	40	42	39

Table 2 Variance analysis of effect of acid treatment on cell wall swelling.

Source	Urea				Zinc chloride			
	SS	Mean Sq.	F	p	SS	Mean Sq.	F	p
Aicd Conc.	6.40	3.20	27.01	<0.01	12.27	6.13	66.09	<0.01
Temp	4.81	2.40	20.29	<0.01	2.64	1.32	14.32	<0.01
Duration	4.62	2.31	19.51	<0.01	10.14	5.07	54.65	<0.01

Fig. 1 indicates that optimum acid pre-treatment condition was treating samples with 10% nitric acid at 100 ^{o}C for 20 minutes and that saturated urea solution was more effective in swelling cell walls than zinc chloride saturated solution. Treating samples with nitric acid at concentration lower than 10% and at low temperatures than 100 ^{o}C was not able to damage the S3 layer sufficiently to allow cell wall to swell. Treating the samples with 15% nitric acid and heating for more than 20 minutes showed much lower cell wall swelling probably because such hash conditions removed substantial amount of materials from the cell wall.

Fig. 2 shows an SEM microphotograph of a fiber tracheid in samples not treated with nitric acid, in which the S3 surface appears smooth and undamaged, whereas as shown in Fig. 3 the S3 microfibrils of fiber tracheid in samples treated with 10% nitric acid at 100 oC for 20 minutes were severely disrupted. Disruption of S3 microfibrils allowed the S2 layer to swell freely inward towards the lumen.

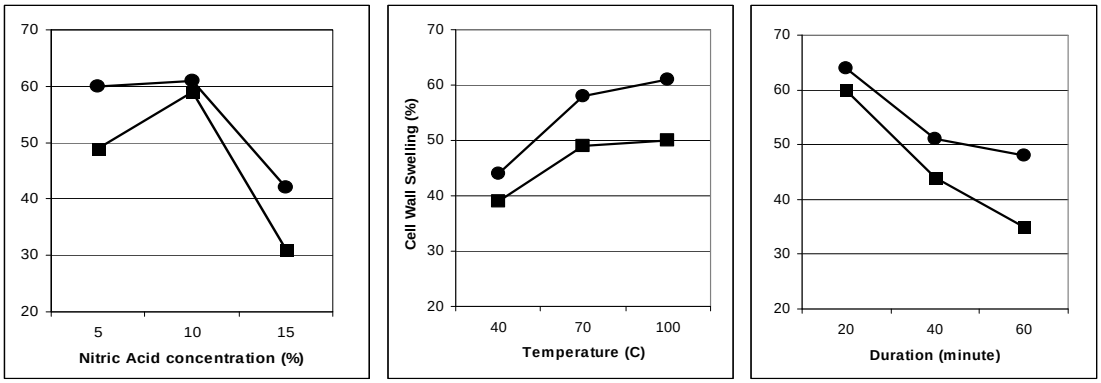

Fig. 1 Effects of nitric acid concentration, temperature and heating time in acid pre-treatment on cell wall swellin.

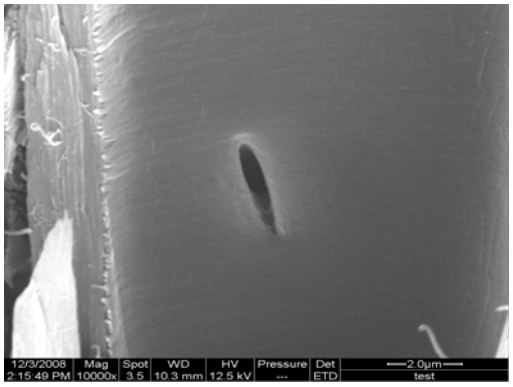

Fig. 2 Untreated fiber tracheid with smooth and undamaged S3 layer.

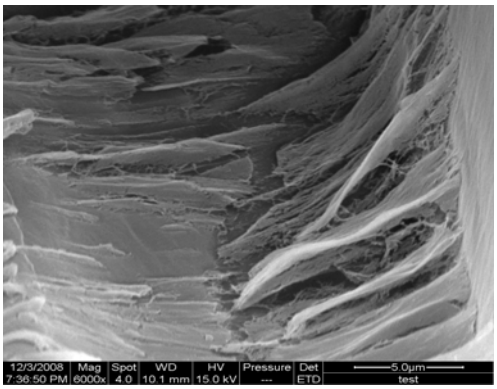

Fig. 3 Nitric acid-treated fiber tracheid with ruptured S3 layer.

Fig. 4 is a light microphotograph of transverse section of untreated *Trema orientalis* wood, showing fiber tracheids with thin walls and large lumen diameters. Fig. 5 shows a transverse section of *Trema orientalis* wood that was acid pre-treated followed by immersing in zinc chloride saturated solution for 3 weeks, where fiber tracheid walls were greatly swollen with much reduced lumen diameter. External swelling of wood is limited due to presence of S1 layer and compound middle lamella. In the treated wood, with S3 layers damaged by the nitric acid treatment, swelling pressure in the S2 layer caused the cell wall to swell toward lumen, resulting in reduced lumen diameter.

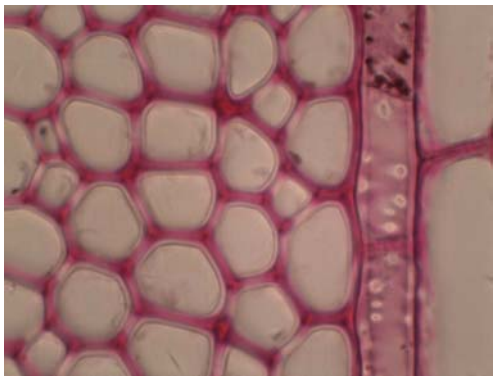

Fig. 4 Transverse section of untreated *Trema orientalis* wood with thin walls and large lumen diameters.

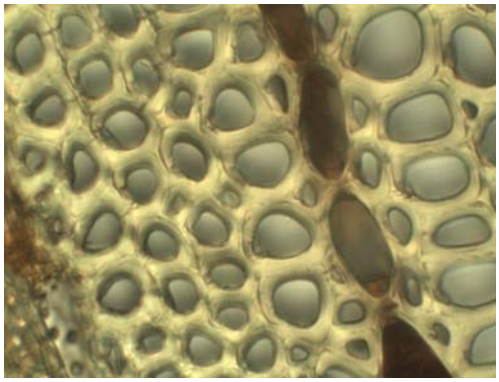

Fig. 5 Acid pre-treated *Trema orientalis* wood followed by $ZnCl_2$ treatment, showing swollen walls and reduced lumen diameter.

4. Conclusions

Pre-treating *Trema orientalis* wood with nitric acid followed by immersing the wood in saturated solutions of urea and zinc chloride was able to swell cell wall up to 75% of the original thickness. Optimum conditions of acid pre-treatment to obtain maximum cell wall swelling was found to be 10% nitric acid and heating at 100 ^{o}C for 20 minutes. SEM observations indicated that acid pre-treatment caused rupture of S3 microfibrils which allowed S2 layers to swell toward lumen. Observations with light microscope also showed that acid and saturated salt solution treatment caused substantial swelling of cell walls with reduced lumen diameters. Critical point drying of the swollen wood would result in a material with additional porosity in the cell wall.

5. Acknowlegement

The authors wish to thank the National Natural Science Foundation of China for supporting this study under Project No. 30630052

6. References

(1) Kuo, M. L., D. D. Stokke, and H. S. McNabb, Jr. 1988. Microscopy of progressive decay of cottonwood by the brown-rot fungus *Gloeophyllum trabeum*. Wood & Fiber Science 20(4):405-414.
(2) Stamm, A. J. 1964. Wood and Cellulose Science. Ronald Press Co., New York.

Variation of Vascular Bundle and Metaxylem Vessel Morphology and their Correlations with Physical-Mechanical Properties of *Phyllostachys pubescens*

Yi-Qiang Wu

College of Materials Science and Engineering, Central South University of Forestry and Technology, Changsha

Abstract: *Phyllostachys pubescens* is the most important bamboo resources used for pulping and paper as well as construction in China. In order to make use of bamboo resources, the diameter of vascular bundle and metaxylem vessel at the tangential and radial directions and physical-mechanical properties of *Phyllostachys pubescens* were determined, Variation patterns of vascular bundle and metaxylem vessel and their correlations with the physical-mechanical properties were carried out. Research results are as follows: 1) Tangential diameter of vascular bundle and metaxylem vessel of the three parts of bamboo in the radial direction is outside >middle>inner, while the radial diameter of metaxylem vessel is almost same.Vascular bundle diameter decreases with the increase of height. 2) Basic density is significantly negatively correlated with radial vascular bundle diameter, negative correlation with tangential metaxylem vessel diameter; Both radial shrinkage-tangential vascular bundle diameter correlation and tangential shrinkage-radial metaxylem vessel diameter correlation were is significantly positive; Both tangential and radial vascular bundle diameter are significantly correlated with thermal diffusion coefficient. Mechanical properties except for shear strength obviously negatively correlated vascular bundle diameter,while significantly positively correlated with metaxylem vessel diameter.

1. Introduction

Phyllostachys pubescens is the main bamboo resource and also is one of the main timber assortment of cultivating pulpwood in China. While researches on its properties is the most basic work to utilize bamboo resource efficiently and deeply[1]. Many researchers at home and abroad have carried on plenty study on it: Zhang Qi-sheng[2] studied on the variation of fiber thickness in different ages to find that fiber thickness increases from inner to outside then reduce when getting the top; and that fiber thickness increases along with the ages increasing. Ma Ling-fei[3] determined the fiber morphology, tissue ratio, cellulose content and basic density and analyzed the variation of the above indicator. Xian Xing-juan[4] explored the relation between age and physical-mechanical properties, the results showing the age is close related to physical-mechanical properties. Tommy and Chung [5, 6] studied the mechanical properties of *Phyllostachys pubescens* to find that the compressive strength is related to the quantity of vascular bundle. Tong Jin[7] explored the effect of content of vascular bundle fiber on wear resistance. From all the studies, we can know that the vascular bundle and vessel are the important constitution of *Phyllostachys pubescens*, and the vascular bundle composing of many thick-wall cells is the key factor that affects the physical-mechanical properties [8,9].

In this paper, we measured tangential and radial diameter of vascular bundle and metaxylem vessel in the experiment, analyzed their variation, and explored the correlation between vascular bundle and metaxylem vessel morphology and main physical-mechanical properties by means of mathematical statistics analysis, to provide important reference for sustainable and reasonable development of bamboo resources.

2. Materials and Methods

(1) Preparation of materials

Five 3-4 years-old *Phyllostachys pubescens* selected from Xing Longshan Village, Long Toupu Town in Hunan Province. After falling down, all specimen bamboos were sawed into segments and were marked ordinally and directionally. All these segments were air dried in the laboratory under the nature condition, then made into test specimens.

(2) Methods of measurement

Measurement of vascular bundle diameter and metaxylem vessel diameter: Permanent microscopic slides on cross section were made in each specie bamboos. Under digital biomicroscope, four points ranging from outer to inner were averagely chosen on one slide, tangential diameter and radial diameter in vascular bundle and those in metaxylem vessel were measured and calculated, all measurements were repeated three times.

(3) Measurement of physical-mechanical properties

Physical-mechanical properties including basic density, shrinkage,compressive strength, shear strength parallel to grain, tensile strength parallel to grain and bending strength are determined according to National Standard GB/T15780-1995.

(4)Measurement of thermal diffusion coefficient

Flash method was adopted with JR-2 Laser Tester, whose measuring accuracy is±5%. Assuming the thickness of the testing material is much smaller than the diameter(0.2 cm<<1.0 cm), and one side of testing specimen was heat equably and quickly, then the shape of temperature-rising curve in opposite side is related to thermal diffusion coefficientα and thickness. Based on this theory, by micro thermocouple, temperature which varies with time is measured, then is transformed into signal which is amplified later and enters A/D converter.The final thermal diffusion coefficient is got by processing these signals in microcomputer.

(5) Analysis of data

All data collected from this experiment were preliminarily processed by Microsoft Excel, and then were analyzed by means of regression analysis and correlation analysis with 12.0 SPSS.

3. Results and Discussion

From the data we obtained in experiment, they shown us that the tangential diameter of vascular bundle and vessel in the outer of bamboo are the most large, then bamboo pulp, last inner of bamboo； the radial diameter of vascular bundle distributed uniform in every part, however, the radial diameter of vessel is most large in the outer of bamboo, then bamboo pulp, last inner of bamboo, this is the same with the variation in tangential direction. The variation of tangential and radial diameter of vascular bundle and vessel in south and north direction are light. In addition, the tangential and radial diameter of vascular bundle and vessel varied lightly in height.

In Table 1, the pearson correlation showed us the relationship between diameter of vascular bundle and vessel and physical-mechanical properties of *Phyllostachys pubescens.* The thermal diffusion coefficient is a very important physical parameter, for it is a critical factor in the process of bamboo-based panel manufacture when hot pressing, as illustrated the thermal diffusion coefficient increased along with the increase of tangential and radical diameter of vascular bundle, at 0.01 level, their correlation coefficients are 0.909, 0.907 respectively, however, the thermal diffusion coefficient decreased when the tangential and radical diameter of vessel increase, at 0.05 level, their correlation coefficients are -0.834, -0.775 respectively.

The correlation between basic density and tangential and radial diameter of vascular bundle and vessel are very significant, their correlation coefficients are -0.729(at 0.05 level), 0.886 (at 0.01 level), -0.837 (at 0.01 level), 0.885(at 0.01 level). As the result showed, the basic density increased along with the decrease of tangential and radical diameter of vascular bundle, but increased when the tangential and radical diameter of vascular bundle increase, because vascular bundle is an important component of bamboo, the diameter of vascular bundle is more large, the space in bamboo wood is more large, resulted in less substance per volume, and contributed to lower basic density. Also this result is in accordance with former research.

As illustrated in Table 1, the radial shrinkage is negatively related to tangential and radial diameter of vascular bundle, the tangential shrinkage is negatively related to tangential and radial diameter of vessel, but the volume shrinkage is not related to tangential and radial diameter of vascular bundle, nor to tangential and radial diameter of vessel.

The correlation between radial diameter of vascular bundle and mechanical properties (BS,TSPG,CS,SS,MOE) of *Phyllostachys pubescens* are significant, at the 0.01 level, their correlation

coefficients are -0.886, -0.879, -0.925, -0.847, -0.856 respectively. The correlation between radial diameter of vascular bundle and mechanical properties (BS,TSPG,CS,MOE) of *Phyllostachys pubescens* are significant, except SS, their correlation coefficients are -0.819, -0.799, -0.833 at 0.05 level, -0.862 at 0.01 level. The correlation between tangential and radial diameter of vessel and BS,TSPG,CS,SS,MOE are significant at 0.01 level, and also the correlation between tangential and radial diameter of vessel are significant, their correlation coefficients are 0.792, 0.724 respectively. These results indicated that the size of vascular bundle and vessel are closely related to the main mechanical properties, this is to say, the size of vascular bundle and vessel can measure main mechanical properties of *Phyllostachys pubescens* to some extent to avoid complicated determination.

Table 1 Pearsons' correlation coefficients.

Index	tangential diameter of vascular bundle	radial diameter of vascular bundle	tangential diameter of vessel	radial diameter of vessel
BD	-0.729(*)	-0.837(**)	0.886(**)	0.885(**)
RS	-0.837(**)	-0.769(*)	0.551(ns)	0.579(ns)
TS	0.697(ns)	0.813(*)	-0.858(**)	-0.870(**)
VS	-0.558(ns)	-0.399(ns)	0.141(ns)	0.061(ns)
TDC	0.909(**)	0.907(**)	-0.834(*)	-0.775(*)
BS	-0.819(*)	-0.886(**)	0.899(**)	0.850(**)
TSPG	-0.799(*)	-0.879(**)	0.918(**)	0.874(**)
CS	-0.833(*)	-0.925(**)	0.891(**)	0.867(**)
SS	-0.657(ns)	-0.847(**)	0.866(**)	0.926(**)
MOE	-0.862(**)	-0.856(**)	0.792(*)	0.724(*)

Note:** at the level of 0.01； * at the level of 0.05； ns presents not significant;BD-basic density; RS-radial shrinkage; TS-tangential shrinkage; VS-volume shrinkage;TDC- thermal diffusion coefficient ; BS- bending strength; TSPG- tensile strength parallel to grain; CS- compressive strength parallel to grain; SS- shearing strength parallel to grain; MOE-modulus of elasticity.

4. Conclusions

(1) Tangential diameter of vascular bundle: outside> middle> inner, they reduce both in outside and middle, and there was no apparent change in inner; radial diameter: middle> outside> inner, with height increase, both tangential and radial diameter of vascular bundle decrease in all these three parts. Tangential and radial diameter of vessel: outside> middle> inner, and there are obvious difference in these three parts; all of them have a trend to increase with height increase.

(2) Vascular bundle diameter is significantly negative-correlated to basic density and radical shrinkage, metaxylem vessel diameter is significantly positive-correlated to basic density but negative to tangential shrinkage, and they are significantly correlated to thermal diffusion coefficients with correlation coefficients being 0.909,0.907,-0.834,-0.775, respectively.

(3) The correlation between tangential diameter of vascular bundle and other four mechanical properties are significant at the level of 0.01, the correlation coefficient to bending modulus of elasticity is -0.862 at the level of 0.05, the correlation coefficient to tensile strength, compressive strength, bending strength are -0.819, -0.799 and -0.833 respectively; the correlation between radical diameter of vascular bundle and all the mechanical properties are significant, the correlation coefficient are -0.886, -0.879, -0.925, -0.847 and

-0.856 respectively. As for the relationship between mechanical properties and metaxylem vessel diameter at the level of 0.01, the tangential diameter of metaxylem vessel is significantly correlated to bending strength, tensile strength, compressive strength and shear strength with correlation coefficient being 0.899,0.918,0.891 and 0.866 respectively, the radial diameter of metaxylem vessel is significantly correlated to bending strength, tensile strength, compressive strength and shear strength with correlation coefficient being 0.850,0.874,0.867 and 0.926 respectively; the tangential and radial diameter of vessel are significantly correlated to bending modulus of elasticity with correlation coefficient being 0.792 and 0.724 respectively.

5. References

(1) W. Liese, FRG.Hamburg: Wood Sci. Technol. Vol. 21(1987), p.189
(2) Q.S. Zhang: Industrial utilization of bamboo in China. China Forestry Pbulishing House. Beijing(1995).
(3) L.F. Ma: Scientia Silvae Sinicae. Vol. 33(1997), p.356
(4) X.J. Xian : Journal of Bamboo Research Vol. 9(1990), p.10
(5) Y.Tommy: Construction and Building Materials Vol. 22 (2008), p.1532
(6) K.F. Chung, W.K. Yu: Eng. Struct. Vol. 24(2002), p.429
(7) J. Tong: Wear. Vol. 259 (2005), p.78
(8) D.Fengel, X.Shao: Wood Sci.Technol. Vol. 18(1984) , p.103
(9) Y.F. Yang, Z. Liu : Journal of Zhejiang Forestry University Vol. 3(1996), p.21

This work was supported by Eleventh Five-Year-Plan National Scientific & Technological Supporting Project (No. 2008BADA9B0102).

Comparative Study of Carbon Storage in *Larix olgenisis* and *Larix kaempferi*

Mingfang Yin[1], Lin Zhao[1] and Weida Yin[2]

[1]College of Forestry, Shenyang Agricultural University, Shenyang

[2]Horticultural Research Institute of Undergraduate College, Chiba University

Abstract: The purpose of this study lies in obtaining the current annual and mean increment of stem volume using stem analysis method, determining the carbon percentage and density of *larix olgensis* and *larix kaempferi* in their different age stages, and probing into the carbon storage process of these two species of trees. Results indicate that at the ages of 48.3 and 49.3 respectively, the stem volume of *larix olgensis* and *larix kaempferi* has the maximum mean increment; the carbon density fluctuations of these two species of trees tend to be basically identical, to put it concretely, *larix olgensis* reaches its peak at the age of 30 and *larix kaempferi* at the age of 35; the current annual carbon storage in *larix kaempferi* is greater than *larix olgensis* but would reach the maximum value at an elder age, to put it concretely, *larix olgensis* is at the age of 30 and *larix kaempferi* at the age of 35; *larix kaempferi* has a lager average carbon storage than *larix olgensis*; at the age of 48.7 and 47.7 respectively, *larix olgensis* and *larix kaempferi* stem volume have the maximum mean increment, which is obtained by fitting in the curve equations on current annual and average carbon storage.

1.Introduction

Over the past two decades, a mass of research work on carbon storage, density and sequestration of the forest ecosystem have been done by scholars worldwide, and significant achievements were accomplished[1-5]. So far, forestry sequestration is chiefly measured in two major ways: standing crop biomass inventory method and forest carbon dioxide flux conversion method [6-7]. The first method is easy to operate and therefore widely used in China，but unsatisfying in precision; the latter one was only applied in recent years in China when the Chinese Academy of Sciences established four carbon dioxide flux fixed-position observation stations[8-9] for typical forest ecosystem in 2002 to analyze the carbon flux over forests at different areas[10-12].

In this discussion, by applying the forest measurement and the biological wood science theories and on the basis of a mass of research achievements made by former research fellows, the dynamic measurement of forest carbon storage is put forward as a new type of concept: according to many studies made by Fang Jingyun et al[13] that the amount of growing stock is closely related with standing tree biomass, and that the annual forest carbon storage is a variable attached to the forest tree volume increment percent [14], we can directly measure the three factors affecting the forest carbon storage, that is, volume of forest tree growth at the age of t, density of dry matter in the forest trees at the age of t and carbon content of dry matter in the forest trees at the age of t, to probe into new research methods for the dynamics of carbon storage in different age stages (5 years for each age stage) which are actually measured based on the volume increment, wood density, carbon content and density, trying to make clear of the variation of carbon storage in forest tree stem.

The purpose of choosing Larix olgensis and Larix kaempferi which are the major tree species for artificial afforestation as the objects to study and classifying carbon storage into current annual carbon storage and average carbon storage and measuring them respectively lies in probing into the law of change in carbon storage during their growth.

2. Geographic and natural conditions, and research method

(1)Geographic and natural conditions

The research was carried out at Dabiangou Forest Farm south of Qingyuan Manchu Autonomous County, Fushun city, Liaoning province (41°59′-42°42′N,124°59′-125°10′E). This area is of the continental monsoon climate, chilly and dry in winter, and hot and rainy in summer. The soil is generally of brown forest soil with a pH of 5.5～6.5.The vegetation is of Changbai broad-leaved mixed forest.

(2) Research method

A. Gathering sample

The sample was cut down at Qingyuan Dabiangou Forest Farm, Liaoning province. Both of the two sample trees are found in pure artificial forests with the age of 45 and density 0.8. Choosing two standard areas of 20 m×30 m for *Larix olgensis* and *Larix kaempferi*, then the diameter and heigh are measured for both tree samples, as a result, their standard diameters at ground levels are 23.4 cm and 25.8 cm respectively. According to their average diameters, three standard tree samples has been chosen from each standard land(Table 1).

Table 1 Schedule of DBH （diameters at breast height）and tree height of sample trees.

Sample tree		DBH (cm)		Tree height(m)
		Outside bark	Inside bark	
Larix olgensis	1	24.5	22.9	27.8
	2	22.0	21.6	22.9
	3	23.6	22.0	24.9
Larix kaempferi.	1	25.9	23.8	24.0
	2	26.2	24.9	26.3
	3	25.4	23.1	28.0

B. Obtaining data

Cut down the sample trees for stem analysis[15]. In the sample preparation workshop at Timber industry Research Institute of Chinese Academy of Forest Sciences, through their piths we cut the discs into sample bars of 1cm in both width and height along north-south direction and then into blocks according to an age span of five years. Measure the accurate length of each block using a vernier caliper, the length value represents the volume of each sample block. Put the sample blocks into a dryer for a baking at (103±2) ℃ for 8h, and choose 2~3 blocks for test weighing for the first time, then weigh the just weighed sample blocks again 2h later. In case the mass difference between the second and the third weighing is within an order of magnitude of 10^{-3}, we can consider the samples are completely dry.

Take out the sample blocks that are cut according to different age spans, and weigh their dry mass after cooling for future use. Put the sample blocks into an FW100 universal high-speed smashing machine for smashing, we obtain fine particles with a diameter of 100 meshes. Pack 10mg of the smashed sample with a tin boat and put it into a Vario EL Ⅲ elemental analyzer[16] to measure the carbon percentage of the sample. The formula is:

$$Cp = \frac{Cc \times m}{V}. \quad (1)$$

where Cp represents carbon density ($g \cdot cm^{-3}$); Cc represents carbon percentage (%); m presents the wood mass (g) of sample blocks cut according to an age span of five years; V represents the volume (cm^3) of sample blocks cut according to an age span of five years.

By this means we obtain the carbon densities in different age spans. Through classification and tabulation of the data obtained using the above method, we obtain the arithmetic average of various indexes of different tree species.

C. Calculation of carbon storage

By reference to the forest measurement theories about the concepts of current annual carbon storage (C_{θ}, kg) and average carbon storage (C_Z, kg), we calculate the carbon storage in two ways, current annual carbon storage and average carbon storage (C_Z, kg). The former means the actual carbon storage in trees in a certain year; the later means the average carbon storage in trees over a certain period. The formula is:

$$C_\theta = Cp \times \theta_A \quad (2)$$

$$C_Z = Cp \times Z_A \quad (3)$$

Where θ_A presents the mean volume increment(m^3); Cp represents carbon density ($kg \cdot m^{-3}$); Z_A represents the current annual volume increment(m^3).

All analyzed by means of SPSS 13.0 and equation-fitted by means of curve essessstimation.

3. Results and Analyses

(1) Sample tree volume increment

It can be seen from Fig. 1 that the volume increment of both *larix olgensis* and *larix kaempferi* increases without interruption and comes into a rapid growth stage since the 10th year. Their growth speeds down more or less after 25 years later and reaches their peaks at the age of 35. After that, the mean increment of both tree species remains to increase while the current annual increment tends to be a significant decline. In the view of the forest measurement, neither tree species can be regarded as being quantitatively mature at the age of 45, as is related to the site condition and microclimate of the sample plot. Moreover, *larix kaempferi* prevails over *larix olgensis* in growth trend and speed.

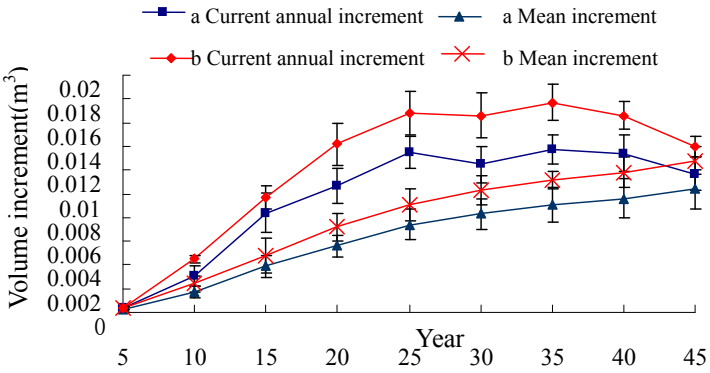

Fig. 1 Current annual increment and mean increment of *larix olgensis* (a) and *larix kaempferi* (b).

By fitting the current annual increment and mean increment of both tree species (Table 2), according to the values of R^2 and F, as well as the systematic error, we conclude that the quadric equation has a better fitting effect. The quantitative maturity ages of *larix olgensis* and *larix kaempferi* volume are 48.3 and 49.3 years respectively.

Table 2 Fitting equations on current annual increment and mean increment of *larix olgensis* and *larix kaempferi.*

Tree species	Fitting equation							
	Current annual increment	R^2	F	Systematic error (%)	Mean increment	R^2	F	Systematic error (%)
L. olgensis	$y = -0.0004 x^2 + 0.0057 x - 0.0053$	0.9779**	132.759	0.93	$y = -0.0001 x^2 + 0.0025 x - 0.0024$	0.9954**	650.387	0.76
L. kaempferi	$y = -0.0005 x^2 + 0.0075 x - 0.0073$	0.9795**	281.812	1.60	$y = -0.0001 x^2 + 0.0031 x - 0.0028$	0.9966**	871.743	0.52

The systematic error means the error in precision detection for equation fitting; ** $P < 0.01$.

(2) Carbon density of both tree species

The changes in density of both tree species tend to be basically identical, that is, the carbon density increases with the increase in tree age and reaches the peak at the age of 25, then decreases gradually. Of them, *Larix olgensis* gets a maximum carbon density at the age of 30, while *Larix kaempferi* at the age of 35.

(3) Carbon storage in both tree species

It can be seen from Fig. 2 that the current annual carbon storage in *larix olgensis* and *larix kaempferi* increases with the increase in tree age, and drops down slowly when reaching their peaks. Of them, the current annual carbon storage in *larix olgensis* reaches its peak (4.013 kg) at the age of 30 while *larix kaempferi at the age of 35* (5.151 kg), that is, the rate of current annual carbon storage in both tree species reaches their peaks at the ages of 30 and 35 respectively. At the same tree age (above 5 years), the current annual carbon storage and the mean carbon storage at different age periods in *larix kaempferi* are both larger than *larix olgensis*.

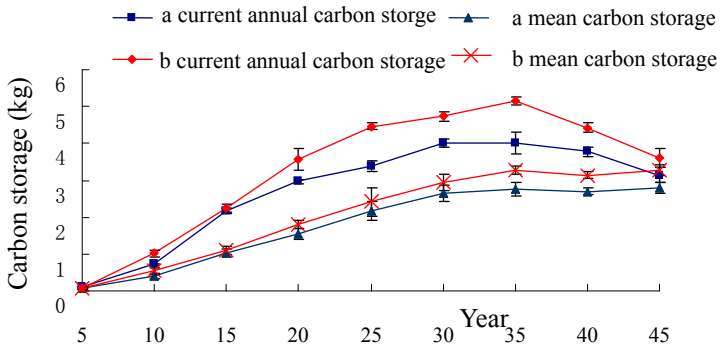

Fig. 2 Curves of carbon storage in *Larix olgensis*(a) and *Larix kaempferi*(b) at different ages.

As for their increase trends, the mean carbon storage in both tree species increases with the increase in age, but doesn't reach their peaks. Through calculation, the two curves of current annual carbon storage and the mean carbon storage in *Larix olgensis* and *Larix kaempferi* are intersected at the 48.7 and 47.7 years respectively.

4. Conclusion and Discussion

We can obtain the current annual carbon storage and the mean carbon storage in *Larix olgensis* and *Larix kaempferi* at different age stages using the forest measurement combined with chemical experimental methods and they are of distinct difference.The changes in carbon density that are obtained by calculating the carbon density of both tree species at different age stages is in conformity with the laws of biological wood science: *Larix olgensis* grows slower than *Larix kaempferi*, but with a higher density than the later; the laws of changes in carbon density of both tree species are of distinct difference, with a difference of 5 years when reaching their maximum values.

The carbon storage is subject to such two factors as carbon density and current annual increment, and the carbon storage maturity age that is worked out by means of fitting mathematical modeling can reflect the overall carbon accumulation capacity of each tree species, at the same time, be used for reference of afforestation aiming at carbon sequestration.

The study of the carbon storage maturity in different tree species helps select the optimal tree species in the process of carbon sequestration trading, and therefore decide on the forest management technology for carbon sequestration trading so as to gain a higher carbon storage at the same time period. In this discussion, the carbon storage dynamic analysis method is used, which rectifies the shortcomings of previously used carbon storage measuring methods and better reflects the carbon storage in forest at different time points, offering a new method for the assessment of changes in carbon storage in forest.

5. References

(1) Dixon RK, Brown S, Houghton RA, *et al*. Carbon pools and flux of global forest ecosystem. *Science,* 1994,263: 185-190

(2) Fang J-Y. Forest productivity in China and its response to global climate change. *Acta Phytoecologica Sinica* , 2000, 24 (5): 513-517 (in Chinese)

(3) Fang J-Y, Chen A-P. Dynamic forest biomass carbon pools in China and their significance. *Acta Botanica Sinica*, 2001, 43(9)：967-973 (in Chinese)

(4) Liu H,Lei R-D. Research methods and advances of carbon storage and balance in forest ecosystems of China. *Acta Botanica Boreali-occidentalia Sinica*,2005,25(4):835-843(in Chinese)

(5) Liu G-H,Fu B-J,Fang J-Y. Carbon dynamics of Chinese forests and its contribution to global carbon balance. *Acta Ecologica Sinica* , 2000, 20(5): 733-740 (in Chinese)

(6) Valentini R,Matteucci G,Dolman AJ, *et al*. Respiration as the main determinant of carbon balance in European forests.*Nature,*2000,404：861-865.

(7) Malhi Y,Baldocchi DD, Jarvis PG. The carbon balance of tropical, temperate and boreal forests. *Plant, Cell and Environment,* 1999, 22: 715-740

(8) Wu J-B,Zhang Y-S,Guan D-X. Methods and progress of research on CO_2 flux of forest ecosystem. *Journal of Northeast Forestry University* , 2003, 31(6): 49-51 (in Chinese)

(9) Wang W-J,Shi F-C,Zu Y-G,*et al*. Construction and development of CO_2 flux networks on terrestrial ecosystem. *Journal of Northeast Forestry University* , 2002, 30(4): 57-61 (in Chinese)

(10) Yang Y-H,Bi X-D. Benefit of CO_2 fixation by the forests in Hebei Province.*Chinese Journal of Ecology* , 1996, 15(4): 51-54 (in Chinese)

(11) Wang X-K ，Feng Z-W . The potential to sequester atmospheric carbon through forest ecosystems in China. *Chinese Journal of Ecology* , 2000, 19(4): 72-74 (in Chinese)

(12) Wu J-B , Guan D-X , Su X-M , *et al.* CO_2 turbulent exchange in a broadleaved Korean pine forest in Changbai Mountains. *Chinese Journal of Applied Ecology* , 2007, 18 (5): 951-956 (in Chinese)

(13) Fang J-Y,Chen A-P Zhao S-Q Ci J-L. Estimation of Forest Biomass in China: Some Explanation about the Article Science Written by Fang, et al [J]. *Acta Phytoecologica Sinica* 2002,26(2): 243～249 (in Chinese)

(14) Lang k-J, Li C-S, Ying Y etc. Ten theories and methods of ecological benefit evaluation for forestry ecological engineering [J]. *Journal of Northeast Forestry University* 2000, 28(1)(in Chinese)

(15) Meng X-Y . Forest Mensuration. Beijing: China Forestry Press, 1996 (in Chinese)

(16) Dong D-E , Li T-H . Measurement of carbon sulfur element in the coal by the Va

Predicting Hygroscopic Warping of Sugar Maple Sawn Timber by Finite Element Analysis

Yiren Wang and Shih-Hao Lee

Dept. of Forest Products Science & Furniture Engineering, National Chiayi University, Chiayi

Abstract: The features of wood such as anisotropy and inhomogeneity make the behaviors of timber subjected to moisture variation more complicated. One of them is the shape stability that is very significant in the use of solid wood. Warping, defined as the out-of-plane deformation of an initially flat panel, is a critical problem associated with the use of solid wood.

A three-dimensional finite element model was developed to predict the hygroscopic warping of sugar maple sawn timber. This specially developed finite element analysis is applied here to predict warping due to moisture content gradient of solid wood (sugar maple). Detailed model development and computer simulation results are presented.

The results of this study might offer a better understanding of timber warping and the ideas how to reduce the magnitude of timber warping.

1. Introduction

Wood is a hygroscopic, anisotropic and inhomogeneous material. When it is exposed to moisture variation it will cause deformations [3]. The common deformation is warping. Warping is defined as the out-of-plane deformation of an initially flat panel. It is always due to built-in unbalance in hygroscopic swelling forces or sometimes in thermal forces, triggered by change in moisture content and temperature [4]. The types of warping such as bow, cup, crook and twist are most concerned since severe warping of finished products will significantly increase the cost of manufacturing and lower the consumer's confidence in using wood products [1].

To improve this issue it is important to clarify how the material properties, its internal structure and environmental conditions affect this deformation process. Therefore, the complex behavior of wood makes computer simulation necessary. A three-dimensional finite element model is developed here to predict the hygroscopic warping of sugar maple sawn timber.

The commercial software Ansys is used in this study so that the finite element model and the deformed geometry could be displayed graphically. The objectives of this study are to describe the analysis method and show the finite element method applied to the warping of a solid wood.

2. The practical warping problem-Warping of solid wood plate

Assume that a solid wood plate (sugar maple) is used to simulate the warping of solid wood due to moisture content gradient. Its dimension is 30 cm long, 30 cm wide and 3 cm thick and is shown in Fig. 1.

The assumed imbalance is from the following moisture content gradient:

+8% from the bottom surface to 1/4 thickness; +6% from the 1/4 thickness to the 1/2 thickness; +4% from the 1/2 thickness to the 3/4 thickness; +2% from the 3/4 thickness to the top surface.

An initial moisture content, 12%, is assumed for the whole plate. The Poisson's ratio and the hygroscopic expansion are assumed to remain unchanged with moisture content change, as shown in the following:

ν_{LT}=0.5, ν_{TR}=0.42, ν_{LR}=0.46; α_T=0.0029, α_L=0.00015, α_R=0.0015

The Young's moduli (E) and shear moduli (G.) are affected by the moisture content. The appropriate adjustments were made according to the following equation [2] and are shown in Table 1.

$$E=E_{12}*(E_{12}/E_{GR})^{-((M-12)/(M_p-12))}$$

Where: E=MOE at MC=M; E_{12}=MOE at MC=12%;

E_{GR} = minimum MOE at MC = Mp, which is somewhat less than FSP

Mp=MC at which the modulus reaches its minimum value

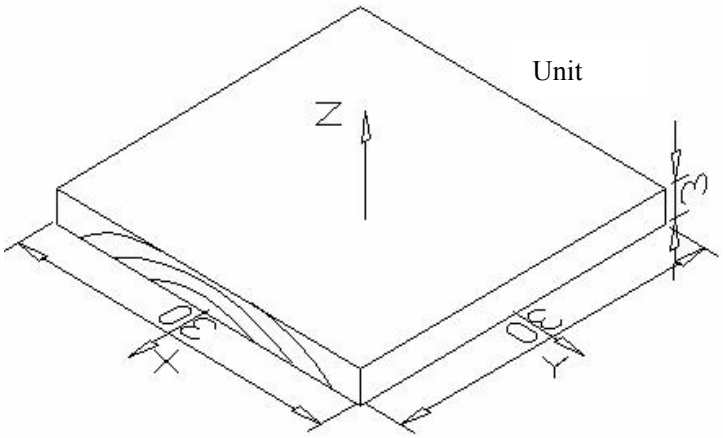

Fig. 1 Sugar maple plate for finite element modeling of panel warping.

Table 1. Young's moduli (E) and shear moduli (G) of Sugar maple plate.

Moduli (10^9N/mm^2)	the bottom surface to 1/4 thickness	the 1/4 thickness to the 1/2 thickness	the 1/2 thickness to the 3/4 thickness	the 3/4 thickness to the top surface
E_L	12.248	12.621	13.005	13.401
E_T	0.486	0.528	0.574	0.624
E_R	1.002	1.071	1.146	1.225
G_{LR}	0.883	0.914	0.946	0.978
G_{LT}	0.640	0.666	0.694	0.723
G_{RT}	0.210	0.220	0.231	0.243

3. Finite element modeling of hygroscopic warping of solid wood

The governinng equations for describing the mathematical aspect of this problem are derived by researchers [5]. The finite element modeling of hygroscopic warping of solid wood was conducted by commercial software, Ansys. A three-dimensional orthotropic solid element was developed to model and simulate the warping of solid wood due to moisture content gradient. The principal material directions of wood are assumed perfectly oriented with the Cartesian coordinate system and wood growth rings are assumed perfectly flat. The mesh is displayed in Fig. 2, by using Ansys preprocessing. The commercial software Ansys is implemented in this study so that the finite element model and the deformed geometry could be displayed graphically.

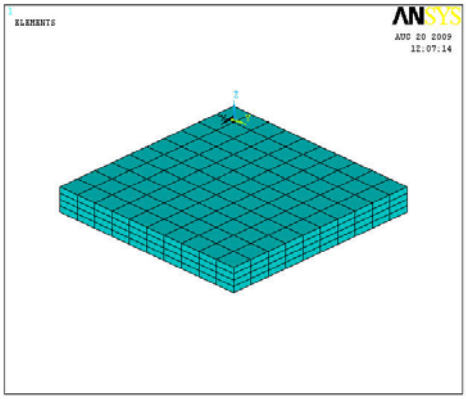

Fig. 2 The finite element mesh of Sugar maple plate.

4. Results and Discussion.

The results of the analysis are shown in Fig. 3, which displayed the displacement Uz of the deformed body versus the un-deformed edge. The shading indicate the extent of the warping, which can be read on the horizontal scale.

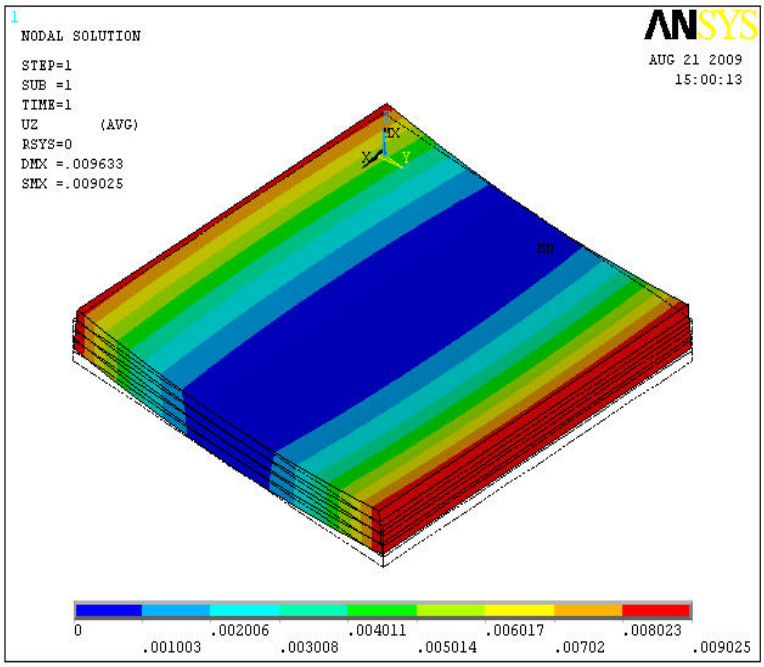

Fig. 3 The Z-direction displacement for warping of Sugar maple plate.

5. Conclusion

The hygroscopic warping of orthotropic material due to moisture content gradient was modeled and simulated successfully by the finite element method. This simulation can help the practitioner understand the complex warping behavior and provided the guidelines to reduce the magnitude of warping.

6. References

(1) Cai, Z. and J. R. Dickens (2004) Wood composite warping: modeling and simulation. Wood and Fiber Science 36(2): 174-185.

(2) Forest Products Laboratory: Wood Handbook (1987), Agric. Handbook No. 72. USDA Forest Serv. , Washington, D.C., 466p.

(3) Ormarsson, S., O. Dahlblom, and H. Petersson (1998) A numerical study of the shape stability of sawn timber subjected to moisture variation Part 1: Theory. Wood Science and Technology 32: 325-334.

(4) Suchsland, O. and J. D. McNatt (1986) Computer simulation of laminated wood panel warping. Forest Products Journal 36(11/12): 16-23.

(5) Tong, Y. and Suchsland, O. (1993) Application of finite element analysis to panel warping. Holz als Roh-und Werkstoff 51:55-57.

The Effect of Different Soil Type on the Wood Properties of *Populus×euramericana* cv.'74/76'

Rongjun Zhao[1], Benhua Fei[2], Haiqing Ren[1], Xiaomei Huo[1] and Xianbao Cheng[1]

[1]Research Institute of Wood Industry, Chinese Academy of Forestry, Beijing

[2] Beijing Forestry Machinery Research Institute of The State Forestry Administration, Beijing

Abstract: In this paper，wood anatomical characteristics, chemical compositions and physical and mechanical properties of *Populus×euramericana* cv.'74/76' were measured and analyzed the influence of two soil type on wood properties. The results showed that soil type had significant effect on wood cell wall thickness and cell lumen while the effect of soil type on fiber length and microfibril angle could be ignored. For poplar, cellulose content of poplar grown in sandy soil was more slightly but fiber length was shorter than that grown in black alkali soil, the difference is not significant based on standard of papermaking. Moreover, both of modulus of elasticity and density were not significant differences under the same condition and average annual growth quantities almost equaled. Integrated analysis showed that poplar is good papermaking material for its fast growth and strong adaptation to environment.

1. Introduction

Poplar is one of the most important afforestation tree species in our country ,it has a broader planting area that accounting for 1/5 of the total area of plantation，which is 4 times than the total area in other parts of the world(Zhang et al.,2003). The *Populus×euramericana* cv.'74/76' (107 poplar)was bred successfully in 1990 which brought in 1984 by the Chinese academy of Forestry and planted widely in North China and other places because of its high height , straight trunk, strong capacity of anti-pest and diseases resistance.

Various conditions are contributed to the change of the wood anatomical characteristics, chemical compositions and physical and mechanical properties, the soil type is an critical influence factor(Liu et al.,2001). In order to instruct the oriented cultivation of plantation and accelerate the extensive plantation of the 107 poplar，we study the influence of different soil type on the wood properties. However, many domestic scholars have done some researches on the variation rule of the length of wood fiber(Fei et al.,1994;Zhao et al.,1999), there are a few of papers about the systematic researches of wood properties of 107 poplar. In this paper, selecting 107 poplar from the different soil texture in Beijing，we discussed the different wood properties of poplar in two soil type and the influence on the properties of paper-making and board, for looking forward to provide a theoretical basis of the orientated breeding of poplar plantation and wood processing.

2. Material and methods

The *Populus×euramericana* cv.'74/76' wood samples examined in this study were obtained from shunyi and miyun in Beijing, the soil style were black alkali soil and sandy loam. According to GB1927-91, 5 representative trees selected from each plot, at the breast height (1.3m) cutted two discs which thickness is 5cm, made wood samples and test wood properties.

3. Results and discussion

(1) The influence of soil texture on the fiber morphology and Microfibril angle(MFA)

Fig. 1 showed the wood fiber alteration tendency of the 107 poplar, it indicated that the fiber length of 107 poplar was increasing with the age, the relationship between the length and growing age were linear regression, so the growing age is an important factor to affect the length of wood fiber.

In Fig. 1, the width of wood fiber was increasing from the pith to the bark, but the fiber width from black alkali soil had a decline tend at the 5th year. The analysis of variance indicted that the wood fiber width had no significant difference between the two styles of soil. The cell wall thickness of wood fiber was increasing from pith to bark at the breast height, but the increasing degree was small; at the same growing age, the cell wall

thickness of wood fiber from the black alkali soil fields was larger than that from the sandy loam fields. The lumen diameter in tangential direction of wood fibers was increasing fast in the first two years, after the second year, for the samples selected from sandy loam, its' lumen diameter in tangential direction was diminishing year by year, but for the samples selected from black alkali soil, the trend was increasing at first and then begin to descend. By analyzing we can find out that the lumen diameter in tangential direction also had a remarkable difference under different soil conditions.

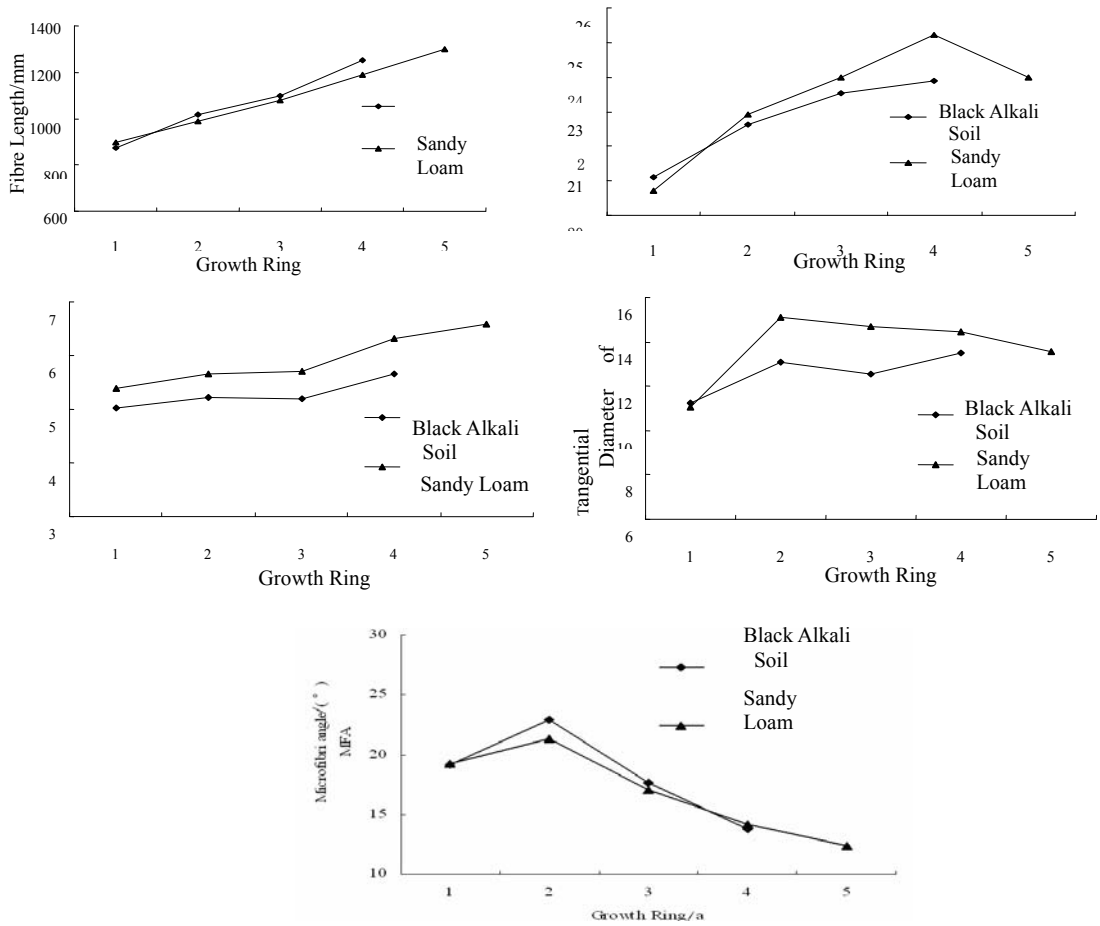

Fig.1 The Infiuence of different soil texture on fibre morphology.

Table 1 The Morphological Characteristics of Wood Fibre on Different Soil Texture Condition.

Soil Texture	Fibre Length/μm		Fibre Width/μm		Cell Wall Thickness/μm		Diameter of Cell Lumen/μm	
	Average	Variation coefficient	Average	Variation coefficient	Average	Variation coefficient	Average	Variation coefficient
Black Alkali Soil	1056.20	17.60	22.77	14.27	5.28	16.10	12.61	26.72
Sandy Soil	1087.21	17.83	23.36	15.71	5.92	18.41	13.92	28.95

In a word, the fiber shape of 107 poplar wood from the black alkali soil was slightness, the cell lumen was smaller and the cell wall was thinner, but the fiber of 107 poplar from sandy loam was opposite, though the fiber shape was distinctness under different soil conditions, there were no significant difference overall, and the

average annual increment was the same on the whole (Table 1), therefore, the growth of the 107 poplar was rapid under two different soil conditions. This result indicated that this tree species has a strong ability to adapt to the environment.

Table 2 The average of MFA on different soil texture condition.

Soil Texture	Growth Ring of Sample				
	R1	R2	R3	R4	R5
Black Alkali Soil	19.16°	22.90°	17.63°	13.74°	－－
Sandy Soil	19.24°	21.35°	17.08°	14.19°	12.41°

(2) The influence of soil texture on the chemical components

Cellulose is the most important chemical component of wood cell wall, but also it is the most essential chemical composition of pulp and paper at the same time. The content of cellulose in the raw material directly influence on the pulp yield.

Table 3 Comparison of wood chemical contents between the different soil texture.

Soil Texture	Ash%	Alcohol Benzene%	Cellulose%	Lignin%	Pentosan%
Black Alkali Soil	0.44	4.03	46.55	26.83	19.05
Sandy Soil	0.51	3.82	49.49	25.01	18.50

The lignin can affect the humidity and swelling of fiber in the papermaking process, the more lignin is generally resulting in the worse hydrophilicity of pulp, and the more difficulty of beating and the lower bonding between fibers, thus, it is difficult to obtain high quality papers when the pulp have a high lignin content. According to the analysis, the content of lignin of the 107 poplar selected from black alkali soil were higher than that from sandy loam, which was not beneficial to production. Alcohol benzene extractive of wood has directly effect on the pulping, bleaching, whiteness of pulp-bleaching, stability of whiteness, waste recovery and utilization. In the Table 4, we can see that the content of extractive in the 107 poplar selected from black alkali soil is higher than that from sandy loam, but the difference between them is very small.

(3) The physical and mechanical properties

Wood density is a key index to wood property. MOE is a significant index to evaluate the possibility of wood as the veneer panel and building materials. The Table5 and 6 showed the test results of 107 poplar from different soil type.

Table4 Comparison of physical and mechanical properties between the different soil texture.

Soil Texture	Average MOE in Static Bending of the former four years（GPa）	Average MOE in Static Bending of the Former Five years（GPa）	Average Air-Dry Density(g/cm^3)	The Variance Analysis
Black Alkali Soil	9.046	————	0.403	F＜Fcrit 2.46＜3.97
Sandy Soil	9.222	9.415	0.400	

Table 5 Comparison of physical and mechanical properties between the different soil texture in different heights.

Soil Texture	Average MOE in Static Bending at the Height of 1.3m（GPa）	Average MOE in Static Bending at the Height of 3.3m（GPa）	Average MOE in Static Bending at the Height of 5.3m（GPa）
Black Alkali Soil	8.462	9.202	10.178
Sandy Soil	8.999	9.573	9.841

From Table 5 we can see that air-dry density of poplar in the two kinds of site conditions are consistent on the whole. Average value of MOE of 5-year-old poplar is better than that of 4-year-old, the variance analysis indicated that the MOE is no significant difference between the two sites. The Table 6 showing the changing trend of MOE of 107 poplar from two different soil conditions along the tree trunk, it concluded that MOE of poplars were increasing with the height (from 1.3m to 1.7m), it can increase wood stiffness and support the weight of tree top that improve the wind resistance of trees.

4. Summary

According to the wood properties of 107 poplar in two different soil type, we analyzed that different soil type had significant impact on the cell wall thickness and cell lumen, but it wasn't on the fiber length and MFA. Referring to the standard of pulping and papermaking, the cellulose content of 107 poplar from sandy soil was higher but shorter fiber length than that of black alkali soil. Taking physical and mechanical properties into account, there are no significant differences between density and MOE, the average annual growth quantities were consistent in two kinds of soil type, it indicated that different soil type had no significant influence on the density and MOE.

For analyzing systematically, the results showed that the 107 poplar was good for papermaking as an fast growing specie and had strong ability of adaptation that can be planted in north part of China widely.

5. References

(1) Zhang Q W and Li J H. New Varieties of poplar wood for timber industry (China Forestry Publications, BeiJin 2003)
(2) Liu S Q, Jiang Z H and Bao F C. Scientia Silvae Sinicae. Vol37(2), p90(2001)
(3) Fei,B H. Journal of Northeast Forestry University.Vol22(4), p61(1994)
(4) Zhao R J, Guo J R andYang P H. Journal of Northwest Forestry University. Vol14(1), p6(1994)

This study was supported by the "948" project of State Forestry Administration (2006-4-96, 2006-4-C01)

The Research on Variation of Green Density and Bark Percentage of Fast-growing Eucalyptus of Different Ages

Feng Xu, Yunlin Fu, Jianju Luo, Yingjian Li, Songwu Chen, Yinyou Mo, Guidan Chen and Yinluan Qin

Forestry college, Guangxi University, Nanning

Abstract: The variation of green density and bark percentage was studied in this essay. The green density was tested by drainage, and bark percentage was tested by measuring volume and quality. The research showed that: the green density of five-year, six-year and seven-year fast-growing eucalyptus was 1.033g/cm^3, 1.037 g/cm^3,1.036 g/cm^3 respectively, and the variation was unremarkable among different ages. The bark volume percentage of five year, six year, seven year was 17.56%、16.29%、13.94% respectively, and the variation was significant among different ages. The bark quality percentage of five year, six year, seven year was 18.34%、14.57%、11.21% respectively, and the variation was significant among different ages.

1. Introduction

Eucalyptus was imported into China in the late 19 century and developed very fast. The growing area has been more than 2000 thousand hm^2 [1~2]. Studying green density of eucalyptus can know the variation of green density and provide reference for wood transportation. The research on bark percentage can ensure the proper lumbering age of eucalyptus, and provide basic data for eucalyptus planting and processing.

2. Material and method

(1) Test sample collection

In Mountain Tianping Forest Farm, Guigang City of Guangxi, 75 eucalyptus trees of 5 ages, 6 ages and 7 ages were collected, each group including 25 respectively. The sample trees were sawed into 7 circular plates of 5cm thickness at 0m, 1.3m, 3.3m, 5.3m and 7.3m, 9.3m、11.3m. The circular plates were put into plastic bags after sawing so that the moisture would not evaporate.

(2) The bark percentage testing

The bark volume percentage was accounted in as follows:

$$V_v\% = \frac{\pi R_b{}^2 H - \pi R_w{}^2 H}{\pi R^2{}_b H} * 100$$

Vv: the bark bulk percentage Rb: radius with bark

Rw: radius without bark H: circular plate thickness

The bark quality percentage was accounted in as follows:

$$V_q\% = \frac{G_b - G_w}{G_b} * 100$$

Vq: the bark quality percentage; Gb:weight with bark; Gw: weight without bark

(3) Green density testing

The green density was tested by drainage. One quarter of circular plate in the northeast direction was divided into pith-part, middle-part and sapwood-part respectively, and 3-5 samples were tested in the same part. The result was analyzed according to pith-part, middle-part, sapwood-part and mean respectively of all tested samples; meanwhile, the mean of green density of 5 age, 6 age and 7 age was counted.

3. The result and analysis

(1) Density variation

The radial variation of green density of 5 ages showed that the average of green density of pith-part, middle-part and sapwood-part was 1.023g/cm^3, 1.029 g/cm^3, 1.048 g/cm^3 respectively.

The longitudinal variation of green density of 5 ages showed that the average of green density with tree height 0m, 1.3m,3.3m,5.3m,7.3m was 1.038 g/cm^3,1.038 g/cm^3,1.026 g/cm^3,1.035 g/cm^3,1.026 g/cm^3 respectively.

The radial variation of green density of 6 ages showed that the average of green density of pith-part, middle-part, sapwood-part was 1.026 g/cm^3, 1.028 g/cm^3,1.058 g/cm^3 respectively.

The longitudinal variation of green density of 6 ages showed that the average of green density with tree height 0m,1.3m,3.3m,5.3m,7.3m,9.3m was 1.031 g/cm^3,1.020 g/cm^3,1.041 g/cm^3,1.036 g/cm^3,1.047 g/cm^3,1.051 g/cm^3 respectively.

The radial variation of green density of 7 ages showed that the average of green density of pith-part, middle-part, sapwood-part was 1.014g/cm^3, 1.032g/cm^3, 1.062g/cm^3 respectively.

The longitudinal variation of green density of 7 ages showed that the average of green density with tree height 0m, 1.3 m, 3.3 m, 5.3 m, 7.3 m, 9.3 m, 11.3 m was 1.061 g/cm^3,1.034 g/cm^3,1.040 g/cm^3,1.023 g/cm^3,1.028 g/cm^3,1.020 g/cm^3,1.047 g/cm^3 respectively.

The Variance analysis in the following Table1 showed that the variation of green density among different age was insignificant.

Table 1 Variance analysis of green density.

Source	Degrees of Freedom	Sum of Squares	Mean Square	F	$F_{0.05}$
Among-group	2	0.00095	0.00048	0.83	3.40
Within-group	72	0.042	0.00058		
Total	74	0.042			

(2) Variation of bark percentage

The relationship between balk volume percentage and tree height was showed as Fig. 1. The balk volume percentage decreased with increasing height, and it was 17.56%,16.29%,13.94% for 5 year, 6 year, 7 year respectively in 0 tree height.

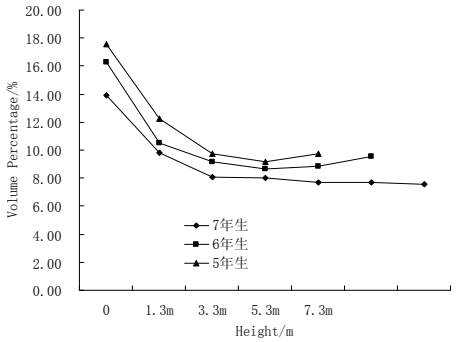

Fig. 1 The relationship between balk volume tree height.

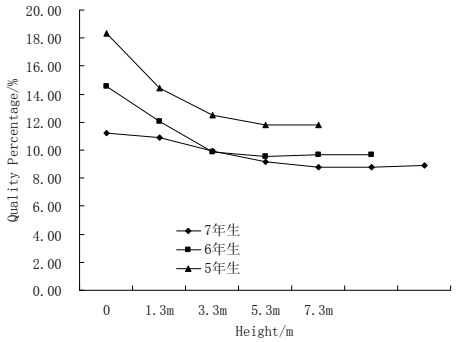

Fig. 2 The relationship between balk percentage and quality percentage and tree height.

The relationship between bark quality percentage and tree height was showed as Fig. 2. The bark quality percentage decreased with increasing height, and it was 18.34%,14.57%,11.21% for 5 year, 6 year, 7 year respectively in 0 tree height.

Table 2 Variance analysis of bark bulk percentage.

Source	Degrees of Freedom	Sum of Squares	Mean Square	F	$F_{0.05}$
Among-group	2	0.0095	0.0047	26.74*	3.40
Within-group	72	0.013	0.00018		
Total	74	0.022			

The Variance analysis in Table 2 showed that the variation of bark volume percentage among different ages was significant

Table 3 Variance analysis of bark quality percentage.

Source	Degrees of Freedom	Sum of Squares	Mean Square	F	$F_{0.05}$
Among-group	2	0.018	0.0090	39.65*	3.40
Within-group	72	0.016	0.00023		
Total	74	0.034			

The Variance analysis as Table2 showed that the variation of bark bulk percentage among different age was significant

4. Conclusion

The green density was 1.033g/cm^3,1.037 g/cm^3,1.036 g/cm^3 for 5 year, 6 year, 7 year respectively. And the variation of green density among different ages was insignificant.

The balk volume percentage was 17.56%, 16.29%, 13.94% for 5 year, 6 year, 7 year respectively. And the variation of bark bulk percentage among different ages was significant.

The balk quality percentage was 18.34%,14.57%,11.21% for 5 year, 6 year, 7 year respectively. And the variation of bark quality percentage among different ages was significant.

5. References

(1) YU Fu-Ke; HUANG Xin-Hui; WANG Ke-Qin, et al. An overview of ecological degradation and restoration of Eucalyptus plantation. *Chinese Journal of Eco-Agriculture*, 2009, 17（2）: 393~398

(2) Li Long-zhe, Yang Cai-xi, Song Zuo-mei, et al. Performance of Eucalyptus Lumber after Resin Impregnation and Heat Treatment. *Wood Industry*, 2009, 23（3）: 40~42

The Application of Multimedia Timer in Data Acquisition of Log Shape

Hong-E Ren, Ni-Hong Wang and Yan Wu
Information and Computer Engineering College, Northeast Forestry University, Harbin

Abstract: This paper introduces how to collect the output values from the angle sensor real time with the help of data acquisition card Advantech PCI-1711 in the measurement system MQK3102 for the shape of log. And it also demonstrates the programming method with Visual C++. Comparing with three methods used for controlling the frequency of sampling and allowing for the sampling accuracy in this system as well, it was put forward that Multimedia Timer is optimal for timing precisely in the process of data acquisition. The minimum timing accuracy can be raised up to one millisecond.

1. Principle of the measurement system MQK3102 for the shape of log

There is a detecting frame which is an important part in the measurement machine. Eight detecting pendulum bars are arranged in circle on the detecting frame at the center section of the machine. A roller with very short diameter is installed at the bottom end of each pendulum bar to contact the surface of log, and an angle sensor is installed on the mandrel at the fixed end of each pendulum bar. When the log moves to the detecting frame, one of its ends pushes the eight pendulum bars, and then the eight contact rollers fall onto the log. The fluctuation on the surface of log causes the pendulum bars to swing, thus leading to the change of the output values from the angle sensor. Those output values of voltage were collected at intervals and the samplings were saved in the computer at the same time. Fig. 1 shows the workflow of the measurement system MQK3102 for the shape of log.

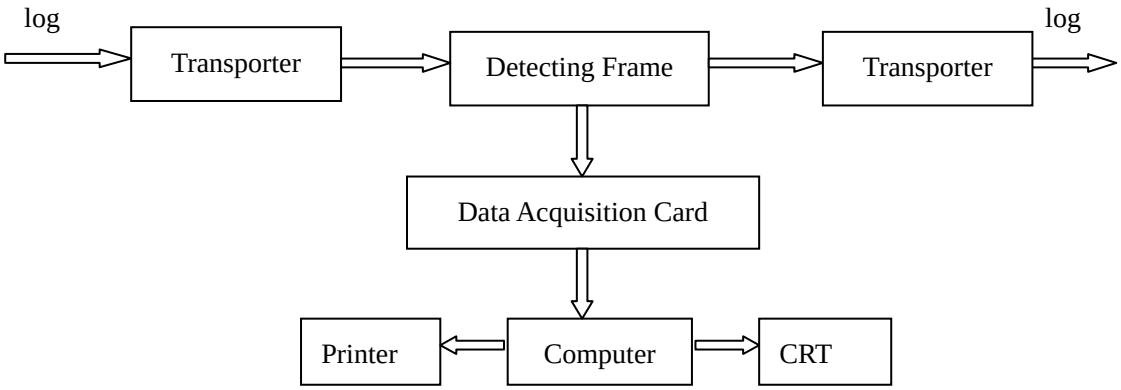

Fig. 1 Workflow of the Measurement System MQK3102 for the Shape of Log.

After analysis and calculation, these voltage values were converted to the coordinate values of the sampling points on the cross section of log. The shape of log cross section can be clearly stimulated by curve fitting. Accordingly, the whole body shape of log can also be simulated approximately by the cross sections along the length direction of log.

2. Real-time data acquisition

In order to acquire the output values from eight angle sensors real time, data acquisition card Advantech PCI-1711 was used because of its low loss and multifunction.

3. Settings of Hardware

In this system we used AI_0-AI_7 as analog input channels which were separately connected to the output end of eight sensors. And the two input ends of the sensors were connected with DC supply. The earthing grips of the

sensors were connected with AIG on the data acquisition card. Because the output values of angle sensor are from 0 to 5 volt, the gaining for analog input was set to be one which corresponds to the input voltage range from -10 to 10 volt.

4. Programming implementation.

There are mainly two kinds of programming methods for plug-in DA&C cards of Advantech Automation Corp.. One way is writing programs by oneself to directly control the registers, and another way is to use ADSAPI32.DLL provided by Advantech which includes many functions for I/O operation of hardware [1]. The second method was used in this system to improve the efficiency. Internal trigger is used for the programming of AI operation [2]. First, the file "Adsapi32.lib" should be added into the project created by Visual C++, and the library function "DRIVER.H" must be put in the project folder and included in the source file so that all the library functions provided by Advantech can be used for programming. The program flow diagram of data acquisition with Advantech PCI-1711 is shown by Fig. 2.

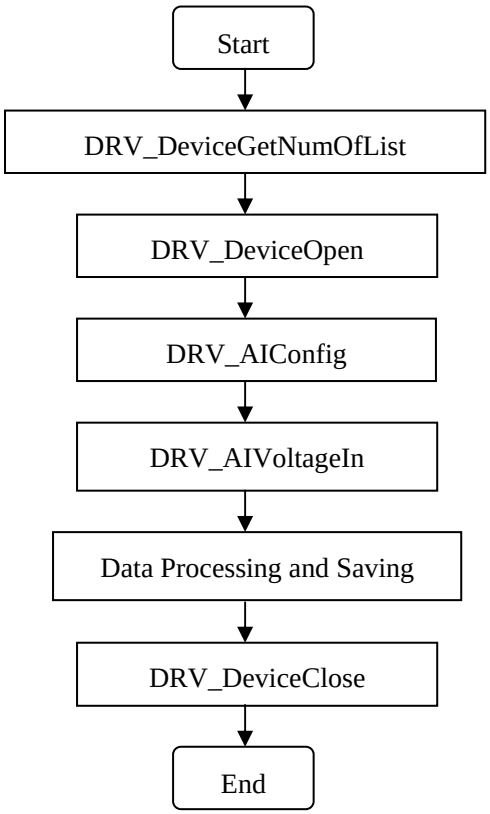

Fig. 2 Program Flow of Data Acquisition with Advantech PCI-1711.

5. Controlling the frequency of sampling with multimedia timer

In data acquisition and processing system controlled by computer, the information always needs to be acquired timely and processed precisely. So the accuracy of sampling time is the key point for the whole control system to work well. There are three methods generally used to control the sampling frequency as follows:

(1) Windows Timer is a traditional way with which the user sends the message WM_TIMER to the message queue and the process of data acquisition is completed in the function. The minimum timing accuracy of this traditional Timer is just 54.945 ms [3] and the message WM_TIMER has the lowest priority of all so this Timer can be only used for general timing.

(2) It is the second way that data acquisition is running as an independent thread. But the priority of this thread must be higher than before, which is dangerous for thread operation because critical resources can be easily

destroyed. In addition, this way has 20 ms delay [4].

(3) Multimedia Timer is the third way. Compared with traditional Timer, the Multimedia Timer has the minimum timing accuracy up to one millisecond because it can set the initial value of T/C0 of 8253 according to the required accuracy. Furthermore, Multimedia Timer does not depend on message mechanism. Its independent thread can directly call the callback function after a number of interrupt requests and does not have to wait until the message queue is empty. So timer interruption can be responded timely.

In this system the feed rate of log on the transporter is 11.00m/min, and here suppose that D represents sample interval on the log, then the sample period of the system represented by T can be obtained from the Eq. 1:

$$T = D/(11.00\times10^{-3}/60\times10^{-3}) = 5.45D \tag{1}$$

Generally, the whole body shape of log will be simulated clearly when the sample interval on the log is15mm. The closer the sample interval is, the better the simulating effect of the shape of log will be. Here five different kinds of sample intervals and respective sample periods are listed in Table 1 as follows:

Table 1 Sample Period of the System.

D [mm]	1	2	5	10	15
T [ms]	5.45	10.91	27.27	54.55	81.82

As shown in Table 1, four kinds of sample period are lower than the minimum timing accuracy of traditional Timer (54.945 ms). But Multimedia Timer whose minimum timing accuracy is 1ms can satisfy all the five kinds of sample period. So in this system Multimedia Timer is used to control the sampling frequency and also has shown a good effect.

6. Summary

(1) Realize the key technology of data acquisition in the measurement system for the shape of log.

(2) Take advantage of Multimedia Timer in the process of data acquisition and improve the timing accuracy.

7. References

(1) PC-Lab Card PCI-1711 Multifunction Data Acquisition Card User's Manual. Advantech Technology Inc. (1993). (in Chinese)

(2) X.F.Peng, C.E.Yang: Information Technology (2001), p. 51. (in Chinese)

(3) F.L.Chang, J.Liu: Computer Applications Vol.23 (2003), p. 177. (in Chinese)

(4) J.Li, J.W.Yang and X.Qian: Computer Applications Vol.20 (2000), p. 67. (in Chinese)

(5) J.Shi, X.Q.Bian and M.Y.Fu: Computer Applications Vol.21 (2001), p. 233. (in Chinese)

(6) B.Y.Yang, B.H.Zhang and X.X.Chu: Computer Engineering Vol.26 (2000), p. 153. (in Chinese)

The Surface Longitudinal Growth Strain of Reaction wood Induced by Artificial Inclination in Poplar I-107 and Loblolly Pine

Shengquan Liu and Yamei Liu

School of Forestry & Landscape Architecture, Anhui Agricultural University, Hefei

Abstract: Sixty one-year-old saplings of poplar I-107 (*Populus× euramericana* cv. "74/76") and Loblolly pine (*pinus taeda* L.) separately were planted in the garden and were artificially inclined at the angles of 0°, 15°, 30°, 45° and 60° from the vertical in growth season. The results revealed that the surface longitudinal growth strain increased with the angle of the trunk to a certain point (15°or 30°), but then decreased or constant. In different seasons the surface longitudinal growth strain increased from spring to winter and decreased from winter to spring.

1. Introduction

Along with the structure of forest has turned from natural forest to plantation forest, how to improve the wood quality and utilization of plantation wood become important tasks all over the world. Reaction wood is regarded as the main problems which affect the character and machining of wood in wood research fields [1, 2]. This wood, generally considered as abnormal tissue, is produced by the cambium in reaction to a gravitational stimulus induced by the displacement of an axis from its equilibrium position [3, 4] and typically forms in leaning or crooked trunks and branches, angiosperms produce tension wood generating high tensile stresses on their upper face and gymnosperms produce compression wood generating high compressive stresses on their lower face [5, 6].

Although growth stress of reaction wood has been largely described in the literature [7, 8], but in most cases, adult trees are concerned. There have little reports about growth stress of reaction wood by artificial inclination. This study focused on growth strain variation of reaction wood in poplar I-107 (*Populus× euramericana* cv. "74/76") and Loblolly pine (*pinus taeda* L.) induced by artificial inclination for one year.

2. Materials and methods

Experiments were conducted in 2007 in a field owned by Anhui Agricultural University, China. Sixty one-year-old saplings of poplar I-107 and sixty three-year-old saplings of Loblolly pine. were selected as materials, they were planted in the pots. These Saplings average 145cm long, 11mm in diameter when planted. They were divided into five groups, twelve saplings for each group, In the middle of May, the pots were artificially inclined at the angles of 0°,15°,30°,45°and 60° from the vertical (Fig. 1).

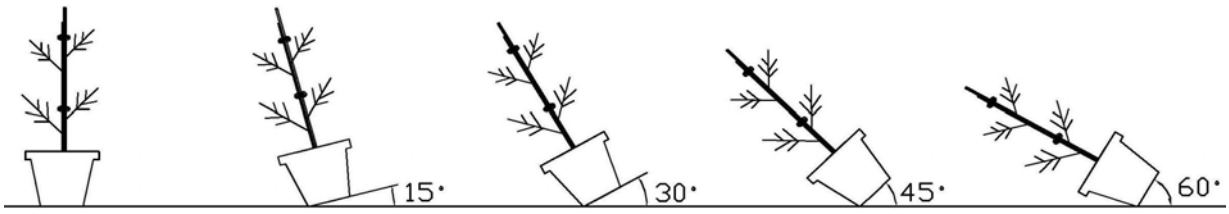

Fig. 1 Schematic diagram for artificial inclination of saplings.

To avoid any mechanical disturbance, the position of each sapling was maintained by a pole attached to the stem above the ground.

The surface longitudinal growth strain was measured with strain gauges on the upper side of poplar I-107 leaning stem and lower side of *pinus taeda* L. leaning stem; the smooth outer surface of the secondary xylem was exposed by removing the bark, cambial zone, and differentiating xylem with a knife, so as not to scratch the xylem surface. A 2-mm long strain gauge（Minebea, B-FAE-2S-12-T11）was glued to the xylem surface and

connected to a strain meter in 2 gauge-2 wire mode. The measurement precision was ±0.001%. A groove was cut to the depth of the current growth layer (1-2mm) close to each side of the strain gauge to release the growth stress. The distance from the edge of the gauge to the groove was 2mm. The growth strain was measured every three months from September in 2007 to September in 2008.

3. Results and discussion

For poplar I-107 and Loblolly pine., the released strain increased with the angle of inclined up to 15°or 30°, and then remained constant or decreased (Fig. 2~3). These trends were observed at all measuring time. When a tree grows eccentrically and produces reaction wood, thicken is promoted on the reaction wood side, and inhibited on the opposite side [9]. Yoshida (2000) reported tension wood and growth stress induced by artificial inclination in *Liriodendron tulipifera* Linn. and *Prunus spachiana* Kitamura f. *ascendens* Kitamura, still concluded that growth stress generated by inclined is limited [10]. The results in this paper were not in accordance with their conclusions.

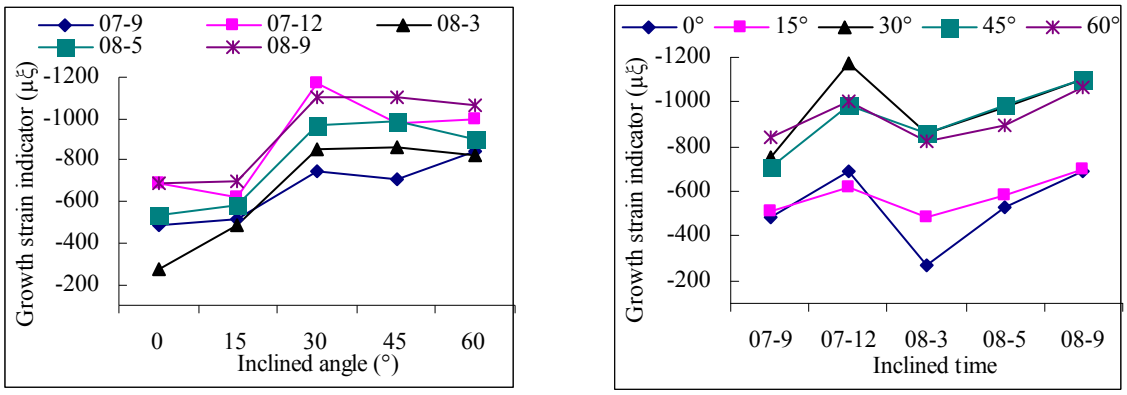

Fig. 2 The influence of inclined angle and inclined time on surface longitudinal growth strain of poplar I-107.

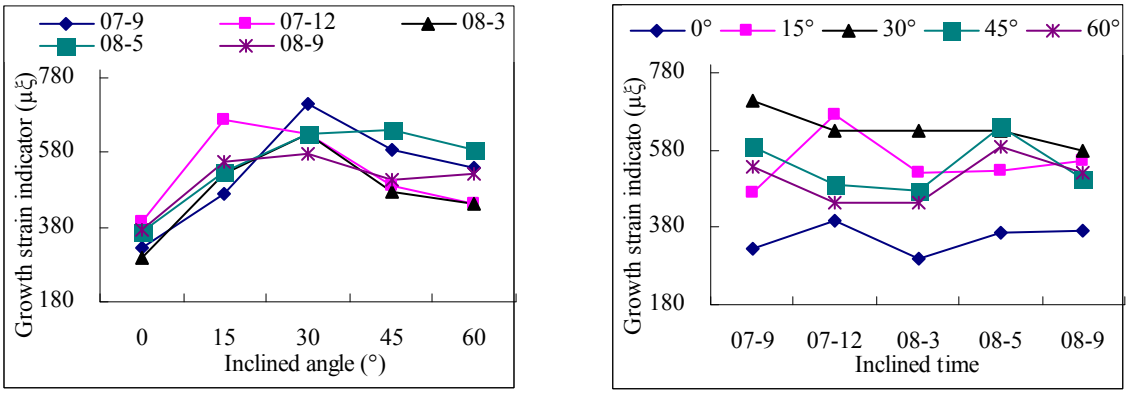

Fig. 3 The influence of inclined angle and inclined time on surface longitudinal growth strain of *pinus taeda* L.

For poplar I-107 and Loblolly pine., from 07-9 to 07-12, the growth strain increased, and then from 07-12 to 08-3, there were reducing tenancy, from 08-3 to 08-9, another increasing tenancy (Fig. 2~3), then the tenancy may alternative in further study. Changes aroused by different seasons From spring to autumn, the growth strain value increased; from autumn to winter, the value increased, but from winter to spring, the value decreased. The reason may be from winter to spring is in period of dormancy, the growth of tree become slowly. And there were fluctuations in Loblolly pine. These may be influenced by the environment conditions like wind or low temperature changes.

In the all, the surface longitudinal growth strain increased with the angle of the trunk at 15°or 30°, but then decreased or constant. The results disagree with the former report that growth stress generated by inclination is

limited. The accelerated growth would strongly induce sufficient upward moment to return the axis of the trunk to the vertical. In different seasons the surface longitudinal growth strain increased from spring to winter and decreased from winter to spring.

4. References

(1) D.W. Einspahr: The influence of short-rotation forestry on pulp and paper quality. I. Short-rotation conifers. II. Short-rotation hardwoods. [J]. Tappi, 59(6) (1976), 135-142.

(2) A.J.Panshin and C. De Zeeuw: Textbook of Wood Technology, 4th ed. McGraw-Hill, New York, NY. (1980).

(3) A.B.Wardrop: The reaction anatomy of arborescent angiosperms, in: Zimmermann M.H. (Ed.), The formation of wood in forest tree, Academic Press, New York, (1964) pp. 405–456.

(4) J.B.Fisher and J.W.Stevenson: Occurence of reaction wood in branches of Dicotyledons and its role in tree architecture, Bot. Gaz.142 (1981) 82–95.

(5) Y.Trénard and P.guéneau : Relations entre contraintes de croissance longitudinales et bois de tension dans le hêtre (Fagus sylvatica L.). Holzforschung 29(6) (1975),217-223.

(6) F. Sassus :Déformations de maturation et propriétés dubois de tension chez le hêtre et le peuplier:Mesures et modèles. PhDThdsis. ENGREF, Montpellier. (1998).

(7) H. Yamamoto: Generation mechanism of growth stresses in wood cell walls: Roles of lignin deposition and cellulose mcrofilril during cell wall maturation. Wood Science and Technology, 32(1998), 171-182.

(8) D. Jullien and J .Gril: Growth strain assessment at the periphery of small-diameter trees using the two-grooves method: influence of operating parameters estimated by numerical simulations. Wood Sci Technol, 42(2008), 551–565.

(9) W.A.Côté and A.C.Jr, Day: Anatomy and ultrastructure of reaction wood. In: Côté WA Jr (ed) Cellular ultrastructure of woody plants. Syracuse University Press, Syracuse, (1965), pp 391–418.

(10) M. Yoshida, T. Okuda and T .Okuyama: Tension wood and growth stress induced by artificial inclination in Liriodendron tulipifera Linn. and Prunus spachiana Kitamura f. ascendens Kitamura. Ann For Sci 57(2000a), 739–746.

Analysis and Characterization of Dimensional Stability and Crystallinity of Super Heat-Treated Larix SPP

Weilun Sun and Jian Li

Key laboratory of Bio-based Material Science and Technology, Ministry of Education, Northeast Forestry University, Harbin

Abstract: To investigate the dimensional stability, crystallinity and interrelation between them, the ASE, crystallinity and characteristic of FT-IR of super heat-treated Larix SPP were determined and characterized. Results showed that the value of ASE increased along with the heat temperatures increasing ranging from 180 to 220℃ and was beyond 60%, but when the heat-treated medium was nitrogen, the value of ASE was lower than that of air. The spectrum of FT-IR demonstrated that the stretching vibration of –OH groups at 3380cm^{-1} was diminished accompanying the enhancing heat temperatures and obviously changed ;The relative intensity of carbonyl groups at 1730cm^{-1} decreased with the increasing temperatures; At the same treated situation, the hydroxide and carbonyl groups in the nitrogen were lower than those of oxygen. The tendency of crystallinity of super heat-treated Laris SPP was firstly increased, then decreased and finally increased. The value of crystallinity in the nitrogen was higher than that of air and over 65% under identical circumstances. The prosperities of moisture absorption reduced and the dimensional stability increased when the Laris SPP was underwent super heat-treatment. New way was provided for better use of Laris SPP with abundant storage on the basis of the studied results.

1. Introduction

Larix SPP. with naturally wide distribution, strong growth adaptability, powerful mechanical property and better wearability, as well as an important forestry species of Pinaceae Larix, mainly grow in Northeast China and Inner Mongolia. It is widely used in building and other industrial fields. But with the larger shrinkage and difficultly unreleased growth stress, Larix SPP. is limited to use in much more extensive fields, especially in furniture application [1-2].

The thermal modification of wood has long been recognized as a potentially useful method to improve the dimensional stabilization of wood and increase its decay resistance. Further studies of this technology led to the development of several commercial processes, such as ‘Lignostone’ and ‘Lignifol’ in Germany, and ‘Staypak’ and ‘Staybwood’ in the United States. More recently, several commercial processes have been introduced in Europe. These are the Thermowood process in Finland, the Plato process in Holland, and the Perdure process and Retification in France [3-6]. At present this technology has been drawn wider researcher attentions coping from the technology, materials, structural differences, the mechanism to other aspects [7-9].

Larix SPP. was treated at different thermal temperatures and different treated media (heat-treated temperature ranging from 180 to 240℃， heat-treated time was 4h). Fourier transform infrared spectrometer and X-ray diffraction (XRD) were used to characterize the chemical components and the variation characteristics of crystallography. The value of ASE was used to determine the dimensional stability.

2. Material and methods

(1)Material

Larix SPP.: 50 years old .Experimental size: 20×20×20mm

(2) Thermo Wood process

The Thermo Wood process can be divided into three main phases:

Phase 1. Drying

Temperature increased to 103℃ at 20°/min and kept for 24h until the moisture content in the wood decreases to nearly zero.

Phase 2. Heat treatment

Once high-temperature drying has taken place, the temperature inside the oven is increased to required objective temperature. When the target level has been reached, the temperature remains constant for 4 hours depending on the end-use application.

Phase 3. Cooling and moisture conditioning

The final stage is to lower the temperature to room temperature naturally re-moisturising takes place to bring the wood moisture content to a useable level, 4–7%.

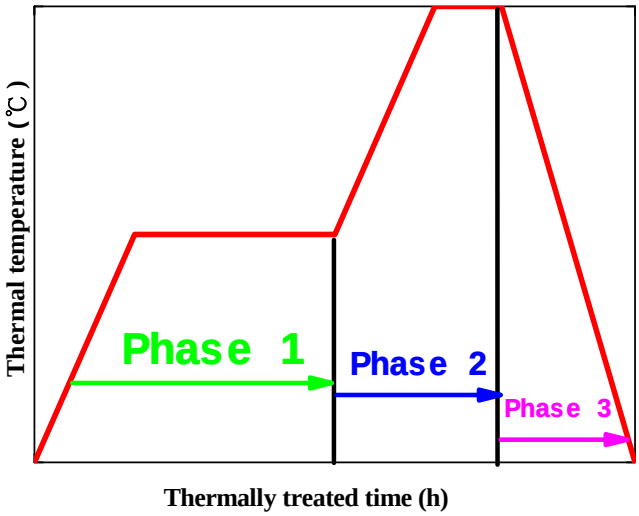

Fig. 1 Diagram of the production process.

3. Results and Discussions

(1) Characteristics of FT-IR spectra of super heat-treated Larix SPP. under different treated media

It can be observed that the vibration intensity of OH groups at around 3380 cm^{-1} diminished along with the elevation of heat treatment temperatures and changed obviously, which illuminated that the quantities of hydroxyl groups decreased with the increasing temperatures. Therefore the hydroscopic property dropped and the dimensional stability increased after the wood determined to thermal treatment.

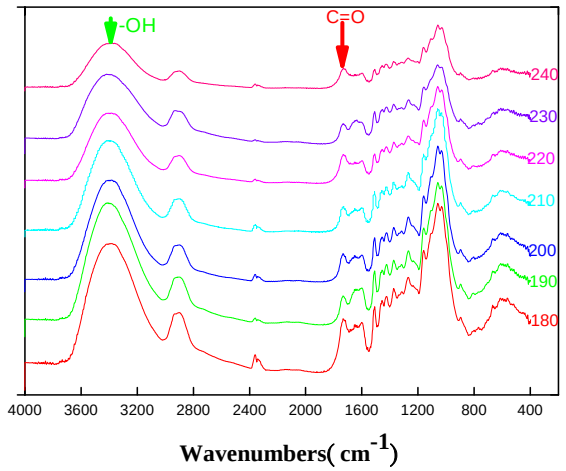

Fig. 2 FT-IR spectra of treated wood under air.

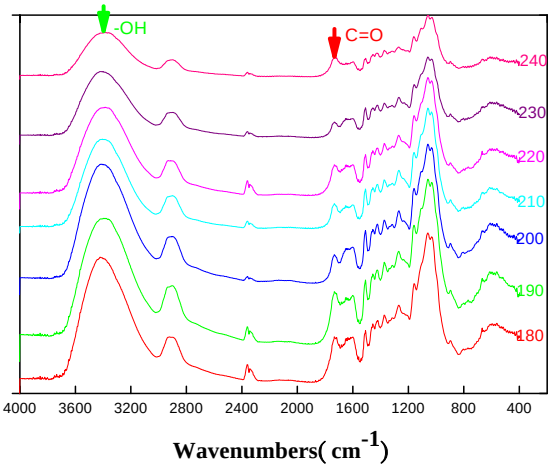

Fig. 3 FT-IR spectra of treated wood under nitrogen.

The stretching vibrations of both acetyl groups at around 1730 cm^{-1} and the carboxyl groups changed quite obviously along with the enhancement of heated temperature. These absorption peaks of C=O are the characteristic absorption peaks of hemicellulose, which suggested that the chemical components of

hemicellulose underwent thermal decomposition resulting in the chemical compositions changed. At the same time, some insoluble water chemical matters emerged during the thermal decomposition of hemicellulose leading to the dimensional improvement of thermal modified wood.

The intensities of both hydroxyl groups at around 3380 cm^{-1} and acetyl groups at around 1730 cm^{-1} under the N_2 atmosphere are lower than those of air. The possible reasons may describe the existence of N_2 can hinder the degradation process of some chemical groups. With the latency owing to the existence of N_2 of some chemical components, however, the dimensional stability of thermal wood enhanced but with the limited reduction of mechanical strength.

(2) Crystalline features of heated wood

It is observed fromTable 1 that the diffraction angle of 002 face is in the vicinity 22.3 °(21.96-22.64°) and the crystalline width is about 4nm(4.02-4.32nm). Segal method is used to calculate the relative crystallinity of cellulose. The variations of thermal wood are firstly increasing, then decreasing and increasing again at last. The changes of crystallinity are very obvious. The value of crystallinity is up to 65%. The main ascriptions are due to the increase areas of cellulose surfaces and the re-crystallization of microfibrils.

Table 1 Crystalline features of super heat-treated Larix SPP.

Thermal medium	Temperature(℃)	Angle of 002 face（°）	Relative crystllinty（%）	Crystalline width（nm）
air	180	22.2	50.77	4.04
	190	22.34	52.48	4.07
	200	22.47	56.46	4.11
	210	22.52	57.88	4.13
	220	22.35	43.59	4.05
	230	22.09	62.13	4.21
	240	21.96	64.15	4.3
N_2	180	22.22	51.98	4.02
	190	22.19	54.6	4.05
	200	22.38	57.92	4.17
	210	22.41	61.58	4.21
	220	22.64	63.72	4.3
	230	22.54	47.18	4.06
	240	22.38	67.29	4.32

(3) Thermal effects on the dimensional stability

It is revealed that(shown in Fig. 4), whether the heat treatment medium is AIR or N_2, the value of ASE increase with the increasing temperatures, which suggested that dimensional stability of wood has been enhanced of Larix SPP. after super heat-treatments. It is also indicated that the ASE of AIR is lower than that of N_2 at the range from 180 to 220℃， but thereafter the value of ASE is higher than that of AIR.

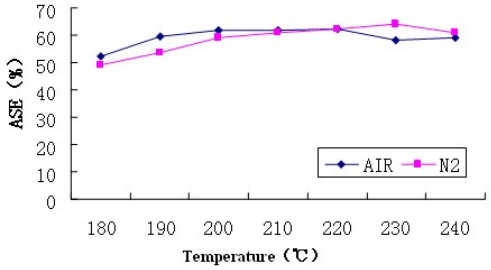

Fig. 4 Variations of ASE at different temperatures.

4. Conclusions

(1) The stretching vibration intensity of - OH groups at around 3380cm^{-1} decreased and changed significantly with the rise of heat treatment temperatures within the thermal media of air and N_2 from the indication of FT-IR spectra, while, the absorption intensity of carbonyl groups at around 1730 cm^{-1} also decreased with increasing temperature. Under the same conditions, the absorption peak intensity of hydroxyl and carbonyl groups under the protection of N_2 is higher than that of air.

(2) The crystallinity of super heat-treated Larix SPP. in different thermal media showed the trend of first increases, then decreases and increases again accompanying the enhancement of heated temperatures. Under the same conditions, the crystallinity of thermal wood in the N_2 is greater than that of air.

(3) The ASE of thermally modified wood increased with the increasing temperatures at range from 180 t0 220℃ and at the same the value of ASE is beyond 60%. But the ASE of thermal wood in the N_2 is lower than that of air at the same scope.

(4) The hygroscopic property decreased, while, the dimensional stability of super heat-treated Larix SPP. increased after heat treatment.

5. References

(1) Jian Li. Wood Preservation. Beijing: Science Press, 2006:155-166

(2) Jian Li. Wood Spectrum. Beijing: Science Press, 2003:104-120

(3) Kamdem DP, Pizzi A, Jermannaud A..Holz als Roh- und Werkstoff, 2002, 60:1-6

(4) Weiland JJ, Guyonnet R. Holz als Roh- und Werkstoff, 2003, 61:21-20

(5) Sivonen H, Maunu SL, Sundholm F, Ja¨msa S, Viitaniemi P. Holzforschung, 2002, 56:648-54

(6) Stamm A J, Hansen L A. Industrial and Engineering Chemistry, 1937, 7:831-833

(7) Kollman F, Schneider A. Holz.als Roh-und werkstoff, 1963, 21:77-85

(8) Bourgois J, Guyonnet R. Wood Science and Technology, 1988, 22:143-155

(9) Bourgois J, Janin G, Guyonnet R. Holzforschung, 1991, 45: 377-382

Evaluation of Dynamic Young's Modulus of Shuttle-Shaped Column with Non-uniform Section Properties Using Flexural Vibration Test

Chih-Lung Cho and Yang-He Huang
National I-Lan University, I-Lan

Abstract: The purpose of this study is to evaluate the dynamic modulus of elasticity (DMOE) of shuttle-shaped column used in historical building in Taiwan. The natural frequencies of various vibration modes of shuttle-shaped column made of *Cunninghamia konishii* were determined by flexural vibration test. The equivalent moment of inertia and area of cross-section of each specimen was determined according to Galerkin's approximate method and these will be used to calculate the Young's modulus.

The results showed that natural frequencies with respect to each flexural vibration mode could be identified accurately using modal analysis. The equivalent moment of inertia of shuttle-shaped columns with respect to Galerkin's approximate method decreased in a curve trend as the modes of vibration increasing and those of equivalent area of cross-section would be increased. The mean absolute percentage differences between predicted and measured natural frequencies of first, second, third, fourth, and fifth flexural vibration mode for shuttled-shaped columns are 1.59%, 2.84%, 3.22%, 3.42%, and 4.05%, respectively. The DMOE determined from higher vibration mode frequencies are lower than that from fundamental frequency, no matter the specimens is round column or shuttle-shaped column. The mean absolute percentage differences between DMOE of round and shuttle-shaped columns with regard to the first, second, third, fourth, and fifth flexural vibration mode are 3.38%, 5.83%, 6.59%, 7.20%, and 8.58%, respectively. This study suggests that the DMOE of shuttle-shaped column determined from fundamental frequencies would be more precisely than the others.

1. Introduction

Non-uniform beams with cross-section varying in a continuous or non-continuous manner along their lengths are used in many structural applications, such as marimba bar, baseball bats, and shuttle-shaped column in traditional historical building in an effort to achieve an optimum function. The effect of mass, section area and moment of inertia on the natural frequencies of different flexural vibration modes would be dependent on the cross-section varying in a beam. A reliable method to determine the dynamic modulus of elasticity of wooden members at different natural frequencies with respect to their equivalent moment of inertia and area of cross-section are required. Accurate Young's modulus of non-uniform member could be induced according to above mentioned and the properties of wooden member could be substantial evaluated precisely. The purpose of this study is to evaluate the dynamic modulus of elasticity of shuttle-shaped column used in historical building in Taiwan. The natural frequencies of various vibration modes of shuttle-shaped column made of *Cunninghamia konishii* were determined by flexural vibration test. The equivalent moment of inertia and area of cross-section of each specimen was determined according to Galerkin's approximate method and these will be used to calculate the Young's modulus.

2. Materials and methods

Ten Luanta fir (*Cunninghamia konishii*) specimens of round columns with 3cm in diameter, and 60 cm in length were prepared for this study. The specimens were conditioned at 20℃ and 65% relative humidity for more than a month prior to measure their properties. The first five resonant frequencies of each round column under free-free flexural vibration were determined from modal analysis. The shuttle-shaped columns were then made from each round column. The dimension of shuttle-shaped column is shown in Fig. 1.

(1) Flexural vibration test

Each of round or shuttle-shaped columns was supported horizontally via two rubber bands to simulate the free-free flexural vibration test. The specimen was impacted with an impact-induced hammer at an end along central line. The time-domain signals from vibration detectors were introduced to modal analysis and the first

five resonant frequencies of specimen were identified. The value of Young's modulus according to Euler beam theory was calculated. The equivalent moment of inertia and area of cross-section of each shuttle-shaped column was determined according to Galerkin's approximate method and these will be used to calculate the Young's modulus.

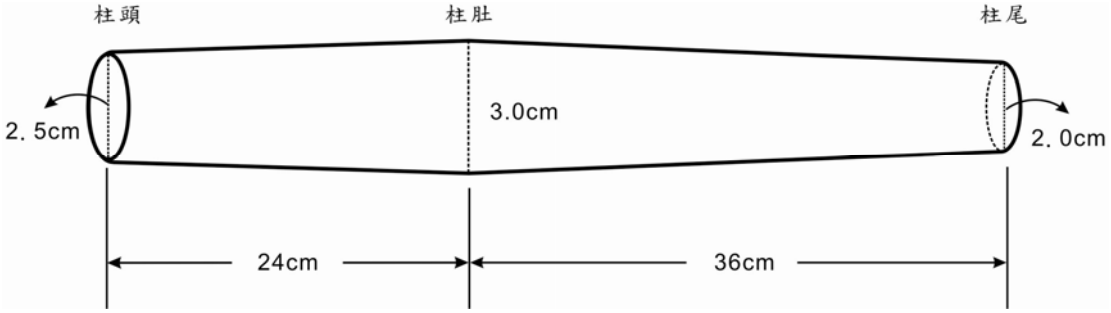

Fig.1 The dimensions of shuttle-shaped column.

3. Results and discussion

Table 1 shows the comparison of resonant frequencies for round and shuttle-shaped columns as obtained from flexural vibration test. The fundamental frequency of each shuttle-shaped column is higher than that of round column, but the other resonant frequencies of shuttle-column are lower than those of round column. The mean predicted resonant frequencies of the shuttle-shaped columns determined from the Young's modulus of round columns and Galerkin's approximate method are shown in Table 2. It indicates that the relative percentage differences between predicted and measured resonant frequencies of shuttle-shaped are less than 4% for the first five vibration modes. It reveals that Galerkin's approximate method could be reliably used to evaluate the vibration properties of non-uniform wooden materials with cross-section varying in a continuous manner along their length.

Table 1 Resonant frequency of round and shuttled-shaped columns at each flexural vibration mode.

Vibration mode	Resonant frequency (Hz)	
	Round column	Shuttle-shaped column
Mode 1	347	366
Mode 2	924	898
Mode 3	1718	1633
Mode 4	2668	2537
Mode 5	3726	3540

Table 2 Comparisons of predicted resonant frequencies of shuttle-shaped column to those of experimental values.

Vibration mode	Resonant frequency (Hz)		
	Predicted	Measured	Percentage difference (%)
Mode 1	360	366	1.59
Mode 2	883	898	2.84
Mode 3	1620	1633	3.22
Mode 4	2468	2537	3.42
Mode 5	3423	3540	4.05

The mean values of Young's modulus of round and shuttle-shaped columns at various vibration modes are shown in Table 3. The Young's modulus determined from higher vibration mode frequencies are lower than that from fundamental frequency, no matter the specimen is a round column or a shuttle-shaped column. The mean

relative percentage differences between the Young's modulus of round and shuttle-shaped columns with respective to first, second, third, fourth, and fifth flexural vibration mode frequencies are 3.38%, 5.38%, 6.59%, 7.20%, and 8.58%, respectively.

Table 3 Dynamic modulus of elasticity determined from each flexural vibration mode of round and shuttle-shaped column.

Vibration mode	Dynamic modulus of elasticity (GPa)		
	Round column	Shuttle-shaped column	Percentage difference (%)
Mode 1	7.95	8.22	3.38
Mode 2	7.42	7.69	5.83
Mode 3	6.67	6.95	6.59
Mode 4	5.88	6.22	7.20
Mode 5	5.14	5.50	8.58

4. Conclusions

According to the experimental results determined by flexural vibration method and Galerkin's method, the conclusions from this study are as follows:

(1) Based on Euler beam theory and Galerkin's approximately method, it was observed that a high correlation existed between the predicted and measured Young's modulus of shuttle-shaped columns.

(2) The values of Young's modulus obtained from flexural vibration method for round and shuttle-shaped column were more accurate by determining from fundamental frequency.

5. References

(1) Jategaonkar R. and P.S. Chehil(1989) Natural frequencies of a beam with varying section properties. J. of Sound and Vibration 133(2):303-322.

(2) Perstorper M. (1993) Dynamic modal tests of timber evaluation according to Euler and Timoshenko theories. 9th International Symposium on Nondestructive Testing of Wood. Madison, WI. P.45-54.

Structural Analysis of Chuan-dou and Truss-frame Wood Houses in Liouguei Area

Chun Chou and Ming-Chung Lee
Forest Utilization Division, Taiwan Forestry Research Institute, Taipei

Abstract: Structures of 5 wood-frame houses built between 1910 and 1960 were investigated. Two of them belong to chuan-dou style with T- and L-shape roofs. The other three are truss framed with gable, hip, and octagonal roofs, respectively. Species used for structural members included Taiwan red cypress, China fir, Japanese cedar, Formosan michelia, and some hardwood species as roof posts. Nails, dowels, bolts, dog irons, fish plate bolts, steel strips, and wood blocks were used as connectors. End joints used included snake head, scarf with tenon, tapered scarf, and dovetail. Lap joints used included dovetail, halved tenon, and halved tenon with tongue. Static bending and compression tests were conducted on small specimens from structural members after the destruction of T-shape, chuan-dou house in 1996. The results showed that tie beam had the largest residue bending strength ratio, and China fir floor beam the least.

1. Introduction

Most traditional Chinese buildings were constructed by wood and are noted for their comfort in living, ability to withstand earthquake, and aesthetic appeal. Many wood-frame houses were built in Taiwan before 1960. This trend, however, changed to non-wood structures afterwards. Wood houses are getting back to trend with the elevating of living standards and the demand for higher living quality. Recent studies concerning traditional Chinese buildings focused mostly on the palace and religious structures. Studies on residential buildings, especially in Taiwan, are relatively few. The purpose of this study, therefore, is to understand the structures of some residential buildings in Taiwan by investigating 5 existing buildings in Liouguei Research Center.

2. Materials and methods

Of the five buildings investigated, one located in Liouguei Research Center, the others in Shanping Work Station. One or more of the following steps was adopted for individual buildings.

(1) The layout was plotted. Defects, such as decay, weathering, structural member failure, were recorded.
(2) The foundation, floor system, wall system, and roof system were investigated. The joint types connecting structural members were also noted.
(3) Species and dimensions of structural member were recorded.
(4) Small, clear, static bending specimens were cut from selected structural members in different locations. Specimens were conditioned to a MC of 12% and subjected to static bending tests.

3. Results and discussion

The first building, with a T-shape and gable roof, was built in 1937 and disassembled in 1996. The dismantlement took 29 labor-days including waste disposal and removal. Purlins were supported directly by roof posts which indicated a chuan-dou framing. A peripheral 45-cm-high concrete strip wall with ventilation openings composed the foundation. On top of this wall were Taiwan red cypress (*Chamaecyparis formosensis*) sills which have strong decay resistance. To enhance the decay resistance of sills, creosote was spread on sill's surface. Floor beams and joists were supported by sills and floor posts. Tatamis were placed on top of strip floorings. Japanese cedar (*Cryptomeria japonica*) was used as columns which tenonned into sills in the bottom and supported end cross beams or tie beams on the top. Bamboo plastered wall was applied as interior wall and weather boards as outside wall. Roof posts were supported by China fir (*Cunnnghamia lancelata*) tie beams which sat on Japanese cedar end cross beams. On top of roof posts were purlins, rafters, roof sheathings, felts, and sheet metal roofings.

Small specimens were cut from selected sills, floor beams, columns, end-cross beams, tie beams, and purlins

for static bending tests. The residual strength ratio, tested value compared to listed values, is shown in the following table. In general, bending strength of structural member retains more of its original value than that of modulus of elasticity. As for the species used, Taiwan red cypress is best. As for the type of structural member, the residual strength ratio decreases in the order of tie beam, sill, Taiwan red cypress floor beam, purlin, end cross beam, column, and China fir floor beam.

Table 1 Residual Strength ratio in %.

	Species	MOR	MOE
Sill	R. Cypress	84.2	65.4
Floor beam	R. Cypress	80.3	47.5
Floor beam	C. China	49.2	47.1
Wall Column	J. Cedar	61.6	45.9
End cross beam	J. Cedar	67.0	53.8
Tie beam	C. China	91.0	77.6
Purlin	J. Cedar	79.8	58.3

The second building, L-shape with both gable and hip roofs, is chuan-dou frame and was built in 1914. A peripheral 48-cm-high concrete stripe wall with ventilation openings was used as foundation. Creosote-coated Taiwan red cypress sills were fastened to stripe wall by anchoring bolts. The framing of floor, wall, and roof systems are similar to those of the first building. The intersection of the L-shape roof formed a hip roof instead of a gable roof.

The third building, built in 1950's and disassembled in 2005, had a gable roof composed by 11 king post trusses. A peripheral 27-cm-high concrete strip wall on a concrete slab formed the foundation. Creosote-coated Taiwan red cypress was used for sills as in the above buildings. Japanese cedar served as column that tenonned into sills in the bottom and supported end cross beams in the top. This building was used as a warehouse. The top surface of concrete foundation was used as floor. No interior wall or ceiling existed. Tar-coated strip weather boards formed the exterior wall sheathing. A concave of approximately 5 mm in the spring wood portion of weather board due to weathering was observed. All structural members except sills are heavily infested by termite, the reason for demolition.

The fourth building, built in 1952, has an octagonal layout with truss-frame roof. A peripheral 27-cm-high concrete strip wall on a concrete slab formed the foundation. Wood frame sat atop a 77-cm-high brick wall, which effectively kept moisture and termite away, built on top of concrete strip wall. Octagonal roof contained two king post trusses. The octagonal shape was formed by purlins extended out to different lengths on upper chords of truss. The structural members in this building were Formosan michelia (*Michelia formosana*).

The fifth building, with truss-frame hip roof, is a 2-story construction built in 1959. The lower level was reinforced brick wall on concrete foundation. Floor beams of 2nd floor were support by sills laid on top of brick wall. Joist and strip flooring along with floor beams formed the floor system. Bamboo plastered wall between columns formed the wall system. The major structure of hip roof was 3 king post trusses. The structural members in this building were Formosan michelia.

In review of the five buildings investigated, several protective measures were adopted by traditional Chinese residential buildings to protect them from decay and termite. These measures include elevated floor system, decay-resistant species for structural member in contact with ground, tar-coated exposed part of structural member, and sheet metal covered exported portion of member.

The Motion Analysis of the Sub-nanometer Wood Flour in the Processing

Yan Ma

Forestry and Woodworking Machinery Engineering Technology Center，Northeast Forestry University，Harbin

Abstract：In this paper the concept of particle size of sub-nanometer wood flour is proposed. The preparation process of sub-nanometer wood flour is analyzed , the equipment structure and principle are discussed in view of a larger practical significance of the sub-nanometer.

1. Introduction

Putting forword Nano-technology represents a new level of people's awareness, if the nano-science is compared with a wood cell in the wood science, the equivalent diameter of a wood cell is about 3×10^{-6}meter, corresponding to 30000 nm and 30 μm or so[1]. From the macro-geometry of the timber into the cells of wood, the specific micro-scale research of the sub-nanometer wood flour is the first step for wood science matching towards the nano-technology[2].The form of nano Ultrafine particles of the timber is wood shape, wood nano-solid materials is the wood polymer nano-ultrafine particles made of solid wood-based materials.

2. The definition of sub-nanometer wood flour and the analysis of processing form

In this paper, the dimension of particle envelope diameter which defines nano and wood sub-nanometer wood flour should range from 1000 to 40000 nm, the particle between 1000 ~ 8000 nm is called the nano-particles, the particle between 8000 ~ 20000 nm is called the sub-nanometer wood flour particles, the particle between 20000 ~ 40000 nm is called the ultra-fine wood flour, the particle more than 40000 nm is called ordinary wood flour.
The wood flour which is more than 8000 nm and less than 40000 nm is defined as sub-nanometer wood flour. In the application of wood flour, the sub-nanometer wood flour still has many uses. When different cutting approach are taken, different structures of wood flour can be formed, the wood flour which is formed by method of cutting in this paper is basically the sub-nanometer wood flour. sub-nanometer wood flour are closely related with wood flour particle size and shape, needing a comprehensive analysis. If we define the end-scale of sub-nanometer wood flour less than 8000nm, as a result of the anisotropic wood fiber,the length of wood flour particles formed along the direction of fiber length may reach 25000 nm. Analysis from the shape,it is Likely to form the shape of a long crystal structure.

As the picture below:

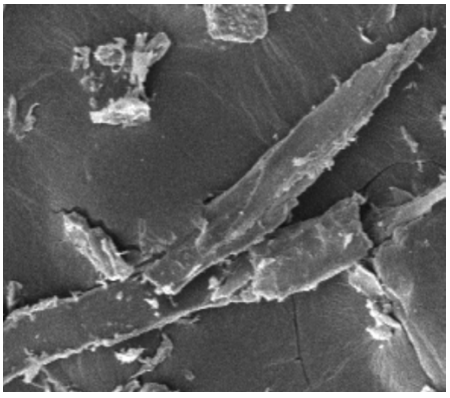

Fig. 1 The sub-nanometer wood flour of long crystal shape.

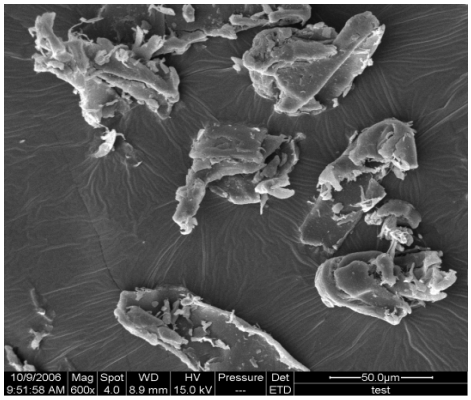

Fig. 2 Fine particle of nano wood flour.

The size of fine nano wood flour particle is less than 2000 nm, the direction of particles along the length of fiber along the direction of fiber length can be less than 3000 nm, being close to square shape in view of shape.

The preparation process of sub-nanometer wood flour is the process of cutting、impacting and smashing the

sawdust or shredded wood fiber,with the use of high-speed cutting tool, along with the generation of new surface of wood flour particles. The equipment which is used to prepare sub-nanometer wood flour atopted the means that high-speed electro-spindle drives high-speed rotation,rotating using a sharp, small-wedge-angle knife[3, 4].The production of sub-nanometer wood flour is using cutting tool to cut wood so as to crack into the shape of fiber cross-section as shown in Fig. 3.

Fig. 3 The cross-section shape of wood cracking fiber.

3. Analysis on the equipment structure and principle of the sub-nanometer wood flour

The sub-nanometer wood flour processing equipment, from the feeding to discharging, that is, directly from raw materials to finished products,three fans and loading head collect wood flour of different mesh numbers from three different parts of the export.

The whole structure and principle of the sub-nanometer wood flour processing equipment is shown in the Fig. 4.

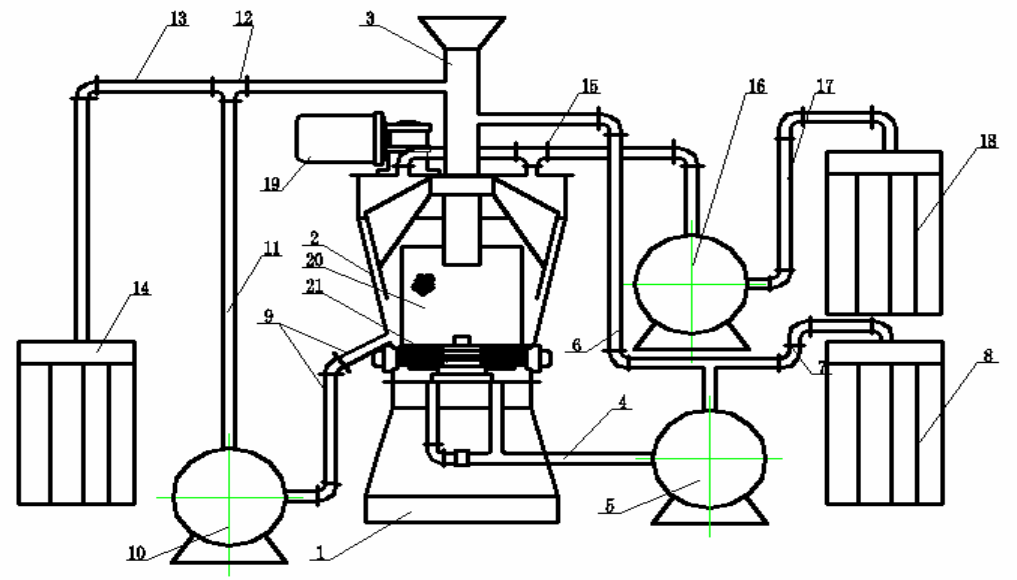

1.base 2.stock bin 3.feed inlet 4.discharging one 5.fan one 6.feed pipe one 7.aggregate one 8.loading head one 9. discharging two 10.fan two 11.pipeline 12.feed pipe two 13. aggregate two 14. loading head two 15. discharging three 16.fan three 17. aggregate three 18. loading head three 19.scraping plates system 20.screen 21.tool group

Fig. 4 The picture of structure and principle of wood flour cracking for cutting method.

Raw materials is directly fed into the screen in the chamber 2 from the hopper 3, in Room 2 in the early period, ultra-fine wood flour particle is crushed mainly by shear stress that formed by high-speed rotary tool in the tool group and fixed units, when the processing to a certain particle size of about 1mm, the raw materials are mainly subjected to both the collision and the shear stress so as to grind further. As a result of gravity, some parts of materials will be gradually deposited at the bottom of the crushing chamber,at this time the 1st fan 5 has

brought out the high-speed airflow ,and it can take out the materials, which is re-transported through the feed tube 6 to Room 2 to smash once again.

When the material is processed to the provisions of the particle size, the wood flour which has met the qualification will be filtered out through the screen in the chamber 2 under the negative pressure of fan 2, extremely fine wood flour is adsorbed to the wall of chamber 2, some flour is absorbed in the screen, and then is scraped through the scraping plates system 19 and deposited to the bottom of the chamber 2. the high-speed air flow generated by the second fan 10 is taken out from discharging two , and is transported to the loading head two through the aggregate two,and then becomes the finished product that can be removed directly after packaging[5].

4. The analysis on the process of cutting and crushing of the sub-nanometer wood flour

In this article, the equipment of sub-nanometer wood flour for cutting has one Electro-spindle in all, power of 2.2KW, directly driving 4 knives for ultra-high-speed rotating, and another worm gear reducer rotates through a pair of gear driving the scraper[6]. Three Typhoon aircrafts whose air volume is controlled by three throttle valves collect material from three different directions , fan one and fan three are controlled by their own three way ball valves.There is an electromagnetic pilot operated valve for regulation of pressure difference inside and outside the equipment after the end of processing .

5. Conclusion

(1) the particle size between 8000 nm to 40000 nm of the wood flour is defined as sub-nanometer wood flour.
(2) In this paper, the grading equipment and the grinding equipment will be combined into one system, which will filter out the sub-nanometer wood flour constantly which have reached the requirements of mesh number , while the wood flour not meeting the requirements will be put back into the grinding room and processed circularly.
(3) In this paper, the theory of cutting the main axis of rotation is put forword, and practical design made the theory verify.

6. References

(1) Wanghui,Mayan,Yangchunmei and Renchangqing: Wood processing machinery, Vol.6 (2005)
(2) Zhaoguangjie: Beijing Forestry University, vol. Z1 (2002)
(3) Liu L M, Qi Z N: J Appl. Polym. Sci., Vol.71 (1999), p. 1133
(4) ZHAOG J, L W H: Forestry Studies in China, Vol. 5 (2003), p. 44-48
(5) Zhujichun,Litingshou and Zhudonglin: Refractory materials, Vol. 03 (1996)
(6) Liuweiping and Chenmisong: Journal of Southern Institute of Metallurgy, Vol. 01 (2002)

National Natural Science Foundation Project "sub-nanometer best mesh wood flour and cell lysis modeling correlation analysis" (30,800,869) Funding.

Preparation and Properties of Carbon Fibers from the Liqueided Wood

Xiaojun Ma[1], Guangjie Zhao[2] and Zhong Liu[3]

[1] Department of Packaging & Printing Engineering, Tianjin University of Science & Technology, Tianjin

[2] Department of Material Science and Technology, Beijing Forestry University, Beijing

[3] College of Material Science & Chemical Engineering, Tianjin University of Science & Technology, Tianjin

Abstract: After melt-spinning by adding hexamethylenetetramine and the curing treatment, carbon fibers (LWCFs) were prepared from the phenolated wood by using of direct carbonization method. The structure characterization of LWCFs was studied by SEM, FTIR and X-ray analysis. The results show that the crystallite size $La_{(100)}$ of LWCFs increases with temperature increasing, whereas the interlayer spacing (d_{002}) gradually decreases during carbonization. It is also found that Although the structure of the precursor has been changed at 500℃ and 800℃ respectively, the bands at 1632 cm^{-1} and 1454cm^{-1} corresponding to the characteristic vibrations of aromatic ring still exist during carbonization. LWCFs at 1000℃ have smooth surface and an ellipse cross-section. At the same time, LWCFs with tensile strength of 1.7GPa, Modulus of 159GPa and yield of 60% are obtained.

1. Materials and methods

(1) Preparation of carbon fibers from liquefied wood

Wood meals (20-80 mesh) of Chinese Fir (Cunninghamia lanceolata (Lamb.)) were dried in an oven at 105℃ for 24 h, and mixed with phenol containing 8wt% H3PO4 as a reaction catalyst. The ratio was wood/phenol=1/6 by weight. The mixture was liquefied by holding at 160°C for 2.5h. Subsequently, hexamethylenetetramrae was added to liquefied wood by 5wt% and allowed to stand for 5min after heating to 120°C in 40min to prepare spinning solution.

After melt-spinning, the spun filaments were cured by soaking in an acid solution HCHO and HCl as main components at 95°C for 4h, washed with demonized water and finally dried at 90°C for 2h. The precursors were carbonized for 2 hours by heating from a room temperature to 1000°C at a heating rate 4°C min-1 in a stream of nitrogen. Carbon fibers from liquefied wood were prepared.

(2) Analysis of the samples

The cross-section of LWCFs was observed with a scanning electron microscope (S-3000N, Hitach Company in Japan). Infrared spectra were recorded on Brukert Tensor27 spectrometer using the KBr disk technique. The X-ray analyses of the fibers before and after carbonization were carried out at room temperature on a Powder X-ray Diffractometer (XRD-6000, Shimadzu Company in Japan). Tensile strength was measured by electrical tensile strength apparatus (YG004N, Hongda spinning apparatus factory, china), the data shown are average value for 20 fibers.

2. Results and discussion

Fig. 1 shows SEM photographs of LWCFs. As can be seen from Fig. 1a, the surface of LWCFs is smooth, and the micropore, attachment or groove structure is not observed. The cross section shown in Fig.1b is elliptical pattern due to the squareness bobbin during melt- spinning process.

Fig. 2 shows the relationship between carbonization temperature and mechanical properties of LWCFs. With carbonization temperature increasing, tensile strength and modulus of LWCFs obviously improve, while elongation at break rapidly reduces. The yields of carbon fibers from liquefied wood are 53.6 ~ 57.3% from 800 to 1100°C. It is clear that the yield of LWCFs is higher than that of lignin based carbon fibers. By orthogonal test, tensile strength, modulus and yield of carbon fibers from liquefied wood is 1.22~1.7GPa, 114~176GPa and 55.8%, respectively.

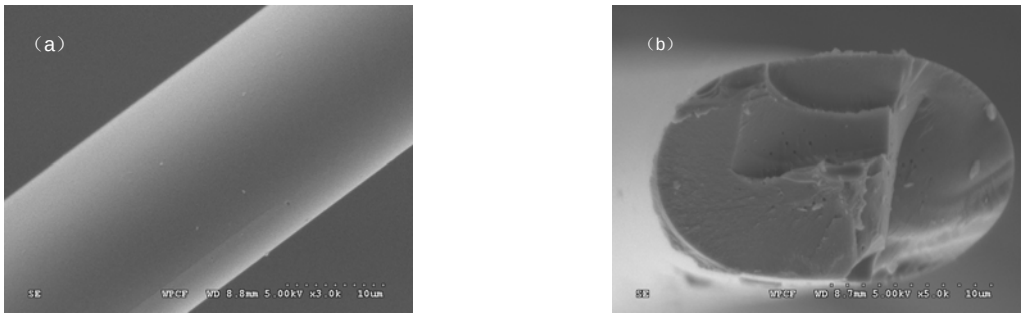

Fig.1 SEM photographs of LWCFs: (a) side surface, (b) crossing section.

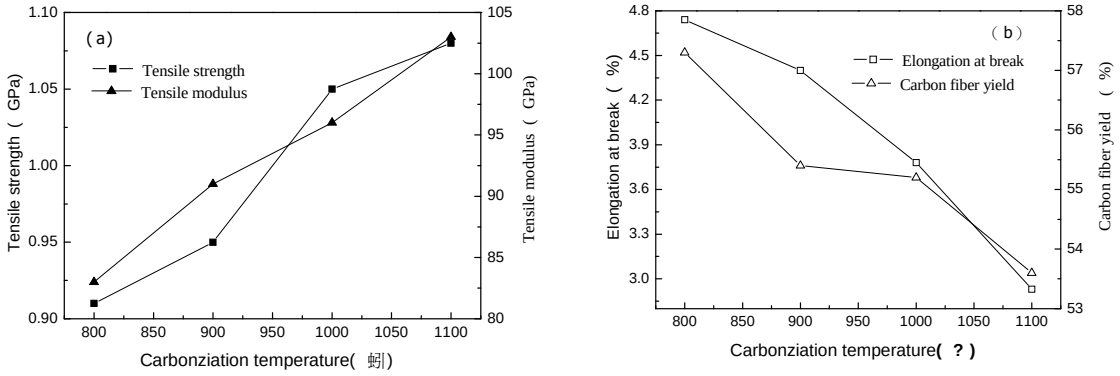

Fig. 2 Mechanical properties of LWCFs.

Fig. 3 shows FTIR spectra of fibers at various stages. During carbonization, the intensity of absorption peak at 3426 cm-1 assigned to O-H stretching band in LWFs, gradually weakens and shifts to 3444 cm-1 (at 1000°C). The absorption peaks at 2922 and 2852cm-1 (mainly methylene bridge) increase and then slowly reduce with temperature increasing. At 1000°C, the bands at 1353 cm-1 assigned to O-H, 1222 cm-1 attributed to C-O and 1002 cm-1 assigned to hydroxide methyl group have completely vanished. In addition, the absorption peaks at 754 and 832 cm-1 basically disappear at 1000°C while the weak absorption peak at 880 cm-1 is still visible. These results indicate that the network crosslinking structure of the fibers is broken due to the scission of methylene bridge of benzene ring and the formation of many condensed rings during carbonization. However, the absorption peaks at 1632 and 1454cm-1, which are corresponding to the characteristic vibrations of aromatic ring, still exist at 1000°C, indicating that the carbonization of the precursors from liquefied wood is a typical non-graphitizing course.

Fig. 4 shows the X-ray diffraction profiles of LWCFs at various temperatures. There is an evident difference between the precursors and LWCFs. It can be seen that the diffraction of 002 peak only exists in the precursors. With the increasing temperature, 002 peak in LWCFs becomes obviously wide. While above 400°C, 100 peak around 44.3°in LWCFs begins to appear and gradually strengthens with temperature increasing. From the above results, it is clear that structure of the fibers has been completely changed during carbonization.

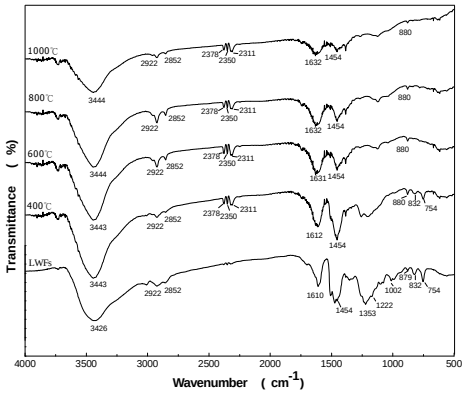

Fig. 3 FTIR spectra of fibers at all stages.

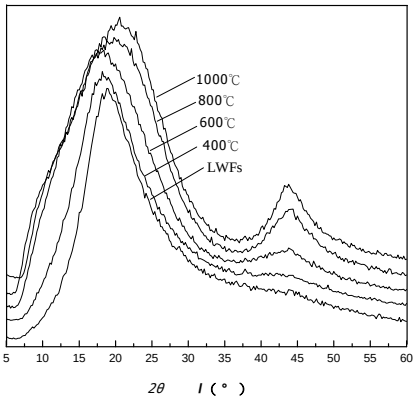

Fig. 4 X-ray diffraction patterns of LWFs and LWCFs.

As shown from Table 1, The crystallite size $La_{(100)}$ of LWCFs increases with temperature increasing, whereas the interlayer spacing (d_{002}) gradually decreases during carbonization. The results indicate that the microstructure evolution of LWCFs is more complex than other carbon fibers.

Table 1 X-ray diffraction structure parameters.

HTT (°C)	$2\theta(002)$(°)	$d_{(002)}$ (nm)	$Lc_{(002)}$(nm)	$2\theta(100)$(°)	$L_{a(100)}$(nm)
400	18.2	0.4870	0.8034	43.6	2.4697
600	18.4	0.4817	0.6599	43.6	2.9738
800	19.8	0.4480	0.6182	44.5	3.2424
1000	20.6	0.4306	0.6411	44.7	3.4829

3. Acknowledgement

This research was financially supported by National Natural Science Foundation of PR China (No. 30471351).

4. References

(1) C. E. Byrne and D. C. Nagle: Carbon Vol.35 (1997), p. 259
(2) K. Sudo, K. Shimizu, N. Nakashima and A. Yokoyama: J. Applied Polymer Sci.Vol.48 (1992), p. 1485
(3) S. Kubo, Y. Uraki and Y. Sano: Carbon Vol.36 (1998) , p.1119
(4) X.J. Ma and G.J. Zhao: Wood and Fiber Science Vol.40 (2008), p.470
(5) X.J. Ma and G.J. Zhao: Fibers and Polymers Vol.9 (2008), p.405
(6) J. F. Kadla, S. Kubo and R. A. Venditti: Carbon Vol.40 (2002), p.2913
(7) M. H. Alma, M. Yoshioka and Y. Yao: Mokuzai Gakkaishi Vol.41 (1995), p.741

Modification of Wheat Straw Through Steam Explosion Treatment

Guangping Han[1], Shunxin Fu[1], James Deng[2] and Tony Zhang[3]

[1]Material Science and Engineering College, Northeast Forestry University, Harbin

[2]FPInnovations - Forintek Division, Québec, QC G1P 4R4, Canada

[3]FPInnovations - Forintek Division, 2665 East Mall, Vancouver, BC V6T 1W5, Canada

Abstract: Steam explosion treatments were used to modify straw fiber attributes for panel manufacturing. In particular, the effect of steam temperature and retention time on morphology, acidity, wettability, and ash and silicon contents of wheat straws was studied. The results showed that the pH value of the untreated wheat straw fibre was nearly 7 and the pH values and acid buffer capacities of straws were greatly reduced after steam explosion treatments. This indicated that the acidity of straws increased after steam explosion treatments. The dynamic contact angle of the straws before the treatment was nearly 90 degree, indicating that the straw materials without treatment are more hydrophobic. After steam explosion treatments, the contact angle of straws was significantly reduced, showing that the surface wettability of the treated straws was improved. The ash and silicon contents of straws were also significantly reduced by steam explosion treatments. The improved acidity and wettabillity as well as decreased silicon content would contribute to the improved bondability between straw particles and water-soluble adhesive binders.

1. Introduction

In general, crop materials such as straws, sugar cane, and bast fibers (flax and hemp) have lower cellulose and lignin contents, but higher pentosan content than wood [1]. The ash content of all crop materials is significantly higher than that of wood [2，3]. More than 90% of the ash in wheat straw was silica [4]. The chemical composition of crop fibers, especially high ash content, has limited the use of these crop materials as raw fiber materials for panel manufacture [4]. In addition, crop materials commonly contain high levels of extractives, which may influence the curing behavior of adhesives [5]. The pH and acid buffering capacity of aqueous extracts from the non-wood lignocellulosic materials are significantly higher than those of softwood, which increases the gel time of urea- formaldehyde (UF) resin and causes bonding difficulty [6]. The presence of extractives can also influence the wettability of materials [7，8]. The low wettability is related to the existence of nonpolar extractives [9]. Generally, there is a waxy layer on the crop material surface [4, 5]. The water-soluble UF resin is chemically incompatible with the straw material and it is probably the main factor responsible for the reduction of bond quality.

The overall goal of this work was to investigate the feasibility of improving the bondability between steam explosion pre-treated wheat straw and UF resin. The specific objective was to evaluate the effects of different treatment conditions (i.e., steam temperature and retention time) on the morphology, acidity, wettability, and chemical properties of wheat straw.

2. Materials and methods

(1) Raw materials and preparation

Wheat straw was collected from Quebec, Canada. The air-dried wheat straw was hammer-milled and screened to attain furnish with an average length of 25 mm. Subsequently, all the straw material was presoaked in water at 20^{o}C for 12 hours prior to steam explosion treatment.

(2) Steam explosion treatment

The presoaked wheat straw was treated under various steam explosion conditions. Steam temperature was 190^{o}C and 200^{o}C and the retention time was 2 min and 3 min. The treatment was conducted using a specially designed steam explosion vessel at the pilot plant of the Eastern Laboratory of the FPInnovations-Forintek Division.

(3) Evaluation of pH and buffer capacity

The pH, acid and base buffer capacity were evaluated for wheat straw from various steam explosion treatments. Straw particles were ground using a small Wiley grinding mill (model 4) and sieved to pass a 40-mesh screen. The sieved straw samples (15 g dried weight) were refluxed in a 200 ml of boiling distilled water for 20 min. The mixture was filtered under vacuum and then diluted to 500 ml. This filtrate solution was used for pH and buffer capacity measurements. A Corning Pinnacle 530 pH meter was calibrated with pH 7.00 and 4.00 standard buffer solutions for acid buffer capacity determination, and with pH 7.00 and 10.00 for base buffer capacity determination. Each filtrate (100 ml) was titrated twice using a 25-ml burette with a standard 0.025 N H2SO4 solution until reaching pH 3.00 for acid buffering capacity measurement. For base buffer capacity, each filtrate was titrated twice with a standard 0.025 N NaOH solution until reaching pH 11. The initial pH was recorded prior to each titration. The buffering capacity, expressed as total milliequivalents (mEq) of acid (or base) per 100 g of oven dried (OD) sample needed to lower the pH to 3.00 (or 11.00).

(4) Measurement of wettability

Dynamic contact angles were measured to evaluate the wettability of the straw material treated under various steam explosion conditions. The wettability of water onto the straw samples was determined using the capillary rising height method. Oven-dried sample (0.05±0.005 g) was loaded into the cyclindric glass tube, which was closed at one end with a porous glass sieve. The sample glass tube was then hung on a microbalance and the weight of the samples together with the tube was tarred to zero. The test liquid under the glass tube, maintained at 20^{o}C, was brought into the sample by penetrating through the glass sieve and wet the sample. The test liquid reservoir rose up to contact with the sample at a rate of 4.5 mm/min. The balance detected the weight increase as a function of time until steady state was reached. Six replications were performed in the measurement of each condition.

(5) Ash and silicon content

The ash and silicon contents of wheat straw material treated under various steam explosion conditions were analyzed in accordance with ASTM D 1102 Standard (ASTM 2007). Four samples of straw material with each steam explosion treatment were used for the determination of ash and silicon contents. To determine the ash content, each sample entailed an18-h combustion at 800°C followed by an acid digestion of the total ash.

3. Results and Discussion

(1) Effect of steam explosion treatments on acidity properties of wheat straw

The pH value of untreated wheat straw material (control sample) was 6.83. After steam explosion treatments, the pH values and acid buffer capacities of straw decreased remarkably. The pH value of the treated straw under 200^{o}C for 3 min was reduced to 4.98 from 6.83 of the control sample. Acid buffer capacities were lowered from 16.25 of the control sample to 6.88 for the water-soaked sample and to 4.16 for 190^{o}C/2 min treatment. The results indicate that the acidity of wheat straw material was increased after steam explosion treatment. It can be predicated that the better acidity properties of the treated straw particles will help improve the bondability between straw particles and the acid-setting UF resin, and thus the performances of straw particleboards.

(2) Effect of steam explosion treatments on wettability of wheat straw

The average values of dynamic contact angles of wheat straw after various treatments are shown in Fig. 1. The contact angle of the straw before treatment was nearly 90 degrees, indicating that water hardly wet the straw material. This means that the raw material without treatment is more hydrophobic. It clearly shows that the contact angles after steam explosion treatments decreased, indicating the improved surface wettability. This is probably due to the damaged waxy layer and the exposed highly reactive hydroxyl groups of the straw material resulted from steam explosion treatment. The wettability of wheat straw, which is prerequisite for the good adhesion between the straw fibers and binder, depends on many factors, such as the porosity, hygroscopicity, and

chemical composition of the straw. The improved wettability of treated straw samples could also be attributed to the fact that the surface of the material becomes more porous due to explosion effect caused by the sudden release of steam at the end of treatment. The better wettability of treated straw would contribute to the improvement of the bondability between straw particles and water-soluble UF resin, thus to improved performances of the products.

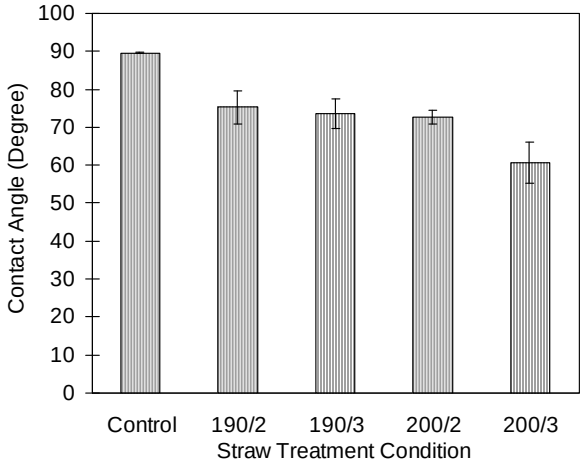

Fig. 1 Contact angles of wheat straws before and after various steam explosion treatments.

(3) Effect of steam explosion treatments on chemical properties of wheat straw

Fig. 2 shows the ash and silicon contents of the steam explosion treated wheat straw. The ash content of the straw sample before treatment was 5.8%, which is much higher than wood (normally less than 1%). It was reported that more than 90% of the ash in the wheat straw was silica (Sauter 1996). Sawatari et al. (1996) concluded that the silicon atoms in rice and wheat straws were extremely concentrated in the surface layer. The chemical composition of straws, especially the high ash content, has a negative impact on the use of straws as raw materials for panel manufacture (Markessini et al. 1997). After steam explosion treatments, the ash and silicon contents decreased significantly. This means that part of ash was removed via steam release. As ash is hydrophobic, the removal of ash from wheat straw will contribute to the improvement in its wettability and consequently better bondability between wheat straw and water-soluble UF resin.

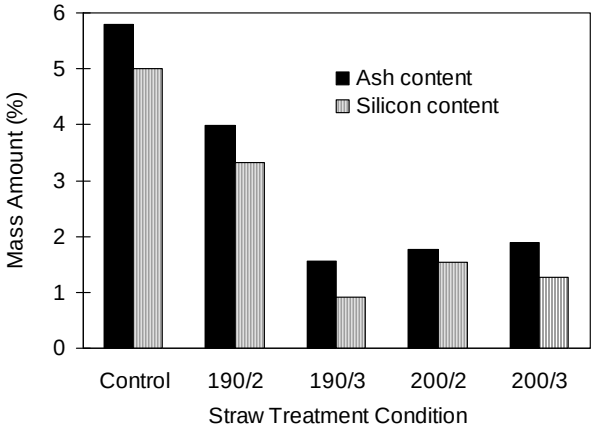

Fig. 2 Ash and silicon contents of wheat straws before and after steam explosion treatments.

4. Summary

Steam explosion treatment can be a feasible approach to improve the bonding strength between wheat straw material and adhesive binders. After steam explosion treatments, the proportions of large particles decreased while fiber bundles increased. Higher steam temperature and longer retention time resulted in more homogeneous fiber-like material. It was found that the pH values and acid buffer capacities of straw were greatly reduced, indicating the increased acidity of the treated straw. The straw material before treatment was more hydrophobic. The dynamic contact angles after steam explosion treatments decreased significantly, indicating that the surface wettability of the treated straw was improved. The ash and silicon contents of the treated straw were significantly reduced through steam explosion. The improved acidity and wettabillity as well as the decreased silicon content would contribute to the improvement in bondability between straw particles and water-soluble UF resins.

5. Acknowledgements

The financial support on this project by Science and Technique Bureau of Heilongjiang Province (Grant No. GB07B503) and the Programme of Introducing Talents of Discipline to Universities ("111 Programme") is acknowledged.

6. References

(1) Rowell Roger M., 1996. Composites from agri-based resources. In: Proceedings, No.7286 the Use of Recycled Wood and Paper in Building Applications. Madison WI, Forest Products Society. pp. 217-222.

(2) Youngquist, J.A., English, B.E., Spelter, H., Chow, P., 1993. Agricultural fibers in composition panels. In: Proceedings, 27th International Particleboard/Composite materials Symposium. Washington State Univ. Washington, USA. pp. 133-152.

(3) Youngquist, J.A., Krzysik, A.M., English, B.W., Spelter, H.N., Chow, P., 1996. Agricultural fibers for use in building components. In: Proceedings, No.7286 the Use of Recycled Wood and Paper in Building Applications. Madison WI, Forest Products Society. pp. 123-134.

(4) Sauter, S.L., 1996. Developing composites from wheat straw. In: Proceedings, 30th International Particleboard/Composite materials Symposium. Washington State Univ. Washington, USA. pp. 197-214.

(5) Loxton, C., Hague, J., 1996. Utilization of agricultural crop materials in panel products. In: Proceedings, No.7286 the Use of Recycled Wood and Paper in Building Applications. Madison WI, Forest Products Society. pp. 190-192.

(6) Hague J., Mclauchlin A., Richard Q., 1998. Agri-materials for panel products: A technical assessment for their viability. In: Proceedings of the 32th International Particleboard/Composite materials Symposium., Washington State Univ., Washington, USA. pp. 151-159.

(7) Young, R.A., 1976. Wettability of wood pulp fiber. Wood Fiber Sci. 8, 120-128.

(8) Hes, C-Y, Kuo, M-L, 1988. Influence of extractives on wood gluing and finishing – a review. Forest Prod. J. 38, 52-56.

(9) Nguyen, T., Johns, W.E., 1979. The effects of aging and extractives on the surface free energy of Douglas-fir and red wood. Wood Sci. Technol. 13, 29-40.

Preparation and Antibacterial Efficiency of Metallized Activated Carbon

Jin-Cherng Huang, Yi-Hsuan Liu, Ying-Fu Chang, Syun-Wun Ruan, Ya-Nan Wang and Su-Ling Liu

Department of Forest Product Science, National Chiayi University, Chiayi

Abrstract: Preparation of antibacterial activated carbon was performed in this study using an ethylene glycol reduction method, a glucose reduction method and a physical method, by mixing silver nitrate, zinc nitrate and nanosized zinc oxide with activated carbon respectively. Scanning electron microscopy (SEM) was employed to assess the surface structure, while measuring number of *Escherichia coli* (*E. coli*) and *Staphylococcus aureus* (*S. aureus*) in order to understand the basic properties and antibacterial efficiency of metallized activated carbon. In the SEM graphs with the same concentrations, activated carbon made with ethylene glycol reduction method had less silver whereas that made with glucose reduction method had more silver, in their aggregate states; thus, the glucose water solution has better reducibility on silver nitrate; after being treated with nanosized zinc oxide, it dispersed on the surface of activated carbon in the form of tiny particles, tended not to plug the pores of the activated carbon. The iodine value of metallized activated carbon decreased with the rise in concentration of metal. The activated carbon's antibacterial effect on *E. coli* and *S. aureus* under various treatment conditions showed that activated carbon without metallizing does not possess an antibacterial effect and would increase the growth of bacterial in water. The metal content in metallized activated carbon is positively correlated with solution concentration. With the same silver nitrate concentration, the rate of bacteriostasis on *E. coli* deoxidized by glycol was merely 66.7%, whereas it could reach 70.7%~100% if deoxidized by glucose. So the antibacterial effect when using the glucose reduction method is better than that of the ethylene glycol reduction method. To prepare the activated carbon with silver and zinc using glucose reduction, experimental results showed that those made with 0.005M silver nitrate had the rate of bacteriostasis as high as 100%, while the activated carbon with zinc made with 1.5M zinc nitrite did not; this proved that silver has a better antibacterial effect than zinc. However all the sample materials treated with nanometer zinc oxide method at 200℃ had a bacteriostasis rate of 99.9%.

1. Introduction

In early times, bamboo was often used to build fences and buildings because of its stiffness and excellent hardness. When it was substituted by plastic products, bamboo was seen as a cheaper, but inferior product. If there is no revolution in the bamboo industry, it will face bankruptcy and cause a disastrous loss in assets; this research therefore studies and activated carbon sample from bamboo. Liu (2008) studied the carbonization and activation temperatures for different parts of *Phyllostachys edulis* and *Bambusa stenostachya*(Thorng bamboo). In their results, it was found that the best temperatures for carbonization and activation were 550°C and 800°C respectively.

When activated carbon is used in waste water treatment or tap water processing, bacteria can reproduce on the activated carbon during water purification due to its excellent bio-compatibility; this can easily impose secondary pollution (Park & Jang,2003). Many metals possess bacteriostatic or sterilizing properties. Xu(2004) pointed out that the main antibacterial metals would be silver (Ag), copper (Cu) and zinc (Zn).

Liu *et al.*(2008) prepared Ag-activated carbon and Cu-activated carbon via reduction using glycol. It was found that an Ag concentration of 0.001M metallised on activated carbon would provide excellent antibacterial effects - better than Cu-activated carbon. Their work also showed that Zn possesses a lower antibacterial effect, but is cheaper to produce. By preparing ZnO on the nanometer scale, it's the antibacterial effect can be enchanced. Wu (2007) pointed out that nanosized ZnO can act as a highly efficiency disinfectant. Their experiments confirmed that 1% of nanosized ZnO could killed 98.86% of *Staphylococcus aureus* (*S.* aureus) in 5 minutes and could killed 99.93% of *Escherichia coli* (*E.* coli). Thus in this research, lower toxicity Zn was used instead of Ag and Cu to be metallised on the surface of activated carbon.

2. Material and method

(1) Experimental materials

A. Commercial activated carbon, made from coconut shell activated carbon, provided by LI JING VISCARB CO.,LTD

B. Prepared activated carbon

(A)40-60 mesh-sieved activated carbon from hard shell of *Sapindus Mukorossi* as raw material.

(B)20-40 mesh-sieved activated carbon from *Bambusa stenostachya* as raw material.

(2) Methods

The schematic layout of the experimental methods is shown in Fig1.

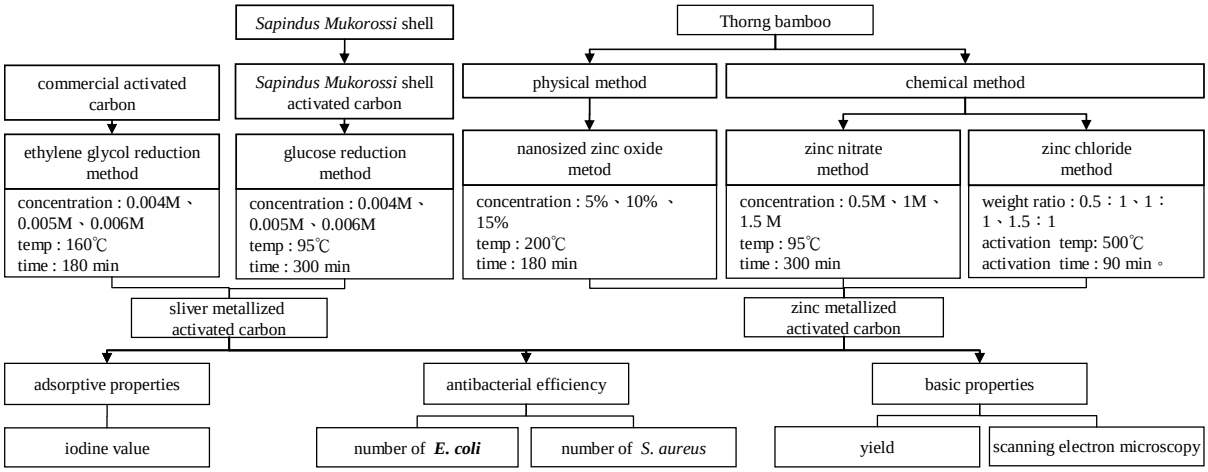

Fig. 1 The preparation and properties of metallized activated carbon.

3. Results and discussion

(1) Char yield and weight increment

Table 1 tabulates the char yields of Zn-activated carbon during different calcinations. From the table, we note that the char yields of chemical activation were higher than the physical activation. Furthermore, their weights increased with increasing concentration regardless of whether Nano ZnO or ZnO was sythesised by using zinc nitrate. For Nano ZnO under the same concentration, its weight at 200^{o}C was greater than 800^{o}C.

(2) Iodiane value

Liu (2008) pointed out that the Thorng bamboo, processed at 550^{o}C for carbonization and 800^{o}C for activation, possessed a mainly mesoporous structure with a pore diameter of about 8nm. From Table 2, we can see that the iodine value for inactivated charcoal was only 60.6 mg/g and it had very few pores. Steam activation at 800^{o}C provided a distinct enhancement in the iodine value, reaching 772 mg/g. The adsorption of iodine on commercial activated carbon is generally 600~1000 mg/g (Wu *et al.*, 1999). From this research, ZnO-5 reached the commercial standard; furthermore, using zinc chloride as an activating agent, the iodine value increased slightly when the consumption of zinc chloride was greater. This is because zinc chloride can permeate into raw materials, allowing for their expansion. During carbonization, chloride and hydrogen in the raw materials reacted and formed hydrochloric acid or steam so that there are no other hydrocarbon or oxide compounds clogging the pores. (Liu, 1998).

Table 1 The yield and weight percent gain after treatment of metallized activated carbon.

Item		carbonization temperature (℃)	activation temperature (℃)	yield (%)	weight percent gain after treatment (%)
carbon		550	—	26.73 (0.01)	—
bamboo activated carbon			800	11.29 (0.02)	—
Sapindus Mukorossi shell activated carbon		500	800	14.39 (0.99)	—
zinc chloride method	ZnCl2-50	500	500	48.15 (2.47)	—
	ZnCl2-100			55.08 (3.03)	—
	ZnCl2-150			59.50 (0.85)	—
nanosized zinc oxide method (800℃ treated)	ZnO-5	550	800	—	8.37 (3.66)
	ZnO-10			—	26.37 (3.94)
	ZnO-15			—	52.67 (5.93)
nanosized zinc oxide method (200℃ treated)	ZnO-5	550	800	—	43.35 (1.62)
	ZnO-10			—	56.53 (2.65)
	ZnO-15			—	73.33 (3.20)
zinc nitrate method	$Zn(NO_3)_2$-0.5	550	800	—	47.47 (3.13)
	$Zn(NO_3)_2$-1			—	62.87 (2.86)
	$Zn(NO_3)_2$-1.5			—	78.73 (5.20)

note：( ) are standard deviation

Table 2 Iodine value of metallized activated carbon.

Item		materials	carbonization temperature(℃)	activation temperature(℃)	iodine value (mg/g)
carbon		—	550	—	60.61 (1.59)
bamboo activated carbon		—		800	772.84 (6.36)
Sapindus Mukorossi shell activated carbon		—	550	800	558.36 (2.24)
nanosized zinc oxide method (800℃ treated)	ZnO-5	zinc	550	800	697.26 (1.49)
	ZnO-10				686.08 (3.30)
	ZnO-15				644.00 (4.97)
nanosized zinc oxide method (200℃ treated)	ZnO-5	zinc	550	800	607.81 (5.19)
	ZnO-10				561.71 (7.06)
	ZnO-15				518.02 (3.23)
zinc chloride method	ZnCl2-50	zinc	500	500	567.72 (2.40)
	ZnCl2-100				585.53 (2.64)
	ZnCl2-150				590.06 (1.52)
zinc nitrate method	Zn()2-0.5	zinc	550	800	307.49 (4.57)
	Zn(NO3)2-1				293.10 (3.15)
	Zn(NO3)2-1.5				283.69 (2.45)
Ethylene glycol reduction method	$AgNO_3$-0.004	sliver	—	—	573 (6.5)
	$AgNO_3$-0.005				556 (8.5)
	$AgNO_3$-0.006				552 (7.3)

note：( ) are standard deviation

(3) Scanning electron microscope (SEM) observations

Fig. 2 illustrates the SEM images of Ag-activated carbon using: (A) glycol and (B) glucose as a reducing agent. It clearly shows that while using glucose as a reducing agent, Ag metal was undergoing agglomeration. Fig. 3 depicts the SEM images of Zn-activated carbon from bamboo. The agglomerate of metallic Zn was found on activated carbon after the reduction of zinc nitrate using glucose. In Figure (A), the surface of activated carbon is covered by a thin layer of film, which blocks some of the pores. It was postulated that the thin film formed between the glucose and Zn. In Figure (B), many pores were found for the activated carbon processed via chemical activation after low temperature carbonization at 500^{o}C. In Figure (C), it clearly shows that Nanosized ZnO was well-dispersed on the surface of activated carbon and the granular size of ZnO was smaller than the pores of activated carbon. This indicated that the Nanosized ZnO would not easily clog of the pores of activated carbon.

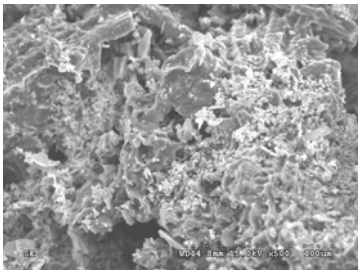

(A) ethylene glycol reduction method (x0.5X)

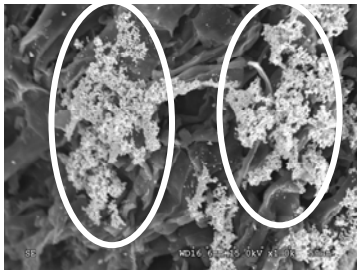

(B) glucose reduction method (x1.0K)

Fig. 2 SEM micro photos of different methods treated sliver metalized activated carbon.

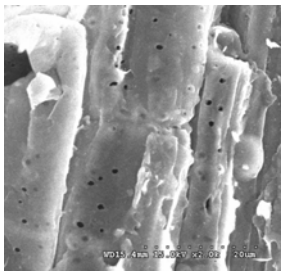

(A) zinc nitrate method (x2.0K)

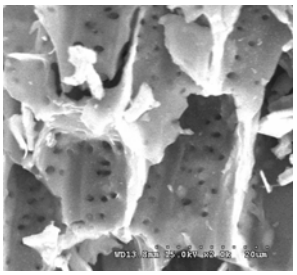

(B) zinc chloride method (x2.0K)

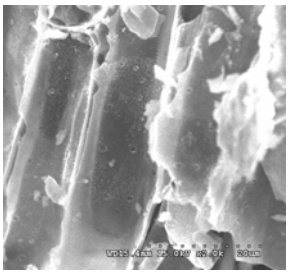

(C) nanosized zinc oxide method (x2.0K)

Fig. 3 SEM micro photos of different methods treated zinc metalized activated carbon.

(4) Bacteriostasis experiment

Table 3 tabulated the bacteriostatic effect of Ag-Activated Carbon on *E.* coli and S. aureus. In the cases of using glucose as a reducing agent, all samples could provide a 100% bacteriostatic effect, except 0.004M. For *E.*coli, samples using glucose as a reducing agent performed better bacteriostatic effect than those that used glycol. From Table 4, in Nano ZnO samples, the number of bacteria colonies was lower than the blank samples, and hence it demonstrated that Nano ZnO displays a bacteriostatic effect. The Nano ZnO was prepared by using zinc chloride at 200^{o}C displayed a 99.9% bacteriostatic effect. According to Hisashi Tamai *et al.* (2000), bacteria can grow on the surface of activated carbon and occupy the base of activated carbon, causing bacterial pollution in water. This could possibly explain why the control samples perform slightly better than the blank samples.

Table 3 The antibacterial efficiency of sliver metalized activated carbon at *E. coli* and *S. aureus*.

Item	carbonization temperature (℃)	activation temperature (℃)	concentration 0f $AgNO_3$ (M)	the number of bacteria (10^9 CFU/ml)		bacteriostatic ratio (%)	
				E. coli	*S. aureus*	*E. coli*	*S. aureus*
			drinking water	1.65 (0.11)	1.94 (0.19)	—	—
glucose reduction method	550	800	AC water	2.09 (0.33)	2.27 (0.13)	—	—
			0.004	0.04 (0.02)	0.05 (0.01)	98.1	97.8
			0.005	0.00 (0.00)	0.00 (0.00)	100.0	100.0
			0.006	0.00 (0.00)	0.00 (0.00)	100.0	100.0
ethylene glycol reduction method	—	—	drinking water	1.10×10^2	—	—	—
			AC water	1.05×10^2	—	—	—
			0.004	3.5×10^1	—	66.7	—
			0.005	3.5×10^1	—	66.7	—
			0.006	3.5×10^1	—	66.7	—

note：( ) are standard deviation.　AC water is activation carbon water

Table 4 The antibacterial efficiency of zinc metalized activated carbon at *E.* coli and *S.* aureus.

Item		the number of bacteria (CFU/ml)		bacteriostatic ratio (%)	
		E. coli	*S. aureus*	*E. coli*	*S. aureus*
water		2.91×10^5 (0.12)	3.06×10^5 (0.03)	—	—
Bamboo activated carbon		3.56×10^5 (0.06)	3.61×10^5 (0.11)	—	—
nanosized zinc oxide method (800℃ treated)	ZnO-5	2.86×10^5 (0.15)	2.26×10^5 (0.12)	16.6	32.1
	ZnO-10	2.16×10^5 (0.06)	2.16×10^5 (0.25)	37.0	35.1
	ZnO-15	2.86×10^5 (0.06)	2.20×10^5 (0.20)	16.6	33.9
nanosized zinc oxide method (200℃ treated)	ZnO-5	2.90 (2.71)	2.16×10^2 (0.17)	99.9	99.9
	ZnO-10	1.37 (0.15)	1.33 (0.15)	99.9	99.9
	ZnO-15	4.67 (2.08)	3.37 (4.01)	99.9	99.9
zinc chloride method	$ZnCl_2$-50	1.08×10^2 (0.06)	7.10×10^1 (0.26)	99.9	99.9
	$ZnCl_2$-100	3.57×10^1 (1.34)	4.53×10^1 (0.21)	99.9	99.9
	$ZnCl_2$-150	1.83×10^1 (0.25)	1.37×10^1 (0.12)	99.9	99.9
zinc nitrate method	$Zn(NO_3)_2$-0.5	3.00×10^2 (2.00)	6.67×10^2 (1.53)	99.0	99.2
	$Zn(NO_3)_2$-1	5.00×10^2 (2.65)	1.73×10^3 (0.31)	99.3	98.0
	$Zn(NO_3)_2$-1.5	4.43×10^3 (0.91)	5.88×10^4 (0.03)	94.1	31.1

note：( ) are standard deviation

Thermal Conversion of Wood Chip in a 150 kWth Bubbling Fluidized Bed Gasification Pilot Plant

Keng-Tung Wu[1], Helmar Tepper[2], Matthias Gohla[2], Bert Lemin[2], Lutz Hoyer[2] and Hom-Ti Lee[3]

[1] Department of Forestry, National Chung Hsing University, Taichung

[2] Department of Process and Plant Engineering, Fraunhofer Institute for Factory Operation and Automation, Germany

[3] Energy & Environment Research Laboratories, Industrial Technology Research Institute, Hsinchu

1. Introduction

Biomass is the largest renewable energy source and the fourth largest primary energy supply in the world. The gasification, the environmental-beneficial process, then could be considered as a technology to recover energy from biomass and waste. In Taiwan, because the forest waste is the high quality biomass, the utilization of the waste should be enhanced. The small scale gasification then is also considered as a core technology to recover energy from the agriculture wastes in Taiwan.

In Germany, the wood chips can be gasified in a small decentralized unit with a thermal output between 1-10 MW to produce power and heat cost-effectively. The wood processing industry can be considered for implementation of this development. In combination with appropriate syngas processing, the advanced gasification system can be connected with an internal combustion engine-generator to produce electricity. This form of energy conversion can achieve a higher efficiency than the conventional steam power processes based on the same condition (e.g. power range) and it requires the lower investment and operating costs.

The objective of this study is to ensure and analyze the performance of this gasifier. All experiments were carried out in a 150 kWth atmospheric bubbling fluidised bed gasification pilot plant, WSV 400 (Wirbelschichtvergaser mit 400 mm Bettdurchmesser) located at German Fraunhofer Institute for Factory Operation and Automation (IFF). In addition, a catalytic reformer and a wet scrubber are installed with the gasifier to investigate the tar conversion or removal. The utilization of the syngas in an engine for power generation is also studied. It is expected that the results of this investigation would provide some valuable information in developing the gasification technology for small power and heat systems in Taiwan and Germany.

2. Experimental

(1) Configuration of the gasification pilot plant

The 150 kWth bubbling fluidised bed gasifier employed in this study consists 9 main units including the air supply, fuel supply, fluidized bed gasifier, cyclone, catalytic reformer, wet scrubber, combustion chamber, gas engine, and measurement devices, which is designed for the low calorific fuels (e.g. biomass and waste) with a size up to 50 mm.

The fluidized bed gasification reactor, with a diameter of 0.4 m in the bed region, 0.6 m in the freeboard region, and a total high of 3 m, is constructed of the heat resistant steel covered with a thermal insulation on the outer surface to limit heat loss. A screw feeder with 90 mm in diameter is used for fuel feeding. A silo filled with nitrogen above the screw feeder is employed for the fuel storage. Air supplied by a compressor is used as gasification agent. The air is pre-heated by the electric heaters during heating up the gasification reactor only. The average operation temperature for gasification is 800 to 900°C at an air equivalence ratio (ER) between 0.2 to 0.5. The raw syngas leaves the gasification reactor at the top then through a cyclone for the primary cleaning. The ash and unburned char with a size larger than 10 μm are separated from the cyclone for removal.

The produced syngas is used in a combustion chamber or in a gas engine. For syngas utilization in gas engines, the tar contained within the raw syngas should be converted into the light hydrocarbons (e.g. CO and H_2) or be removed. Connected with the cyclone, a full stream catalytic reformer consisted of honeycomb reforming

catalysts is used for the secondary cleaning. The tar in the reformer with the steam at a higher temperature (above 900°C) is converted into the light hydrocarbons. However, the reforming efficiency can not be sufficient for the syngas utilization in a gas engine with the internal combustion. Therefore, a wet scrubbing system installed after the reformer is used for final cleaning of the syngas. A special engine for the low calorific syngas is installed to investigate the utilization of the produced gases for power generation. This engine with an electricity output of 30 kW is a modified gas engine with an internal combustion operated with the Diesel's principle.

The components of the syngas, such as CO, CO_2, H_2 and CH_4 is analyzed by employing a series of separated gas analyzers for the characterisation of syngas quality. The tar is sampling automatically and analyzed by a Ratfisch Analysensysteme GmbH Tar Analyser TA 120-3 with a flame ionization detector.

(2) Fuel and bed material

The wood chips from the pine were employed as the feeding fuel with a size of 3.5 cm × 2.5 cm approximately. The wood chips contained 36.53 *wt.*% carbon, 5.39 *wt.*% hydrogen, 30.37 *wt.*% oxygen mainly. The moisture of wood chips was 26.5 *wt.*% with a higher heating value of 15.68 MJ/kg before feeding. Olivine was employed as the bed material in this study. The average mean size of the olivine was between 0.4 to 0.6 mm in diameter.

3. Results and discussion

(1) Gasification Temperature Profile

At the initial state, the temperature profile within whole gasifier was almost uniform around 800-900^{o}C, but the temperatures at the freeboard decreased afterwards. However, the temperatures finally kept at constant mostly between 700-800^{o}C. The decrease in the temperatures is caused by the endothermic reactions during the gasification. Nevertheless, the temperatures in the bed region increased up to 900^{o}C.

It is suggested that the most combustion (exothermic reactions) of wood chips occurred in the bed region to provide the heat source for gasification upon the bed region. The high volatile contents of wood chips may react within the freeboard region, although the fluidized bed provides the well-mix conditions for reactions in the bed region. However, in order to enhance the gasification reaction completely, a small amount of the secondary air was injected into the freeboard. It also led to the descent of the temperature by the endothermic reactions.

(2) Syngas Quality

Tar can be defined as all organics boiling at temperatures above that of benzene, i.e. all hydrocarbons consisted in the syngas excluding gaseous ones (C1 -C6). As mentioned above, the tar should be converted or removed from the syngas before utilization for the gas engine. To investigate the possibility of tar conversion or removal, a catalytic reformer and a wet scrubber were employed.

For a test run at ER = 0.32 without any catalytic reforming, the average composition of the syngas was about 5.57 *vol.*% H_2, 15.66 *vol.*% CO, 14.97 *vol.*% CO_2, 3.95 *vol.*% CH_4 and 0.39 *vol.*% O_2. The average lower heating value of the syngas was around 3.86 MJ/Nm^3.

Operated at the higher temperatures (above 900°C) in the reformer, it is possible to convert tars in a reaction with steam into the gaseous hydrocarbons, i.e. carbon monoxide and hydrogen. The advantages of this reforming process are that the tar is converted to usable gases without formation of hazardous residues, and the syngas retains the chemically bonded energy content of the tar, and tar is converted to usable gases without formation of hazardous residues. More than 95% of the existing tar can be converted with such a reforming process. After the reformer, the tar in the raw syngas can be reduced from 10 g/m^3 to 0.5 g/m^3 below. Except removing the tar, a wet scrubbing system is installed after the reformer for separation of the solid particles from the syngas and for cooling down the syngas to the ambient temperature before entering the gas engine. For this purpose an organic scrubbing liquid must be used. However, the disadvantage is that the tar-contained liquid residues can not be re-used as the ignition oil in some special gas engines.

Fig. 1 shows the effect of the reformer temperature on the syngas composition. It can be seen that the amount of CO increases with increasing the temperature, but CH_4 shows the reverse tendency. The variation of H_2 concentration is slightly. The effect of the reformer temperature on the tar content in the syngas is shown in Fig. 2. It is obvious that the tar content decreases with increasing the operation temperature of the reformer. However, although at the higher operation temperature (>900^{o}C), a small amount of syngas would be burned for proving the heat source to heating the reformer, the heating value of the syngas after the reformer could reach 4.41 MJ/Nm^3, which is higher than that without catalytic reforming.

For power generation using the syngas produced shown above, the gas engine was in operation around 45 minutes with an electricity output of 13 kWe (around 8 kWe from the syngas and 5 kWe from the ignition oil) for the first 20 minutes, and with an electricity output of 20 kWe (around 15 kWe from the syngas and 5 kWe from the ignition oil) for the last 25 minutes. The maximum electricity output of the engine is 30 kWe.

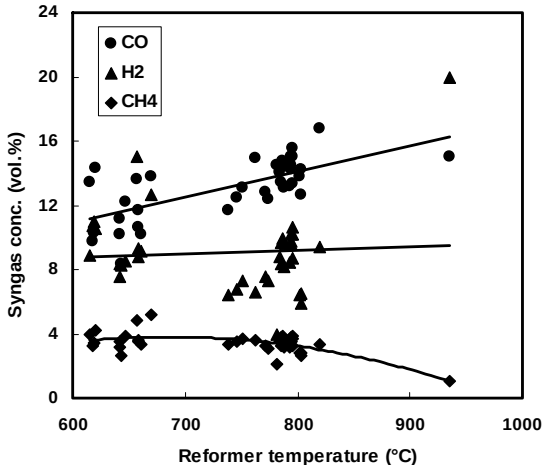

Fig. 1 Effect of the reformer temperature on the syngas composition.

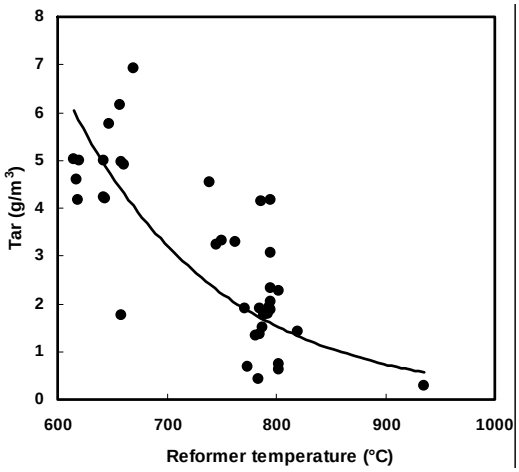

Fig. 2 Effect of the reformer temperature on the tar content in the syngas.

4. Conclusions

The gasification of the wood chips has been carried out in a 40 cm I.D. bubbling fluidized bed gasification system. A catalytic reformer and a wet scrubber are employed to investigate the possibility of tar conversion or removal in the syngas for power generation. The results show that the tar can be converted into the gaseous by the catalytic reformer effectively. The tar content decreased with increasing the reformer temperature obviously. The amount of CO increased with increasing the reformer temperature, but CH_4 showed the reverse tendency. The heating value of the syngas after the reformer was higher than that without catalytic reforming. The electricity output can reach around 15 kWe by the syngas form a 30 kWe gas engine. The power by gasification of biomass is feasible.

5. Acknowledgements

The authors K.-T. Wu and H. T. Lee acknowledge financial support provided by the Bureau of Energy, MOEA, R.O.C. Special thanks are due to the German Arbeitsgemeinschaft industrieller Forschungsvereinigungen (AiF) “Otto-von-Guericke” for supporting the research project “Fuel gas treatment for the energetic utilization of scrap wood using bubbling fluidized bed gasification” at Fraunhofer Institute for Factory Operation and Automation (IFF).

Removal of Heavy Metal Ions from Aqueous Solutions by Thermally Modified Bamboo Waste

Fu-Lan Hsu[1], Gwo-Shyong Hwang[1], and Hong-Lin Lee[2]

[1] Division of Forest Chemistry, Taiwan Forestry Research Institute

[2]Graduate Institute of Bioresources, National Pingtung University of Science and Technology

Abstract: The heavy metal removal efficiency of *Phyllostachys pubescens* was greatly influenced by thermal treatment. After exposed to 200, 250, 300, 350, 400, 500, 600, 700, 800, 900, or 1000℃ for 60 min, thermally modified *P. pubescens* waste exhibited 3 different stages of heavy metal removal efficiency. First, the heavy metal removal ability increased as the heating temperature increased, and reached to maximum at 300℃. Cu (II), Pb (II), Cd (II), and Ni (II)-removal efficiencies were greatly improved as compared to the untreated controls from 18.23, 47.76, 35.80 and 12.96 to 72.09, 92.72, 82.46 and 57.78%, respectively. Secondly, metal removal ability of *P. pubescens* was significantly decreased at around 400℃. Its metal removal efficiencies decreased to 10.03, 30.67, 8.55 and 0.66% for Cu (II), Pb (II), Cd (II), and Ni (II), respectively, showing less efficiency than the untreated controls. Thirdly, the heavy metal removal ability of treated bamboo increased again as heated from 500 to 1000℃. By thermal modification, *P. pubescens* waste not only can remove toxic heavy metals, but also can release essential elements suck as K (I), Ca (II), Mg (II), and Na (I). It is potential for thermally modified *P. pubescens* as a boiabsorbent because of its efficiency and safety.

1. Introduction

Heavy metals, which are not biodegradable and are readily accumulated in living tissues, cause a variety of diseases and disorders (Walker *et al*., 2001). Conventional methods for removing heavy metals from industrial effluents are too expensive and not suitable for treating large volume of wastewater with low heavy metal concentration. Cost-effective alternative technologies for treating heavy metal-contaminated wastes are needed (Seco *et al*., 1999; Chu and Hashim, 2000). Inexpensive biological materials such as algae (Holan *et al*., 1993), sawdust (Dikshit, 1989), exhausted tea, exhausted coffee and bark (Masri *et al*., 1974; Randall *et al*., 1974) have been recognized to possess the potential efficiency to adsorb heavy metals. Bamboo, a cheap and rapidly renewable lignocellulosic material, is abundant in Taiwan. The purpose of this research is to evaluate the heavy metal removal efficiency of thermally modified bamboo (*P. pubescens*) waste.

2. Methods

Bamboo specimens, *P. pubescens*, were collected, chipped, sieved and then were transferred into an oven at 200, 250, 300, 350, 400, 500, 600, 700, 800, 900, or 1000℃ for 60 min. Standard metal ion solutions of copper [Cu (II)], lead [Pb (II)], cadmium [Cd (II)], nickel [Ni (II)], and 23-element-mixture (Ag, Al, Ba, Bi, Ca, Cd, Co, Cr, Cu, Fe, Ga, In, K, Li, Mg, Mn, Na, Ni, Pb, Sr, Tl, Y, and Zn) were purchased from Merck (Darmstadt, Germany) and diluted to 10 ppm prior to the metal removal test. To evaluate heavy metal ion removal ability of thermally modified *P. pubescens*, 0.4 grams of treated and untreated specimens were mixed with 20 mL for each of 10 ppm metal solutions. After thoroughly mixing, metal ion concentrations in the filtrate were determined by inductively coupled plasma atomic emission spectroscopy (ICP-AES, Spectro Ciros 120, Kleve, Germany) and the removal efficiency was calculated according to the following equations (Yang et al. 2005).

Removal efficiency (%) = (Cb-Ca) ÷ Cb × 100, where Cb and Ca are the concentrations of metal ions before and after adsorption (mg L^{-1}).

In order to evaluate the metals released from thermally modified *P. pubescens* wastes, 1 gram of treated specimen was immersed in 20 mL of distilled water for one day. After thoroughly mixing, metal ion concentrations in the filtrate were also determined by ICP-AES.

3. Results

Results of effect of thermal modification on metal-removal ability of *P. pubescens* wastes were shown in Fig. 1.(A) revealed that as the heating temperature increased to 300℃, the heavy metal removal ability increased. This may be ascribed to the less-adsorptive-portions of bamboo, cellulose and hemicellulose, have been gradually removed during the heating process. In the meantime, the-most-adsorptive-portion, lignin, was exposed and contributed to improve the heavy metal adsorption ability. At around 400℃, metal removal ability of *P. pubescens* was significantly decreased resulting from the loss of most metal removal functional groups. As the temperature increased from 500 to 1000℃, the heavy metal removal ability of treated bamboo increased again. Apparently, the metal removal mechanism of 500 to 1000℃ modified *P. pubescens* was mainly dependent on the physical property, such as the increment of interior mini pores and contact surface, rather than the chemical property. Fig. 1(B) showed that effect of thermal modification on metal-removal ability of *P. pubescens* wastes from mixed aqueous solutions exhibited almost the same tendency as from the individual aqueous solutions. Whereas, the 250-350℃ treated *P. pubescens* wastes lost Cd (II) and Ni (II) removal ability in mixed aqueous solutions. Results from Table 1 showed that thermally modified *P. pubescens* wastes released large amount of K and trace amount of Ca, Mg, and Na. The 900℃-treated *P. pubescens* released more metals than the 500℃-treated *P. pubescens*. Metal released from thermally modified *P. pubescens* wastes decreased as leaching test increased.

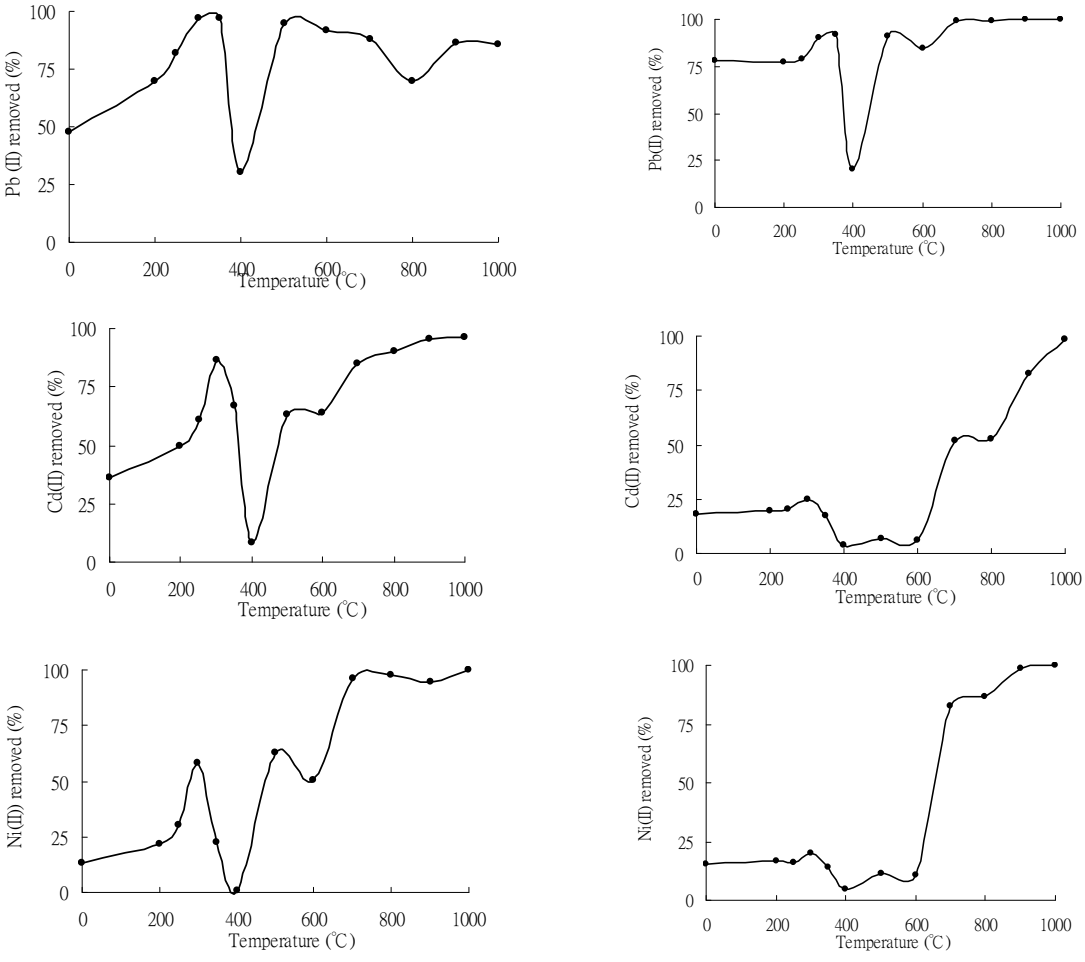

（A）from individual aqueous solutions （B）from mixed aqueous solutions.

Fig. 1 Effects of thermal modification on metal-removal ability of *Phyllostachys pubescens* wastes.

Table 1 Metals (ppm) released from the 500 and 900℃ thermally modified *Phyllostachys pubescens* wastes.

	500℃				900℃			
	K	Ca	Mg	Na	K	Ca	Mg	Na
1st leaching	60.91	0.84	1.15	0.58	143.06	2.07	0.87	1.03
2nd leaching	22.50	0.00	0.00	0.45	31.70	2.03	0.53	0.60
3rd leaching	6.19	0.00	0.00	0.45	6.28	0.73	0.05	0.50
4th leaching	5.41	0.00	0.00	0.45	6.76	0.86	0.03	0.59

4. Conclusion

By thermal modification, the heavy metal removal efficiency of *P. pubescens* can be greatly increased. At below 300℃, *P. pubescens* remained its chemical metal removal ability, and was easily saturated in mixed aqueous solutions, especially for Cd (II) and Ni (II). Thermal treatment at 400℃ should be avoided since *P. pubescens* lost its heavy metal removal ability. By increasing the heating temperature from 500 to 1000℃, *P. pubescens* re-gained its metal removal ability, and it was not easy to be saturated in mixed aqueous solutions. Besides, thermally modified *P. pubescens* released essential elements suck as K (I), Ca (II), Mg (II), and Na (I). Apparently, thermally modified *P. pubescens* possess potential as a boiabsorbent because of its metal removal efficiency and safety.

5. References

(1) Chu K. H. and M. A. Hashim. 2000. Adsorption of copper(II) and ETDA-chelated copper(II) onto granular activated carbons. J ChemTechnol Biotechnol 75:1054-1060.

(2) Dikshit V. P. 1989. Removal of chromium (VI) by adsorption using saw-dust. Nat Acad Sci Lett 12:419-421.

(3) Holan Z. R., B. Volesky and I. Prasetyo. 1993. Biosorption of cadmium by biomass of marine algae. Biotechnol Bioeng 41:819-825.

(4) Masri M. S., F. W. Reuter and M. Friedman. 1974. Binding of metal cations by natural substances. J Appl Polym Sci 18:675-681.

(5) Seco A., C. Gabaldon, P. Marzal and A. Aucejo. 1999. Effect of pH, cation concentration and sorbent concentration on cadmium and copper removal by a granular activated carbon. J Chem Technol Biotechnol 74:911-918.

(6) Walker C. H., S. P. Hopkin, R. M. Sibly and D. B. Peakall. 2001. Principles of ecotoxicology (2nd ed). London: Taylor and Francis. p 3-22.

(7) Yang T. C., C. F. Li, S. S. Chou and C. C. Chou. 2005. Adsorption of metal cations by water-soluble N-alkylated disaccharide chitosan derivatives. J Appl Polym Sci 98:564-570.

Mosquito Larvicidal Activities of Extractives from Different Plant Parts of *Cryptomeria Japonica*

Sen-Sung Cheng[1], Hui-Jing Gu[2] and Shang-Tzen Chang[2]

[1] The Experimental Forest, National Taiwan University.

[2] School of Forestry and Resource Conservation, National Taiwan University.

1. Introduction

Mosquitoes are responsible for the spread of more diseases than any other group of arthropods. The incidence of dengue, one of the mosquito-transmitted diseases, has increased tremendously in recent years. *Aedes aegypti* and *Aedes albopictus* are two main species of mosquitoes responsible for dengue fever in Taiwan. In recent years, dengue fever has increased significantly in Taiwan resulting in significant research interest in mosquito control, especially through the use of compounds from plants. The Japanese cedar (*Cryptomeria japonica* D. Don) is well known in Taiwan as an important plantation tree species because of its durability for exterior construction and its beautiful yellowish-red heartwood color. Due to its industrial importance, its constituents have been investigated in numerous studies. Besides its good quality, *C. japonica* also showed great biological activities, including antifungal, antibacterial, antitermiticidal, antimite and anti-inflammatory activities from many researchers. The aim of this study, mosquito larvicidal activities of extractives from different plant parts of *C. japonica* against *A. aegypti* and *A. albopictus* were investigated.

2. Experimental

Leaf, wood and bark from a 43-year-old Japanese cedar tree (*Cryptomeria japonica* D. Don) were collected in February 2005 at the Experimental Forest of National Taiwan University located in Nantou County in Central Taiwan. The essential oils of different plant parts of *C. japonica* were subjected to water distillation in a Clevenger-type apparatus for 6 h. The contents of the essential oils were determined and their chemical compositions were analyzed by GC and GC-MS. In addition, wood, bark and leaf chips of *C. japonica* were prepared from freshly cut trees and soaked in ethanol at ambient temperature. The plant extracts were evaporated to dryness in a rotary vacuum evaporator. The ethanolic extract (EtOH extract) of wood was separated into *n*-hexane (Hex.), ethyl acetate (EtOAc), *n*-butanol (BuOH) and water-soluble fractions for subsequent bioassay by liquid-liquid partitions.

The concentration of dimethyl sulfoxide (DMSO) used as solvent control in the assay was 1%. Extractives at the concentrations of 400, 200, 100, 50 and 25 μg/mL were tested and each compound was tested at 100, 50, 25 and 12.5 μg/mL. Controls were also used for each assay, which involved treating larvae with water or with 1% DMSO in water. Ten larvae of fourth-instar were placed in a 30-mL disposable plastic cup containing 20 mL distilled water and exposed to different concentrations of extracts and each compound for 24 h. Mortality was recorded after 24 h of exposure and the larvae were starved within this period. The percentage of mortality was corrected for control mortality using Abbott's formula and the results were plotted on log/probability paper using the method of Finney. Toxicity and effect were reported as LC_{50} and LC_{90}, representing the concentrations in μg/mL with 50 and 90% larvae mortality rate in 24 h, respectively. Four replications for each treatment were performed.

3. Results and discussion

Among three essential oils and three ethanolic extracts from *C. japonica*, leaf essential oil from *C. japonica* exhibited the most effectiveness against both *A. aegypti* and *A. albopictus* larvae at 24 h with an LC_{50} value of 59.6 μg/mL and 42.7 μg/mL, respectively (Fig. 1), followed by wood ethanolic extract. From the results of GC and GC-MS analyses, β-elemol (20.48%) and 16-kaurene (20.23%) were the dominant constituents of leaf essential oil. In addition, the 15 constituents of *C. japonica* were also tested individually against the two mosquito larvae (Table 2). Among them, α-terpinene (LC_{50} = 14.7 μg/mL) exhibits the best larvicidal effect

against *A. aegypti* and limonene (LC_{50} = 15.0 μg/mL) shows an excellent inhibitory action against *A. albopictus* larvae. These results revealed that the leaf essential oil and its effective constituents might be considered as a potent source for the production of fine natural larvicides.

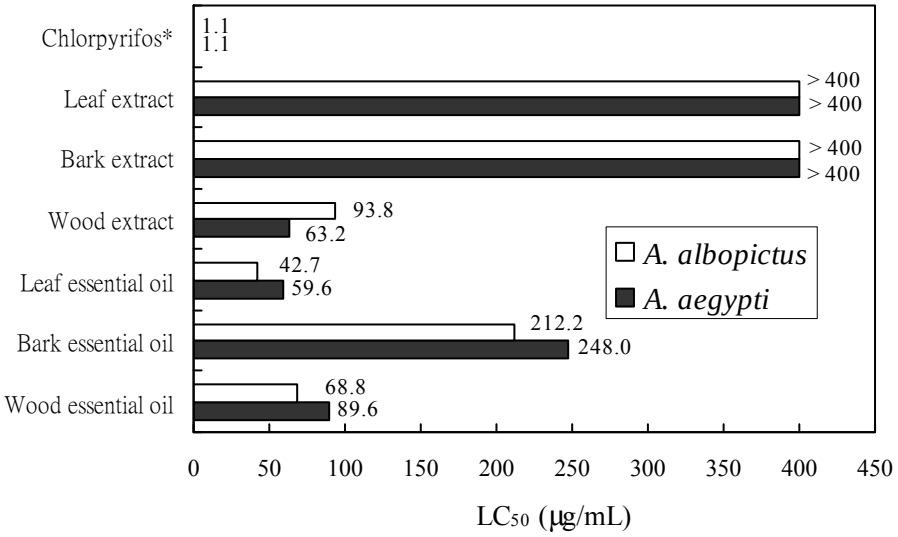

Fig. 1 50% of lethal concentrations (LC_{50}) of extractives from different plant parts of *C. japonica* against fourth instar larvae of *A. aegypti* and *A. albopictus* after 24 h test.

* Positive control

Table 2 LC_{50} and LC_{90} values (μg/mL) of fifteen constituents of leaf essential oil from *C. japonica* against *A. aegypti* larvae and *A. albopictus* larvae after 24 h test.

Compounds	*A. aegypti*		*A. albopictus*	
	LC_{50}	LC_{90}	LC_{50}	LC_{90}
α-Pinene	79.1	> 100.0	74.0	> 100.0
3-Carene	25.3	69.4	24.1	62.3
β-Myrcene	35.8	> 100.0	27.0	75.4
Limonene	19.4	50.4	15.0	34.0
α-Terpinene	14.7	39.5	25.2	53.2
γ-Terpinene	26.8	68.7	22.8	57.4
(-)-Terpinen-4-ol	> 100.0	> 100.0	> 100.0	> 100.0
Terpinolene	32.1	83.6	22.0	55.5
β-Eudesmol	> 100.0	> 100.0	> 100.0	> 100.0
β-Elemol	> 100.0	> 100.0	> 100.0	> 100.0
16-Kaurene	57.0	95.0	56.5	92.5
Ferruginol	> 100.0	> 100.0	> 100.0	> 100.0
epi-Cubebol	77.5	> 100.0	63.8	96.3
Cubebol	60.1	> 100.0	50.0	90.6
Isopimarol	> 100.0	> 100.0	> 100.0	> 100.0
Chlorpyrifos*	1.3	3.4	1.1	2.3

* Positive control.

The Role of Reactive Oxygen Species (ROS) Free Radicals in Boards Made from Laccase-treated Bamboo Powders

Chun-De Jin

Department of Wood Science and Technology, Zhejiang Forestry University, Hangzhou

Abstract: The reactive oxygen species (ROS) free radicals produced from laccase-treated bamboo was analyzed by electron spin resonance (ESR). The wet-process bamboo particleboards were made from the laccase-treated powder by hot pressing and board properties were analyzed with the methods in the national standard. By single factor experiment, the relationship between the ROS free radicals and the board properties is researched. It is found that the concentration of ROS free radicals produced with laccase is closely to the properties of bamboo powder board. The ROS free radicals produced in the laccase-bamboo catalyzed oxidation reaction play an important role in the board strength. By measurement of the ROS free radical in the reaction system: pure sample main chemical components and pure laccase, it is proved that laccase help the degradation of lignin to produce ROS free radicals and can't catalyze oxidation of cellulose and hemicelluloses.

1. Introduction

Moso bamboo is one of the worldwide most important bamboo species and China has 90% of the world's total moso bamboo area. Because of its rapid growth rate, excellent specific strength, easy machinability and resource richness, it is used widely as a raw material for furniture, construction, handicrafts, and pulp. The traditional method of using urea-formaldehyde resin adhesive or phenolic-formaldehyde resin adhesive to produce wood-based panel will bring the formaldehyde and phenol gas. So it is important to research a new way to make wood-based panel. In this paper, we use the method of laccase treatment to make bamboo particleboard. The effects of free radical in the chemical reactive on the board strength and the source of ROS free radical generated in the wood-laccase treatment system are studied.

2. Materials and methods

(1) Materials

Aspergillus laccase was bought from Novozyme China Investment Co., Ltd, Denmark. Enzyme activity was measured in units (U). The enzyme preparation had an activity of 362.8 U/ml. Moso bamboo particles were supplied by Hangzhou Baifu Bamboo Flooring Limited Company. The Bamboo particles moisture content was 8.4%. Bamboo particle was milled to powder. The bamboo milled wood lignin (MWL), xylan, filter paper and pure cotton were prepared. For the isolation of bamboo MWL the samples were extracted with acetone, dried and ball-milled according to Bjorkman. Xylan from beech wood was purchased from Sigma–Aldrich Inc (Shanghai, China). Filter paper and pure cotton were purchased from China. The spin trap N-benzylidene-tert-butylamine N-oxide (PBN) was purchased from Sigma–Aldrich Inc (Beijing, China). The ABTS was supplied by Sigma–Aldrich Inc. (Beijing, China). All other reagents were purchased from China and were analytical grade.

(2) Methods

A. Bamboo particleboards making and testing

Bamboo powder was suspended in 0.2M disodium hydrogen phosphate citric acid buffer. The suspension was vortically mixed up and then incubated by water bath heating for a certain period. The water contained in the bamboo powder firstly was extruded by paving and shaping in a mold on a filter screen. Then wet-process particleboards (dimension size 20cm×20cm ×10mm) with a target density of 0.70g/cm^3 were made from the laccase-treated powder by hot pressing under the following conditions: 3.0MPa of pressure, 200℃ of temperature and 140℃ of mat core temperature. The boards were tested for IB, MOR and TS by the methods in Chinese state standard GB/T 17657-1999.

B. Laccase treatment for ESR and ROS measurement

0.045g bamboo powder was suspended in 400μl 0.2M disodium hydrogen phosphate–citric acid buffer. 40mM PBN solution and laccase was added. The suspension with a total volume of 500 μl was vortically mixed up and then incubated by water bath heating for a certain period. 300μl ethyl acetate was added to the reaction mixture, shaken for 1 min, and centrifuged at 10 000g for 4 min. The organic solvent layer was withdrawn into a quartz tube with 2.5 mm diameter for determination of ROS on an ESR spectrometer. The experimental factors and levels are shown in Table 1. For the single factor experiment, it was designed as by respectively fixing 4 factors' level and changing the levels of the other fifth factor. Each experiment was repeated for 3 times.45g of bamboo MWL, xylan, filter paper and pure cotton were used to instead the bamboo powder by laccase treatment. Laccase dosage is 3×10^{-3}U/g and the other treatment conditions keep invariant. ESR measurements were performed on a spectrometer (200DSRC; Brucker Instruments, Germany) at room temperature. The PBN–ROS complex in the organic solvent layer was measured in a 2.5mm internal diameter quartz tube at 25℃. During measurement the effective volume for sampling organic solvent was 60μl.The conditions for ESR detection were as follows: X-band; 100 kHz modulation with 3.2 G amplitude; microwave power, 20mW; central magnetic field 3 385 G, scan width 400 G, time constant 0.3s, and scan time 4 min. The whole height of triplet hyperfine structure, namely the three peaks in each ESR signal, was taken as the concentration of ROS free radicals (c). Each test has at least three replications.

Table 1 Experimental factors and levels.

Factors	Levels				
	1	2	3	4	5
Laccase dosage (u/g)	0	10	20	30	40
pH value	3	4	5	6	7
Incubation time (h)	0.5	1	2	3	4
Incubation temperature (℃)	40	50	60	70	80
Cu^{2+} concentration (mM)	0	10	20	30	40

U/g means the amount of laccase activity (u) designed for per g dry substance.

3. Results and discussion

(1) Effects of ROS free radicals on the strength (IB, MOR and TS) of boards

Fig. 1~3 shows the relations between the properties of bamboo particleboards and the ROS free radical levels. The concentration of ROS free radials and IB or MOR is logarithmic function relationship. The concentration of ROS free radials and TS is hyperbola function relationship. The correlation indexes are all above 0.88. ANOVA analysis indicates there is significant difference between ROS concentration values of bamboo powder treated by laccase and the properties of bamboo particleboards respectively at P=0.01. So the ROS free radicals produced in the laccase treatment has a great effect on the bonding force between bamboo powders.

Enzymatic catalyzed bonding is linked to the oxidative generation of stable radicals in lignin, and it has been suggested that the radicals can cause cross-linking or loosening of the lignin structure. Laccase catalyzes a one-electron oxidation of phenolic hydroxyl groups while reducing oxygen, yielding phenoxy radicals and water. In the course of chemical reaction, the ROS free radicals were produced. The probability to occur the reaction between bamboo powders increase because more ROS free radicals produced bring more phenolic hydroxyl groups. The polycondensation from bamboo chemical components by laccase oxidation will happen and give the bonding force between bamboo powders. Enhance the IB and MOR of boards increase with the ROS free radicals. Hydrophilic group on the surface of bamboo powders decrease when the amount of ROS free radicals increases, so TS of the bamboo particleboards decrease.

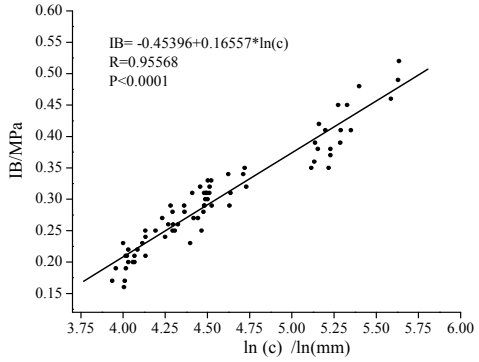

Fig.1 Relation between concentration of ROS free radicals and IB of the boards.

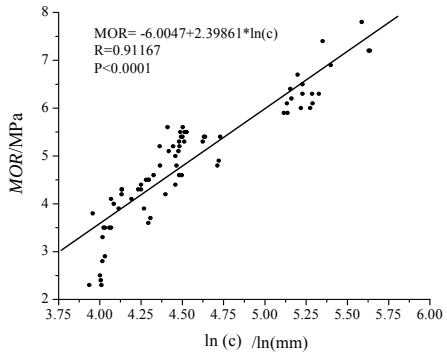

Fig.2 Relation between concentration of ROS free radicals and MOR of the board.

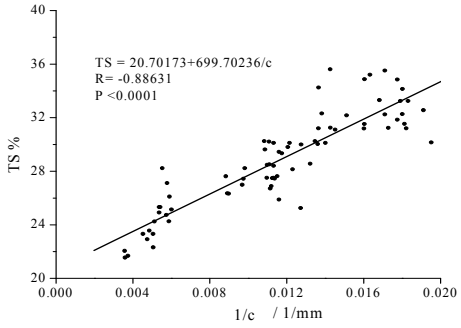

Fig.3 Relation between concentration of ROS free radicals and TS of the boards.

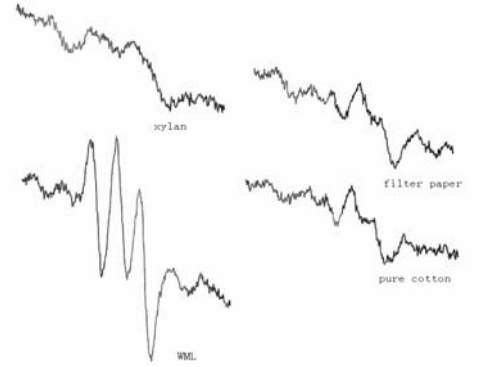

Fig.4 ESR signal of the three main chemical composition of bamboo treated by laccase.

(2) Measurement of the ROS level in pure samples of various main components

To improve the speculation and give the direct evidence, bamboo milled wood lignin (Lignin), filter paper or pure cotton (Cellulose) and xylan (Hemicelluloses) are treated by laccase and detected the free radicals produced from each of the three main chemical compositions by ESR. The results are showed in Fig. 4. It is found that only when lignin reacted with laccase can produce ROS free radicals while cellulose and hemicelluloses can't produce ROS free radicals. It is firstly proved by ESR that the ROS free radicals produced were produced from lignin. That means that laccase only reacted with lignin to produce ROS free radicals and that laccase can not react with cellulose or hemicelluloses to produce ROS free radicals.

4. Conclusions

It is firstly proved by ESR that the ROS free radicals produced in the laccase-treated bamboo were only produced from lignin. Laccase treatment helps the degradation of lignin to produce ROS free radicals and can't catalyze oxidation of cellulose and hemicelluloses. The more ROS free radicals produced in the laccase treatment system, the greater the strength of boards made by laccase-treated bamboo powders. We confirm reaction mechanism involving ROS-mediated attack on the part of lignin indirectly accessible for the enzyme and solubilized low-molecular mass lignin which functions as reactive compounds like adhesives, clinging back to the bamboo powder surface, could accordingly describe laccase-catalyzed oxidation of powder surface.

5. References

(1) Bjorkman A. Studies on freely divided wood. Part 1. Extraction of lignin with neutral solvents. Svensk Papperstid. 59, p.477-485(1956).
(2) CAO YL, GUO P, XU YC, et al. Simultaneous detection of NO and ROS by ESR in biological systems. Methods in Enzymology 39, p.387-394(2005).
(3) Capani F, Aguirre F, Loidl CF, et al. Farach BH, Pecci-Saavedra J. Changes in reactive oxygen species (ROS) production in rat brain during global perinatal asphyxia: an ESR study. Brain Research 914, p.204-207 (2001).
(4) Felby C, Lars SP, Nielsen BR. Enhanced auto adhesion of wood fibers using phenol oxidases. Holzforsehung 51, p.281-286(1997b).
(5) Viikari L, et al. (1998) World patent. WO 98/31763(1998).
(6) Yamaguchi H., Maeda Y., Sakata I. Bonding among woody fibers by use of enzymatic phenol dehydrogenative polymerization. Mokuzai Gakkaishi 40, p.185–190(1994).
(7) ZHOU GW, LI JN, CHEN YS, et al. Determination of reactive oxygen species generated in laccase catalyzed oxidation of wood fibers from Chinese fir (Cunninghamia lanceolata) by electron spin resonance spectrometry. Bioresource Technology 100, p.505-508(2009).

The Study on the Key Manufacturing Technology of BOSB

Wan-Si Fu
Beijing Forestry Machinery Research Institute of the State Forestry Administration, Beijing

Abstract: This paper illustrated the necessity of developing BOSB (Bamboo Oriented Strand Board). It was found that the technology, equipment research and development of bamboo flaking, particle drying and gluing are the key manufacturing technology problems of BOSB after analysis. Moreover, it put forward the methods of solving the problems.

1. Introduction

BOSB (Bamboo Oriented Strand Board） is a new kind of composite board, being made by drying, gluing and orienting some specific bamboo strands which are flaked by special manufacture equipments. China has the biggest bamboo plantation area and is the richest country of bamboo resources and bamboo production in the world. Based on the results of research, BOSB has the better properties than OSB (Oriented Strand Board), and is helpful for development of other bamboo byproducts, which can reduce the conflict between supply and consumption of wood.

2. Analysis of difficulties in BOSB research and manufacture technology

Bamboo is special in both physiologic and physical construction, with bamboo inner knots, small diameter, thin wall and internal empty, big tapering grade, which result to the thin flake, specific shaped and easily be destroyed. So comparing with wood-based OSB, BOSB manufacturing needs more special technology and equipments. So far, the key and difficult technology in BOSB manufacturing is bamboo flaking, bamboo flakes drying, gluing technology and the corresponding equipments.

There two main difficulties in oriental flaking and equipments. One is how to exactly locate and clamp the bamboo strand to avoid the loosening, scattering during flaking after the bamboo oriented arrangement put into the BOSB flaker. The other is how to minimize the probability of the breaking of bamboo flakes during flaking. This phenomenon is the result of some low inner linking strength between single fiber, which is very vulnerable to the impact and crossing interaction.

The main difficulties techniques and equipments of bamboo in flakes drying and gluing are: BOSB bamboo flakes are long, thin and the shape is specific, which together results in breaking, stress, combustion and even explosion during bamboo flakes drying. During gluing, the adhesive can not be spreaded uniformly; all mentioned above badly affect BOSB production and products quality.

3. Discussion the solution of key manufacturing technology of BOSB

(1) Bamboo flaking technology

A. Methods and principle of bamboo flaking

During the processing of BOSB, bamboo should be cut radially, so that the influence of the outer of bamboo on gluing will be minimal and manufacture can be conducted automatically. As Fig. 1 shows, bamboo is rifted cut, and then be removed bamboo knot, arranged and at last lapped one layer by layer. Flaking direction should be radial or approximately radial in order to gain some specific bamboo flakes. With the aim of producing bamboo flakes suitable for BOSB, raw bamboo should be cut into some specific length and then be slit, primarily cut the inner knots to make the bamboo pieces（Fig. 1(a). Before being put into flakes, bamboo pieces should be piled up and clamped to specific orders and directions by special mechanical parts (Fig.1 (b)).

The flaking efficiency should be improved as much as possible on condition of the good bamboo flakes, the bamboo is flaked by “Rotary Cutting”, but many bamboo flakes can be gained by every flaking (Fig.2). The length of “Type A” cutting-knife (Fig. 3(a)) should be the same as that “Type B” scoring-knife (Fig.3(b))during flaking. Meanwhile, “Type A” should locate lower than” Type B” in the same axis, also they should flake the

bamboo alternately and be installed along the same axis one by another

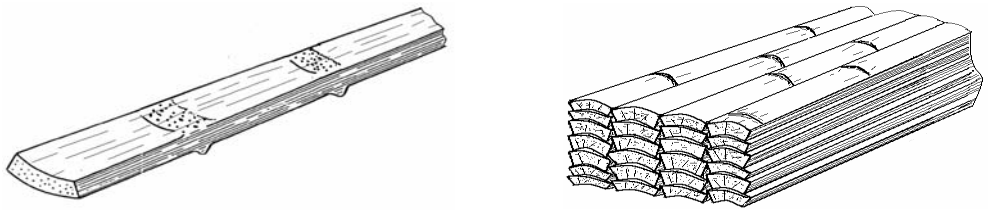

(a) The bamboo pieces without knots

(b) The specific orders and directions bamboo pieces

Fig. 1 Piling up of bamboo pieces.

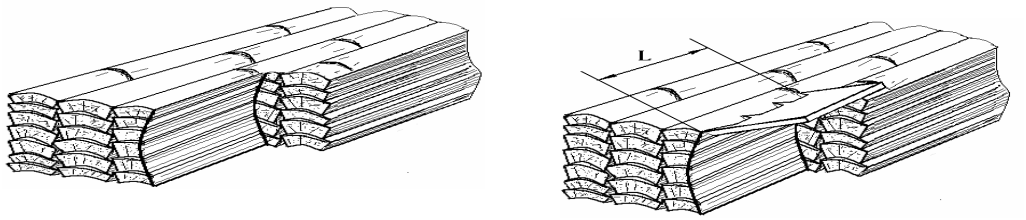

（a）Before flaking the bamboo pieces

（b）“Type B” scoring-knife flaking the bamboo pieces

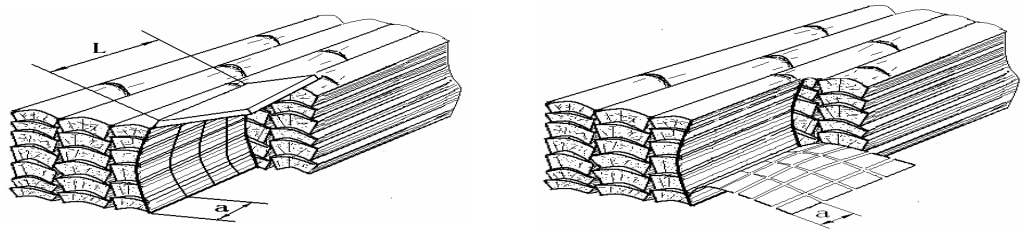

（c）“Type A” cutting-knife flaking the bamboo pieces

（d）After flaking the bamboo pieces

Fig. 2 Method of bamboo flaking.

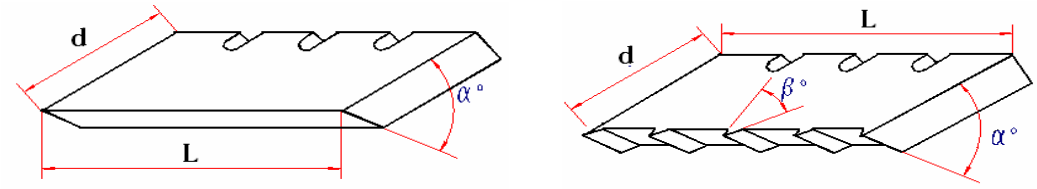

（a）Sketch map of cutting-knife (Type A)

（b）Sketch map of scoring-knife for fixed length (Type B)

Fig. 3 The two types knifes sketch map of BOSB Flaker.

B. Design of the BOSB flaker

Compared with wood, bamboo does not have inner solid, and wood has the high strength and toughness characteristics between the fibers, so it can not be used by general wood disc or drum chipper. In order to solve these problems, it could adopt the flaking principle with external ring, and bamboo pieces which have entered into the flaker are restricted by three side’s directions. BOSB flaker working principle is as Fig. 4.

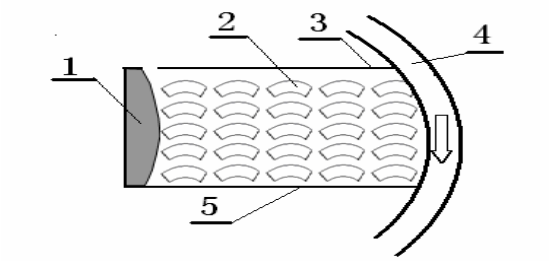

1－Arc shaped baffle;2－Bamboo pieces;3－Floating pressure plate;4－Knife ring;5－Fixed pressure plate.

Fig. 4 Processing mechanism of BOSB Flaker.

Design principles are as follows: knife ring (4) is rotating in high-speed, at the same time, knifes installed in the knives ring are flaking bamboo. In the flaking processing, floating pressure plate (3) and fixed pressure plate (5) in the knife ring make movement (4) in parallel with the movement of knife ring. Bamboo pieces (2) are pressed to knife ring (4) by arc shaped baffle (1),in order to make flake bamboo in fixed length and thickness.

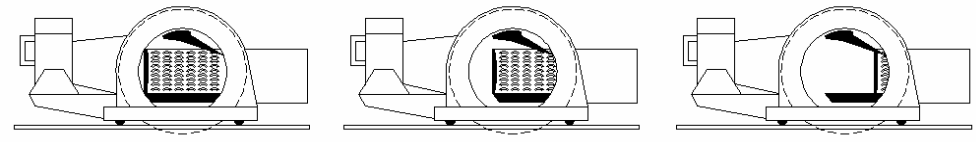

(a) The beginning of flaking (b) The middle of flaking (c) The end of flaking

Fig. 5 Sketch map of Processing of BOSB flaker.

The BOSB flaker working principle are as follows: at the beginning of flaking, the position of knife ring and bamboo pieces is as Fig. 5(a), the frame drives floating pressure plate (3) and fixed pressure plate (5) in the knife ring to make movement in parallel with the movement of knife ring pointing to the direction of bamboo pieces while knife ring (4) rotating in high-speed. The position of middle of flaking is as Fig. 5(b),when it continue to feed knife and bamboo pieces, position as Fig. 5(c),so it finishes a flaking stroke. Then knife ring (4), floating pressure plate (3) and fixed pressure plate in the knife ring (5) simultaneous return to the beginning of position as Fig. 5(a) rapidly, in order to wait for the next feeding bamboo pieces, moreover, it makes the next flaking stroke, and so back and forth.

(2) Discussion the drying equipment of BOSB flakes

As followings, drying equipment of BOSB flakes has its own features though it has common features as wood OSB: the flakes of BOSB are thinner and the shape is more specific than that of wood OSB, which makes BOSB flakes fragile more easily. So rotor drier and roller drier are used to accelerate drying rate and minimize the breaking of BOSB flakes, but the rotational speed of rotor drier and roller drier is slower rate than that of wood OSB. As BOSB flakes are thin and specific which can easily make BOSB flakes deform during drying and influence gluing and forming, the drying temperature is generally lower to avoid deformation resulting from drying stress. Length of rotor or roller of drier for BOSB flakes should be longer to avoid their influence on drying rate and processing capacity of drier processing. Anti-fire and anti-explosive control system should be installed in drying system of BOSB flakes, as BOSB flakes is more combustible compared with wood OSB flakes.

(3) Gluing equipment of BOSB and its features

Wood roller atomization glue blend machine is used in BOSB manufacture in order to improve gluing quality and manufacture efficiency as well as minimize flakes breaking. To ensure the technique available, Wood roller automatic glue blending machine must be improved technically: as the shape of BOSB flakes are quite big, the

mount of nozzle and the distance between nozzles should be both increased.

4. Conclusions

Raw material of BOSB is not only richer and cheaper, but also has lower power consumption. More importantly, BOSB manufacture technique can refers to that of wood OSB, so research and manufacture of BOSB is very necessary and available from such views as environment protection, ecology, manufacture technique and application.

The raw material of BOSB is very different from that of wood OSB in both physiological and physical construction. BOSB manufacture technique needs special flaking equipment, drying and gluing equipments for bamboo's thin wall, internal empty, inner knots, big tapering grade, and different property between the outer and inner of bamboo body.

A Study on the Bending Deflection Properties of Bamboo Particle/wood Fiber Board

Jian Han
Central South University of Forestry and Technology, Changsha

Abstract: This paper researched a kind of composition board that was made up of bamboo particle and wood fiber in proportion to 65%：35%.The bending deflection properties of this bamboo particle/wood fiber composition board in the state simply supported were investigated. The deflection function model（ω）was proposed,and the deflection function was related with load（q）,plane size of board and coordinate of any point inside board.The deflection of any point inside board had a linear relationship with the load.The bending deformation of board was symmetric,and the deflection values at both sides of board were basically equal.The calculation values of the model were agreed with the test results very well, the errors of both were changed from 1.3% to 11.7%, and the mean error was 5.87% through comparing the test results with the theoretical calculation.

1. Introduction

Study on mechanical property of wood-based composition board was payed widely attention with developing of wood-structure building.Research by Mingzhu Pan proved that the composition board produced by straw and wood fiber had better mechanical property than single straw fiber board[1].Xinjuan Xian discovered that the stretching、pressing and bending properties of composition material constituted by bamboo and resin were higher[2].To bending mechanical property of wood-based composition material,zhiliang Cheng considered when load acted on frame member,the stress at each point of frame member could be determined according to elasticity theory or model experiment.This paper will investigate generic bending properties of bamboo particle/ wood fiber composition board（abbreviating bamboo/ wood composition board）through theory calculate and experiment.

2. Properties of bamboo/wood composition board

The bamboo/wood composition board is a kind of material which is made out of residual of bamboo and wood.The bamboo particle is a kind of small stick sized 10~30mm,State of the wood fiber is mainly fiber bunch.The shape of bamboo particle and wood fiber are represented in Fig. 1.

Bamboo particle

Wood fiber

Mixture of bamboo particle and wood fiber

Fig. 1 Bamboo particle and wood fiber.

The structure of bamboo/wood composition board has some properties as follows:（1）The bamboo particle and wood fiber constitute a mixture which is uniform on macroscopy and not uniform on microscopy[4].（2）The product is a kind of orthotropic material which has different properties in perpendicular direction of the board，and has the same properties in plane direction of the board.（3）The product is a kind of lamella,due to its length and width far surpassing thickness.（4）The bending deformation of the material is a elastic deformation while

load is small[5].

3. Establishing of deflection model of bamboo/wood composition board

The bamboo/wood composition board sized 2440×1220×10~30（mm）can be treated as small deformation lamella within elastic deformation[6],and the strainedcondition of the test piece of the bamboo/wood composition board and the coordinates are shown in Fig. 2.

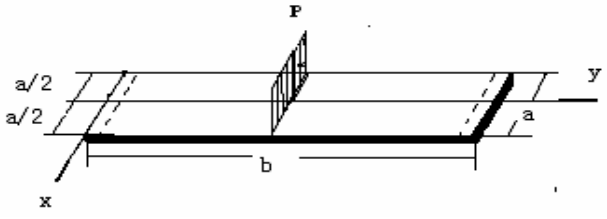

Fig. 2 The suffered force state of the test piece.

Load（P）actes vertically on central section of test piece in Fig. 2,and unit linear pressure q_0 = P/a.Test piece is simply-supported,and limit condition:y = 0、b，$\omega(x，0)=\omega(x,b)=0$。Mathematical model of bending deflection [7] is presented as fallow:

$$\omega(x,y)=\sum_{n=1}^{\infty}\varphi_n(x)\sin\frac{n\pi y}{b} \qquad (1)$$

in（1），$\varphi_n = C_1 ch(\lambda x)+C_2(\lambda x)sh(\lambda x)+C_3 sh(\lambda x)+C_4(\lambda x)ch(\lambda x)+\frac{4qb^4}{n^5\pi^5 D}$ （2）

taking（2）into（1）：

$$\omega(x,y)=\sum_{n=1}^{\infty}\left[C_1 ch(\lambda x)+C_2(\lambda x)sh(\lambda x)+C_3 sh(\lambda x)+C_4(\lambda x)ch(\lambda x)\right]\sin(\lambda y) + \frac{4qb^4}{\pi^5 D}\sum_{n=1,3,5..}^{\infty}\frac{1}{n^5}\sin(\lambda y) \qquad (3)$$

in（3） $\lambda=\frac{n\pi}{b}$， $D=\frac{Et^3}{12(1-\mu^2)}$（$E$-elastic modulus of material, μ-Poisson ratio of material, t- thickness of board）.on limit condition: x =± a/2，establishing and solving equations set,getting:

$$C_1=-\frac{\left(4+a\lambda th(\phi)\right)qb^4}{\pi^5 D n^5 ch(\phi)},\quad C_2=\frac{2qb^4}{\pi^5 D n^5 ch(\phi)},\quad C_3=C_4=0$$

taking C_1、C_2、C_3、C_4 into（3）, getting the expression of deflection functionω（x，y）：

$$\omega(x,y)=\frac{4qb^4}{\pi^5 D}\sum_{n=1\cdot3\cdot5\cdots}^{\infty}\frac{1}{n^5}\left[1-\frac{2+\phi th(\phi)}{2ch(\phi)}ch(\lambda x)+\frac{\lambda x}{2ch(\phi)}sh(\lambda x)\right]\sin\lambda y \qquad (4)$$

in(4) $\phi=\frac{a}{2}\lambda$

Equation（4）shows that deflection function（ω）is related with load（q）、plane size（a、b）and coordinates of any point inside board，and deflection function（ω）has linear relation with lateral direction load（q）.
Describing of experiment and calculation example

The bamboo used for experiment is residuum of plyllostachys pubescens,and tree species of wood fiber is pinus massomiana.The weight proportion of bamboo particle to wood fiber is 65% 35%,and the adhesive is urea-formaldehyde resin,and the amount of adhesive used is 10% based on the total amounts of bamboo particle and wood fiber dried. Main instruments:MWD-50 mechanics performance testing instrument、BY602X2/150T hot-press machin, etc. Product test follows the standard for particle board（GB/T 4897.4-2003）.Four test pieces

were made to each board,and the test pieces size is 240×45×13（mm）.10N is taked as a load unit, maximum load is 500N,and speed of loading is 0.1mm/min.The test results is given in Table 1.

Table 1 The test results of the bending deflection of the pieaces.

Load（N）		0	50	100	150	200	250	300	350	400	450	500
Deflection（mm）	Board 1	0	0.24	0.47	0.70	0.91	1.12	1.32	1.53	1.74	1.95	2.15
	Board 2	0	0.29	0.54	0.74	0.95	1.16	1.35	1.57	1.75	1.96	2.16
	Board 3	0	0.21	0.43	0.65	0.86	1.07	1.26	1.44	1.66	1.88	2.08
	Board 4	0	0.32	0.52	0.75	0.97	1.18	1.38	1.58	1.77	1.95	2.17

Taking the load as the independent variable（x）, and the deflection as the dependent variable（y），the regression analysis to the test datas is represented in Table 2.

Table 2 The regression analysis of load and bending deflection.

Test piece number	Sample amount	Regression sum of squares	Remain sum of squares	F numeral value	Related coefficient	α	Regression equation
Board 1	50	20.016	0.012	78750.62	0.999	0.01	$y = 0.059 + 0.004x$
Board 2	50	18.965	0.016	59709.66	0.999	0.01	$y = 0.057 + 0.004x$
Board 3	50	19.012	0.016	56763.74	0.999	0.01	$y = 0.045 + 0.004x$
Board 4	50	18.683	0.016	56310.87	0.999	0.01	$y = 0.083 + 0.004x$

The deflection of the test pieces is notable linear correlation with load according to regression analysis,which is in accord with the established deflection model.Taking the correlation parameters into（4）and calculating,the datas of calculation and test is represented inTable 3.

Table 3 The comparison of the theory calculation and test results .

Load（N）	50	100	150	200	250	300	350	400	450	500
Calculation deflection（mm）	0.234	0.468	0.701	0.935	1.170	1.403	1.637	1.870	2.104	2.338
Test deflection（mm）	0.265	0.490	0.710	0.923	1.133	1.330	1.530	1.740	1.940	2.150
Difference value（mm）	-0.031	-0.022	-0.009	0.012	0.037	0.073	0.107	0.13	0.154	0.188
Error（%）	-11.7	-4.5	-1.3	1.3	3.3	5.5	7.0	7.5	7.9	8.7

The absolute value of the minimum error is 1.3%,the maximum is 11.7%,and the average is 5.87% according to comparing the calculation with the test datas,which testifed that the datas of calculation and test inosculate better.

4. Conclusion

(1) The established deflection model of the bamboo/wood composition board,which relate to the load state、the plane size of the board and the plane coordinate of any poin inside board when the bending deformation of this board is among a small circle,represents the change discipline of the bending deflection of this board that is a kind of orthotropic material.

(2) The bending deflection model shows that the deflection（ω）has linear relationship with the load（q），and the regression analysis of the test results proves that the defelection of this material has remarkable linear relationship with load,too,which gives evidence of that the deflection model is correct.

(3) The absolute value of the minimum error is 1.3%，maximum is 11.7%,and average is 5.87% according to compare the calculation results with the test datas of bamboo/wood composition boad,which testify that the datas of calculation and test can inosculate better.

5. References

(1) Mingzhu Pan, Dingguo Zhou. Complex technology and performance of the Straw/wood density fibreboard[J]. Journal of Nanjing forestry university, 2006,30（2）:25~28

(2) Xingjuan Xian, F. G. Shin. Evaluation of mechanical Behaviour and application of bamboo reinforced plastic composites[J]. Advanced in mechanics, 1989,19（4）:515~519

(3) Zhiliang Cheng. Stress Analysis theory of fibre composite material component[J]. Journal of Sichuan university, 2000,32（4）:15~19

(4) Xie Z, Sheng J, Wan Z. Mechanical properties and morphology of poly propylene/polystyrene blends[J]. J Macromol Sci phys, 2001,B40(2): 251~261

(5) Yinghua Zhao, Jinzhong Wang. Damage process and elastoplastic constitutive relations of interface of composite materials[J]. Actamateriae composite sinica, 1999, 16（4）:130~135

(6) R. M. Jonth. Mechanics of composite material[M].Shanghai: science and technology publishing house, 1981

(7) Jialong Wu. Mechanics of elasticity[M]. Shanghai: Publishing house of Tongji university, 2002

Preliminary Study on Structural Bamboo Panels from Laminated Circumferential Sections

Wanli Cheng[1], Baiping Liu[1], Jie Gao[1], Guangping Han[1] and Jianbo Zhou[2]

[1]Material Science and Engineering College, Northeast Forestry University, Harbin

[2]Beijing Forestry Machinery Research Institute, Beijing

Abstract: Bamboo has been widely used in the manufacture of composites such as plywood, particleboard, and oriented strand board (OSB). The utilization rate of bamboo in plywood manufacture is only 17-25% due to the hollow structure of bamboo. This study aims at developing a new structural bamboo panel, which is made from laminated circumferential sections. The bamboo utilization rate of this new product will be significantly enhanced, targeting at 75%. Boards were manufactured by laminating glued circumferential sections in the thickness direction using a high-frequency press. The effects of adhesive type, resin loading level, and pressing condition on the physical and mechanical properties were investigated. The results showed that the properties of panels made with phenol-formaldehyde (PF) resin were slightly lower than those of panels with polymeric diisocyanato-diphenylmethane (pMDI) resin, but both results can meet the requirements of laminated veneer lumber standard. The study indicated that panels had satisfied properties when PF resin loading level was at 250 g/m^2. The optimum conditions of high-frequency pressing was as follows: specific pressure: 2.0MPa, press time: 25s/mm, plate voltage: 4200V, screen current: 1.5A.

1. Introduction

China has abundant bamboo resources, which account for the largest planting area, output and stock volume of live bamboo in the world [1]. The total bamboo production will reach to 31 million tons in 2010, which can replace wood production of 28 million m^3 [2]. The conflict between wood supply and demand has become increasingly significant. Bamboo is one of the fastest renewable plants with a maturity cycle of 3–4 years. Bamboo has excellent mechanical properties in comparison with its weight due to longitudinally aligned fibers [3, 4]. The utilization potential of this material for traditional unstructured composite panel manufacture has been explored [5, 6]. However, such superior mechanical properties have not been well drawn for structural bamboo panels. The use of bamboo in such products can help reduce the demand for wood materials and environmental impacts associated with wood harvesting. The objective of this study was to develop a new structural bamboo panel, which is made from laminated circumferential sections. The adhesive type, resin loading level, and pressing condition on the physical and mechanical properties were investigated.

2. Materials and methods

(1) Raw materials and preparation

Moso bamboo was collected from Hunan Province, China. Bamboo stems were first cut into circumferential sections with a radius of 50mm, and then treated with preservatives. After removing knots, inner and outer layers, the circumferential sections were processed into smooth surfaces. Phenol-formaldehyde (PF) resin with 45% solid content and diisocyanato-diphenylmethane (pMDI) resin were used.

(2) Board manufacture and Performance evaluation

Structural bamboo panels were fabricated by the lamination of glued circumferential sections along the thickness direction. The panels were pressed using a high-frequency press (Fig. 1). The manufacture parameters are shown in Table 1. The physical and mechanical properties of panels were tested in accordance with the state Standard of Test method of Evaluating the Properties of Wood-based Panels and Surface Decorated Wood-based Panels (GB/ T 17657-1999).

Table 1 Manufacture parameters for laminated bamboo panels made from circumferential sections.

Panel ID	Specific Pressure （MPa ）	Adhesive Types	Resin Loading Levels (g/m^2)	Pressing Time (s/mm)	High-Frequency Voltage (V)
1	2.0	PF	300	15	6300
2	2.5	PF	300	30	4200
3	3.0	PF	300	30	4200
4	2.0	PF	200	30	4200
5	2.0	PF	250	15	6300
6	2.0	PF	300	15	6300
7	2.0	pMDI	200	15	6300
8	2.0	pMDI	250	15	6300
9	2.0	pMDI	300	15	6300

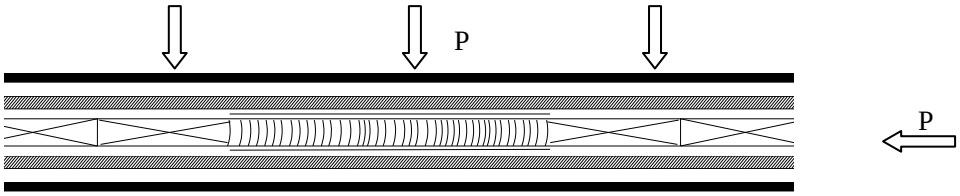

Fig. 1 The laminated bamboo panels under high-frequency press.

3. Results and discussion

(1) The effect of resin type and loading level on panel properties

The relationship between resin application rate and bending properties is shown in Fig. 2. Generally, the properties of panels made with PF resin were slightly lower than those of panels with pMDI resin, but both results can meet the requirements of laminated veneer lumber standard.

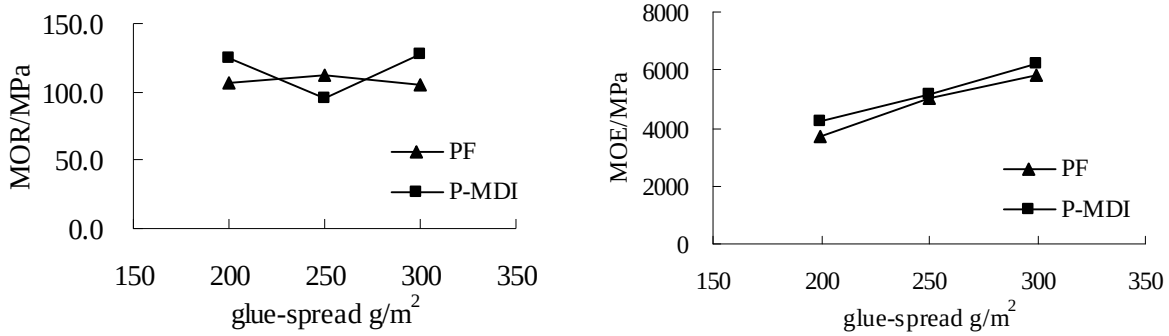

Fig. 2 The effect of resin type and loading level on bending properties of structural bamboo panels.

(2) The effect of specific pressure on panel properties

Since bamboo's density is closely relative to bamboo species, age, diameter, stalk positions, and the changes while growing [7], specific pressure has little impact on the panel density. In addition, bamboo's hardness is so high that the effect of specific pressure on panel's moisture content, thickness swelling and bonding strength is of little significance. Fig. 3 shows MOR and MOE of structural bamboo panels under various pressing pressures. The panels had the lowest bending properties under a specific pressure of 2.5MPa, while it shows similar MOR

values at 2.0MPa and 3.0MPa. Considering the energy consumption and production cost, 2.0MPa would be the premium specific pressure condition.

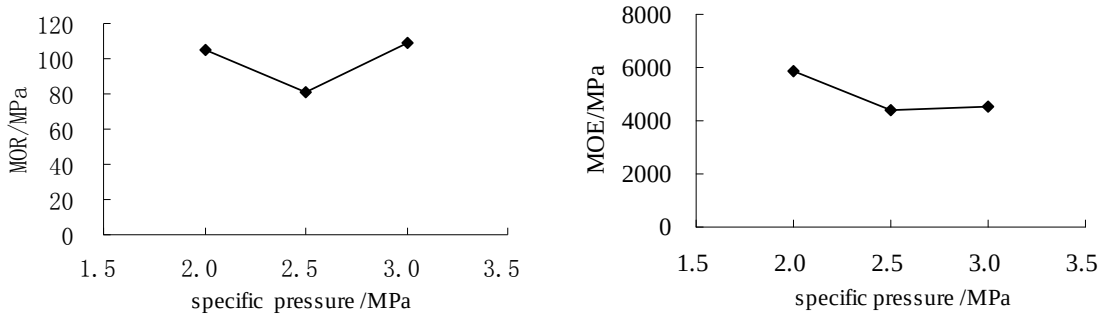

Fig. 3 The effect of specific pressure on bending properties of structural bamboo panels.

4. Conclusions

A new structural bamboo panel from laminated circumferential sections was made. The resin type, its loading level, and pressing condition on the physical and mechanical properties of the panels were investigated. It is concluded as follows:

(1) Generally, the properties of panels made with PF resin were slightly lower than those of panels with pMDI resin, but both results can meet the requirements of laminated veneer lumber standard. To reduce production cost, PF resin is more practical.

(2) The panels had satisfied properties when PF resin loading level was at 250 g/m^2.

(3) The panels showed the lowest bending properties at a pressing pressure of 2.5MPa, and similar MOR values at 2.0MPa and 3.0MPa. To reduce the energy consumption and production cost, 2.0MPa is considered as the premium specific pressure.

(4) The premium press conditions: pressing time of 30s/mm, screen voltage of 4200V, plate current of 1.5A.

5. Acknowledgements

The financial support from “the 11th 5-Year Plan” Chinese Science Support Key Project. (Grant No. 2006BAD11A16-03-01) and the Programme of Introducing Talents of Discipline to Universities (“111 Programme”) is highly acknowledged.

6. References

(1) Xie Yifa. Xie Guishui. Yao Qingqun. Present situation and outlook of bamboo resources utilization in China (2004) Chinese Journal of Tropical Agriculture 24(6): 46-52.

(2) Cheng Xiucai. Reinforcing mechanisms and application prospects of bamboo/plastic composite materials (2007) International Wood Industry 37(11): 45-47.

(3) Okubo K, Fuji T, Yamashita N (2005) JSEM Int J 48(4): 199.

(4) Kawai S, Ohmori Y, Han G, Adachi K, Takatoshi K (2001) A trial of manufacturing high-strength bamboo fiber composites. In: Symposium on utilization of agricultural and forestry residues. Nanjing, China, pp 124–129.

(5) Ma L, Kawai S, Sasaki H (1999) Mokuzai Gakkaishi 45(1): 25.

(6) Zhang M, Kawai S, Yusuf S, Imamura Y, Sasaki H (1997) Mokuzai Gakkaishi 43(4): 318.

(7) Xu Youming, Hao Peiying, Liu Qingping (2003) Advances of bamboo properties and their resources exploitation and utilization. Journal of Northeast Forestry University 31(5): 71-77.

50, 000m^3/a Continuous Rolling Thin MDF Production Line Processing Equipment

Hang Xing
DongDa Forestry Technique Equip. Co., Ltd. Harbin

1. Preface

Since 2001, the China-MDF-Productivity have kept a continuously and fast growth. By the end of 2008, the capacity is up to 30. 45 million m³/a, among them 52 continuous plat-press MDF lines, capacity in total 7.60 million m^3, 25% of the gross MDF; 46 cont-roller MDF lines, capacity 2.15 million m³, 7% of the gross. The cont-roller MDF is favored by the investors. In 2008, 21 con-roller lines were into production, 45.6% of China existing cont-roller lines. In the condition of the numerous amount of cont-roller lines in production in so short time, additionally the shortage of the related textbooks and papers, and training materials, I indeed believe that the necessary to introduce the line in system. Due to the restriction of fiberboard below 50, 000 m^3/a according to *the Guiding Objectives of Industrial Restructuring* announced by the National Development and Reform Commission, herein the 50, 000 cubic meter is as the model to introduce.

2. Raw material、accessory and heat energy

(1) Raw material

MDF is based on wood fiber as main raw material, second to acaroids stalk fiber. Materials are from small-diameter wood, thinning, bucking residues, processing residues (such as slab、core wood、waste veneer、and leftover bits and pieces), lop wood (diameter at above 5cm), the recycle old wood (such as old car plate、old house log), and etc, bark content is no less 8%.

(2) Accessory

Urea-formaldehyde resin adhesive, paraffin, ammonium chloride, ammonia.

(3) Heat energy

Saturated steam

3. Process

The dry process goes to all the China MDF plants, new erected and rebuilt. The main difference between dry and wet process lays in the different medium during fiber conveying and mats shaped, wet for water, dry air flow.

(1) Raw material preparation

This section, including chipping、storing、screening、and watering, is to offer qualified chip for thermo finer to use.

(2) Fiber preparation and glue blending sections

A. Fiber separation

Fiber preparation includes fiber separation、glue blending and paraffin applying、fiber drying and storing, so as to supply plough board preparation. Due to differences on materials and ways of fiber separation, the quality of gained fiber is widely different. The MDF is subject to the fiber quality, the full consideration should be on material species, fiber yield, and energy consumption.

B. Fiber paraffin applying and glue blending

The essence of fiber wax handling is to do the fiber waterproof, and the paraffin is the kind of waterproof agent that the most common used and in good effectiveness.

For gluing uniform and maintaining the fixed rate, a complete calculation device is set to gluing system, additionally interlocking with the conveying screw of thermo finer, so that glue impregnating into fiber blow

valve at uniform rate. The glue, impregnated into blow valve under pressure, and the fiber, simultaneously into blow valve under vapor pressure, are mixed uniformly, for the purpose of glue blending.

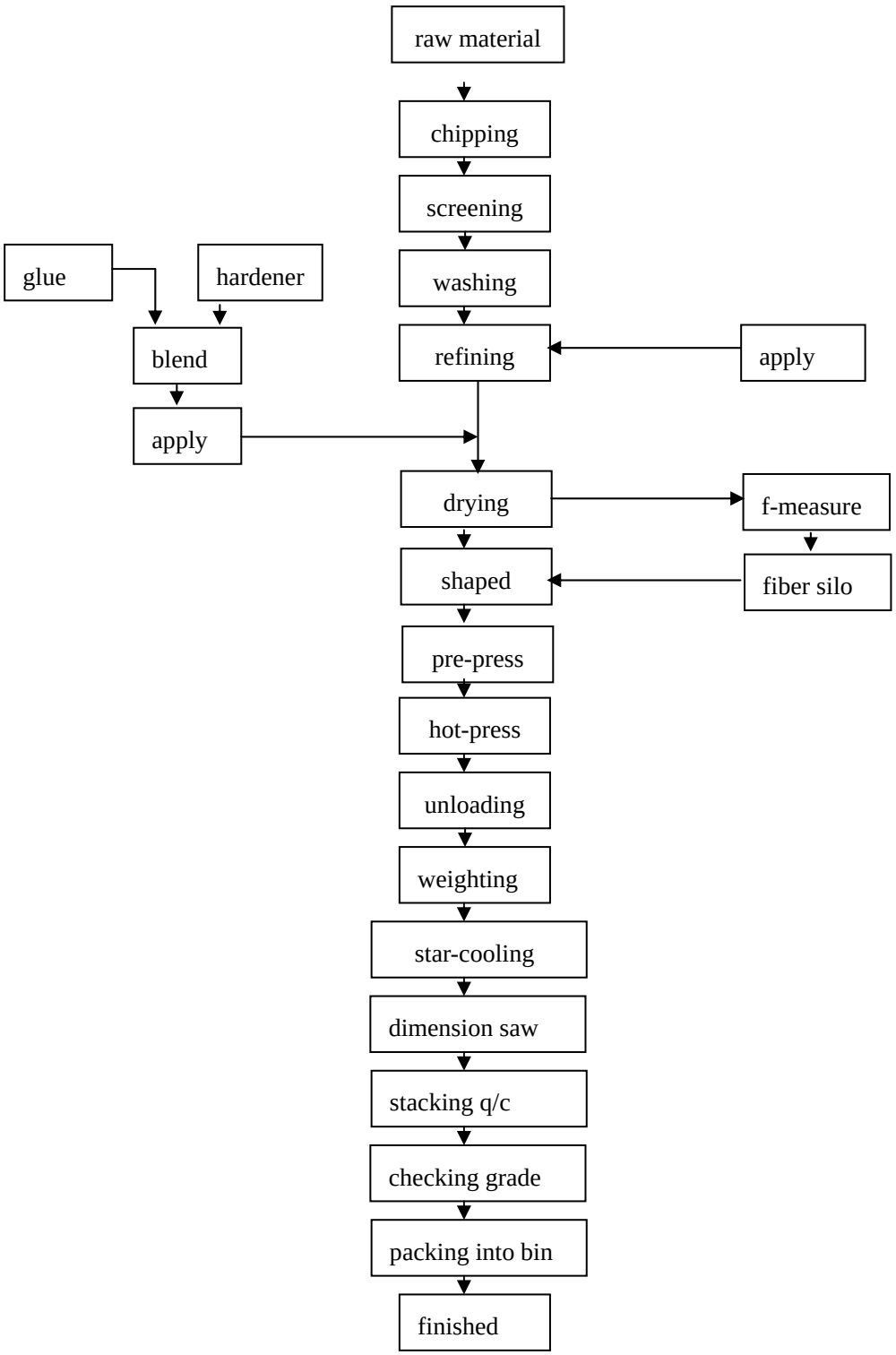

50, 000m^3 /a Cont-roller MDF line process flowchart

C. Fiber drying

The moisture content of refiner-discharged-fiber is around 50%, besides the moisture of gluing into the system, the final moisture content is more up to 60%, however, the following section requires the content to 5~10%, thus it is a must to dry in order to convey and shape.

The fiber is mixed with hot air in the dry pipe so that the fiber is dried in the suspend condition; generally speaking, the final moisture content is around 10%. In order to pretend the fire, the auto-detect device is set in the drier pipe, for the purpose of auto-fire-alarm and auto-spurring water to be out the fire.

Through the heavy cyclone separating, the dried fiber is down to screw conveyor through pipe. On the condition of emergency (fire), screw conveyor can be reversed to unload the fiber forward to waste fiber house. At last the dried fiber is conveyed into dry-fiber-silo through vapor for the use of forming shaping.

(3) Forming & hot-press section

A. Forming and pre-press

In the process of MDF production, forming of mats is in the important role. The qualified formed mats dominate the quality MDF.

The fiber, stored in the dried silo, was conveyed into mechanical former silo through the air, produced by parabolic roller. According to molding speed, the fiber-loading in the silo was adjusted. The landed fiber was formed uniformly on the wire-belt through needle roller, so the continuous mats are shaped.

The pre-pressed mats were through the process of longitudinal sawing, and by conveyor conveyed into continuous roller. The mats moisture content was detected by the moisture meter, installed on the top of the conveyor, so that the right hot-press flowchart was to be drawn up. Additionally, the metal detector and densitometer were also set on the line, in case of the density, the un-proper moisture content, or the existing metal into the conveyor but turn into the waste carrier. The good mats were continuous pressed into shape once only by the cont-roller press, and conveyed onto the star-cooler for cooling.

B. Hot-press

In the MDF line, hot-press is the most important process. In China, there are three types of hot-press, which is batch-flat-press hot press, continuous flat hot press, and cont-roller hot press (generally used as the 1.6-10mm thin MDF). The features of the last type hot-press are the complete synchronous in running speed during the processes of mats-shaped、pre-press、pre-hot、hot-press、cooling、and etc, and among them the advantages are the followings: equipment simplification; unlimited on the finished length; small damage on cross trimming; high productivity and unrelated with board thickness; tolerance only ±0.15; no sanding so the low consumption on material; low consumption on power; centered by PLC, so than guarantee the good quality on MDF and low consumption and high efficiency operation.

(4) Finished board preparation section

The rough board, out of the star-cooler, are sawed into the 4×8 sized board by longitudinal and transversal saw, then the sized board are through the processes of stacking、storing、checking、grading、and storage into warehouse.

The sawed complete board to be used as the baseboard of veneer, the sanding is necessary, generally the sanding token place after 48 hours stacking, the sanded boards are to test grade, and storing into warehouse.

4. Conclusion

The technology development of China artificial board mechanical unit on cont-roller MDF has contributed to the investors' approval since 2005, so comes to the dozens of lines. However, in China the line is still new to many people. So, herein, as the example of output 50, 000m3/a, I briefly introduce the production process as to contribute this line popular to the insiders.

The Decay Resistance Properties of *P. ussuriensis Kom* Lumber Impregnated with Preservative by Roller-compression

Yao-Xing Sun and Shi-Cheng Zhang
Department of Wood Engineering, Beihua University, Ji Lin

Abstract: *P. ussuriensis* Kom green lumbers were impregnated with the water-borne preservative of DDAC and boride by the roller-compression, whose compression rate was from 10% to 50%. With the rise of compression rate, both the penetration depth of preservative and the retention quantity of preservative of experimental mass increased while the rate of mass loss decreased. The penetration depth perpendicular to the grain was more than 3.9 mm whereas that parallel to the grain of wood was more than 10mm with compression rate of 30% and up. With compression rate of 30%, the retention quantity of preservative of mass impregnated with DDAC (thickness of 1%) was 8.743 kg/m^3 and the rate of mass loss was 14.36%; while those with boride (thickness of 2%) were 8.743 kg/m^3 and 14.36%.

1. Introduction

It is a new technique used to impregnate preservative into wood[1]. lumbers go forward between two rollers in the preservative liquid, the Dimension of lumbers reduce in the direction of compression because of compression, with the rotation of the rollers, the water and air in the wood gap was pushed out of wood, when the compressed part leave the rollers, wood may restore the original shape and size, in the wood vacuum come into being, the preservative was absorbed into the wood on account of the vacuum, the impregnated wood processing was completed[2-4]. In this study, the water-saturated *P. ussuriensis* Kom timber was processed with the impregnation-roller-compression method through two water-borne preservative (DDAC and boride) and different compression ratio. The impregnation depth、retention and mass loss ratio was measured, and the wood decay resistance levels was ascertained.

2. Materials and methods

P. ussuriensis Kom limbers with similar structure、non-section scar、straight uniform texture was selected. The standard radial and tangential limber was manufactured, the limber impregnated by dye was cut five parts for the compression ratio 10%, 20%, 30%, 40% and 50% . The limber was cut longitudinally six parts for impregnating preservative. One of them was as untreated samples, the other part of the samples were treated to impregnate preservative with the compression ratio from 10% to 50%.Test size of sample was 150mm (L)×80mm (W) × 20mm (T).The roller-compression-impregnation processing was operated at room temperature; before processing, the wood was water-saturated , after that, the specimen was dried quickly.

The two water-based preservative : DDAC, the concentration of 1%; boride, the concentration of 2%.

Dye: Acid Red GC.I 18050 MW 509. 41, the concentration of 0.3%.

Tested bacterial is [Coriolus versioolor (Fr.) Cooke].

The parameter of roller-compression machine (roller diameter is 200 mm, the roller speed is 13 r / min).

The absolute dry specimen was vertically, horizontally cut for testing the impregnation depth; the impregnation depth of red dye was measured by point in different compression ratio along the radial、the tangential and parallel to grain.

The method of making sample、test and mass loss ratio calculating was executed in accordance with the national standard "Method for laboratory test of natural decay resistance of woods (GB / T 13942. 1-92) ".
The calculation methods of the retention is the formula (1).

$$R = \frac{W_0 - W}{V} \qquad (1)$$

R-- retention, kg/m^3;
W_0-- the absolutely dry quality after impregnated by preservative, kg;
W-- the absolutely dry quality before impregnated by preservative , kg;
V-- The cubage of sample, m^3.

3. Results and discussion

The impregnation depth with different compression ratio and different compression direction

Table 1 impregnated depth of different compression direction and different compression ratio.

Compression ratio [%] (compression direction)	Impregnated depth [mm]		
	parallel to grain	radial	tangential
10% (radial)	1.1	0.9	0.5
10% (tangential)	0.9	0.6	0.8
20% (radial)	3.1	2.0	1.4
20% (tangential)	2.8	1.3	1.5
30% (radial)	11	5.5	3.9
30% (tangential)	10	4.8	5.1
40% (radial)	17	6.0	4.5
40% (tangential)	16	5.5	6.0
50% (radial)	23	8.5	7.0
50% (tangential)	24	8.0	8.1

From Table 1, for the roller-compression-impregnation treatment, the radial and tangential depth was varied by compression direction, the impregnated depth was slightly bigger in the compression direction; With the increase of compression ratio, the radial、tangential and parallel to grain depth increase, when the compression ratio was 30 percent and above, this increase is evident, particularly in the depth of parallel to grain. When the compression ratio is 10%, the depth of the radial and tangential was between 0.5and 0.9mm, the depth of parallel to grain was between 0.9 and 1.1mm; when the compression ratio is 20%, the impregnate depth of radial and tangential was between 1.3 and 2.0mm, the depth of parallel to grain was between 2.8 and 3.1mm; when the compression ratio was 30% above, the depth of radial and tangential was above 3.9 mm, the depth of parallel to grain above 10mm.

According to Chinese standards-the use of wood preservative treatment and classification requirements (LY / T 1636-2005) , when the compression ratio was above 30%, the treated wood attains the requirement of C3 .

4. Retention

The retention of *P. ussuriensis* Kom lumber in different compression ratio was Table 2.

Table 2 shows that, for two water-soluble wood preservatives of DDAC and boride, with the increase of compression ratio , the retention increased, and the retention of borides were less than that of DDAC with the same compression ratios.

According to" Use category and specification for preservative-treated wood (LY/T 1636-2005)" ,for DDAC preservatives, the treated wood with the compression ratio 10% can meet the requirements of category C3; that with the compression ratio 20% can reach requirements of category C4A, and that with the compression ratio 20% can reach the application requirements of C4B . For boride preservatives, the treated wood with the compression ratio 30% can reach the category C1.

Loss ratio

Through experimental research, the mass loss ratio of *P. ussuriensis* Kom specimens treated by rollers-compression was showed in Table 3 (the sample with the compression ratio 0 was untreated).

At the same time, according to the national standards (GB/T 13942.1-92) "Method for laboratory test of

natural decay resistance of woods ", the decay resistance grades of treated wood and untreated one was determined.

Table 2 Net dry salt retention of roller-pressure process.

Compression ratio	Retention (kg /m^3)	
(%)	DDAC	Boride
10	5.336	1.650
20	6.520	2.692
30	8.743	3.322
40	11.901	3.788
50	14.887	4.377

Table 3 Preservation grade and loss rate of *P.ussuriensis* Kom.

Compression radio	DDAC		Boride	
(%)	Loss rate (%)	Preservation grade	Loss rate (%)	Preservation grade
0	31.82	Ⅲ	32.79	Ⅲ
10	26.51	Ⅲ	20.24	Ⅱ
20	20.42	Ⅱ	17.65	Ⅱ
30	14.36	Ⅱ	9.92	Ⅰ
40	9.83	Ⅰ	9.03	Ⅰ
50	7.22	Ⅰ	6.50	Ⅰ

For DDAC preservatives, the grade of the treated wood with the compression ratio 20% and above can attain to the level of "Ⅱ", that with the compression radio 40% and above can reach the level of "Ⅰ"; for boride preservatives, that with the compression ratio10% can attain the level of "Ⅱ", and that with 30% and above can reach "Ⅰ".

5. Conclusions

The study on the preservatives impregnation depth with different compression ratio showed that with the rise of compression ratio, the preservative depth increases, in the compression direction the depth was slightly larger; when the compression ratio of 30% and above of radial and tangential compression, the radial and tangential impregnated depth was above 3.9 mm, the depth of parallel to grain was above 10mm.

The studies on the decay properties and the retention of *P. ussuriensis* Kom wood treated by rollers-compression have shown that for DDAC preservative, the treated wood with compression ratio 20% and above attains to the decay resistance level "Ⅱ", and that with the compression radio 40% and above reached the level "Ⅰ". the treated wood with compression ratio 10% can meet the requirements of C3, that with the compression ratio 20% can reach category C4A, and that with the compression ratio 40% can reach C4B . For boride preservatives, the retention with the compression ratio 30% can reach the category C1.

6. References

(1) Adachi K, Inoue M, Kanayama K，et al.Water removal of wet veneer by roller pressing[J]. Journal of Wood Science,2004,50(6):479—483.

(2) SUN Yao-xing, LIU Yi-xing and FANG Gui-zhen. Shape Variance Regularity of *P. ussuriensis* Kom Lumber Processed by Roller Compression[J].Journal of Northeast Forestry University, 2005,33(2):20—21,42.

(3) SUN Yao-xing, LIU Yi-xing.Variation of Density and Shrinkage Rate of Popular Sample Compressed by Rollers[J].China Wood Industry, 2007,21(6):13—16

(4) SUN Yao-xing, LIU Yi-xing. Research on Variance of the Mechanics Strength of *Populus ussuriensis* Lumber Compressed by Roller[J].Forestry Science and Technology,2008,33(4)：37—41

The Application of Nano-materials in Wood Preservation

Shicheng Zhang
Traffic and Construction Engineering Academy of Beihua University , Jilin

Abstract: In the field of wood protection, wood preservation has the most widely application to economize wood resources which played a key role of preventing decay and extending usage span. As inorganic modifier, the nano-materials have good performance of fire and decay resistant without toxicity. Apart from the preservation property, other good performances can be obtained when wood are combined with the nano-materials. In this paper, the nano-materials, wood inorganic composite materials as well as its application are introduced briefly.

1. Introduction

In the field of wood protection, the main preservations is cresol quality oil, which contain oil-soluble pentachlorophenol, copper naphthenate, tin organic compounds. The water-soluble preservations is adopted for the compound such as copper chrome arsenic (CCA), copper chromium boron (CCB), about tens of kinds. In tradition, these preservatives in use is effective to prevent harmful micro-organisms , yet it is bad for human and animal and the environment, so it caused more and more attention. This kind of anti-toxic and losing of preservatives will be replaced by the new, non-toxic to humans and the environment by friendly and efficient alternative preservatives. In recent years the use of nano-TiO_2, ZnO and other semiconductor photocatalytic degradation of pollutants elimination has become an active research direction. Its photocatalytic degradation to the ultimate non-toxic tasteless generated CO_2, H_2O and a number of simple inorganic substances [1]. However there are flammable timber, size stability, anisotropy, such as variability in the processing and use of a number of intractable problems. So the use of nano-materials for the manufacture of new types of modified composite wood will strengthen the wood preservative, bactericidal, fire-retardant properties, etc. At the same time it will increase the dimensional stability and the intensity.

2. Application of nano-materials

Nano-materials are that the size of the microstructure of materials is less than 100 nm and show the performance of some special materials. Due to the specificity of its structure, such as large surface area, as well as a series of new effects which contain small size effect, interface effect, quantum effect and the quantum tunneling effect, the nano-materials show difference from the unique properties of traditional materials.

In the household [2] of the gap the timber is divided into permanent and transient gap. Some researchers [3] divide into: macro-voids, micro-and mesoscopic gap by the size of the gap in the timber. Nano-mesoscopic gap or gaps exist in softwood bordered pits edge plug holes, pits a single pit membrane pores, dry or moist state of the timber wall voids, under the state-run expansion of microfibril gap, with microfibril scale for the smallest gap. Timber in the presence of nano-scale gap means that the timber itself accept nanoparticles (powder), nanotubes, nanorods and other nano-structural units of the same order of magnitude inherent in space, rather than deliberately cut.

The concept of nanocomposites is the dispersed phase size has the one-dimensional composite material 100nm. Nanocomposites is different from the conventional inorganic filler / polymer composites of materials, which is not a simple mixture between inorganic and organic, but which is complexed between them in two-phase interface between the more strong or weak hydrogen bonds or combined with Van der Waals force[4]. Therefore, the timber as a natural organic polymer materials and inorganic nano-composite materials constituting a wood-based inorganic nanocomposites with nano-materials should not only particle size effect, surface effect, such as nature, but also the rigidity of the inorganic, dimensionally stable and thermal stability and toughness of wood processing and dielectric environment, as well as the unique characteristics of the blend together, so that result a number of specific performance. Therefore nano-technology and its application in the wood science will

be concerned as one high-tech, and the wood-based inorganic nano-materials will be given the new features, at the same time wood-preserving will be brought new prospects for development.

3. Wood - inorganic composite materials (WIC)

In recent years, in order to overcome these inherent shortcomings of wood, physical, chemical or mechanical methods of processing or handling of timber are used to give more new features of the timber. Inorganic composites of wood are to strengthen the body as inorganic substances in a certain way, dispersed in the matrix of the wood as wood / inorganic composite materials. (Wood inorganic composites, WIC). As a result of the inorganic filler material can suppress the thermal decomposition of wood to prevent decay really mycelium growth and termite damage, etc, composite wood will be good anti-decay and termite resistance, dimensional stability and flame retardant, at the same time as a result timber contains a certain amount of inorganic substances, which can also increase the strength [5]. Wood and other composite materials or substances enlarge the use of their advantages, to make up for the shortcomings of each other through a variety of processing complex together well. Complex patterns at the time of the general come down to three: stratification, mixing, infiltration [6]. Among them, the timber can be maintained to maximize the performance of the infiltration of the original compound.

4. Inorganic Nanocomposite Applications

Wood / inorganic composite materials are rare earth modified preparation method, sodium silicate submerged timber, double-ion diffusion method, intercalation, sol - gel method (Sol-gel process). The sol - gel method is widely used at home and abroad in recent years, WIC infiltration method of preparation. It is of some organic compounds such as alkoxy silane precursor, such as submerged timber, and wood and their water (or add the alcohol solvent) to form a uniform solution, solute and water (alcohol) or alcohol have a hydrolysis reaction, the reaction products of sodium gathered a few meters into the particles and the composition of sol, with the hydrolysis (alcoholysis) - polycondensation reaction and curing of various sizes generated (about 100nm) and the structure of the sol particles, by dry xerogel after that inorganic composites have been of such timber. In China, Wang Xi-Cheng [7] by the sol - gel method and the method of in situ composite made of the level in the cells of the wood-based composite materials silica, and its mechanical properties, dimensional stability and flame resistant properties are improved to varying degrees.

The study found alkoxy silane in the form of wood cell wall is a selective gel, wood cells combined with the higher water content, the formation of more gel also showed the effect of dimensional stability and flame retardant the better. Studies have reported that the use of ultrasound gel processing technology to improve the timber's weight gain rate of 15% ~ 30%. Cell wall formation in the gel only a smaller weight gain rate on the dimensional stability of wood, fire-retardant and anti-termite has a great impact. Cavity formation in the cells of the silica gel is on the dimensional stability of wood, fire-retardant nature of the effect of no obvious improvement, but showed strong anti-termite properties.

With compression - decompression so that infiltration of 5% sodium silicate in the timber, and then treated wood immersed in saturated aluminum sulfate, calcium chloride solution, insoluble reaction sediments, this method can be used for preparation of silicide surgery. X-ray electron microprobe analysis form insoluble silicate deposition in the main cavity and the catheter in tracheid. Preparation of inorganic composites have good fire-retardant materials and anti-fungal properties, but the enhanced moisture absorption.

The basis of previous studies, using 5% barium chloride react with sodium silicate, sodium silicate 30% of the reaction with boric acid and borax can also be the preparation of inorganic wood composite material, these composite materials is similar to the moisture absorption and material, However, it has a better anti-expansion of capacity, although the decrease in bending strength, but not affected by the elastic modulus and excellent dimensional stability. Reaction with boric acid and borax prepared WIC also have good flame-retardant and decay resistance. With boric acid, boron trioxide prepared WIC has relatively small moisture absorption, anti-swelling and good flame resistance and decay resistance.

The use of acetic anhydride, and C, respectively, deal with the North American Liriodendron chinense anhydride (Liriodendrorit, liPiferal) Preparation of acetylated wood acylation and C after the sodium silicate solution and then dipping their processing, composite materials prepared by the timber and wood-based composite acid material. These two composite materials with acid acylation and C compared to the timber, the solution treated with sodium silicate composite material Compatibilizer rate, anti-inflation rate of wetlands and low resistance, but due to silica condensate the existence of plastic, which has a special composite material is still an excellent dimensional stability. Generated as a result of the weight of silica gel by re-rate on the flame retardant has played an important role, sodium silicate solution to deal with composite materials than the material of the oxygen index. Acetylated wood after treatment, the swelling in the wet state can be reduced by 1/3-1/2, under the water can be reduced by1/6 to 1/5, have improved dimensional stability, and timber decay and pest resistance, and strength and also improve the acoustics.

5. Wood - the modification of inorganic composite materials

Different ways of the timber - inorganic composite materials have a significant effect in the dimensional stability, flame retardance, heat resistance, decay resistance and anti-fungal properties, and so on, but on the other hand, there may be have the shortcomings which can not be ignored, so the composite materials that will be modified further. For example, TMSAH Japanese cypress (Chamaecy Parisobtuse Endl) is treated by sol - gel method and adding anti-microbial, for inorganic composite material of wood, which does well on inhibition from the brown-rot bacteria, but does not inhibit from white-rot fungi inhibition. However HFOETMOS- Composite wood added with the modifier HFOETMOS has a high hydrophobic nature which enhance the antibacterial properties of the wood on the brown-rot fungus and the white-rot fungus produced inhibition. In the view of the way that WIC is prepared from the infiltration, the sol - gel method is often used in recent years. Composite-inorganic materials of wood are made by adding flame retardant, antibacterial.

6. Conclusion

Wood-preserving traditional referred to anti-corrosion, pest control, mold, anti-chemical is dealed with timber, sheet or wood products with the way of atmospheric or pressure leaching. Wood-preserving is an important way of the conservation of forest resources and is an important part in forest-products processing industry. However, the corrosion of traditional methods only has a single effect, at the same time it may be toxic to the environment which can cause a certain degree of pollution. The timber has the ability to adapt with the nano-materials naturally, which will be applied to the wood, which not only can be achieved a good preservative effect, but also able to set the structure of wood materials, functional materials, eco-friendly materials in one timber to enhance performance, expanding its purposes.

7. References

(1) ShouXin Liu. *Regeneration of Activated Carbon-ray technology and TiO_2 - Mechanism of activated carbon synergy*: [dissertation]. Harbin: Northeast Forestry University Institute of Materials Science and Engineering, 2002.
(2) Second, households wan. *Wood structure no gap*. Materials, 1973,22:903 ~ 907.
(3) Zhao Guangjie. *Timber in the nanometer scale, nano-wood and timber - inorganic nanocomposites*. Journal of Beijing Forestry University. 2002,24 (5 / 6) 204 ~ 207.
(4) XU Guo-cai, ZHANG Li-de. Nanocomposites. Beijing: Chemical Industry Press, 2002.1 ~ 3.
(5) Chen Zhilin, Wang Qun. *Inorganic composites of wood composite technology and the performance closed*. All Materials Journal, 2003,4 (4): 128 ~ 132
(6) Li Jian, Wu Yuzhang. *Inorganic composites and composite wood based panels closed*. China's timber, 2001, (3): 5 ~ 54.
(7) Wang Xi-Cheng. *Prepared by chemical wood-based composite materials silicon dioxide*. China Building Material Science and Technology, 1998, 3 (7): 23 ~ 25.

Synthesis of A Rosin Amide and Its Inhibition to Wood Decay Fungi

Shujun Li[1], Shuangyue Li[1], Hanxi Ding[2], Jing Wang[1] and Dan Liu[1]

[1] Key laboratory of Biobased material Science and technology of Ministry of Education, Northeast Forestry University, Harbin

[2] Beijing Xinxilida Company, Beijing

Abstract: In this paper, rosin was used as raw material to prepare a wood preservitive candidate. First, rosin was modified by acryl acid with the weight ratio of 4.5:1. Then the modified rosin reacted with diethyltriamine (DETA) and a rosin amide (RA) derivative was produced at the conditions as follows: modified rosin and DETA mole ratio of 1:3.5, dimethylbenzene as water carrying agent, reaction temperature of 160-180℃, and reaction time of 8h. The chemical structure of the product as RA was identified by FTIR, EI-MS, and 1H NMR analysis. The anti fungal activity of its derivative was determined by paper-disc method with wood decay fungi such as *Trametes versicolor, Gloeophyllum trabeum, Aspergillus niger* and *Paecilomyces variotii*. The anti-fungal experiment results signified that the derivative is active to these fungi, especially *Paecilomyces variotii*. RA's surface properties were also tested. Its critical micelle concentration was 8.0×10^{-4} mol/L, surface tension was 39.161 mN/m, emulsifying ability was 1320 s, foam hight was 135mm, emulsion stabilizing ability was 125 mm. Since it is produced easily from rosin, which is renewable and not expensive, RA could be a potential wood preservative. Further study is planning.

1. Introduction

The need for wood is increasing while wood resource is declining, so wood preservation is more and more important. Generally speaking, wood treated with preservatives could last at least 5 times or even up to 10 times longer than untreated wood. Wood preservation is an important way for saving forest resource. However, many wood preservatives are toxic and could pollute the environment. This industry needs new non- or low toxic, efficient, environment friendly wood preservatives.

Rosin，which comes from softwood, is an important raw material for chemical industry. With turpentine, it exists as oleoresin in the resin canals of certain conifers, especially pine. When the tree is wounded, the oleoresin is secreted as a viscous fluid to protect the wound from insect/fungous attack. After a few days, the viscous fluid solidified because turpetine is volatile and the most residue is rosin. In Southern China, people collect the secreted oleorein and separate it into rosin and turpentine by distillation. Naturally, rosin is a protector for wood. However, rosin is not an efficient wood preservative. In wood protection field, rosin was applied only to inhibit bleaching of wood preservatives and moisture absorption of wood[1,2]. Fortunately, resin acids, the main components of rosin, have a carboxyl group and two double bonds. So rosin could be modified to improve its bioactivity[3-5]. There were some studies about bioactive dehydrogenated rosin derivatives and some of them are very active to bacteria, but the raw material, dehydrogenated abietic acid, is a medical intermediate and too expensive to be used for wood protection. Wood preservatives based on rosin should get more attention.

In this paper, a bioactive rosin derivative, rosin amide, was synthesized and its bioactivity to some wood decay fungi and its surfactant properties wwere also tested.

2. Experimental methods

(1) Materials

The raw material, gum rosin, was in industrial grade. Others, such as acrylic acid, p-hydroquinone, diethyltriamine (DETA), dimethylbenzene and so on, were reagents in analytical grade.

(2) Methods

A. Synthesis

First, gum rosin was modified by acrylic acid under nitrogen with p-Hydroquinone as the

anti-polymerized agent. When rosin was heated up to 230℃, acrylic acid was added slowly till the weight ratio of rosin to acrylic acid was 4.5:1. The system was kept for another 3h[6,7]. The modified rosin was yellowish glassy solid. In order to remove unreacted acryl acid and p-hydroquinone, the cool modified rosin was ground, washed with high purity water, and oven-dried at 103±2℃. Its acid value was 242.6 mgKOH/g. Then the modified rosin was reacted with DETA. Their mole ratio was 1:3.5. Dimethylbenzene was the water carrying agent. The reaction lasted for 8h at 160-180℃. The reaction equations are as follows:

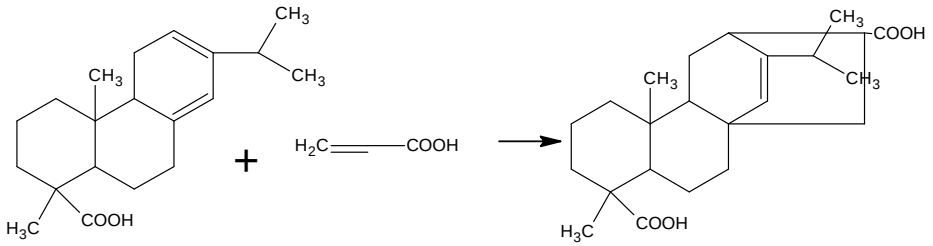

(1)

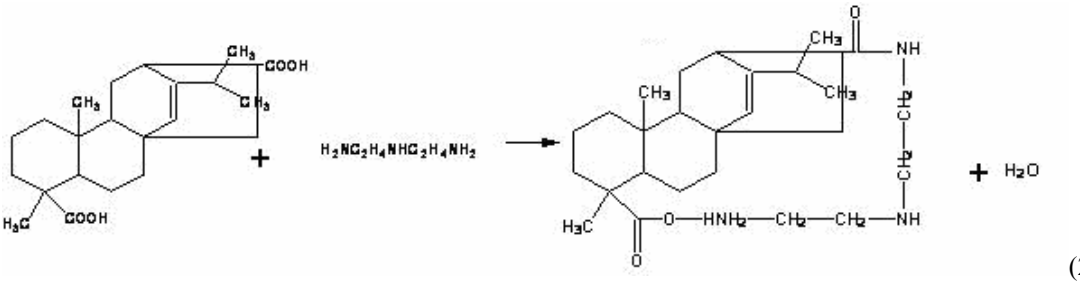

(2)

B. Chemical structure characterization

FTIR and MS were used to identify the chemical structure of the product. FTIR analysis was performed on an Magna 560 FTIR spectrometer, which was made by Nicolet company, and KBr press method was used. MS conditions on API 3000 made by Applied Biosystems company for analysis were: scan range of 400~900 m/z, 1.5 scans/s. ^{1}H NMR analysis was taken on a DRX-400 spectrometer, which was made by BRUKER company, with $CDCl_3$ as its solvent, tetramethylsilane (TMS) as its interior standard.

C. Decay resistance

The anti fungal activity of RA was determined by digging a hole of 7 mm diameter at the center of 1.5 % potato dextrose agar (PDA) in plastic perti dishes previously inoculated with actively growing mycelium of *Trametes versicolor*, *Gloeophyllum trabeum, Aspergillus niger* and *Paecilomyces variotii*. The fungi were inoculated in the plates by mixing a suspension of mycelium and spores of a given fungus with cooled, but still molten PDA. The aqueous solutions of RA were prepared with 2.0, 4.0, 8.0, 16.0 and 32.0 mg of RA derivative/mL of water. Then 60 uL of solutions were injected into the holes, respectively. Each product concentration was replicated on 10 discs and the plates were incubated at 28 ℃ for 2 to 7 days, depending on the growth rate of the test fungus. The effect of RA on growth was determined by measuring the diameter of inhibation halos.

D. Surfactant properties

During experiments, we found RA was surface-active. So its surface tension, emulsion forming and stabilizing abilities were also tested.

3. Results and Discussion

(1) Chemical structure of the product

Fig. 1 shows the spectra of the product, RA. The following FTIR spectral data could be observed: 3350~3280cm^{-1}(N—H stretch), 2930~2860cm^{-1}(C—H stretch), ~1640cm^{-1}(C=O stretch), ~1560cm^{-1} (bending

vibration of N—H), 1450~1380cm^{-1} (bending vibration of C—H), 1350~1320cm^{-1} (C—N stretch). There are special peaks for C=N, N—H, not the peaks for C=O, indicates that mostly the modified rosin by acryl acid reacted with DETA and RA was produced[8,9]. According to Fig. 2, EI-MS spectrum of the product, $[M+H]^+$ was m/z 461, plus the following data of ^{1}H NMR, signifies the product is RA.

^{1}H NMR analysis data: δ1.01(3H,-CH_3), δ2.81(3H,-CH_2-C-N-), δ2.78(2H,-C-CH_2-N), δ1.99(2H,-C-C-NH-C-C), δ5.33(1H,-C=C-CH-), δ3.34(1H,-C(=O)-N-C-CH-N-), δ8.01(1H,-C(=O)-NH-), δ3.36(5H,-CH_2), δ1.42(2H,-CH_2-), δ1.25(4H,-CH_3-).

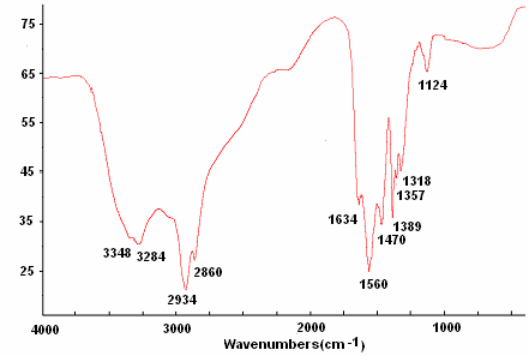

Fig. 1 FTIR spectrum of the product.

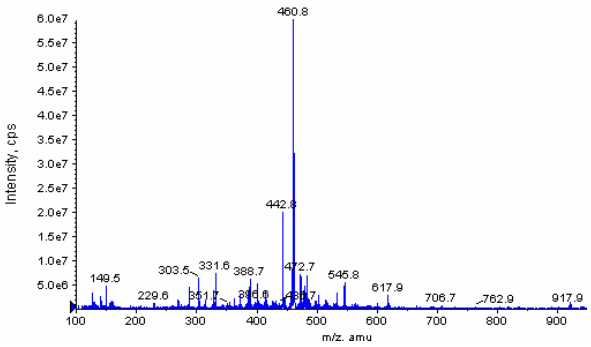

Fig. 2 EI-MS spectrum of the product.

(2) Fungal toxicity

The resistance of the product to some wood stain fungi (*Aspergillus niger, Paecilomyces variotii)* and wood decay fungi *(Trametes versicolor and Gloeophyllum trabeum*) was illustrated in Table 1. In these experiments, the product of RA showed good anti-fungal activity to all the tested fungi. With the concentration increasing, the anti-fungal activity also increased. RA was active to all those fungi when its concentration was greater than 1.60mg/mL. It was more efficient to *Paecilomyces variotii*. Even when the concentration was as low as 0.80mg/mL, the resistance to this fungous was visible.

Table 1 Halo diameters of RA on growth of selected wood decay fungi on PDA, mm.

	Concentration of the product,RA 〔mg•mL^{-1}〕					
Fungus	control	2.0	4.0	8.0	16.0	32.0
Aspergillus niger	0	5	9	12	17	22
Paecilomyces variotii	0	18	19	27	31	44
Trametes versicolor	0	13	24	26	33	37
Gloeophyllum trabeum	0	27	29	35	38	42

(3) Surfactant properties

Surface properties of the target product had been studied through the means of electric conductivity and surface tension. 8.0×10^{-4} mol/L of critical micelle concentration(CMC), 39.161 mN/m of surface tension, 1320 s of emulsifying ability, 135mm of foam hight, 125 mm of emulsion stabilizing ability, signifies RA has nice surface-activity.

4. Conclusions

A rosin amide was synthesized with rosin as raw material. Its chemical structure was identified by FTIR, EI-MS, and ^{1}H NMR analysis. Its resistance to some wood decay fungi was tested by bioassay *in vitro*. All results showed that the rosin amide is effective to protect wood from the decay fungi. Meanwhile, RA also has nice surface-activity. Since rosin is abundant in China, renewable, cheap, environment-friendly, it has a promising future as a potential wood preservative.

5. References

(1) Schultz, P. T., Nicholas, D. D., and Shi, J. 2007. Water repellency and dimensional stability of wood treated with waterborne resin acids/TOR. IRG paper 07-40364

(2) Roussel, C., Haluk, J-P., Pizzi, A., Thevenon, M-F. 2000. Copper based wood preservative---- A new approach using fixation with resin acids of rosin. IRG paper 00-30249

(3) SONG, Z. 1994. Development of fine chemicals from Chinese gum oleoresin. Chemistry and Industry of Forest Products, 14(1):68-73.

(4) Liang, M. and Ye, J. 2000. Synthesis and performances of quaternary ammonium cationic surfactants with dehydroabietyl group. Chemical World, 2000(3):138-141.

(5) Ding, X. 2006. Studies on synthesis, structure and biological activities of rosin derivatives. Nanjing Forestry University

(6) Mei, P., Hu, L., Gao, Q., Ai, J., Chen, W. 2007. Synthesis and properties evaluation on quaternary ammonium of bis-imidazoline as acid corrosion inhibitor. Journal of Oil and Gas Technology, 29(4):140-143

(7) Wu, W., Zhao, X., and Wen, P. 2007. Study on synthetical techniques of acrylic modified rosin. Forestry Science&Technology, 32(1):59-61

(8) Xie, H. and Cheng, Z. 1998. Research on preparation of acrylpimaric acid type polyurethane paint. Chemistry and Industry of Forest Products, 18(3):67-73

(9) Li, C., Dun, Z., Wang, F. 2007. Performance study of a series of carboxylated imidozoline phosphate. Fine Chemicals, 24(11):1064-1068.

Identification and Preservation of Wood in Wooden Cultural Heritage Protection in China

Guanwu Zhou[1], Xinfang Duan[1], Danyang Luo[1,2], Jianing Li[1,2] and Dajun Shang[1,2]

[1] Research Institute of Wood Industry, Chinese Academy of Forestry, Beijing

[2] Northwest Agriculture & Forestry University, Shaanxi

Abstracts: China is one of the biggest cultural heritage country in the world. China's wood science and technology researchers make good progress in identification and preservation of wood in wooden cultural heritage protection. The research works about wood identification and wood deterioration of wooden heritage protection, non-destructive evaluation of safety conditions, wood preservation for wooden cultural heritages in China are summarized this paper. More communication and cooperation between wood science institutions and agencies of culture heritage conservation are required

1. Introduction

China is one of the countries with more than 5000 years history in the world. There are many cultural heritage or relics in China. In China, the non-movable cultural heritages or relics can be defined by 3 levels according to their value. They are National Key Cultural Relic Protection Unit, Province Level Key Cultural Relic Protection unit, and City or County Level Key Cultural Relic Protection Unit. Since 1961, the State Council of China declared six times of National Key Cultural Relics Preservation Units. Until June 2006, the total National Key Cultural Relic Protection Units are 2351. The total number of Province Level Key Cultural Relic Protection units are 7000, City or County Level Key Cultural Relic Protection Units are 60,000. There are 400,000 Cultural Relics 400,000 sites after a national Census, among them ancient architecture accounts for 80,000, wooden constructions only accounts for one third of which.

Up to July, 2008, there have been 37 Chinese cultural relics and natural landscapes listed in the *World Heritage List*. Among them, 7 sites are natural heritages, and 25 are cultural heritages; 1 site is cultural landscape; 4 cultural sites bear the double status of both natural heritage and cultural heritage. Up to July of 2008, there have been altogether 878 world heritage sites distributed in 138 countries. When it comes to the numbers of world heritage sites, China ranks the third right after Italy and Spain in the world.

2. Wood identification of wooden cultural heritages

Wood is one kind of natural material which mankind has been using for long times. As natural biomaterial, there are many wood species for different end uses, also wood properties has great variations among tree species, same tree for same wood species, etc.. Besides, wood is easy biodegradation caused by fungi, insects and termites. So during wooden cultural protection, it is necessary and important to get the correct information of the wood species. Only after having a deep knowledge of the characteristics of the wood, an effective plan of conservation, maintenance and restoration can be worked out. Based on this understanding, wood identification provides basis for choosing wood species when the conservation plan of ancient wooden structure is worked out or when wood members require replacement. Wood identification is an essential measure in the process of determining any properties of ancient wooden relics, because through it we obtain information on natural durability, physical and mechanical performances, uses, workability, aesthetical characteristics, and timber origins. It is feasible to identify the wood species from macrostructure by naked eye and microstructure by means of a microscope.

Some works on wood identification of wooden cultural heritages can be seen in Table 1.From Talbe 1,there were 14 wood species used in Forbidden City construction, in which 8 softwoods and 8 hardwoods. Also, Ipil (*Intsia spp.*) and *Cynometra spp.*that were not China's native tree species were imported from southeast Asia at that times; For the ancient wood structures in Tibet and Qinhai Province, such as Potala Palace, Norbu Linka and The Kumbum Monastery, the woods of the ancient wooden structures were logged and transported from

neighboring forest, such as southeast Tibet and east Qinghai Province. Also we can found that poplar and willow wood which has not good natural durability were used in building at that time due to the lack of understanding of wood durability; For the coffin wood unearthed, cypress woods with yellow color frequently used especially in tombs of emperors and kings because yellow color was for members of imperial family exclusively in ancient times.

3. Research of deterioration of wooden cultural heritage

Ancient wood structures are susceptible to deterioration and insect infestation. Either the choosing of wood preserving and insect prevention techniques or to draw up plans of wood preserving and insect prevention depend on the state and types of wood decay and insect attack. Wood members in ancient wood structures are subject to infestation by a wide variety of termites and beetles. In Tibet, we found that wood damaged mainly by insects of Scolytoidea, Bostrychidae and Anobiidae, not termites. And the most decay fungi in wood members of ancient wood structures such as Potala Palace are *Poria placenta*, *Coniphora cerebella*, and *Merulius aureus.* But in South China, the termite can cause the serious damage to ancient wood structures.

4. Non-destructive Evaluation of safety conditions for ancient wood structures

Based on the evaluation of safety conditions, decisions on planning of the restoration and maintenance and on whether the ancient wood member is maintained or replaced can be made. Evaluation of safety conditions is composed of 2 parts: (1) determining environmental conditions (the surroundings and moisture content of wood) and the biological deterioration level (the defects of wood members including decay and insect infestation); (2) The safety of the strength properties of wooden structure, especially the measurement of the residual strength properties of wooden members to assess the reliability, safety and service life of wood structure.

Nowadays the on-site evaluation of safety conditions is based on visual inspection of the timber member, nondestructive measurement of one or more physical-mechanical properties, or on an appropriate combination of both the above methods. Non-destructive evaluation methods currently used in china to evaluate the safety conditions for ancient wooden structures include Resistograph,

Stress wave method, ultrasonic wave method and surface stiffness detecting method (Xinfang Duan *et al.* 2002, Xinfang Duan *et al.* 2005a, Xinfang Duan *et al.* 2005b). These inspection methods were used in most of the above-mentioned protection of wooden cultural heritages, all non-destructive testing methods and visual inspection were combined.

Nowadays the on-site evaluation of safety conditions is based on visual inspection of the timber member, nondestructive measurement of one or more physical-mechanical properties, or on an appropriate combination of both the above methods. Non-destructive evaluation methods currently used in china to evaluate the safety conditions for ancient wooden structures include Resistograph, stress wave method, ultrasonic wave method and surface stiffness detecting method (Xinfang Duan *et al.* 2002, Xinfang Duan *et al.* 2005a, Xinfang Duan *et al.* 2005b). These inspection methods were used in most of the above-mentioned protection of wooden cultural heritages, all non-destructive testing methods and visual inspection were combined.

5. Wood preservation for ancient wood structures

The wood preservation treatment methods for ancient wood structure maintenance in use today include the following: (1) vacuum/pressure process; (2) hot-and-cold open tank treatment; (3) immersion treatment; (4) brush treatment; (5) drop treatment by drip (suspension bottle);(6)spraying treatment; (7) injection treatment; (8) fumigation.

Treated wood by vacuum/pressure process is the substitutes (newly-used wood members) for the rotten or insect damaged ancient wood members. The highest wood preservation plant (about 3700 meters above sea level) in the world, namely The Wood Preservation Plant for the Three Engineering Projects of Cultural relics' Protection and Maintenance in Tibet Autonomous Region, was built in 1990 at Lhasa, Tibet. Until 2005, 5500 m^3 of wood rafters (approximately 20,000 pieces) and other kinds of wood members have been pressure-treated in

Tibet for Potala Palace and Norbu Linka Maintenance in past 2002-2005.The plant have completed about 10,000 m^3 pressure-treated wood for new substitutes of wood members since 1990.The treated wood species in this plant are larch *(Larix spp.)*,cypress (Cupressaceae), spruce *(Picea spp.)*, pine *(Pinus spp.)*, poplar *(Populus spp.)*, sea buckthorn *(Hippophae spp.)*, and willow *(Salix spp.)*.All those woods are logged from southeast Tibet, not mainland China or imported from foreign countries (Xinfang Duan 2006).

Immersion treatment, brush treatment, drop treatment by drip and spraying treatment involve the on-site wood preservation treatment of unmovable wooden members or artifacts, which was used in the conservation of The Potala Palace, The Kumbum Monastery,The Forbidden City etc. During maintenance of The Potala Palace in 2002-2005, 20,000 m^2 of various wood members treated by on-site wood preservation treatment methods(Xinfang Duan 2006). And for the Forbidden City maintenance in 2003-2005 ,40,000 m^2 of various wood members treated by on-site wood preservation treatment methods, too.

Table 1 The results of wood identification of some wooden cultural heritages in China.

Wooden cultural heritage	Location	Types of wood members or others	Wood species
The Forbidden City (Yufeng Yang 2006)	Beijing	posts, beams, purlins, square posts linking two columns	Larch (*Larix spp.*), Silver fir (*Abies spp.*), Spruce (*Picea spp.*), Cypress (*Cupressus spp.*), pine(*Pinus spp.*) Chinese fir (*Cunninghamia spp.*), Juniper (*Sabina spp*), Golden Larch (*Pseudolarix spp*); Zhennan (*Phoebe zhennan*), Amur Linden (*Tilia amurensis*), Machilus (*Machilus* Nees), Big-fruited Litse (*Litsea lancilimba*), Ipil (*Intsia spp.*), (*Cynometra spp.*)
The Potala Palace (Xinfang Duan, *et al* ,2006)	Lhasa, Tibet Autonomous Region	rafters	poplar (*Populus spp.*), willow (*Salix spp.*), sea buckthorn (*Hippophae spp.*), cypress (*CUPRESSACEAE*), larch (*Larix spp.*), pine (*Pinus spp.*), spruce (*Picea spp.*)
		wood flooring	walnut (*Juglans spp.*), cypress (*Cupressaceae*)
The Norbu Linka(Xinfang Duan, *et al* 2006)	Lhasa, Tibet Autonomous Region	rafters	poplar (*Populus spp.*), willow (*Salix spp.*), sea buckthorn (*Hippophae spp.*)
		purlins, beams and posts	larch (*Larix spp.*), pine (*Pinus spp.*), spruce (*Picea spp.*)
The Kumbum Monastery (Xinfang Duan, *et al* 2006)	Qinghai Province	rafters	poplar (*Populus spp.*), spruce (*Picea spp.*)
		purlins, beams and posts	larch (*Larix spp.*), spruce (*Picea spp.*)
		wood flooring	cypress (*Cupressaceae*)
The No. 1 in'gong mausoleum (An Peijun *et al.* 1990)	Fengxiang County, Shaanxi Province	Wood charcoal and coffin wood	Chinese Arbor-vitae (*Platycladus orientalis* (L.) Franco), Sawtooth Oak (*Quercus spp.)*
Laoshan Han Dynasty Tomb (Rongfeng Huang *et al.* 2004)	Beijing	wall built by piling up wood and coffin wood	Cypress (*Cupressus spp.)*, Chinese Arbor-vitae (*Platycladus orientalis*), Sawtooth Oak (*Quercus acutissima.),* Chinese Scholar Tree(*Sophora japonica*.), Maple (*Acer spp.*),Chinese chestnut (*Castanea mollissima.*), Chinese Pine (*Pinus tabulaeformis*)

6. References

(1) Peijun An, Zhicai Zhao, Wei Han. (1990) Unearthed woods from No. 1 Qin'gong mausoleum at Fengxiang, Shaanxi. Journal of Northwestern Forestry College. 5(2):10-16.

(2) Rongfeng Huang, Fucheng Bao, *et al*. (2004) Dendrochronology research on excavated woods of Laoshan Han tomb. Scientia Silvae Sinicae. 40(5):168-174.
(3) Xinfang Duan, Yudong Li, Ping Wang. (2002) Review of NDE Technology as Applied to Wood Preservation. China wood industry. China Wood Industry. 16(5):14-16.
(4) Xinfang Duan, Ping Wang, Guanwu Zhou *et al*. (2005a) Nondestructive detection of decay and insect attacked ancient wood members in Tibet by stress wave methods. Proceedings of international symposium on research and effective Utilization of bio-based materials. Harbin. 2005:566-571.
(5) Xinfang Duan, Ping Wang, Guanwu Zhou *et al*. (2005b) Nondestructive evaluation of dynamic MOE of ancient wooden structure members by stress wave method. Proceedings of international symposium on research and effective Utilization of bio-based materials. Harbin. 2005:572-575.
(6) Xinfang Duan, Ping Wang. (2006) Progress of the wood preserving in the 3 projects of cultural relics' protection and maintenance in Tibet. Proceedings for the seminar of the publicizing and implementation of new national standards on wood preservation and workshop on the development of treated wood industry. Beijing. 2006:40-41.
(7) Yufeng Yang. (2006) Six ancient structures of the Forbidden City will be face-lifted in this year. Beijing Morning Post. 2006-2-11.

Strengthening and Fire-retardant Treatment Technology for Plantation Wood of Poplar

Junliang Liu[1] and Yubo Chai

Research Institute of Wood Industry Chinese Academy of Forestry, Beijing

Abstract: With Melamine、Methanol and Urea as the main materials, a type of clear and colorless impregnating-solution（MMFU）, which had good water solubility and strong permeability, was made through low temperature and long time synthesis process. And adding a certain proportion of Boric Acid and Borax into MMFU, a multifunctional solution used for wood strengthening and fire-retardant modification was obtained. Then plantation wood of poplar was modified with the multifunctional solution under vacuum -- pressure impregnating treatment, and according to the national standard GB 1927~1943-2009 and GB 8624~2006, properties of treated wood were measured including density、MOR、MOE and fire-resistance property. The results showed that the density of treated poplar was 580kg/m^3, MOE and MOR had increased by 40% and 80% separately compared with untreated wood, and fire-resistance property reached level Ⅲ

1. Introduction

The area of forest plantations reaches about 53million hectares in China, accounting for 40% of plantations in the world, ranking the first in the world. Due to the deficiencies of wood produced by plantations, such as high growth stress, deformation and cracking, texture soft, low density and so on, the application scope of plantations is limited to some extent and the added value of product is reduced, like Poplar, Fir, Eucalypts, Masson Pine and so forth .Thus, it is necessary to find an effective technique to modify the properties of plantation wood and meanwhile add decay-resistance, fire-resistance property and other new functions to wood as well as increase plantation wood dimensional stability[3.4]. Therefore it opens up a new path for effective use of plantation and can also substitute natural precious wood to relieve the contradiction between demand and supply of wood[5].

Plantation wood enhance-fire-retardant treatment technique is a sort of wood impregnating treatment techniques, which blend water-soluble low molecular weight melamine-modified urea-formaldehyde resin (abbreviated as MMFU solution)with boric acid, borax and other additives in a specified proportion into a kind of multifunctional wood modification agent with a good penetration and environmental friendly[1.2].Through vacuum-pressure impregnation processing and post-drying treatment, enhanced-fire-retardant material is obtained. Thus this technique can not only enhance the density and strength of plantation, but also improve dimensional stability and workability, and meanwhile make wood have a good fire-resistance and decay-resistance.

2. Materials and methods

(1) Test materials

The material that was used in this experiment was plantation wood of poplar grown in Yuan-jiang City Hunan Province. The air density of poplar was 390 kg/m^3 and dimensions of samples were1000×140×30mm (L×T×R). In addition, the main agents, which dealt with the wood, composed of melamine, formaldehyde, urea, methanol, boric acid, brax, dextrine, camphor tree sap and water.

(2) Test equipments

Capacity of reactor used for preparing adhesive was 30L, produced by Wu-xi yun tong shi hua zhuang bei corporation in Jiangsu Province. The type of vacuum – pressure impregnating instrument made by IHI Corporation is SBK-45OB, which owned the highest pressure1.96MPa and volume was.25 m^3. The volume of lumber kiln was 10 m^3 .

(3) Test methods

A. The performance index of physical mechanics: the weight percentage gain (WPG) formula is as follows:

$$W = \frac{G_2 - G_1}{G_1} \times 100\%$$

Where w is the weight percentage gain; G1 is the over-dry weigh of sample before processing; G2 is the over-dry weigh of sample after processing.

While according to the national standard GB 1933-91《Method of determination of the density of wood》, GB 1932-91《Method for determination of the shrinkage of wood》, GB1936.2-91《Method for determination of modulus of elasticity》 and GB 1936.1-91《Method of testing in bending strength of wood》,other indexes, like density, shrinkage, MOR and MOE, are measured.

B. Testing of fire-resistance property: According to the national standard GB 8624-2006 《Classification for burning behavior of building materials and products》and the standard of Taiwan CNS 《Method of test for incombustibility of interior finish material of buildings》, the fire-resistance property is measured. The dimensions of sample are 220×220×25.4 mm, and the total number of sample is nine, which is divided into three parallel groups.

C. Testing of formaldehyde content: The formaldehyde content is measured through the national standard GB 18580《Test method of Formaldehyde Emission Content》, and the dimensions of sample are 150×50×20 mm, and the total number of sample is thirty, which is divided into three parallel groups.

3. Results and discussion

(1) Resin synthesis and solution preparation

A. Resin synthesis (abbreviated as MMFU solution): The mole ratio of main components: melamine: formaldehyde: urea: methanol=1:2.6:1.2:2.8. The synthesizing process: □Add melamine and formaldehyde into three-neck flask, and adjust pH value to 9.5 using sodium hydroxide solution.; □ Control the reaction temperature increase to about 80℃ in 30 min, and the reaction process lasted 40 minutes; □As the temperature decreased to 70℃, adjust pH value of solution above 12 using sodium hydroxide solution; □Add urea and methanol to the solution, and react 60 minutes, then make the solution cool to 65℃ and adjust pH value to 9.2 or so; □Add urea to the solution and dissolve 10 minutes, then adjust pH value to 7.5 by hydrochloric acid. 30 minutes later, dissolve the solution using water and react 60 to 90 minutes. When the solution was dissolved to six times compared with original solution, adjust pH value of solution to 10.5-11.0 again, and finally MMFU solution was obtained.

B. Solution preparation：Based on the formal experiment, the multifunctional modified solution was composed of 20% melamine modified urea formaldehyde resin, 2% boric acid, 3% borax, 5% dextrine, 5% agent(camphor tree sap)and 65% water.

(2) Vacuuming & pressing treatment and wood drying

A. Vacuuming & Pressing treatment

Put timber into tank and then vacuum for 40 minutes (the vacuum degree was 0.095MPa). And then in a vacuum state, the prepared liquid was soaked slowly into the treatment tank, when finished, keep the tank for 30 minutes. Use pressure pump pressed until the pressure in the tank reached to 0.8-1.0MPa, keeping the pressure for 120 minutes, and then release pressure and discharge the liquid.

B.Wood drying

After the samples, which were removed from treatment tank, were air dry for a period of time（about 2 weeks）. And then take them into drying kiln(about 20 days). Finally modified wood was obtained.

(3) Physical and mechanical properties indexes:

The results of growth rates, density, dry shrinkage, MOE, MOR and formaldehyde content of modified wood were shown in Table 1.

Table 1 Results of physical and mechanical properties and formaldehyde content of modified wood.

Items	Growth rates (%)	density (g/cm^3)	shrinkage (%)		MOE ($MPa \times 10^3$)	MOR (MPa)	Formaldehyde content (mg/L)
			radial direction	longitudinal direction			
Results	42	0.63	3.71	1.79	11.2	103.4	0.3

(4) Fire-resistance property:

Results of fire-resistance of modified wood were shown in the Table 2.

Table 2 Results of fire -resistance of the modified wood.

Test items		Results			Severity rating
Sample number		1	2	3	
Length×Width×Thickness (mm)		220×220×25.4	220×220×25.4	220×220×25.4	……
Heating time（min）		6	6	6	6
Weight before test（g）		744.1	720.6	697.2	……
Weight after test（g）		697.8	675.0	654.3	……
Weight loss of heated （g）		46.3	45.6	42.9	……
The time of discharge temperature curve exceed standard curve（min/sec）		3’07”	3’15”	3’11”	None exceed
Coefficient of fuming（CA）		44.7	43.2	46.2	Under 120
The time of residual flame（s）		25	26	21	Under 30
conclusion	It matches fire-resistance grade III of CNS6532《Method of test for incombustibility of interior finish material of buildings》				

4. Comprehensive analysis

The results of experiment showed that, through vacuum-pressure impregnating treatment and using multifunctional modified wood solution, the performance indexes of plantation Poplar improved obviously. Dimensional stability of wood is increased by 30% or so, MOR and MOE are increased by 30% and 80% respectively, and hardness and abrasion resistance are also improved. Meanwhile free-formaldehyde content of treated wood can reach to E_0 standard (≤0.3 mg/L). In addition, the wood also has fire-resistance function. The average value of coefficient of fuming is 44.0, which is much lower than severity rating 120. The average time of residual flame is 24 seconds, which is also lower than severity rating 30 seconds. By now the treatment cost of each cubic meter poplar is 600-800 yuan at the market price. Furthermore, the treatment solution has advantages of good permeability, colorless, tasteless and environmental friendly.

5. References

(1) H.R.Liu,J.L.Liu. Heat Transfer in Resin Impregnated Poplar LVL during Hot-pressing. CHINA WOOD INDUSTRY.2008, 22（1）:

(2) Y.B.Chai, H.R.Liu,J.L.Liu. Study on physical and mechanical properties of poplar modified by phenol-formaldehyde resin. Chinese forestry science and technology，2008，7（1）：82-87

(3) S.G.H.an， R.Z.HUANG. Modification of Melamine Formaldehyde Resin for Paper Impregnation. CHINA WOOD INDUSTRY. 2009，23（4）：12－15

(4) H.F .TAN， H.X.GUO. Performance of Poplar Wood Impregnated with Organic and Inorganic Additives. CHINA WOOD INDUSTRY. 2009，23（4）：40－42

(5) G.Z.Fang. Function Improvement of Wood. Publishing house of chemical industry (Beijing),2008

Bonding Performance of Wood Treated by Cold Plasma

HongyanWang, Hui Wang, Guanben Du and Hong Lei
Southwest Forestry University, Kunming

1. Introduction

The bonding performance of wood is greatly affected by the characteristics of wood surface. A lot of work has been done to improve the bonding performance with the method of wood surface treatment. Plasma treatment is one of the most attractive and promising technology in all of the wood surface treatment methods. Plasma technology was introduced to wood science in the beginning of 1990s [1, 2]. Du G.B *et al* [3-7] has already done a systematic study work on the utilization of microwave plasma in the field of wood and bamboo. The main research results are concentrated the study of the chemical composition on the surface of wood being treated by plasma and its effects on the wettability of wood surface. The possibility of using some plasma to initiate polymerization reaction on the surface of wood was studied, too. However, the report on the effects of plasma treatment on the bonding performance of wood is limited. Huang *et al* studied the bonding performance of bamboo treated by plasma and the results showed that plasma treatment could improve the bonding performance effectively [8, 9].

Plasma treatment could activate the surface of wood, then improve the wettability of wood and introduce functional chemical groups to wood, which could improve the resulted bonding performance [3, 7]. The chemical composition on the surface of wood with or without N_2 cold plasma treatment and the shear strength performance with different plasma gases resources were studied in this paper.

2. Material and methods

Yunnan Pine (*pinus yunnanensis*) from Kunming Forestry Industry Company with moisture content 10%~12% was used in this paper. Specimens were cut to the dimension 50×15×6mm. Melamine-urea-formaldehyde resins were prepared in lab with molar ratio (M+U)/F=1.88. Resin characteristics are then solids content being 60%, viscosity 350mPa·s measured at 22 °C. The latent hardener NH_4Cl was mixed with resins before utilization.

Wood with and without plasma treated was cut to specimens with desired dimension. Plywood with these specimens was prepared in the lab. The glue-spread used was of 350 g/m^2 of liquid glue-mix double glue line. Pressing time was 6 minutes at 110°C and 1 MPa pressure. The plywood was cut according to the standard EN 314. The panels, after being aged for some time, were tested for dry shear strength according to standard specification GB/T17657-2003. Some samples were prepared for X-ray photoelectron spectroscopy (XPS) analysis.

Nitrogen, oxygen, ammonia and argon were chosen to be used as plasma gases resources in this paper. Power for the treatment is 50 watt. The samples were treated under the vaccum condition for 3min. During the treatment, the gas flow was controlled by keeping the vaccum degree stable.

Samples with and without treatment were analyzed by XPS. The measurements were carried out under the following conditions: Mg radiation was used. The operation electric parameters are 15kv and 20mA. Curve fitting was done by the method of Gussian and Loentzian.

3. Results and discussion

(1) XPS analysis

From XPS results bonding energy of inner electrons for almost all elements except H and He can be calculated. Therefore, chemical composition on the surface and their relative content can be gotten since each element has a specific bonding energy. Wood is mainly made of cellulose, hemicellulose, lignin and the main chemical elements for wood are C, H, O. The elemental composition of wood surface untreated or treated by cold plasma could be seen in Table 1. Their XPS spectra results were given, too (Fig. 2 and Fig. 3).

Table 1 Elemental composition on wood surface untreated/treated by cold plasma.

Samples	Elemental composition (%)			
	C	O	N	O/C
Untreated wood	77.41	22.59	0	0.29
Treated wood	63.28	29.41	7.26	0.46

Both in Fig. 1 and Fig. 2, strong absorption peaks could be seen in two zones: one is at 284～290 eV, the other is at 531～534 eV. They could be attributed to elements C and O from the wood composition itself, respectively. While besides the two peaks, when compare the two figures, a new peak could be seen at 400～400.5 eV after the wood sample being treated by N_2. It was normally attributed to N atom, specifically coming from the group of -NH_2. It appeared that the new element N was introduced to the wood surface after plasma treatment when using N_2 as the plasma resource. The newly N element proportion is 7.26% on the total content of all of the elements with obvious peaks in the spectra. It possibly existed on the surface of wood through the formation of -NH_2 group. On the surface of treated wood, the proportion of C decreased, while that of O increased. Hence, the ratio of O/C increased from 0.29 to 0.46 after plasma treatment. It seemed that a great deal of oxygenated groups or peroxides were generated on the wood surface after this treatment.

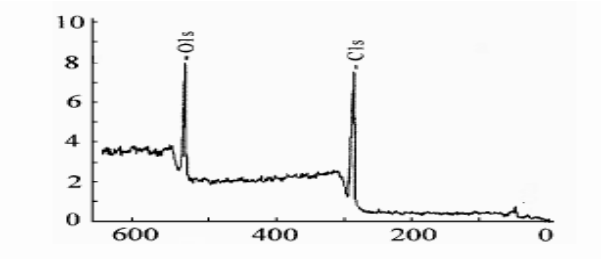

Fig. 1 XPS spectra of untreated wood surface.

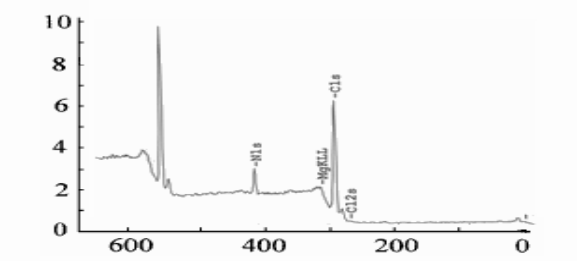

Fig. 2 XPS spectra of treated wood surface.

(2) C1s spectra analysis of untreated/ treated wood surface

C1s spectra analysis is a branch of XPS analysis. The C1s spectra of untreated and treated wood surface could be seen in Fig. 3 and Fig. 4, respectively, and the relative specific data were summarized in Table 2.

According to the different types of groups and their position appearing in the XPS C1s spectra analysis, the carbon atoms for wood normally could be divided into four parts [3]: C_1 corresponded to carbon atoms bonded only with other carbon or hydrogen, which mainly come from lignin phenyl propane, aliphatic acids, fats, waxes, etc. And their binding energy (BE) was about 285 eV. C_2 attributed the carbon atoms bonded with one oxygen atom, mainly from the carbon atoms bonded with the hydroxyl, and it had a comparable BE with C_1 and it was 286.5 eV. C_3 come from carbon atoms bonded with a carbonyl or two non-carbonyl oxygen atoms. They were characteristics peaks when the chemical composition on wood surface being oxidized. Its BE was about 88 eV. C_4 was the carbon atoms bonded with a carbonyl and a non-carbonyl oxygen atom, normally being attributed carboxyl groups. Its BE was above 289 eV.

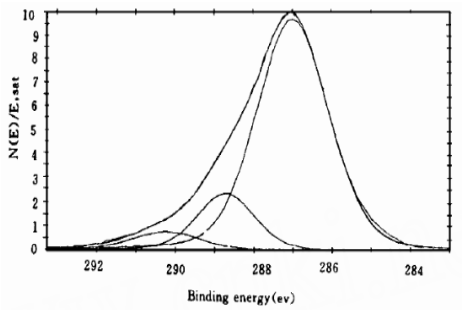

Fig. 3 C1s spectra of untreated wood.

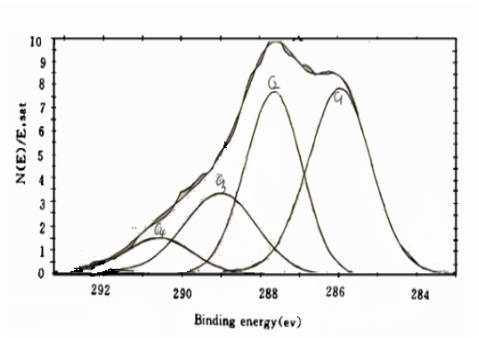

Fig. 4 C1s spectra of treated wood.

Table 2 Bonding energy, C1s peak area ratio of wood untreated/treated with N_2 by cold plasma.

Samples	Untreated wood		Treated wood	
	Bonding energy (eV)	Peak area (%)	Bonding energy (eV)	Peak area (%)
C_1	284. 79	61. 96	284.73	40.45
C_2	286. 44	28. 52	286.26	33.36
C_3	287. 96	9. 52	287.50	18.74
C_4	—	—	288.96	7.45

There were three main peaks for the wood untreated from the spectra results. According to the analysis above, they could be attributed to C_1,C_2 and C_3 and their proportion on the three total content of carbon atoms are 61.96%，28.52% and 9.52%, respectively. The spectra results meant that the carbon atoms in wood untreated are mainly in the form of C_1. After treated by cold plasma(see Fig.4), some changes had happened on the proportion of the three kind of carbon atoms. The proportion for C_1 decreased, while for both C_2 and C_3 it increased. Another obvious difference was the appearance of a new peak, which were C_4. The proportion for C_4 was 7.45%. The increase of the proportion of C_2 meant the increase of hydroxyl on the surface of wood, which was favorable to the modification of wood wettability. Carbonyl group which was formed in the plasma treatment was responsible for the increase of proportion of C_3. What's more, the increase for C_2 had some effects on the change of proportion of C_3. The appearance of C_4 meant that wood surface was oxidized by the plasma treatment. In all, the plasma treatment caused the appearance of more groups with oxygen.

(3) Bonding Performance Analysis

In this study, wood samples were treated by four different plasma resource gases. From Table 3, all shear strength for the panels treated by plasma was increased when compared with that of control. However, the increase extent was different with different treatment gases. From the results of Table 3, it seemed that the best strength come from treatment with Argon. The strength improved nearly 20% with argon, while with oxygen 13%, and with Nitrogen and ammonia about 16%.

At present, although to find the reason for the strength increase is rather difficult, it is meaningful to the work in the future. P. Rehn *et al* [10] found that the hydrophilic property of wood surface increased when treated wood with He, N_2 and Ar cold plasma, which was helpful to the improvement of strength performance. However, according to the results of G. Du *et al*, it seemed that the reason for the increase on the strength was not only from the modification of wood surface and the introduction of group of -NH_2. According to the results of earlier work of G. Du *et al*, it was found that in all of the four gas plasma treatment it was oxygen plasma that improve the wettability of wood surface more obviously than the other three gases. However, the result from Table 3 showed that the increase for bond strength for oxygen was the least in all of the four gases for the plasma treatment. They also found that whatever gas was used, new groups with N could be seen from the chemical composition analysis. These groups normally were attributed to –NH_2, which could react with amino resins adhesive. However, it seemed that the introduction of –NH_2 should not be responsible for the increase of bond strength, at least should not be the only reason for that. More –NH_2 was formed when N_2 and NH_3 was used for the plasma treatment than other gases, while the strength for former was less than that of Ar. The plasma treatment with Ar could increase the strength of bamboo-based panels greatly, too, which will be reported in later papers. In all, the mechanism for cold plasma treatment to increase shear strength was very complicated.

Table 3 Results of shear strength of plywood with plasma treatment.

Treated gas	—	O_2	NH_3	N_2	Ar
Shear strength（MPa）	6.23	7.02	7.11	7.24	7.41

4. Conclusions

Cold plasma treatment was used for wood in this paper. The chemical composition and their proportion on the surface of wood showed some differences between the samples treated or untreated by plasma. For the former, atomic ratio O/C has increased, and more groups were oxidized or more peroxides were formed on the surface of wood. After treatment with plasma, the N element was introduced to the wood surface and it was attributed to the group of $–NH_2$. Shear strength of the panels with treated wood increased by about 20% with different plasma resource gas. However, the effects on the bond strength with different plasma gases were different. With the same treatment time, the effects on the bond strength for the four plasma gases used in this paper were $O_2<NH_3<N_2<Ar$. While the modification mechanism for cold plasma treatment with different resource gases were not yet clear.

5. Acknowledgements

The authors thank the financial support from NCET-06-0825 and NSFC 30671638.

6. References

(1) D.L. Chao and E. Sjoblom, in: J.Appl.Polym. Sci., Polymer Symposium Vol. 46 (1990), p: 461
(2) H.Y. Chen and E. Zavarin, in: Chem.Tech. Vol.16 (1990), p: 387
(3) G. Du, Y. Hua, Y. Cui and Z. Wang, in: Scientia Silvae Sinicae,Vol 35 (1999), p: 104
(4) G. Du, Z. Yang and J. Qiu, in: Scientia silvae sinicae, Vol 40(2004), p.148
(5) G. Du, Y. Hua and Z. Wang, in: Scientia Silvae Sinicae, Vol 35 (1999), p:95
(6) G. Du, Z. Sun and L. Huang, in: Journal of Northeast Forestry University, Vol 35(2007), p: 31
(7) G. Du, Y. Hua and Z. Wang, in: China Wood Industry, Vol 12(1998), p: 17
(8) H. Huang, L. Xue, X. Lu and L.Dong, in: J. of Nanjing Forestry University,Vol 30 (2006), p: 23
(9) H. Huang, X. Lu, L. Xue, Z. Zeng and X. Liang, in: Journal of Zhejiang Forestry University, Vol 23 (2006), p: 486
(10) P. Rehn and W. Viol, in: Holz als Rohund Werkstoff, Vol 61(2003):145

Current Status of Shrub Utilization in Desert in China

Ximing Wang
Inner Mongolia Agricultural University, Hohhot

Abstract: This paper discusses the feasibility of building special company of wood based panel in desert zone, rational utilization on desert plant resource, controlling、opening up and getting coordination generalization and sustainability of development in desert zone. The special company of desert industry has got huge economic benefit, and peasants have got obvious income. That has excited the peasants of planting desert plant, and has improved local ecological environment benefit and furthered the development of sand industry.

1. Introduction

Mr. Qian xuesen, a famous scientist in China, advocates developing sand industry in our country. He analyzed and studied resource advantage by a new idea and new thinking methods, and managed the ecological economic system of desert zone with new controlling methods and opening model. Based on the planting industry、animal husbandry、oil、natural gas and coal industry, we can build and form the agricultural industry with dense knowledge by modern science and technology including chemical、physical and biological method、fixing and converting solar energy by photosynthesis.

Decades, we were working as the direction of sand industry by Qian, we are going to study how to control and utilize the 1530000km2 desert in China. The predecessor minister of Native Forestry Ministry named Xu Youfang said that the next work of controlling and preventing desert must convert the simply prevent and fix sand into the track of exploit desert resource when he summarized the experience of controlling desert. Under the situation of establishing socialist market economy, we must not only controlling and utilization desert, but also building great oasis and arriving in a new stage of improving ecological environment, and get coin、cotton、egg etc from desert. Professors who was controlling desert studied Mr. Qian's sand industry theory in 1994, and suggested that human being must treat desert with a new thinking mode. With the improvement of engineering and environment consciousness, it is necessary to think over that the method of controlling desert expansion and decreasing windy plague is not the single way to prevent people from sand disaster. Mr. Qian's theory of sand industry has made a platform for controlling desert and opening up the value of desert resources. Sand industry's important symptom rooting on this basis is that it should be utilized the special nature condition completely to promote the efficiency in converting living things into solar energy. Therefore the development of desert zone can get harmonized、compositive and persisted ecosystem. Because the working style of sand industry is directed by the socialism market economy, the special economic efficiency and values can be got in special situation. In order to develop the sand industry, we must build the professional sand industry company, firstly develop the technology of sand industry, advance industry and utilize reasonability plant resource and other resource in desert.

In former times, Inner Mongolia Forestry College has studied the utilization of drought and half-drought zone in Inner Mongolia. According to the sand industry theory suggested by Mr. Qian Xuesen, we have built salix particleboard producing line in Mao Wusu desert under the support of Yi Meng government in 1989. This work has broken an effective path to synthesis utilization of desert plant resource. More importance is that while enterprises made great economic benefits, the peasants have got more income from the salix, which has raised peasants' zeal of planting salix. Therefore salix particleboard project is a new sand industry to prompt public economic and improve public ecologic environment. Inner Mongolia Daily Newspaper reported on 15th December 1996 that all output values of forestry production of Dong Sheng city in 1986 has been over 28 950 000 ¥, the profit and tax has been 360 000¥, peasants earn 130 000 ¥ of Salix, and some individual units' income has over 10 000 ¥, average unit's salix income was half of their all incomes. Before the foundation of salix particleboard factory, Man Lai village's annual forestation area is 2km2, while the forestation area in 1990 is up

to the double. Now, salix particleboard enterprise has become the head corporation in Dong Sheng city, and the important method to control the Mao Wusu desert has becoming a part of sand theory of Mr. Qian Xuesen.

2. The state of plant resource in mao wusu desert

Mao Wusu desert, which area is over 4000km2, is on the drought and half-drought zone in north and middle of China. It is a fragile and complex ecologic system of nature-economy-society. The rock and sand of Cretaceous period are abundant, which has become the main material of this desert. Wind、light、heat、soil、water and coal resources are rich, especially the groundwater is plentiful, therefore the sand plant resource is abundant, such as salix、black salix、hankow salix、little leaf pea shrub plant resource are very rich. The plant cover ratio in desert is over 30~50%, and the main species is salix、black salix and little leaf pea shrub etc.

The investigating results of salix resource in Yi Meng show that the area of salix forestry is 5333km2. The biological properties of salix ask to be cut to regrow per 3~5yr, and 0.75~5.25kg salix trunk can be cut every square meter. So the yield in this area is 4 000 000~28 000 000t. Nowadays, 5 product lines have been built in desert zone, which could exhaust 50 000 000kg salix trunk every year, and the remainder have not be used in reason. Especially some redundant salix trunk has no ways to be used; the peasants will not cut salix for decades. With the time goes by, salix would be old、decline and blast if it wasn't be cut immediately. According to the investigation, 1160km2 salix forestry is wasted naturally because the cost of labor is more than the salix trunk's economy cost, Therefore, in this zone whose traffic is inconvenient, more and more forest couldn't be chucked away. To sum up, in order to improve the ecologic environment and increase the receipt of peasants, salix resource must be exploited immediately and rationally.

3. The study on opening up and utilizing the salix resource

Shrub growing in Mao Wusu and Ku Buqi desert in the west of Inner Mongolia Municipality, such as salix、little leaf pea shrub, have lignified, so it is possible to open up and utilize the desert plant resource. First of all, shrub's structure and characteristics have been studied. Secondly, base on the structure and characteristics of shrubs, the direction of plant resource utilization are to be made sure.

The sorts are as follows:

(1) Whole kinds basketry, laminated lumber, recombined lumber
(2) Clip kinds particleboard, veneer complex board, cement-particleboard, gypsum-particleboard, slag-particleboard
(3) fiber kinds pulp paper, hard board, middle density fiber board

If industrialisation comes to truth, developing to certain scope and layout the factory in reason, the utilization of desert plant resource would be sustained.

4. Developing shrub wood based panel indutry, promoting forestry industrialization in desert

The practice of utilizing desert plant resource shows that developing the shrub wood based panel industry is a main technological path, for it's a lower invest, faster efficiency, and its economic, social and ecological benefits are all obvious. After reforming and opening, the technological path we chose is reasonable to open up and utilize the desert plant resource. What we have done will protect the brittle ecologic environment and promote the well-ordered cycle of ecologic system. It is well known that the found of industrial base must bring the increase of population, the establishing of road and traffic, the instauration of energy device and communication and so forth, which is bound to destroy the ecologic environment. Therefore the choosing of the technological path of synthesis father the desert namely development of sand industry must be coordinated with public economic development. The experience of Dong Sheng particleboard factories tell us that the development of shrub wood based panel industry is not only could utilize fully resource or convert the advantage of resource into the economic advantage, but also increase the peasants' income and achieve a balance of ecology. To some extend, we achieved our aim: controlling the desert and develop sand industry.

The raw materials of traditional wood based panel production are from forestry. In recent years, with the decreasing of forestry, most scientist and technologist have opened up many new materials of wood based panel continuously. Through decades' working, the third forestry resource has been opened out, which is include the shrub from desert、stalk and residue of agricultural production (except for bamboo resource). The sunflower trunk、hemp stalk、flax stalk, sugarcane residues etc. based panels, and little leaf pea shrub、salix wood based panel have been studied successfully one after another. The producing technology of salix wood particleboard, which was developed by Inner Mongolia Forestry Collage, was supported by Dong Sheng city government. In our country the first salix particleboard product line has been established in Dong Sheng city, and it is the first forestry industrial enterprise in desert zone in our country also. Based on the judge of plant resource by forestry experts, this line's designing capacity is 5000m^3, which exhaust 5500t salix trunk every year and the total investment is 3 760 000 ¥. Because salix's color is white and the kind of raw material is united, the production's quality could meet the standard of country. The production quality is similar to wood based particleboard, while the cost is lower than wood, so this factory got benefits over 1 000 000 ¥ in 1992. This factory's practical producing result shows that the diameter of raw material supplying zone is 10 km, and 150 000 m^2 salix forest can supply this factory abundantly. The purchase by this factory bring mass income for peasants, which stimulate their positivity of planting salix, so that the area of salix in Dong Sheng city is twice more than in 1990. The direct result of father desert is that the man enters while the sand back off. The forestry industry in Dong Sheng city made a greatly solid step to industrialization. Using for reference of the successful experience of Man Lai particleboard after 1992 in Dong Sheng city, Wu Shen banner and Yi banner have built 4 particleboard producing lines. Therefore the salix particleboard product has been the mainstay industry. And the company of salix particleboard has been the fourth group after coal industry、chemistry industry and architecture material industry. We may gratulate that salix particleboard factories are built and vast forest resources are surrounded, and the sand industry theory of Mr. Qian Xuesen is the first to develop in western desert zone of Inner Mongolia.

5. The assurance of sustained utilization of desert shrub resource is reasonable layout of shrub wood based panel enterprise

People have got the illumination from the successful experience of salix particleboard. Some enterprisers including foreign investors knew the salix particleboard project and appraised it highly. Mr. Huang Wenzhang who come from Hong Kong chose salix particleboard as his first investment item after investigated his investment projects in Dong Sheng city in 1992, and determined to construct Sheng Jia shrub wood based panel company cooperated with Dong Sheng city government. A coal group took a fancy to salix particleboard project too, and set up a 10 000 m^3 salix particleboard product line around 1994. It is well known that, the distance between Man Lai and Dong sheng is 45km, and Dong Sheng city is not a central locus of salix resource. After all the product lines have been built up, the supply of raw material becoming a serious problem. In order to protect salix resource further more, Dong Sheng city government took some firm actions, and required particleboard factories to scatter their raw material base. So the choose of the site of factory must be reasonable and every raw material base's capability radiuses is within 20~50km; the production scale within 10 000~15 400 m3 is in order for particleboard factories. Furthermore, forestry department and particleboard enterprises should make corresponding policy to assure the quality of particleboard and the continuable utilization of salix resource.

Aim at the raw material, enterprise must insist on a principle: three kinds of raw material may be accepted and three kinds couldn't be drew in. Firstly, the salix trunk which diameter is over 2cm is eligible, while the truck's age of salix, which is under 3 years, will be incompetent. Secondly, black truck cut in winter is eligible, while the yellow truck felled in grow period will be unqualified. The last, the peasant who hold the exploitation license is eligible, the others will be underproof. Under the control of these rules, the layout of particleboard factories is becoming reasonable. While the peasants' direct economic benefits are bond with shrubs resource, they could protect and manage the desert shrub resource consciously.

According to the successful experience of salix particleboard factories and the state of resource in the west of Inner Mongolia, if half of the salix raw material could be utilized enough every year, it would satisfy with the

supplement of a 70000m^3/y particleboard factory. Calculating as recent price, the output value is about 7 billion ¥ and the benefit and tax is over 1.05 billion ¥ every year. Particleboard produced by shrub can replace 2 100 000 m^3 log (this quantity is equal to half of the wood production in Big Xing'an Mountain forestry zone) every year. These particleboards delay effectively the contradiction of supply and inquire of wood in western region. The more importance is these factories could provide 4500~7000 stations for persons. All these would bring the desert zone into rich where economy and culture is behindhand. Undoubtedly, the desert will turn into oasis sooner or later by our persistent efforts.

In conclusion, utilizing desert shrub resource rationally and developing shrub wood based panel industry is an important measure to deal desert with a whole new thinking style and concept, it is a inevitable technological path to develop the forestry industry in desert region also.

6. References

(1) Li Yunzhang, 1994. To develop wood based paned Using salix stick.
(2) Journal of Inner Mongolia Forestry College.
(3) Yang Yanping, 1997. Wood industry and sand industry A perch of articles.
(4) People daily newspaper, 1994.
(5) Inner Mongolia Daily, 1996.
(6) Qian Xuesen. Sand industry theory article's perch.

Development and Application of High-Valued Wood Products Made of Fast-Growing Poplar

Wei Xu, Zhi-Hui Wu and Yu-Shu Chen
College of Furniture and Industrial Design, NanJing Forestry University, Nanjing

Abstract: In recent years, wood of greatly value are decreasing continuously. However, the percentage of low-grade wood or fast-growing species are increasing. The utilization of fast-growing species is one of the significant themes of investigation in wood industry. Fast-growing poplar (southern type poplar) which have been planted successfully and grown over a wide area in China are well known as famous fast-growing species of the most important commercial trees and industrial timber. In this paper, the distributions of plantation resources and methods of industrial utilization of fast-growing poplar in China were analyzed, respectively. High-valued wood products made of fast-growing poplar will be an inevitable trend in wood industry, including wood-based panel, engineered wood, solid wood door, curved laminated veneer lumber, and wood floor, in the 21st century. In this paper, varieties of poplar products inclued poplar composites board, poplar floor, poplar technological door, curved laminated veneer poplar molding components and poplar scientific wood were introduced. On the basis of research and application, the author emphatically analyzed multi-layer wood floorings made of fast-growing poplar veneer and MDF, curved furniture components made of poplar veneer, sofa frame maed from poplar composites board.

1. Introduction

The 20th century was the time for rapid development of the industrial world and vast accumulation of wealth. It was also the time when forests were destroyed and decreased sharply in terms of forest area. It has become a more and more concerned issue whether timber plantation can meet the demand of sustainable development of human society.

The natural wood resources are shrinking more and more, while the wood consumption of industrial use is keeping increasing with the economic development and growing population. China is a country short of wood resources while the consumption of wood is keeping increasing all the time. At present, it consumes about 370 million cubic meters annually in China. As we all know, such a huge wood demand cannot fully rely on natural forests. To solve the contradiction between supply and demand of wood resources, which disturbing the nation production, the Chinese government has always been insisting on planting fast-growing wood resources on a wide scale.

In the past 20 years, because greatly valued and very durable timbers are decreasing continuously and the percentages of plantation wood or fast-growing species are increasing, the wood resource for industrial production is gradually changing from natural wood resources to plantation wood resources. Therefore, how to use plantation wood to produce high quality wood composite is focused on.

In many plantation wood species of China, Fast-growing poplar is a special plantation wood species. The purpose of this paper was to analyze the resource distributions and industrial utilization of fast-growing poplar in China. High-valued wood products made of fast-growing poplar will be an inevitable trend in wood industry, including wood-based panel, engineered wood, solid wood door, curved laminated veneer lumber, and wood floor, in the 21st century.

2. Varieties of poplar products

As demand for timber increased, the supply of natural wood can no longer meet the demand. The lack of virgin forest makes the use of valuable timber becoming an extravagant hope, so those valuable timber replaced by a variety of fast-growing Poplar Glulam and Poplar wood composite. The emergence of such material ease the shortage of natural wood and it is beneficial to environmental protection, sustainable development of ecological environment. This material has some advantages of solid wood and overcomes shortcomings of

natural wood such as: dry-shrinkage and wet-expansion, not fire-resistant, low intensity. By the way, its low cost is welcomed by consumers. Varieties of poplar products include poplar composites board, poplar floor(multi-ply solid flooring and intensive composite floor), poplar technological door, curved laminated veneer poplar molding components, and poplar scientific wood.

3. Development of high-valued wood products made of poplar

(1) Use fast-growing poplar veneer and MDF to produce multi-layer wood floorings

A. Structural design of multi-layer wood floorings made of fast-growing poplar

At present, multi-layer wood floorings were commonly divided into two categories, one included three layers, and the other included multiple layers. Three-layer wood flooring was a kind of groove floor composed of ripping solid wood sheet as surface layer, solid wood panel as core layer, veneer as bottom; multi-layer wood flooring is composed of Sliced wood sheet (also ripping sheet) as surface layer, plywood as base material.

(A)Structural design of multi-layer wood floorings that used poplar veneer as the substrate

In order to overcome the above-mentioned common defects of multi-layer wood floorings, during the researching, the author directly selected poplar veneer, designed structure, formed multi-ply slab and then used complex gluing and pressing process to made them into substrate (they could be either an odd-numbered layer or be an even-numbered layer of specially designed, special slab) on the basis of multi-ply composite structure of the floor with the thickness requirements rather than select the formed multi-ply plywood as the substrate, then overlaid double-sided surface (overlaid the upper surface with high-quality veneer chipping, lower surface with ordinary peeling veneer), to ensure the shape stability and structure symmetry of multi-ply parquet. The structure was shown in Fig. 1.

(a) odd-numbered layer (b) even-numbered layer

1、5-painting layer 2-decorative sliced wood sheet 3-multi-ply veneer 4-peeling veneer

Fig. 1 The structure of multi-ply parquet use poplar veneer as substrate.

(B)Structural design of multi-layer wood floorings that used poplar veneer and HDF as the substrate

In order to make full use of fast-growing wood or small diameter log, waste material and other resources, to improve the comprehensive utilization of raw materials, to achieve high quality decorative effect of high-grade multi-layer wood floorings or solid wood floorings, the author made some new attempt and improvement, made research on the manufacturing technology of high quality multi-layer wood floorings which used poplar veneer and HDF as raw material, developed high-grade multi-layer wood floorings made of poplar veneer and HDF. The structure was shown in Fig. 2.

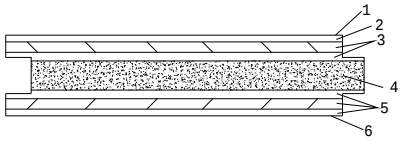

1、6-painting 2- decorative sliced wood sheet 3、5-multi-ply veneer 4-HDF

Fig. 2 The structure of multi-ply parquet use poplar veneer & HDP as substrate.

(2) Processing of multi-layer wood floorings made of poplar veneer

A. Processes of multi- layer wood floorings that used poplar veneer as the substrate

Specific production process was shown in Fig. 3:

1）raw poplar log→ peeling→ drying & leveling→ conditioning→ cutting ,splicing and selecting
pre-pressing ←slab forming ←gluing ←
hot pressing→ substrate cooling(conditioning)→ surface sanding
2）sliced sheet(wood peel)→ drying→ conditioning→ cutting ,splicing and selecting→ gluing
slab forming→ hot and gluing presssubstrate cooling(conditioning)→ dissecting→ conditioning
→ vertical and horizontal groove or tenon slot processing→ (back deformation slot cutting) → surface sanding→ (back and both sides painting)→ UV painting decoration→ inspection and grading→ packing→ products storage

Fig. 3 The "overlap together and gluing press twice" process of Multi-layer wood floorings use poplar veneer as substrate.

B. Processes of multi- layer wood floorings that used poplar veneer and HDF as the substrate

Specific production process was shown in Fig. 4:

1）raw poplar log→ peeling→ drying & leveling→ conditioning→ cutting ,splicing and selecting
2) poplar HDP→ conditioning→ cutting→ gluing
slab forming→ pre-press→ hot pressing→ substrate cooling(conditioning)→ surface sanding
3）sliced sheet(wood peel)→ drying→ conditioning→ cutting ,splicing and selecting→ gluing
slab forming→ hot and gluing presssubstrate cooling(conditioning)→ dissecting→ conditioning
→ vertical and horizontal groove or tenon slot processing→ (back deformation slot cutting) → surface sanding→ (back and both sides painting)→ UV painting decoration→ inspection and grading→ packing→ products storage

Fig. 4 The "overlap together and gluing press twice" process of Multi-layer wood floorings use poplar veneer & HDP as substrate.

(3) Use poplar veneer to produce curved furniture components

The processing of veneer bending and gluing was as follow: use multi-layer veneer with glue, and then combined according to the use of functional and human-scale ergonomics and needs for product design and structural design; compress and bend in particular mould and then gluing and molding, then made into various shapes of parts and components with different radius and curvature. The veneer bending and gluing was wildly used in bending components of chairs, sofas, tables and other furniture. This kind of products that had good dimensional stability can increase the utilization of timber.

(a)whole plate of seat surface backrest

(b)divided plate of seat surface backrest

(c)bending crosspiece of chairs

Fig. 5 Types of curved furniture components made of laminated poplar veneer.

In the past, domestic enterprises mainly used Manchurian Ash, Birch, and Linden and imports hardwood of high-quality. However, resources are scarce in recent years, in order to meet the needs of the market, so new raw material resource must be developed. Therefore, the author studied the manufacturing technology of bending and gluing curved furniture components which made of Italian Poplar and developed the curved furniture components that made of poplar veneer successfully. As Fig. 5 show, there were different types of curved furniture components made of laminated poplar veneer. By the process exploration, performance test and promoting the industrialization, the author summarized some factors that affect the quality of components as follow:（1）moisture of veneer；（2）thickness of veneer;（3）precision of the mould；（4）adhesive；（5）pressure application；（6）hot pressing technology；（7）assemble time

(4) Use poplar composites board to produce sofa frame

The main technological process was as follow（Fig. 6）:

material preparing→ discharge→ sawing→ buffing

seat frame assembling (the lower plate, upper plate, cross-file plate, column plate)
back frame assembling (cross-file plate, top plate, column plate)
arm frame assembling（arm top plate, arm front and back plate, cross-file plate）

→ integrated assembling→ trimming→ inspection→ finished products

Fig. 6　Technological process of sofa frame made of poplar composites.

As Fig. 7 showed, integral leisure sofa frame that made of poplar plywood, the up layer 1 and the down layer 3 of whose seat frame were spliced by some poplar plywood respectively, interface was trapezoidal, fixed by nail gun; the up and down layers of poplar composites board were fixed by column 2, each column 2 followed by staggered and closed to the up and down layers of poplar plywood 1 and 3 inside and outside. Back frame was composed by some backrest cross-file plate 5, backrest top plate 6 and backrest column, also fixed by nail gun, and the curved shape of whose components depended on the needs of sofa modeling. Handrail frame was composed by handrail top plate 8, arm column 9, cross-file 10 and arm front plate11.

1-seat frame down layer plate　2-seat frame column plate　3-seat frame up layer plate
4-seat frame cross-file plate　5-backrest cross-file plate　6-backrest top plate　7-backrest column plate
8-handrail top plate　9-handrail column plate　10-handrail cross-file plate　11-handrail front plate

Fig. 7　Structural frame of sofa made of poplar multiply wood.

4. Conclusion

Using poplar to produce furniture and wood products with high additional value achieved that the usage of poplar was turned from general use to high- grade use, non-load-bearing components to load-bearing components, nail-pattern structure to forming parts removable structure. It enlarged the fields of poplar wood processing and usage; also, it increased the added value and technology of poplar products. It achieved the target that using soft poplar as hard, using crude wood as precision, using poor material as fine. It was significant that poplar which was fast-growing, crude and soft gradually replaced those high-grade solid woods. So, how to use

poplar recourses and use wood modification and composite materials technology; study and develop poplar wood products with high additional value; as well as promote industrialization and form a large scale of specialization; replace high-grade solid woods materials and products; improve the additional value of poplar products and expend their application scope; upgrade the processing level of “Poplar Industry” will be a very important direction of development.

5. References

(1) Hua Yuhua, Hong Zhongli and Associates, The synthetic utilization of fast-growing poplar in wood based panels production, Proceedings of Properties and Utilization of Fast-growing Trees, Nanjing, China, 1994,10:185-189.
(2) Kai Wang, Xuhe Chen, Guangqi Chen, Recent research developments in processing and utilization of poplar wood in China, Proceedings of Properties and Utilization of Fast-growing Trees, Nanjing, China, 1994, 10:26-31.
(3) Wu ZH, Furuno T, Zhang BY, Properties of curved laminated veneer lumber made of fast-growing species with radio frequency heating for use in furniture, J Wood Sci, 1998, 44(4): 275-281.
(4) Wang Mingxiu, The industrial timber plantation of southern type poplar, Proceedings of China-Japan Symposium of Forming and Utilization of Fast-growing Trees, Nanjing, China, 2000, 5:1-4.
(5) Zhang Qinli, The processing and utilization of southern type poplar in China, Proceedings of China-Japan Symposium of Forming and Utilization of Fast-growing Trees, Nanjing, China, 2000, 5:83-86.
(6) Deng Lining, Outlook of China’s panel industry, China Forest Products Industry, 2003, 30:13-15.
(7) Yuhua Hua, Researches on bio-composites in China, Proceedings of the 7th Pacific Rim Bio-based Composites Symposium, Nanjing, China, 2004, 10:1~7.
(8) Qian Xiaoyu, Discussion on sustainable development of wood resources in China, China Wood-based Panels, 2005, 12(5): 8-11.
(9) Wu Zhihui, Xu Wei,Chen yushu,The technology for engineered solid wood flooring made of fast-growing poplar veneers and HDF, China forest products industry, 2008,35(2):29-33.
(10) Wu Zhihui, Xu Wei,Chen yushu,Quality requirement and control of engineered solid wood flooring made of fast-growing plplar veneers and HDF, China forest products industry ,2008,35(3):29-33.
(11) Xu Wei, Wu Zhihui, Test and analysis of mechnical properties of wood based panel applied on the structural frame in the sofa, China forest products industry, 2009,36(1):25-28.

Optimized Study on Technics Parameter of Wheatstalk/Polystyrene Composite

Min Xu, Jian Li and Yi-xing Liu

Key Laboratory of Bio-based Material Science and Technology of Ministry of Education, Northeast Forestry University, Harbin

Abstract: Wheat stalk and recycled polystyrene(PS) were used as raw material to hot press composite. Such as hot-pressing cycle time, density of composite, and ratio of PS to adhesive content were considered to affect composite properties by orthogonal experimental design and factors. Results showed that those factors made different effects. On the basis of available data, optimized process condition was confirmed : Hot press time of 7min, hot temperature of 190℃, PS proportion of 35%, and the amount of 3%,were a better combination when board density was 0.6 g/cm³or 0.65 g/cm³,the resulted composite meet the requirement of national standard.

1. Introduction

Wheat straw is a main kind of agricultural residue in many areas of the world. For example, there are more than one hundred million tons every year in China. However, most of them have not been reasonably used. One of the most unreasonable treatments is to burn wheat straw. Burning wheat straw not only wastes resource, but also pollutes the air, and disturbs the traffic safety of airport and highway. On the other hand, with the development of plastic industry, the problem of how to treat recycled plastic are increasingly serious [1]. It is reported that more than 40,000,000 tons plastic are required to recycle in the world every year [2]. Developing the manufacturing process of wheat straw/PS composite will be significantly important for reasonably utilizing agricultural residues, protecting environment and water resource, resolving the contradiction among human, resource and environment, and establishing a sustainable developing society [3].

In this paper, wheat straw and recycled polypropylene was cool-mixed and then hot-pressed to prepare wheat straw/recycled polypropylene composite and the optimal processing factors for preparing this composite was investigated.

2. Materials and methods

(1) Materials

A.Wheat straw

Wheat straw was stacked in lab for about 5 months and its moisture content (MC) was 5%. In processing, the MC of straw was conditioned to 10% before cutting into particles of 2mm to 4mm long. These particles were screened(Table 1).Only those between +4 # --40 # were conditioned to 14% MC for further using.

Table 1 Classifying value of straw shaving.

screen mesh	+4 #	+8 # -4 #	+16 # -8 #	+20 # -16 #	+40 # -20 #	-40 #
proportion/%	3.4	4.6	41.4	19.4	19.6	11.6

B. Plastic

Recycled PS pellets were shivered by a pulverizer. Particles over 40 # mesh were used.

C. Adhesive

Diphenyl methane diisocyanate（MDI）was used as adhesive and acetone as solvent. Polytetrafluoroethylene mylar film was used in hot pressing in case finished board stick to hot press platen.

(2) Methods

A. Process flow

Wheat straw was sprayed with MDI that solved in acetone and then mixed with PS uniformly. After manually spread, the mat was cold-pressed and then hot-pressed into 11mm board. After conditioned at 25℃ and 60% relative humidity, the mechanical properties of the board were measured according to Chinese National Standard (GB/T4897.1-4897.7-2003).

B. Preliminary experiment

The orthogonal experiments were conducted. In which hot pressing cycle time, composite density, portion of PS (with wide value range) was considered as effecting factors. The orthogonal experiment was designed as hot press time (5min, 7min, 9 min), density (0.55 g/cm^3, 0.60g/cm^3, 0.65 g/cm^3) and polystyrene proportion (0, 25%, 40%).

C. Fine experiment

Based on the results of the preliminary experiment, a fine experiment was designed as Table 2 to study the effects of PS portion, hot pressing temperature and adhesive content.

Table 2 Level of experiment factors.

Factors	Polystyrene proportion/%	Hot press temperature /℃	Adhesive content /%
1	25	185	4.5
2	30	190	3.5
3	35	195	2.5
Fixed factors	temperature：190℃	PS proportion： 30%	PS proportion：30%
1	density：0.6 g/cm³	density：0.6 g/cm³	density：0.6 g/cm³
2	time：7min	time：7min	time：7min
3	adhesive content：3.5%	adhesive content：3.5%	temperature：190℃

(3) Tests of the boards

According to Particleboard National Standard (GB/T4897.1-4897.7-2003), the properties such as internal bond strength (IB), modulus of rupture (MOR), modulus of elasticity (MOE), thickness swelling (TS), and moisture content (MC) were measured for evaluating board quality.

3. Results and discussion

Results of the orthogonal test, the k of the change factors and variance analysis were listed in Table 3, Table 4 and Table 5.

Table 3 Results of the test.

No.	IB/MPa	MOR/MPa	MOE/MPa	2hTS/%	MC/%
1	0.17	18.22	1864.33	4.04	4.81
2	0.30	21.49	1807.02	2.08	2.51
3	0.23	19.58	2206.02	1.14	1.48
4	0.24	18.65	1971.91	7.24	1.60
5	0.54	20.49	1935.11	3.52	1.39
6	0.29	25.91	2936.60	7.43	2.89
7	0.26	13.88	575.39	4.53	1.10
8	0.22	20.15	2266.86	5.46	1.52
9	0.42	26.73	2764.30	3.30	0.30

Table 4 The k of the change factors.

Average/k	level	time/min	density/g/cm³	PS Proportion /%
IB/MPa	k1	0.24	0.25	0.23
	k2	0.39	0.35	0.34
	k3	0.28	0.31	0.35
MOR/MPa	k1	19.76	16.92	21.43
	k2	21.82	20.84	22.29
	k3	20.34	24.07	18.12
2hTS/%	k1	2.59	6.06	5.75
	k2	6.06	3.69	4.21
	k3	5.11	4.02	3.80
W/%	k1	2.94	2.56	3.07
	k2	1.95	1.80	1.56
	k3	1.12	1.65	1.39

Table 5 The variance analysis and significance influence.

Factors	IB/Mpa	MOR/Mpa	2hTS/%	MC/%
Pressing time	0.53	2.66	9.38 **	4.89 *
Density	1.54	24.78 **	4.78 *	1.39
PS proportion	0.42	7.14 *	4.01 *	5.06 *
		F • (2,11)=3.98	F • (2,11)=7.21	

**: the high significant effect of factor. *: significant effect of factor. F: the significant value of factor

As table 5 showed, the effect of hot press time, density of board, PS proportion on IB was not significant. The effect of density on MOR was highly significant. PS proportion had significantly affected MOR. The effect of PS proportion on MOR was significant. The effect of hot pressing cycle time on TS was highly significant. The effect of density and PS proportion to MC was significant.

(1) The effect of PS proportion on mechanical properties

Table 6 The variance analysis of Polystyrene proportion.

PS proportion /%	IB/MPa	MOR/MPa	MC/%	2hTS/%
25	0.49	32.76	4.17	2.50
30	0.53	34.22	2.25	1.41
35	0.60	37.70	2.23	1.30
F	5.82*	0.10	0.94	6.02*

As Table 6 showed, the effect of PS proportion on IB was significant. The more PS used as bonding material, the higher IB was. PS was a nonpolar material. When PS content increased, wheat straw were enwrapped better the polymer, so it is difficult for water to permeate, and swelling decreased.

(2) The effect of hot pressing temperature on mechanical properties

Table 7 The variance analysis of temperature.

temperature/℃	IB/MPa	MOR/MPa	MC/%	2hTS/%
185	0.55	34.22	2.25	2.30
190	0.75	43.05	0.72	1.46
195	0.66	34.78	1.44	1.40
F	5.83*	30.82**	1.09	1.08

As table 7 showed, the effect of temperature on IB was significant; the effect of temperature on MOR was highly significant. When temperature raised from 185℃ to 190℃, PS melted better and strengthen the bonding between wheat straw and plastic, so IB and MOR were improved. When temperature further increased to 195℃, strength was lower. This is because higher temperature melted the plastic in the surface layer and MDI solidified quickly, which is difficult for inner water to evaporate out of the mat. Additionally, higher temperature caused wheat straw to degrade.

When temperature raised from 185 to 190℃, the MC of the composite declined because water evaporated out of the mat more quickly with temperature rising,. The more water came out, the lower the MC was. While temperature increased to 195℃, surface layer melted too quickly, hindering the water come out form the mat because the temperature was too high. The higher the temperature was, the lower the TS was. This was because that the higher the temperature was, the better the plastic melted. However, it was difficult for water to penetrate into the board.

(3) Effect of adhesive

Table 8 indicated that the effect of adhesive content on IB was significant. When adhesive was added, bonding strength was better between wheat straw and PS, so IB was improved. The effect of adhesive content on other properties of the board was not significant.

Table 8 The variance analysis of resin content.

resin content /%	IB/MPa	MOR/MPa	MC/%	2hTS/%
4.5	0.83	39.06	0.65	1.30
3.5	0.78	37.33	1.74	1.50
2.5	0.53	32.14	1.49	1.80
F	5.64*	1.14	1.12	0.98

(4) The optimal technical factors

The optimized technical parameters were summarized as in Table 9.

Table 9 Optimized parameter of process.

Condition	time/min	PS proportion/%	temperature/℃	Resin content/%	Density/g/cm^3
Value	7	35	190	3.5	6.0 / 6.5

(5) Verifying experiment

Using to the optimal parameters listed in Table 11, wheat straw/PS composites were prepared. Their properties are showed inTable 10.

Table 10 Properties of wheat straw/PP composite.

Density/g/cm³	IB/MPa	MOR/MPa	MC/%	2hTS/%	24 hTS/%
0.60	0.40	20.33	1.07	2.11	5.32
0.65	0.42	20.43	1.02	2.01	4.07

As Table 10 showed, when board density was 0.6 g/cm³ and 0.65 g/cm³, all the mechanical properties of the composite met the National Standard (GB/T4897.1-4897.7-2003) except IB.

4. Conclusions

(1) Wheat straw particleboard can be made with wheat straw and recycled PS, and the mechanical properties met the Chinese National Standard.

(2) Adding PS could reduce the needed quantity of MDI and reduce the cost of the manufacture of wheat straw particleboard.

(3) The optimal process parameters were studied: hot pressing recycle time was 7 minutes, temperature was 190℃, PS proportion was 35%, resin content was 3%, density was 0.6 g/cm³ and 0.65 g/cm³, which will provide a foundation for the future study.

5. References

(1) Liang-BH, Mott-L,Shaler-SM, Caneba-GT. Properties of transfer-molded wood-fiber polystyrene composites. Wood-and-Fiber-Science. 1994, 26: 3, 382-389

(2) Mehrabzadeh M., Farahmand F., Recycling of Commingled Plastic Waste Containing Polypropylene, Polyethylene and Paper. Journal of Polymer Science. 2000, 80: 2573-2577

(3) Clemons C., Composites in the United States. The Interfacing of Two Industries. 2001, 20(8): 697-717

Torque Rheological Properties of Bamboo Flour/PP Composites

Wenbin Yang and Enhui Chen
Material and Engineering College, Fujian Agricultural and Forestry University, Fuzhou

Abstract: The rheological behavior of plant flour reinforced thermoplastics composites is very important to practical industry, however few research especially research about bamboo flour reinforced polypropylene(PP) composites is available regarding rheological field. In this paper, the torque rheometer made in Shanghai was used to examine the flow behavior of bamboo flour filled PP composites. The orthogonal test was adopted to analyze how three factors(weight percentage of bamboo, weight percentage of MAPP and rotate speed) influence the behavior of composites. The result indicated that bamboo flour filled PP composites was pseudo-plastics or shear-thinning flow under the experimental condition investigated. The effect of weight percentage of bamboo on rheological peoperties was signigficant,but the effect of both of the rest of two factors on rheological was not significant under the given experimental condition.

1. Introduction

Plant fiber reinforced thermoplastic composites has been a hot topic and practices in both wood industry and plastic industry in the past decade owing to the economic advantage and its reinforcing possibility as filler for thermoplastic. The commercial markets for this composites are mostly frequently termed wood plastic composites(WPC) both in North America and China. The experts predicted that industrial added value of WPC in China would reach up to 80 billion yuan by 2010[1]. However, most of plant fiber used in WPC are wood fiber[2-5]. In Fujian Province of China, there is very plenty of bamboo with high strength and modulus, and its specific strength and modulus are from 220MPa·cm^3/g to 23MPa·cm^3/g respectively[6]. And also, it could be cut in shorter cycle than wood. But just a few paper about bamboo fiber filled plastic composites could be found[7]. Many technical issues regarding WPCs have been well studied. Because the melt rheology is critical to WPC processing issuses but poorly understood by WPC industries, the objectives of this research are to investigate the effect of content of bamboo flour, types of coupling agent, rotate speed on rheological properties of bamboo flour filled polypropylene composites.

2. Materials and methods

(1) Materials and instrument

Bamboo flour pretreatment: bamboo flour was screened by 20 mesh screener and dried for 8 hours at 100 ℃; Polypropylene: 225 type, which is commercially available from Nanjing Jin Ling Plastic Chemical industry Ltd.; Coupling agent: MAPP; Lubricant: stearic acid.

The torque rheological properties was carried out by using torque rheometer(XSS-300, made by Shanghai Kechuang Plastic Machinery Ltd. of China).

(2) Methods

Because the complicated interaction of each constituent among composites, the orthogonal experiment was adopted to analyze the torque rheological properties of composites. The selection of factors and levels for experiment were shown in Table 1. The arrangement based on table 1 was shown in Table 2.

Bamboo flour filled polypropylene composites was mixed inside confined space by using torque rheometer as shown in Fig.1. There are three heating parts in mixer(Fig. 1), front heating panel, middle heating region, back heating panel, in which the temperature was set at 190℃； 190℃； 185℃ respectively. At the same time, the pre-blended compound which were consist of bamboo flour, polypropylene, coupling agent and lubricant were prepared based on Table 2 under room temperature for the torque test. The weight of lubricant was 2% of polypropylene's in all testing plans. When the temperature at each heating region reach the set temperature, the pre-blended compound based on experimental design were pour into torque mixer,then the torque of bamboo

flour filled PP could be acquired.

Table 1 Factors and levels of orthogonal experiment with MAPP as coupling agent.

Factors / levels	bamboo /%(PP based)	MAPP/%(bamboo based)	Rotate speed/rpm
1	20	2	45
2	30	4	55
3	40	6	65

3. Results and discussion

(1) Determination of fluid type of composites

The typical rheological behavior of bamboo/PP composites in the process of its melting was shown in Fig.1 during which the weight of bamboo is 30% of PP's, rotate speed was 55rpm. There are two curves in Fig.1 for temperature vs. time(lower one) and torque vs. time(upper one) respectively. Because of the limited space of mixer, the compound must be added in two batches. The torque profile shown in Fig. 1 could be divided into 4 stages. In the first stage, the pre-blended compound was put into mixer first time, the torque was increased dramatically and the first peak of torque occurred because of adding the solid compound while the temperature decreased rapidly ,which is caused by adding the cold compound and endothermal melting process. In the second stage, the polypropylene began to melt and bamboo flour dispersed in the PP matrix, the torque began to decrease along with the constant increase of temperature. When the polypropylene melt down and bamboo flour were dispersed completely, the torque fell down quickly to certain value, at this time the compound was put into mixer second time. In the third stage after second feeding, because of adding the solid compound into melt compound, fluidity of composites decreased and resulted in rapid increase of torque while the temperature declined, which is caused by the adding of compound with room temperature. The second peak of torque occurred soon after charging of compound. In last stage, the torque declined fast while the temperature rised. Along with the PP melt down thoroughly, the torque decreased dramatically and then leveled off while the temperature rised then stabilized.

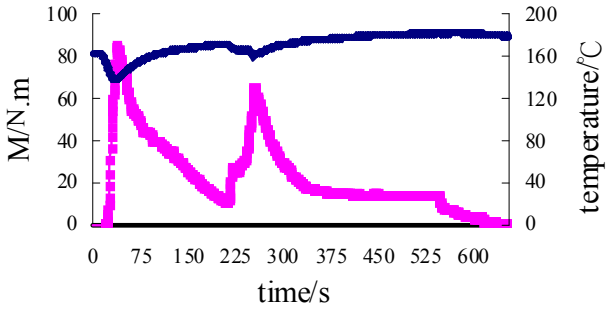

Fig. 1 Mixing torque profile of composites.

In order to determine the type of fluid for composites, the formulation [12] which is an empirical method brought forward by Marquez to calibrate the measuring head of a torque-rheometer to obtain the power-law parameters of polymer melts was shown below and based on the classical power law model where the power law index *n* is directly evaluated from a set of data containing angular velocity *S,* torque *M*, and the consistency index *m*

$$M = C(n)mS^n \tag{1}$$

Because there is a relationship between angular velocity and rotate speed:

$$\text{Angular velocity} = 2\pi \times \text{rotate speed} \quad (2)$$

we can calculate out "*n*" and "*C(n)m*" if corresponding value from Table 3 were substituted into equation (1) and equation (2). The calculating result is that *n*=0.269 and *C(n)m*=2.70 respectively. According to the value of *n*, we can decide that the fluid type of composites is pseudoplastic melt. So it doesn't have yield stress and would be shear thinned fluid from the power function equation (3):

$$\tau = K\gamma^{a} \quad (3)$$

Where,

K——fluid consistency; *a*——non-Newton index;

τ——shearing stress; *γ*——shearing rate

Table 3 The result of torque at 2 kinds of rotate speed.

bamboo /%(PP based)	MAPP/%(bamboo based)	Rotate speed/rpm	Equilibrium torque/N.m
20	2	55	13
20	2	65	13.6

(2) Analysis of results of orthogonal test

Equilibrium torque of composites based on designed orthogonal test were listed in Table 4. Based on Table 2 and Table 4, the range analysis for the orthogonal test was made on which the Intuitive analysis Fig. 2 about the three influencing factors were based. As we know, bamboo flour would not melt at the designed temperature but the PP has melted, so the bamboo flour adding into PP would hinder melted PP from flowing. The result in table 5 was coincident with this viewpoint. The maximum range among three influencing factors is 7.9 for bamboo which showed that the weight percentage of bamboo was the first effecting factor on rheological behavior of bamboo/PP composites. From Fig. 2(a), we could find that the equibrium torque increased remarkably with the increase of bamboo's weight percentage because of the increasing viscosity of the melt. This can be attributed to the increase in slip resistance between the additional bamboo particles that are contained within the melt. This result is in agreement with results found for both HDPE-wood systems [13,14] and other highly filled plastics [15,16]. Variance analysis results revealed that the effect of weight percentage of bamboo on torque was extremely significant(shown in Table 5).

Table 4 The results of orthogonal test based on Table 2.

Plans	1	2	3	4	5	6	7	8	9
Equilibrium torque/N.m	7.9	10.3	10.9	15.4	15.5	13.7	18.5	16.6	17.7

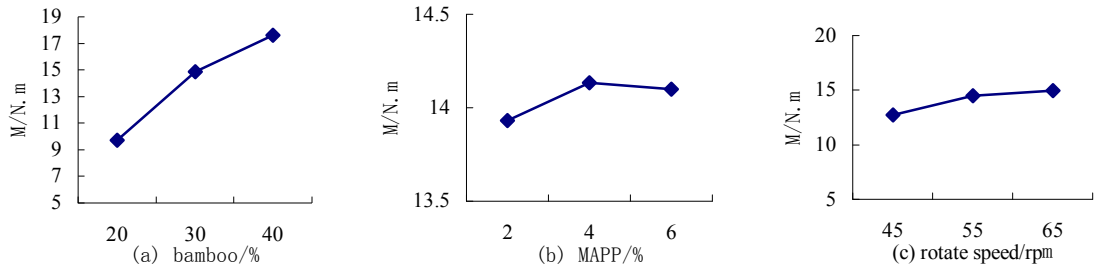

Fig. 2 Intuitive analysis about the three influencing factors.

The torque increased with the increasing rotate speed as shown in Fig. 2(c), this result could be explained by

the increase of shear stress and rotate speed because it was pseudoplastic melt proved previously. There is a good agreement for the experimental torque with other people's work. Li's experiment demonstrated that the torque of PVC melt increased with the rotate speed[17]. But variance analysis in Table 5 showed that the effect of rotate speed on torque of composites is not significant, this could be possibly attributed to the low range of rotate speed designed in orthogonal test.

In order to improve the affinity and adhesion between plant fiber and thermoplastic matrices in production in order to improve the mechanical properties of composites, chemical coupling agents especially MAPP have often been employed [18-20]. As shown in Table 5, the range of MAPP is the least among three influencing factors and only 0.200 when the weight percentage of MAPP varied from 2wt%-6wt%. The effect of weight percentage of MAPP on the torque is presented on Fig. 2(b). When weight percentage of MAPP increased from 2wt% to 4wt%, the torque increased slightly, but decreased slightly when weight percentage of MAPP increased sequentially from 4wt% to 6wt%. Variance analysis in Table 5 indicated that the weight percentage of MAPP is not a significant influencing factor. This result is similar to the result in Sonia's experiment. He found that the functionalized polyolefins showed flow behavior similar to that of PP homopolymer[21]. It could possibly been attributed to the existence of lubricant which weakened the contribution of MAPP on composite torque.

Table 5 Variance Analysis.

Factors	Sum of deviation square	Free degree	Ratio of F	Significant
bamboo /%(PP based)	96.576	2	162.040	*
MAPP/%(bamboo based)	0.069	2	0.116	
Rotate speed/rpm	8.242	2	13.829	
erros	0.60	2		

Note：$F_{0.05}(2,2)=19.000$; $F_{0.10}(2,2)=9.000$; $F_{0.01}(2,2)=99.000$

4. Conclusion

(1) Melt type of bamboo flour/PP composites is pseudoplastic.
(2) Weight percentage of bamboo is significant effecting factor on torque of composites, the torque of composites increases with the increase of weight percentage of bamboo.
(3) Although rotate speed in the range of designed test didn't significantly influence the torque of composites, the torque of composites increased with the increasing rotate speed.
(4) The MAPP did not significantly influence the torque of composites in the range of test.

Viscoelastic Properties of MAPP-modified Wood Flour /Polypropylene Composites

Jin-zhen Cao, Wei-Yue Xu, Lei Wang and Guang-jie Zhao
Faculty of Material Science and Technology, Beijing Forestry University, Beijing

Abstract: The viscoelastic properties of MAPP ()-modified wood flour / polypropylene composite (MAPP-WPC) were investigated by both compression stress relaxation method and dynamic mechanical analysis (DMA). Three wood to polymer ratios (40:60, 60:40, and 80:20) and five MAPP loading levels (0, 1, 2, 4, 8 %) were used to study their effects on the viscoelastic properties of MAPP-WPC. The results showed that: (1) higher wood to polymer ratio corresponds to higher stress relaxation for unmodified WPC. The modification with MAPP has obvious effect on the stress relaxation of MAPP-WPC at higher wood to polymer ratios (60:40 and 80:20), but almost no effect at a wood to polymer ratio of 40: 60. The optimal MAPP loading level for the wood to polymer ratio of 60:40 appears at 1 %; (2) the storage modulus reaches the maximum at a MAPP loading level of 1 % for wood to polymer ratios of 40:60 and 60:40, while for wood to polymer ratio of 80:20, higher storage modulus is observed at higher MAPP loading levels, which is quite consistent with the stress relaxation results. The results suggested that a suitable loading level of MAPP has a positive effect on the viscoelastic properties of WPC at higher wood to polymer ratios. Excessive MAPP loading would result in adverse effect.

1. Introduction

In recent years, wood flour/PP composites have received considerable attention from both academic and commercial sides. Since wood flour is hydrophilic and PP is hydrophobic, there is problem with compatibility between these two materials. Usually, this problem can be alleviated by surface treatment of wood fibers or adding coupling agent [1-2]. There are a lot of research concerning the mechanical properties of wood flour/PP composites and the effect of coupling agent on the mechanical properties [3-5]. However, the viscoelastic properties of wood flour/PP composites have seldom been investigated. The viscoelastic properties of a material are highly related to its short-term or long-term dimensional stability under static or dynamic loadings. Nunez et al. [6-7] once studied the creep and dynamic mechanical behavior of wood flour/PP composites, and they found that the creep deformation was generally reduced with the addition of wood flour, except at very high filler concentrations because of filler-wetting and dispersion problems. In this study, we proposed to study the compressive stress relaxation and also the dynamic mechanical behavior of wood flour/PP composites at different wood to polymer ratios and different maleated polypropylene (MAPP) loading levels, and therefore, to investigate the effect of MAPP on long-term deformation or dynamic deformation at different wood to polymer ratios.

2. Materials and Methods

(1) Preparation of MAPP-WPC.

The MAPP-WPC was prepared by using the wood flour of poplar (*Populus tomentasa*. Carr) with a size over 100 mesh and polypropylene flour as raw materials and MAPP as the coupling agent. The selected wood to polymer ratios were 80:20, 60:40, and 40:60, respectively. At a same wood to polymer ratio, five different MAPP loading levels were used, which are respectively 0, 1, 2, 4, and 8% of the total weight of wood and polymer. After weighing, the wood flour, PP flour and MAPP were put into the high-speed mixer. The mixture was then dried in an oven for 2 h and taken out for hand matting. A laboratory hot press was used to compress the mat at 180 ℃ and 4MPa for 6 min. Polyfluortetraethylene (PTFE) membrane was used as demoulding material during hot-pressing. After hot pressing, the formed mat was pressed at 20 ℃ and 4 MPa for another 6 min. The same

This study is financially supported by the National Natural Science Foundation of China (NSFC) No. 30871966.

method was used to prepare the mats of wood and PP controls.

(2) Stress relaxation determination

The stress relaxation tests were performed on a self-designed equipment, which was composed by electric system, mechanical system (including the compression plates), heating system, cooling system, and control system. In this study, the air-dried WPC or wood and PP controls were fixed at first in the compression plates and then compressed for 20% of the original thickness. After compression, the stress produced inside the sample was detected by the sensor and transmitted to the computer, which was recorded as f(0). The temperature during the tests keeps at 26 ± 1℃. The test duration for each sample was 3000 s. Therefore, the stress inside the sample after 3000 s was also recorded as f(3000). The percentage of relaxed stress was then calculated by [f(0)-f(3000)]/f(0)×100%. For each condition, five measurements were carried out and their average value was taken as the final result.

(3) DMA determination

The viscoelastic properties of oven-dried WPC or wood and PP controls were performed on a dynamic mechanical analyzer (DMA-242C) by using 3-point bending mode. The temperature ranged from -40℃ to 150℃, and the frequency kept at 5 Hz. The data were collected automatically by the equipment and transformed to figures.

3. Results and Discussion

(1) Stress relaxation of MAPP-WPC

The percentage of relaxed stress at 3000 s based on the initial stress was recorded for MAPP-WPC with different wood to polymer ratios and MAPP loading levels, together with the wood and polymer controls. As shown in Fig. 1, pure polypropylene (PP) and wood both appear higher stress relaxation than their composites, suggesting that the long-time deformation can be improved by combining these two materials together. For unmodified WPC (No MAPP), the higher wood to polymer ratio corresponds to higher stress relaxation. However, after the addition of MAPP, different changing trend was observed. At lower wood to polymer ratio, for example, 40: 60, MAPP has negligible influence on the stress relaxation of MAPP-WPC; while at the wood to polymer ratio of 60:40, the influence from MAPP became significant and the lowest stress relaxation appeared at MAPP loading of 1%; when the wood percentage reached 80%, the stress relaxation was obviously reduced by the addition of MAPP and it decreased continuously with the increasing MAPP loading within the experiment range in this study. It suggests that the optimal loading of MAPP for a superior anti-deformation WPC is highly dependent on the wood to polymer ratio. At low wood to polymer ratio, the addition of MAPP can not reduce the long-term deformation of wood/polypropylene composite. For wood percentages higher than 60%, MAPP can play a significant role in improving the long-term performance. There is an optimal loading of MAPP, which depends on the wood to polymer ratio.

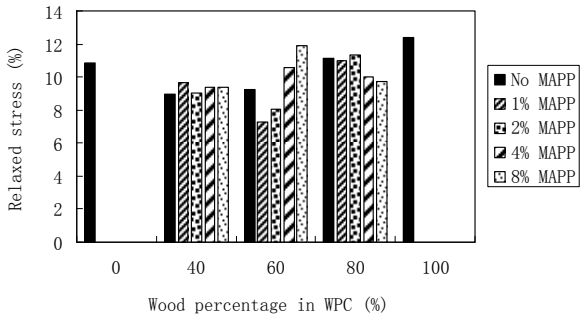

Fig. 1 The percentages of relaxed stress after 3000 s for MAPP-WPC with different wood percentages and MAPP loadings. Wood percentage of 0 % and 100 % represent polypropylene and wood controls, respectively.

(2) DMA analysis of MAPP-WPC

The storage modulus E′ and loss factor tanδ of wood/PP composites and wood, PP controls were determined within the temperature range from -40 to 150 ℃. The temperature spectra at wood to polymer ratios of 60:40 are shown in Fig. 2 as an example. The ability of the samples against deformation can be shown by the viscoelastic properties. The storage modulus represents the elastic part of the sample, and higher storage modulus corresponds to higher resistance to deformation; while the loss factor represents the viscous part of the sample, and higher loss factor means easier deformation.

As shown in Fig. 2a, E′ of wood flour almost keeps unchanged within the whole temperature range, while E′ of PP decreases obviously with the increasing temperature. It suggests that the deformation of PP is much more temperature-sensitive than wood. At higher temperatures, the deformation of PP is much more significant. The critical temperature seems appear at around 15 ℃, below which PP is stable than wood but above which reverse result can be observed.

The storage modulus of wood/PP composites are much higher than PP control, which means that the dimensional stability would be improved by combining these two materials together. The curves appear similar trend with PP control, namely, E′ decreases obviously with the increasing temperature. Compared with wood control, E′ of wood/PP composites shows much higher value than it at relatively lower temperatures. The intersection points of the E′ curves of wood/PP composites and wood control are found from 90 to 110 ℃ for ratio of 60:40, which is much higher than 15 ℃ for PP control. Therefore, within usually used temperature range, the dimensional stability of wood/PP composites is higher than both wood and PP controls.

The addition of MAPP also has effect on the storage modulus of wood/PP composites, especially at lower temperatures. At wood to polymer ratio of 60:40, the highest storage modulus was observed for MAPP-WPC at a MAPP loading of 1%. Excessive MAPP loading has a negative effect on increasing storage modulus. The curves of storage modulus at wood to polymer ratio of 80:20 were not given here for space limitation, which showed highest storage modulus at the highest MAPP loading used in this study. Therefore, the effect of MAPP on storage modulus is dependent on the wood to polymer ratio. It is much obvious and more MAPP is required to improve the elastic properties of wood/PP composite at higher wood to polymer ratio. This result is consistent with the stress relaxation result.

The loss factor of wood, PP, and MAPP-WPC are shown in Fig. 2b. As shown in the figure, the loss factor of wood control has not changed much within the measured temperature range, while for PP control two peaks were observed respectively around 0 ℃ and 80 ℃. However, at higher wood to polymer ratios such as 60:40, both peaks disappeared and the curves were more inclined to wood control.

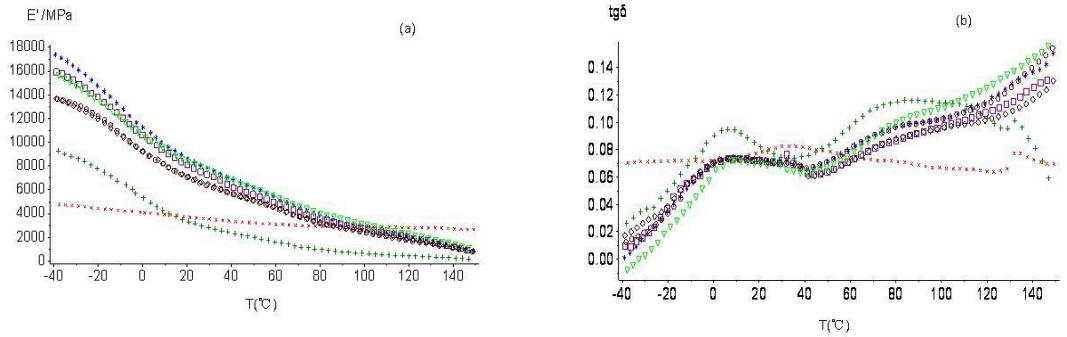

▽: No MAPP; *: 1% MAPP; □: 2% MAPP; ○: 4% MAPP; ◇: 8% MAPP; +: polypropylene control; ×: wood powder control.

Fig. 2 Temperature spectra of storage modulus (a) and loss factor (b) of MAPP-WPC with different MAPP loadings at a wood to polymer ratio of 60:40.

4. Summary

The viscoelastic properties of MAPP-modified wood/PP composites observed from both stress relaxation and DMA approaches are quite consistent in the following aspects. First, the composition of wood and PP can improve the dimensional stability compared with wood and PP controls; secondly, at lower wood to polymer ratios, the effect of MAPP is not obvious; while at higher wood to polymer ratios, MAPP shows significant effect on improving the dimensional stability; Finally, there is an optimal MAPP loading for wood/PP composites. For wood to polymer ratio of 60:40, the optimal MAPP loading appears at 1%. Excessive MAPP loading would result in adverse effect.

5. References

(1) Bledzki A. K., Gassan J.: Prog Polym Sci., Vol. 24(1999) p. 22-274
(2) Filex, J. M., Gatenholm P.: Appl. Polym. Sci., Vol. 42(1991)p. 609-620
(3) Kokta B. V.，Raj R.G.，Daneault C.: Polymer-Plastics Technology and Engineering, Vol. 28 (1989）p. 247-259
(4) Krzysik A.M., Youngquist J.A.: International Journal of Adhesion and Adhesives，Vol.11 (1991) p. 235-240
(5) Qin T., Huang L., Li G.: Journal of Forestry Research, Vol. 16 (2005) p. 241-244
(6) Nunez A. J., Kenny J. M., Reboredo M. M., et al.: Polymer Engineering and Science, Vol. 42 (2002) p. 733-742
(7) Nunez A. J., Marcovich N. E., Aranguren M. I.: Polymer Engineering and Science, Vol. 44 (2004) p.1594-1603

Effects of Carbonization Temperatures in an Earthen Kiln on the Properties of Bamboo Charcoal

Gwo-Shyong Hwang, Chin-Mei Lee, Hsin-Yi Yu and Ying-Shen Wang
Division of Forestry Utilization, Taiwan Forestry Research Institute. Taipei

Abstract: Moso bamboo, Makino bamboo and Ma bamboo were used for charcoal making in an earthen kiln. The bamboo specimens cut to 4-6 cm in width and 20 cm in length were put into a cylinder made by stainless steel. Five cylinders were piled up to 1 m in height. The carbonization temperature in each cylinder was respectively measured using a K-type thermocouple. In order to investigate the properties of bamboo charcoal affected by the carbonization temperature difference in the earthen kiln, PH, true density, electric resistivity and specific surface area tests were performed for specimens sampled from the different cylinder. From the results of the processes of carbonization temperatures at each cylinder in the earthen kiln, the curves of different temperatures were obtained. The highest carbonization temperature in each cylinder at end of carbonizing was 774℃, 745℃, 695℃, 609℃ and 537℃, respectively, from the top to the bottom. The pH of bamboo charcoals were at the range of 0.96-10.26 and were not obviously affected by the species and carbonization temperature. The true density of bamboo charcoal increased with the increase of carbonization temperature. The electric resistivity of three kinds of bamboo charcoal decreased significantly with the increase of carbonization temperature. For any kind of bamboo charcoal, the specific surface area increased with the increase of carbonization temperature.

1. Introduction

Bamboo charcoal has a wide variety of applications, for example, humidity control, deoderization, fresh-keeping, water purification, soil improvement etc. Bamboo charcoal offer us not only a good environment for life, but also a raw material to industries for developing new products.

In order to solve the downcast prosperity problem of bamboo processing industries, investigation of the local industries on the products of bamboo charcoals and manufacture of high quality charcoals by local bamboo species are very essential.

Taiwan forestry research institute (TFRI) has started to develop bamboo charcoal making from 2002 to use the domestic bamboo effectively. The earthen kiln building technology and the charcoal making technology reached maturity after a half year. TFRI built 16 seat charcoal kilns in Taiwan until 2008 and taught charcoal making technology to the farmer group for promoting domestic bamboo charcoal industry. Recently, we have published some research papers in Taiwan (Lin et al. 2004, Hwang et al. 2004, Hwang et al. 2006).

2. Materials and methods

Moso bamboo, Makino bamboo and Ma bamboo cut to 4-6 cm in width and 20 cm in length after heat-treating with smoke and air-drying were used for charcoal making with difference of temperature in an earthen kiln. The kiln was 2.8 m wide and 2.8 m long and 1.4 m high with an arch-type ceiling is shown in Fig. 1. Three kinds of bamboo specimens were put into a cylinder made by stainless steel, bored 5 mm holes in diameter, with 20 cm in diameter and 20 cm in height. Five cylinders piled up to 1 m in height were installed at rear part in 30 centimeters away from the bottom of the chimney flue at rear part of kiln. The carbonization temperature in each cylinder was respectively measured using a K-type thermo -couple. In order to investigate the properties of bamboo charcoal affected by the carbonization temperature difference in the earthen kiln, PH, true density, electric resistivity and specific surface area tests were performed for specimens sampled from the different cylinder.

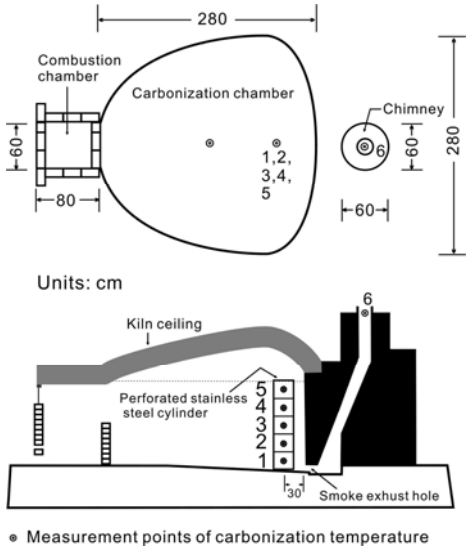

Fig. 1 Dimensions of the earthen kiln and measurement points (No.1-6) of carbonization temperature.

3. Results and discussion

The properties of material for test are shown in Table 1 shows the specific gravity of Moso bamboo, Makino bamboo and Ma bamboo is 0.91, 0.87 and 0.78, respectively.

Table 1. Properties of bamboo for test.

Species	Moisture Content (%)	Specific gravity	Thickness of culm wall (mm)
Moso bamboo	9.43	0.87	10.01
Makino bamboo	10.77	0.91	6.86
Ma bamboo	10.93	0.78	11.38

From the results of the processes of carbonization temperatures at each cylinder in the earthen kiln, the curves of different temperatures are showed in Fig. 2. The carbonization speed of bamboo in the upper was earlier and more rapid than those in the lower. The highest carbonization temperature in each cylinder at end of carbonizing was 774℃, 745℃, 695℃, 609℃ and 537℃, respectively, from the top to the bottom. The pH of bamboo charcoals shown in Table 2 were at the range of 0.96-10.26 and were not obviously affected by the bamboo species and carbonization temperature. The true density of bamboo.

charcoal shown in Table 3 increased with the increase of carbonization temperature. At the same carbonization temperature, the true density of Ma bamboo charcoal was the greatest, and the Makino bamboo charcoal was the next, and the Moso bamboo charcoal was the smallest. The electric resistivity of three kinds of bamboo charcoal shown in Table 4 decreased significantly with the increase of carbonization temperature, but the electric resistivity of Makino bamboo charcoal was smaller than those of Moso bamboo charcoal and Ma bamboo charcoal at the same carbonization temperature. The results for the specific surface area performance of the three kinds of bamboo charcoal with different carbonization temperature are shown in Table 5. Table 5 indicate the specific surface area increased with the increase of carbonization temperature for any kind of bamboo charcoal.

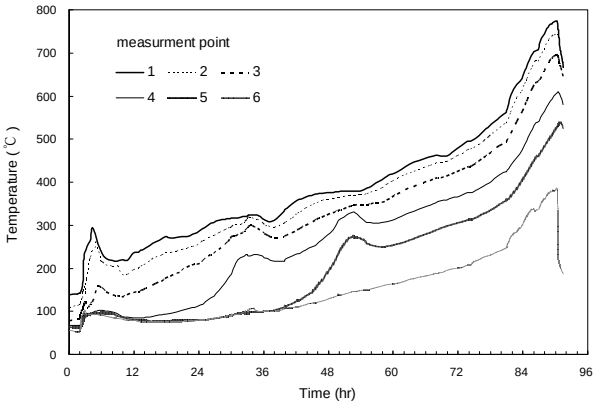

Fig. 2 Temperature curves of the carbonization processes. (measurement points 1-6 are shown in Fig. 1).

Table 2. The PH of bamboo charcoal at different carbonization temperature.

Carbonization temperature (℃)	pH		
	Moso bamboo	Makino bamboo	Ma bamboo
774	9.88	9.94	10.26
745	9.12	9.46	9.96
695	8.96	9.18	9.46
609	9.37	9.10	9.66
537	9.54	9.61	9.66

Table 3. The true density of bamboo charcoal at different carbonization temperature.

Carbonization temperature (℃)	true density (g/cm^3)		
	Moso bamboo	Makino bamboo	Ma bamboo
774	1.95	1.96	2.04
745	1.87	1.90	1.91
695	1.76	1.77	1.79
609	1.58	1.61	1.62
537	1.51	1.52	1.52

Table 4. Electric resistivity of bamboo charcoal at different carbonization temperature.

Carbonization temperature (℃)	Electric resistivity (Ω·cm)		
	Moso bamboo	Makino bamboo	Ma bamboo
774	1.2×10^{0}	0.8×10^{0}	1.6×10^{0}
745	1.3×10^{0}	1.1×10^{0}	2.2×10^{0}
695	3.2×10^{1}	1.9×10^{1}	3.7×10^{1}
609	9.0×10^{4}	8.3×10^{3}	1.1×10^{4}
537	1.4×10^{6}	8.9×10^{5}	1.0×10^{6}

Table 5. The specific surface area of bamboo charcoal at different carbonization temperature.

Carbonization temperature (℃)	Specific surface area (m^2/g)		
	Moso bamboo	Makino bamboo	Ma bamboo
774	369.71	358.01	408.83
745	294.45	273.42	304.66
695	215.27	226.91	197.42
609	183.36	92.91	144.37
537	67.13	23.85	42.94

4. Literature cited

(1) Lin YJ, Hwang GS, Yu HY. 2004. Cost analysis for the building of bamboo charcoal kiln. Qua J Chinese For 37(2):195-204.

(2) Hwang GS, Yu HY, Toba A. 2004. Effects of carbonization temperatures in an earthen kiln on the true density and electric resistivity of Makino bamboo charcoal. Taiwan J For Sci 19(3):237-245.

(3) Hwang GS, Ho CL, Yu HY, Su YC. 2006 Bamboo vinegar collected during charcoal making with an earthen kiln and its basic properties. Taiwan J For Sci 21(4):547~57.

Study on the Visco-elastic Behavior of Rice Husk/HDPE Composites

Dagang Li[1], Jing Yongtao[1] and Zenyuan Wu[2]

[1] Nanjing Forestry University, Nanjing Long Pan Road 159, 210037, China

[2] Nanjing Jufeng Advanced Materials Co., LTD, 210042, China

Abstract: As a new kind of material, the WPC (Wood and Plastic Composite) has absorbed more and more attention from people. But the impediment to utilize these materials is the lack of comprehension about the performance of WPC. Two aspects are included in this paper, the first interest is the long-term creep performance of the WPC by using the short-term creep testing procedure; second is the time temperature superposition of WPC.

1. Introduction

Wood-plastic composites, which are described as thermoplastics reinforced with wood fiber, have been produced in China for several years. Although the industrial demand for WPC in structural applications is no match for that of traditional materials like steel, concrete, or timber, the market has steadily grown over with the discovery and understanding of some of the structural advantages associated with WPC. Many natural fibers, including jute, wheat, hemp, flax straw, sugarcane, etc., can be combined with plastics to improve mechanical performance and dimensional and thermal stability. WPC utilizes the natural fiber of wood flour as an alternative to synthetic filler, which creates a renewable and biodegradable composite with lower density, less abrasiveness, and lower cost. Plastic wastes are a major component of global municipal solid waste and provide a new and promising raw material source for the manufacture of WPC. Recyclable plastics that melt and can be processed below the degradation temperature of wood are normally suitable for use in extrusion of WPC.

2. Visco-elastic models and prony series model of the WPC

In order to describe more complex viscoelastic behavior, models utilizing combinations of springs (Hookeian behavior) and dashpots (time dependent behavior) in parallel or series, or combinations of both have been developed. The Kelvin and Maxwell models are mentioned as Fig.1. A Prony Series can be described as N Kelvin elements (springs and dashpots in parallel) in series with a lone spring, as shown in Fig. 2 and equation (1).

$$D(t) = D_0 + \sum_{i=1}^{n} D_i[1 - e^{\frac{-t}{\tau i}}] \qquad (1)$$

Where: D_0 and D_i, are positive constants, and where τ_i is the retardation time.

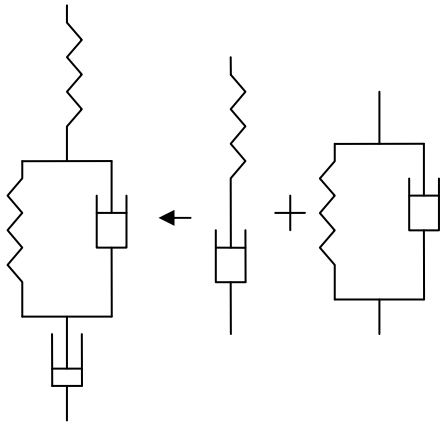

Fig.1 Four-element mechanics model

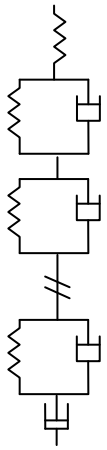

Fig. 2 Multiple elements mechanics model

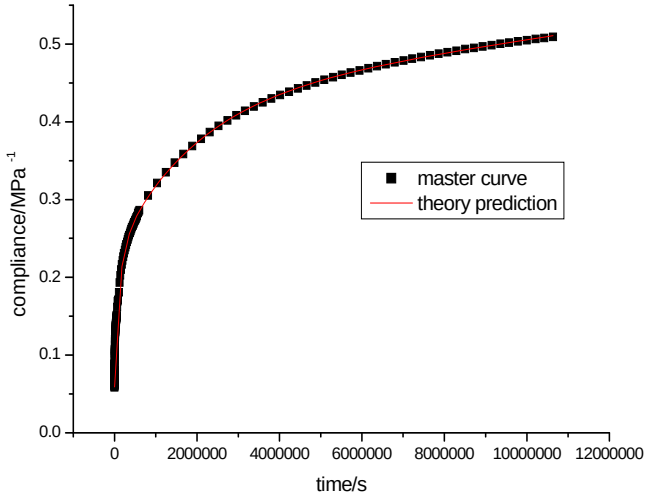

Fig. 3 Ten–elements model and fitting constants.

The spring dashpot models are very versatile in that additional stiffness and damping mechanisms can model varying modes of viscoelastic response occurring in long duration tests when compared to the power law model which models only one mode. There are many other forms of the time dependent compliance used to model viscoelastic behavior which will be explored in the next section.

We have modeled the behavior of WPC with viscoplastic models, compared a non-linear viscoelastic model consisting of a spring and nine Kelvin elements and a viscoplastic model that assumes that both elastic and inelastic deformation occur at all stages of loading. The viscoplastic model was found to better fit rapid loading and loading rate changes.

The short term creep behavior of rice husk/ HDPE under different temperatures and stresses were studied. Fig. 3 showed that the creep behavior of WPC were stress equivalence principle for short term creep, we could gain the compliance master curve at 55℃. The ten-element model was utilized and it was proved that this model could fit the master curve efficiently. The ten-element model is:

$$D(t) = D_0 + D_1(1 - e^{\frac{-t}{\tau 1}}) + D_2(1 - e^{\frac{-t}{\tau 2}}) + D_3(1 - e^{\frac{-t}{\tau 3}}) + D_4(1 - e^{\frac{-t}{\tau 4}}) + \frac{t}{\eta_5} \qquad (2)$$

3. Time-temperature dependence of WPC

Creep behavior of WPC is strongly dependent on the amount of stress, time and temperature. The WPC has the characters of the simple thermo-rheologic materials. There are three parts are included in the short-term creep curve: elastic phase、visco-elastic phase and viscous phase. We can utilize the TTSP to predict the long-term creep performance, then get the mechanic models and the mathematics formula. Using time-temperature superposition principle, the flexural creep compliance master curve of rice husk/ HDPE composites at 25℃ are obtained.

The time temperature superposition principle (TTSP) proposes that temperature effects may be described by altering the time scale of the viscoelastic response. This means that the creep data recorded at a reference temperature and shifted according to where $a_T(T)$ is the time shift factor, can represent the viscoelastic creep at a temperature T, providing the data is available over a long period of time.

$$\log a_T = \frac{-C_1(T - T_s)}{C_2 + T - T_s} \qquad (3)$$

The first was developed by Williams, Landel, and Ferry for temperature dependence of the relaxation modulus of a polymer or composite and is known as the WLF equation which can be expressed as where $C1$ and $C2$ are material dependent constants, T is the temperature at which the shift factor is desired, Ts is the reference

temperature and $a_T(T)$ is the time shift factor, or horizontal shift factor.

According to the Fig.7 we can get the C_1 and C_2 is 13.6、150.55, than equation (2) change into follow as equation (3).

$$\log \alpha_T = \frac{-13.6(T - T_s)}{150.55 + T - T_s} \quad (4)$$

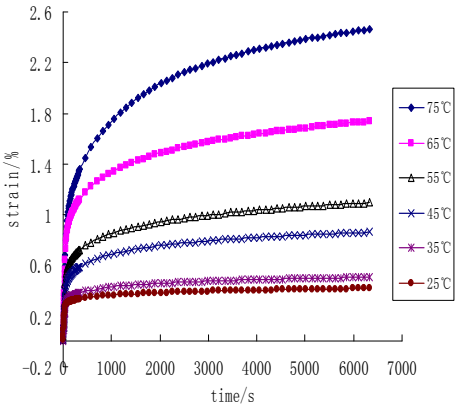

Fig. 4 Bending creep strain curves of WPC.

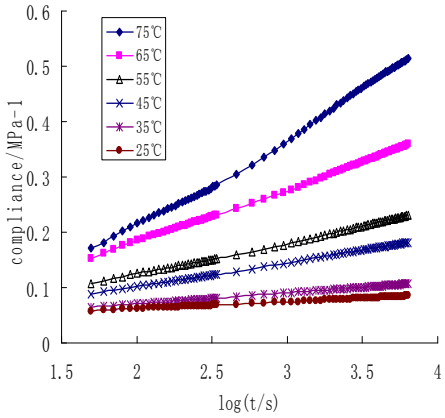

Fig. 5 Compliance curves of WPC.

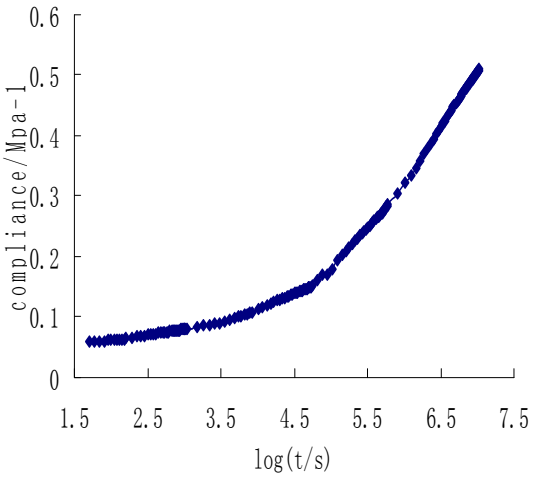

Fig. 6 Master curve of WPC.

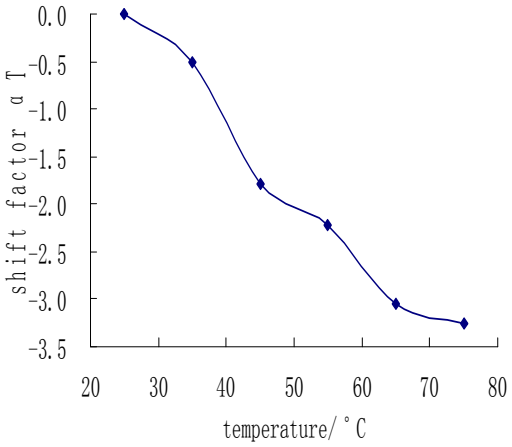

Fig. 7 Effect of temperature on shift factor.

4. Acknowledgements

This work was supported by the National Natural Science Foundation of China (No. 30871968). (Title: Nano-mechanics of Biomass / plastic composite material), (from 2009 to 2011).

5. References

(1) Jiang Yong-tao, Li Da-gang, Wu Zen-yuan, Ding Jian-sheng: Effect of Temperature on Flexural Creep Behavior of Rice Husk/HDPE Composites: Journal of Building Materials, Vol. 11, No.6, (2008), p.695-698

(2) Jiang Yong-tao, Li Da-gang, Wu Zen-yuan, Ding Jian-sheng: Study of the Creep Behavior of Rice Husk/High Density Polyethylene Composites: Packaging Engineering, Vol. 29, No.8, (2008), p. 4-6

(3) Jiang Yong-tao, Li Da-gang, Wu Zen-yuan, Ding Jian-sheng: Effect of Temperature on Two Kinds of Wood Plastic Composites: Forestry Machinery & Woodworking Equipment, Vol.36, No.3, (2008), p. 24-27.

(4) Jiang Yong-tao, Li Da-gang, Yan Wei-li, Wei Wei: Study on fracture property of bamboo and plastic composites with different compounding formula under temperature effect: New Building Materials, Vol.36,

No. 12 (2008), p.78-80
(5) Jiang Yong-tao, Li Da-gang, Wu Zen-yuan, Ding Jian-sheng: Study on Creep Behavior and Stress Relaxation Property of WPC: Forestry Machinery & Woodworking Equipment, Vol.37, No.4, (2009)
(6) Tian Xian-ling, Li Da-gang, Jiang Yong-tao, He Qiang, Wu Chun-yu: Study of Creep Behavior of Wood/Plastic Composite by Different Loading: China Plastic Industry, Vol.36, No.10 (2008), p.43-46
(7) Zhou Xia-xing, Li Da-gang: Fracture Mechanism of Plastic-wood Floors under Fatigue and Creep Interaction: Forestry Machinery & Woodworking Equipment, Vol.37, No.3, (2009), p.15-17

Study on Impacts of pH Value to Paulownia Wood Stain

Delong Chang, Yuyan Li, Nan Liu , Weihua Hu, Wenhao Huang, Fuhai Li and Yunling Zhang

Paulownia Research Center of China, Zhengzhou

Abstract: Impacts of acid and alkali on paulownia wood were studied, and the effects of weak alkali solution on stain prevention of paulownia wood were tested and analyzed. It shows that pH value affects paulownia wood color, and that white value of paulownia wood is prone to decrease and chromatism rises under acidity condition. Whiteness of paulownia wood rises and chromatism decreases under alkalescence condition, color and luster obviously tend to be bright. The alkali solution with concentration of 0.25% can promote the penetrability of paulownia wood, dissolve some extractives containing stain precursor chemicals, strengthen stain prevention of paulownia wood, but can not contaminate board surface. Anti-stain reagent has effect on prevention stain of paulownia wood, but only using it for controlling paulownia wood stain would induce stain-returning phenomenon, using weak alkali solution and anti-stain reagent has better effect than just using reagent only, the treatment by concentration of 0.25% weak alkali solution with anti-stain reagent can make controlling effect even both inside and outside.

1. Introduction

Paulownia is one of important species with fast growth and high yield oriented to industry uses in China, paulownia wood is widely used in furniture-making, decorating materials, musical instruments manufacture (JIANG Jianping, 1990), etc. Brown or black stain often appears on the surface of paulownia wood during processing and using. Discoloration seriously affects paulownia utilization, and it can cause huge loss due to being lowed grade and being cut price caused by stain (CHENG Junqing, 1983a; CHENG Junqing, 1983b; ZU Bosun, *et al*. 1991). It was found during our research that pH value of paulownia wood plays an important role in anti-stain and decoloring. Thus through changing pH valuve of paulownia wood, the fungi and enzyme activity can be inhibited, penetrability be promoted, and the effect of anti-stain and decoloring will be obviously enhanced.

2. Materials and methods

(1) Test materials

Test wood sample: Paulownia *elongata* 20 trees, age 10 a, 13 m, DBH(diameter at breast height) 38 cm, test sample dimensions are as follows: 100 mm x 100 mm x 50 mm(L x R x T), 30 mm x20 mm x 10 mm, 20 mm × 20 mm × 100 mm test pieces (no-stain) are stored in a refrigerator for use. Apparatus for measuring color: The system of international light committee L^*, a^*, b^* is adopted, L^*(brightness), TW(white value), △E(chromatism) etc. are measured with TC-PⅡG chromatism meter.

(2) Methods

A. Impacts of pH value to paulownia wood color

Various acid and alkali solutions with different pH are made, paulownia wood pieces for decay experiment are put in the solution for 24 hours with vacuum and pressure treatments till being consistent both inside and outside. Decay test is carried out after sterilization of twelve groups with six pieces each treated, wood color is measured after six weeks (CHANG Delong, *et al*. 1998; WILCOX W W, 1964.).

B. Effect of alkali solution to penetration of paulownia wood

Orthogonal experiment is adopted, concentration and time are designed for three levels including two affecting factors totalling 9 experiments (Table 1), each test has three repeats, the average of the three repeats is the result. The results are analyzed with the two factors variance method considering interaction,

penetrability is measured with gas flow rising replaced by water moving up (CHENG Junqing. 1983a).

Table 1 test factors and levels.

Factor	level		
	1	2	3
Concentration （%）	0.01	0.05	0.25
Time （h）	12	24	48

3. Results and discussions

(1) Impacts of pH value to paulownia wood color

The pH－$\triangle E^*$ in Fig. 1 shows that general chromatism rises slowly when pH is between 3.5~5 in pulownia wood, and that it rises fast when pH value is between 5~6, and that it reaches the top when pH value is at 6. Wood is seriously affected with the lowest white value because fungi can easily grow and enzyme activity is high under the condition of pH value being between 4~6 (LI Jian, 1999; Michikazu Ota, 1991; ZHOU Huiming, 1989); General chromatism lowers down slowly when pH value is between 6.1~6.5, it sharp decreases when pH value is between 6.6~7.5, and falls gradually when pH value is over 7.5. It tells us from the above digits that general chromatism changes obviously when the wood is under acid condition, and the wood color goes toward dark direction. And the stain can be inhibited and color becomes well accompanied by lowering chromatism and rising white value under the condition of pH value over 6 toward alkalescence. That is the key factor for fungi growth that takes place change, fungi and enzyme activity are prohibited, wood hemi-cellulous and low glycosanes degrade slowly (ZHOU Huiming, 1989; ZU Bosun, *et al.* 1991), and produce little stain radical groups causing small chromatism. Thus, anti-stain effect can be achieved by changing wood pH value appropriately, making the wood being under alkali condition.

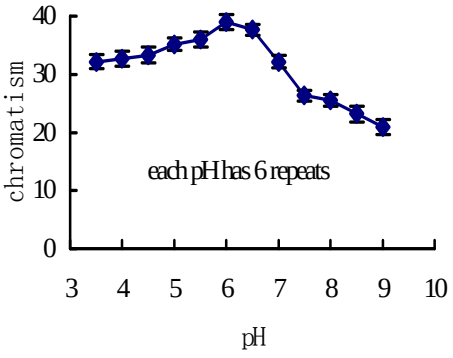

Fig. 1 pH-Chromatism curve.

(2) Impacts of weak alkali solution to penetrability of paulownia wood

Table 2 Osmosis variance analysis.

Variance source	Liberty degree	Independent difference square sum	Mean square	Mean square ratio	F	Significance
Concentration	2	1946.73	973.37	12.9	$F_{0.05}$=6.94	extremely
Time	2	1444.38	722.9	9.58	$F_{0.05}$=6.94	extremely
Surplus	4	301.78	75.45			

Table 2 shows that alkali solution has significant effect to paulownia wood penetrability, which is enhanced with the increase of concentration and prolonging dipping time. The penetrability with concentration of 0.25%, 48 hours immerging is the best among all treatments. All the nine experiments indicate that weak alkali solution can promote the penetrability of paulownia wood, increase osmosis of paulownia wood through dissolving and water swelling. Water swelling can open some hydrogen bonds on the cell wall of cellulose and hemi-cellulose, and increase the interspace on the cell wall, and thus enhance the wood penetrability. Besides, some molecules of low polymerization take place dissolution, especially small cellulose and hemi-cellulose and some carbohydrate are dissolved in the non-crystal zone, therefore they can promote osmosis of paulownia wood (LI Jian, 2002; LU Wenda, 1993). Consequently, weak alkali solution has extracting function to low polymerization including stain usher substances, which makes the extracts in cell wall and aperture pit be solved out, thus increases the penetrability of paulownia wood, promotes the effect of anti-stain on paulownia wood.

4. Conclusions

The pH value affects paulownia wood color, which becomes worse under acid condition, the chromatism of paulownia wood rises from 30 to 40; Wood stain can be inhibited under alkali condition, color becomes good, the chromatism treated by weak alkali solution and anti-stain reagent decreases from 40 to 21 that being near its natural color.

Some inner extractives containing stain precursors can be dissolved by 0.25% weak alkali solution, which can promote paulownia penetrability, enhance the anti-stain effect of controlling stain but can not contaminate the paulownia wood.

5. References

(1) CHANG Delong, Chen Yuhe, Hu Weihua, et al. 1998. Ascertaining stain type of Paulownia wood and Identification of stain fungi[J]. Beijing:Wood industry, 12(2):20-21,32.
(2) CHENG Junqing. 1983a, The study on paulownia wood properties and usage,[J]. Beijing:Scientia Silvae Sinicae, 19(1):57~63.
(3) CHENG Junqing. 1983b, The study on paulownia wood properties and usage,[J]. Beijing:Scientia Silvae Sinicae, 19(3):284~291.
(4) JIANG Jianping. 1990. Paulownia plantation scienc. Beijing: Chinese Publishing House.
(5) LI Jian. 1999. Wood protection science. Habin:Northeast Forestry University Publishing House.
(6) LI Jian. 2002. Wood science. Beijing:High Education House.
(7) LU Wenda. 1993. Wood modification technology. Habin:Northeast Forestry University Publishing House.
(8) Michikazu Ota . 1991. The chemistry of color changes in kiri wood(Paulownia tomentosa steud.) II.， Mokuzai Gakkaishi ， 37(3):254-260.
(9) WILCOX W W, 1964. Some methods used in studying microbiological deterioration of wood[J]. U.S. Forest service research note, FPL-063.
(10) ZHOU Huiming. 1989. Wood antidecay. Beijing:Chinese Publishing House.
(11) ZU Bosu, Xu Lulu, Zhou Qin, et al. 1991.The prilimary test of anti-stain of Paulownia wood[J]. Beijing:Wood industry, 5（3）：29—33.

A Simple Process for Electroless Plating Nickel-phosphorus Film on Wood Veneer

Lijuan Wang, JianLi and Yixing Liu

Key Laboratory of Bio-based Material Science and Technology of Ministry of Education, Northeast Forestry University, Harbin

Abstract: A facile electroless Ni-P plating process for preparing EMI shielding wood-based composite was studied. In the process, the activation was combined with the electroless deposition in the plating bath. It is a simple and environmentally friendly method that Ni-P film was easily deposited on the surface of birch veneer. The plated specimens were observed by SEM that the film is uniform, compact and continuous. EDS results shows that the coating contains 3.32wt% phosphorus and 96.68wt% nickel. It is indicated by XRD analysis that the film on birch veneer is crystalline. It is considered that the crystalline structure is related to the lower phosphorus content of the film. It is measured that the birch veneer plated with crystalline Ni-P coating has better electrical conductivity and electromagnetic shielding performance.

1. Introduction

Wood is a kind of important biomass material for its better heat insulation, sound insulation, moisture control and excellent mechanical strength. However, its application is limited because it is non-conducting and has no performance of electromagnetic shielding. Electrolessly nickel-plated wood veneer with excellent properties of wood and metal can be widely used in electromagnetic shielding and anti-static fields. Some researches [1-10] have been carried out. Especially, the activation methods have attracted more attention of some researchers [11].

The non-catalytic substrate has to be catalyzed to produce catalytic nuclei before the electroless deposition. This is the process of activation in which the catalytic nuclei will act as nucleation centers to initiate the autocatalytic deposition of metal. Since good catalysis is the key for the electroless plating process and will directly affect the quality of the film. In fact, $PdCl_2$-$SnCl_2$ colloid is the most prevalent catalyst in commercial use. However, Pd is very expensive and the colloid is not always stable, which improves the cost and makes the plating process uncontrollable. In order to save Pd and decrease the cost, many attempts were made to employ Ni activation, in which two methods are widely investigated. One is that Ni^0 was produced on the substrate absorbed Ni^{2+} by thermal treatment at higher temperature [12-16], the other is that Ni^{2+} on the surface of the substrate was reduced to Ni^0 by $NaBH_4$ in two separate steps [17-18].

In the present work, a simple electroless plating process was employed to prepare metallized wood veneer for electromagnetic interference (EMI) shielding without $PdCl_2$-$SnCl_2$ colloid activation. In the process, wood veneers were pretreated with sodium borohydrice ($NaBH_4$) and hung in air for 1min, then directly submersed in the plating solution. The activation and nickel plating process were combined and completed in one bath. It is a very simple, facile and low-cost method. The film on wood veneer was characterized by Scan Electron Microscopy (SEM-EDAX) and X-ray diffraction (XRD). The electrical performances of plated veneers were also measured.

2. Experimental method

(1) Material and specimens

Wood veneers of 0.6mm thickness were purchased from a plywood factory. All the chemicals used were of analytical grade purity.

The veneers were polished by emery papers to remove fine fiber or dust on the surface. Then cut into square of 50mm×50mm for measuring electrical conductivity. And specimens for electromagnetic shielding effectiveness (ESE) were cut according to Chinese industrial standard SJ20524-1995 as shown in Fig. 1.

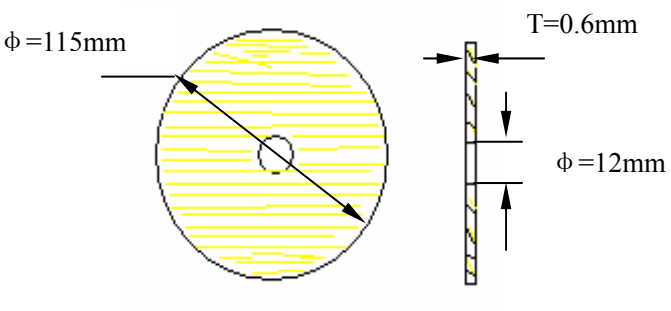

Fig.1 Schematic of the sample.

(2) Activation and plating

In the process, firstly, specimens were dipped in $NaBH_4$ solution containing 5g/L sodium hydroxide (NaOH) for certain time at room temperature; next, hung in air for $NaBH_4$ diffusing to the inner pores. The time is about 1min; and then; put into the plating bath. The composition of electroless bath and the operation conditions are listed in Table1. The pH of the bath was adjusted using $NH_3 \cdot H_2O$.

(3) Surface characterization

The surface morphologies and element compositions of the coatings were characterized by SEM (Quanta 200) and an X-ray energy dispersive spectrometer (EDS)(EDAX). Specimens were not sprayed with gold prior to analysis. Additionally, the phase structure for the coating was clarified by X-ray diffraction(XRD, Rigaku D/max 2200 diffractometer) using Cu K_α radiation generator setting of 40kv and 30mA.

(4) Measurement of electrical performances

The surface resistivity of the metallized wood veneers was evaluated by using the method designed according to Chinese National Military Standard GJB2604-96. The shielding effectiveness of the plated veneers was measured by using the method of Chinese industrial standard SJ20524-95. Angilent E4402B spectrum analyzer and standard butt coaxial cable line with flange were used to detect the generation of incidence electromagnetic waves and the transmission of electromagnetic waves.

Table 1 Composition and operation condition of electroless plating.

Chemicals	Content/g/L
$NiSO_4 \cdot 6H_2O$	25-35
$NaH_2PO_2 \cdot H_2O$	25-35
Complexing agent	25
Buffering agent	30
Thiourea	0.002
pH	8.5
Temperature(℃)	68
Time (min)	20

3. Results and discussions

(1) Morphology and composition analysis

Fig.2 shows the morphology of the birch veneer. As shown in Fig. 2 (a), wood veneer before plating has complicated porous structure. A lot of pores, whose shape and diameter are different, can be observed. It can be seen from Fig. 2 (b) that the entire surface including some pore structure is covered with uniform and continuous coating which has obvious metallic sheen. Because of a layer of coating on surface of birch veneer, morphology of surface film shown in Fig2 (b) is brighter than that in Fig. 2 (a). It is also found that pores still exist and not filled by the coating after plating. It can be observed in Fig. 2(c) that the coating is comprised of countless unit cells whose diameters are about 1~3μm at high magnification. They deposit together closely so that the coating

is smoother. According to the mechanism of electroless deposition, each unit cell is assembled with atoms which are reduced during the plating reaction.

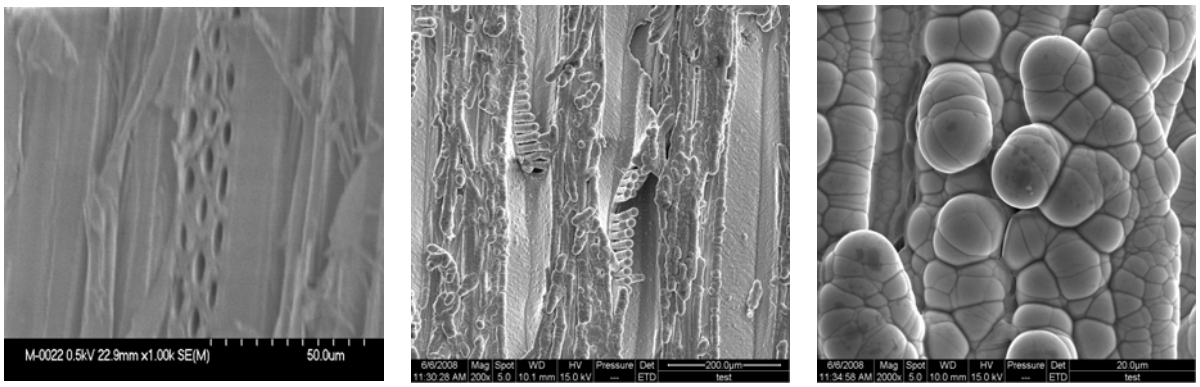

Fig. 2 SEM photographs of birch veneer (a) before plating, (b and c) after plating.

Fig. 3 shows the EDS spectrum of the plated birch veneer. Peaks of carbon and oxygen are from wood, and nickel and phosphorus are attributed to the coating. In the beginning of the process, $NaBH_4$ on veneers reacts with Ni^{2+} as main salt in the plating solution, which Ni^0 is initiated immediately and to catalyze the subsequent electroless Ni-P co-deposition. It is proved by EDS results that the film is consist of Ni-P alloy. However, boron element wasn't checked. It is indicated that the reaction took place when specimens with $NaBH_4$ were placed in the plating solution. It can be written as: $2Ni^{2+} + BH_4^- + 2H_2O \rightarrow 2Ni^0 + 2H_2\uparrow + BO_2^- + 4H^+$. There was no boron depositing together with Ni^0 in the activation stage.

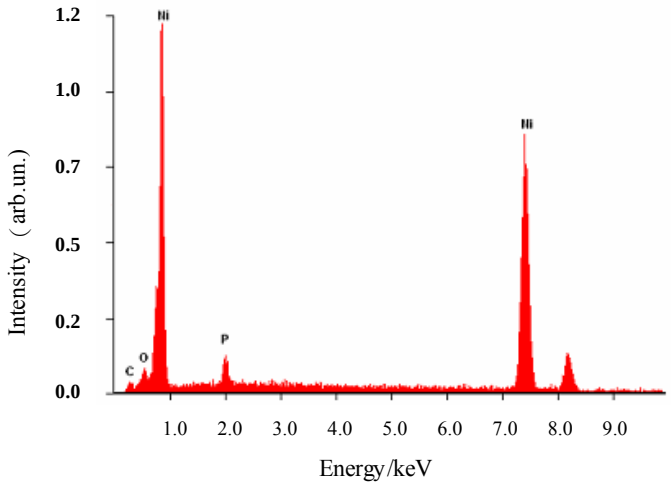

Fig. 3 EDS spectrum of the plated birch veneer.

(2) XRD analysis

Fig. 4 shows the XRD pattern of birch veneer before and after plating. The strong peak in Fig.4(a) at 2θ=22°is characteristic peak of birch veneer. The sharp peaks at 2θ=44.48°, 51.56°and 76.64°, which are observed in Fig. 4(b), are attributed to Ni (111), Ni (200) and Ni (220) which shows the face centered cubic phase of nickel (JCPDS: 04-0850) and indicates the crystalline nature of the film. This result is mainly related to lower P content and largely attributed to little distortion of crystalline of Ni caused by P atoms. Comparing XRD patterns shown in Fig.4 (a) and (b), the characteristic peak intensity of the plated birch veneer is decreased obviously. The result indicates that birch veneer is entirely and compactly covered by Ni-P coating and the thickness reaches at least to μm.

(3) Electrical performance analysis

It is measured the surface resistivity of the plated specimens is 145.4mΩ/cm^2, which shows excellent electrical conductivity. Therefore, plated veneer can shield more electromagnetic wave. Fig. 5 shows the ESE is higher than 60 dB in the frequencies from 10MHz to 1.5GHz. The result show that the plated birch veneer has electromagnetic shielding performance and can be used in some special application, which can broaden application range of wood veneer.

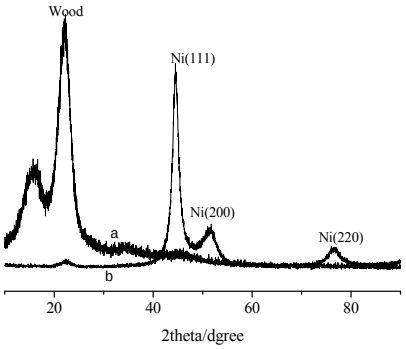

Fig. 4 X-ray diffraction pattern of the plated birch veneer (a) before plating, (b) after plating.

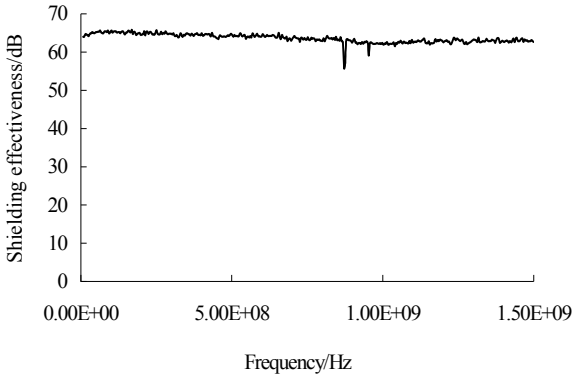

Fig. 5 Electromagnetic shielding effectiveness of the plated birch veneer.

4. Conclusion

A facile process for nickel electroless plating on birch veneer has been achieved. This process was carried out by combining activation with electroless plating in one bath. It is found that uniform, compact and continuous film with crystalline structure was obtained by using this process. Plated birch veneer has better electrical conductivity and electromagnetic shielding performance. This process is a facile, low-cost and well-controlled method, which is promising for large-scale commercial manufacturing.

5. References

(1) Nagasawa, C. and Kumagai:Y. J. Wood Sci Vol.**35**(1989): 1092–9
(2) Nagasawa, C., Kumagai, Y., Koshizaki, N., and Kanbe, T: J. Wood Sci Vol.**38**(1992): 256–63
(3) Nagasawa, C., Kumagai, Y., Urabe, K: J wood sci Vol.**36**(1990): 531–7
(4) Nagasawa, C., Kumagai, Y., Urabe, K. J: Wood Sci Vol.**37**(1991):158–63
(5) Nagasawa, C., Kumagai, Y., Urabe, K., and Shinagawa, S. J: Porous Mater (1999):247-254
(6) Nagasawa, C., Umehara, H., Koshizaki, N. J: Wood Sci, Vol.**40**(1991):1092–9
(7) Wang LJ, Li J, Liu YX: Mater sci Technol No.6(2006):296-9
(8) Wang LJ, Li J: Scientia Silvae Sinicae No.12(2007):311-5
(9) Wang LJ, Li J, Liu YX: J Mater Eng No.4(2008)56-60
(10) Huang JT, Zhao GJ: J Beijing Forestry Univ No.3(2004):97-101
(11) Gao GQ, Huang JT: J Inner Mongolia Agric Univ No.1(2007):95-8
(12) Li LB, An MZ: J Alloy and Compd Vol.46(2008):85-91
(13) Li LB, An MZ, Wu GH: Surf Coat Technol Vol.200(2008):5102-12
(14) Tang XJ, Bi CL, Han CX: Mater Lett (2009)
(15) Wang SL, Wu HH: Chin J Appl Chem No.5(2003):491-2
(16) Shao Q, Yang YX, Ge SS: Funct Mater No.12(2007):2001-3
(17) Hu GH, Wu HH, Yang FZ: Electrochem No.1(2006):25-8
(18) Lai DZ, Chen WX, Yao YF: J Text Res No.1(2006):34-7

Study on the Computer Color Matching of Birch Veneer for Dyeing

Minghui Guo[1], Xuemei Guan[2] and Xin Guan[1]

[1] Key Laboratory of Bio-based Material Science and technology(Northeast Forestry University)，Ministry of Education, Harbin

[2] Information and Computer Engineering College, Northeast Forestry University, Harbin

Abstract: Birch Veneer was taken to study dye forecast formula using three stimulate value method of computer technology based on Kubelka-Munk theory. Red sandalwood: reactive brilliant red X-3B 0.116%; reactive yellow X-R 0.219%; reactive blue X-R 0.032%. Black rosewood: 0.461%; 0.544%; 0.177% respectively. Black walnut: 0.119%; 0.206%; 0.077% respectively. Teak: 0.122%; 0.400%; 0.082% respectively. It was found that the method was very effective for wood dyeing, and the formula was found after few times, and the error was less than 5%.

1. Introduction

(1) General

Color matching is an important part of wood dyeing. During this process, the general synthesis of color matching is based on traditional color mixing theory, which is an artificial matching color way. With the people's increasing demand for wood dyeing, computer color matching will be used in it to speed up the rate of bringing formula of dye, improve the efficiency and save cost [1-2]. In this paper, birch veneer was taken to study computer color matching technology based on three stimulate value method and Kubelka-Munk theory. The purpose of the study was obtaining the prediction formula of valuable material and exploring for the wood staining methods in computer color matching.

(2) Theoretical Basis. Kubelka-Munk Theory

When the illumination light projected onto the opaque substrate (wood), most of it went into the internal matrix and occurred absorption and scattering, apart from a small number of it reflecting. Based on it, Kubelka and Munk proposed Kubelka-Munk theory:

$$(K/S)\lambda=[1-R(\lambda)]2/2R(\lambda) \quad (1)$$

Where: K was the absorption coefficient, and S was the scattering coefficient, and R (λ) was the reflectivity on wavelength λ. This theory was the basis of measuring colors.

(3) Three Stimulate Value Method

The specific approaches of three stimulate value method were like that: firstly, select the number of colors used to color the different dyes, Which were generally three types of dyes (In this study, red, yellow, blue three colors for the color of the reactive dye). The definition of the following vectors and matrix like that:

$$t=\begin{bmatrix} X \\ Y \\ Z \end{bmatrix} \quad T=\begin{bmatrix} \overline{x_{400}} & \overline{x_{420}} & \cdots & \overline{x_{700}} \\ \overline{y_{400}} & \overline{y_{420}} & \cdots & \overline{y_{700}} \\ \overline{z_{400}} & \overline{z_{420}} & \cdots & \overline{z_{700}} \end{bmatrix} \quad E=\begin{bmatrix} E_{400} & 0 & \cdots & 0 \\ 0 & E_{420} & \cdots & 0 \\ \cdots & \cdots & \cdots & \cdots \\ 0 & 0 & \cdots & E_{700} \end{bmatrix} \quad r^{(s)}=\begin{bmatrix} R^s_{400} \\ R^s_{420} \\ \vdots \\ R^s_{700} \end{bmatrix} \quad r^{(m)}=\begin{bmatrix} R^m_{400} \\ R^m_{420} \\ \vdots \\ R^m_{700} \end{bmatrix}$$

T was the matrix of tristimulus values of CIE1964 standard, and t was the vector of tristimulus values of target of precious wood, and E was the matrix of relative spectral distribution function of CIE standard source. R was the spectral reflectivity, subscript denoted wavelength with nm as a unit, and $r^{(s)}$ was spectral reflectance vector of precious wood, and $r^{(m)}$ was spectral reflectivity of dyeing veneer[3-4]. The intention of three stimulate value method was that made the tristimulus values of dyeing veneer and precious wood homology, and the purpose of color matching was reached and elicited formula(2):

$$TE[r(s)-r(m)]=0 \quad (2)$$

Then the following vectors and matrix were defined:

$$f=\begin{bmatrix}(K/S)_{400}\\(K/S)_{420}\\\vdots\\(K/S)_{700}\end{bmatrix}\quad D=\begin{bmatrix}d_{400}&0&\cdots&0\\0&d_{420}&\cdots&0\\\cdots&\cdots&\cdots&\cdots\\0&0&\cdots&d_{700}\end{bmatrix}\quad C=\begin{bmatrix}C_1\\C_2\\C_3\end{bmatrix}\quad \Phi=\begin{bmatrix}(K/S)^1_{400}&(K/S)^2_{400}&(K/S)^3_{400}\\(K/S)^1_{420}&(K/S)^2_{420}&(K/S)^3_{420}\\\cdots&\cdots&\cdots\\(K/S)^1_{700}&(K/S)^2_{700}&(K/S)^3_{700}\end{bmatrix}$$

Where, (i = 400，420…700nm), and C was vector of dye strength (1,2,3 were three dye respectively). According to these vectors and matrix, formula for calculating concentration of color matching dyes was derived as formula(3). Detailed theory might be see references [3].

$$C=(TED\Phi)^{-1}TED\left[f^{(s)}-f^{(t)}\right] \tag{3}$$

2. Materials and methods

(1) Experimental materials

This paper chose red sandalwood style, black rosewood, black walnut and teak as target precious wood. Samples (birch veneer) purchased from Harbin, Heilongjiang. And the thick was 0.6mm, the size of was 100 × 50mm. The reactive red dye X-3B, Reactive Yellow XR, Reactive Blue XR, agent using JFC, the use of salt (NaCl) as both agent and promoting agent, fixing agent for the soda ash (Na_2CO_3) were used.

(2) Experiment Design

Samples depurated by sand paper and preparation of dyeing liquor with dye (calculational concentration), penetrant JFC (0.1% concentration), half of NaCl (2% concentration) and distilled water, liquor ratio of dyeing liquor is 10:1[6]. Timing when dyeing temperature was 75℃, the other half of NaCl was put in dyeing liquor when 10min would reached dyeing time. Samples were treated with sodium carbonate when dyeing time was 60min, then the beaker was took out after 30min. Dyeing veneers were cleaned by distilled water till the washing liquid was no color, then airing and color measurement[7].

(3) Measuring Method

Tristimulus values (*X*, *Y* and *Z*) and spectral reflectivity (*R*) of the surfaces of the four precious wood, birch veneers before dyeing and after dyeing with reactive brilliant red, reactive yellow and reactive blue separately were measure by spectrophotometer, wavelength interval was 20nm and wavelength range was from 400nm to 700nm. Average veneer surface was measured three dots and the average value was calculated.

3. Results and discussion

(1) Measuring results for tristimulus value of Surface reflectance

Table 1 showed the spectral reflectivity of the surfaces of the four precious wood, birch veneers and dyeing birch veneers. Table 2 showed the tristimulus values of the four precious wood, others were not required.

(2) Computer color matching and dyeing

According to basic data, using a computer to calculate and determined the relevant data in the formula (3) and calculated respective dye strength, received the theoretical ratio to simulate precious wood. Using this ratio to dye birch veneers and compared with target wood, collated dyeing prescriptive, which the whole process of birch veneer was dyeing to simulate precious wood.

A. Searching and calculation of color matching parameters

(A) The relative spectral distribution function of CIE standard source D65 was received from related records (Guoxing He, Color Science), then T and E were determined. Table 3 shows the results.

(B) According to formula $d_i = -\frac{2R_i^2}{1-R_i^2}$ (i = 400，420…700nm) and Table 2, d value of precious wood was calculated in every wavelength and matrix D was determined. Table 4 showed the result.

(C)According to Kubelka-Munk theory and Table 1, averages of K/S value of precious wood, birch veneers and dyeing veneers were calculated, matrix φ, vector $f^{(s)}$ and vector $f^{(t)}$ were determined.

Table 1 Surface reflectivity.

Wavelength (nm)	Reflectivity							
	Red sandalwood	Black rosewood	Black walnut	Teak	Plain veneer	Red dye veneer	Yellow dye veneer	Blue dye veneer
400	0.057000	0.022200	0.048500	0.033533	0.574333	0.114333	0.057167	0.118200
420	0.058500	0.022833	0.052133	0.035533	0.618333	0.104100	0.053233	0.172267
440	0.060400	0.023533	0.056200	0.038233	0.663867	0.091033	0.056000	0.224333
460	0.062967	0.024433	0.061100	0.042333	0.718767	0.073500	0.068800	0.269000
480	0.065067	0.025067	0.064533	0.046967	0.759767	0.056033	0.097333	0.261100
500	0.071133	0.026400	0.067967	0.054533	0.776433	0.046300	0.164900	0.181067
520	0.081300	0.029167	0.075200	0.067300	0.792700	0.038633	0.288633	0.130333
540	0.097467	0.032633	0.083700	0.080367	0.802033	0.028000	0.427567	0.099067
560	0.126533	0.037867	0.096733	0.094167	0.809333	0.037667	0.524933	0.070833
580	0.158400	0.045067	0.112100	0.109000	0.802400	0.093567	0.580600	0.060167
600	0.193767	0.057100	0.127333	0.126767	0.812667	0.257000	0.619400	0.054700
620	0.235400	0.076900	0.145467	0.148233	0.830333	0.477167	0.652200	0.053433
640	0.272867	0.100933	0.164667	0.166967	0.832467	0.614333	0.672967	0.057667
660	0.301800	0.127133	0.182500	0.180800	0.820533	0.663433	0.676067	0.067900
680	0.312000	0.133367	0.187733	0.185933	0.822600	0.701433	0.682967	0.068833
700	0.315700	0.135133	0.189400	0.187400	0.826200	0.719167	0.686300	0.069433

Table 2 Tristimulus values of the four precious wood.

Tristimulus values	Tree species			
	Red sandalwood	Black rosewood	Black walnut	Teak
X	15.34	4.88	10.41	10.00
Y	13.19	4.15	9.68	9.16
Z	6.87	2.59	6.34	4.44

B. Determine the ratio of dye

(A) Determined approximate ratio C of dye strength according to formula (3), and Table 5 showed the results.

(B) Dyeing birch veneers according to theoretical ratio of dye, the averages of tristimulus values were measured, then calculating the difference Δt of tristimulus values to target precious wood, and deducing formula (4) and (5):

$$\Delta C = [TED\Phi]^{-}\Delta t \quad (4)$$

$$C^* = C + \Delta C \quad (5)$$

Error was exist after determining new dye ratio according to formula (5), so adjusted again. Table 6 shows the results after two adjustment, it shows that relative error of tristimulus values is less than 5%, and it's difficult to distinguish between the naked eye. Table 7 shows the final dye ratio.

Table 3 Tristimulus values of matrix T and relative spectral distribution of standard source.

Wavelength（nm）	CIE1964standard observer tristimulus values			E
	$\overline{X}$	$\overline{Y}$	$\overline{Z}$	
400	0.0191	0.002	0.086	82.8
420	0.2045	0.0214	0.9725	93.4
440	0.3837	0.0621	1.9673	104.9
460	0.3023	0.1282	1.7454	117.8
480	0.0805	0.2536	0.7721	115.9
500	0.0038	0.4608	0.2185	109.4
520	0.1177	0.7618	0.0607	104.8
540	0.3768	0.962	0.0137	104.4
560	0.7052	0.9973	0	100
580	1.0142	0.8689	0	95.8
600	1.124	0.6583	0	90
620	0.8563	0.3981	0	87.7
640	0.4316	0.1798	0	83.7
660	0.1526	0.0603	0	80.2
680	0.0409	0.0159	0	78.3
700	0.0096	0.0037	0	71.6

Table 4 d value of precious wood.

Wavelength（nm）	d value			
	Red sandalwood	Black rosewood	Black walnut	Teak
400	-0.00652	-0.00099	-0.00472	-0.00225
420	-0.00687	-0.00104	-0.00545	-0.00253
440	-0.00732	-0.00111	-0.00634	-0.00293
460	-0.00796	-0.00119	-0.00749	-0.00359
480	-0.0085	-0.00126	-0.00836	-0.00442
500	-0.01017	-0.00139	-0.00928	-0.00597
520	-0.01331	-0.0017	-0.01137	-0.0091
540	-0.01918	-0.00213	-0.01411	-0.013
560	-0.03254	-0.00287	-0.01889	-0.01789
580	-0.05147	-0.00407	-0.02545	-0.02405
600	-0.07802	-0.00654	-0.03296	-0.03266
620	-0.11733	-0.0119	-0.04324	-0.04493
640	-0.16089	-0.02058	-0.05574	-0.05735
660	-0.20042	-0.03286	-0.06891	-0.06759
680	-0.21568	-0.03622	-0.07306	-0.07162
700	-0.2214	-0.0372	-0.07441	-0.07279

Table 5 Dye ratio of birch veneer simulation precious wood.

Dye type	Red sandalwood	Black rosewood	Black walnut	Teak
Reactive brilliant red	0.138%	0.503%	0.142%	0.141%
Reactive yellow	0.226%	0.524%	0.227%	0.405%
Reactive blue	0.036%	0.189%	0.092%	0.092%

Table 6 Tristimulus values of dye veneer surface after adjustment.

Tristimulus values	Imitation rosewood veneer	Imitation black rosewood veneer	Imitation black walnut veneer	Imitation teak veneer
X	14.94	5.12	10.52	10.16
Y	13.31	4.13	9.91	8.95
Z	6.56	2.66	6.35	4.29

Table 7 Dye ratio of birch veneer simulation precious wood after adjustment.

Dye type	Red sandalwood	Black rosewood	Black walnut	Teak
Reactive brilliant red	0.116%	0.461%	0.119%	0.122%
Reactive yellow	0.219%	0.544%	0.206%	0.400%
Reactive blue	0.032%	0.177%	0.077%	0.082%

Other birch veneers were dyed by the use of this prescription and the difference was controlled in 8%. Although it still had some difference between the final products and the target precious wood, adjustment many times could regulate the difference. Due to system error and human error, the final color of dye birch veneer was alterability, for instance, the same species, there were differences between different batches; the same batches, there were differences between different trees; the same trees, there were differences between different parts. So this study chose the result of two adjustment as the final outcome of dye.

4. Conclusion

Tristimulus values and Kubelka-Munk theory as the core of computer color matching technology and theoretical pillar used in many industry widely. This paper chose birch veneer as object of study and previous dyeing as basic research, discussed color matching method to simulate precious wood and achieved remarkable results. Specific conclusions are as follows:

(1) Computer color matching technology on the basic of tristimulus values and Kubelka-Munk theory could forecast dye ratio, and it had a little difference between actual ratios and the results. Tristimulus values errors were less than 5% after two adjustments. It showed that tristimulus values for color matching technology was completely suitable for wood dye, and it was superior to artificial color matching and orthogonal experimental color matching, dyeing results were satisfactory.

(2) After adjustments, dye strength ratio of birch veneers to simulate precious wood was as follows: Red sandalwood: reactive brilliant red X-3B 0.116%; reactive yellow X-R 0.219%; reactive blue X-R 0.032%. Black rosewood: 0.461%; 0.544%; 0.177% respectively. Black walnut: 0.119%; 0.206%; 0.077% respectively. Teak: 0.122%; 0.400%; 0.082% respectively.

This study had received some achievement, but there were still some inadequacies. Due to Kubelka-Munk theory was ideal formula, the errors were inevitable. It needed study in-depth to establish an accurate model in accordance with material own characteristics. In addition, color matching model didn't consider that the structure of wood itself impacts on dyeing.

5. References

(1) Changsheng Li, Dianwen Wang, Yanhui Wu. Study on Measurement of Forest Ecological Benefit of China. Protection Forest Science and Technology, Vol. 2(2005),p. 1-3

(2) Zhonghua Yin, Minghua Tian. Analysis of Gains or Losses of Chinese Timber Imports in Great Quantities. Forestry Economics, Vol. 9 (2006),p. 47-50

(3) Guoxing He. Color Science. Shanghai: East China University Press (2004), p. 140-180

(4) Qi Liao, Yuan Liu etc. Dyeing Technology of Poplar Veneer with Reactive Dyes. China Wood Industry, Vol. 19(4) (2005), p. 39-41

(5) Allen E. Basic Equations Used in Computer Color Matching.Journal of the Optical Society of America, Vol. 56(9) (1966), p. 1256-1259
(6) Chunsheng Li, Jinlin Wang. Computer Color Matching Technique for Wood Dyeing. China Wood Industry, Vol. 6 (2006), p. 5-7
(7) Lin Wu, Zhiming Yu. Preliminary Study on Application of Computer Color Testing and Color Matching Technology in Wood Dyeing. China Wood-Based Panels, Vol. 8 (2006), p. 17-20

Study on the Surface Finishes Methods of Wood Based Panel to Reduce the Emission of TVOC and Formaldehyde

Feng Chen, Jun Shen and Xueyao Su
Material Science and Engineering College, Northeast Forestry University, Harbin

Abstract: Chemical contaminants, such as TVOC and formaldehyde, from wood-based panel are the main sources of indoor air pollution. How to reduce their emission is the hot spot for domestic and foreign scholars. This article namely starts with Secondary Processing of wood based panel. Through the experiment, we choose particleboards just manufacture from factory as substrate and select five commonly finishes methods including mlamine-impregnated paper, vinyl decorative paper, veneer finishes, polypropylene water paintings coatings and polyurethane water paintings coatings. The emission curves and equilibrium concentrations of TVOC and formaldehyde of surface finishes of wood based panel were obtained and measured using an airtight glassed dryer and environmental chamber. The experiment results can be used to compare the difficult effectiveness of barriers and evaluate the emission characteristics of surface finished wood-based panel.

1. Introduction

The second manufacturers on the surface of the wood-based panel, such as the surface finishes which act as vapor diffusion barrier, also lower emissions of VOCs from wood composites[1]. Besides, release mechanisms of raw wood composites have successfully been preliminarily studied by our previous research team based on the production process, but the particleboard with surface finishing have been not investigated. The overall goals of this program were to investigate the Release Characteristics by different surfaces finishes methods to develop strategies to compare the barrier impacts of these surface finishes methods on the particleboards.

2. Materials and methods

The test materials, newly manufactured raw particle boards, were obtained from Suiha Wood Composite plant supplying 1.22- by 2.44-m panels. Within 24-h,these were cut from the center of panel into 0.23- by 0.24-m squares and wrapped in aluminum foil. The small pieces then were shipped to the laboratory. The edge of test specimens was sealed with aluminum tape to prevent the rapid release of VOCs and formaldehyde from edges of samples. All samples were then surface- finished on the raw specimen, all illustrated in Table 1, and wrapped with aluminum foil and put in a first polyethylene bag. Then the wrapped test specimens were then inserted in -30℃ refrigerator before detection[2].

Table 1 Description of surface finishing specimens.

Material	Material ID	Parameter
Melamine paper	A.	0.20mm thickness(80g)
	B.	0.20mm thickness (120g) with
Wood veneer	C.	0.20mm thickness pine veneer
	D.	0.15mm thickness walnut veneer
polyethylene film paper	E.	0.11 mm thickness
Water-based polypropylene coating	F.	wet film thickness 0.4mm(undercoat)
	G.	wet film thickness 0.4mm(topcoat)
Water-based Polyurethane emulsion coating	H.	wet film thickness 0.4mm(undercoat)
	I.	wet film thickness 0.4mm(topcoat)

Two methods, the airtight cabin method and ventilation cabin method, for the concentration detection of TVOC and formaldehyde are used. The first method was to keep the airtight condition and to detect the gradually emission value of the specimen in the first 6 hours and total concentration one day later. The second method was that keep the ventilated condition of 23±0.5℃, 45±5%RH, air velocity 0.3 m/sec and ventilation rate 1.0 air changes per hour. The sink effects of the chamber was low for many VOCs because of polished aluminum surface[3].

3. Results and discussions

Fig. 1 presents the TVOC concentration from A to E in the first 6 hours with the airtight cabin method. By comparing the concentration curves in six hours, various effects to minimize TVOC emissions from A to E are as follows: (1)polyethylene film paper was the best among the 5 finishing methods. The next were melamine paper (80g) and melamine paper (120g). Wood veneer's effect was the worst. (2) TVOC concentration of melamine paper and polyethylene film paper specimens were under that of the raw particleboard. (3) The result showed that when using the UF adhesive in hot pressing the veneer the barrier effect was affected by the curing time of adhesive. (4) From the Fig. 2, the total value show that the barrier effect of polyethylene film paper particle board is best among the five finishing materials. Melamine impregnated paper (120g) is slightly better than melamine impregnated paper (80g).

From the Fig. 3, when using the water-based coating, because of the actual drying time is long, the value is much larger than that of raw particleboard. The TVOC barrier effect of the water-based is not obvious.

The results of the formaldehyde barrier in the airtight cabin are plotted in Fig. 4. The tests showed inaccurate results only by the 2 digits at most after decimal point of Formaldehyde INTERSCAN-4160 analyzer. Nevertheless, the barrier effect of formaldehyde is better.

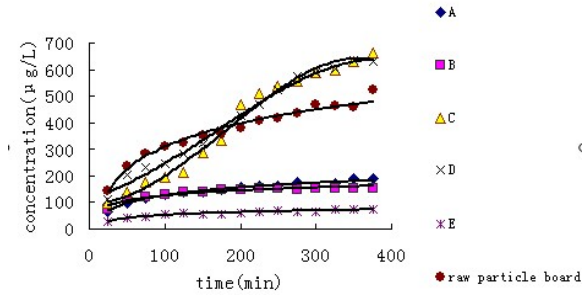

Fig. 1 TVOC emission concentration measured for from A to E.

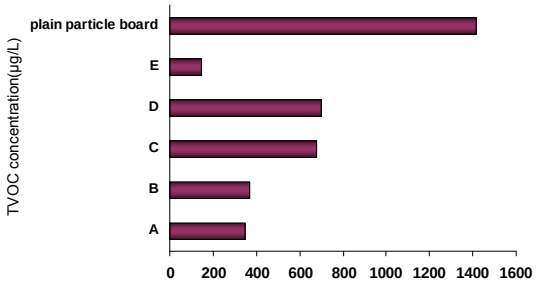

Fig. 2 TVOC emission concentration measured after 1d.

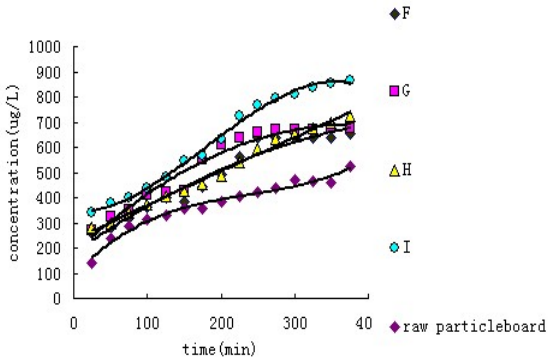

Fig. 3 TVOC concentration in 6 hours.

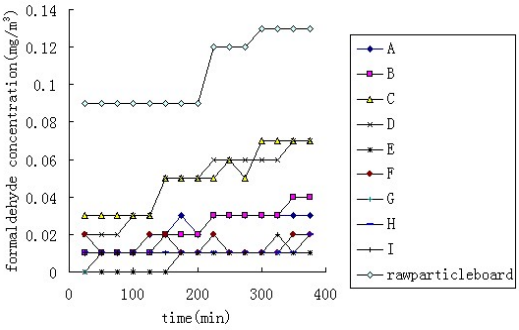

Fig. 4 Formaldehyde emission concentration measured in 6 hours.

The specimen in the ventilation cabin is detected until the value reached equilibrium concentration when there was no significant difference between values ($p<0.05$). When achieving equilibrium concentration, the Table 2 shows the barrier effect results.

By the data from the Table 2, the formaldehyde reduction of melamine paper and polyethylene film paper particleboard is higher than 99%, and reduction of pine and walnut veneer is about 67%. While the water-based polypropylene coating particleboard and water-based polyurethane emulsion coating particleboards have little reductions that are 16.7% and 25%.

Table 2 Finished panel reduction in TVOC and formaldehyde emissions.

Surface finishing	TVOC ($\mu g \cdot L^{-1}$)	Reduction (%)	Formaldehyde (mg/m^3)	Reduction (%)
Melamine paper(80g)	41	-85.2%	0	>99%
Melamine paper(120g)	27	-90.3%	0	>99%
Pine veneer	39	-85.9%	0.04	66.7%
Walnut veneer	73	-73.6%	0.04	66.7%
polyethylene film paper	15	-94.6%	0	>99%
Water-based polypropylene coating(under coat)	147	-46.9%	0.10	16.7%
Water-based polypropylene coating(top coat)	291	+5.1%	0.10	16.7%
Water-based Polyurethane Emulsion coating (under coat)	115	-58.5%	0.09	25%
Water-based Polyurethane Emulsion coating (top coat)	348	+25.6%	0.09	25%
raw particleboard	277	——	0.12	——

4. Summary

According to the concentration time curve of airtight cabin experiment, there was logarithmic relationship between the time and concentration, and at last the curve was close to a straight line.

The results of airtight cabin experiment method showed that apart from the water-based paint and veneer whose adhesive containing volatile organic compounds which were used in the hot-press of veneer, the barrier effect with the airtight cabin method and the ventilation cabin method have the relationship. polyethylene film paper is the best finishing material to reduce the release of TVOC and reduce TVOC emissions by 94.6%, and the formaldehyde emission by over 99%; The barrier effect of melamine papers lower than that of polyethylene film but above the veneer paper. The barrier effect of melamine paper(120g) better than 80g which is related to their density; the reductions of formaldehyde emission of Pine wood veneer and walnut are equal, but reduction of TVOC emissions the of pine 12.3% higher than the walnut. Compared with the walnut, the pine veneer was better, which was due to the porosity of pine. From table 2, water-based polyurethane emulsion paint on the formaldehyde release of the closure rate of 25%, slightly better than the modified water-based acrylic acid emulsion paint closure rate of 17%; The closed effect of under coat reduce by 46.9% and 58.5% ,while the barrier effect of topcoat was not better.

The next stage of research would further study the market selection of several typical finishing materials (such as PVC veneer, pre-paint paper, decoration oil-based wood, light-curing paint, powder coating). Further

qualitative and quantitative analysis will be conducted in the ventilation conditions, investigating the the attenuation change of the monomer composition of VOCs, and explore mechanism of VOCs barriers with surface finishes methods.

5. References

(1) Alpha Barry, Diane Corneau. Effectiveness of barriers to minimize VOC emissions including formaldehyde [J]. Forest Products Journal, 2006,56(9): 38-42.

(2) Triangle Park NC. Using small environmental test chambers to characterize organic emissions from indoor materials and products [J]. EPA, August 1989.

(3) Hai Guo, Frank Murray, Shun-Cheng Lee. Emissions of total volatile organic compounds from pressed wood products in an environmental chamber [J].Building and Environment, 2002, (37): 1117–1126.

Effect of Finger Joint on the Tensile Strength of Lamina

Min-Chyuan Yeh , Yu-Li Lin and Yung-Chin Huang
Dept. of Wood Science & Design National Pingtung Univ. of Sci. & Tech. Pingtung

1. Introduction

The structural performance of glued laminated lumber (glulam) is determined by the layout and strength properties of laminae during the process of product development. Usually the end joints are required for extending the lengthwise lamina for the glulam with a long span. Chang et al. (1991) indicated that the strength of a scarf joint is 20~47% lower than that of a finger joint, and the butt joint showed 70% lower. Furthermore, one of key affecting the strength of laminae is the finger joint processing technique. Several factors including the geometry of finger formation, types of adhesives, wood species, density or grade of lumber, and orientation of finger need to be considered in order to improve the finger joint efficiency. Many research works deal with the finger joints of wood for the non-structural purposes or applications and evaluated based on the bending test. In this study, the structural members with finger joints were evaluated with tensile approach to get more information about joint.

2. Methods

Five wood species including Japanese cedar (*Cryptomeria japonica*, J), hemlock (*Tsuga heterophylla*), Douglas fir (*Pseudotsuga menziessii*, D), southern yellow pine (*Pinus* spp., P) and SPF (spruce-pine-fir) were selected for preparing the size of 33 X 81 X 1200 mm specimens. Three finger lengths including 18, 21, and 24 mm with tip width of 0.95, 1.3, and 0.65 mm, respectively, and at the same tooth spacing of 6 mm were processed using finger jointer (KMFJ-400, Chuan Chier Industrial Co.). The finger orientations during the assembly included vertical (V) and horizontal (H) directions. Resorcinol phenol formaldehyde adhesive (D-40, solid content: 60%, Wood Glue Co.) was applied with para-formaldehyde powder for the finger jointing of lumbers. A tensile test was performed for the finger jointed specimens and solid wood using a tensile testing machine (KH-3000, Kuang Hsin Co.)

3. Results

The overall efficiency of finger joint evaluated by tensile tests for five wood species was 61.4%, while Douglas fir showed the highest joint efficiency, 79.3%. The highest tensile strength was found for finger jointed southern yellow pine, followed by Douglas fir, and then hemlock and SPF, and the lowest for Japanese cedar (Table 1). There was no significant difference in tensile strength of specimens jointed with finger oriented either vertically or horizontally. Furthermore, the specimens jointed with 18-mm finger showed 11.2% higher in tensile strength than that of jointed with 21-mm finger and had similar performance to the 24-mm finger treatment.

Table 1. Tensile strength of the finger jointed lamina.

Species	Orientation	Finger length(mm)	Replication	Tensile strength(MPa)	Statistics
J	H	21	11	22.1	A
J	V	21	10	24.0	A
J	H	18	10	24.2	A
J	H	24	11	25.2	A
J	V	24	10	26.2	A
J	V	18	10	26.5	A
SPF	H	21	10	28.5	AB
SPF	V	21	12	33.3	BC
SPF	V	18	10	33.7	BCD
H	V	24	10	33.8	BCD
H	V	18	12	34.0	BCD
H	V	21	11	34.7	BCDE
SPF	H	24	9	35.3	BCDEF
D	V	21	9	35.7	CDEF
H	H	18	11	36.1	CDEF
D	H	24	11	36.3	CDEF
H	H	21	9	37.3	CDEF
SPF	H	18	10	37.4	CDEF
D	H	18	11	39.3	CDEFG
SPF	V	24	9	41.0	DEFG
H	H	24	10	41.9	EFG
D	H	21	11	42.7	FG
D	V	24	10	45.0	G
S	V	21	11	45.6	G
S	H	24	12	45.8	G
D	V	18	11	46.0	G
S	H	21	11	54.9	H
S	H	18	12	56.2	H
S	V	24	12	56.5	H
S	V	18	12	61.0	H

Predicting the Developmental Trends of Wood-based Materials in China Using AHP and the BCG Matrix

Jian Li, Wenshuai Chen, Haipeng Yu and Yixing Liu
Northeast Forestry University, Harbin

Abstract: To predict the developmental trends of wood-based materials in China, an analytic hierarchy model was constructed, taking into consideration resource and the environment, as well as social and economic systems, and the weighted values of evaluation indexes were also determined. Five catalogues, totaling 15 kinds of wood-based materials, were scored based on the analytic hierarchy process (AHP). Then a comprehensive analysis in the criteria-level combinatorial space was conducted by integrated with the Boston Consulting Group (BCG) matrix. Consequently, the developmental trends of wood-based materials in China were predicted. The results showed that (1) all the judgment matrixes have satisfied consistency requirements, which proves that applying AHP in predicting the developmental trends of wood-based materials is feasible; (2) the comprehensive analysis of the criteria-level combinatorial space by integration with the BCG matrix put the materials into relevant catalogues and locates them at different quadrants; and (3) in the future, solid woods will become a cow, wood-based panels will become a cow or turn into a dog and wood recombination materials could possibly turn into any type. New types of wood-based materials will overcome many difficulties and become a star and non-wood plant panels will face some unexpected influences.

1. Introduction

With increasing product requirements and decreasing supply, the developmental trends of different wood-based materials, such as wood-based panels (Hua 2008), wood plastic composites (Guo et al. 2008), wood ceramics (Tao et al. 2006), and these materials' applications in buildings (Yu and Chen 2009), bridges (Smith 2007), furniture (Scholz et al. 2007), decorations (Chen and Yu 2009), packaging (Zhang 2008), structural materials (Fridley and Asce 2002) and functional eco-materials (Zhao 2006) have gained more attention. Therefore, accurately forecasting the developmental trends can guide us to produce wood-based materials scientifically and utilize wood resources efficiently. However, there are many factors influencing the developmental trends, including raw materials, processing, environmental pollution, product properties, economic benefits, and others, and each of these factors consists of many sub-factors (Yu and Chen 2009). As all of these factors are needed for rational statistics and analysis, the forecasting work becomes very complicated and difficult.

AHP initially breaks down a complex multi-criteria decision- making problem into a hierarchy of interrelated decision elements (criteria and decision alternatives) (Saaty 1994). It has been successfully used in some fields related to wood-based materials, such as the expert analysis of forest industry strategies (Elfvengren et al. 2007), the location choices of furniture companies (Burdurlu and Ejder 2003), forest-certification cases (Kurttila et al. 2000), and so on.

Compared with AHP, the BCG matrix can help with resource allocations (Yang, 2007) and can be used in portfolio analysis (Hambrick, 1982), as well as planning (Kopf et al. 1993). The matrix can also be used to forecast the developmental trends in some relevant fields (Singh 2004).

The objective of this study was to combine AHP and the BCG matrix in predicting the developmental trends of wood-based materials in China. The paper began by scoring 15 kinds of materials by combining tangible and intangible analyses with AHP, and then analyzing them by using the BCG matrix. We then presented the predictions and conclusions.

2. Scoring the materials using AHP

(1) Constructing a hierarchy model

According to AHP (Saaty 1994), a complex decision-making problem was structured as a hierarchy, and the

objective, criteria and alternatives were arranged in a hierarchical structure similar to a family tree. In this study, the hierarchy model with a standard format was illustrated as Fig. 1.

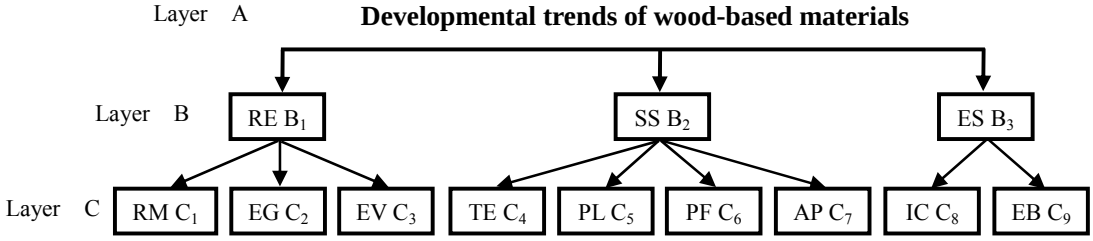

Fig. 1 The hierarchy model of wood-based materials

The first level (objective) referred to the developmental trends of wood-based materials. The objective was divided into three main criteria: resource and environment system (RE), social system (SS) and economic system (ES). Each of these criteria consists of the following sub-criteria:

- RE: raw material (RM), energy (EG) and environment (EV)
- SS: technique (TE), policy (PL), performance (PF) and application (AP)
- ES: investment cost (IC) and economic benefit (EB)

(2) Constructing judgment matrixes

After developing the hierarchy model, 15 experts were invited to establish the pairwise comparison matrix and measure the relative importance of each matrix by using Saaty's (1994 and 1999) 1~9 scale. The pairwise comparison matrix and the comparison results of each matrix were shown in Tables 1~ 4.

Table 1 Judgment matrix A-B.

A	B_1	B_2	B_3
B_1	1	1/3	2
B_2	3	1	4
B_3	1/2	1/4	1

Table 2 Judgment matrix B_1-C.

B_1	C_1	C_2	C_3
C_1	1	1/3	1/8
C_2	3	1	1/5
C_3	8	5	1

Table 3 Judgment matrix B_2 –C.

B_2	C_4	C_5	C_6	C_7
C_4	1	3	1/2	1/3
C_5	1/3	1	1/5	1/6
C_6	2	5	1	1/2
C_7	3	6	2	1

Table 4 Judgment matrix B_3-C.

B_3	C_8	C_9	B_3
C_8	1	1/5	C_8
C_9	5	1	C_9

(3) Confirming the index's weight and checking the consistency

After the comparison matrixes have been formed, the indicator's weight *W* needed to be confirmed. Then, the consistency ratio (CR) was calculated by CR=CI/RI to verify the coherence of the judgment matrix to be accepted, which must be about 0.10 or less. All of the results were illustrated in Tables 5 and 6.

(4) Comprehensive scores

The five categories, which consist of 15 kinds of wood-based materials were numbered and marked in a matrix *P* according to the sub-criteria indexes by the experts. Then, the sub-criteria level score of each material was calculated by multiplying the weighted value of the sub-criteria index and its correlative mark in the matrix *P*. Finally, the total score of each material was counted by summing up the sub-criteria level scores (in Table 7).

Table 5 Local priorities of management options.

Matrix	f1	f2	f3	f4	λ	CI	RI	CR	Consistency
A—B	0.24	0.62	0.14		3.02	0.01	0.58	0.02	Satisfactory
B_1—C	0.08	0.19	0.74		3.04	0.02	0.58	0.04	
B_2—C	0.16	0.06	0.29	0.48	4.03	0.01	0.96	0.01	
B_3—C	0.17	0.83			2.00	0.00	0.00		

Table 6 Global priorities of options.

C	B			weight	sort
	B_1	B_2	B_3		
	0.24	0.62	0.14		
C_1	0.08			0.018	9
C_2	0.19			0.045	6
C_3	0.74			0.177	3
C_4		0.16		0.102	5
C_5		0.06		0.040	7
C_6		0.29		0.181	2
C_7		0.48		0.297	1
C_8			0.17	0.023	8
C_9			0.83	0.117	4

Table 7 *Comprehensive score of 15 kinds of materials.*

Sorting	Number	Materials	Sub-criteria indexes									Total score
			C_1	C_2	C_3	C_4	C_5	C_6	C_7	C_8	C_9	
Solid woods	1	Solid wood	0.04	0.09	1.41	0.72	0.16	1.09	1.79	0.12	0.68	6.09
	2	Solid wood floor	0.02	0.05	1.06	0.52	0.24	1.46	1.49	0.16	0.91	5.89
	3	Veneer	0.07	0.14	1.23	0.72	0.24	0.55	2.09	0.14	0.80	5.97
Wood-based materials	4	Plywood	0.05	0.18	0.53	0.82	0.28	0.55	2.38	0.14	0.80	5.73
	5	Particleboard	0.16	0.18	0.53	0.82	0.36	0.36	2.38	0.09	0.80	5.69
	6	MDF	0.16	0.14	0.53	0.82	0.36	0.36	2.38	0.09	0.80	5.65
Wood recombination materials	7	LVL	0.11	0.14	1.06	0.31	0.24	1.64	1.19	0.09	0.46	5.23
	8	Glued laminated timber	0.13	0.14	1.06	0.41	0.24	1.64	1.19	0.09	0.46	5.35
	9	OSB	0.16	0.18	1.06	0.31	0.32	1.46	0.89	0.09	0.34	4.81
New types of wood-based materials	10	Recombinant Wood	0.09	0.32	1.23	0.21	0.36	1.09	0.89	0.09	0.68	4.97
	11	WPC	0.13	0.27	1.06	0.31	0.24	1.09	1.19	0.12	0.80	5.20
	12	Thermowood	0.11	0.09	1.23	0.31	0.28	1.09	0.89	0.14	0.80	4.94
Non-wood plant panels	13	Flax residue fiberboard	0.14	0.14	0.53	0.41	0.36	0.55	0.89	0.09	0.46	3.57
	14	Straw particleboard	0.14	0.14	0.53	0.52	0.36	0.55	0.89	0.09	0.46	3.67
	15	Bagasse Particleboard	0.13	0.14	0.53	0.52	0.32	0.55	0.89	0.09	0.46	3.61

3. Predicting developmental trends with the BCG matrix

(1) BCG-matrix analysis in a combinatorial space

In the criteria level combinatorial space, five categories of 15 kinds of wood-based materials were comprehensively analyzed by integrated with the BCG matrix based on the scores from AHP (Fig. 2~4). The boundaries of different quadrants were determined by the experts.

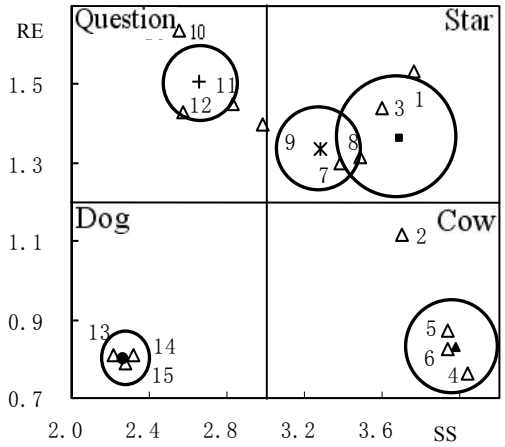

Fig. 2 RE-SS combinatorial space.

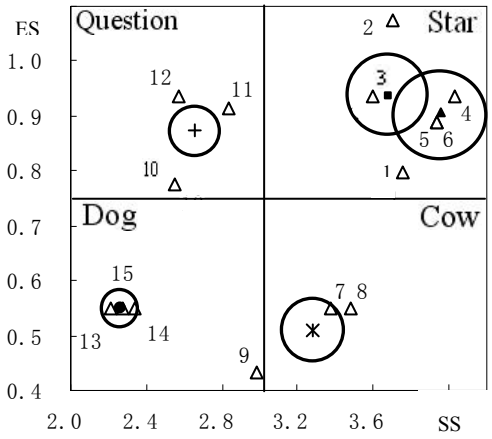

Fig. 3 ES - SS combinational space.

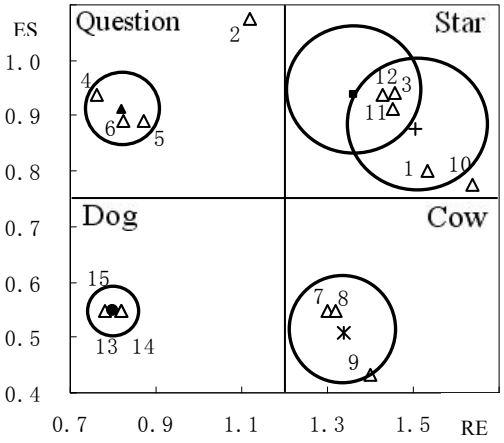

Fig. 4 ES-RE combinational space.

The figures showed that solid woods were distributed with high scores in the star quadrant grid at each space, illustrating that the solid woods are popular materials in China. Wood-based panels were distributed in different quadrants at different combinatorial spaces: cow quadrant in the RE-SS space, star quadrant in the ES-SS space and question mark quadrant in the ES-RE space, which showed that this kind of material had obvious advantages and disadvantages. At present, wood-based panels are widely used because of their low price. However, the volatile organic compound (VOC) pollution problem needs to be solved. Most of the wood recombination materials were distributed near the cross quadrant, demonstrating that their present developmental situation in China is not stable, and the future developmental trend is still very vague. New types of wood-based materials were mainly distributed in the question mark quadrant and turned into the star quadrant in the ES-RE space, which indicates that this kind of material has great developmental potential and space in China. However, during the developmental process, these materials will face many problems. All the non-wood plant panels were located in the dog area, suggesting that the development of this kind of material has to solve many problems. All of the analytical results based on the BCG matrix had a uniform consistency with the results of the comprehensive scores from AHP.

(2) Forecasting developmental trends

Considering the present status of wood-based materials in China, a developmental trend gram based on the BCG matrix analysis was created (see Fig. 5). As can be seen, solid woods will still develop as a star in the long term. With the maturation of wood processing technology and the competition from new types of wood products, the solid woods will gradually shift into a cow. Wood-based panels will have a good space to develop within a short time and will reach their developmental peak soon. This kind of material will become a cow in the future if the environment pollution problem is solved scientifically. However, if the economic benefit can not compensate for the pollution problems, wood-based panels will eventually be replaced by new types of products or other materials. At that time, wood-based panels will turn into dog products, or disappear from the wood-based materials. The developmental trends of wood recombination materials are very complex. If we can develop this kind of product and make it suitable for China's conditions and domestic market, the materials will become a star or cow in the near future. They can also turn into a question mark if their comprehensive performance is still unable to satisfy consumer's demand, and then the developing space will be narrow. In a short time, new types of wood-based materials will be faced many difficulties, and certain fluctuations will exist in the developmental process. With technological innovation, the materials will gradually transit into the tomorrow star of wood-based materials. But in the developmental process, the upgrading of products will also be very fierce. Non-wood plant panels will be developed as dog products over the long term. Product performance and applications, economic benefits and development scale are all important factors that will restrict the development of these materials. However, cheap and sufficient raw materials ensure they will not be eliminated. With major progress in technology, the materials will turn into a question mark or a cow. Otherwise, they will disappear from the wood-based materials.

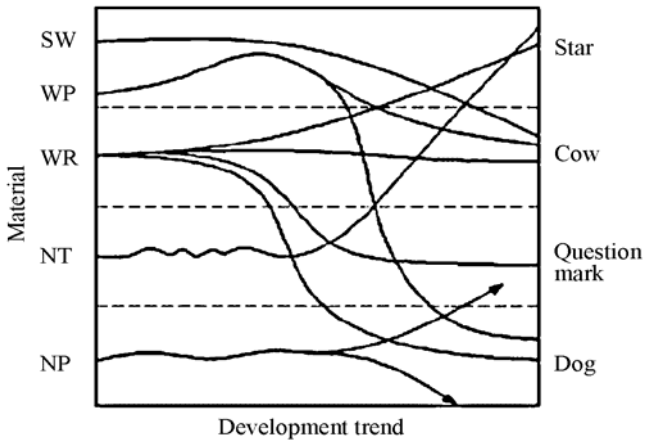

Fig. 5 Developmental trends of wood-based materials.

4. Summary

This study applied AHP to score five categories that consisted of 15 kinds of wood-based materials in China, and then gave a comprehensive analysis in the criteria level combinatorial space with the BCG matrix. Finally, the predictive results of the developmental trends of wood-based materials in China were attained. The results showed that: in the future, solid woods will become a cow, and wood-based panels may turn into a cow or shift into a dog. The developmental trends of wood recombination materials are very complicated and the materials can change into any type. New types of wood-based materials will become a tomorrow star, while non-wood plant panels will face many problems in the developmental process.

Effects of Weathering on the Surface Properties of Wood-Plastic Composites Manufactured by Injection Molding

Pei-Yu Kuo, Huei-Chin Shiue, Jin-Hau Chen and Song-Yung Wang

Biomaterial Physical *Laboratory*, School of Forestry and Resource Conservation, National Taiwan University, Taipei

Abstract: In the world, the most of the applications of WPCs (Wood-Plastic Composites) are in outdoors applications so it is imperative to understand the durability of WPCs. The purpose of this study was to investigate the effect of accelerated and outdoor weathering on functional groups and surface characteristics of WPCs by Fourier Transform Infrared Spectroscopy (FTIR) Diffuse reflection mode (Drift) and Scanning Electron Microscope (SEM). Material compositions includes different plastic-based (Low density Polyethylene, LDPE; Polypropylene, PP; Recycled Polypropylene, RP) and different plastic/wood ratios (3/7, 5/5, 7/3). The results showed that after weathering WF/LDPE composites have fewer cracks than WF/PP and WF/RP composites observing by SEM. In FTIR spectroscopy, under different plastic/wood ratios, there were obvious peaks nearby 3400 cm^{-1}, 2900 cm^{-1} which have been used to characterize the surface of wood because of the increased amount of wood flour on WPCs surface. Moreover, peaks between 1160-1040 cm^{-1} and 1600-1500 cm^{-1} became unobvious because of the weathering of lignin.

1. Introduction

Recently, natural-fiber-reinforced polymers have attracted the attention of researchers because of their advantages over established materials. Plant fibers are biodegradable and readily available, and, compared with glass fibers, their attributes include low cost, low-density, lower abrasive nature, higher specific strength, and higher modulus of elasticity. However, although WPCs have displayed so many advantages, still, there are some unsolved or partially solved problems, like their weathering properties which can't be ignored for outdoor application. Therefore, this study focuses on surface characteristics of WPCs to clarify which kind of material compositions would have more resistance of weathering.

2. Materials and methods

(1) Materials

LDPE (low-density polyethylene), PP (polypropylene) and RPP (recycled polypropylene) were used as the plastic matrices. Wood flour was selected for this study, namely commercial SPF. The flour was then dried for 24 h at 103 ± 2 ℃ in an oven. One additive was used in this study, namely MAPP (Maleic Anhydride Polypropylene) as coupling agent and the amount is 3% of the each batch.

(2) Methods

The compositions of the tested WPCs are indicated in Table 1. The constituent materials were first combined in a mixer according to Table 1. The mixing speed, temperature, and time were 55 rpm, 180 ℃, and 5-10 min, respectively. Wood–plastic particles were produced using a pelletizer and then dried for 24 h at 60℃ in an oven prior to injection molding into tension and flexural bar test samples.

After drying, the wood–plastic particles were placed in an injection molding machine in order to manufacture tension and flexural bar test samples.

Table 1 Composition of tested WPCs.

Specimen Code	Plastic matrix	Wood flour	Specimen Code	Plastic matrix	Wood flour	Specimen Code	Plastic matrix	Wood flour
PE 30	29.1 % PE	67.9%	PP 30	29.1 % PP	67.9%	RP 30	29.1 % RP	67.9%
PE 50	48.5 % PE	48.5%	PP 50	48.5 % PP	48.5%	RP 50	48.5 % RP	48.5%
PE 70	67.9 % PE	29.1 %	PP 70	67.9 % PP	29.1 %	RP 70	67.9 % RP	29.1 %

3. Results and discussion

(1) Morphology of the composite surface with SEM

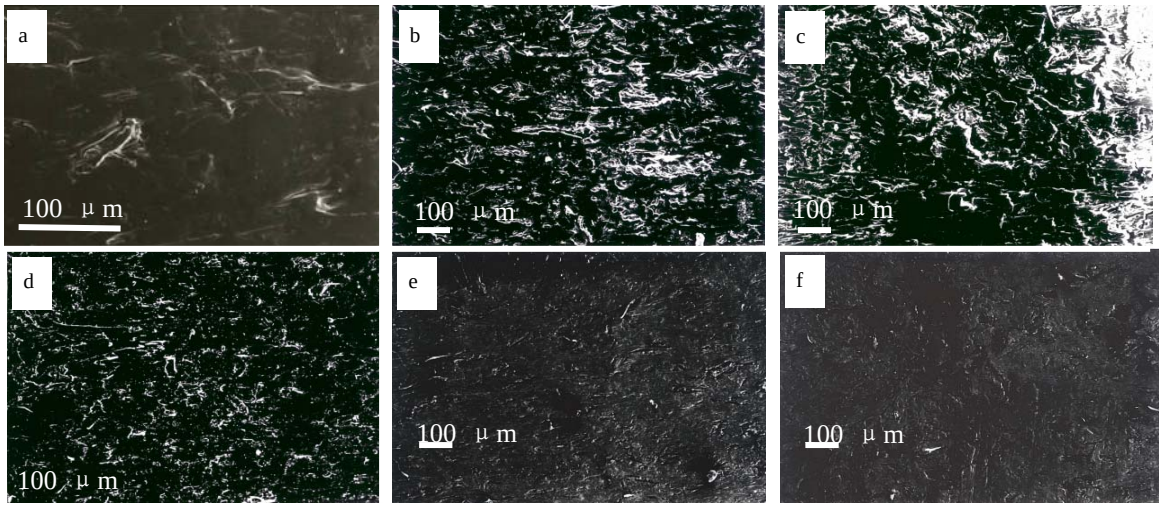

Fig. 1 Scanning electron micrographs of injection molded WF/LDPE composite surfaces (a) before weathering (b) after 360 h of accelerated weathering (c) after 1080 h of accelerated weathering (d) after 9 months of indoor weathering (e) after 5 months of outdoor weathering (f) after 9 months of outdoor weathering.

Before exposure the injection molded composites surface (Fig. 1a) was smooth, and LDPE flow over wood particles was evident. After accelerated and outdoor weathering the surface was degraded (Fig. 1b, c, e and f). Accelerated weathering seems to affect plastic matrix more serious than outdoor weathering because plastic matrix has more breaks on surface. In comparison with indoor weathering (Fig. 1d) which cause a white powder, accelerated and outdoor weathering surface have more cracks in the interface.

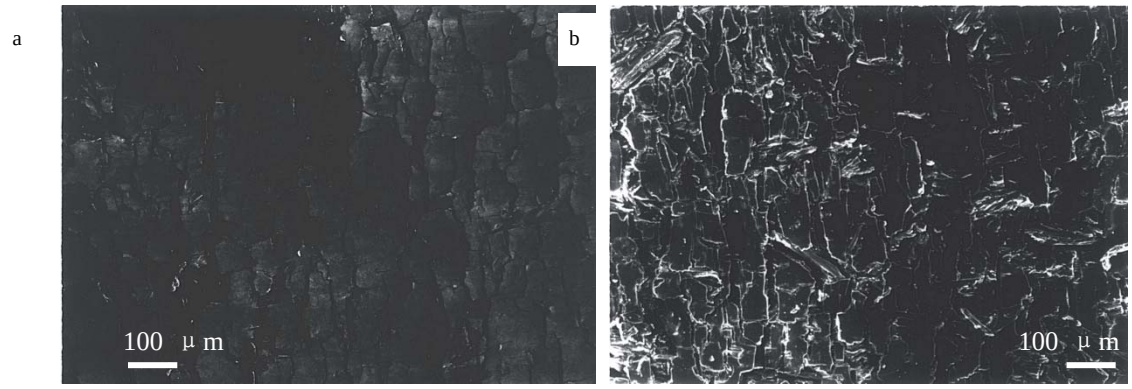

Fig. 2 Scanning electron micrographs of injection molded WF/PP (a) and WF/RP (b) composite surfaces after outdoor weathering five months.

In WF/LDPE composite surfaces, there are more cracks on interfaces. In WF/PP (Fig. 2a) and WF/RP (Fig. 2b) composite surfaces, there are more cracks on matrix. Protrusion was cause by wood particles swelling and shrinking after absorbing and desorbing moisture and Photo-degradation can cause surface cracking. [1]

(2) Surface characteristics of WPCs with FTIR

The infrared spectra of the WPCs surfaces revealed that some bands appeared or disappeared by weathering, appeared peak like 1735 cm^{-1} (C=O stretching in acetyl or carbonyl group)and disappeared peaks like 1500 cm^{-1} to 1700cm^{-1}, and the ratio of peaks had also changed. In Fig. a and Fig. c, specimens, which have more wood

flour, also have more obvious peaks of wood. For example, in comparison with PE 70, PE 30 has several peaks only belonged to wood, such as 2900 cm^{-1}, 1800-1500 cm^{-1} [2]. However, after outdoor weathering, the function groups of three different wood/ plastic ratio look all the same.

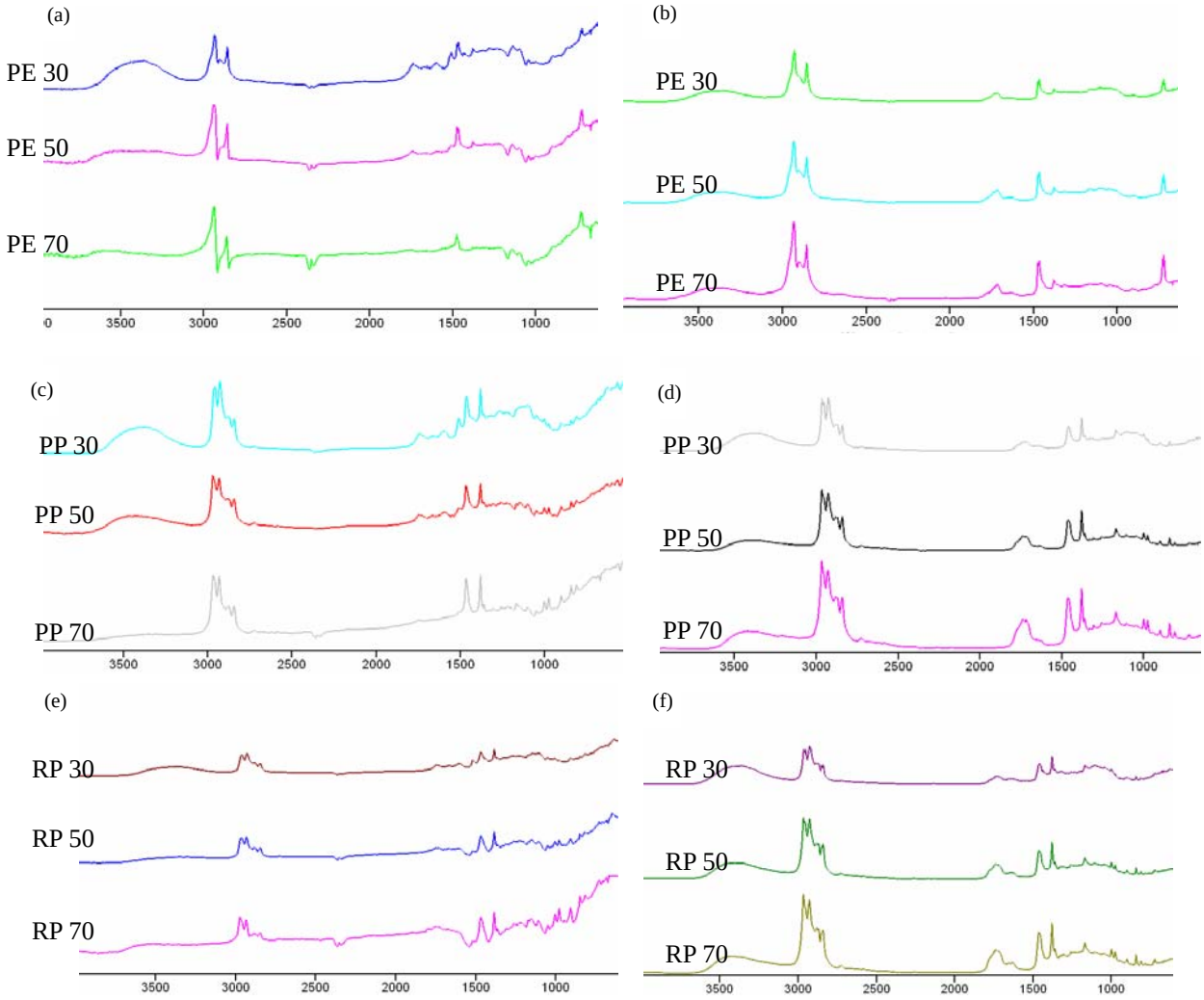

Fig. 3 FTIR spectra of WF/LDPE, WF/PP and WF/RP composites before weathering (Fig. a, c, e) and after five months outdoor weathering (Fig. b, d, f).

4. Reference

(1) Nicole M. Stark, Laurent M. Matuana. Characterization of weathered wood-plastic composite surfaces using FTIR spectroscopy, contact angle, and XPS. Polymer Degradation and Stability, 2007, 92:1883-1890.

(2) Pandey KK. A study of chemical structure of soft and hardwood and wood polymers by FTIR spectroscopy. J Appl Polym Sci 1999, 71(12): 1969-1975

Properties of Dominant, Intermediate and Suppressed Woods in the Japanese Cedar Stand

Jin-Hau Chen and Song-Yung Wang

Biomaterial Physical *Laboratory*, School of Forestry and Resource Conservation, National Taiwan University, Taipei

Abstracts: The research is to know the properties of dominant, intermediate and suppressed woods in the Japanese cedar stand. On the other hand, the relationship between nondestructive and destructive test must be established. The result showed that the density, compressive strength, MOR, DMOE and MOE of dominant woods were the lowest. In those tests, the suppressed woods were the highest. There was no difference among dominant, intermediate and suppressed woods in the MOR values. But, in the compressive strength, DMOE and MOE tests, There were difference between dominant and suppressed woods. Density and among MOR, DMOE and MOE were significantly positive liner relationship. But Density and Pilodyn were significantly negative liner relationship. Among three kinds wave tests were significantly positive liner relationship. MOE and all kinds wave test were significantly positive liner relationship. And so did between MOE and DMOE. Otherwise, in standing woods, the test values were not affected by measured position.

1. Introduction

Japanese cedar (*Cryptomeria japonica*) is important plantation specie in Taiwan. So, to understand the properties of Japanese cedar is front burner. However, even trees grown in the same sites, but each tree was much different. Thus, trees were distinguished from dominant, intermediated and suppressed trees by investigating the DBH of all trees. Using nondestructive test including ultrasonic wave, stress wave and soft X-ray measured trees to know each tree properties. Nondestructive test was popular in the recent year [1-2]. Finally, Using destructive test including bending and compressive strength knew mechanical properties. Then, mechanical strength bridged nondestructive test. One day, nondestructive test can replace destructive test and it becomes more convenient.

2. Material and methods

(1) Material

Japanese cedar is in the Chi-Lan Mt. area, northeastern Taiwan. The study site was located in Compartment no. 20, Tai-Ping-Shan Working Circle of the Forestry Development Department of the Veterans Affairs Commission. The site has an average elevation of 1100 m, and the land gradient is between 15° and 35°. The bedrock is quartzite and shale, and soils are gray and tawny clay loam which produces deep and fertile topsoil. The mean annual temperature near the Yuan-Yang Lake Nature Reserve of Chi-Lan-Shan was 13 ℃, and the mean annual relative humidity was 89% during 1994 and 1996; in addition, the total precipitation in 1994 was 4066 mm.

(2) Methods

First of all, the stand must be investigated the DBH of all trees. Then, standing trees were distinguished from dominant, intermediated and suppressed trees by DBH. Standing trees were measured by nondestructive tests which include ultrasonic wave test, pilodyn test, and Factometer compressive strength test. Next step, standing trees were cut and tuned into sampling woods (2*2*32 cm). Sampling woods were measured by some nondestructive tests including ultrasonic wave test, tap tone test, transversal vibration test, and soft X-ray which could get nine ring characteristics. Then, sampling trees were measured by destructive tests including bending test and compress test. Finally, the data of mechanical strength bridged nondestructive test. And, to know which factors affected bending or compressive strength important. The nondestructive tests which were the best way know the properties of standing trees.

3. Results and discussion

Table 1 Difference of ultrasonic wave velocity and compressive strength among dominant, intermediated and suppressed tree.

	V（m/s）	P（mm）	σ_{cf}（kgf/cm^2）
suppressed	2976 [a]	19.44 [a]	320 [a]
intermediated	2834 [ab]	22.20 [ab]	288 [ab]
dominant	2614 [b]	23.79 [b]	268 [b]

In the ultrasonic wave velocity and compressive strength sides, suppressed tree was the largest and dominant tree was the lowest. The suppressed tree of Pilodyn penetration depth was the lowest. In general, penetration was lower and density was larger. Then, density and compressive strength were positively liner relationship. In those tests, there was difference between the suppressed tree and the dominant tree. The intermediated tree has no differences from the suppressed tree and the dominant tree.

Table 2 Difference of sampling wood's properties among dominant, intermediated, and suppressed wood.

	D (g/cm^3)	V (m/s)	DMOE (kgf/cm^2)	Tv (m/s)	Tt (m/s)	P (mm)	MOR (kgf/cm^2)	MOE (kgf/cm^2)
Suppressed	0.412 [a]	4405 [a]	82330 [a]	4039 [a]	4419 [a]	13.88 [a]	601 [a]	52980[a]
Intermediated	0.408 [a]	4334 [a]	80960 [a]	3968 [a]	4338 [a]	14.48 [ab]	581 [a]	52010[a]
Dominant	0.406 [a]	3991 [b]	70820 [b]	3670 [b]	3938 [b]	15.36 [b]	571 [a]	43060[b]

In the density and MOR sides, the suppressed wood was the largest and dominant wood was the lowest. There were no differences among the suppressed wood, the intermediated wood and the dominant wood. In the ultrasonic wave velocity, DMOE, Tv, Tt and MOE sides, the suppressed wood was the largest and dominant wood was the lowest. The dominant wood was difference from the suppressed wood and the intermediated wood. In Pilodyn test, the intermediated tree has no differences from the suppressed tree.

Table 3 The r values of the sampling wood properties.

	D	V	DMOE	Tv	Tt	MOR	MOE	P
D	1							
V	-0.03	1						
DMOE	0.31	0.93	1					
Tv	0.02	0.98	0.93	1				
Tt	-0.04	0.96	0.89	0.97	1			
MOR	0.56	0.43	0.60	0.48	0.44	1		
MOE	0.33	0.79	0.87	0.82	0.78	0.61	1	
P	-0.55	-0.49	0.29	-0.48	-0.49	-0.11	0.19	1

Density and MOR had a positively liner relationship. Ultrasonic wave velocity had the positively liner relationships among DOME, Tv, Tt and MOE. DMOE had the positively liner relationships among Tv, Tt, MOR and MOE. Tv had the positively liner relationships between Tt and MOE. Tt and MOE had a positively liner relationship. Pilodyn and density had a negatively liner relationships.

4. Conclusions

The result showed that the density, compressive strength, MOR, DMOE and MOE of dominant woods were the lowest. In those tests, the suppressed woods were the highest. There were no differences among dominant, intermediate and suppressed woods in the MOR values. But, in the compressive strength, DMOE and MOE tests, There were difference between dominant and suppressed woods. Density and among MOR, DMOE and MOE were significantly positive liner relationship. But Density and Pilodyn were significantly negative liner relationship. Among three kinds wave tests were significantly positive liner relationship. MOE and all kinds wave test were significantly positive liner relationship. And so did between MOE and DMOE.

5. Reference

(1) Wang, S. Y. and S. T. Chuang. Experimental data correlation of the dynamic elastic modulus, velocity and density of solid wood as a function of moisture content above fiber saturation point. Holzforschung. 54:309-314.

(2) Wang S. Y., C. J. Lin and C. M. Chiu. Evaluation of wood quality of Taiwania trees grown with different thinning and pruning treatments using the ultrasonic-wave method. Wood Fiber and Science. 37(2):192-200.

Flammability and Related Properties of Double-diffused Plywood

Sheau-Horng Lin

Department of Wood Science and Design, Pingtung University of Science and Technology, Pingtung

Abstract： Red lauan(*Shorea* spp.) veneers, 0.65 mm thick, and 2.7 mm thick radiata pine(*Pinus radiata*) veneers were double diffused with nine inorganic salts as the first solutions and subsequently with diammonium phosphate（DAP） as the second solution. Four millimeter thick flame retardant plywood was manufactured after one side MUF glue spreading. Flame retardant performance and the improving efficiency in bond shearing strength of the plywoods were carefully examined. Veneers treated with magnesium and zinc sulfates gave the highest increment in weight, those treated with boric acid, boron oxide and sodium tetraborate showed the least. Specimens weight gain increased with the concentration of the second solution, DAP.The flame retardant performance of all the plywoods double diffused with nine saturated first solutions before the second solutions of three different concentrations fulfilled the performance examination. The flame retardant grades of the treated plywoods were all promoted to the second level, except those diffused with zinc sulfate and 10% DAP. All except three (those treated with aluminum,magnesium, zinc sulfates and subsequently with 30 % DAP) flame retardant plywoods met the regulation of Type Ⅲ products. Bond shearing strength loss percentage ranked from 9.9 to 74.2 % for all the plywoods produced; more than two-thirds of the treated specimens passed Type Ⅱ requirement, according to CNS 8060 standard. Their average bond shearing strength loss percentage were 10.5-67.7 %.

1. Introduction

Red lauan and radiata pine veneers were chosen as the raw materials in this study, double diffused with nine saturated salt solutions before impregnation concentrations with DAP of three as the 2nd treatment. Four millimeters thick flameproof plywoods were made after spreading MUF resin as adhesives. The flame retardant performance and its improving efficiency were examined followed by the determination of the bond shearing strength of the final products.

2. Materials and methods

(1) Materials

Air-dry, 0.65 mm thick rotary red lauan veneers and 2.7 mm thick radiate pine veneers were dimensioned into 320 mm×320 mm for the infiltration of chemical solutions. The nine saturated first solutions applied were 35.0 %, $ZnSO_4$; 48.0 %, $Al_2(SO_4)_3$; 60 %, $MgSO_4$; 43.0 %, $BaCl_2$; 40 %, $CaCl_2$; 55.0 %, $MgCl_2$; 5.0 %, H_3BO_3; 4.5 %, $Na_2B_4O_7$; and 4.5 %, B_2O_3.DAP was chosen as the 2nd solution. Market melamine urea formaldehyde resin was introduced wheat flour the extender, 10 % NH_4Cl the hardener to as the adhesives and manufacture double-diffused plywoods.

(2) Methods

A. The weight gains (WGs %) of the veneers were calculated.

B.A spreading amount of 183.0 g/m^2 melamine urea formaldehyde resin (MUF) was introduced onto a surface of the treated veneers before 10 minutes cold press at 10 kgf/cm^2 and hot press at 115 -120 ℃ (1 minute for 1 mm thickness). Four millimeter thick 3-ply flame retardant plywood was thus manufactured.

C.Flame retardant performance of the plywoods with a flammability 45 degree tester (Model FL-45MC) according to CNS 8736 (1997) and CNS-7614 (1994).

D. The bond shearing strength of the treated plywood were obtained according to CNS 11668 (1997) and CNS 8060, respectively.

3. Results and discussion

(1) The combustion performance of the untreated plywoods and the weight gain of the treated plywood

It was perceivable from Fig. 1 that, among the nine first solutions, magnesium sulfate gave the highest weight gain (38.78 %) and sodium tetraborate the lowest(16.89 %), indicating the difficulty for the latter to diffuse into the specimens.

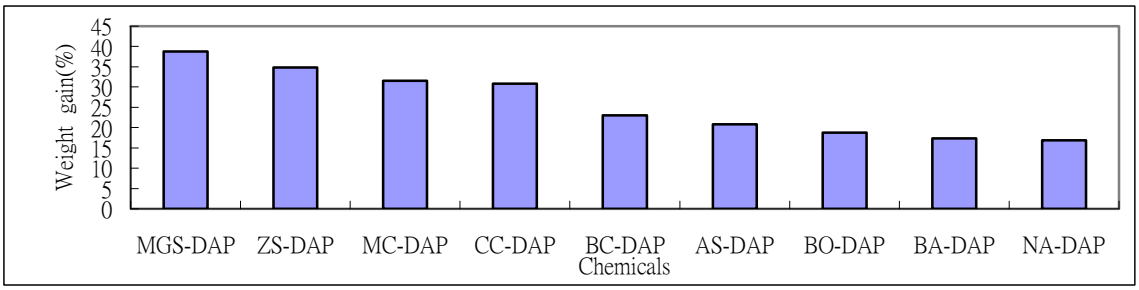

（In which MGS is $MgSO_4$, ZS is $ZnSO_4$, MC is $MgCl_2$, CC is $CaCl_2$, BC is $BaCl_2$, AS is $Al_2(SO_4)_3$, BO is B_2O_3, BA is H_3BO_3 while NA is $Na_2B_2O_7$. DAP is diammonium phosphate）

Fig.1 Weight gain of double diffusion treated plywood.

(2) The flame retardant performance of the double-diffused plywoods

All the treated plywoods passed the flame retardant test regulated in CNS 11668 and were categorized as third or second grade FR after CNS 7614, indicating that the combination of chemicals applied in this study did improve plywoods'flame retardant performance. (Table 2).

Table 2 The flame retardant performance and estimated results of double diffusion treated plywood.

Chemicals	Board thickness (mm)	MC (%)	Sp.gr	WG (%)	Flame retardant performance CA (cm^2)	CL (cm)	AF (sec)	AG (sec)	MLP (%)	Estimated results CNS 8736	CNS 7614
Control	3.9	8.3	0.6	—	134.2	17.3	62.6	63.3	7.6	X	X^+
AS-DAP_{20}	4.3	7.3	0.6	20.9	25.1	7.5	0.0	0.0	0.6	O^a	2
ZS-DAP_{20}	4.3	7.6	0.6	32.3	21.2	7.4	0.0	1.2	1.2	O	2
MGS-DAP_{20}	4.3	7.9	0.7	37.2	24.2	7.3	1.3	1.6	1.2	O	2
BC-DAP_{20}	3.9	9.6	0.7	20.3	23.4	7.2	0.0	0.0	1.1	O	2
CC-DAP_{20}	3.6	9.7	0.7	29.1	37.7	8.8	0.0	9.0	2.5	O	2
MC-DAP_{20}	4.1	9.0	0.7	30.5	22.8	7.0	0.0	0.0	1.3	O	2
BA-DAP_{20}	4.3	10.0	0.7	18.1	24.2	7.3	0.0	0.0	0.9	O	2
NA-DAP_{20}	4.4	7.6	0.6	17.6	31.5	8.3	0.0	0.0	0.9	O	2
BO-DAP_{20}	4.3	9.7	0.7	19.2	23.4	7.0	0.0	0.0	0.7	O	2

(3) Bond shearing strength of the treated plywood

A positive relation was established between the concentration of the second impregnation solution and the weight gain of the treated plywoods. The carbonized area, carbonized length and mass lose percent were also improved with increasing weight gain (Table 3). Similar results were obtained in the studies of other flammability and fire-retardant plywoods (Lin and Wang, 1992, 1993, 2001~2003).

Table 3 The bond shearing strength of flame retardant plywood.

Chemicals & conc.(%)	Type Ⅲ			Type Ⅱ		
	τ(kgf/cm^2)	L_1(%)	WFR(%)	τ(kgf/cm^2)	L_2(%)	WFR(%)
Control	18.2	----	100	12.4	----	90
AS-DAP_{10}	8.1	55.5	85	6.2*	50.0	60
AS-DAP_{20}	7.9	56.6	80	6.0*	51.6	65
AS-DAP_{30}	7.1*	60.9	80	5.3*	57.3	60
ZS-DAP_{10}	8.4	53.8	85	7.2*	41.9	70
ZS-DAP_{20}	7.9	56.6	85	5.2*	58.1	60
ZS-DAP_{30}	4.7*	74.2	60	4.0*	67.7	50
MGS-DAP_{10}	10.9	40.1	90	8.1	34.7	70
MGS-DAP_{20}	10.0	45.1	90	7.2*	41.9	65
MGS-DAP_{30}	7.2*	60.0	80	6.1*	50.8	60
BC-DAP_{10}	16.4	9.9	100	11.1	10.5	85
BC-DAP_{20}	13.1	28.0	95	10.5	15.3	80
BC-DAP_{30}	11.9	34.6	85	8.7	29.8	75
CC-DAP_{10}	13.8	24.2	95	10.2	17.7	85
CC-DAP_{20}	12.2	32.9	85	9.3	25.0	80
CC-DAP_{30}	11.3	37.9	80	8.1	34.7	75
MC-DAP_{10}	15.0	17.6	100	11.0	11.3	85
MC-DAP_{20}	14.5	20.3	100	10.5	15.3	85
MC-DAP_{30}	11.8	35.2	90	8.2	33.9	78
BA-DAP_{10}	14.7	19.2	100	10.1	18.5	85
BA-DAP_{20}	12.4	31.9	95	9.8	20.9	80
BA-DAP_{30}	9.60	47.3	90	8.1	34.7	80
NA-DAP_{10}	12.5	31.3	95	10.8	12.9	85
NA-DAP_{20}	11.6	36.3	95	9.4	27.4	80
NA-DAP_{30}	11.0	39.6	90	8.2	33.9	80
BO-DAP_{10}	16.0	12.1	100	10.8	12.9	80
BO-DAP_{20}	13.2	27.5	100	10.2	17.7	80
BO-DAP_{30}	10.9	40.1	90	8.0	35.5	70

τ (kgf/cm^2):Bond shearing strength；L_1 & L_2 :Loss percent of bond shearing strength；WFR(%):Wood failure ratio；＊ Represents failure from standard

4. References

(1) Lin, S.H.and H.H.Wang (1992) The manufacturing of fire-resistance plywood and investigation of gluability. Forest Products Industries 11(4):68-80.

(2) Lin, S.H.and H.H.Wang (1993) The flameproof, gluability and hygroscopic of composite treated plywood. Q.Jour.Chin.For. 26(2):79-94.

(3) Lin, S.H., H.H.Wang and J.W.Perng (1997) The manufacturing of 9 mm-thick fire retardant-treated plywood. Q.Jour.Chin.For. 30(4):437-444.

(4) Lin, S.H., H.H.Wang and K.J.Hong (2001) Improvement on the flame retardant performance of the double-diffusion treated plywood. Forest Products Industries 21(2):135-144.

(5) Lin, S.H., H.H.Wang and K.J.Hong (2002) Improving efficiency of flameproof performance on double diffusion treated plywood. Q.Jour.Chin.For. 35(3):321-330

(6) Lin, S.H.(2003) Study on the improving efficiency of incombustibility of plywood treated by fire retardants double diffusion method. The Dept. of Forestry, National Chung-Hsing University, Doctoral Dissertation. 255 pp.

Assessment of Temperature and Relative Humidity Conditioning Performance of Interior Decorative Materials in Container under Ventilation Condition

Lang-Dong Lin[1], Song-Yung Wang[2], Miao-Fen Yan[2] and Ming-Jer Tsai[2]

[1] Department of Forest Products Science, National Chiayi University, Chiayi

[2] School of Forestry and Resource Conservation, College of Bio-Resource and Agriculture, National Taiwan University, Taipei

Abstract: The purpose of this study was to examine the temperature and relative humidity (RH) conditioning performance of wood panels (used as interior decorative materials) in container under ventilation condition. Hourly temperature and RH values were recorded in a living environment based on the data of average values from 1974 to 1990 for the Taipei area. Thirty-six interior finishing materials, attached to one inside surface of a 35-cm^3 simulation aluminum container with a controllable ventilation opening (10.5 X 8.5 cm), were used. During the daily experimental period, programmable ventilation was performed from the 5^{th} to 8^{th} hour for exposure to a high humidity. The results revealed that a significantly lower average RH (in comparison with control group and climate condition) was indicated in the sealed container lined with various wood species and some wood-based materials, while a significantly higher average RH was observed in the sealed container lined with inorganic materials after ventilation under a humid condition. The hygroscopic conditioning performance of the decorative materials could be classified into three types, in accordance with b values (humidity conditioning performance index). The RH changing ratio decreased curvilinearly with increasing panel thickness and A/V values (surface area of interior decorative materials attached to container/inside air volume of container), whereas b values increased with increasing panel thickness and A/V values in the sealed container.

1. Introduction

In modern society, more and more people are spending most of their time indoors. Therefore, interior climate qualities in residences, offices and other non-industrial indoor environments have become an issue of increasing concern, as an important aspect of indoor environment. In general, the interior climate of a living environment is controlled by a combination of room temperature, relative humidity (RH), ventilation, air circulation and heat radiation. It is recognized that these factors can be influenced by the design and construction of the building or the materials used and facilities installed. However, when the relationship between the materials used and interior climate was considered, the effect of room humidity was greater than that of room temperature.

To explore the temperature and RH conditioning effects of interior decorative materials, Wang and Tsai [1] investigated 36 interior finish materials attached to a single inside surface of a sealed 35-cm^3 simulation aluminum container. The temperature and RH vibration in the closed aluminum container was mainly caused by the temperature changes outside the aluminum container and thermal conductivity during the daily experimental period. Actually, natural ventilation is a widely used cooling scheme for buildings. It provides a thermal, comfortable environment by refreshing the indoor air with outdoor air without using mechanical power thus reducing the energy consumption in buildings [2,3]. It also improves the indoor air quality, avoiding the Sick Building Syndrome caused by a poor design of active ventilation systems [4]. As a result, it has attracted a considerable amount of interest from researchers and building designers in the recent years.

Therefore, to assess temperature and RH conditioning performance of interior decorative materials in container under ventilation condition, the environmental chamber used in our former study [1] was programmed with average hourly temperature and RH values from 1974 to 1990 for the Taipei area. Programmable ventilation was performed through an opening in the sealed container from the 5^{th} to 8^{th} experimental hour (for exposure to high humidity) during the daily experimental period (Fig. 1). Thirty-six materials were tested and data derived from temperature and RH changes inside the sealed container were used (Fig. 2). The temperature and RH conditioning performance of various materials, and wood panels with different thicknesses and A/V values

(surface area of interior decorative materials attached to container/inside air volume of container) were evaluated under ventilation condition.

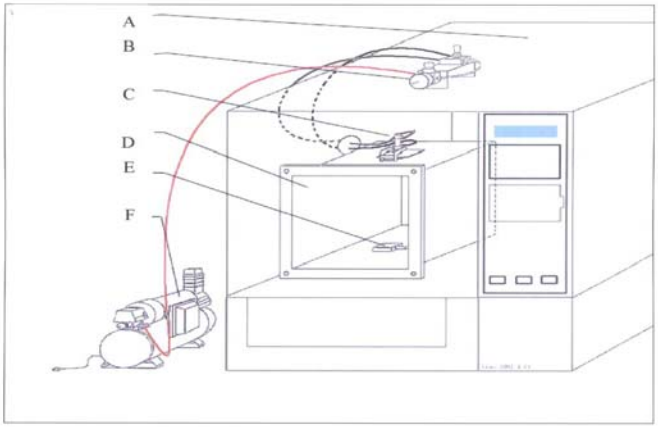

A: Computer-controlled environmental chamber; B: Controllable valve of opening on aluminum container; C: Controllable opening on aluminum container; D: Aluminum container; E: Temperature and RH detector; F: Air compressor

Fig. 1Diagram of experimental set-up.

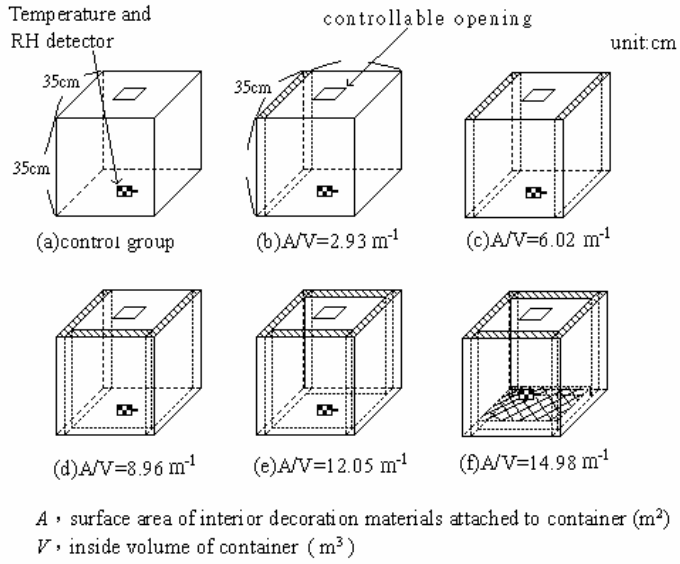

Fig. 2 Experimental aluminum container (35 cm^3) without any lining material (a), and with one–five pieces of wood panel (b–f) lining its inner wall.

2. Results and discussion

(1) Efficiency index of various decorative materials

In general, temperature changing ratios and average temperature rarely altered. A possible reason for this is the fact that the A/V value was 2.87–2.99 m^{-1}. Heat energy was transferred inward from the other five sides of the aluminum container owing to thermal conductivity, thermal convection and heat radiation. However, smaller RH changing ratios were found in the following test samples: five untreated solid woods of different species, plywood, insulation fiberboard and paper overlaid fiberboard. Higher RH changing ratios were seen in materials combined and/or coated (sprayed) with adhesives, although their surfaces still had wooden characteristics: these materials included particleboard, MDF (medium density fiberboard), fiberboard, OSB (oriented strand board),

concrete board and plaster fiberboard. When the surface of wood-based materials was treated with resin or inorganic material (e.g. glass, or marbles), relatively larger RH changing ratios were seen.

The average RH in a sealed container under ventilation condition showed significant differences in comparison with the results of our former study in a closing condition [1]. A significantly higher average RH was observed in inorganic materials (75.5%–80.6%). This is because moisture in a sealed container could not be absorbed by inorganic materials after ventilation under a humid climate condition. However, a significantly lower average RH (in comparison with control group and climate condition) was indicated in five untreated solid wood (70.1%–72.7%) and some wood-based materials. This phenomenon might be due to the fact that the untreated solid woods of different species could absorb much moisture resulted from ventilation under a humid climate condition; therefore, the lower average RH in a sealed container after ventilation under a humid climate condition could be obtained.

(2) Efficiency index of various panel thicknesses

The changes in temperature and RH with time inside an aluminum container lined with Japanese cedar or red oak panel (A/V 2.88–3.04 m^{-1}) of different thicknesses after ventilation are summarized as follows. It was found that $\Delta T_1/\Delta T_2$ ranged from 0.97 to 1.20 for Japanese cedar and from 1.07 to 1.24 for red oak panels. The values were similar to those of the control (1.11). A poor temperature conditioning performance was found between various panel thicknesses. In comparison to control group (24.6 °C), a significant change of average temperature was also not observed in our study. It was found that the average temperature ranged from 24.1 °C to 24.7 °C for Japanese cedar and from 24.1 °C to 24.9 °C for red oak panels. For the RH conditioning performance, it showed that the $\Delta RH_1/\Delta RH_2$ value ranged from 0.24 to 0.56 for Japanese cedar panels of various thicknesses and from 0.22 to 0.63 for red oak panel. For the aluminum container without specimens inside, the $\Delta RH_1/\Delta RH_2$ value was 0.83. In comparison to control group (74.5%), a significantly lower average RH was indicated in various thicknesses for Japanese cedar panel (69.1%–72.7%) and for red oak panel (68.5%–70.1%), respectively. This is because moisture could be absorbed by wood after closing the opening in the container. It was concluded that a thickness of as little as 0.3 cm was sufficient to display the RH conditioning performance of wood panels.

(3)Efficiency index of various A/V values

Changes in temperature and RH with time inside an aluminum container lined with Japanese cedar or red oak panels (thickness: 0.9 cm) at various A/V values after ventilation were as follows. The $\Delta T_1/\Delta T_2$ ranged from 1.06 to 1.42 for Japanese cedar and from 1.03 to 1.20 for red oak panels. The values were similar to those of the control (1.11). There was, therefore, no conditioning effect on temperature, even when the A/V value reached 14.98 m^{-1}. In terms of the conditioning effect on RH, the $\Delta RH_1/\Delta RH_2$ decreased as A/V value increased. The $\Delta RH_1/\Delta RH_2$ values were 0.58–0.45 for Japanese cedar and 0.70–0.55 for red oak panels. For the aluminum container without a specimen inside, the $\Delta RH_1/\Delta RH_2$ was 0.83. In comparison to control group, a significant change of average temperature was also not observed in our study. However, a significant lower average RH was indicated in various A/V values for Japanese cedar panel (67.6%–72.7%) and for red oak panel (65.8%–70.1%), respectively. For the aluminum container without specimens inside, the average RH value was 74.5%. Thus, an A/V value of as little as 2.93 m^{-1} provided a conditioning effect on RH.

3. References

(1) Wang SY, Tsai MJ. Assessment of temperature and relative humidity conditioning performances of interior decoration materials. J Wood Sci 1998; 44: 267–274.

(2) Zhao R, Xia Y. Effective non-isothermal and intermittent air movement on human thermal responses. Proceedings of Room Vent 98. Stockholm, 1998; vol. 2, pp 351–357.

(3) Busch JF. A tale of two populations: thermal comfort in air-conditioned and naturally ventilated oDces in Thailand. Energy and Buildings 1992; 18: 35–49.

(4) Finnegan JJ, Pickering CAC, Burge PS. The sick building syndrome: prevalence studies. British Medical Journal 1984; 289:1573–1575.

Leachability, Metal Corrosion and Termite-resistance of Wood Treated with Copper-based Preservative

Lang-Dong Lin[1], Yi-Fu Chen[2], Song-Yung Wang[2] and Ming-Jer Tsai[2]

[1]Department of Forest Products Science, National Chiayi University, Chiayi

[2] School of Forestry and Resource Conservation, College of Bio-Resources and Agriculture, National Taiwan University, Taipei, Taiwan.

Abstract: Health-awareness and concern for the environment have resulted in voluntary removal of chromated copper arsenate (CCA) from wood preservatives in residential applications worldwide. Copper-based preservatives have been formulated as replacements, but these may not provide a permanent solution to all of the related problems, including copper contamination of aquatic environments and corrosion of fasteners. In this study, the copper retention (before and after the leaching process) of five softwood specimens vacuum-treated with alkaline copper quaternary (ACQ) and copper azole (CA) at three target retention levels were investigated by X-ray fluorescence studies. The metal corrosion and termite (*Coptotermes formosanus*) resistance of treated specimens were studied under laboratory conditions. Except for treated Japanese larch wood, the copper retentions of the other wood specimens were able to meet the target copper retention values (use classes 2–4) in CNS 3000. The copper leaching rates were 6.92–19.54% for ACQ-treated wood and 9.38–22.46% for CA-treated wood. The metal corrosion rates of iron nails due to corrosion tests (CNS 6717) were influenced significantly by the 1.2% ACQ and 1.2% CA treatments; whereas the metal corrosion rates of zinc-galvanized steel nails were less than 2 and could meet the tested standard. Even though the ACQ and CA treatments caused higher copper leaching rates from the treated specimens, they also increased termite mortalities and reduced the mass loss significantly after termite-resistance tests (JIS K 1571).

1. Introduction

Biodegradation of wood by termites is recognized as one of the most serious problems for wood utilization in countries such as Taiwan, Japan, and parts of the United States (Cheng et al., 2007). Many toxic wood preservatives were used in the past in attempts to minimize termite damage. Recognition of risks for human health and potential damage of the environment have prompted changes of the types of preservatives used commercially in recent years. The use of preservatives that include arsenic, chromium and other heavy metals has decreased in most European countries and in North America (Humar et al., 2006).

Some alternative methods, including chemical modification and the use of arsenic/chromium-free preservatives, are developed to enhance the durability of wood without the use of conventional toxic biocides. Chemical modification is accomplished by reacting the wood with selected chemicals, which modify the cell wall wood polymers without leaving toxic residues within the wood. The use of chemical modification to stabilize wood against the activities of decay organisms has been the subject of numerous studies. Arsenic/chromium-free alternatives based on copper compounds have been also introduced recently as alternative chemicals, because copper exhibits good biocidal activity. Some of these new preservative systems include alkaline copper quaternary (ACQ), copper azole (CA), ammoniacal copper citrate (CC), copper dimethyl-dithio-carbamate (CDDC), and Cu-HDO ((bis-(*N*-cyclohexyldiazeniumdioxy)-copper). There have been some reports about the properties of penetration, retention, leaching, resistance to fungi and termites and long-term field test of some softwood and hardwood treated with these new preservatives (Temiz et al., 2005; Yildiz, 2007).

However, copper-based preservatives may not provide a permanent solution to all related problems; some of these issues include concern over copper in aquatic environments and corrosion of fasteners (Arango et al., 2006). In this study, copper retention (before and after the leaching process) of five softwood specimens vacuum-treated with ACQ and CA at three target retention levels were investigated by X-ray fluorescence studies. The metal corrosion and termite (*Coptotermes formosanus*) resistance of treated specimens were studied

under laboratory conditions. These results can provide information for estimating applicability of copper-based preservatives in architectural design.

2. Results and discussion

(1) Copper retention of treated wood specimens after the leaching process

Except for treated Japanese larch wood, the copper retentions of the other wood specimens were able to meet the target copper retention values (use classes 2–4) in CNS 3000. The treated Japanese larch wood was able to meet the target copper retention values (use classes 2 and 3) in CNS 3000 because of resins in the tracheids of Japanese larch. Generally, the copper retentions of treated specimens increase with an increase of preservative concentration. A high coefficient of relationship (r = 0.9763) between copper retention and preservative concentration was found. Taking specimen density into consideration, there was a negative linear relationship (r = 0.7074) between copper retention of treated specimens and density of the wood.

Except for treated Japanese larch wood, the copper retention of the other wood specimens after the leaching process met the target copper retention values for use classes 2–4 in CNS 3000. After the leaching process, the treated Japanese larch wood could meet the target copper retention value only for use classes 2 and 3 in CNS 3000. For all ACQ- and CA-treated wood specimens, the copper leaching rates were 6.92–19.54% and 9.38–22.46%, respectively. Generally, the copper leaching rates of treated specimens increased with increased concentration of treated preservative, possibly because of better copper fixation when the wood was treated with lower concentrations of preservatives.

(2) Metal corrosion

Fig. 1 shows metal corrosion rate of wood treated with ACQ and CA. The result indicates that the metal corrosion rate of the iron nails due to corrosion was influenced significantly by the treatment with 1.2% ACQ and 1.2% CA (metal corrosion rate > 2). This is because serious metal corrosion may be caused by ammonia and chloride in the preservatives tested. The metal corrosion rates of the zinc-galvanized nails after the corrosion tests were less than 2 (Fig. 1). The rates showed no significant difference among specimens treated with 0.3% ACQ, 0.6% ACQ, 0.3% CA, and 0.6% CA (1.17–1.22%). However, a significant difference was found between 1.2% ACQ (or 1.2% CA)-treated specimens (1.59-1.62%) and the other specimens.

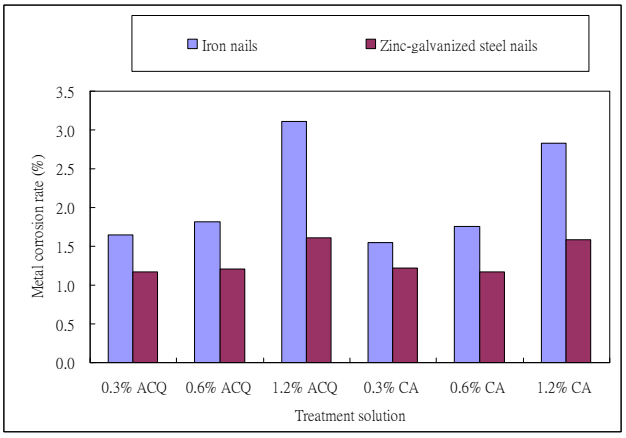

Fig. 1 Metal corrosion rate of wood treated with alkaline copper quaternary (ACQ) and copper azole (CA).

(3) Termite- resistance of untreated specimens

The termite-resistance tests showed that untreated Japanese larch suffered the greatest mean mass loss (mean 13.94%) and had the lowest termite mortality (9.5%) (a positive relationship (r = 0.6442) between specific gravity and mass loss, but a negative correlation between termite mortality and mass loss (r = 0.6923), and between specific gravity and termite mortality (r = 0.5970)).

(4) Termite-resistance of treated specimens

Even at low retention values, ACQ- and CA-treated specimens showed lower mass loss and greater termite mortality in comparison to those shown by the untreated specimens. Even though the leaching process caused higher leaching rates of copper from the treated specimens, ACQ and CA treatments also increased termite mortality significantly and reduced the mass loss.

We examined the relationship between termite mortality, mass loss, and specific gravity using linear statistical analysis. According to this test, the mass loss and the termite mortality of treated specimens were inversely associated (r = 0.5972). The rate of termite mortality and specific gravity were also inversely related (r = 0.3292), while mass loss had a marginally positive association with specific gravity (r = 0.2629).

3. References

(1) Arango, R.A., Green, F., Hintz, K., Lebow, P.K., Miller, R.B., 2006. Natural durability of tropical and native woods against termite damage by *Reticulitermes flavipes* (Kollar). International Biodeterioration & Biodegradation 57 (3), 146–150.

(2) Chang, S.T., Wang, S.Y., Wu, C.L., Su, Y.C., Kuo, Y.H., 1999. Antifungal compounds in the ethyl acetate soluble fraction of the extractives of Taiwania (*Taiwania cryptomerioides* Hayata) heartwood. Holzforschung 53, 487–490.

(3) Humar, M., Peek, R.D., Jermer, J., 2006. Regulations in the European Union with emphasis on Germany, Sweden, and Slovenia. In: Solo-Gabriele, H., Townsend, T., Taylor and Francis, Editors, Environmental Impacts of Preservative-Treated Wood, Boca Raton, pp. 37–57.

(4) Temiz, A., Yıldız, Ü.C., Gezer, E.D., Yıldız, S., Dizman, E., 2005. Leaching characteristics of alder wood treated with copper based wood preservatives. In: Proceedings of the IRG 36th annual meeting. 24–28 April 2005, Bangalore, India, IRG/WP 05-50225.

(5) Yildiz, S., 2007. Retention and penetration evaluation of some softwood species treated with copper azole. Building and Environment 42(6), 2305–2310.

Effects of Low Molecular-weight Phenol Resin Treatment on the Vibration Properties of Sitka Spruce Plate

Chih-Lung Cho
National I-Lan University, I-Lan

Abstract: This study investigated the vibration properties of quarter-cut Sitka spruce plates treated with three kinds of low molecular-weight phenol resin (LPR) concentrations (5%, 10%, 20%) by non-pressure process. Resonant frequencies of modes (1, 1), (0, 2), and (2, 0) were measured by Chladni plate vibration method to evaluate acoustic properties of Sitka spruce.

The experimental results indicated that moisture contents of chemically treated specimens in equilibrium with 20℃ temperature and 65% relative humidity were 4.6% ~ 7.0% lower than those of untreated specimens. The decreased percentages were proportional to chemical concentrations. The hygroscopic ability of Sitka spruce impregnated with LPR was reduced significantly. The density of test specimen was slightly increased while increasing chemical concentration. Resonant frequencies of different modes, modulus of elasticity and shear modulus of chemically treated plates were increased significantly. The physical properties were improved greater for modulus of elasticity in the radial direction and shear modulus than for modulus of elasticity in the longitudinal direction. Consequently, the ratios of Young's modulus to the shear modulus were reduced. Specific modulus of elasticity in the longitudinal and radial direction and specific shear modulus usually used as important evaluated parameters for acoustic properties of stringed instruments were increased about 11%, 27% and 21%, respectively. From the points of specific modulus and chemical cost, we suggest the more appropriate concentration of LPR used for improvement of acoustic properties of Sitka spruce plate is 5%.

1. Introduction

Wood of the Picea genus has been used as the material for the manufacturing of musical instruments since ancient times. It was primarily used for the top plate of stringed instruments and sounding board of pianos. Improvement of the acoustic properties of low quality wood for musical instruments is very important. This would solve a problem originating in the short supply and expensive cost of high quality wood for musical instruments. This study investigated the vibration properties of quarter-cut Sitka spruce plates treated with three kinds of LPR concentrations (5%, 10%, 20%) by non-pressure process. Resonant frequencies of modes (1, 1), (0, 2), and (2, 0) were measured by Chladni plate vibration method to evaluate acoustic properties of Sitka spruce.

2. Materials and methods

(1) Wood samples

Forty-five quarter-cut plates made of Sitka spruce with a dimension of 410 (L) ×250 (R) × 6 (T) (mm) were prepared for LPR treatment. Wood samples were divided into three subsets for treating with 5%, 10%, and 20% weight concentrations of LPR solution, respectively.

(2) Chladin plate vibration method

A 60 watt loudspeaker was mounted horizontally on a stand under a 20 cm hole in a heavy table top so that the speaker frame was close to the table but did not actually touch it. A thin pad of soft polyurethane foam was tucked between the edge of the speaker and the table. The vibration equipment consisted of an audio generator, a power amplifier capable of 30 to 40 watt output, and a digital frequency counter. The Sitka spruce plate was mounted over the hole in the table on some soft pads with respect to the vibration modes. The plate and the speaker should be as close as possible for good coupling through the air. Fine-grain wood flour was sprinkled on the top of the plate so that when resonant vibrations occur, the flour would bounce out of the actively moving areas (antinodes) and pile up in the quiet areas (nodes). Fig. 1 shows the (1, 1), (0, 2), and (2, 0) vibration modes obtained by Chladni plate vibration method. Mounting points of soft pads and speaker placement for making

each of these three modes appear in plates are shown in Fig. 2.

(1, 1) mode (0, 2) mode (2, 1) mode

Fig. 1 Chladni patterns of different vibration modes.

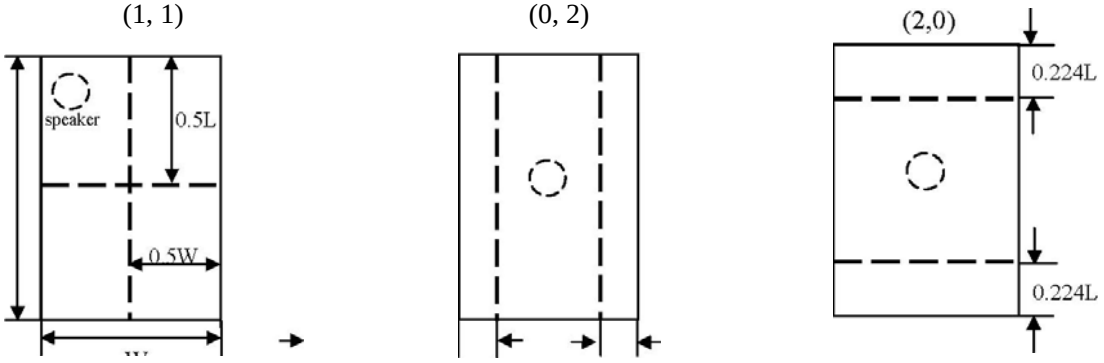

Fig. 2 The large circles show the position of the plate over the speaker cone. Dash lines indicate the nodal lines of different modes of free plates.

3. Results and discussions

(1) Variations of moisture content and density of treated specimens

The moisture contents of specimens treated with 5%, 10%, and 20% weight concentrations of LPR solution in equilibrium with 20℃ temperature and 65% relative humidity were 4.6%, 6.4%, and 7.0% lower than those of untreated ones. The hygroscopic ability of Sitka spruce impregnated with LPR solution was reduced significantly. The densities of specimens were slightly increased while increasing chemical concentrations.

(2) Resonant frequencies at various vibration modes

Table 1 shows the (1, 1), (0, 2), and (2, 0) mode frequencies of control and treated specimens. Whatever concentrations of LPR solution were used, resonant frequencies were increased significantly after treatment. The (2, 0) mode frequency was slightly increased from 2.95% to 5.43% on average, while the increased percents of (1, 1) and (0, 2) mode frequencies were higher in comparison to that of (2, 0) mode frequency. This indicates the thickness of LPR treated Sitka spruce used for plates of stringed instruments could be reduced to achieve the objective frequency and to increase the sound loudness.

(3) Acoustical properties

Table 2 shows the values of modulus of elasticity and shear modulus of chemically treated specimens are greater than those of control specimens. The increased percents of stiffness in the radial direction and of shear modulus of plate were more remarkable than that of stiffness in the longitudinal direction. The values of specific

modulus of elasticity in the longitudinal direction, in the radial direction, and the specific shear modulus of treated specimens, usually used as important parameters for acoustical properties evaluation of stringed instruments, were increased about 11%, 27%, and 21%, respectively.

Table 1 Resonant frequencies of control and treated quarter-cut Sitka spruce plates.

Specimens	Subset	EMC (%)	Density (kg/m3)	(1, 1) (Hz)	(0, 2) (Hz)	(2, 0) Hz
Control	A	12.1	440	64.8	111	184
	B	12.3	430	64.1	110	187
	C	11.9	443	64.0	112	187
Treated	LPR 5%	7.51	455	71.1	125	194
	LPR 10%	5.87	459	70.2	122	196
	LPR 20%	4.88	499	71.8	128	192

Table 2 The values of modulus of elasticity and shear modulus of control and treated quarter-cut Sitka spruce plates.

Specimens	Subset	EMC (%)	Density (kg/m3)	E_L (GPa)	E_L (GPa)	G_{LR} (GPa)
Control	A	12.1	440	11.07	0.62	0.48
	B	12.3	430	11.03	0.59	0.46
	C	11.9	443	11.13	0.63	0.46
Treated	LPR 5%	7.51	455	12.73	0.82	0.60
	LPR 10%	5.87	459	12.94	0.78	0.58
	LPR 20%	4.88	499	13.22	0.91	0.65

E_L: modulus of elasticity in the longitudinal direction.

$E_{L:}$ modulus of elasticity in the radial direction.

G_{LR}: shear modulus of the LR plane.

4. Conclusions

Corresponding to the experimental results determined by Chladin pattern method and of their statistical analysis, the conclusions from this study are as follows:

(1) The Chladin pattern method provides a simpler approach for measurement of important mode frequencies of wooden plates.

(2) The increase in the values of modulus of elasticity in the radial direction of Sitka spruce plate after LPR treatment was greater than that in the longitudinal direction.

(3) A 5% weight concentration of LPR solution would be an optimal selection to improve the acoustical properties of wooden plates used for musical instruments.

5. References

(1) Bucur, V. (1995). Acoustic of wood. P. 135-140. CRC press.

(2) Hutchin, M. C. (2000). Plate tuning for the violin maker. CAS J. 4(1): 52-60.

(3) Yano H, H. Kajita and K. Minato (1994). Chemical treatment of wood for musical instruments. J. of Acoust. Soc. Am. 96(6): 3380-3391.

Leachability of Commercial Ammoniacal Copper Quat and Micronized Copper Quat Used in Taiwan

Chih-Lung Cho, Ya-Lih Lin, Jun-Yan Shen and Li-Chun Lin
Department of Forestry and Natural Resources, National Ilan University

Abstract: In order to fulfill the desire of Taiwan wood preservation industry of obtaining domestic research information to verify the possible leaching property improvement of Micronized Copper Quat (MCQ) declared by Osmose Inc., the leaching test were followed by CNS 6717. The test was conducted using southern yellow pine (SYP, *Pinus* spp.) wood blocks with currently used commercial Chromated Copper Arsenate (CCA), Ammoniacal Copper Quat (ACQ), MCQ, and Copper Azole (CA) and of varied preservative retentions.

Results indicate that among treated SYP blocks, the average leaching percentage of MCQ treated blocks with varied retentions is the lowest (4.94%), followed by the CCA treated blocks (5.42%, statistically indifferent with MCQ treated ones), and then the ACQ treated blocks (10.19%). Components of CCA, ACQ, and MCQ did not leach in proportion to the active ingredient composition of these preservatives. The percentage of Cu compound leached from CCA treated SYP blocks was the highest among the three active ingredients in CCA, followed by Cr compound then As compound. The quats made up over 90% of the leachate leached from ACQ and MCQ treated SYP wood blocks. Dispersed micronized copper compound in MCQ leached less (0.40%) from the treated SYP blocks than from the soluble copper compound in ACQ treated blocks (0.69%), however, the less leachability of the DDAC in MCQ (14.15%) than the BKC in ACQ (22.31%) counts significantly for the less leachability of MCQ than ACQ.

When the leachability of CA was estimated by the percentage of Cu leached from treated SYP wood blocks, CA seems to possess the lowest leaching percentage than other preservatives tested.

1. Introduction

MCQ (Micronized Copper Quat) was imported to Taiwan in 2007 as a substitution/competitor of ACQ. Comparing to ACQ with MCQ, the major differences are: 1. instead of dissolving in the preservative solutions as Cu compounds do in ACQ, micronized Cu compound particles (less than 1000 nm) are dispersed in the preservative solutions with the aid of polymer dispersing agents; 2. the substitution of the chlorine in DDAC with carbonate; and 3. free from ammonia and/or amine in preservative solutions (Freeman and McIntyre 2008). Arguments on the advantages of MCQ over ACQ or vice versa have been pronounced by individual supporters. Tests have been conducted to verify the properties announced. In this article, results from preservative leaching test of commercial CCA, ACQ, and MCQ currently used in Taiwan are reported and the leachabilities of the preservatives are compared. The Cu leaching property of commercially used CA (Copper Azole) preservative is also mentioned.

2. Materials and methods

(1) Wood blocks

Southern yellow pine (SYP) wood blocks with a dimension of 20 × 20 × 20 (mm) were used.

(2) Preservatives

CCA (CNS 14495 CCA No. 3, Arch Inc.), ACQ (CNS 14495 ACQ No.1, Koshii Inc.), MCQ (Osmose Inc.), and CA (AWPA P5-04 CA-B, Arch Inc.) solutions were prepared to perform the SYP treated wood blocks with preservative retentions of 12.0, 9.6, 6.4, 4.0, and 2.4 kg/m^3.

(3) Wood block treatment and leaching test

Wood block treatment and leaching test were performed according to CNS 6717.

(4) Retention and leachate analysis

Unleached treated wood blocks were grounded into pass a 20 mesh sieve powder, and followed by wet ashing procedure (CNS 14730) or extraction (AWPA A37-08) into samples for analysis. The metallic components and

quats in the sample were quantified by ICP and titration respectively. Leachate solutions were analyzed directly without pretreatments.

3. Results and discussions

(1) Total preservative leached

Preservatives and their components leached from treated SYP blocks are summarized in Table 1. The average leaching percentage of CCA, ACQ, and MCQ treated SYP blocks of varied retentions shows that MCQ has the least preservative leaching percentage (4.94%), and ACQ has the highest (10.19%) while CCA (5.42%) is only numerically slightly higher than MCQ and is statistically of no difference.

The preservative leachability seems decreased as the preservative retentions of the treated blocks increase for these three preservatives. However, the absolute amounts (kg/m^3) of preservatives leached from the higher retention blocks were as expected, higher than the lower retention blocks.

Table 1 Average leaching percentages of preservatives and their components leached from treated SYP blocks.

Preser-vative	Preservative and component leached in relate to the original retention (%)				retention reduced
CCA	CrO_3	CuO	As_2O_5	Total	(kg/m^3)
	5.84	8.76	3.01	5.42	0.285
ACQ		CuO	BKC	Total	(kg/m^3)
		0.69	22.31	10.19	0.553
MCQ		CuO	DDAC	Total	(kg/m^3)
		0.40	14.15	4.94	0.234
CA				Cu	
				0.773	

(2) Components of preservatives leached

It is obvious that the components of all the preservatives tested did not leach equally (Table 1). The average leaching percentage of the five retentions reveals CCA treated SYP blocks that As_2O_5 leached least (3.01%), while CuO leached the most (8.76%) and CrO_3 was in between (5.84%). This feature also holds for blocks of all the five retentions individually (Fig. 1).

The difference between the two components (CuO and Quat) in ACQ and MCQ was notable. The average percents of quats leached were 22.32% and 14.15% for ACQ and MCQ respectively, and 0.69% and 0.40% for CuO.

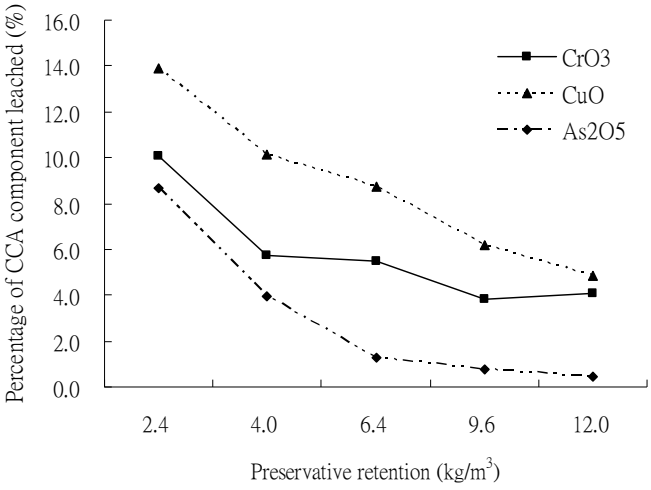

Fig. 1 Percentage of individual component leached from CCA treated SYP blocks.

(3) Leachability of CA

Since tebuconazole makes up only 3.1% of the CA treating solution, referring to the average leaching percentage of copper leached from CA treated SYP blocks of varied preservative retentions was 0.773% (table 1), even if all the tebuconazole were leached, it still makes CA treated SYP blocks possess the lowest preservative leaching percentage (a maximum of 3.873%, approximately) than blocks treated with the other three chemical tested.

The total percentage of Cu compounds leached from SYP blocks treated with ACQ, MCQ and CA (the Cu/organic compound type preservatives) were 0.69%, 0.40%, and 0.77%, respectively. This indicates that with a different fixation mechanism from the ethanolamine and/or ammonium solvent type preservatives, the micronized Cu compounds in MCQ seemed to fix better than the other two preservatives did in the SYP blocks.

4. Conclusions

Among CCA, ACQ, and MCQ, MCQ leached the least (4.94%) from the treated SYP wood blocks tested, followed by CCA (5.42%, statistically indifferent with MCQ) then ACQ (10.19%). The components of CCA, ACQ, and MCQ did not leach in proportion to the active ingredient compositions of these preservatives. The percentage of Cu compounds leached from CCA treated SYP blocks was the highest among those of the three active ingredients in CCA, followed by Cr compounds and then As compounds.

The quats made up over 90% of the leachate leached from ACQ and MCQ treated SYP blocks. The less leachability of the DDAC in MCQ than the BKC in ACQ counts significantly for the better fixation property of MCQ over ACQ.

When the leachability of CA was estimated by the copper leached from treated SYP blocks, CA seems to possess the lowest leaching percentage than the other three preservatives tested.

5. Literature cited

(1) American Wood Protection Association. 2008. AWPA Standard A37-08, P5-08.
(2) ureau of Standards, Metrology, and Inspection. 2000. CNS 6717, 14495, 14730.
(3) Freeman MH, McIntyre CR. 2008. A comprehensive review of copper-based wood preservatives with a focus on new micronized or dispersed copper systems. Forest Prod J. 58(11):6-27.

Effect of Phosphoryl Triamide Treatments on the Mechanical Properties and Dimensional Stability of Woodflour-polypropylene Composites

Chin-Yin Hwang[1], Wen-Jun Ku[1] and Hong-Lin Lee[2]

[1]Taiwan Forestry Research Institute

[2]National Pingtung University of Science and Technology

Abstract: The purpose of this study is to investigate effects of phosphoryl triamide treatment on the flexural properties, internal bond strength, and dimensional stability of woodflour-plastic composites. Factors investigated also included woodflour loading, fire retardant type, and concentration. Results showed that fire retardant treatments adversely affected flexural properties, internal bond strength, and dimensional stability of composites panels. All the measured properties were improved at higher polypropylene (PP) contents improved flexural strength, internal bond strength, and dimensional stability of woodflour-PP composites.

Woodflour-plastic composites have received considerable attention from industry because of their desirable features such as desirable processability, light-weight, dimensional stability, decay resistance, etc. A wide range of properties can be achieved to meet consumer demands by manipulating components formulation and processing factors; however, fire performance of woodflour-plastic composites has been a critical issue. Previous studies have shown that thermal properties, decay and termite resistance of the phosphoryl triamide-treated wood have greatly improved. In this study, mechanical properties and dimensional stability of the phosphoryl triamide-treated woodflour-plastic composites were investigated.

Air-dried China-fir (*Cunninghamia lanceolata Lamb*.) woodflour was pressure impregnated with fire retardants with various concentration levels using a full-cell pressure process. The treated woodflours were then dried, hand-mixed with polypropylene (PP) powder, and subjected to panel fabrication by blending furnish with UF resin, prepressing, hot pressing, and cold setting procedures. A total of 105 panels were made, with 5 replicates for each of the 21 treatment combinations, including 3 woodflour loadings (WFL, 100, 80, and 60%) and 7 concentration levels: untreated (control, CTL), 2 concentration levels for Dricon® (1%, D1; 2%, D2), tripropyl phosphoramide (1%, P1; 2%, P2), and triphenyl phosphoramide (1%, A1; 2%, A2), respectively. Properties investigated including 3-point flexural modulus of rupture (MORb), flexural modulus of elasticity (MOEb), internal bond strength (IB) without (IB0) and with 24 hr water soaking (IB24). Dimensional stability measured comprised of water absorption (WA), thickness swelling (TS) and linear expansion after (LE) after 2 (WA2, TS2, LE2) and 24 hrs (WA24, TS24, LE24) water soaking.

Fig. 1 illustrates the flexural properties of the fire-retardant-treated woodflour-polypropylene composites (WF-PP composites). The average flexural MORs of all treatment combinations were between 119~307 kgf/cm^2. It can be seen in Figure 1 that fire retardant treatments adversely affect the flexural MORs of the WF-PP composites at 2 higher levels of WFL; whereas the adverse effect of fire retardant treatment becomes unnoticeable at WFL=60%. Addition of PP profoundly enhanced flexural MORs of the composite panels, with or without fire retardant treatments. Composites with 40% PP content exhibited highest flexural MORs among all PP levels. Treatment P showed less reduction in the flexural MORs of composite panels, as compared to the other 2 counterpart fire retardants. Average flexural MOEs of the WF-PP composites ranged from 63,200 to 98,900 kgf/cm^2. However, in comparison with the flexural MORs, the adverse effect of fire retardant treatment on flexural MOEs was less pronounced. It is worth noting that WF-PP composites treated with commercially available fire retardant Dricon® (D) showed lower flexural MORs and flexural MOEs than fire retardants A and P.

IB test results showed that average IB0 and IB24 for all treatment combinations ranged from 1.7 to 7.6 kgf/cm^2 and 0.2 to 6.0 kgf/cm^2, respectively (Fig. 2). At 100% WFL, IB0s of the WF-PP composites treated by fire retardants A and D were negatively affected. Conversely, fire retardant treatments showed higher IB0s over the untreated (CTL) composite panels at 2 lower WFL levels. Addition of PP gradually increased IB0s of WF-PP

composites, 60% WFL exhibited the highest IB0s among all WFL levels. After 24 hrs water soaking, IBs of the WF-PP composites dropped considerably. The overall average IB retention, calculated by IB24/IB0*100%, were about 43.6%. Considering WFL effect, average IB retentions decreased from 66.9, 37.5, to 29.7% as WFL increased, implying addition of PP strengthened the IB of the WF-PP composites. However, average IB retentions for the 3 fire retardants were in a order of A (50.7%) ≒ CTL(50.9%) > P (41.7%) > D (33.1%). This result suggested that WFL and fire retardant type collectively affected the IBs of WF-PP composites.

Results of dimensional stability tests are listed in Fig. 3~5. Fig. 3~5 demonstrate that the average dimensional stability for all treatment combinations range from 6.3 to 98.0% for WA2, and 27.5 to 113.4% for WA24; 4.6 to 50.7% for TS2, and 8.4 to 60.0% for TS24; and 0.1 to 1.2% for LE2, and 0.2 to 1.4% for LE24, respectively. At 100% WFL, fire retardant treatments D and P showed higher WA2, WA24, TS2, TS24, LE2, and LE24 than untreated panels (CTL), while treatment A displayed lower WA2, TS2, and LE2 than CTL, but became equivalent to those of CTL at WA24, TS24, and LE24. Among the 3fire retardants, Dricon® (D)-treated WF-PP composites showed higher water uptake, thickness swelling, linear expansion than triphenyl phosphoramide (A) and tripropyl phosphoramide (P). Increasing the PP proportion reduced the water uptake, thickness swelling, and linear expansion of WF-PP composites and offset the adverse effect of fire retardant treatment on dimensional stability. At 60% WFL, CTL panels showed slightly higher WA2, WA24, TS2, TS24, LE2, and LE24 than those of fire retardant treated counter composites.

In conclusion, fire retardant treatment showed adverse effects on the flexural properties, internal bond strength, and dimensional stability of composites panels, especially for Dricon®. As PP was incorporated in the system, flexural MOR, internal bond strength, and dimensional stability of WF-PP composites was greatly improved, the effects were most pronounced at PP level = 40%.

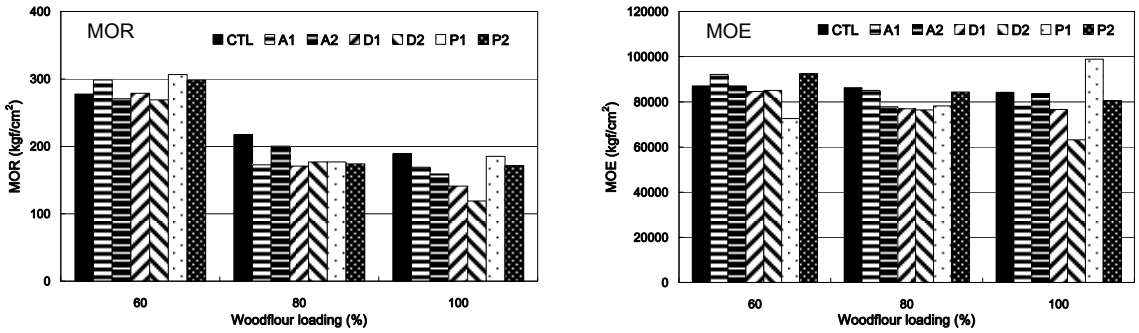

Fig. 1 Effect of fire retardant type, fire retardant concentration, and woodflour loading on the flexural MOR(left) and MOE (right) of WF-PP composites.

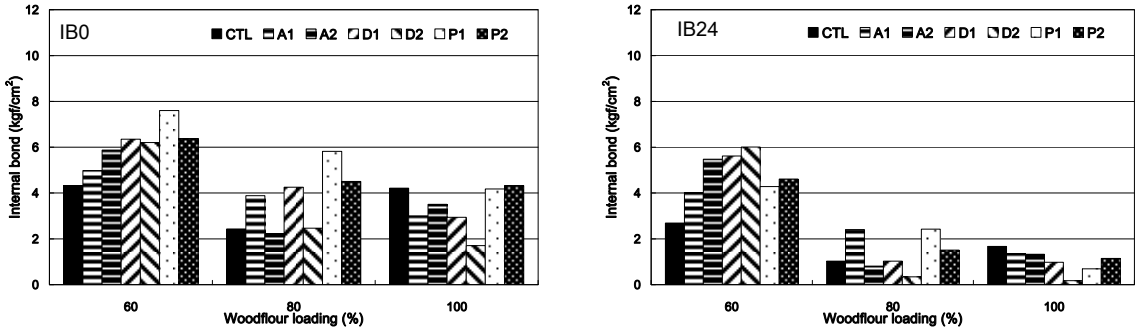

Fig. 2 Effect of fire retardant type, fire retardant concentration, and woodflour loading on the internal bond of WF-PP composites before (left) and after 24-hr water soaking (right).

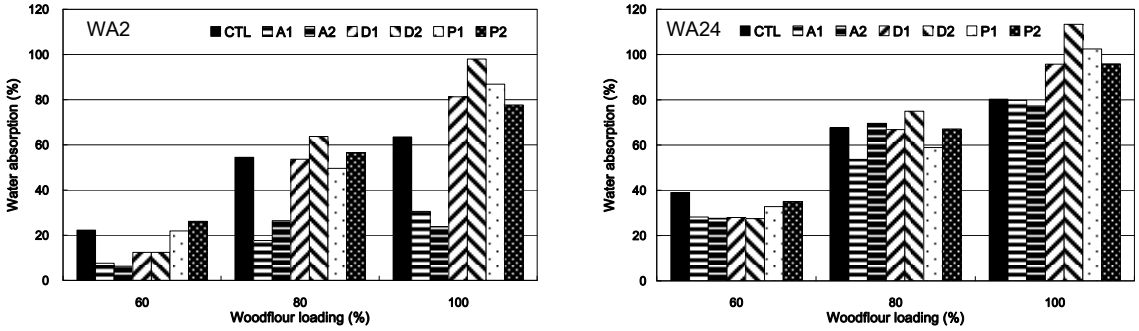

Fig. 3 Effect of fire retardant type, fire retardant concentration, and woodflour loading on the 2-hr (left) and 24-hr (right) water absorption of WF-PP composites.

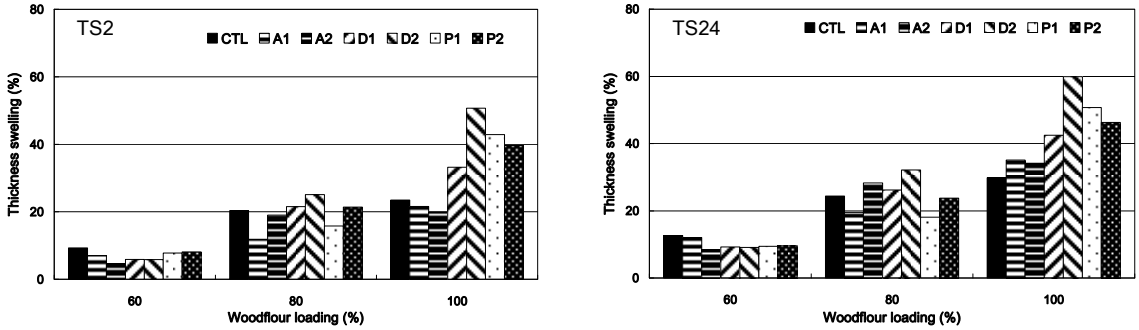

Fig. 4 Effect of fire retardant type, fire retardant concentration, and woodflour loading on the 2-hr (left) and 24-hr (right) thickness swelling of WF-PP composites.

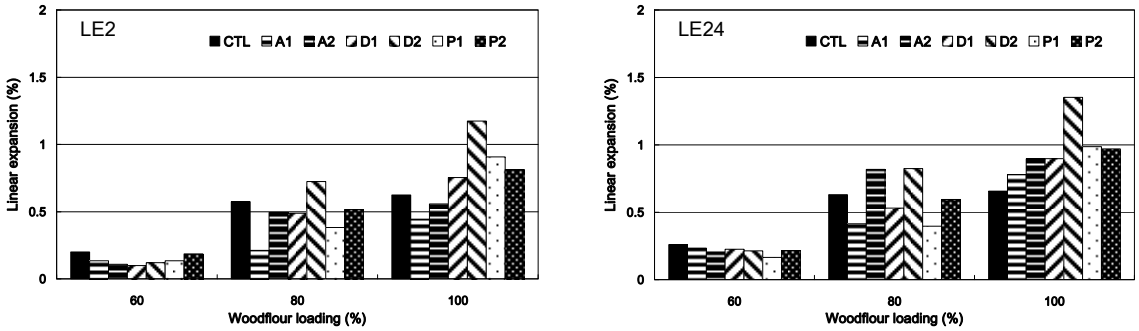

Fig. 5 Effect of fire retardant type, fire retardant concentration, and woodflour loading on the 2-hr (left) and 24-hr (right) linear expansion of WF-PP composites.

The Volatile Flavor Components from Shiitake Mushrooms Grown on the Medium of *Cunninghamia lanceolata*

Jui-Chung Shieh
Taiwan Forestry Research Institute, Taipi

Abstract: The purpose of this study was to explore the volatile components and the scents in shiitake mushrooms [*Lentinus edodes* (Berk.) Sing.] grown on the logs of *Cunninghamia lanceolata* Hook., *Castanopsis hystrix* A. DC., the mixed sawdusts of *Cun.lanceolata* and *Cas. Hystrix*, and pure sawdust of *Cas. hystrix.* Forty eight volatile compounds were obtained from shiitake growing on the different cultivation media in this study. The major compounds of the scents were 1-octen-3-o1 and 1,2,4-trithiolane. The various cultivation media furnished different contents of volatile compounds in shiitake. The total amounts of S-compounds in shiitake revealed the better sensual quality or scents of shiitake mushroom grown on the coniferous material. The content of 1,2,4-trithiolane in shiitake increased with increasing time and temperature during the drying process. Greater contents of C_8 compounds were observed in the mushroom caps than in the mushroom stems. There were no significant differences in the total amounts of sulfurous compounds between mushroom caps and stems.

1. Introduction

Shiitake mushroom *[Lentinus edodes* (Berk.) Sing.] in its origin is a natural food growing in the forest. Because naturally grown shiitake was insufficient in quantity, an artificial cultivation technology was developed to grow shiitake on logs such as those of Fagaceae. Because of shortages of logs in the last decades, the cultivation was swiched to grow it on sawdust medium and on logs other than those of Fagaceae. Unfortunately, broad leaved trees have been cut extensively in recent years. Meanwhile, the consumption of shiitake was increasing; therefore, production costs of logs and sawdust medium increased greatly. The author found that *Cunninghamia lanceolata* Hook. could be used to cultivate shiitake under some circumstances. Lately, we also found that the yield of shiitake increased in the sawdust medium of *Cun. lanceolata* containing a certain portion of the traditional sawdusts, which really reduced the production cost of shiitake.

Components of the scents of shiitake can be divided into two groups ; one is the sulfur compounds and the other is the alcohols having eight-carbons (C_8).The major components of the former were cyclic sulfurous compounds such as 1,2,4-trithiolane (C_2H_4 S_3), and those of the latter were 1-octen-3-o1 and 2--octen-1—o1. Only a slight scent was present in the shiitake before drying. However, enzyme could be activated by the elevated temperature in the drying process which triggers the scent precursors to form the scent of shiitake. The present study attempted to explore the volatile components and scents in shiitake grown on different cultivation media, especially on coniferous materials as well as on traditional materials,*Castanopsis hystrix* A. DC.

2. Material and methods

(1) Mαterials

The shiitake used in this study can be divided into two groups. The first is grown on the logs of *Cun. lanceolata* and/or *Cas. hystrix.* The other is grown on the mixed sawdusts of *Cun. lanceolata* and *Cas. hystrix* and of *Cas. hystrix* only.

(2) Gas chromatograph-Mass spectromety(GC-MS)

Volatile compounds of the shiitake mushroom were extracted from the homogenized fresh mushrooms, then fractionated by silica gel-column chromatography, and further analyzed by GC and GC-MS.

3. Results and discussion

(1) Volatile compounds identified in shiitake mush-Rooms

The results of GC and GC-MS analyses of the volatile compounds are shown in Fig. 1 and Table 1.

The identified compounds in Table 1 can be divided into three groups:

A. Eight-carbon compounds containing alcohols such as 1-octen-3-one, 3-octanol,1-octen-3-o1,1-octanol, cis-3-octen-1-ol,and cis-2-octen-1-o1 were present in the volatiles of shiitake. The results were similar to those described by Chen and others.

B. Sulfur compounds such as dimethyl trisulfide,methyl (methylthio) methyl disulfide,1,2,4-trithiolane,and 1,2,4,6-tetrathiepane were present in the volatile compounds of shiitake. The results were similar to those described in the report by Chen and others.

C. Thirty terpenes and other compounds such as α-pinene,3-hexanone,etc.were listed on Table 1.

(2) Comparison of the compounds identified in the shiitake grown on log and sawdust bags

Contents of the volatile compounds in 100 g of fresh shiitake from *Cun.lanceolata* logs,*Cas. hystrix* logs,mixed sawdust of *Cun. lanceolata* and *Cas. Hystrix*,and sawdust of *Cas. hystrix* were 50,66,46,and 43 mg, respectively. The identified compounds were listed on Table 2 and Fig. 1. Shiitake mushroom flavor is complex in nature and displays well over 41 components as shown in Table 1. Sulfur compounds and C_8 compounds are the major components in the volatile compounds of shiitake, and they are the major compounds affecting the scent of shiitake. Therefore, they must be noticed and studied. Among C_8 components, 1-octen-3-o1 appears as a general mushroom flavor. Among sulfur components, 1,2,4-trithiolane possesses the special odor of shiitake.

As shown in Table 2, 1-octen-3-ol which accounted for 68.42% of the volatile compounds in shiitake from logs of *Cas. hystrix*, followed by 53.79% of those from the mixed sawdusts of *Cun. lanceolata* and *Cas. hystrix*, 46.38% of those from the sawdusts of *Cas. hystry*, 44.33% of those from the logs of *Cun. lanceolata*, was the major component. The content of *cis*-2-octen-1-ol,which was one of important C_8 compounds in the volatile components of shiitake grown on the logs of *Cun. lanceolata,* the logs of *Cas. hystrix*, the mixed sawdusts of *Cun. lanceolata,* and *Cas. hystrix,* and the sawdust of *Cas. hystrix,* were 5.78, 5.55, 4.11,and 3.54%, respectively. The C_8 components of 59.15% in the volatile compounds of shiitake from the logs of *Cun. lanceolata* were less than those of 79.25% from the logs of *Cas. Hystrix.* 1,2,4- Trithiolane contents in the volatile compounds of fresh shiitake grown on the logs of *Cun. lanceola*, the mixed sawdusts of *Cun. lanceolata* and *Cas. hystrix,* the sawdusts of *Cas. hystrx*, and the logs of *Cas. hystrix* were 21.50, 12.06, 6.58, and 0.1%, respectively.

The total sulfur components (21.61%) in the volatile compounds of shiitake from the logs of *Cun. lanceolata* was greater than those of 0.80% from the logs of *Cas. hystrix.* The sulfur compounds of 12.92% in those from the mixed sawdusts of *Cun. lanceolata* plus *Cas. hystrix* were also more than those (7.07%) from the sawdusts of *Cas. hystrix.*

Large percentages of linalool, cinnamic aldehyde, decane, and cedrol were present in shiitake mushrooms (Table 2) grown on the coniferous and traditional materials. It was obvious that the contents of the volatile compounds, especially terpene components, in shiitake were different from those by the various cultivation medium.

Among them, cedrol was the major component in the essential oil of *Cun. lanceolata,* and had the characteristic odor of the wood of this species. Therefore, if *Cun. lanceolata* logs or the proper amount of its sawdust is used for shiitake cultivation, it may promote the special odor of shiitake mushrooms. From the facts described above, it can be concluded that the sensual quality or scents of shiitake from the logs of *Cun. lanceolata* are much better than those of conventional ones, because shiitake grown on the logs of *Cun. lanceolata* or mixed sawdusts of *Cun. lanceolata* and *Cas. hystrix* contains more sulfur compounds (1,2,4-trithio-Iane) and cedrol than the conventional media *(Cas. hystrix)*

Table 1. Volatile compounds identified in shiitake mushroom by capillary gas chromatograph-mass spectrometry.

Peak Nos.	Identified compounds	m. wt.[a]	m. f.[b]	Base peaks	Main[c] fragments m/z
1	α-pinene	136	$C_{10}H_{16}$	93	91, 92, 77, 41, 79
2	3-hexanone	100	$C_6H_{12}O$	57	43, 71, 100
3	camphene	136	$C_{10}H_{16}$	93	121, 41, 79, 67, 107
4	2-hexanone	100	$C_6H_{12}O$	43	58, 71, 100
5	3-methyl-3-pentanol	102	$C_6H_{14}O$	73	55, 45, 43, 87
6	β-pinene	136	$C_{10}H_{16}$	93	69, 41, 79
7	sabinene	136	$C_{10}H_{16}$	93	77, 91, 41, 79
8	3-hexanol	102	$C_6H_{14}O$	59	55, 31, 43, 73
9	limonene	136	$C_{10}H_{16}$	68	67, 93, 45, 79, 121
10	2-hexanol	102	$C_6H_{14}O$	45	69, 87, 84
11	2-methyl-2-(1-methylethl)-oxirane	100	$C_6H_{12}O$	43	71, 58, 85, 100
12	1-octen-3-one	126	$C_8H_{14}O$	70	55, 97, 43, 83
13	3-octanone	128	$C_8H_{16}O$	43	57, 71, 72, 99, 128
14	p-cymene	134	$C_{10}H_{14}$	119	134, 91, 45
15	dodecane	170	$C_{12}H_{26}$	43	57, 71, 85, 99
16	1-hexen-3-ol	100	$C_6H_{12}O$	57	71, 41, 58, 56, 43, 67
17	dimethyl trisulfide	126	$C_2H_6S_3$	126	45, 79, 47, 64, 111
18	3-octanol	130	$C_8H_{18}O$	59	55, 83, 101, 41
19	4-methoxytoluene	122	$C_8H_{10}O$	122	121, 77, 107, 79, 91
20	1-octen-3-ol	128	$C_8H_{16}O$	57	43, 72, 85, 99
21	benzaldehyde	106	C_7H_6O	77	105, 106, 77, 51
22	linalool	154	$C_{10}H_{18}O$	71	93, 55, 41, 43, 69, 80
23	2,2-dimethylpentanal	114	$C_7H_{14}O$	43	57, 72, 85, 89
24	1-octanol	130	$C_8H_{18}O$	41	43, 56, 55, 69, 70, 84
25	1-propoxy-hexane	144	$C_9H_{20}O$	43	85, 59, 73
26	4-terpineol	154	$C_{10}H_{18}O$	71	43, 111, 93, 55, 86
27	ethyl benzoate	150	$C_9H_{10}O_2$	105	77, 122, 150
28	cis-2-octen-1-ol	128	$C_8H_{16}O$	57	41, 81, 68, 95, 110
29	methyl (methylthio) methyl disulfide	140	$C_3H_8S_3$	61	45, 46, 140
30	3-hexene-2,5-diol	116	$C_6H_{12}O_2$	43	55, 83
31	tridecane	184	$C_{13}H_{28}$	57	43, 71, 85
33	1,2,4-trithiolane	124	$C_2H_4S_3$	45	78, 124
34	3-phenylpropanal	134	$C_9H_{10}O$	91	92, 134, 105, 78, 65
35	geraniol	154	$C_{10}H_{18}O$	69	41, 68, 93, 121, 136
36	decane	142	$C_{10}H_{22}$	57	43, 71, 41, 85
37	2-phenylbut-2-enal	146	$C_{10}H_{10}O$	117	115, 146, 91, 78
38	cinnamic aldehyde	132	C_9H_8O	131	103, 77, 51
39	veridiflorol	222	$C_{15}H_{26}O$	43	109, 69, 81, 55, 161
40	cedrol	222	$C_{15}H_{26}O$	43	95, 151, 152, 41, 69, 81
41	1,2,4,6-tetrathiepane	170	$C_3H_6S_4$	78	170, 124, 78, 45, 172, 126

[a] m. wt.: Melecular weight. [b] m. f.: Molecular formula. [c] Main fragment in decreasing intensity order and number indicates relative percentages of the base peaks.

Table 2. Variation of the volatile compounds in fresh shiitake grown on the various cultivation media.

Peak Nos.	Compounds	Shiitake grown on media			
		Logs of *C. l.*[a] %	Logs of *C. h.*[b] %	Mixed sawdusts of *C. l.* and *C. h.*[c] %	Sawdust of *C. h.*[d] %
	Eight-carbon components (%):				
12	1-octen-3-one	Trace	Trace	Trace	0.15
13	3-octanone	3.70[e]	2.25	4.79	3.84
18	3-octanol	3.97	0.32	6.67	5.49
20	1-octen-3-ol	44.33	68.42	53.79	46.38
24	1-octanol	1.37	2.71	0.74	1.12
24-1	*cis*-3-octen-1-ol	Trace	Trace	0.47	0.29
28	*cis*-2-octen-1-ol	5.78	5.55	4.11	3.54
	Total amount of 8-C conponents	59.15	79.25	70.57	60.81
	Sulfurous components (%):				
17	dimethyl trisulfide	Trace	Trace	0.43	0.30
29	methyl (methylthio) methyl disulfide	0.06	0.60	0.28	0.19
33	1,2,4-trithiolane	21.50	0.10	12.06	6.58
41	1,2,4,6-tetrathiepane	0.05	0.10	0.15	Trace
	Total amount of S-components	21.61	0.80	12.92	7.07
	Terpene and other compounds (%):				
3	camphene	Trace	1.51	0.47	0.38
6	β-pinene	0.04	1.61	0.10	0.48
9	limonene	Trace	0.58	0.30	0.40
10	2-hexanol	0.08	0.90	0.51	2.29
11	2-hexanone	0.11	1.28	0.56	2.02
16	1-hexen-3-ol	Trace	0.51	Trace	0.54
22	linalool	1.45	1.50	4.93	10.86
34	3-phenylpropanal	0.45	0.50	0.48	1.53
36	decane	12.00	0.80	Trace	Trace
37	2-phenylbut-2-enal	0.03	0.10	0.47	1.07
38	cinnamic aldehyde	0.41	0.60	3.50	10.29
39	veridiflorol	0.80	5.70	0.15	0.90
40	cedrol	3.51	2.56	4.32	0.17
	Total amounts of terpene and other components	18.88	18.15	15.79	30.93

[a] Logs of *C. l.*=logs of *Cun. lanceolata.* [b] Logs of *C. h.*=logs of *Cas. hystrix.* [c] Mixed sawdusts of *C. l.* and *C. h.*=The mixed sawdusts of *Cun. lanceolata* and *Cas. hystrix.* [d] Sawdust of *C.h.*=The sawdust of *Cas. hystrix.* [e] Counted by digital integrator; the method of area normalization was used in the quantification of each volatile component in shiitake mushrooms.

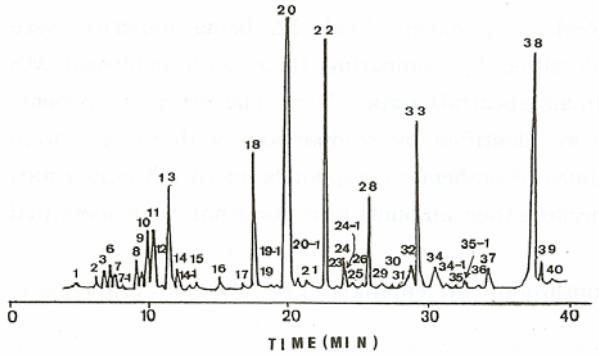

Fig. 1. Chromatogram of the volatile components in shiitake mushrooms grown on the sawdust of *Cas. hystrix.*

(3) Changes of the volatile compounds during the drying process

Each 200 g samples from the mixed sawdust of *Cun. lanceolata* plus *Cas. hystrix.* was collected randomly at 0, 2, 4, 6, 8, 10 and 12 h during the drying process. After extraction with chloroform, the volatile compounds in each sample were 70, 105, 130, 140, 230, 190, and 170 mg, respectively. The content variations of 1-octen-3-ol in the volatile components in shiitake during the drying process were 56.80, 56.67, 28.52, 1.33, 0.98, 0.20, and 0.19%, respectively. Therefore, Contents of 1-octen-3-o1 decreased with the increases of drying times and tempera tures. Conversely, the contents of 1,2,4-trithiolane increased with increases of drying times and

temperatures from 12.06% before drying to 44.58% after 6 h of drying. However, it decreased thereafter to 10.92% after another 6 h of drying. the content of 1-octen-3-o1 (Peak 20) in the volatile components of shiitake grown on the logs of *Cun. lanceolata* decreased from 44.33% for fresh shiitake to 0.1% after drying, and the content of 1,2,4-trithiolane (Peak 33) increased from 21.50% for fresh shiitake to 90.55% after drying.

The total content of C_8 compounds also decreased with the increases of drying times and temperatures. On the other hand, the total content of sulfurous compounds increased with the increases of drying times and temperatures untill 6 h of drying. However, it decreased after 6 h of drying until 12 h of drying. This might be because of the inactivation of enzyme (s) by the higher temperatures, and the less moisture in the drying mushrooms or by the interaction of both factors. Because, enzymes have their appropriate temperatures for reactions, enzyme protein might be inactivated at the drying temperature of 55°C in the late stage.

During drying processes, lenthionine may be produced first in the tissue, but this may be followed by chemical decomposition to remove the 2S (-S-S) to give 1,2,4-trithiolane(Fig. 2). The increase in the yield of 1,2,4-trithiolane during the drying process was suggested to be the results of chemical decomposition.

From Fig. 3, the largest total amount of the S-compounds of shiitake, which accounted for 30% of the shiitake moisture during process of drying, was observed after 6 h of drying. It revealed that the best time of drying was 6 h, but shiitake containing much moisture easily decay in a short time. In the late stage during the process of shiitake drying, the total amounts of S-components and shiitake moisture were reduced gradually with drying time. When shiitake moisture after 10 h of drying reduced to 15%, it may easily be kept for longer times to be used as food. Therefore, the drying of shiitake for 10 h is suggested to be best in the process of drying.

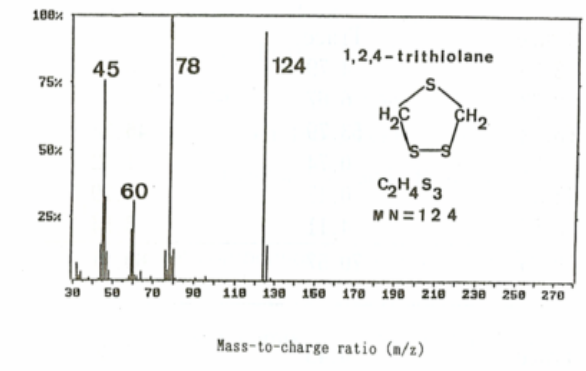

Fig. 2 Mass spectrum of 1,2,4-trithiolane in the volatile components of shiitake mushrooms on the logs of *Cun. Lanceolata.*

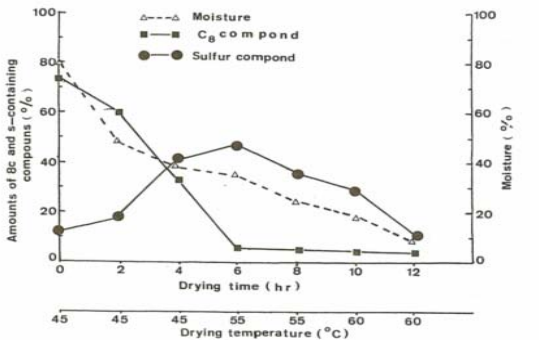

Fig. 3 Changes of the total amounts C_8 and sulfurous compounds in the volatile compounds of shiitake during the shiitake drying process.

(4) Differences between the volatile scents in the stems and those the caps

The mushroom caps contain twice the amounts of C_8 components in mushroom stems. However, there are no significant differences in the amounts of sulfurous compounds in mushroom caps and stems. The contents of α-cedrol in the mushroom caps was more than that in the mushroom stems. There also are no significant differences in other terpenes, except for cedrol, between mushroom cap and stem.

4. Conclusions

(1) Fourty-eight compounds were identified in the volatile scents of shiitake growing on various cultivation media as shown in Table 1. The major components of shiitake scents were 1-octen-3-o1 and 1,2,4-trithio-lane. The presence of 18 volatile components such as cedrol and limonene were reported for the first time in shiitake grown on *Cun. lanceolata* material.

(2) The total content (21.61%) of sulfurous compounds in the volatiles of shiitake grown on the logs of *Cun. lanceolata* was much more than that (0.80%) on the logs of *Cas. hystrix.* On the other hand, the total content (12.92%) of sulfurous compounds in the volatiles of shiitake grown on the mixed sawdust

of *Cun.lanceolate* and *Cas. hystrix* was more than that (7.07%) on the sawdust of *Cas. hystrix*. Therefore, the sensual quality or scents of shiitake grown on the coniferous material was better than that on the traditional material.

(3) The total content of C_8 compounds decreased with increases of drying times and temperatures. On the other hand, the total amount of sulfurous compounds increased with increases of drying times and temperatures after 6h of dring. However, it decresed in the late stage of the drying process.

(4) The total amount of C_8 compounds in the mushroom caps was more than that in the mushroom stems. However, there were no significant differences in the total amounts of sulfurous compounds in mushroom caps and stems.

Preparation and Property of Wood Polymer Composite with a Two-step Method

Yi-Xing Liu [1], Jian Li [1], Yong-Feng Li[1] and Xiang-Ming Wang [2]

[1]Key Laboratory of Bio-based Material Science and Technology of Ministry of Education, Northeast Forestry University, Harbin

[2]FPInnovations-Forintek Division, Quebec, Canada

Abstract: Wood as a porous structure has weak durability and unsatisfactory mechanical properties which limits its utilization. For this reason, the study presents a two-step method to prepare a new modified wood material—*Wood Polymer Composite*. *Maleic anhydride*(*Man*) firstly penetrates into the porous structure of wood, followed by a reaction with wood cell walls. Then, *Styrene*(*St*) with some *Man* and a few amount of initiator, *AIBN*, permeate through the whole wood and react with the above modified wood. The structural characterization of *wood polymer composite* with SEM and FTIR indicates that Man reacts successfully with the hydroxyl group of wood cell wall by its anhydride group, and further reacts fully with styrene as a free radical copolymerization form by its double bond; and thus the polymer fills in wood cell lumina as a solid form, which combines the wood cell walls without any evident crack. The testing results of properties show that the mechanical properties of wood polymer composite increase by about 50%-250% over those of unmodified wood, and its durability improve 1.9-4.89 times than untreated wood.

1. Introduction

Wood as a renewable natural material of biological origin possesses a natural porous structure like honeycomb which endues it with some excellent mechanical properties and a friendly environmental characteristic. However, wood is constituted by biomorphic cells with essential cell walls which have abundant functional groups—hydroxyl groups. As the hygroscopic characteristic of hydroxyl group[1-2], wood is vulnerable to degradation[3] and susceptible to change in dimension[4], which greatly limits its life of utilization.

In order to improve the durability and mechanical properties of wood for longer utilization and wider application, this study presents a new method to reduce the amount of hydroxyl groups with preparing a wood-based composite material called wood polymer composite: with the porous structure of wood as a template, *Maleic anhydride*(*Man*), firstly penetrates into wood cell lumina. After reacting with wood cell wall under a certain condition for *Man*, *Styrene* (*St*) and *Man* are further impregnated into wood cell lumina and reacts with the above treated wood. However, this area of study is very limited[5].

2. Reacting principle

Man is selected to reduce the hydroxyl groups on inner cell walls for the first reacting step, and *St* is used to reinforce the strength of wood for the second step. The reacting principle is expressed as the following formula 1.

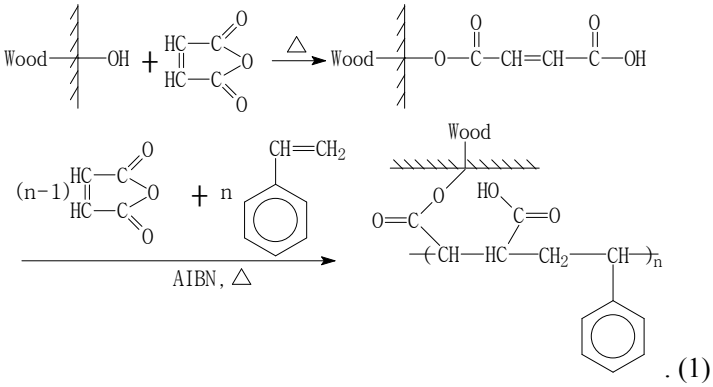

. (1)

3. Material and Methods

(1) Material

Man and *AIBN* were both recrystallized before use. *St* as a reagent of analytical grade was cleaned with sodium hydroxide, and was subsequently distilled under a negative pressure for further purification before use. Wood samples were all cut from *Populus ussuriensis Kom*. The impregnating equipment was self-made.

(2)Methods

First, *Man* was dissolved in acetone for a mixed solution with a 10% concentration; then the wood samples in different sizes were immerged in the mixed solution under conditions of a vacuum of approximate 0.08MPa for 20min, and a following pressure of approximate 0.8MPa for 20min. The impregnated samples were further wrapped in aluminum foils and heated to 100℃~110℃ for 2h. On the second step, *St* firstly mixed with *Man* which was dissolved in acetone with a 50% concentration, and *AIBN* as an initiator was also dissolved in the mixed solution, accounting for about 0.5% of total of *St* and *Man* in weight. The amount of *St* equalled the total of *Man* used on the two steps. Then the mixed solution was impregnated into the wood treated by *Man* under the above impregnating conditions. Following this, the treated samples were wrapped in aluminum foils and further heated to 75℃~85℃ for 6h~8h. The *Wood Polymer Composites* were eventually obtained through the above procedure.

4. Results and discussion

(1) Structure characterization with SEM

Fig.1a shows clearly that wood has a structure of porosity in different sizes called wood cell lumina. Fig.1b shows that after the monomers copolymerizing in the porous structure through the above two-step processes, polymers sufficiently fill in wood cell lumina as a solid form. The polymers contact wood cell walls tightly without any obvious crack which indicates that there's an intensive interaction between polymers and wood cell walls. This interaction may either be physical or chemical, which needs to be further testified by FTIR.

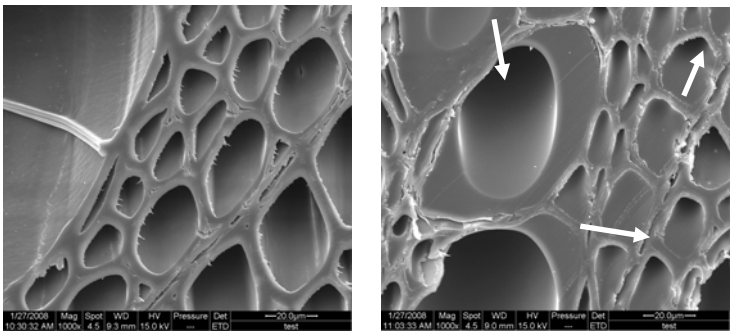

a 1000×untreated wood　　b 1000×wood polymer composite

Fig. 1 SEM morphologies of untreated *wood* and *wood polymer composite.*

(2) Characterization with FTIR

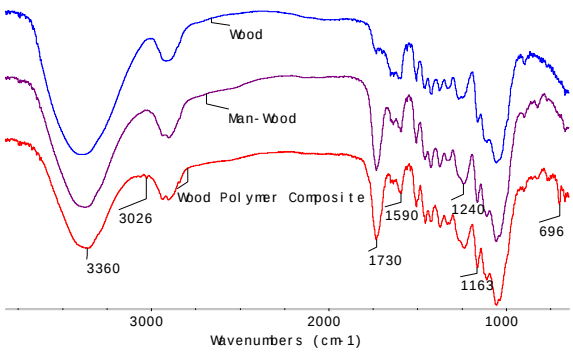

Fig. 2 FTIR spectra of wood and the two types of wood composites.

Fig. 2 shows that compared with *wood*, the band intensities of hydroxyl groups at about 3360cm^{-1} for *Man-Wood* and *Wood Polymer Composite* are degressive, while the band intensities of carbonyl groups at about 1730cm^{-1} for the two wood composites are both quite higher and almost same in degree, which indicate that *Man* reacts with the hydroxyl group of wood cell wall as formula 1, and because of this, the ratio of hydroxyl groups in wood cell walls is reduced. The appearance of a slight peak at 3026cm^{-1} for Ar-H stretching vibration and a peak at 696cm^{-1} for *Ar-H* out-of-plane bending wagging(δ_{Ar-H}) in *Wood Polymer Composite* gives a full evidence for the reaction of St with *Man*. The information about a slightly enhanced peak at 1597cm^{-1} for aromatic skeletal vibration showing in *Wood Polymer Composite* also proves that *St* polymerises with *Man* by their double bonds. The band intensities of C(=O)—O at 1240cm^{-1} and C—O at 1163cm^{-1} in both *Man-Wood* and *Wood Polymer Composite* were higher than that of *Wood* respectively, which also proves that *Man* reacts with the hydroxyl group in wood cell wall. In conclusion, From Fig. 2, it can be known that *Man* and *St* copolymerise in wood cell lumen by their double bonds; meanwhile, the resultant polymers finally bond wood cell walls in a chemical level with a fully complex effect.

(3) Mechanical properties

Table 1 Mechanical properties of wood and Wood Polymer Composite[a]

Mechanical Properties / Sample Name	Static Bending Strength [MPa] (Tangential Section)		Abrasion Resistance [mm] (Tangential Section)		Compression Strength [MPa] (Parallel to Grain)		Hardness [N] (Tangential Section)	
	Mean	Times	Mean	Times	Mean	Times	Mean	Times
Wood	57.47	—	0.101	—	51.43	—	893	—
Wood Polymer Composite	87.93	1.53	0.028	3.51	96.69	1.88	1857	2.08

[a] Mean value is the average for five samples

Table 1 shows that the static bending strength, abrasion resistance, compression strength and hardness of *Wood Polymer Composite* are respectively improved 53%, 88%, 251%and 108% over those of untreated Wood. The above comparison results prove that the produced polymer in wood greatly enhances the mechanical properties of wood, which would broaden the application range of wood.

(4) Durability

Table 2 Decay resistance and dimensional stability of Wood and Wood Polymer Composite[a]

Decay Resistance	Weight loss percentage [%]	Enhanced Times	Volume Swelling Efficiency (soaked in water for 720h)[%]	Enhanced Times
Wood	79.28	—	13.21%	—
Wood Polymer Composite	13.46	4.89	4.56	1.9

[a] value is the average for five samples

Table 2 shows that comparing with *Wood*, the decay resistance and the dimensional stability of *Wood Polymer Composite* are respectively improved 4.89 and 1.9 times, which indicate that the durability of *Wood* is remarkably enhanced. This is the necessary result of polymer reacting with the hydroxyl group of wood cell wall as shown in Fig. 2.

5. Conclusion

The above results show that with the two-step method, polymer produced in situ wood porous structure highly improves the mechanical properties of *Wood*, and also reacts sufficiently with wood cell walls which brings about an excellent durability for *Wood*. As a result, wood modified with this method would become a

promising material which can be widely used in the areas of construction, traffic and furniture.

6. Acknowledgement

This work was financially supported by the Programme of Introducing Talents of Discipline to Universities ("111 Programme").

7. References

(1) Eiichi Obataya, Sakae Shibutani, Kazuya Minato. Swelling of acetylated wood Ⅱ:effects of delignification on solvent adsorption of acetylated wood. Journal of Wood Science, 2007, 53: 408~411

(2) Hui-Ting Chang, Shang-Tzen Chang. Moisture excluding efficiency and dimensional stability of wood improved by acylation. Bioresource Technology, 2002, 85: 201~204

(3) Kartal S. N., Yoshimura T., Imamura Y.. Decay and termite resistance of boron-treated and chemically modified wood by in situ co-polymerization of allyl glycidyl ether(AGE) with methyl methacrylate(MMA). Internation Biodeterioration & Biodegradation, 2004, 53: 111-117

(4) Rashmi R. Devi, Ilias Ali, Maji T. K.. Chemical modification of rubber wood with styrene in combination with a crosslinker: effect on dimensional stability and strength property. Bioresource Technology, 2003, 88: 185~188

(5) Ümit C.Yildiz, Sibel Yildiz, Enqin D. Gezer. Mechanical properties and decay resistance of wood-polymer composites prepared from fast growing species in Turkey[J]. Bioresouce Technotogy, 2005, (96), 1003-1011

New Varieties of *Cinnamomum Osmophloeum* Chemical Classification and Antioxidant Activity

Kun-Yuan Hong[1], Chun-Ya Lin[2], Siou-Sian Lin[2] and Yu-Hui Wu[1]

[1] Division of Forest Chemistry, Taiwan Forestry Research Institute, Taipei

[2] Institute of Forest Environment and Resources, National Taiwan University, Taipei

Abstract: *Cinnamomum osmophloeum* were unique and rare plants, with a wide range of biological activity. Over the past differences in chemical composition is divided into nine chemical strains. In this study, according to new varieties of *Cinnamomum osmophloeum* are divided into 'small round leaf', 'small curled leaf' , 'large curled leaf', and 'veins of gold leaf' and *Cinnamomum osmophloeum* with a garden of ornamental value. These new varieties in 2004, had seedlings from the seed breeding.

By gas chromatography mass spectrometry(GC-MS) analysis, we can totally understood, 'small round leaves' *Cinnamomum osmophloeum* retention time in 23.37 min (KI = 1492) with the control group clearly marked linalool type of difference. 'Small curled leaf', 'large curled leaf, and ' gold veins' in *Cinnamomum osmophloeum* retention time 19.61 min (KI = 1374), had a common principal component. Principal component analysis based on the chemical can confirm the new species, and can be 'vein of gold leaf' and 'the two varieties of cinnamon combined together, and show 'small round leaves', 'small curled leaf' and 'large curled leaf' identified as a new chemical strain.

Measured by the Total phenol content, DPPH, total flavonoid content can realized linalool type of antioxidant capacity and polyphenolic content, was significantly less than those of new chemical strain.

1. Result and discussion

From Fig.1 to Fig. 5 showing that the typical and variation of *Cinnamomum osmophloeum* , there are significant differences in leaf morphology. From Fig 6 and Table 1 also shows result in great differences from the target element contains linalool, cinnamaldehyde, α-copaene. Therefore, analyzing based on morphology, volatile components and antioxidant activities, can confirm that there does exit a new variants and have diversity of chemical strains in *Cinnamomum osmophloeum*.

Fig. 1 *Cinnamomum osmophloeum.*

Fig. 2 New Varieties of "Short leaves".

Fig. 3 New Varieties of "Small curled leaves".

Fig. 4 New Varieties of "Large curled leaves".

Fig. 5 New Varieties of "Yellow vein".

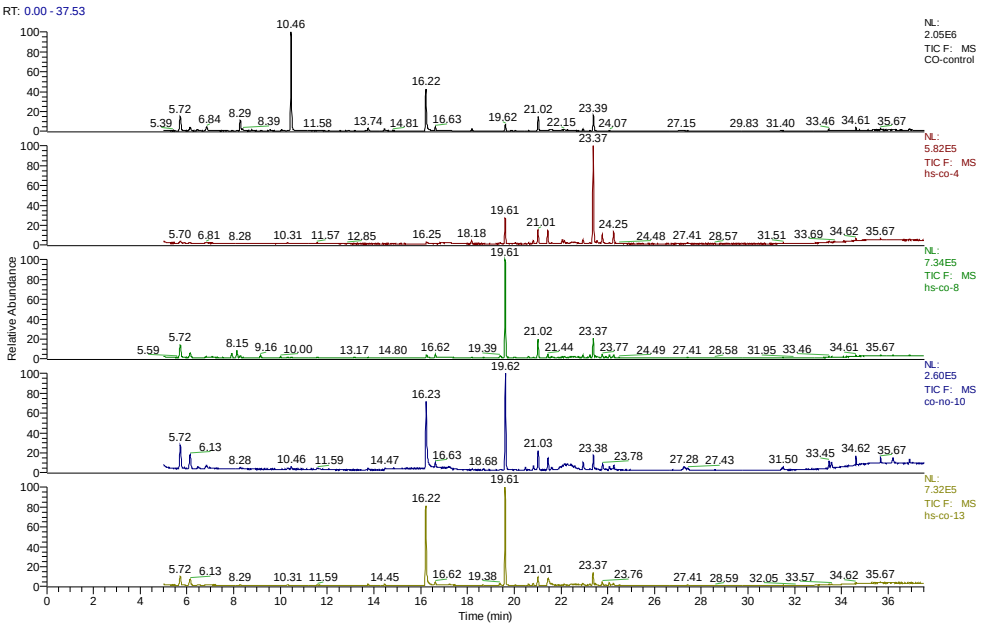

Fig. 6 Gas chromatogram for all different specimens of *Cinnamomum osmophloeum.*

Table 1. The RI, KI value, and relative compounds on different samples.

Sample	RI	KI	Compound
Control	10.46	1098	linalool
HS-4	19.61	1374	α-copaene
	23.37	1492	sesquiterpenes
HS-8	19.61	1374	α-copaene
HS-10	16.23	1272	cinnamaldehyde
	19.62	1374	α-copaene
HS-13	16.22	1271	cinnamaldehyde
	19.61	1374	α-copaene

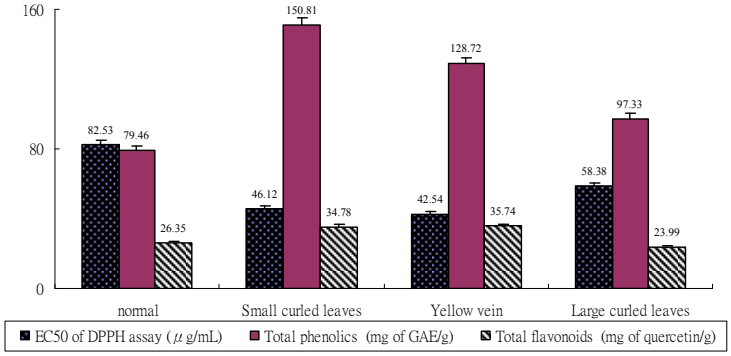

Fig. 7 Plant antioxidant activity of leaf methanol extract from different *Cinnamomum osmophloeum* specimens.

2009海峽兩岸林產科技研討會論文集

Cross Strait Forest Products Technology Symposium
Proceedings of the 2009

發 行 人　黃裕星
總 編 輯　王益真
執行編輯　何振隆、葉民權、徐光平
責任美編　許明峰
出版單位　行政院農業委員會林業試驗所
地　　址　10066台北市中正區南海路53號
電　　話　02-2303-9978
傳　　真　02-2314-2234
網　　址　http://www.tfri.gov.tw
印　　刷　麥克馬林有限公司
展 售 處　國家書店
　　10455台北市松江路209號1樓 (02)2518-0207
　　五南文化廣場：台中總店
　　40042台中市中山區中山路6號3樓 (04)2226-0330
出版日期　中華民國九十八年十一月 初版
工 本 費　新台幣200元整
ISBN　978-986-02-0752-1
GPN　1009803364